THE UNIVERSITY
of EDINBURGH

Investigations of Novel Dimerisations and Brevianamide-type Alkaloids

Degree of Doctor of Philosophy

Helen Jones

School of Chemistry

The University of Edinburgh 2021

Declaration

I declare that:

a) that the thesis has been composed by the student, and

b) either that the work is the student's own, or, if the student has been a member of a research group, that the student has made a substantial contribution to the work, such contribution being clearly indicated, and

c) that the work has not been submitted for any other degree or professional qualification except as specified, and

d) that any included publications are the student's own work, except where indicated throughout

Helen Jones, 24 January 2022

Acknowledgements

Firstly, I would like to thank my supervisor Prof. Andrew Lawrence for the opportunity to work on these projects and all his assistance given during my PhD.

I would like to thank all members of the Lawrence group past and present that I have worked alongside. With special thanks to Peter DaBell (Dabsy) and Jake Stuart for the top banter in and outside of the lab. As well as Dr Josh Homer for being a glowing source of positivity and encouragement and for making the long nights and weekends up in N2.16 bearable. To Dr David Jones for sharing his wealth of knowledge and for the much needed support given during the final stages of my PhD. And of course for his unwavering patience when proof reading the first drafts of my thesis!

A special thanks to Jacob for his endless and tirless support, encouragement and tolerance of me day-in-day out during my PhD.

Finally, I would like to thank my family for their unwavering support and unconditional love throughout my time in Edinburgh.

Abbreviations

$[\alpha]_D^T$	specific rotation, T °C, sodium D line
ΔG	Gibbs free energy
δ	chemical shift
12-crown-4	1,4,7,10-tetraoxacyclododecane
18-crown-6	1,4,7,10,13,16-hexaoxacyclooctadecane
9-BBN	9-borabicyclo[3.3.1]nonane
Ac	acetyl
acac	acetylacetonate anion
AIBN	2,2′-azobis(2-methylpropionitrile)
app.	apparent
aq.	aqueous
Bn	benzyl
BOC	tert-butyloxycarbonyl
BOX	bis(oxazoline) ligands
BP	boiling point
br.	broad
cat.	catalytic
cat*	chiral catalyst
Cbz	benzyl chloroformate
CIP	counter ion pairs
CLA	chiral lithium amide
COSY	correlation spectroscopy
CuTC	copper thiophene carboxylate
d.r.	diastereomeric ratio
DABCO	1,4-diazabicyclo[2.2.2]octane

DBU	1,8-diazabicyclo[5.4.0]undec-7-ene
DCC	*N*,*N*′-dicyclohexylcarbodiimide
DDQ	2,3-dichloro-5,6-dicyano-p-benzoquinone
DEAD	diethylazodicarboxylate
DEATMS	(diethylamino)trimethylsilane
DFT	density functional theory
dia-	diastereomer
DIBAL-H	diisobutylaluminium hydride
DIPT	diisopropyltryptamine
DKR	dynamic kinetic resolution
DMAP	4-(dimethylamino)pyridine
DMF	*N*,*N*-dimethylformamide
DMP	Dess–Martin periodinane
DMSO	dimethyl sulfoxide
dppf	1,1′-bis(diphenylphosphino)ferrocene
e.e.	enantiomeric excess
e.r.	enantiomeric ratio
E	generic electrophile
EDC	1-ethyl-3-(3-dimethylaminopropyl)carbodiimide
EDG	electron donating group
EI	electron ionisation
EI^+	electron ionisation (positive mode)
epi-	epimer
Equiv.	equivalents
ESI	electrospray ionisation
ESI^-	electrospray ionisation (negative mode)
ESI^+	electrospray ionisation (positive mode)

EWG	electron withdrawing group
H-bond	hydrogen bond
HATU	1-[bis(dimethylamino)methylene]-1*H*-1,2,3-triazolo[4,5-*b*]pyridinium 3-oxid hexafluorophosphate
HDMS	hexamethyldisilazane
hept	heptet
HMBC	heteronuclear multiple-bond correlation
HMPA	hexamethylphosphoramide
HOBt	hydroxybenzotriazole
HPLC	high performance liquid chromatography
HRMS	high-resolution mass spectrometry
HSQC	heteronuclear single-quantum correlation
hν	photochemical irradiation
i-	*iso*-
IHB	ionic hydrogen bond
IMDA	intramolecular Diels–Alder
IR	infrared
IPA	isopropyl alcohol
J	coupling constant
JohnPhos	(2-biphenylyl)di-*tert*-butylphosphine
L*	chiral ligand
LA*	chiral Lewis acid
LDA	lithium diisopropylamine
LG	leaving group
LLS	longest linear sequence
NHPI	*N*-hydroxyphthalimide
nr	no reaction
[M]	molecular ion

m/z	mass to charge ratio
*m*CPBA	*meta*-chloroperberzoic acid
MHz	megahertz
MoOPH	oxodiperoxymolybdenum(pyridine)-(hexamethylphosphoric triamide)
MP	melting point
MS	molecular sieves
MTBE	methyl *tert*-butyl ether
MW	molecular weight
NBS	*N*-bromosuccinimide
NCS	*N*-chlorosuccinimide
NIS	*N*-iodosuccinimide
NMP	*N*-methyl-2-pyrrolidone
NMR	nuclear magnetic resonance
NOESY	nuclear Overhauser effect spectroscopy
Nu	generic nucleophile
[O]	oxidation
P_1-*t*-Bu	*tert*-butylimino-tris(dimethylamino)phosphorane
p-TSA	*para*-toluenesulfonic acid
p-Ts	*para*-toluenesulfinate
petrol	petroleum ether 40-60 °C
PG	generic protecting group
Ph	Phenyl
Phth	phthaloyl
PIFA	(bis(trifluoroacetoxy)iodo)benzene
Piv	pivaloyl
PMB	*para*-methoxybenzyl
POM	pivaloxymethyl

ppm	parts per million
quant.	quantitative yield
R	generic alkyl group
r.r	regioisomer ratio
recry.	recrystallization
R_f	retention factor
RSM	recovered starting material
rt	room temperature
SM	starting material
S_N2'	nucleophilic conjugate substitution
SSIP	solvent separated ion pairs
TADDOL	α,α,α',α'-tetraaryl-2,2-disubstituted 1,3-dioxolane-4,5-dimethanol
taut.	tautomerisation
TBAF	*tetra*-*n*-butylammonium flouride
TBS	*tert*-butyldimethylsilyl
Tf	trifluoromethylsulphonyl
TFA	trifluoroacetic acid
TFAA	trifluoroacetic anhydride
THF	tetrahydrofuran
TLC	thin layer chromatography
TMEDA	*N*′-tetramethylethylenediamine
TMS	trimethylsilyl
t_R	retention time
Ts	*para*-toluenesulfonyl
TS	transition state
TsOH	tosic acid
UV	ultraviolet

ν_{max}	IR absorption maximum
w/u	work-up
w/v	weight per volume
w/w	weight per weight
X	generic halogen/leaving group

Lay Summary

Chapters 1-3: Enantiomers are two molecules that possess the same chemical connectivity, but are non-superimposable mirror images of each other. In chemistry it is often beneficial, for medicinal purposes, to make compounds as a single enantiomer. Although each enantiomer looks identical, they can have starkly different biological activities and some of which can lead to potentially adverse side effects when used in medication. Chemical methods to separate enantiomers have historically been considered difficult to execute and wasteful through low product recovery or poor separation. Extensive work has been sought to combat these known limitations, by developing new approaches for the production of single enantiomers – a field known as asymmetric synthesis.

Within chapter **2** and **3** we discuss efforts towards creating a fundamentally new and more efficient approach towards the synthesis of single enantiomers. Each chapter details the application of this new approach to different chemical reactions and the optimisation of the reactions to achieve the most effective method for single enantiomer production.

Chapters 4-7: Chemical compounds that are derived from microorganisms, animals and plants are referred to as natural products. The brevianamides are a family of natural products produced by fungi. In 1969 they were first isolated and have since sparked much interest regarding their origin and chemical synthesis. This is because members of the family have been shown to possess a wide range of biological activities. Despite extensive chemical research, not all of the members have been made synthetically in a laboratory. The aim of this project was to produce a short and concise synthetic route to members of the brevianamide natural product family.

Chapters **4-7** describe the successful synthesis of several of these complex natural products, in addition to efforts towards the synthesis of other members. Through these investigations we have been able to develop a better understanding of their origins and have been able to produce workable quantities to test for more biological activities these molecules may possess.

Abstract

This thesis describes work towards two discrete projects; Chapter 1-3 methodology development of enantioconvergent reactions, Chapter 5-7 total synthesis of brevianamide type natural products. Both of these studies are linked through the underlying theme of the development of novel dimerisations.

Chapter 1-3

Classically, asymmetric synthesis has relied upon kinetic resolutions to deal with racemic starting materials. Unfortunately, the use of kinetic resolutions is limited to a maximum 50% yield, which represents a serious inefficiency in modern chemical synthesis. Enantioconvergent reactions offer a method to circumvent this limitation and afford a single enantioenriched product in a maximum theoretical yield of 100%. However, all currently known methods for achieving enantioconvergency are limited in their substrate scope; the starting materials invariably contain stereogenic elements that are amenable to mutation or ablation and are currently unable to contain multiple stereogenic centres. We aimed to overcome this long-standing limitation by developing stereoretentive-enantioconvergent reactions, which would allow the use of racemic substrates with multiple robust stereogenic elements. The new approach would feature a symmetry-breaking dimerisation of racemic starting materials to form of a non-*meso* dimeric product.

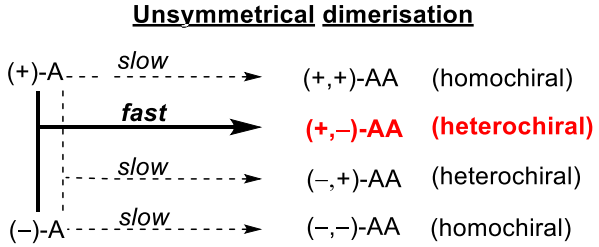

To accomplish this we targeted dimerisations that are inherently heterochiral-selective (*i.e.*, opposite enantiomers dimerise), and developed methods to make these reactions enantioconvergent. This thesis will describe our investigations into previously known

heterochiral-selective dimerisations; an *aza*-Darzens dimerization (Chapter 2) and a Diels–Alder dimerization (Chapter 3), and efforts to make them enantioconvergent including the success of performing the first stereoretenetive enantioconvergent *aza*-Darzens reaction.

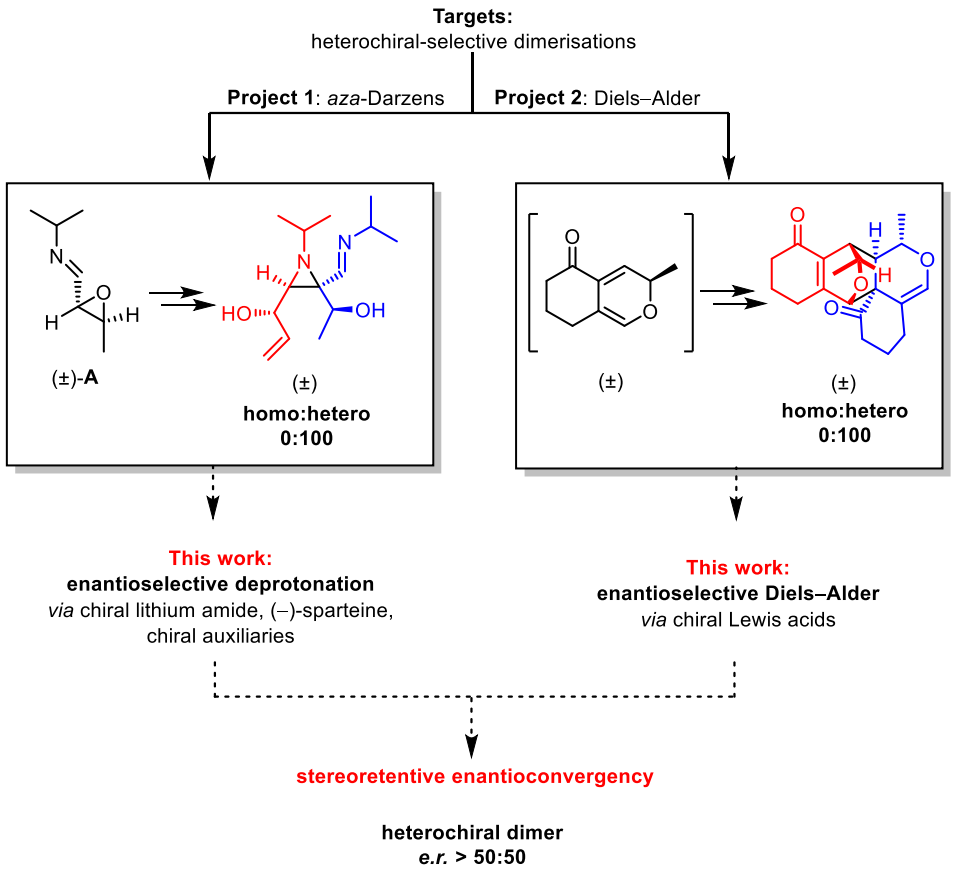

Chapter 4-7

The brevianamides are a family of alkaloid natural products extracted from the *Aspergillus* and *Pencillium* fungi. The brevianamides were the first natural products, isolated in 1969, to contain the archetypal bicyclo[2.2.2]diazaoctane ring. Since their first isolation their complex structure and varied biological activities have inspired many total syntheses. Despite decades of experimentation, the synthesis of many members of the brevianamide family have yet to be conquered and many unanswered questions remain about their biosynthetic origin.

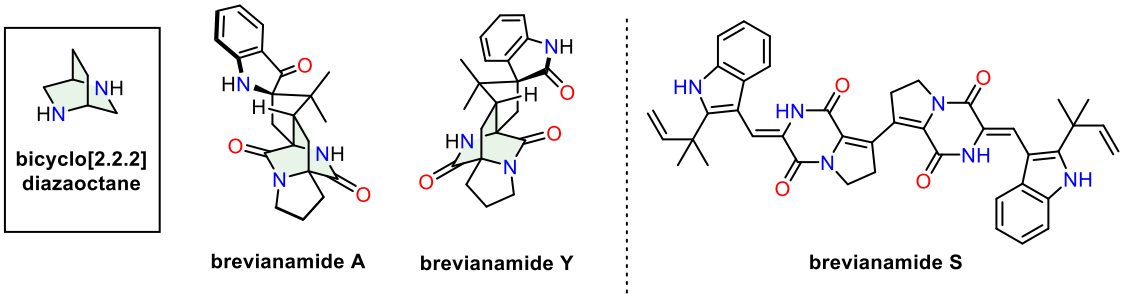

In 2020 the Lawrence group published the first total synthesis of brevianamide A, over 50 years since its isolation. This thesis continues the Lawrence group's work and describes the efforts towards the first total synthesis of a dimeric member of the natural product family, in addition to the concise bioinspired total synthesis of other members. These studies also provided new mechanistic insights into the key domino reaction pathway believed to be biosynthetically responsible for constructing the core bicyclo[2.2.2]diazaoctane motif.

Table of Contents

Chapter 1: Stereoretentive Enantioconvergent Reactions Introduction

Nature's high specificity is derived through chiral control. This ability to have absolute control over the regio-, chemo-, diastero- and enantio- outcomes of organic reactions has long been recognised as a target across multiple disciplines of synthetic chemistry. The high demand from the pharmaceutical and the agricultural industry to produce optically pure compounds has provided a major driving force in the development of these new asymmetric synthesis methods. Despite remarkable progress being made in the field since its inception, asymmetric synthesis, i.e., the production of enantioenriched chiral compounds, still remains of high importance, but represents a significant challenge for the synthetic community.

1.1 Asymmetry in Synthesis

Classically, in asymmetric synthesis, the methods used to install new stereogenic elements depend on the nature of the substrate. When starting with an achiral substrate, we can use enantioselective reactions to install a new stereogenic elements, wherein an enantioenriched reagent or catalyst is used to control the absolute configuration of the new stereogenic elements (**Scheme 1.1**).

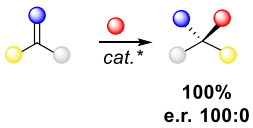

Scheme 1.1: Schematic representation of an enantioselective reaction of a prochiral substrate

A classic example is the Noyori asymmetric hydrogenation of 1,3-keto-esters (**1.1**) (**Scheme 1.2**).[1] The enantioenriched ruthenium complex selectively delivers hydride to one enantiotopic face, with chelation to the neighbouring ester functional group stabilising one diastereomeric transition state over the other to afford a single enantiomer as the product (**1.2**). Despite these reactions playing an

extensive role throughout chemical synthesis, the number of viable prochiral functional groups remains limited.

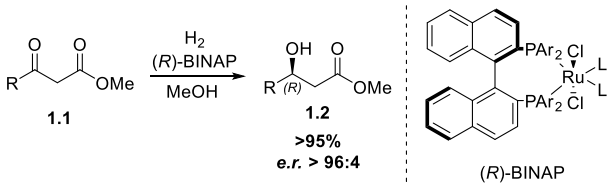

Scheme 1.2: Noyori asymmetric hydrogenation of a 1,3-keto-ester

Starting with a racemic starting material, the situation is much more complex. Typically, we rely on kinetic resolutions which achieve partial or complete separation of a racemate by the virtue of unequal rates of reaction with a chiral reagent or catalyst to afford an enantioenriched product (**Scheme 1.3**).[2]

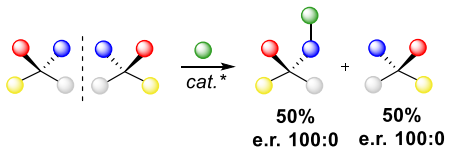

Scheme 1.3: Schematic representation of the kinetic resolution of a racemic mixture

An illustrative example is the kinetic resolution of racemic allylic alcohols (**(±)-1.3**) using the Sharpless asymmetric epoxidation (**Scheme 1.4**).[3] The chiral reagent reacts preferentially with the (*R*)-enantiomer to form the corresponding epoxy alcohol (**1.4**) in enantioenriched form.

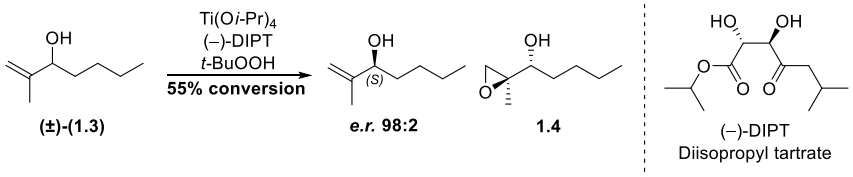

Scheme 1.4: Kinetic resolution of a racemic allylic alcohol *via* the Sharpless asymmetric epoxidation

This protocol of racemate separation has several associated limitations. Firstly, the resolution is restricted to a maximum 50% theoretical yield as one enantiomer of the racemate remains unreacted. Predominately in kinetic resolutions, the unreacted enantiomer is actually the desired product and the other enantiomer, which has undergone the synthetic transformation, is often separated and discarded. This highlights the secondary limitation of step economy, as a step must be added to the reaction sequence solely for the purpose of resolution and not a synthetic transformation. Therefore, though prevalent in academia and industry,[4,5] kinetic resolutions represent a serious inefficiency in modern chemical synthesis when dealing with racemic starting materials.

1.2 Enantioconvergent Reactions

Enantioconvergent reactions avoid the loss associated with kinetic resolutions, by incorporating both enantiomers of the racemic starting material into a single enantioenriched product, which therefore has a maximum theoretical yield of 100% (**Scheme 1.5**). Noyori has previously described this process as an example of "ideal asymmetric catalysis".[6]

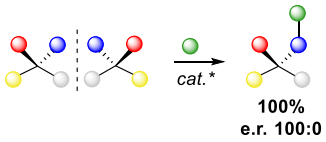

Scheme 1.5: Schematic representation of an enantioconvergent reaction of a racemic mixture

Currently three distinct approaches towards enantioconvergent reactions exist in the literature (**Figure 1.1**).[7] Each of these focuses on a different method to desymmetrise the system by destroying the mirror plane of symmetry that exists between the two enantiomers, either through stereoablation, stereomutation or stereoconvergence.

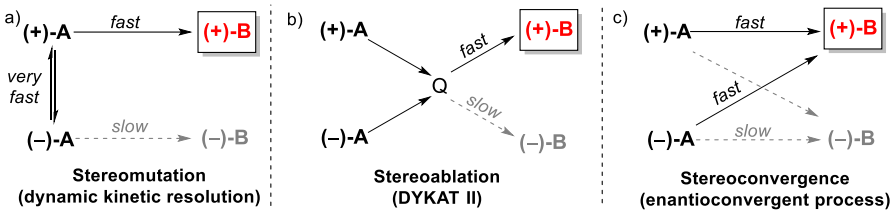

Figure 1.1: Current approaches known towards enantioconvergent synthesis, a) stereomutation, b) stereoablation and c) stereoconvergence

1.2.1 Stereomutation

The most common approach is stereomutation, which is frequently employed in organic synthesis as a dynamic kinetic resolution (DKR) (**Figure 1.1a**).[8] Within this protocol, system-level symmetry is broken *via* a rapidly interconverting equilibrium, thus proceeding through a common achiral intermediate. This ensures a constant turnover to the more reactive enantiomer, which reacts preferentially with a chiral catalyst or reagent to afford the desired product in enantioenriched form. For an effective DKR the rate of racemisation k_{rac} must be equal or greater than the rate of reaction k_a. If $k_{rac} < k_a$ resolution is still possible, but only if k_{rac} is significantly greater than k_b ($k_{rac} >> k_b$) (**Scheme 1.6a**).[9]

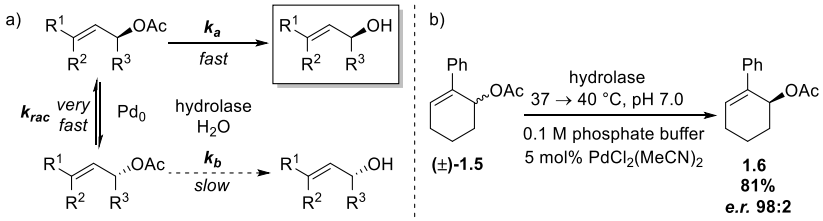

Scheme 1.6: a) Schematic of a stereomutative process b) The transition metal catalysed epimerisation of an allylacetate with the biocatalysed ester hydroylsis

An example of this is the *in situ* transition metal catalysed racemisation of an allylic acetate **(±)-1.5** followed by biocatalysed ester hydrolysis, which yields (−)-allylic alcohol (**1.6**) in 81% yield and e.r. 98:2 (**Scheme 1.6b**).[10]

Nature has an innate stereospecificity, so biosynthetic pathways do not require the use of racemases and as a consequence very few have been found to exist. This is why predominately transition metals are found to be used in the deracemisation step.

1.2.2 Stereoablation

Another approach is through stereoablation, which involves the destruction of the system's intrinsic stereochemistry *via* a chemically stable intermediate (**Q**) followed by a stereoselective reaction to form a single enantiomer as the product (**Figure 1.1b**). The nature of the common intermediate **Q** determines the subclass of these reactions.

If **Q** is achiral, the ensuing stereoselective transformation must be enantioselective and this type of reaction has been defined as stereoablative. An interesting example of a stereoablative reaction is cyclic deracemisation. Previously it has been employed in the deracemisation of α-amino acids (**Scheme 1.7**) which comprises of an enantioselective oxidation to the corresponding imine (**1.7**).[11,12] Imine **1.7** (the achiral intermediate) then undergoes a non-selective back reaction to give both enantiomers of the starting material. Successive cycles of the reaction result in a build-up of enantiomer **1.8**, which therefore increases the overall *e.r.* of the product.

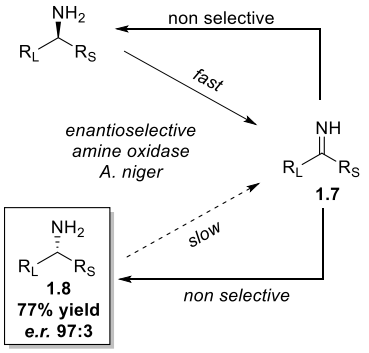

Scheme 1.7: The cyclic deracemisation of α-amino alcohols

However, if the achiral intermediate (**Q**) generated from the racemate is attached to a chiral catalyst it forms a single enantioenriched catalyst-substrate adduct (**ACat***), which is chiral. This external chiral centre now becomes the sole influence on the stereochemical outcome of the reaction and

therefore the final transformation is diastereoselective. These type of reactions were coined by Trost at the turn of the century as dynamic kinetic asymmetric transformation type II (DYKAT II).[13]

A dynamic kinetic asymmetric transformation constitutes a reaction where the intermediate derives from a chiral racemic precursor in which the chirality of the substrate is destroyed. A DYKAT type II reaction is a special form of a DYKAT reaction and is defined by Faber as a resolution proceeding through a single enantiomeric intermediate.[9]

This approach was exemplified by Trost (**Scheme 1.8**) in the enantioconvergent palladium catalysed allylic alkylation of a racemic cyclohexene tetraol (**(±)-1.9**).[14,15] In a stereoselective ionisation, both enantiomers eventually form the same C_2 symmetric δ-allylpalladium complex (**ACat***) albeit, at different rates. The inclusion of an enantiopure ligand on the palladium catalyst determines the outcome of the diastereoselective nucleophilic addition to give a single product **1.10**.

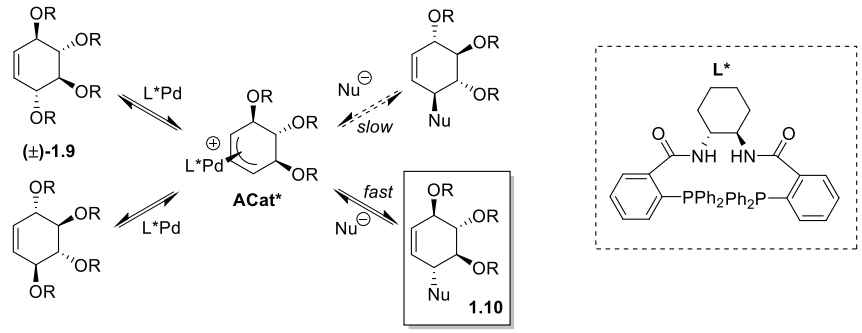

Scheme 1.8: DYKAT type II process. L* = enantiopure ligand, Nu = generic nucleophile

1.2.3 Stereoconvergence

The final known method for enantioconvergence in the literature is direct stereoconvergence, whereby the starting racemate undergoes parallel kinetic resolutions with opposite selectivity to form a single enantioenriched product (**Figure 1.1c**). The stereochemical prerequisites for the chiral catalyst are high as not only must the catalyst exhibit enantioselectivity by having a preference for one enantiomer over the other, but it must also show opposing stereoselectivity with respect to inversion or retention of configuration during the reaction. Consequently these reactions are rare

and currently dominated by biocatalysts. An example of this is shown with the enantio- and stereo-selective hydrolysis of styrene type epoxides **(±)-1.11** (**Scheme 1.9**).[16] One proceeds with inversion and one with retention to give a single enantioenriched diol product of e.r. 95:5 (**1.12**).

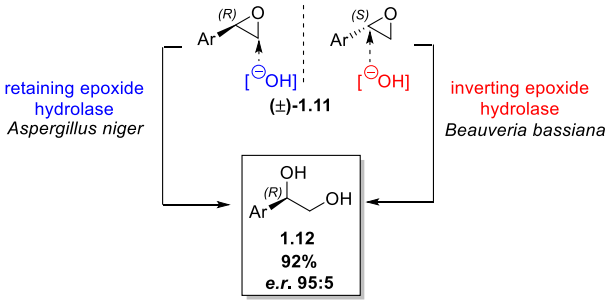

Scheme 1.9: Stereoconvergent biocatalytic hydrolysis of styrene type epoxides

1.3 This Work: Stereoretentive Enantioconvergent Reactions

This project aims to achieve enantioconvergency *via* a new dimerisation approach where no destruction or mutation of the inherent stereochemistry of the racemic mixture need occur.

Dimerisation reactions of racemic samples can lead to an array of different dimeric products with both homo- and hetero- chiral dimerisations possible. A dimerisation can also occur in a symmetrical or unsymmetrical manner. The former is pictorially represented in **Scheme 1.10**, with the new sigma bond formed between groups of the same colour (e.g., white and white, **1.13-1.15**) and the unsymmetrical variant with the newly forming sigma bond between groups of different colours (e.g., white and yellow, **1.16-1.19**).

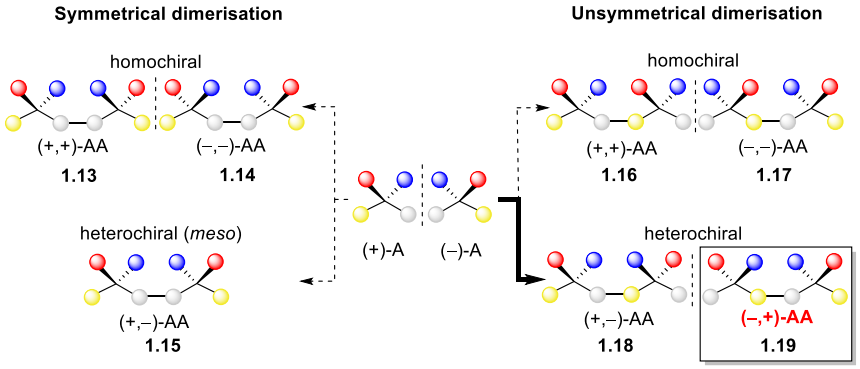

Scheme 1.10: Schematic to show different dimeric combinations possible for a racemic mixture and how to render the dimerisation enantioconvergent

To achieve enantioconvergency both enantiomers of the racemic starting material must be incorporated into the final product and hence the reaction must be inherently heterochiral selective (**Scheme 1.10**). Another prerequisite for enantioconvergency is that the symmetry of the system must be broken during the dimerisation. If the dimerisation occurs in a bilateral symmetrical fashion then the two heterochiral products formed are in fact identical, achiral *meso*-compounds (**1.15**). However, when the system-level symmetry is broken during an unsymmetrical dimerization, then the heterochiral dimers are in fact chiral (**1.18**, **1.19**) and this provides us with the necessary framework to probe whether this could be performed enantioselectively. Thus achieving stereoretentive enantioconvegency.

Conceptually, this represents an exciting new approach to accessing enantiopure materials from racemic starting materials, which is yet to be explored experimentally or theoretically. **Scheme 1.11** summarises this project with the need to focus on known heterochiral selective unsymmetrical dimerisation reactions and the methods to render them enantioselective.

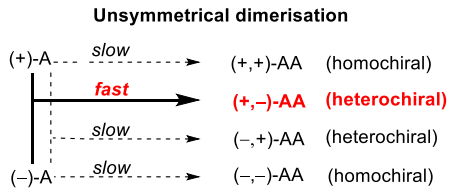

Scheme 1.11: Schematic to show summaries stereoretentive enantioconvergency

1.4 Project 1: *aza*-Darzens

In 2001, Würthwein and co-workers reported a base-induced dimerisation of a racemic imine epoxide, which to their surprise exhibited complete heterochiral selectivity in an unsymmetrical dimerisation (**Scheme 1.12**).[17] The reaction, described by the authors as an *aza*-Darzens process, was serendipitously found when trying to perform a base-induced oxirane opening of **(±)-1.20** to form allylic alcohol **1.21**.

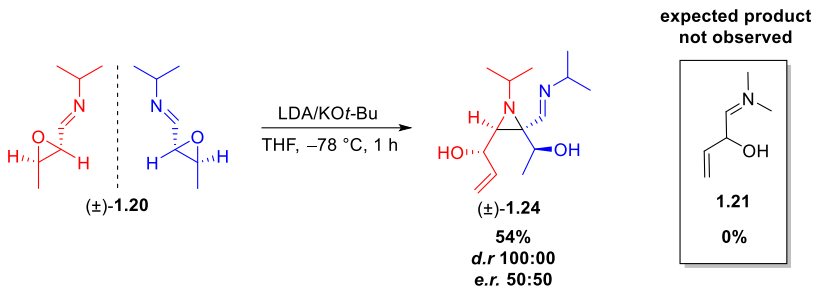

Scheme 1.12: Würthwein's *aza*-Darzens dimerisation

The proposed mechanism of this unexpected dimerisation (**Scheme 1.13**) proceeds *via* deprotonation α- to the epoxide of racemate **(±)-1.20** affording lithiated species **(±)-1.22**, which selectively adds to its antipode in a 1,2-addition step. This adduct then undergoes successive 3-*exo*-tet cyclisation to install the aziridine motif (**(±)-1.23**) and then 3-*exo*-trig ring opening of the epoxide to afford the final product (**(±)-1.24**). To explain the remarkable diastereoselecitivity displayed, Würthwein postulated that an additional lithium ion is chelated between the two epoxides forming a 'decalin-like' 10 membered transition state (**(±)-1.25**). DFT calculations performed on this cationic bislithium TS‡ (**(±)-1.25**) showed that the heterochiral combination is 6.8 kcal/mol lower in energy than the corresponding homochiral couple.

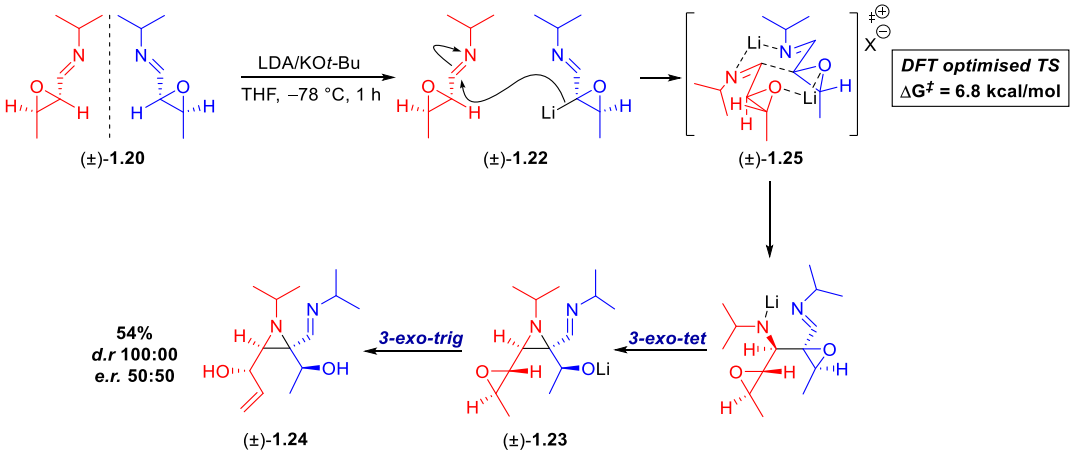

Scheme 1.13: Proposed mechanism of the *aza*-Darzens dimerisation

This *aza*-Darzens reaction presents an attractive, yet simple system for us to investigate initially to establish our new concept of stereoretentive enantioconvergency. In addition to the reaction showing inherent heterochiral selectivity, monomer **(±)-1.20** is easily accessed in two steps from a readily available enal (**1.26**, **Scheme 1.14**).

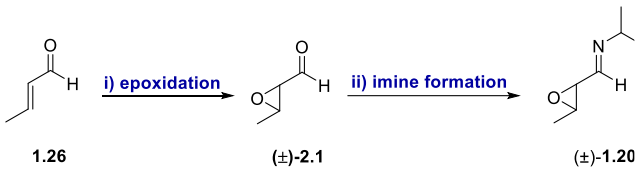

Scheme 1.14: Synthetic route to monomer **(±)-1.20**

1.4.1 Aims of *aza*-Darzens Project

To render this reaction enantioconvergent we plan to substitute the achiral base currently used for a chiral enantiopure alternative to effect an enantioselective deprotonation (**Scheme 1.15**). As Würthwein and co-workers utilized a lithium base in their original work, we decided to focus on chiral lithium amides (CLAs).

The use of CLAs in asymmetric synthesis is well-documented.[18] As a versatile class of reagents, they are able to act as bases, nucleophiles and ligands. Specifically, there are publications reporting the use of CLAs in enantioselective deprotonations α to epoxides.[19] In this project we hope to exploit this previously reported reactivity and apply it to our system to perform an enantioselective deprotonation. Hence, this would provide a gateway to the seminal studies towards establishing stereoretentive enantioconvergency as a novel concept in asymmetric catalysis.

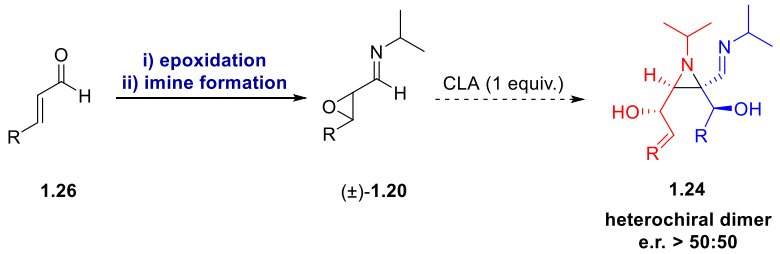

Scheme 1.15: Stereoretentive enantioconvergent variant of Würthwein's *aza*-Darzens dimerisation

1.5 Project 2: Diels−Alder

Alongside these studies, we wish to investigate the highly heterochiral-selective Diels−Alder dimerisation of *2H*-pyrans reported previously by Hayashi and co-workers.[20,21] While exploring the utility of Diels–Alder reactions in the synthesis of an epoxyquinol family of natural products, Hayashi and co-workers noted the heterochiral selective dimerisation as an unwanted side reaction (**Scheme 1.16**).

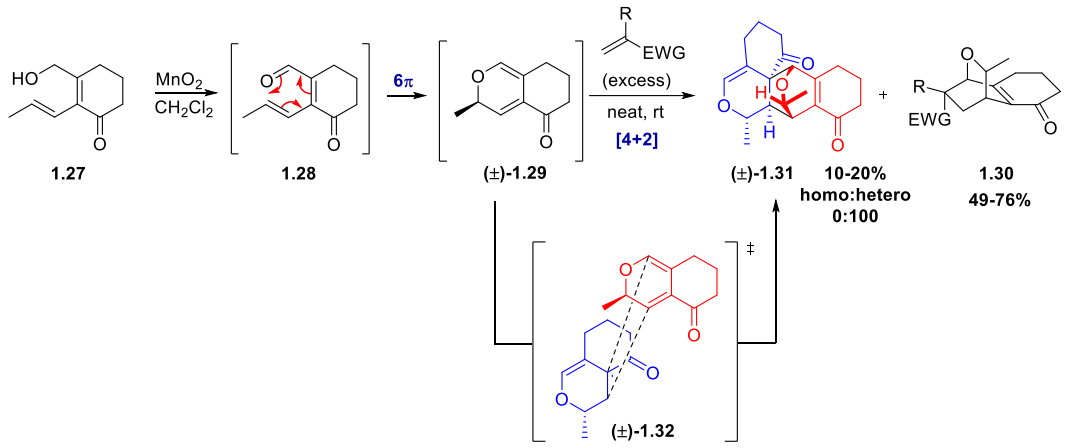

Scheme 1.16: Hayashi's original Diels-Alder reaction with heterochiral dimer side product (**1.31**)

Treatment of alcohol **1.27** with manganese dioxide affords aldehyde **1.28**, which undergoes a spontaneous 6π-electrocyclic ring closure to give 2*H*-pyran **(±)-1.29**. Treatment with an excess of a reactive dienophile traps out the 6π-electrocyclisation product giving predominantly adduct **1.30**. Interestingly, a heterochiral dimerization of the 2*H*-pyran (**(±)-1.31**) also occurs as a minor reaction pathway. The remarkable heterochiral selectivity can be explained by sterics, which induce the highly regio- and *endo*- selective Diels–Alder self dimerisation. The heterochiral combination minimises the steric interactions as the methyl substituents on both the diene and dienophile can occupy space remote to the bond-forming-zone (see proposed transition state (±)**-1.32**, **Scheme 1.16**).

As this Diels–Alder reaction shows a preference for the heterochiral dimerisation product (**(±)-1.31**), it presents an interesting target to potentially prepare in enantioenriched form. The

Diels–Alder cycloaddition is a fundamental reaction in chemical synthesis due to its ability to generate molecular complexity in one simple step through the highly stereo- and regio- selective nature of the reaction. The application of our stereoretentive concept to this system would constitute a significant advance in the utility of this ubiquitous reaction.

1.5.1 Aims of Diels−Alder Project

The use of chiral Lewis acid catalysis is well established for Diels−Alder reactions.[22,23] Given the inherent substrate controlled heterochiral selectivity we only require the chiral Lewis acid catalyst to differentiate between the two enantiomeric transition states in order to form an enantioenriched product (**Scheme 1.17**). Therefore, we have a plethora of potential catalysts to screen, two of which are shown below (**1.33** and **1.34**),[24,25] in hopes of achieving stereoretentive enantioconvergency.

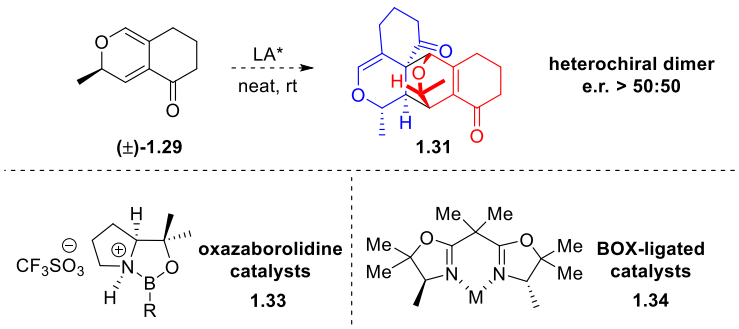

Scheme 1.17: Stereoretentive enantioconvergent variant of Hayashi's Diels-Alder dimerisation

Chapter 2: *aza*-Darzens Results and Discussion

2.1 Synthesis of *aza*-Darzens Monomer ((±)-1.20)

2.1.1 Route 1: Crotonaldehyde

To establish the chemistry that underpins this project, investigations began with the synthesis of (±)-*N*-*iso*propyl-3,4-epoxy-1-*aza*-pent-1-ene monomer (**(±)-1.20**). Following the previously reported synthesis by Würthwein and co-workers,[17] we attempted to reproduce their results forming monomer **(±)-1.20,** *via* epoxidation of crotonaldehyde (**1.26**)[26] and subsequent imine formation (Scheme **2.1**).[17]

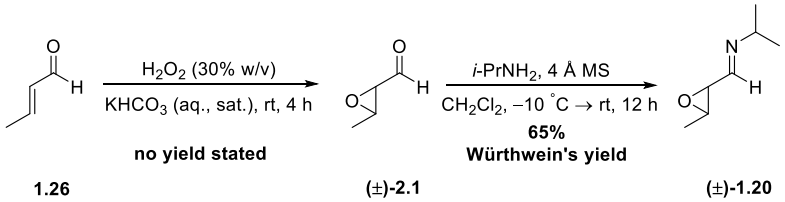

Scheme 2.1: Würthwein's synthesis of monomer **(±)-1.20**

It should be noted that although the synthesis of epoxide **(±)-2.1** must have been achieved by Würthwein and co-workers, the details of their method were not featured in the supplementary information of the paper. Instead the reader was directed to a 1982 paper by Ceroni and Sequin (**Table 2.1**, **Entry 1**).[26] Regrettably, we were never able to reproduce the results of Ceroni and Sequin: the reaction did not go to completion and difficulties in separating the product from the starting material were encountered (**Table 2.1**, **Entry 1**). Attempts at purification by column chromatography resulted in loss of material and attempts at distillation proved unsuccessful, as the starting material (**1.26**) and product (**(±)-2.1**) had similar boiling points (56 °C/93 mbar and 53 °C/80 mbar respectively).[27,28] Furthermore, due to the volatile nature of these compounds, significant loss of material during rotary evaporation was an additional complication.

The need to push the reaction to completion to avoid complications in purification became evident. Using more equivalents of H_2O_2 (**Table 2.1**, **Entries 2-4**) resulted in little difference in conversion

ratios. The best result was obtained when an additional equivalent of H_2O_2 was added after two hours, but still resulted in a non-negligible quantity of unreacted starting material (**Table 2.1**, **Entry 4**).

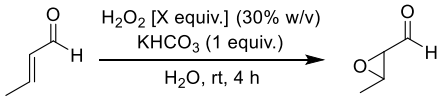

1.26 **(±)-2.1**

Entry	H_2O_2 (X equiv.) at t = 0	H_2O_2 (X equiv.) at t = 2 h	1.26[a]:(±)-2.1[a]
1	1.1	-	11:89
2	2.2	-	25:75
3	3.3	-	31:69
4	1.1	1.1	9:91

Table 2.1: Crotonaldehyde epoxidation, [a] ratios determined by ^{1}H NMR spectroscopy

We considered that one possible reason for the reaction not going to completion was insufficient control of the pH of the reaction; it was later seen that control over pH during epoxidation, of a similar substrate, was imperative to afford product.[29] Further attempts to push the reaction to completion to avoid the purification problems already discussed, by screening alternative reaction conditions (solvent, reagents, time) were also unsuccessful (**Table 2.2**). At this stage it was decided to switch focus to other synthetic approaches (**see Sections 2.1.2 page 15** and **2.1.3 page 16**).

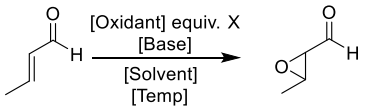

1.26 **(±)-2.1**

Entry	Temp (˚C)	Time (h)	Solvent	Oxidant (X equiv.)	Base (1 M)	1.26[a]:(±)-2.1[a]
1	rt	4	H_2O	H_2O_2 (1.1)	$KHCO_3$	11:89
2	rt	12	H_2O	H_2O_2 (1.1)	$KHCO_3$	10:90
3	rt	4	H_2O	H_2O_2 (3.3)	$KHCO_3$	31:69
4	rt	12	H_2O	H_2O_2 (3.3)	$KHCO_3$	28:72
5	35	48	H_2O	*t*-BuOOH (1.3)	NaOH	21:79
6	rt	12	H_2O/THF (9:1)	H_2O_2 (1.1)	$KHCO_3$	8:92
7	rt	24	H_2O/THF (9:1)	H_2O_2 (1.1)	$KHCO_3$	6:94

Table 2.2: Tested epoxidation conditions of crotonaldehyde, [a] ratios determined by ^{1}H NMR spectroscopy

2.1.2 Route 2: Methyl Crotonate

As the use of crotonaldehyde (**1.26**) as the starting material had proved more challenging than first expected, we decided to explore other routes to synthesise monomer **(±)-1.20**. With not much room for divergence in a synthesis of just two steps, we envisaged starting the synthesis with methyl crotonate (**2.2**). Starting with methyl crotonate (**2.2**) instead of crotonaldehyde (**1.26**) gave us an opportunity to use the alternative oxidant *m*CPBA (due to the more electron rich double bond) in a well-documented literature epoxidation and then use reduction chemistry to access monomer **(±)-1.20** (**Scheme 2.2**).[30,31]

Methyl crotonate **2.2** was successfully epoxidised when refluxed overnight in dichloromethane with *m*CPBA to form the corresponding epoxy ester **(±)-2.3** in a poor yield with many unidentified side products.[30] However, when the solvent was changed to 1,2-dichloroethane this allowed the reaction to take place at a higher temperature, and resulted in a cleaner reaction, forming epoxy ester **(±)-2.3** in 59% yield.[31] Notably, this epoxidation with methyl crotonate was achieved without running into any of the previous problems of incomplete conversion, lengthy reaction times or difficulties in purification found when using crotonaldehyde.

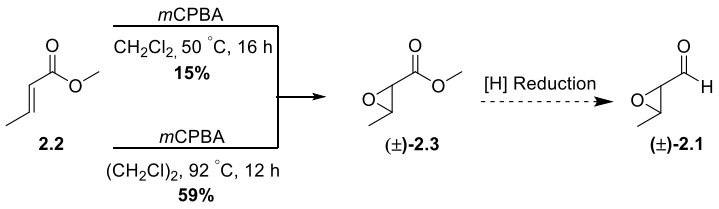

Scheme 2.2: Methyl crotonate route to epoxy aldehyde **(±)-2.1**

It was envisaged that we would carry out direct reduction of the ester functional group to the aldehyde using DIBAL-H (**Scheme 2.3**).[32] Unfortunately, when epoxy ester **(±)-2.3** was submitted to the reaction conditions a complex mixture of products was formed.

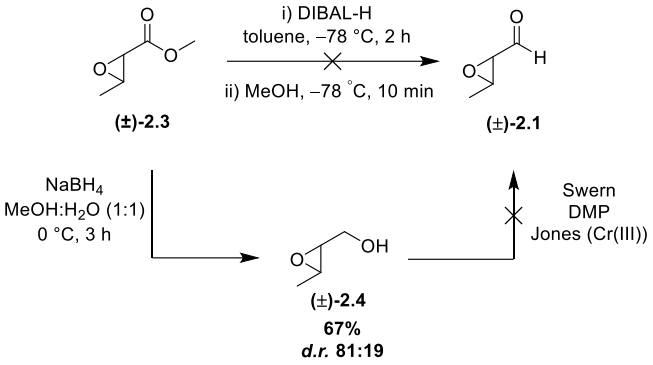

Scheme 2.3: Reduction of epoxy methyl crotonate then oxidation conditions tested to form **(±)-2.1**

Thus, we were forced into the lengthier strategy of over-reduction to the alcohol (**(±)-2.4**) followed by oxidation back to the aldehyde (**(±)-2.1**) (**Scheme 2.3**). Reduction of ketone **(±)-2.3** with sodium borohydride successfully gave alcohol **(±)-2.4** in 67% yield.[33] Regrettably, even though different oxidising conditions were tested (Swern, DMP, Jones oxidation (Cr(III)),[34–36] we were never able to isolate the elusive epoxy aldehyde **(±)-2.1**.

2.1.3 Route 3: Organocatalysis Using Pyrrolidine

With limited success achieved using an alternative starting material, we looked to the use of a catalyst to help speed up reaction times and improve conversion of the original epoxidation of crotonaldehyde (**1.26**). Inspiration came from the work of Cordova *et al.*[37] on the organocatalytic asymmetric epoxidation of α,β-unsaturated aldehydes using proline derivatives. For our system, with no need for asymmetric induction, we looked to use pyrrolidine.

Scheme 2.4 shows the proposed, generally accepted, mechanism for the catalytic cycle.[38] Condensation of the pyrrolidine catalyst with crotonaldehyde forms the more electrophilic iminium ion **2.5**. Subsequent nucleophilic [1,4] addition of the peroxide anion gives enamine intermediate **2.6**, which undergoes a *3-exo-tet* cyclisation to give epoxide **2.7**. Hydrolysis of this iminium

intermediate (**2.7**) produces the desired epoxy aldehyde **(±)-2.1**, and regenerates the pyrrolidine catalyst.

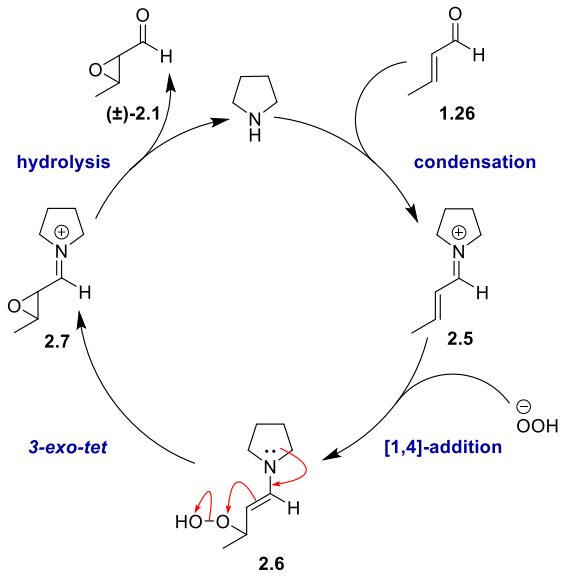

Scheme 2.4: Proposed mechanism of the organocatalysed epoxidation of crotonaldehyde using pyrrolidine

It was found that full conversion could be achieved using just 1 mol% pyrrolidine and leaving the reaction to stir at rt for 2 days (**Table 2.3**). After careful removal of solvent and distillation of the product we recovered epoxide **(±)-2.1** in 32% yield (**Table 2.3**, **Entry 6**). The lower isolated yield compared to the observed NMR conversion is attributed to difficulties during purification resulting in loss of compound.

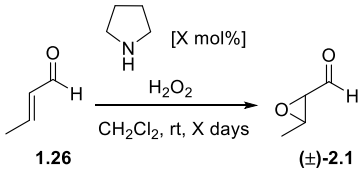

Entry	Pyrrolidine (X mol%)	Time (days)	1.26[a]	(±)-2.1[a]
1	0.1	5	-	100
2	0.1	4	-	100
3	0.1	3	-	100
4	0.1	2	-	100
5	0.1	1	12	88
6	0.01	2	-	100
7	0.005	2	6	96

Table 2.3: Tested crotonaldehyde epoxidation conditions, [a] ratios determined by ^{1}H NMR spectroscopy

Under this new set of conditions, the epoxidation was successfully achieved with 100% conversion and the reaction time was reduced from 5 days to 2 days (**Scheme 2.5**).

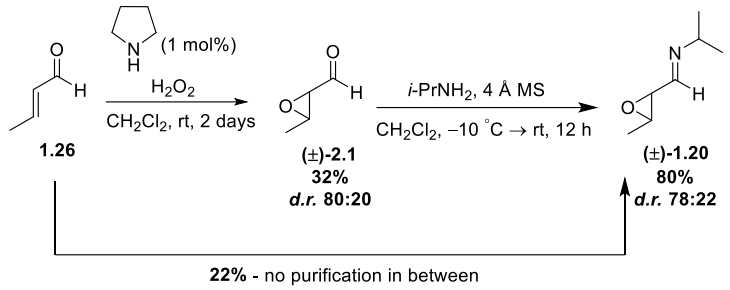

Scheme 2.5: Optimised epoxidation and imine formation conditions for crotonaldehyde

The imine formation step in the synthesis of monomer **(±)-1.20** proved much easier and we were able to form the monomer in an excellent 80% yield, which is higher than that achieved by Würthwein himself (65%).[17] Still suffering with similar difficulties in concentrating the crude epoxidation mixture, we attempted the reaction without purifiying the epoxide **2.1** and achieved a comparable yield of 22% over the two steps (**Scheme 2.5**).

2.2 Monomer Derivatives

After finally achieving the successful synthesis of monomer **(±)-1.20** we looked to the possibility of forming other structural variants. It was anticipated that using less volatile starting materials would present fewer problems in terms of handling and purification. It would also be beneficial to have access to differently substituted monomers (both in terms of varying the substitution of the epoxide and alternative imine groups) for exploring the potential scope of the dimerisation reaction.

2.2.1 *trans*-Hexenal

trans-Hexenal (**2.8**) was selected and the previously described synthesis of monomer **(±)-1.20** using organocatalysis for the epoxidation proved easily amenable, forming the epoxide **(±)-2.9** in 21% yield, under unoptimised conditions. The subsequent imine formation was achieved in 61% yield to afford us our first substituted monomer **(±)-2.10** (**Scheme 2.6**).

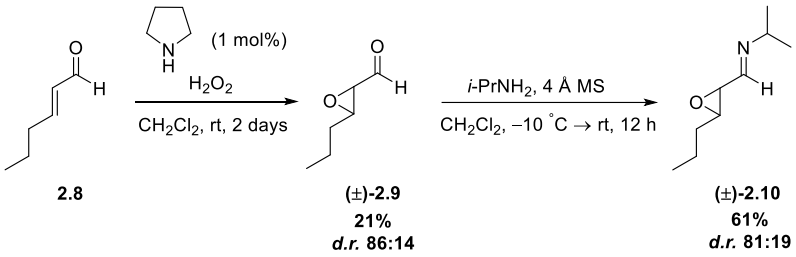

Scheme 2.6: Optimised epoxidation and imine formation conditions for *trans*-hexenal

2.2.2 Cinnamaldehyde

The complications encountered obtaining a pure epoxidation product with the two previous aliphatic enals (**1.26**, **2.8**) encouraged us to try an aromatic enal. Cinnamaldehyde (**2.11**) is an aromatic enal which has a high boiling point (125 °C/ 27 mbar).[40] Our decision was reinforced by literature, as the epoxidation of cinnamaldehyde is also a well-documented transformation with a variety of conditions available to try.[41–43]

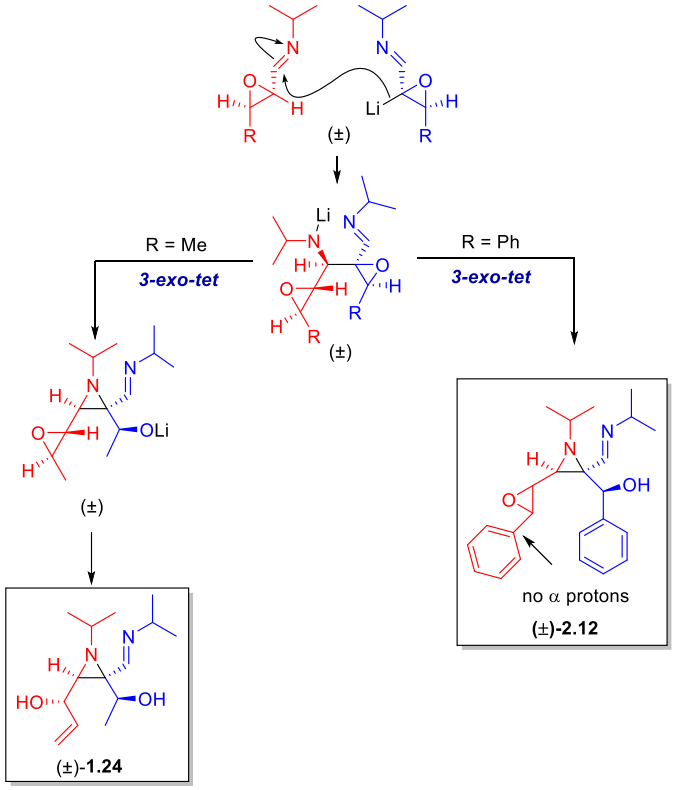

Scheme 2.7: Proposed product for the dimerisation of cinnamaldehyde derived monomer ((±)-**2.12**)

We knew that by using an aromatic enal the dimerisation product formed would be unable to undergo the final *3-exo-trig* opening of the epoxide as no α-hydrogens are available to deprotonate (**Scheme 2.7**). However we were hopeful that the dimerisation may still form with the final product sitting as the epoxide (**(±)-2.12)**.

The first set of conditions for the epoxidation of cinnamaldehyde tested were successful and the product ((±)-**2.13**), as predicted, was a lot more robust to different purification methods (**Scheme 2.8**).

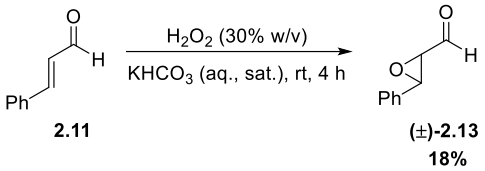

Scheme 2.8: Cinnamaldehyde epoxidation using Würthwein's original conditions

Although epoxide product **(±)-2.12** was now stable to silica, simplifying purification, a further complication was met when we isolated a large amount of a side product. This side product was identified to be benzaldehyde, and was first reported by Wright and co-workers in the kinetic studies of the epoxidation of cinnamaldehyde.[41] Benzaldehyde is believed to be formed by three possible fragmentation reactions (**Scheme 2.9**) of both the product (**(±)-2.13**) and starting material (**(±)-2.11**). With both the concentration of hydroxide and peroxide anions contributing to the amount of side product formed, alternative bases and oxidants were investigated.

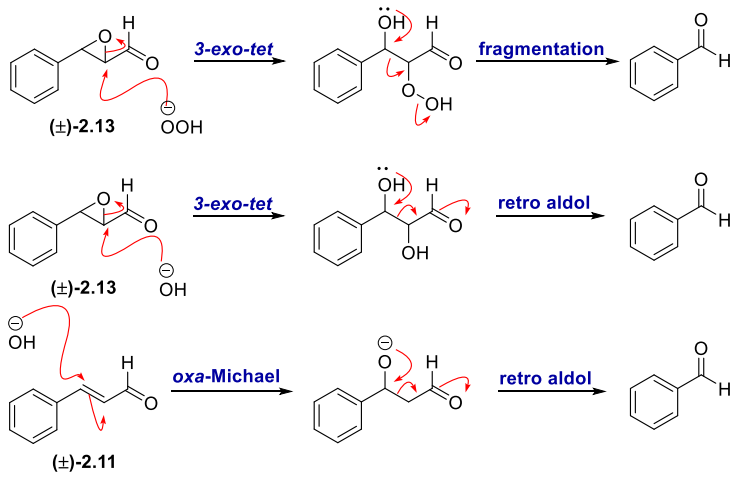

Scheme 2.9: Potential mechanisms for formation of benzaldehyde in the epoxidation of cinnamaldehyde

As mentioned before, the epoxidation of cinnamaldehyde has been performed under a wide range of conditions. **Table 2.4** summarises our efforts to suppress benzaldehyde formation, including the use of non-aqueous bases and alternative oxidants to hydrogen peroxide.

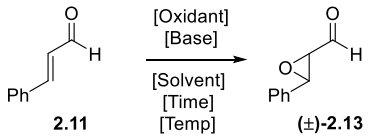

Entry	Temp (˚C)	Time (h)	Solvent	Oxidant (X equiv.)	Base	Results[b]	Ref
1	rt	2	DMSO	*t*-BuOOH (1.3)	Bu_4NF	4%	[44]
2	rt	12	DMSO	*t*-BuOOH (1.3)	Bu_4NF	6%	[44]
3	rt	24	DMSO	*t*-BuOOH (1.3)	Bu_4NF	14%	[44]
4	rt	48	DMSO	*t*-BuOOH (1.3)	Bu_4NF	18%	[44]
5	0 - rt	24	H_2O	H_2O_2 (1.1)	Na_2CO_3	10%	[26]
6	35	48	MeOH	*t*-BuOOH (1.3)	NaOH (1 M)	37%	[45]
7	35	72	MeOH	*t*-BuOOH (1.3)	NaOH (1 M)	32%	[45]

Table 2.4: Tested conditions for cinnamaldehyde epoxidation, [b] yields determined by ^{1}H NMR spectroscopy

The most promising result was found with the use of *tert*-butylhydroperoxide in combination with NaOH as the base (**Table 2.4**, **Entry 6**), which afforded epoxide **(±)-2.13** cleanly in 37% yield. This was followed by the literature reported imine formation using *iso*propylamine and magnesium sulfate as a dehydrating reagent (**Scheme 2.10**) forming **(±)-2.14** in an excellent yield of 91%.

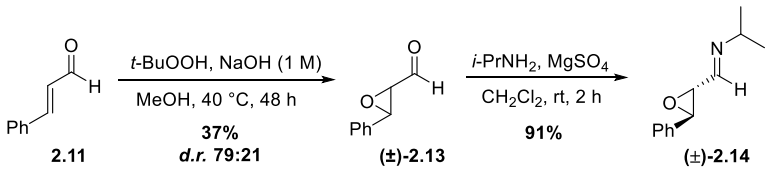

Scheme 2.10: Optimised epoxidation and imine formation conditions for cinnamaldehyde

2.2.3 Alternative Imines

We also investigated the possibility of varying the imine moiety of the imino epoxide. For derivative synthesis other low molecular weight primary amines were used. This meant that an excess of amine could be used which could be removed under reduced pressure, including; *tert*-butylamine (**2.15**) and cyclopropylamine (**2.16**) (**Scheme 2.11**). We were able to successfully form the *tert*-butylamine analogue (**(±)-2.17**) in a 55% yield. However, complications arose in the initial investigation using cyclopropylamine (**2.16**), conducted by Dr David Jones, and further optimisation is required to obtain a second imine variant.

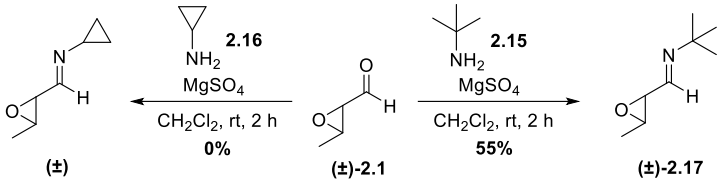

Scheme 2.11: Alternative amines used for imine condensation reaction for form imino epoxides variants

2.3 *aza*-Darzens Dimerisation

In Würthwein's original paper,[17] he describes the protocol for performing the dimerisation using Schlosser's base,[44,46] but later mentions that the same result occurs with just the use of LDA. However, he does not provide a detailed method for how he achieved this.

Initial investigations followed the only dimerisation procedure reported, namely that involving Schlosser's base with crude **(±)-1.20** (due to prior difficulties in acquiring enough starting material) (**Scheme 2.12**).

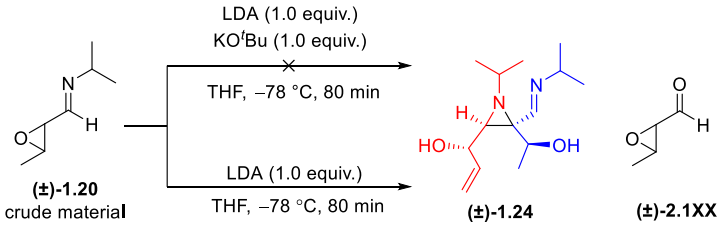

Scheme 2.12: Dimerisation conditions tested

This was unsuccessful with only the hydrolysed imine (**(±)-2.1**) recovered from the reaction mixture. Attempting the dimerisation using LDA as the base initially gave the same unsuccessful result.

There are several possible reasons for the failure of these reactions ranging from purity of the monomer, to the presence of moisture in the reagents, solvents or nitrogen line. With a scalable synthesis and purification protocol of monomer ((±)-**1.20**) being developed, we could now rule out the problem of insufficient purity of the starting monomer. After attaching a drying tube to the nitrogen line and conducting a test lithiation reaction, we could also rule out the possibility of moisture in the nitrogen.

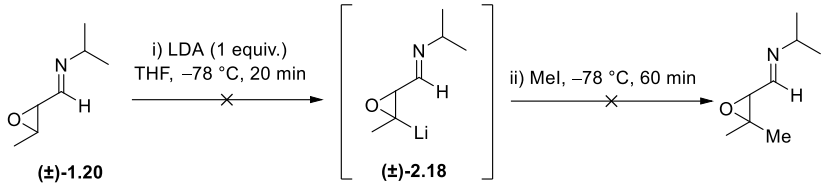

Scheme 2.13: Attempted quenching of lithiated species formed (**(±)-2.18**) with methyl iodide

We proceeded by trying to trap the anion formed after deprotonation for evidence of its existence. This was done conducting the deprotonation and then quenching with methyl iodide to prove the formation of lithiated intermediate **(±)-2.18** (**Scheme 2.13**), but this just resulted in an unidentifiable mixture.

Finally, after freshly distilling all reagents and solvents success occurred when using LDA as the base. The crude reaction mixture was purified using column chromatography and we were able to acquire full characterisation, develop a chiral HPLC assay, and grow high quality crystals for this to gain an X-ray crystal structure of the dimeric product (**Figure 2.1, Spectra 2.1**).

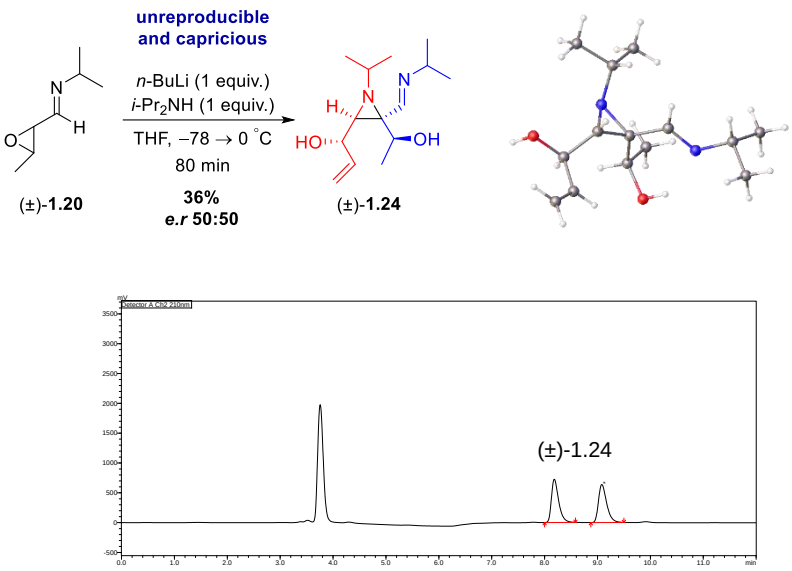

Figure 2.1: *aza*-Darzen dimiersation and X-ray crystal structure and chiral HPLC trace **(±)-1.24** products. Peak at 3.9 min believed to be due to degradation of product while on chiral column.

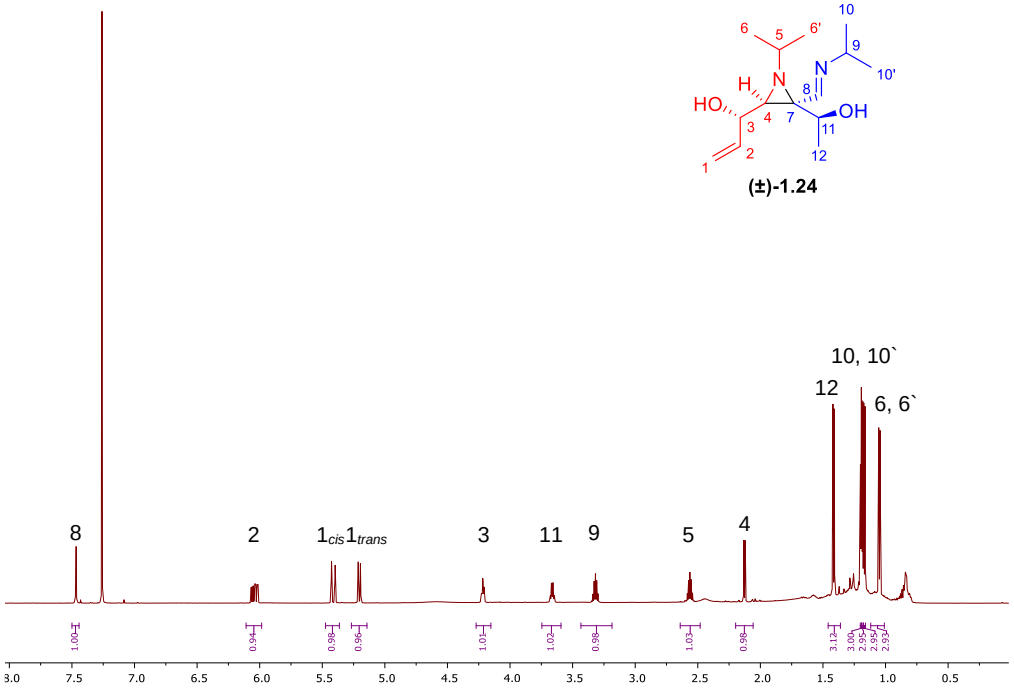

Spectra 2.1: ^{1}H NMR spectrum of dimerisation product **(±)-1.24** ($CDCl_3$, 600 MHz)

The highly temperamental and sensitive nature of the dimerisation made it difficult to draw reliable conclusions from subsequent reactions performed using chiral reagents or alternative monomers.

It was not until we investigated the effect of varying the equivalents that we developed a robust protocol for the dimerisation reaction. By changing the equivalents of LDA to two not only improved the reliability of the reaction but also the isolated yield.

While investigating the effect of varying the equivalents on the reaction it was also noted that when using a substoichiometric amount of LDA a different dimeric product was formed (**Scheme 2.14**). Dimeric product (±)-**2.19**, was found to be the sole product of the reaction which still proceeded through an *aza*-Darzens reaction exhibiting complete heterochiral selectivity. Clearly, without the excess base the final *3-exo-trig* cyclisation cannot occur to give the allylic alcohol dimer product ((±)-**1.24**), instead this results in the epoxide being recovered as the primary product ((±)-**2.19**).

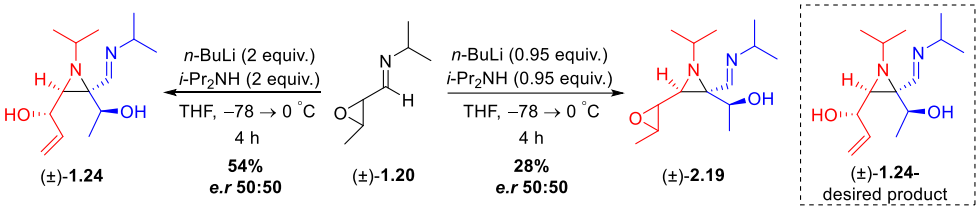

Scheme 2.14: *aza*-Darzens reaction using 0.95 and 2.0 equivalent of LDA to give dimeric epoxide product

It was also noted that facile imine removal was possible when subjecting the final dimeric product ((±)-**1.24**) to mildly acidic conditions, to form aldehyde (±)-**2.20** (**Scheme 2.15**).

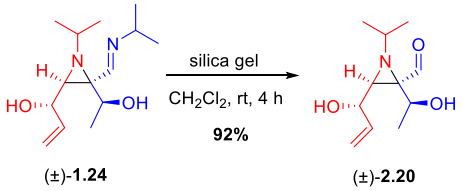

Scheme 2.15: Hydrolysis of imine (±)-**1.24** under mild acidic conditions

With a robust protocol now in hand for performing the dimerisation and controlling the products we now moved to the key step of this project.

2.4 Chiral Reagents or Additives

As described before, the success of this project depends on the ability to perform an enantioselective deprotonation to render the previously reported dimerisation convergent. Würthwein and co-workers originally employed LDA in their dimerisation protocol and the obvious chiral variant of this would be chiral lithium amides (CLAs) (**Figure 2.2a**).

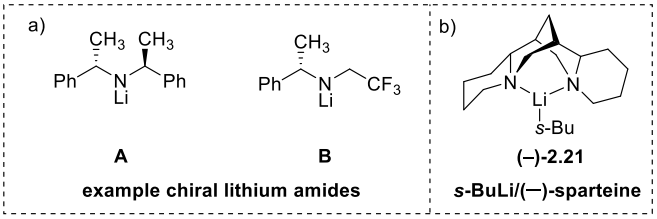

Figure 2.2: Potential reagents to perform an enantioselective deprotonation a) CLAs and b) *s*-BuLi/(–)-sparteine (**(–)-2.21**)

The use of CLAs in asymmetric synthesis was independently introduced Whitesell[47] and Duhamel[48] in the early 1980s, which has resulted in it becoming a valuable tool for the chemical community. CLAs are primarily used as chiral bases, having been shown to be able to discriminate between enantiotopic and diastereotopic protons. Therefore, CLAs appeared a good starting point for our investigations into enantioselective deprotonations.[49] We highlighted two particular CLAs of interest (**Figure 2.2a**) for their previous use in enantioselective deprotonations of epoxides to form allylic alcohols.[19]

We also felt that organolithium reagents, in the presence of (–)-sparteine (**(–)-2.21**), could act as potential alternatives to CLAs (**Figure 2.2b**). Enantiopure organolithium aggregates can be seen to form in the reaction between *sec*-butyllithium and (–)-sparteine (**(–)-2.21**). The use of (–)-sparteine (**(–)-2.21**) (Figure **2.3a**) and diamine surrogates (**Figure 2.3b**) for α-deprotonation of epoxides is well noted in the literature.[18] Particularly noteworthy is the work of Hodgson and co-workers,[50] in the work of desymmetrising *meso*-epoxides (**2.22**) *via* direct deprotonation-electrophile trapping at the unsubstituted terminus to afford chiral epoxides (**2.23, Figure 2.3c**).

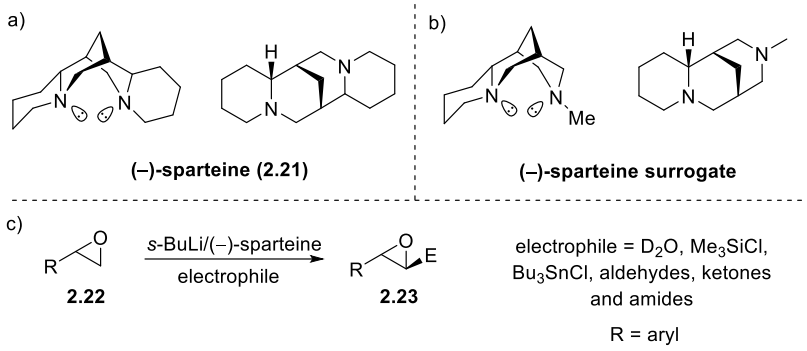

Figure 2.3: Diamines used for enantioselective deprotonations: a) (–)-sparteine and b) (–)-sparteine surrogate c) Hodgson's deprotonation-electrophile trapping of unfunctionalised terminal epoxides with *s*-BuLi/(–)-sparteine

2.5 Screen for Enantioconvergency

Our initial screen of conditions focused on the varying the chiral amine used in the reaction. We selected a range of structurally different chiral amines (**Figure 2.4**) including: Simpkins-type bases (**A** and **B**),[51,52] their derivatives (**C**), diamines (**D**),[53] Koga-type bases (**E** and **F**),[54,55] a proline derived chiral amine (**G**)[56–58] and *sec*-butyllithium/(–)-sparteine (**H**).[50] These different classes of base were also chosen for their ease of synthesis or their commercial availability.

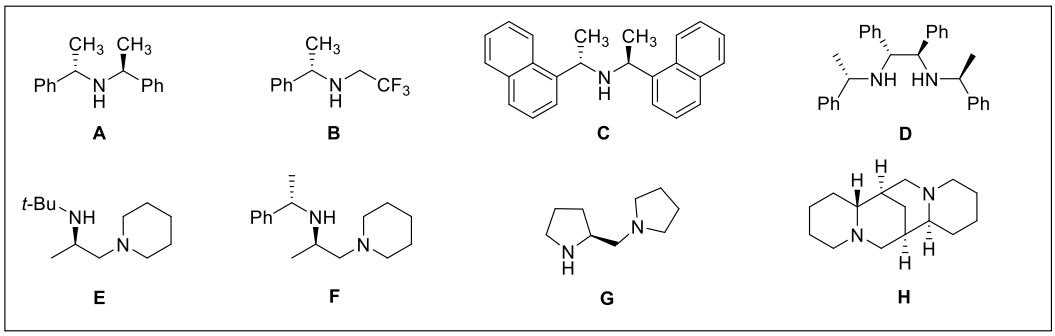

Figure 2.4: Chiral amines used in *aza*-Darzens dimerisation

Chiral amine **B** was chosen as the first enantiopure reagent to synthesise due to its relatively simple four-step synthesis from commercially available starting materials.

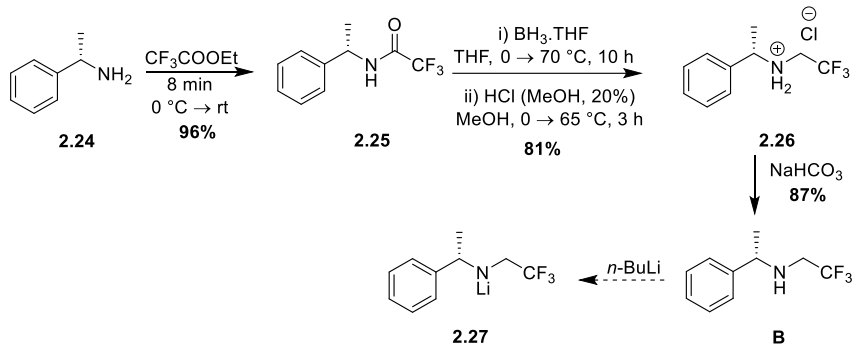

Scheme 2.16: Synthesis of chiral lithium amide precursor **B**

Using the chiral pool strategy developed by Koga and co-workers (**Scheme 2.16**),[59] (*s*)-methylbenzylamine (**2.24**) was trifluoroacetylated under neat conditions to afford chiral amide **2.25** in an excellent 96% yield. Amide **2.25** was then reduced using a borane-THF complex solution and then treated with acid to form the ammonium chloride salt **2.26** in 81% yield. Deprotonation of the salt under mild conditions gave the amine **B**, the precursor for the desired CLA (**2.27**), in 87% yield. From this bench stable precursor the CLA **2.27** can be formed *in situ* by lithiation with *n*-butyllithium when required.

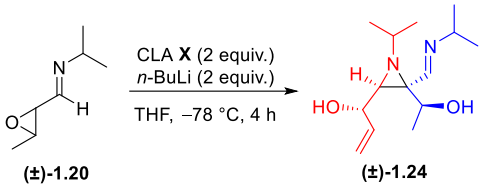

Entry	CLA (2 equiv.)	*e.r.*	Yield
1	**A**	82:18	57%
2	**B**	76:24	40%
3	**C**	trace amount	-
4	**D**	no dimer	n/a
5	**E**	72:28	46%
6	**F**	no dimer	n/a
7	**G**	no dimer	n/a
8	**H**	no dimer	n/a

Table 2.5: Chiral bases used in *aza*-Darzens dimerisation

For the primary screen of inducing enatioconvergency the chiral lithium amide was made *in situ*, *via* the addition of *n*-butyllithium to the chiral amines at –78 °C in THF. Imino epoxide **(±)-1.20**

was added dropwise at –78 °C to the chiral lithium amide and the reaction was slowly warmed to 0 °C. Each reaction was purified *via* column chromatography to get a clean sample of the dimer and to recover the chiral base used. The *e.r.* of the dimer was then determined using chiral HPLC (Chiralpak ID column, 100% hexane, 0.8 mL/min). The results of this are summarised in **Table 2.5**.

From these early studies we discovered that three chiral lithium amides were compatible with the *aza*-Darzen dimerisation (**Table 2.5, Entries 1,2,5**). The best result was found when using Simpkins' first generation CLA (**A**), which gave the dimeric aziridine product in a 57% yield and *e.r.* 82:18 (**Table 2.5, Entry 1**). This was the baseline result for systematically varying the other conditions of the reaction including; temperature, time, equivalents, solvents and potential additives to the reaction, of which the results are summarised in **Table 2.6**.

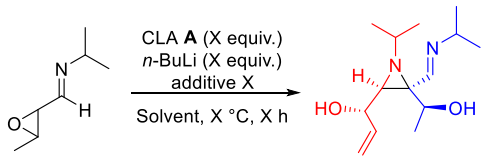

(±)-1.20 (±)-1.24

Entry	Temp (˚C)	Solvent	CLA (2 equiv.)	Additives	Time (h)	*e.r.*	Yield	Ref
1	–78	THF	**A**	-	4	82:18	57%	-
2	–78	toluene	**A**	-	4	trace amount	-	-
3	–78	MTBE	**A**	-	4	no dimer	n/a	-
4	–78	Et_2O	**A**	-	4	77:23	39%	-
5	–78	2-M-THF	**A**	-	4	17:83	51%	-
6	–78	THF	**A**	HMPA	4	no dimer	n/a	[60]
7	–78	THF	**A**	TMEDA	4	80:20	47%	[61]
8	–78	THF	**A**	LiCl	4	86:14	51%	[62]
9	–78	THF	**A**	12-crown-4	4	80:20	49%	-
10	–78	THF	**A**	-	16	75:25	51%	-
11	–78	THF	**A**	-	4	85:15	44%	-
12	–40	THF	**A**	-	4	61:39	52%	-
13	–90	THF	**A**	-	4	86:14	52%	-
14	–95	THF	**A**	-	4	90:10	56%	-
15	–100	THF	**A**	-	4	80:20	52%	-
16	–95	THF	**A** (1 equiv.)	-	4	no dimer	n/a	-
17	–95	THF	**A**	LiCl	4	no dimer	n/a	-
18	–95	THF	**A** (1 equiv.)	LiCl	4	84:16	42%	-

Table 2.6: Screen of conditions used in *aza*-Darzens dimerisation

We started by trialling a range of closely related solvents both in terms of structures and polarity parameters including toluene, MTBE, Et_2O and 2-M-THF (**Table 2.6, Entries 3-5**). The effect of using toluene as the solvent was also investigated (**Table 2.6, Entry 2**), as toluene and THF are the most frequently employed solvents used in chiral lithium amide deprotonations.[63] Though none of these alternative solvents improved the initial hit with THF, there was an intriguing result when the methylated congener (2-M-THF) was used as the solvent. A divergent enantioselectivity was observed, *e.r.* 17:83, using 2-M-THF as the solvent (**Table 2.6, Entry 5**). This is a noteworth result as structurally 2-M-THF is chiral, although used in racemic form as a solvent. Similar solvent effects have been reported previously by Shibasaki and co-workers when investigating enantioselective nitroaldol reactions.[64]

We later looked at the possibility of using additives to improve enantioconvergency. Using additives in combination with chiral lithium amides is well documented in literature.[60–62] They function by disrupting or altering the configuration of the lithium aggregates formed in solution.[65] These aggregates are important as they exert a strong influence on the stereochemical outcome of a reaction. When polar additives like HMPA and TMEDA were added to the reaction it had a detrimental effect on the enantioselectivity of the reaction (**Table 2.6**, **Entries 6** and **7**), with no reaction occurring with the addition of HMPA. However a beneficial salt effect was observed with the addition of a lithium halide to the reaction, *e.r.* 86:14 (**Table 2.6, Entry 8**). 12-crown-4 ether, which is known to show a high selectivity for lithium cations in solution, was also added to the reaction (**Table 2.6, Entry 9**). This proceeded with a slightly diminished *e.r.* of 80:20, but was performed to see if the elimination of lithium ions in solution had an effect on *e.r.*. We were unable to ascertain if all of the lithium cations bound to the crown ether during the reaction, so we cannot comment further on this result.

The effect of temperature on the *e.r.* of the reaction was then investigated. Conducting the reaction at a higher temperature (–40 °C, **Table 2.6**, **Entry 12**) resulted in decreased enantioselectivity. Whereas further cooling the reaction temperature below –78 °C led to an increase in enantioselectivity (**Table 2.6, Entries 13** and **14**). Attempting to perform the reaction at –100 °C

(**Table 2.6, Entry 15**) lead to a decrease in *e.r.* (80:20). This is likely attributed to solubility issues at these lower temperatures causing the reaction to become heterogeneous. The *e.r.* of the reaction peaked at 90:10 when performed at –95°C (**Table 2.6, Entry 14, Scheme 2.17**), and this represented the best result achieved comepleting the first ever stereoretentive enantioconvergent reaction.

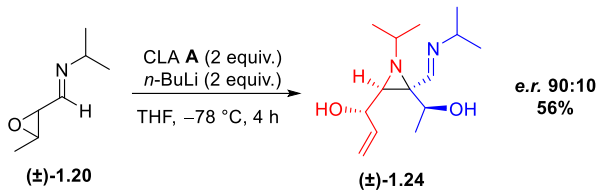

Scheme 2.17: First recorded stereoretentive enantioconvegent dimerisation

2.6 Conclusions

During the course of this project many unforeseen difficulties were encountered from the outset. The majority of these difficulties stemmed from the high volatility and low molecular weights of the compounds required in this synthesis, causing significant loss of material and difficulties in purification.

After screening various conditions and trialling alternative routes (**Sections 2.1.1-2.1.3**, **pages 13-18**) to form epoxide **(±)-1.26**, our efforts were finally rewarded. Monomer **(±)-1.20** was formed through an organocatalysed epoxidation, in 22% yield (**Scheme 2.18**) and the methodology developed, was applied to a further two substituted derivatives (**(±)-2.10**, **(±)-2.14, Sections 2.2.1-2.2.2**, **pages 18-21**).

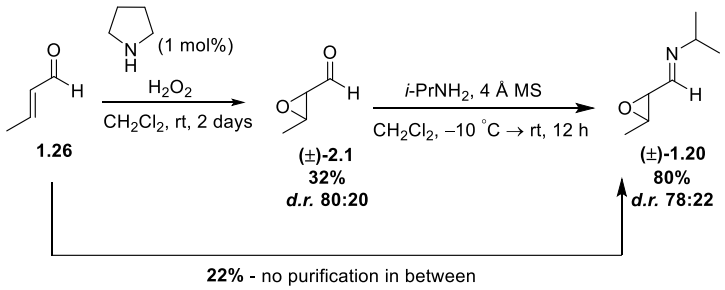

Scheme 2.18: First recorded stereoretentive enantioconvegent dimerisation reaction

We found the nature of the *aza*-Darzens dimerisation to be highly capricious. With the purity of reagents and the dilution of the reaction having a large impact on the outcome of the reaction.

Screening a range of different CLA (**Table 2.5, page 28**) gave an initial hit of ennatioselectivity (82:18 *e.r.*) in the dimerisation (**Table 2.5**, **Entry 1, page 28**). This was later optimised through trialling a wide range of different conditions (**Table 2.6, page 29**). Leading to the optimised conditions for performing the first ever enantioselective stereoretentive dimerisation in a 56% yield and 90:10 *e.r.* (**Scheme 2.19**).

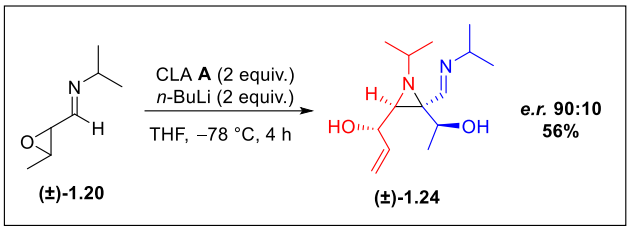

Scheme 2.19: First recorded stereoretentive enantioconvegent dimerisation reaction

2.7 Future Work

The future of this project would be to focus on trying to test the versatility of the enantioselective stereoretentive *aza*-Darzens reaction, by looking towards using variants of the imino epoxide monomer.

Having already synthesised a range of alternative monomers including the use of an alternative imine group (**(±)-2.17**) and varying the substitution of the epoxide (**(±)-2.10** and **(±)-2.14**), conditions could be investigate to perform the heterochiral selective dimerisation (**Scheme 2.20**). If successful this may also lead to a further improvement of the enantioselectivity of the reaction.

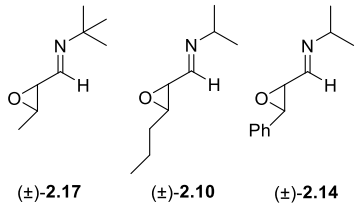

Scheme 2.20: Alternative imine epoxide monomers synthesised

Furthermore, we plan to apply this new concept to other heterochiral selective dimerisations, with the aim of establishing this novel enantioselective stereoretentive approach as method for dealing with dimerisations of racemic starting material.

Chapter 3: Diels–Alder Results and Discussion

3.1 Synthesis of Diels–Alder Monomer

Studies were conducted towards a stereoretentive enantioconvergent Diels–Alder dimerisation (**Scheme 3.1**). This began with the synthesis of precursor monomer **1.27**.

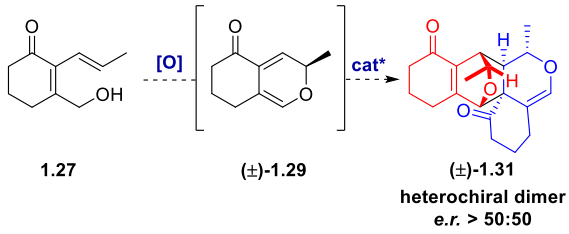

Scheme 3.1: Proposed stereoretentive enantioconvergent Diels–Alder dimerisation

3.1.1 Route 1: Hayashi's Original Route

Hayashi and co-workers reported the formation of Diels–Alder precursor **1.27**, starting from **3.1** in a 9 step synthesis with a 12% overall yield (**Scheme 3.2**).[21] The route proceeded through the converision of 1,3-cyclohexanedione (**3.1**), to the corresponding sulfoxide (**3.2**). The sulfoxide (**3.2**) was able to undergo a Pummerer rearrangement followed by a hydrolysis to afford aldehyde (**3.3**). Reduction of both carbonyls was achieved using Luche conditions, to give di-alcohol **3.4**. The primary alcohol of **3.4** was protected with a TBS group and the secondary alcohol was reoxidised to the ketone (**3.5**). Compound **3.5** was then iodinated to form a suitable coupling partner for a Suzuki–Miyaura cross coupling reaction (**3.6**) used to install the propenyl group. Subsequent alcohol deprotection completed Hayashi's synthesis of the monomer precursor (**1.27**).

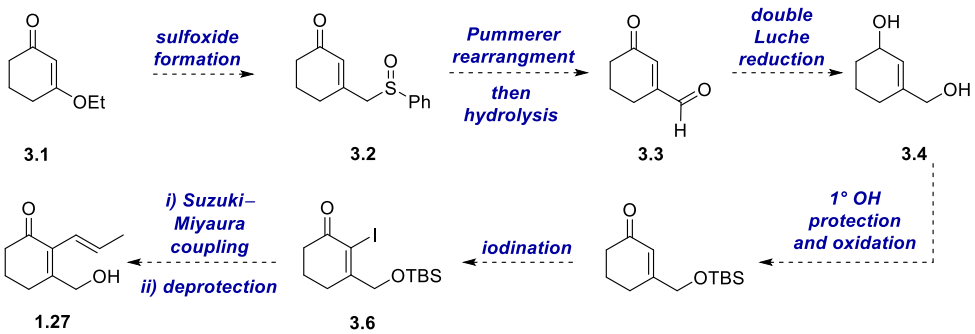

Scheme 3.2: Hayashi's synthesis to monomer precursor **1.27**

As the main focus of the project was to establish our new concept of stereoretentive enantioconvergency, we decided to simply follow Hayashi's original route to the monomer (**Scheme 3.2**). The synthesis began with the preparation of β-keto enol ether **3.1**. Hayashi's original route of heating 1,3-cyclohexanedione (**3.7**) in toluene with ethanol and a catalytic amount of *para*-toluenesulfonic acid had a lengthy reaction time and resulted in a unsatisfactory yield (25%) (**Scheme 3.3**).[66] However, etherifications of cyclic β-diketones in an alcoholic solvent with a catalytic amount of iodine has been shown to afford β-keto enol ethers cleanly and in very high yields, with iodine acting as a weak Lewis acid catalyst.[67] Diketone **3.7**, in the presence of iodine and ethanol, was etherified to give the desired β-keto enol ether (**3.1**) in a 90% yield. Iodine is a necessary additive in this etherification reaction as without it no reaction is seen to occur even after 24 hours.

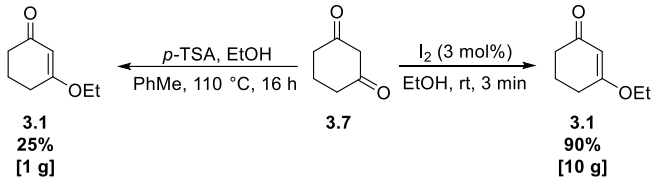

Scheme 3.3: Methods trialled for the etherification of 1,3-cyclohexanedione (**3.7**)

The etherification reaction was scaled up successfully, and we continued to follow Hayashi's route by converting **3.1** into thioether **3.8** *via* the *in situ* deprotonation of thioanisole with *n*-butyllithium (**Scheme 3.4**). The carbanion formed undergoes a Michael addition to the α,β-unsaturated carbonyl and eliminates ethoxide to give **3.8**. In our hands, the reaction proceeded with a lower yield than Hayashi reported (49% vs. 71%), although the reaction was only performed twice.

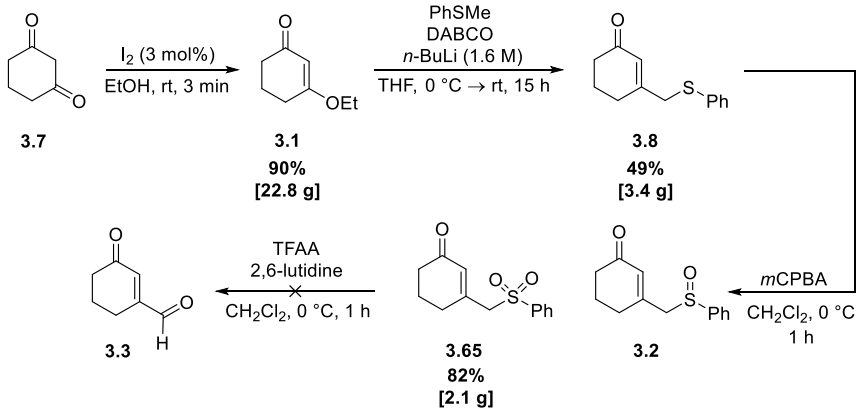

Scheme 3.4: Hayashi's forward synthesis starting from 1,3-cyclohexanedione (**3.7**)

To form the desired sulfoxide (**3.2**), an oxidation with *m*-CPBA was performed. During these early investigations, the product of this reaction was initially misassigned as sulfoxide **3.2**, but sulfone **3.65** was yielded instead due to overoxidation. The ^{1}H and ^{13}C NMR spectra of the corresponding sulfoxide (**3.2**) and sulfone (**3.65**) would likely be very similar and thus leading to our misidentification. Using mass spectroscopy, we detected a mass ion corresponding to the desired sulfone (**3.2**), but this is now attributed to a trace impurity.

Due to obtaining the sulfone **3.65** as the major product, we were unable to perform Hayashi's Pummerer rearrangement of sulfoxide **3.2**, to introduce the required formyl group at the β-position. We were unable to obtain conclusive evidence for the formation of any intermediates in the Pummerer rearrangement we decided to pursue alternative routes to monomer precursor **1.27**.

3.1.2 Route 2: Dithiane Chemistry

Another potential route to form the key aldehyde intermediate (**3.3**), would be using dithiane chemistry. First discovered in 1965 by Corey and Seebach this reaction provides a synthetic trick to add a masked aldehyde to the α,β-unsaturated system through a simple [1,4]-Michael addition.[70,71]

The chemistry works by inverting the natural polarity of the aldehyde C=O bond from electrophilic at carbon to nucleophilic, *via* the dithiane moiety (**Figure 3.1**). This umpolung effect works by utilising sulfur's ability to stabilise α-carbanions through negative hyperconjugation.[72]

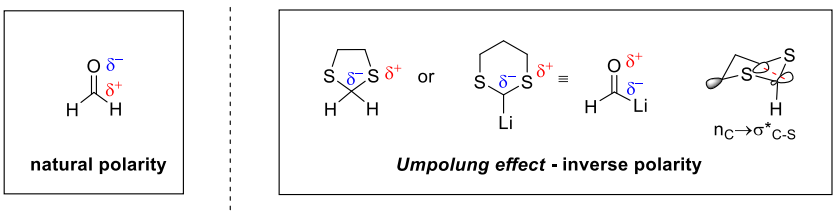

Figure 3.1: Natural Polarity of carbonyl bond vs. inverted polarity of dithiane *via* the umpolung effect using negative hyperconjugation

Using this chemistry would allow the conjugate addition of a dithiane group which could be converted into the desired unsaturated aldehyde product (**3.3**) through an oxidative hydrolysis

(**Scheme 3.5**). By starting with commercially available 2-cyclohexen-1-one (**3.12**), the 1,3-dithiolane can be added in a Michael-type fashion in the presence of a base. The resulting enolate can be trapped with trimethylsilyl chloride to give compound **3.13** or quenched to give the dithiane adduct (**3.14**) directly. Dithiane **3.14** can then be oxidised to unmask the desired conjugated aldehyde (**3.3**).[73]

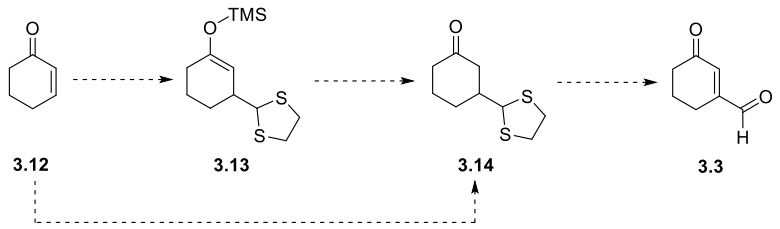

Scheme 3.5: Proposed route to aldehyde **3.3** using dithiane chemistry

We began trying to synthesise the dithiane adduct (**3.14**) directly (**Scheme 3.6a**). This involved reacting enone **3.12** with 1,3-dithiolane and *n*-butyllithium in the presence of HMPA. HMPA (**Scheme 3.6b**) is commonly employed as an additive in reactions to promote the disruption of lithium aggregates.[74] It also has the ability to selectively solvate the lithium cations through the basic nitrogen and oxygen atoms, which can help to accelerate S_N2 reactions through forming more naked anions.[75] Furthermore, Brown and co-workers found that HMPA is crucial for achieving the required [1,4]-regioselectivity in the nucleophilic addition.[76]

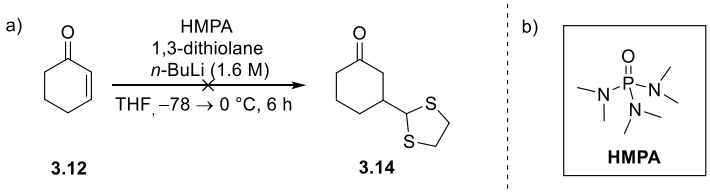

Scheme 3.6: a) Conditions trialled to add 1,3-dithiolane to 2-cyclohexen-1-one (**3.12**) *via* Michael addition b) structure of hexamethylphosphoramide (HMPA)

In 1999, Reich and co-workers determined that the regioselectivity of nucleophile addition to the enone is governed by the structure of the ion-pair interaction of the lithium cation and the dithiane anion.[74] Contact-ion pairs (CIP) with a tight C–Li association typically give [1,2]-addition, whereas solvent-separated ion pairs (SSIP) give predominately give [1,4]-addition (**Figure 3.2**).[77] Due to

HMPA's selective ability to solvate lithium ions it forms a SSIP interaction producing a weaker C–Li bond, which causes the charge of the carbanion to delocalise and form a soft ion. This results in the ion orientating itself at the preferred 'soft' end of the α,β-unsaturated system and therefore reacting in the 4 position.

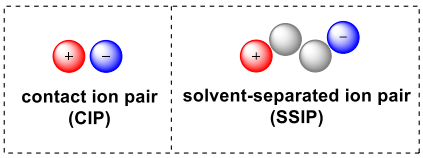

Figure 3.2: Contact ion pair (CIP) *vs* solvent separated ion pair (SSIP) diagram for lithium association

Unfortunately, after many attempts, the dithiolane addition resulted in only recovered starting material. Due to the high reactivity, basicity, and polarity of the organolithium species involved many side reactions can occur and the species is easily quenched with any adventitious moisture present in the reaction.[78] This can result in poor yields and unreacted starting material. Furthermore, 2-lithio-1,3-dithiane species are incredibly sensitive to autoxidation.[79]

The reaction was also performed in the absence of HMPA to see if we could get the [1,2]-addition product (**3.15**) instead (**Scheme 3.7, reaction 1**). If successful, this reaction would have indicated that the HMPA may have been of low purity or had a high moisture content. Regrettably, however, this control reaction also resulted in just recovered starting material.

To discover whether the enolate was formed at all during the reaction we added the quenching reagent of trimethylsilyl chloride so we could isolate the intermediate silyl enol ether (**3.13**) (**Scheme 3.7, reaction 2**). For a third successive time this reaction resulted in only recovered starting material.

In an attempt to avoid the problems associated with such a reactive organolithium species we also tried to perform the reaction with the diorganozinc variant, which acts as milder, less reactive dithiane anion (**Scheme 3.7, reaction 3**).[80]

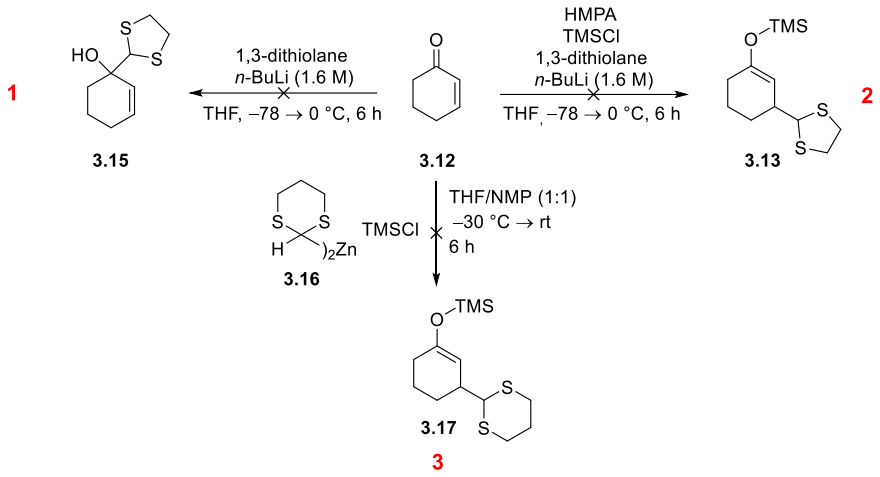

Scheme 3.7: Reactions of cyclohexenone with different molecules dithiane

The diorganozinc species is made *in situ* by simply transmetallating the organolithium reagent **3.16** with zinc bromide. To promote the required [1,4]-addition, NMP is added and it also acts as a co-solvent for the reaction. In another attempt to trap the enolate intermediate, trimethylsilyl chloride was used, but again with no success of forming the desired dithiane adduct (**3.17**).

After unsuccessfully trying a variety of different reaction conditions to form the dithiane adducts (**3.15, 3.13** and **3.17**), it was decided to stop work on this synthetic strategy. Instead, we would explore alternative disconnections to make the Diels–Alder monomer precursor (**1.27**).

3.1.3 Route 3: Birch Reduction

Another possible route explored for the synthesis of the monomer precursor **1.27** utilised a Birch reduction as the key step.

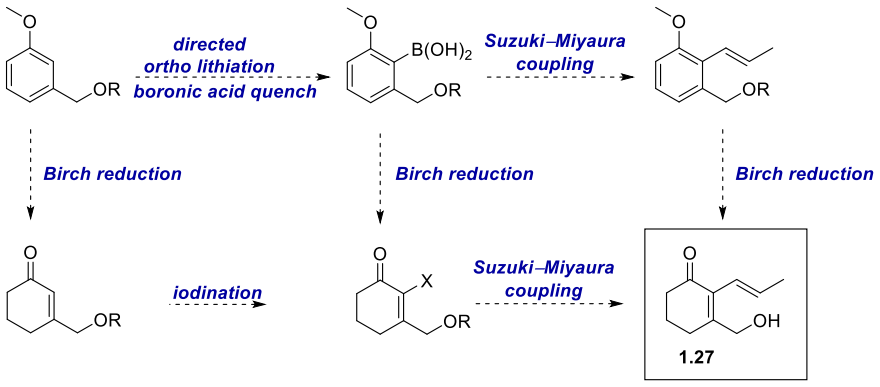

Scheme 3.8: Possible routes to monomer precursor **1.27** *via* Birch reductions (R = H/PG)

The Birch reduction is a [1,4]-reduction of an aromatic compound to the corresponding unconjugated cyclohexadiene by solvated electrons formed *in situ* from alkali metals (Li, K, Na) dissolved in liquid ammonia in the presence of a proton source.[81] The regioselectivity of the reduction depends on the nature of the substituents on the aromatic ring. It has been noted that performing the Birch reduction on an aromatic compound with an EDG present e.g., a methoxy group, without a source of protons present triggers the conversion to an α,β-unsaturated ketone.[82] Therefore, the Birch reduction provides us with an ideal route to form the central α,β-unsaturated ketone moiety needed in monomer **1.27** (**Scheme 3.8**). Furthermore, starting with an aromatic molecule could allow the early installation of the alkenyl group by using a directed *ortho*-lithiation and boronic acid quench, which could also later aid in diversification with substrate and reaction scope.

Investigations into this alternative pathway began with the classic Birch reduction of benzene (**3.18**) to cyclohexadiene (**3.19**) (**Scheme 3.9**). The first trial of the reaction was carried out on the simplest aromatic compound to not only get a feel of the reaction but also to see if the formation of anhydrous liquid ammonia *in situ* was feasible. By reacting a base with an ammonia source in a sealed system, ammonia gas was extruded. The resulting gas was then dried over a connecting packed column of CaO and condensed at −78 °C to produce a steady supply of anhydrous liquid ammonia, which was used in the subsequent Birch reduction. This proved successful on a 1 g scale and formed cyclohexdiene in a moderate 62% yield, but further studies need to be conducted on scaling up the process.

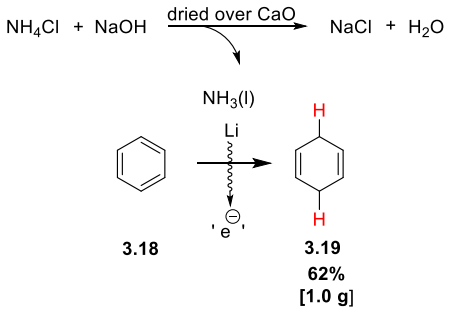

Scheme 3.9: Birch reduction of benzene (**3.18**) using liquid ammonia produced and dried *in situ* from reaction of quaternary ammonium salt with an acid

Moving forward, this procedure was applied to model substrate **3.20** to test the functional group tolerance of the Birch reduction in relation to our system (**Scheme 3.10**). The aromatic compound 3-methoxybenzyl alcohol (**3.20**) was subjected to Birch conditions using ethanol as the proton source. This resulted in a complex mixture of products indicating that this type of substrate is not well suited to Birch reductions.

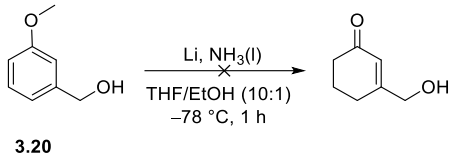

Scheme 3.10: Conditions trialled of Birch reduction on model substrate **3.20**

In addition, forming anhydrous ammonia, although possible, was a laborious and low yielding process which would not be a viable option if scale up was required. Therefore, we stopped pursuing the Birch reduction route.

3.1.4 Route 4: Wohl–Ziegler Bromination

Another method to install the required alcohol functionality could be *via* the allyl bromide analogue **3.21**. This compound could be synthesised starting with commercially available 3-methylcyclohexen-2-one (**3.22**) using the Wohl–Ziegler radical conditions to perform an allylic bromination. This compound (**3.21**) could then be converted into the corresponding alcohol (**3.23**) *via* a nucleophilic substitution (**Scheme 3.11**).

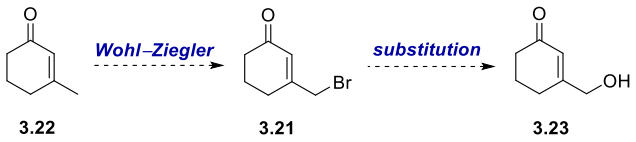

Scheme 3.11: Route proposed to form key intermediate **3.23** *via* Wohl–Ziegler radical bromination and subsequent substitution

The generally accepted mechanism for the Wohl–Ziegler reaction was proposed by Goldfinger in 1953.[83] He proposed a radical-mediated bromination, which uses NBS (**3.24**) as a chain propagator and a source of bromine, to brominate allylic methyl groups. Using NBS (**3.24**) as the bromine source is crucial, as it allows bromine to be released gradually, and therefore provide a source of steady state and low concentration molecular bromine (**Scheme 3.12**).[84] This low concentration of bromine helps to supress the competing reaction of direct bromine addition to the double bond. Moreover, due to the non-polar nature of the carbon tetrachloride solvent this also disfavours direct bromine addition, which would proceed *via* the formation of a cationic bromonium intermediate.

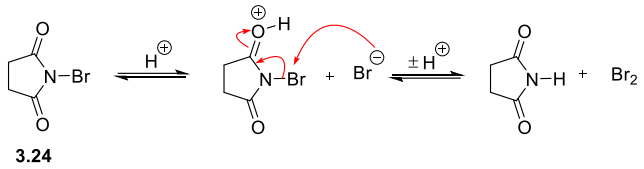

3.24

Scheme 3.12: Proposed mechanism of molecular bromine formation during the Wohl–Ziegler bromination using NBS (**3.24**)

The allylic regioselectivity of the bromination is determined by the hydrogen abstraction step which occurs specifically to give the most stabilised allylic radical.

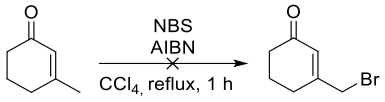

3.22 **3.21**

Scheme 3.13: Conditions trialled for Wohl–Ziegler bromination of **3.22**

We used the adapted literature conditions of AIBN (as the initiator) and NBS in the absence of light and refluxed 3-methylcylcohexen-2-one (**3.22**) for one hour (**Scheme 3.13**). This resulted in an inseparable mixture of products that did not contain bromine, as determined by ^{79}Br NMR spectroscopy. As we were unable to install the required bromine group, we once again looked for another route to form the Diels–Alder precursor (**1.27**).

3.1.5 Route 5: Starting From Cyclohexenone

With no success with the routes pursued so far, we drew inspiration from Olivo and co-workers' work towards the semi-synthesis of the cassane diterpenes, escobarines A (**3.25**) and B (**3.26**).[86] Olivo proposed a semi-synthesis of escobarine A (**3.25**) and B (**3.26**), which starts from the natural product and co-isolate sclareolide (**3.27**) and proceeds through a key cyclohexenone intermediate **3.28** (**Scheme 3.14**). Functionalisation of the C ring of this intermediate would allow access to escobarine A (**3.25**) and B (**3.26**), but also a route to synthesise valuable analogues of the natural product.

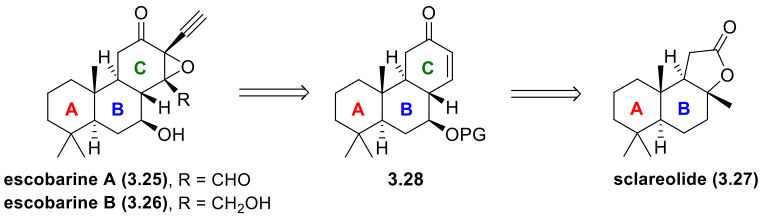

Scheme 3.14: Olivo's semi-synthesis of escobarine A (**3.25**) and B (**3.26**) from sclareolide (**3.27**)

Although Olivo is yet to report a full total synthesis of escobarine A (**3.25**) and B (**3.26**), he has published studies on the construction of the fully functionalised C ring of the natural products.[86] Olivo's synthesis uses α,β-epoxy ketone **3.29**, which can be converted to a model of escobarine B (**3.26**) and escobarine A (**3.25**) (**Scheme 3.15**). To make α,β-epoxy ketone **3.29**, Olivo started with the iodoenone (**3.30**), which was used as a cross-coupling partner in the palladium-catalysed Sonagashira reaction to afford compound **3.31**. Epoxidation of **3.31** followed by deprotected of the primary alcohol gave the fully functionalised ring C of escobarine B (**3.25**).

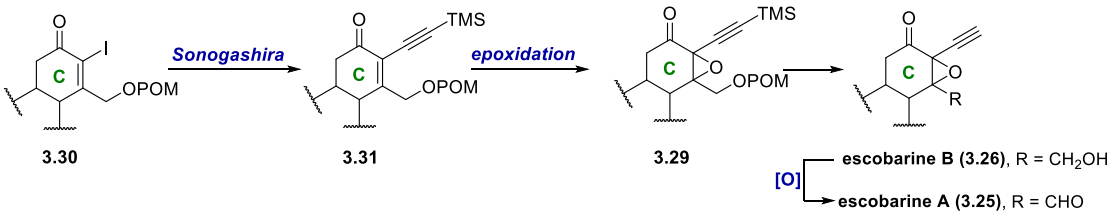

Scheme 3.15: Olivo's model synthesis of the escobarine A (**3.25**) and B (**3.25**) *via* functionalisation of the C ring starting from the key iodoenone intermediate **3.30**

Intermediate **3.30**, which features in Olivo's synthesis, bears a close resemblance to a key intermediate in Hayashi's route to the desired Diels–Alder monomer (**3.6, in Scheme 3.2, page 35**), and only differs by the choice of alcohol protecting group (POM vs. TBS). Synthetically, iodoenone (**3.30**) was accessed by Olivo in 5 steps from commercially available 2-cyclohexen-1-one (**3.12**). This was achieved through tosylation of 2-cyclohexen-1-one (**3.12**) to give sulfone **3.32**. The carbonyl of sulfone **3.32** was then protected (**3.33**) before undergo going an alkylation reaction to afford **3.34**. Subsequent deprotection (**3.35**),and iodination gave iodoenone **3.36** with a 68% overall yield (**Scheme 3.16**).

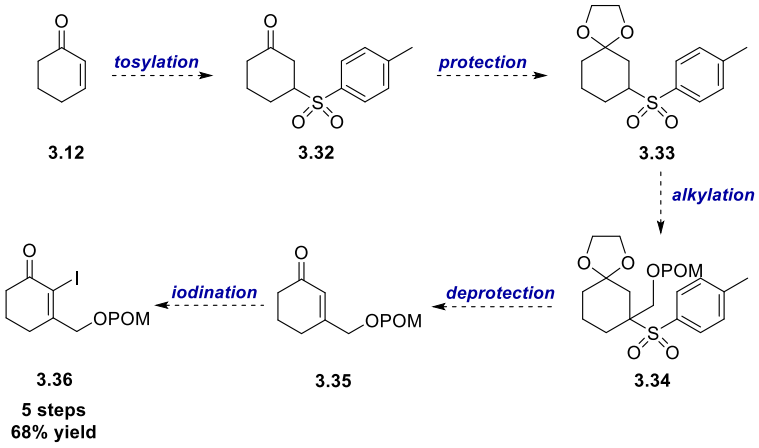

Scheme 3.16: Olivo's synthesis of the key iodoenone intermediate (**3.36**) starting from 2-cyclohexen-1one (**3.12**)

Inspired by Olivo's work, our synthesis started with Michael addition of sodium *para*-toluenesulfinate to 2-cyclohexen-1-one (**3.12**) using a catalytic amount of glacial acetic acid, which afforded aryl sulfone **3.32** in 79% yield on an 11 g scale (**Scheme 3.17**). The protection of the ketone with ethylene glycol at reflux in toluene, with catalytic acid under Dean–Stark conditions gave dioxalane **3.33** in good yield on smaller scale. However, when conducted on a larger scale the yield decreased due to poor conversion. We noted when moving to a larger scale that the refluxing of the reaction was suboptimal even when performed with heating block at higher temperatures.

The azeotropic mixture of toluene and water was unable to reflux up the Dean–Stark apparatus thus meaning that water was not being removed the system.

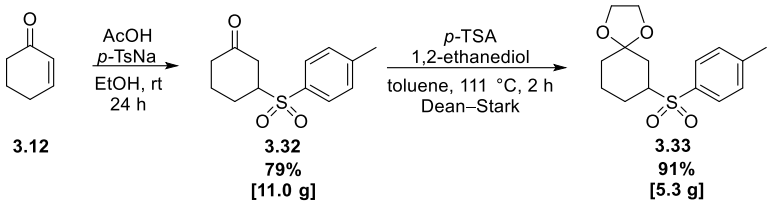

Scheme 3.17: Conditions used for aryl sulfone Michael addition to 2-cyclohexen-1-one (3.12) and subsequent ketone protection

As we were struggling to protect the ketone of compound **3.32** on large scale, alternative conditions and ketal protecting groups were explored. We hoped to exploit the Thorpe–Ingold effect of having a gem-dimethyl/diethyl group on the diol which kinetically favours ring closure due to large gauche interactions in the extended ground state conformation. We examined using 2,2-diethyl/dimethyl-1,3-propanediol as the protecting groups. These diols can be used in combination with dehydrating reagents and Lewis acids to activate the ketone towards addition and dehydration.

Initially we used the commonly employed Lewis acid of boron trifluoride etherate with diethyl-1,3-propanediol as the diol (**Scheme 3.18**).[87] Boron trifluoride etherate was added in excess to sulfone **3.32** to react with the water formed during the reaction and take it out of the equilibrium of the system. The reaction was conducted at room temperature and left to stir overnight, but unfortunately resulted in recovered starting material.

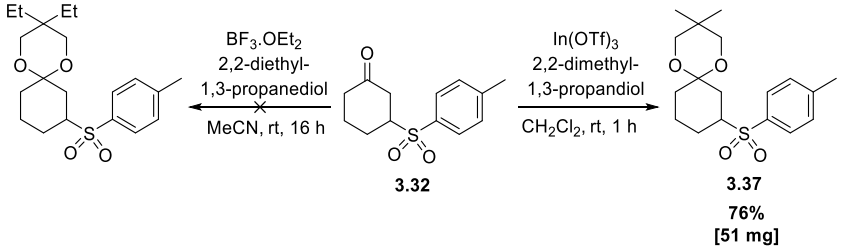

Scheme 3.18: Conditions trialled for alternative methods of ketalisation of **3.32** using Lewis acid sources

We next looked to indium based Lewis acids, as a wide variety of indium salts have been employed to catalyse a range of synthetic transformations.[88] For example, Graham and co-workers have developed a mild method for ketalisation utilising indium triflate.[89] Repeating Graham's work on

our system, we used aryl sulfone **3.32** and 2,2-dimethyl-1,3-propandiol as the diol (**Scheme 3.18**). This procedure worked at ambient temperatures without inert reaction conditions, and the product (**3.37**) was isolated after workup without need for further purification in 76% yield.

To evaluate the use of this diol in our synthesis, we needed to see if its removal was just as easy as its addition. We employed a HF-mediated aryl sulfone elimination and concurrent ketal deprotection reaction.[90] These harsh conditions were applied to compound **3.37** and sadly only an unidentifiable mixture resulted (**Scheme 3.19**).

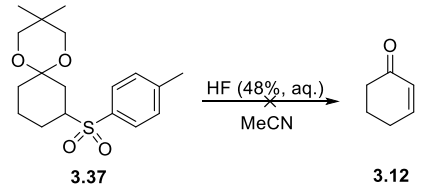

Scheme 3.19: Conditions trialled for removal of ketal protecting group and subsequent aryl sulfone elimination of compound **3.37** using hydrofluoric acid

With the difficulties encountered when trying to change the diol and conditions used for the ketalisation we decide to stick with the original conditions used for the reaction (**Scheme 3.20**). Although this limited us to using 5.0 g batches of starting material it did work well on this scale, giving an excellent yield of ketal **3.33**. When it became necessary to push through large amounts of material, the reaction was repeated multiple times.

Continuing with the forward synthesis to install the pivaloxymethyl (POM) protected β-hydroxymethyl group (**Scheme 3.20**) we again employed sulfur's ability to stabilise α anions. Deprotonation of sulfone **3.33** with *n*-butyllithium was followed by alkyation with chloromethylpivalate to give protected alcohol **3.34**. When this compound was treated with hydrofluoric acid (aq., 48%) we observed a simultaneous ketal deprotection and arylsulfone elimination to give the β-functionalised cyclohexenone **3.35** in excellent 96% yield. Due to the sensitive nature of enone **3.35**, the subsequent α-iodination requires particularly mild conditions of iodine with PIFA, pyridine and BHT. This unusual iodination is believed to work through the formation of a trifluoroacetylhypoiodide species, which can perform mild iodinations under basic

conditions.[91,92] A substoichiometric amount of BHT is required to prevent any unwanted radical reactions occurring. Under these conditions iodoenone **3.36** was formed in a good yield of 87% on >1 g scale.

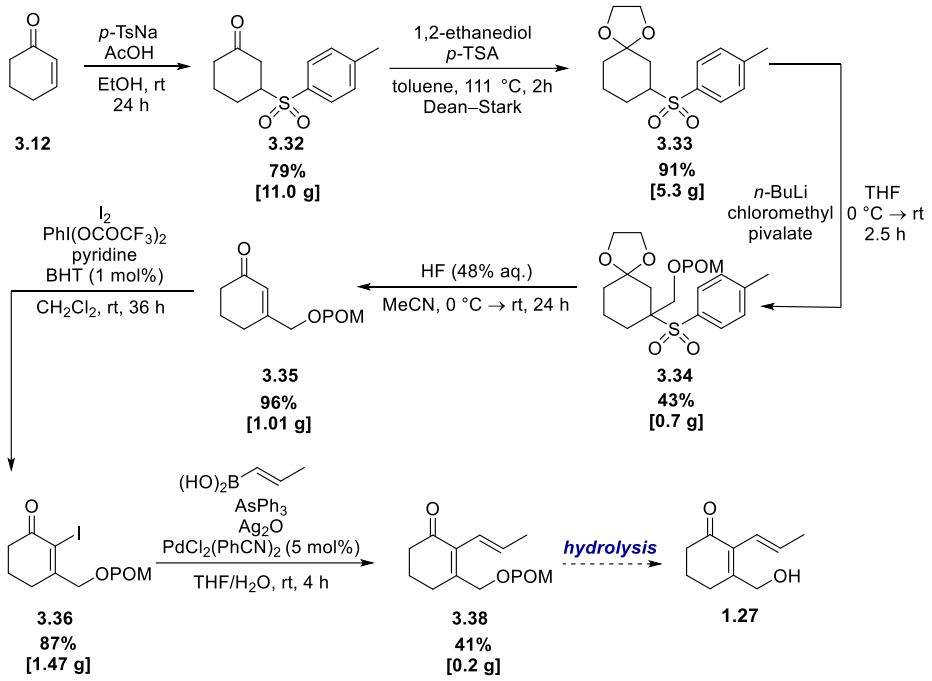

Scheme 3.20: Route for forming POM protected alcohol **3.38** from cylcohexenone (**3.12**)

With the key iodoenone intermediate (**3.36**) in hand this allowed us to continue Hayashi's original route with our altered substrate (*i.e.*, POM protected **3.36**, not TBS protected **3.6**). To install the α-(*E*)-propenyl group a palladium catalysed Suzuki–Miyaura cross coupling reaction with silver (I) oxide and triphenylarsine was used and afforded compound **3.38** in moderate yield (41%). The triphenylarsine ligand is a bulkier alternative to the classic triphenylphosphine ligand, which in some cases has been found to accelerate the transmetallation step in cross-coupling reactions.[93]

3.1.6 Pivaloxymethyl Deprotection

POM protected alcohol **3.38** is a single deprotection step away from the desired Diels–Alder precursor **1.27**. The POM protecting group is a versatile group that can be removed under different conditions, including basic and acidic.

Investigations into the deprotection of **3.38** started with a range of acids and bases summarised in **Table 3.1**. KO*t*-Bu, K_2CO_3, and LiOH resulted in degradation of the starting material (**3.38**) (**Table 3.2, Entries 1-3**). Ammonia in methanol (**Table 3.1, Entry 4**) gave the first indication in the ^1H NMR spectrum of the crude reaction mixture that small amounts of product had formed (SM:P, 94:6). Acidic conditions proved to be far more successful (**Table 3.1, Entry 5-6**). The best result we achieved in these preliminary studies was with TFA (**Table 3.1, Entry 5**), which resulted in a starting material to product ratio of 80:20.

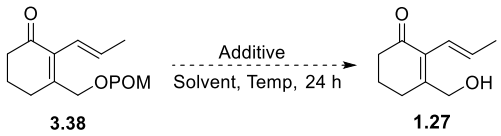

3.38 **1.27**

Entry	Additive	Solvent	Temp	Result (SM:P)
1	KO*t*-Bu	Et_2O	0 °C	decomp.
2	K_2CO_3	MeOH	rt	decomp.
3	LiOH in H_2O	MeOH	rt	decomp.
4	NH_3	MeOH	rt	94:6
5	TFA	-	rt	80:20
6	HCl (aq.)	MeOH	rt	81:19

Table 3.1: Reaction conditions trialled for the POM removal of compound **3.38**

The availability of POM protected Diels–Alder precursor **3.38** was becoming an issue for continued reaction screening efforts. It was decided that removal of the POM group earlier in the synthesis might be an attractive alternative. Indeed, the POM group in compound **3.35** was arguably at its most sterically inaccessible point in the entire synthesis, so earlier removal may be easier. Therefore, efforts to deprotect the alcohol of compound **3.35** were undertaken.

Starting investigation with the removal of the POM group under acidic conditions, we noted no improvement trying this reaction on compound (**3.35**) (**Table 3.2, Entries 1-2**). As we had previously seen product formation using ammonia in methanol we sought to improve this preliminary result by adding a nucleophilic catalyst.[94] When compound **3.35** was subjected to these altered conditions (**Table 3.2, Entry 3**) an enhancement was seen in the starting material to product

ratio (91:9, *cf.* 94:6 without imidazole **Table 3.2, Entry 4**). This inspired us to revisit the previous bases used in **Table 3.1** with the addition of imidazole to catalyse the deprotection. This worked excellently with K_2CO_3, giving over 50% conversion for the first time and increasing the starting material to product ratio to 33:67 (**Table 3.2, Entry 4**). In contrast using LiOH as the base resulted only in recovered starting material (**Table 3.2, Entry 5**). To ensure the reaction was not occurring with imidazole acting as a base itself, a control reaction was performed. This showed it was necessary to add an additional base for any reactivity to occur (**Table 3.2, Entry 6**).

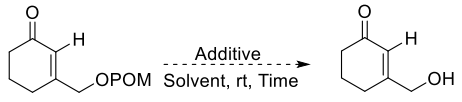

3.35 **3.23**

Entry	Additive	Solvent	Time (h)	Result
1	TFA	-	24	83:17
2	HCl (aq.)	MeOH	24	82:18
3	NH_3/ imidazole	MeOH	24	91:9
4	K_2CO_3/imidazole	MeOH	24	33:67
5	LiOH/imidazole	MeOH	24	RSM
6	imidazole	MeOH	24	RSM
7	K_2CO_3	MeOH	24	43:57
8*	K_2CO_3/imidazole	MeOD	24	deuteration
9*	-	MeOD	24	RSM
10*	K_2CO_3/imidazole	$CDCl_3$	24	RSM
11[#]	K_2CO_3/imidazole	MeOH	24	decomp.

Table 3.2: Reaction conditions trailed for the POM deprotection of compound **3.35**. * Reaction performed on NMR scale. [#] Reaction performed on a larger scale

To determine whether the addition of the nucleophilic catalyst was crucial for the deprotection step, the reaction was performed with K_2CO_3 with the absence of imidazole (**Table 3.2, Entry 7**). This resulted in some formation of product but it was notably not as effective as when K_2CO_3 was used in combination with imidazole (33:67 vs 43:57 respectively).

Attempts were made to follow the reaction by NMR spectroscopy. Initially, we mimicked the reaction conditions using deuterated solvent (methanol-d_4) (**Table 3.2, Entry 8**), but this resulted in deuteration of the starting material in the presence of an external base. Chloroform-*d* was also trialled as a compatible NMR solvent but unfortunately K_2CO_3 was found to be insoluble in this

solvent and no reaction occurred (**Table 3.2, Entry 10**). We concluded that the best conditions involved using K_2CO_3 and imidazole in methanol at room temperature for 24 hours. This gave us a separable mixture of starting material and desired product with an overall yield of 24% on small scale (10 mg). Therefore, these were the conditions chosen for the first scale up of the deprotection (500 mg). Unfortunately, after multiple scale-up attempts there was no success and a lot of starting material was lost. Furthermore, even if this reaction could be conducted on a larger scale the poor yield would severely limit its usefulness. Therefore, this route was reluctantly abandoned.

3.1.7 Alternative Alcohol Protecting Group

As the POM protecting group proved incompatible with our synthesis we looked to the use of other alcohol protecting groups. Hayashi and co-workers found success using the TBS protecting group in the original synthesis of the Diels–Alder precursor (**1.27**), with straightforward protection and deprotection steps. This led us to investigate ways of incorporating a TBS group into our synthesis.

It was found that the synthesis of a methyl TBS variant (**3.39**) of the chloromethylpivalate reagent had previously been reported, although there were only a few examples of its application in organic synthesis (**Scheme 3.21**).[95] The procedure was published in *Organic Syntheses* by Clive and co-workers in 2013, and started from the commercially available ethanethiol (**3.40**). Hemithioacetal **3.41** was formed when ethanethiol was treated with paraformaldehyde. The TBS protecting group was installed to form **3.42**, which undergoes an S_N2 displacement with chloride to give **3.39**.

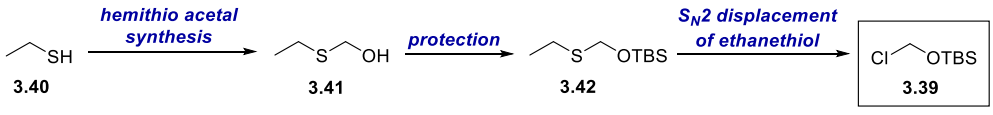

Scheme 3.21: Proposed route to form new electrophile, TBS protected alcohol **3.39** from ethanethiol (**3.40**)

In our hands, ethanethiol (**3.40**) was condensed with paraformaldehyde to give sulfide **3.41**, which due to difficulties in purification was carried through crude for the next reaction (**Scheme 3.22**). Sulfide **3.41** was then treated with trimethylsilyl chloride under basic conditions to protect the

terminal alcohol, giving TBS-protected alcohol (**3.42**) in 96% yield over the two steps. To form the alternative protecting group reagent **3.39** sulfuryl chloride was used a source of chlorine for an S_N2 displacement of ethanethiol. Unfortunately this literature reaction proved unreproducible, after multiple attempts it only resulted in a complex mixture of products, which forced us to abandon this route.

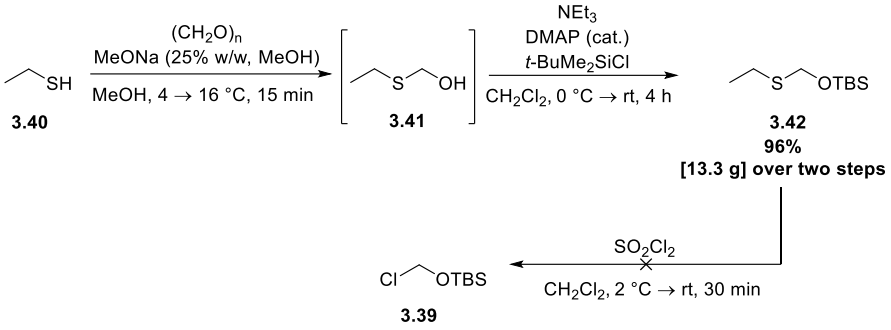

Scheme 3.22: Conditions trialled to form TBS protected alcohol **3.39**

3.1.8 Route to Monomer *via* Unprotected Alcohol

Protection of the primary alcohol in the synthesis was crucial as poor yields had been reported when using the free alcohol in the α-iodination step.[86] Hayashi also opted to use a protected alcohol throughout his synthesis (**3.9, Section 3.1.1, Scheme 3.2, page 35**), suggesting similar problems may occur using the free alcohol in the crucial Suzuki–Miyaura reaction.

Another method to incorporate the TBS-protected alcohol would be to modify our synthesis to install a free alcohol that we could then protect with a TBS group. We previously avoided this protection/deprotection strategy due to step economy. With limited success with all other routes investigated this was the next avenue we chose to pursue.

Repeating the work of Olivo *et al.* (**Scheme 3.23**), the protected aryl sulfone enone **3.33** was formed in two steps from 2-cyclohexen-1-one (**3.12**) in 73% yield.[86] With plenty of **3.33** in hand we opted to add an unprotected alcohol to the β-positon of the cyclohexanone motif using paraformaldehyde as the alcohol surrogate. The first attempt of this reaction worked excellently with complete conversion of **3.33** to the desired product (**3.43**). However, as this reaction was repeated the conversion started to fall off until eventually no formation of the product was observed. All reagents

were purified, and the *n*-butyllithium was titrated to find its exact concentration, but still only recovered starting material was obtained. After a lot of trial and error it was discovered it was imperative that the paraformaldehyde was free from all moisture and was required to be dried under vacuum and over P_2O_5 prior to use. Otherwise any residual moisture present was believed to quench the α-anion formed and result in recovered starting material.

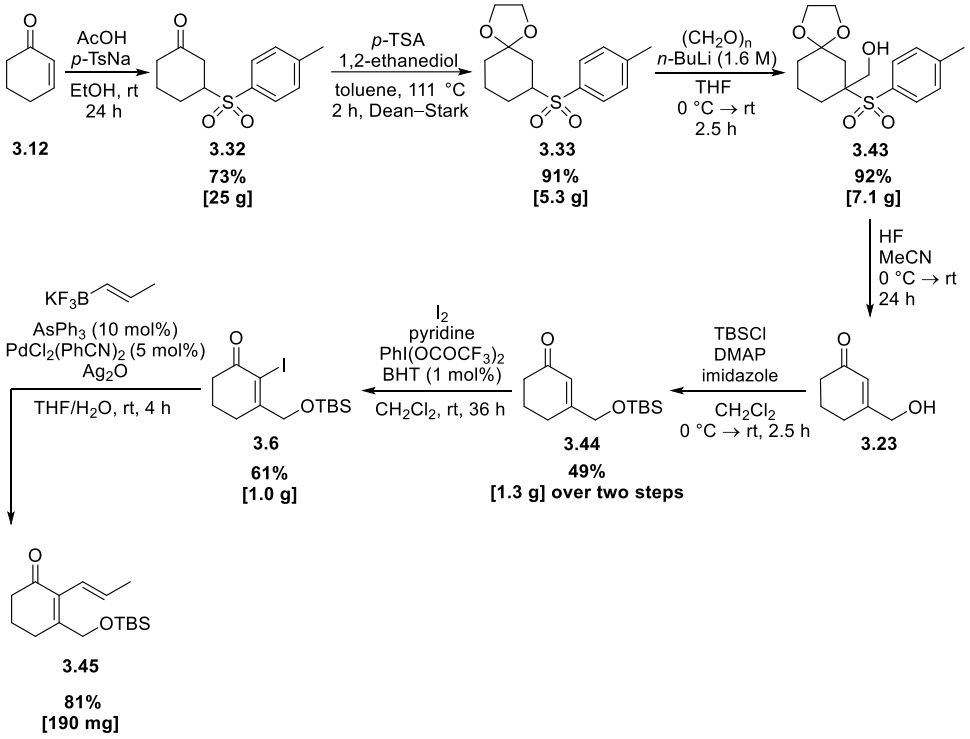

Scheme 3.23: Route to form the TBS protected monomer precursor **3.45** from 2-cyclohexen-1-one **3.12**

With an optimised method to form **3.43** in synthetically useful quantities, the synthesis was continued with the acid-mediated deprotection and simultaneous tosyl elimination to give enone **3.23**. This HF-mediated deprotection with the free alcohol (**3.43**) proved more difficult than previously experienced with the POM protected alcohol (**3.34**). Many side-products were observed, presumably due to acid-catalysed elimination of the primary alcohol, which resulted in a reduced yield and further difficulties with purification. It was found that compound **3.23** would streak on silica columns and began to decompose the longer it sat on the column. To avoid this arduous purification process, the reaction was later telescoped with the subsequent TBS protection. By

combining the two reactions we formed the TBS protected alcohol **3.44** in an improved yield of 49% over the two steps.

This TBS-protected alcohol (**3.44**) was then subjected to the same set of conditions as the POM alcohol (**Scheme 3.23**). The α-iodination and Suzuki–Miyaura cross-coupling reaction exhibited similar reactivity and gave comparable yields to afford compound **3.45**.

For the TBS deprotection of **3.45** we first used Hayashi's procedure involving TBAF in dichloromethane. This worked well but removing the residual *n*-tetrabutylammonium salts left from the TBAF proved difficult. Purification required multiple columns to remove this impurity and resulted in an overall yield of 43% of compound **1.27** (**Scheme 3.24**). Consequently, alternative deprotection conditions were investigated.

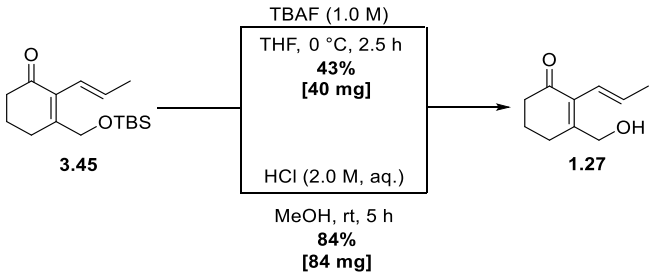

Scheme 3.24: Attempted removal of the TBS protecting group from the primary alcohol (**3.45**) to form the monomer precursor (**1.27**)

It was decided to firstly try the commonly used conditions of HCl in methanol to provide a cleaner deprotection. This worked well resulting in a cleaner ^{1}H NMR spectrum of the crude reaction mixture and straightforward purification to finally give a route to the desired Diels–Alder monomer (**1.27**) precursor in 84% yield (**Scheme 3.25**).

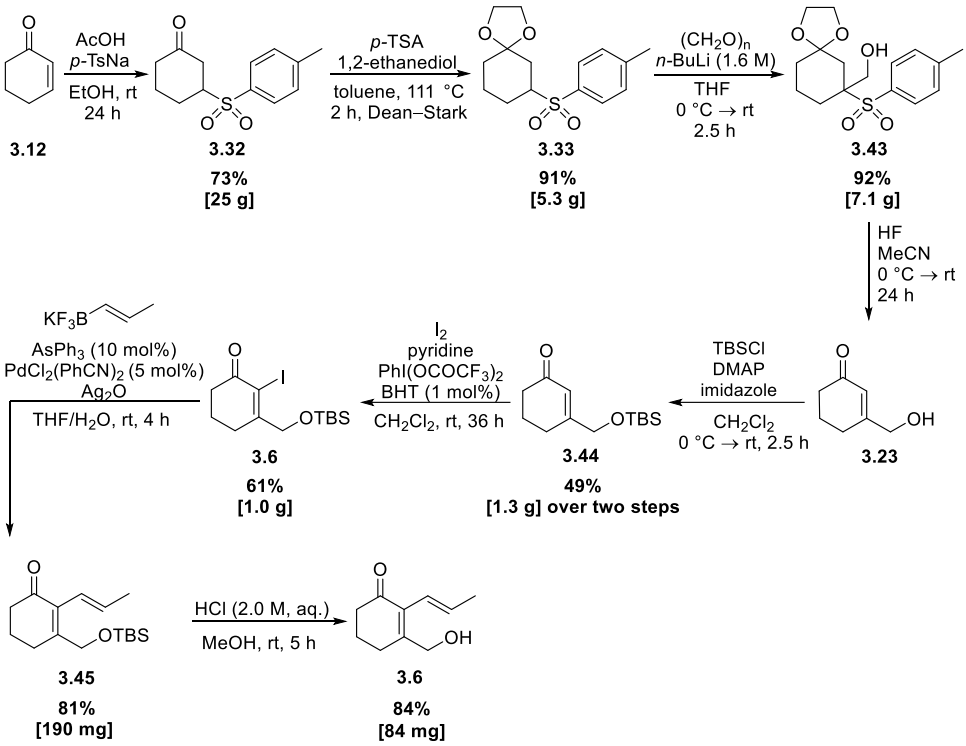

Scheme 3.25: Route summary to form the monomer precursor **1.27** from 2-cyclohexen-1-one (**3.12**) in 8 steps with an overall yield of 1.2%

3.2 Domino *6π*-Electrocylisation/Diels–Alder Dimerisation

After successfully synthesising the Diels–Alder precursor **1.27**, investigations began into the dimerisation reaction itself. The reported heterochiral selective dimerisation starts with the oxidation of the alcohol to the aldehyde which undergoes a domino 6π-electrocyclisation and Diels–Alder dimerisation (**Scheme 3.26**).

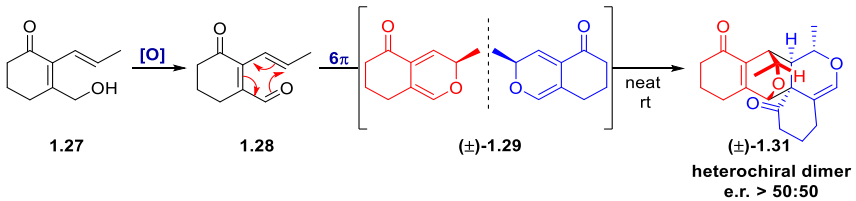

Scheme 3.26: Oxidation of allylic alcohol **1.27** to aldehyde **1.28** followed by domino 6π electrocyclisation/Diels–Alder reaction to give heterochiral dimer product **1.31** in racemic form

This highly selectivity heterochiral dimerisation can be attributed to the methyl groups on both the diene and dienophile wanting to adopt a steric-minimising conformation that lies outside of the bond-forming-zone (**Figure 3.3**). This can only be achieved in a heterochiral pairing of the monomers in an *endo*- type approach.

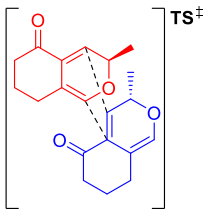

Figure 3.3: Proposed transition state of *endo* selective Diels–Alder reaction of racemic 2*H*-pyran intermediate

To probe this dimerisation reaction ourselves, we first oxidised alcohol **1.27** using activated manganese dioxide (**Scheme 3.27**). Aldehyde **1.28** was isolated and when left to stand at room temperature overnight open to air formed the Diels–Alder product (**(±)-1.31**). Interesting, we noticed an inseparable minor product (**(±)-3.46**) was formed as well, suggesting the selectivity of the Diels–Alder reaction was not as high as Hayashi first reported. We hypothesised that this minor product (**(±)-3.46**) may be the result of a homochiral coupling of monomers in a Diels–Alder reaction.

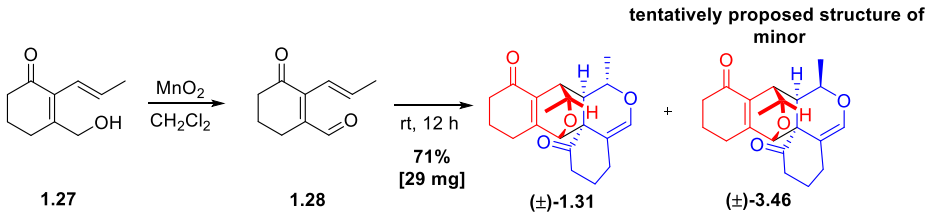

Scheme 3.27: Oxidation of allylic alcohol **1.27** with manganese dioxide

This minor product (**(±)-3.46**) was also confirmed to be racemic by chiral-HPLC as we saw a second set of racemic peaks with a slightly shorter retention time (**Figure 3.4**). Through multiple chiral-HPLC iterations with fraction collecting we were able to separate the two racemic products and successfully characterise the major product. Unfortunately, due to the minor product being formed

in less than 5% yield we were unable to fully characterise this product, but speculate that it is the result of a homochiral Diels–Alder dimerisation.

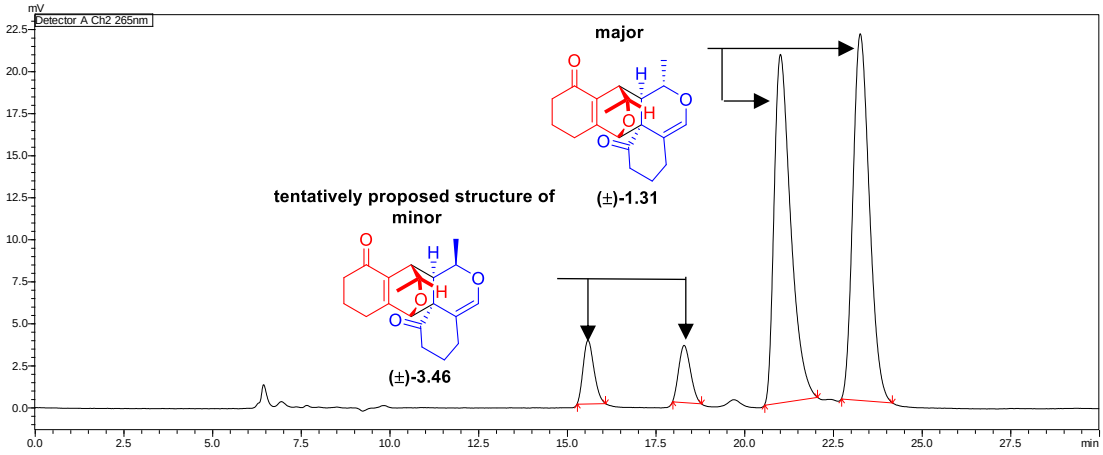

Figure 3.4: Chiral HPLC chromatogram of Diels–Alder dimerisation using Chiralpak OD-H column 87:13 hexane/IPA, 0.5 mL min^{-1}, t_1 = 15.59 min (minor), t_2 = 18.30 min (minor), t_3 = 21.02 min (hetero), t_4 = 23.27 min (hetero)

3.3 Reaction Monitoring Studies of Domino Reaction

Having successfully reproduced the heterochiral dimerisation we wished to study in detail the kinetics of the domino oxidation and *6π*-electrocyclisation/Diels–Alder reaction sequence.

To be able to induce enantioselectivity in our system, we required the rate determining step of the dimerisation to be the Diels–Alder reaction. Enantioselective Diels–Alder reactions are well-documented in the literature, with a range of different of chiral reagents reported.[22] By contrast, an enantioselective *6π*-electrocylisation would be a novel reaction, and therefore represents a significantly more difficult challenge. Due to initial fears that the direct addition of an internal standard may affect the subtleties of the highly selective Diels–Alder dimerisation, we opted for a co-axial monitoring system (**See Appendix 11.1** for details). This involved inserting a thin sealed tube of an internal standard into the NMR tube sample (**Figure 3.5a**).

1,4-Dinitrobenzene was selected as the internal standard of choice due to it producing a single peak at 8.42 ppm (^{1}H NMR spectrum) (**Figure 3.5b**), which didn't overlap with any peaks of interest in the reaction.

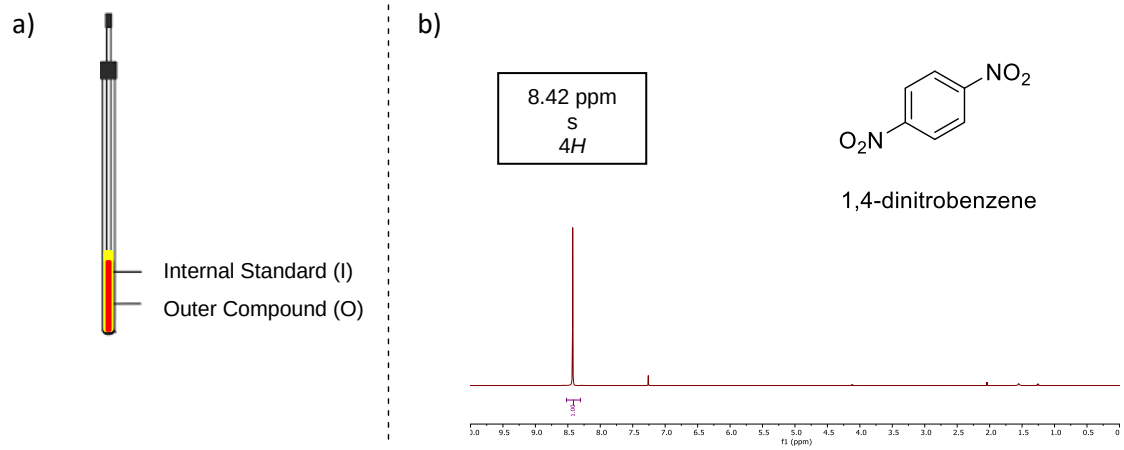

Figure 3.5: a) Coaxial NMR tube set up. b) Internal standard 1,4-dinitrobenzene, ^{1}H NMR spectrum

The oxidation of the alcohol (**1.27**) to the aldehyde with manganese dioxide was repeated (**Figure 3.6**). Care was taken not to expose the crude aldehyde to heat or pressure during the concentration process, which could cause the dimerisation to occur prematurely before NMR data and time points were collected. It was necessary for the NMR reaction to be run in deuterated chloroform instead of under neat conditions, causing the reaction to take place over days instead of hours. During this timed NMR experiment, distinct peaks of the aldehyde (**1.28**) and the major heterochiral (**(±)-1.31**) and tentatively propsed homochiral minor product **(±)-3.46** were monitored over time (**Figure 3.6**). As expected, we noted the conversion of the aldehyde (**1.28**) to the various products over time signalled by the increasing integration of the product peaks with respect to the internal standard added. Yet again there was no evidence of the 2*H*-pyran intermediate forming (**(±)-1.29**). These results were plotted to show conversion over time (**Figure 3.6**).

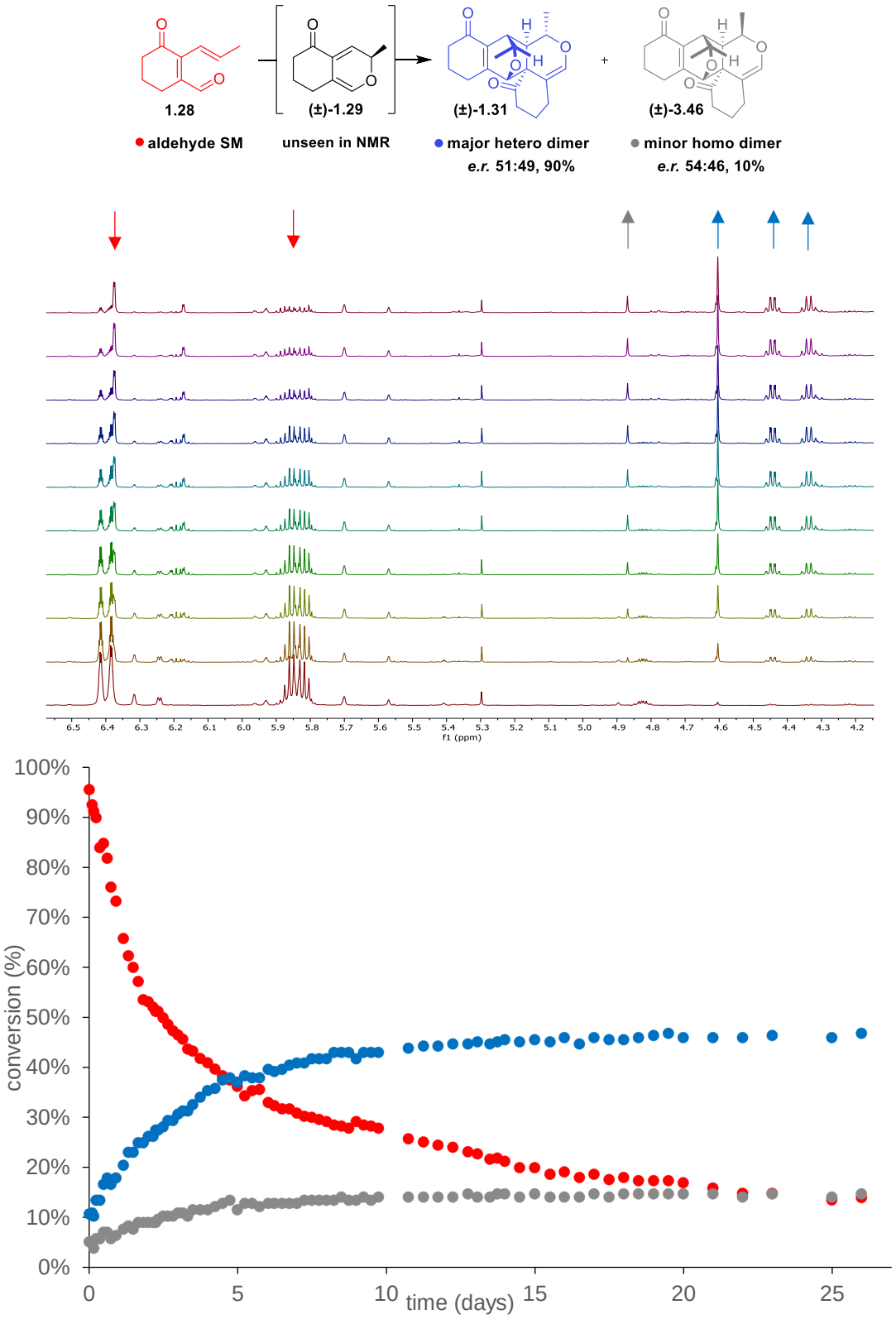

Figure 3.6: Scheme: domino dimerisation reaction and key for spectrum and graph. Minor product postulated structure, Spectra: Timed ^{1}H NMR experiments of domino dimerisation reaction (t=0 at the bottom), Graph: conversion of aldehyde (**1.28**) to dimeric product against time

3.4 Rate Determining Step of Domino Reaction

To use this data to decipher which step of the domino sequence was rate determining, we needed to apply two different types of kinetic scenarios.

First would be the pre-equilibrium approximation (**Scheme 3.28**). This theorem relies upon a fast and reversible equilibrium occurring between the aldehyde (**1.28**) and 2*H*-pyran intermediates (±-**1.29**), finishing with a slower irreversible reaction to the products. This results in the Diels–Alder reaction ultimately being rate determining ($k_1/k_{-1} > k_2$). Based on this assumption, the rate should be proportional to the concentration of starting material (aldehyde, **1.28**) squared. When this is integrated, the rate equation for the pre-equilibrium approximation is obtained.

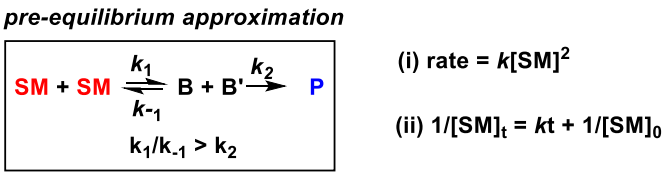

Scheme 3.28: Reaction scheme for pre-equilibrium approximation with (i) rate equations and (ii) integrated rate equation

By applying the pre-equilibrium approximation to our system and plotting 1/[SM] against time we saw a linear relationship between the two (**Graph 3.1**). This suggests that the reaction follows second order kinetics and the rate determining step is the Diels–Alder step. Therefore, through the use of chiral reagents, it may be possible to differentiate between the two enantiomeric transition states and achieve stereoretentive enantioconvergency.

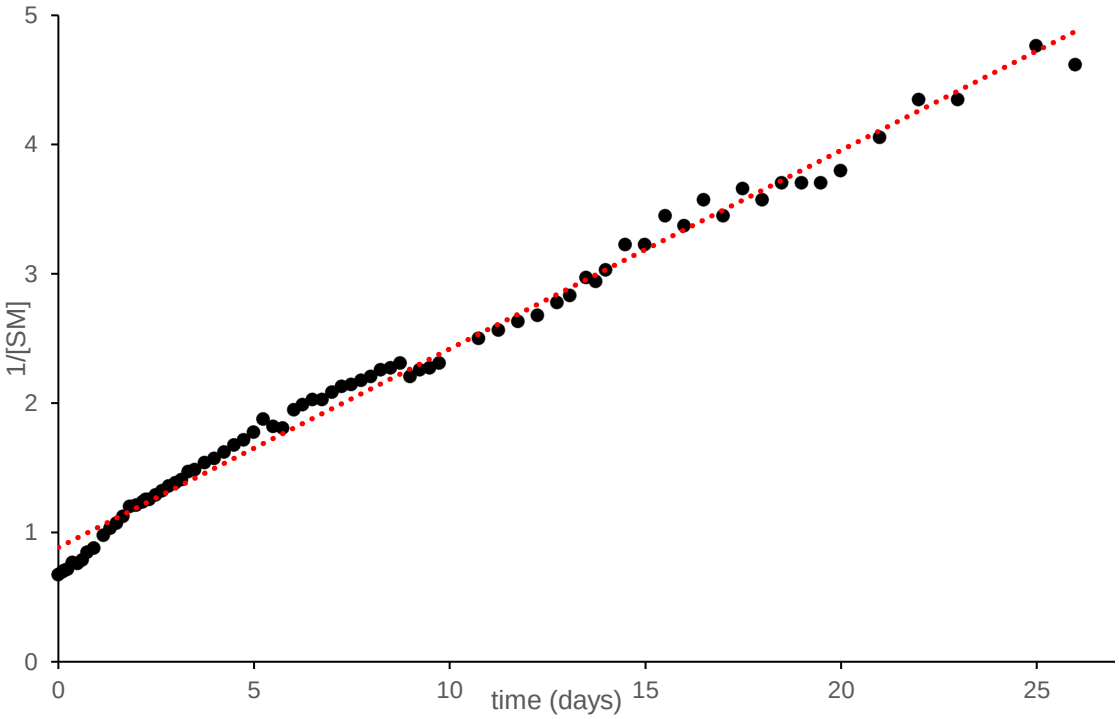

Graph 3.1: Pre-equilibrium approximation

To confirm this result, the Steady State approximation was also applied to our data. This theory involves setting the rate of change of a reaction intermediate to zero by assuming that the intermediate is in very low concentration throughout the reaction as it reacts as soon as it formed ($k_1/k_{-1} < k_2$) (**Scheme 3.29**). When plotting ln[SM] *vs* time this results in a non-linear relationship indicating the reaction does not follow first order kinetics and the 6π-electrocyclisation is not rate determining (**Graph 3.2**).

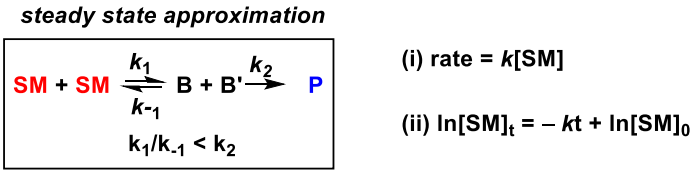

Scheme 3.29: Reaction scheme for steady state approximation with (i) rate equations and (ii) integrated rate equation

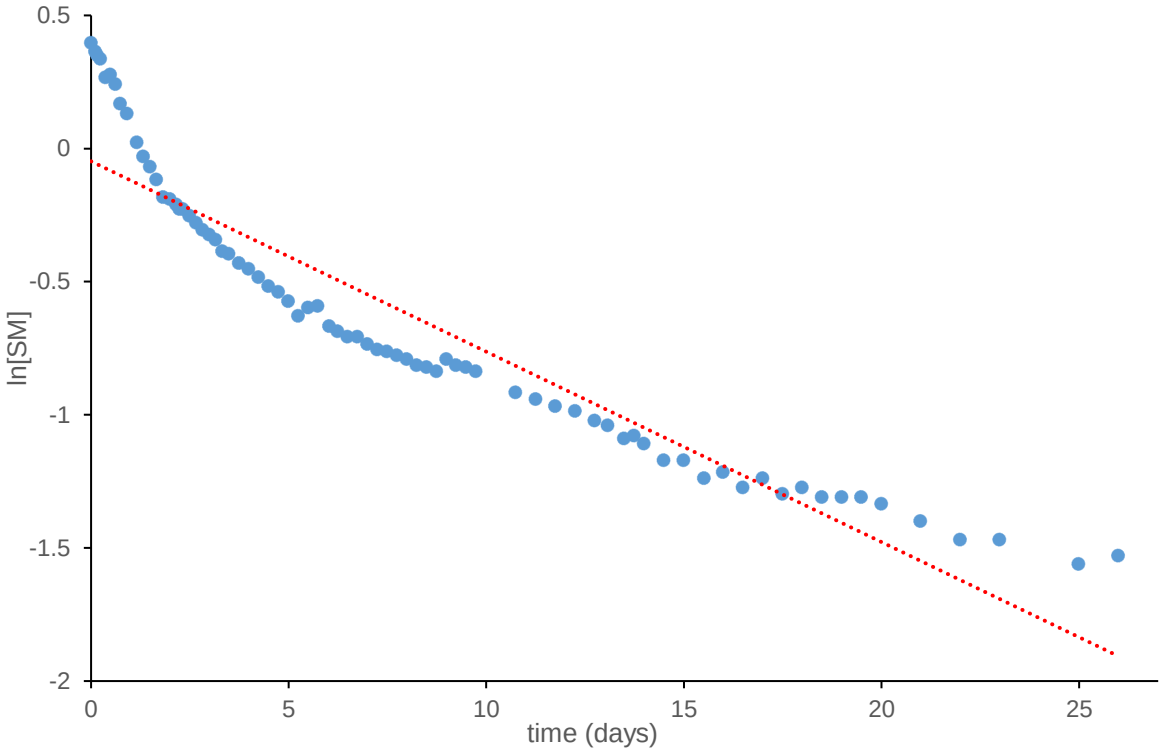

Graph 3.2: Steady state approximation

3.5 Screen for Enantioselective Dimerisation Conditions

With the confirmation of a rate determine step of the domino reaction being the Diels–Alder reaction we could now look to what types of catalyst we could use to perform an enatioselective Diels–Alder reaction.

In literature, to promote a more facile domino *6π*-electrocylcisation/Diels–Alder reaction of similar epoxyquinol-derived compounds, additives such as silica[96,97] or solvents such as MeOH[20,96] have been used. This suggests that the dimerisation might be accelerated through hydrogen bonding, either through the choice of a protic solvent or through using an acidic additive.

To assess whether H-bonding catalysis could be applicable to our system we looked at performing the dimerisation reaction in solvents that varied in polarity and dielectric constants. The dimerisation of **1.28** was performed in each solvent alongside a dimerisation of **1.28** conducted in dichloromethane. The dimerisation in dichloromethane acted as a control reaction to enable us to calculate relative rates and compare the rate of each solvent (**Table 3.3**).

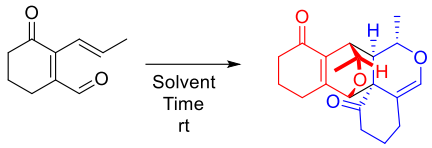

1.28 (±)-1.31

Entry	Solvent	Time (h)	Conversion (%)	Relative rate
1	CH_2Cl_2	48	95	-
2	MeOH	48	97	-
3	CH_2Cl_2	18	30	1.00
4	MeOH	18	82	2.73
5	CH_2Cl_2	18	67	1.00
6	toluene	18	69	1.03
7	CH_2Cl_2	18	87	1.00
8	MeCN	18	38	0.44

Table 3.3: Solvent screen and relative rates calculation for Diels–Alder reaction

To find an appropriate time scale for the dimerization, time points were taken at 48 and 18 hours in dichloromethane and methanol respectively (**Table 3.3, Entry 1-4**). After 48 hours the reactions in both solvents were nearly at completion so this told us very little about their relative rates, but at 18 hours we saw a significant difference. Using the more polar and protic solvent of methanol resulted in a larger NMR conversion to the dimeric product **(±)-1.31**. To test our hypothesis that this dimerisation was susceptible to hydrogen bonding catalysis we surveyed more solvents with varying polarity and hydrogen bonding ability (**Table 3.3, Entry 6, 8**). We established that the relative rate of the reaction did not correlate with the polarity of the chosen solvent (**Figure 3.7**), as we saw the reaction occur fastest in methanol and slowest in acetonitrile. Therefore concluding that this Diels–Alder dimerization may have the potential to be catalysed with induced enantioselectivity using chiral hydrogen-bonding catalysts.

Dielectric constants

MeCN < MeOH < CH_2Cl_2 < toluene
(35.9) (33) (9.1) (2.4)

Relative rate compared to CH_2Cl_2

MeOH < toluene ≈ CH_2Cl_2 < MeCN
(2.73) (1.03) (1.00) (0.44)

Figure 3.7: Solvents organised in varying dielectric constants *vs* relative rate in Diels–Alder reaction

3.5.1 Chiral Hydrogen Bonding Catalysts

In literature we looked for previous examples of hydrogen bonding catalyst used to perform enantioselective Diels–Alder reactions, and found the work of Rawal and co-workers.[98] They were able to perform a hetero-Diels–Alder reaction of aminosiloxydienes and substituted acroleins to afford the Diels–Alder adducts in good yield and enantioselectivity (up to 92% *ee*) (**Scheme 3.30**).

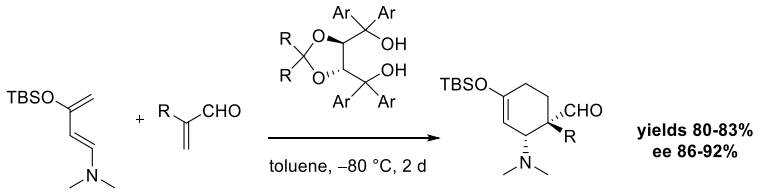

Scheme 3.30: Rawal and coworkers enantioselective Diels–Alder reaction using TADDOLs

This H-bonding catalyst used to promote this type of enantioselective transformation was a TADDOL (tertaaryl-dioxolane-dimethanol) ligand. TADDOLs are chiral diols that possess a core C_2-symmetric dioxolane with flanking aryl groups. TADDOL ligands have a multitude of applications in chemistry, ranging from use as chiral ligands, NMR shift reagents, and dopants for cholesteric liquid crystals.[99,100] This may be due to the TADDOL family encompassing a wide range of compounds due to their ease of modification in synthesis. They can be made in two steps from the corresponding aryl halide, many of which are commercially available.

To investigate if this family of ligands could induce enantioselectivity in our systems we set out to make a library of TADDOLs. This was achieved by treating the L-tartrate derivative (–)-**3.47** with the appropriate Grignard overnight under reflux (**Figure 3.8**). The Grignard reagent used was either commercially available (compounds **3.48, 3.49**) or made *in situ* from the equivalent aryl bromide with magnesium (compounds **3.50**-**3.57**).

With a range of TADDOLs in hand we tested the dimerisation with 10 mol% of the catalyst added. Toluene was used as the preferred solvent as it had performed similarly to dichloromethane in our previous studies (**Table 3.4**), and obviated issues of TADDOL solubility observed when dichloromethane was used.

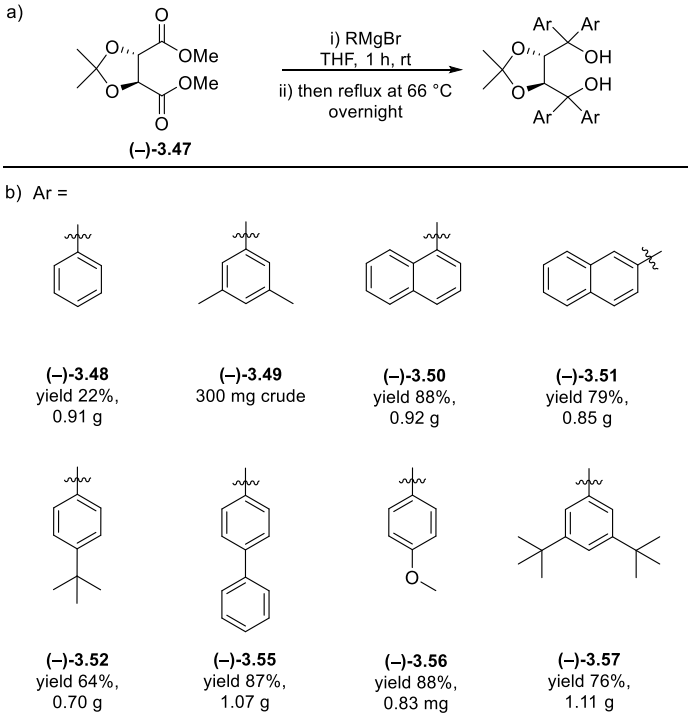

Figure 3.8: a) Typical synthesis of TADDOLs from L-tartrate derivative b) Range of TADDOL ligands synthesised varying the aryl groups

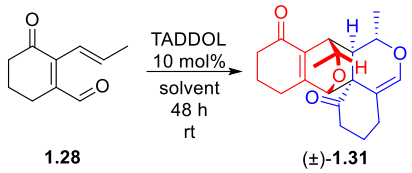

Entry	Ar group	Solvent	Rel Rate	*e.r.*
1	No TADDOL	toluene	1.0	50:50
1	1-naphthyl ((–)-**3.50**)	toluene	3.2	50:50
2	2-naphthyl ((–)-**3.51**)	toluene	3.6	50:50
3	phenyl ((–)-**3.48**)	toluene	3.8	50:50
4	anisole ((–)-**3.56**)	toluene	2.1	50:50
5	4-tert-butylphenyl ((–)-**3.52**)	toluene	1.6	50:50
6	biphenyl ((–)-**3.55**)	CH_2Cl_2	1.8	50:50

Table 3.4: Screen of TADDOL ligands in enantioselective domino *6π*-electrocylisation/Diels–Alder dimerisation

From this small screen, we noted that the TADDOL ligands were compatible with the dimerisation reaction and all the reactions yieldied the heterochiral dimeric product (**(±)-1.31**) in the same diastereomeric ratio as the standard dimerisation. We also noted an enhancement in rate although

this unfortunately did not translate to any enantio-enhancement of the Diels–Alder reaction for this family of ligands.

3.5.2 Thiourea Catalysts

Unsuccessful in our attempts of using TADDOL-type ligands to induce enantioconvergency, we looked to a different class of H-bonding catalyst that have been shown to catalyse enantioselective Diels–Alder reaction; thioureas.

In 2003 Schreiner and coworkers demonstrated the potential of symmetrical thioureas (e.g. **3.58**, **Figure 3.9**) as neutral hydrogen bond donors in catalytic Diels–Alder reactions.[101] These work by lowering the activation energies of Diels–Alder reactions through hydrogen bonds.[102]

Following on from this seminal work, Jacobsen,[103] Takemoto,[104] Nagasawa,[105] and Ricci each developed their own asymmetric variants of Schreiner's thiourea catalysis.[106] These catalysts have now been applied to a wide range of different chemical reactions to induce enantioselectivity including Strecker,[107] Michael,[108] *aza*-Henry,[109] and Baylis–Hillman[110] reactions and more. All exploit the hydrogen bonding donating ability of the thiourea catalysis.

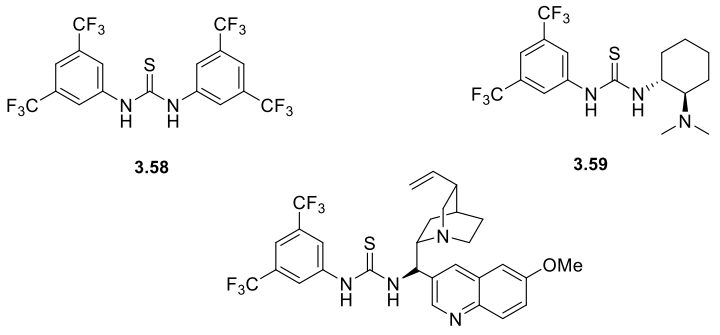

Figure 3.9: A range of different thiourea H-bonding catalyst known to perform enantioselective Diels–Alder reactions

Looking to use these types of neutral hydrogen bond donors in our reaction, we found Schreiner's thiourea[111] and two chiral enantiopure thioureas to be commercially available (**Figure 3.9**).[112]

Thiourea catalysts **3.59**[113,114,115] and **3.60** [116,117,118] have both been shown to act as an effective catalyst in many different asymmetric Diels–Alder reactions.

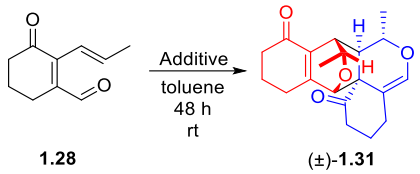

Entry	Additive	Conversion %	Rel. Rate	*e.r.*
1	-	100	1.0	50:50
2	**3.58**	100	2.5	50:50
3	**3.59**	100	2.8	50:50
4	**3.60**	100	2.1	50:50

Table 3.5: Screen of thiourea H-bonding catalysts in enantioselective domino 6π-electrocylisation/Diels–Alder dimerisation

The domino reaction was monitored with the addition of the thiourea catalysts (**3.58-3.60**) to see if there was any rate enhancement or any enantio-induction (**Table 3.5**). Again the catalysts proved to be compatible with the system and all showed a rate enhancement with respect to the standard (**Table 3.5, Entry 1**). Once again, no enantioenrichment with respect to the Diels–Alder reaction was observed.

With both the TADDOL family and thiourea family of H-bonding catalysts proving unsuccessful in inducing enantioselectivity we concluded that although a rate enhancement is exhibited this has no effect on the enantioselectivity of the system.

3.6 Conclusions

Many hurdles were overcome in the synthesis of the monomer **1.**28. Gratifyingly we were able to synthesize the monomer precursor (**1.27**) eventually in a good overall yield of 1.2% over a complex 8 step synthesis (**Scheme 3.31**). During the project we were able to use a broad range of challenging synthetic techniques and procedures to develop this new and robust set of steps.

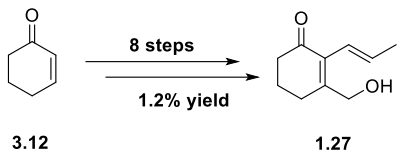

Scheme 3.31: Summary of successful route to monomer precursor **1.27**

Progress was made in understanding the kinetic profile of the domino reaction sequence *via* ^{1}H NMR monitoring experiments. From the data gathered the rate determining step of the domino reaction was successfully confirmed to be the Diels–Alder step. This result proves that this domino reaction sequence could theoretically be made enantioselective through the use of chiral reagents known to perform enantioenriched Diels–Alder reactions.

It was also discovered that the Diels–Alder reaction benefits from a hydrogen bonding effect, which enhances the rate of the reaction under certain conditions. This directed us to try using chiral hydrogen bonding catalyst known to perform enantioselective Diels–Alder reactions (TADDOLs, **Table 3.4** and thioureas, **Table 3.5**). Unfortunately these reactions were unsuccessful in inducing any enantioselectivity. Hence, efforts to attain stereoretentive enantioconvergency on this system evaded us.

3.7 Future Work

Although stereoretentive enatioconvergency has not yet been attained for this reaction, there are many other families of chiral catalyst and reagents that have been shown to achieve enantioselective Diels–Alder reactions.

Work going forward on this project would primarily focus on investigating these other families of chiral additives, for example; chiral Brønsted acid (**3.61**),[119] phosphoric acids (**3.62**),[120] bis(oxazoline) metal complexes[25] (**3.63**) and imidazolidinone MacMillian catalyst (**3.64**)[121,122] to name a few (**Figure 3.10**).

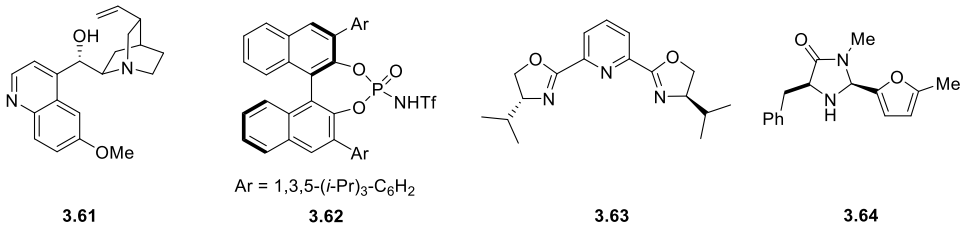

3.61 **3.62** **3.63** **3.64**

Figure 3.10: A range of different chiral catalysts known to perform enantioselective Diels–Alder reactions

There is also the possibility of investigating running the domino reactions at lower temperatures with chiral reagents to see if there was any effect on the *e.r.*. This has previously not been investigated due to limited material available.

If successful in achieving stereoretentive enantioconvergy with this system, we would then focus on developing alternative monomers and to apply the new enantioconvegent methodology. Using the Suzuki–Miyaura cross-coupling reaction as a divergent point in the synthesis would allow us to use alternative boronic coupling partners to diversify our monomer scaffold (**Scheme 3.32**). Creating monomers with larger steric bulk at this key stereogenic centre may help to improve the overall *d.r.* of the Diels–Alder transformation.

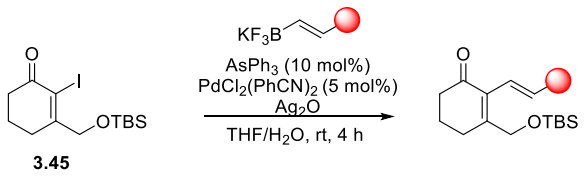

3.45

Scheme 3.32: Divergent Suzuki–Miyaura cross coupling reaction

Chapter 4: Brevianamide Alkaloids Introduction

The brevianamides are a family of fungal metabolites isolated from *Aspergillus* and *Penicillium* fungi.[123] More than 20 different members have been reported since the first examples were isolated in 1969 by Birch and Wright (**Scheme 4.1a**).[124] The brevianamides were the first reported natural products to contain the remarkable bicyclo[2.2.2]diazaoctane architecture. Many related natural product families have since been discovered that possess a bicyclo[2.2.2]diazaoctane core, and now over 100 distinct compounds have been reported to date.[125] These include the closely related natural product families of the stephacidins and the notoamides (**Scheme 4.1b**).[126,127] The brevianamides and other bicyclo[2.2.2]diazaoctane containing alkaloids are of significant interest to the synthetic community as they have intriguing biological activities. In combination with their highly complex structures and fascinating biosynthetic origins they have proven to be attractive synthetic targets spanning numerous decades of research.

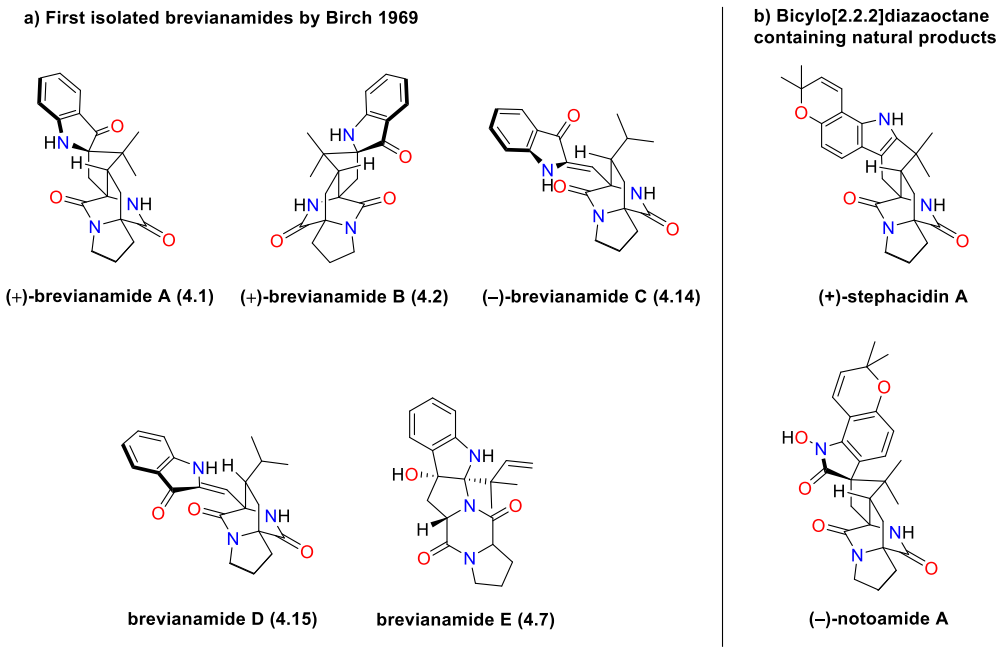

Scheme 4.1: a) The first members of the brevianamide natural product family isolated (A-E) by Birch and Wright in 1969 b) Examples of other natural products containing the bicyclo[2.2.2]diazaoctane motif

Members of the brevianamide family can easily be easily identified by their characteristic diketopiperazine ring and an indole ring bearing a C2-reverse prenyl group. Although these key structural features can be harder to detect in some of the more structurally complex members of the family (due to subsequent rearrangements and cyclisations), their biosynthetic intermediacy is still evident.

Among the first brevianamides isolated by Birch and Wright in 1969,[124] were brevianamide A (**4.1**) and B (**4.2**) found in a diastereomeric ratio of ≳90:10, from the fungus *Pencillium brevicompactum*.[128,129] Structurally, these prenylated alkaloids are diastereomers of each other, and both possess a *(R)*-configured spiro-indoxyl ring and 'psuedo enantiomeric' *anti*-configured bicyclo[2.2.2]diazaoctane core (*anti* refers to the relative configuration of the methine C–H and proximal piperazine nitrogen, see box in **Scheme 4.2**). Potent antifeedant activity against the insect larvae of *Spodoptera frugiperda* (fall armyworm) and *Heliothis virescens* (tobacco budworm) has been recorded for Brevianamide A (**4.1**).[130] Additionally, brevianamide A indicated low overall mammalian toxicity in preliminary screens performed on mice.[131] In contrast, the minor diastereomer, brevianamide B (**4.2**), currently has no recorded biological activity.

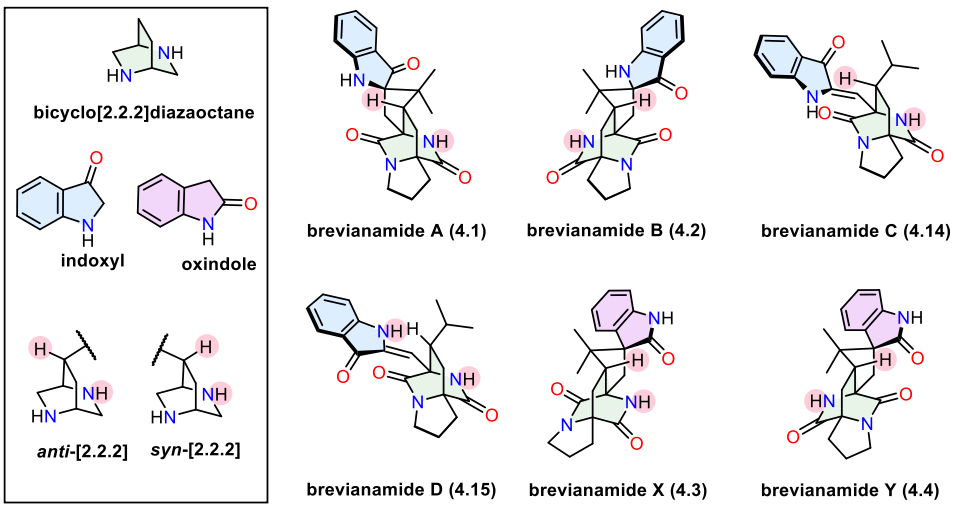

Scheme 4.2: Brevianamide members that contain the bicyclo[2.2.2]diazaoctane ring

In 2017, another two brevianamides, X (**4.3**) and Y (**4.4**), were isolated by Qi and co-workers from the deep-sea-derived *Penicillium brevicompactum* DFFSCS025 and found to contain the bicyclo[2.2.2]diazaoctane system (**Scheme 4.2**).[132] In contrast to brevianamides A (**4.1**) and B (**4.2**), they both contain *spiro*-oxindole rings instead of *spiro*-indoxyl rings. Notably, brevianamide Y (**4.4**) possessed the same *anti*-configured bicyclo[2.2.2]diazaoctane core whereas brevianamide X (**4.3**) has a *syn*-configured core.

4.1 Early Biosynthetic Studies

All members of the brevianamide natural product family are likely derived biosynthetically from a common intermediate, deoxybrevianamide E (**4.5**). Deoxybrevianamide E (**4.5**) is itself a natural product that was isolated by Steyn and co-workers in 1973 from *Penicillium* and *Aspergillus* fungi.[133] The biogenesis of deoxybrevianamide E (**4.5**) begins with the cyclisation of two naturally occurring amino acids, L-proline and L-tryptophan, to form brevianamide F (**4.6**) which features the core 2,5-diketopiperazine ring (**Scheme 4.3**). Turner and co-workers demonstrated this is achieved in nature using the non-ribosomal peptide synthase, brevianamide synthase, which is encoded by gene Afu8g00170.[134] Li and co-workers later showed the C2 reverse prenyl group is introduced by a reverse prenyl transferase which was found to be encoded by the gene cdpC2PT to form deoxybrevianamide E (**4.5**).[135] Deoxybrevianamide E (**4.5**) has been confirmed as a biological precursor for brevianamide A (**4.1**), B (**4.2**) and E (**4.7**) and is assumed to be a precursor for all other members of the family.

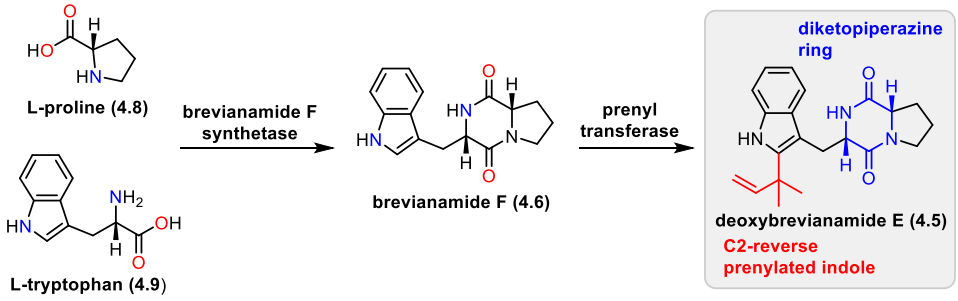

Scheme 4.3: Biosynthesis of the common biosynthetic intermediate deoxybrevianamide E (**4.5**)

With regards to the biogenesis of brevianamide A (**4.1**), Birch conducted feeding studies of the corresponding isotopically labelled L-proline (**4.8**), L-tryptophan (**4.8**) and brevianamide F (**4.6**) to confirm the biosynthetic proposal experimentally (**Scheme 4.4**).[136]

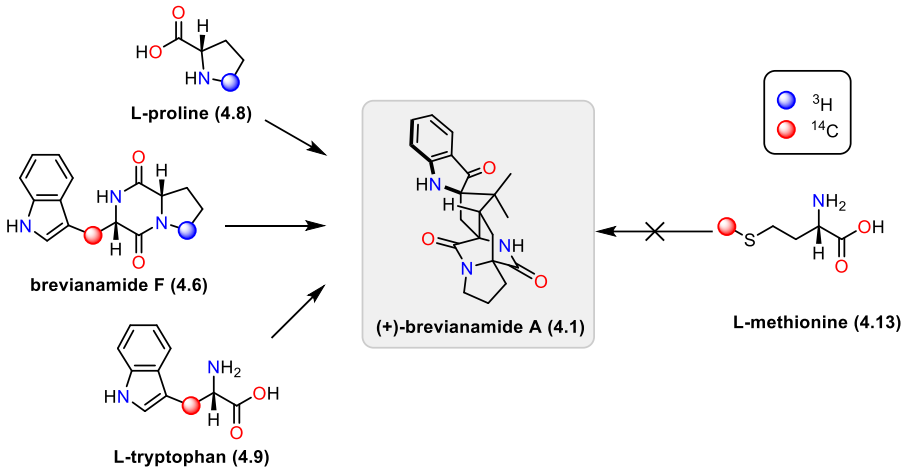

Scheme 4.4: Birch's 1974 biosynthetic feeding studies of brevianamide A (**4.1**)

There has been much debate over the later stages of the biosynthesis of the bicyclo[2.2.2]diazaoctane containing brevianamides. This started shortly after the brevianamides were isolated in 1970, with Sammes and Porter's proposal that the bicyclo[2.2.2]diazaoctane core of brevianamide A (**4.1**) was formed *via* an intramolecular [4+2] cycloaddition (**Scheme 4.5a**).[137] Sammes and Porter conducted model studies on dihydroxypyrazines **4.10** and **4.11** with different dienophiles to form the bicyclo[2.2.2]diazaoctane system in support of their hypothesis (**Scheme 4.5b**). In 1971, Birch countered Sammes' hypothesis with his own biosynthetic proposal which invoked the intermediary of an epidithiapiperazinedione species (**4.12**) (**Scheme 4.5a**).[138] Birch suggested a ring closure could occur with the extrusion of S_2 gas, but did not further suggest how the mechanism would proceed. Birch later noted in biosynthetic feeding studies there was no incorporation of the isotopically labelled amino acid, L-methionine (**4.13**), which ruled out the involvement of a sulfur-containing compound in the biosynthesis (**Scheme 4.4**).[10] Consequently Sammes' proposal of a biosynthetic hetero-Diels–Alder reaction dominated the early speculation surrounding the biogenesis of the biocyclo[2.2.2]diazaoctane containing brevianamides.

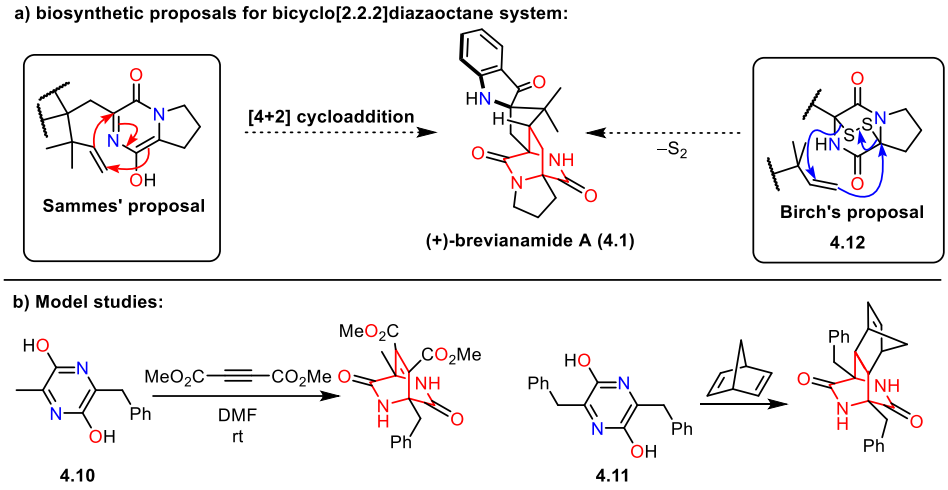

Scheme 4.5: a) Sammes' and Birch's biosynthetic proposals for the synthesis of the bicyclo[2.2.2]diazaoctane scaffold b) Sammes' Model studies of the proposed [4+2] cycloaddition

4.2 Semi Synthesis, (–)-Brevianamide C and D, Birch 1972

In 1972, shortly after isolating the brevianamides, the first semi-synthesis of brevianamides C (**4.14**) and D (**4.15**) was published by Birch and co-workers.[139] Through their isolation studies, Birch noted that when *Penicillium brevicompactum* was grown in the absence of light no formation of brevianamides C (**4.14**) and D (**4.15**) was observed. He hypothesized that these natural products were in fact "photochemical artefacts" of isolation. Birch later proved this hypothesis was correct by subjecting (+)-brevianamide A (**4.1**) to irradiation with visible light (**Scheme 4.6a**), which produced a mixture of brevianamide A, B, C and D (**4.1-4.2,4.14-4.15**). However, under prolonged exposure to visible light (7 hours) the sole products of the reaction were found to be brevianamide C (**4.14**) and D (**4.15**) (**Scheme 4.6b**). Birch suggested the reaction proceeds through a photochemically catalysed radical-mediated ring opening of the 5 membered spirocylic ring (**4.16**). This free radical intermediate (**4.16**) can undergo free rotation, thereby allowing ring closure to reform brevianamide A (**4.1**) or conversion to brevianamide B (**4.2**).

It is important to note that although brevianamide B (**4.2**) was observed as a photolysis product of brevianamide A (**4.1**), during initial photochemical studies when *Penicillium brevicompactum* was grown in the dark brevianamide B (**4.2**) was still isolated in the same ratio.[130] This experiment provide evidence that brevianamide B (**4.2**) is not a "photochemical artefact". Birch also went on

to show that subjecting the major product of irradiation brevianamide C (**4.14**) to further light resulted in more formation of brevianamide D (**4.15**) (**Scheme 4.6c**).

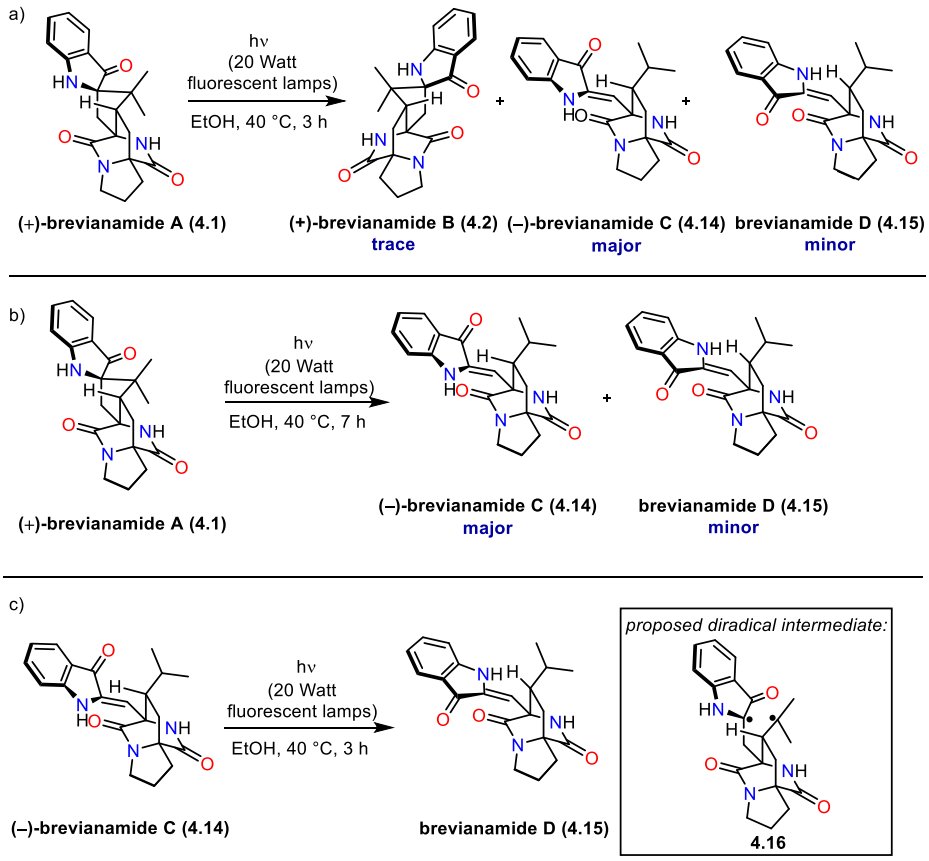

Scheme 4.6: a) Birch's 1972 photolysis of brevianamide A (**4.1**) to brevianamide C (**4.14**) and D (**4.15**) with traces of B (**4.2**) b) Photolysis of brevianamide A (**4.1**) left longer to only yield of brevianamide C (**4.14**) and D (**4.15**) c) Photolysis of brevianamide C (**4.14**) to give a mixture of brevianamide C (**4.14**) and D (**4.15**)

Even though Birch concluded that brevianamide C (**4.14**) and brevianamide D (**4.15**) were the products of a photochemical reaction and not true metabolites of enzymatic origins, they still may have biological importance. Much like brevianamide A (**4.1**), brevianamide D (**4.15**) has shown activity as an insectide.[130] The light sensitive property of brevianamide A (**4.1**) may also bear importance in biological signaling pathways to indicate the presence of light.

4.3 Previous Syntheses of Bicyclo[2.2.2]diazaoctane Containing Brevianamides

4.3.1 Total Synthesis, (–)-Brevianamide B, Williams 1988

Williams and co-workers achieved the first total synthesis of (–)-brevianamide B (**4.2**) in 1988.[140–142] The synthesis utilised a key cationic cyclisation to install the bicyclo[2.2.2]diazaoctane system.

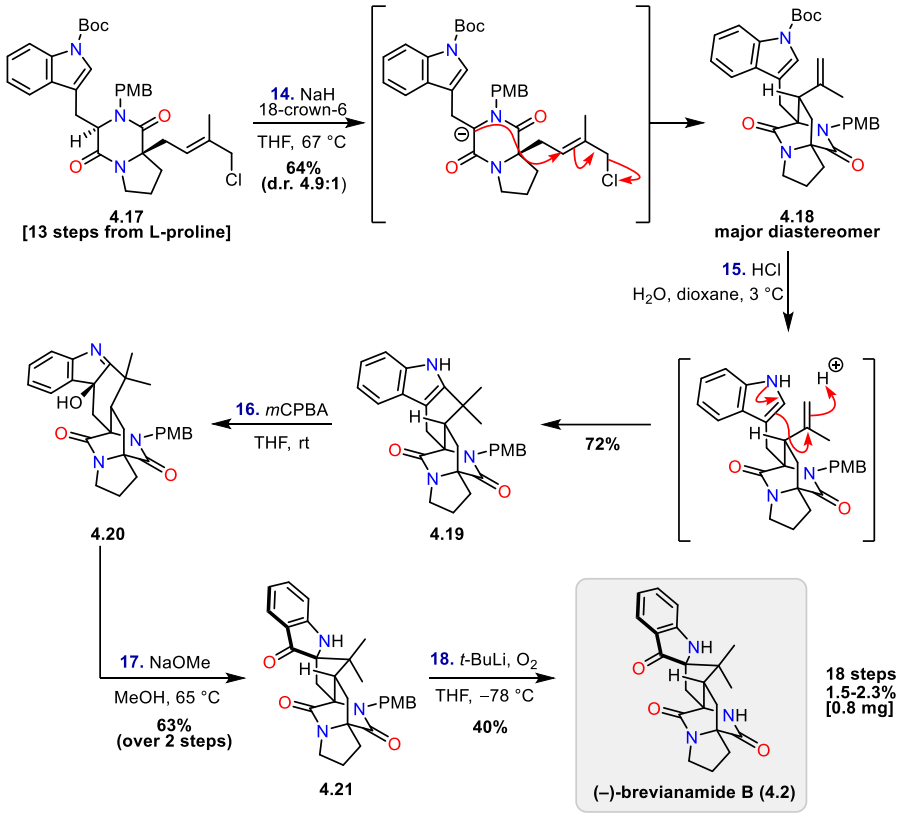

Scheme 4.7: Williams' 1988 synthesis of (–)-brevianamide B (**4.2**)

Their synthesis began from commercially available L-proline (**4.8**), which was converted into the chloro-prenyl-diketopiperazine precursor **4.17** in 13 steps (**Scheme 4.7**). This compound underwent a stereocontrolled S_N2'-cyclisation under basic conditions to form the core bicyclo[2.2.2]diazaoctane scaffold (**4.18**). Williams noted the stereoselectivity of this reaction could be reversed with the exclusion of the 18-crown-6 additive. This effect could be rationalised through the solvent shell surrounding the sodium cation creating a sterically encumbered environment that favours the conformation in which allylic chloride group is directed away. The

major diastereomer (**4.18**) can then undergo the acid-mediated cationic cyclisation and concomitant Boc deprotection to form the fused indole structure **4.19**. Indole oxidation with *m*CPBA favoured the formation of hydroxyindolenine **4.20** as a single diastereomer (convex face of the molecule the same side as the C–H methine of the bridgehead position). Treating **4.20** with sodium methoxide induced a semi pinacol rearrangement to form the indoxyl ring (**4.21**). Finally, PMB deprotection was achieved using *tert*-butyllithium to deprotonate at the benzylic position. The incipient benzylic anion was then quenched with oxygen, which resulted in cleavage of the PMB group, which delivered (–)-brevianamide B (**4.2**) in a total of 18 steps and in an overall yield of 1.5-2.3%. This was the first total synthesis of the unnatural analogue of brevianamide B (**4.2**) and set the benchmark against which future syntheses would be compared. It also marked a challenge for future syntheses as they would have to combat the inherent selectivity of oxidation of indole **4.19** on the convex face of the molecule if they wished to synthesise brevianamide A (**4.1**).

4.3.2 Total Synthesis, (±)-Brevianamide B, Williams 1998

Ten years after their first synthesis, Williams published a second synthesis of (±)-brevianamide B (**4.2**).[143,144] This bioinspired route relied heavily upon Sammes' intramolecular Diels–Alder reaction to form the core bicyclo[2.2.2]diazaoctane motif and was based on Williams' first-generation biosynthetic proposal.[143,145] Williams' first biosynthetic proposal started from deoxybrevianamide E (**4.5**), which is oxidised in a stereoablative manner to afford an achiral azadiene intermediate (**4.22**) (**Scheme 4.8**). Intermediate **4.22** is predicted to undergo the key Sammes-type enantioselective Diels–Alder to form a scalemic mixture of compounds **4.23** and **4.24** with an approximate *e.r.* of 90:10 to account for the observed ratio of the natural products *vide infra*. The resulting enantiomers are each oxidised using an (*R*)-selective indole oxidase to form diasteromers **4.25** and **4.26**. This is followed by a semi-pinacol [1,2] shift to afford a mixture of 'pseudo enantiomers' brevianamide A (**4.1**) and B (**4.2**) in a ratio of approximately 90:10. From the outset Williams' first-generation biosynthetic proposal faced a potential issue as it suggested that the enzymatic oxidation would also have to overcome the innate selectivity observed in their previous synthesis.[140–142]

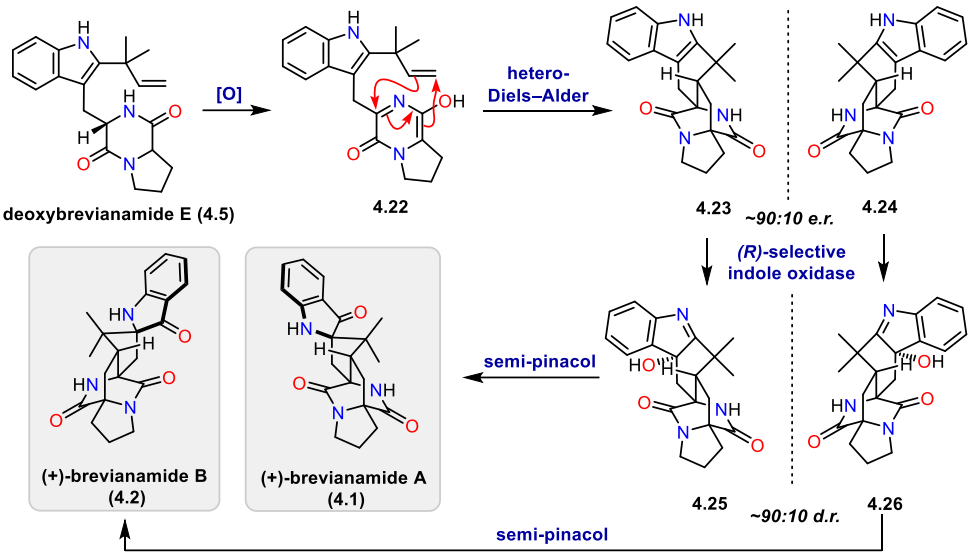

Scheme 4.8: Williams' first generation biosynthetic proposal of brevianamide A (**4.1**) and B (**4.2**), featuring Sammes' intramolecular hetero-Diels–Alder reaction

To probe this chemically, Williams and co-workers involved the compound *epi*-deoxybrevianamide E (**4.27**), which was an intermediate that had previously been synthesised by Kametani and co-workers during a total synthesis of brevianamide E (**4.7**) (**Scheme 4.9**).[146] Following Kametani's published synthesis, Williams formed *epi*-deoxybrevianamide E (±)-(**4.27**), which was converted to the lactim ether (±)-(**4.28**) *via* enol ether formation using trimethyloxonium tetrafluoroborate in 79% yield. The lactim (±)-**4.28** was then oxidised using DDQ to form azadiene (±)-**4.29**. Subjecting the azadiene to basic conditions initiated the intramolecular Diels–Alder reaction to form compound (±)-**4.20** as the minor diastereomer. From here, Williams used the same type of late-stage indole oxidation to give (±)-**4.31** *via* a semi pinacol rearrangement as used in their first synthesis. Finally, treatment with acid deprotected the lactim-ether to furnish (±)-brevianamide B (**4.2**) in 12 steps and an overall yield of 2.8%.

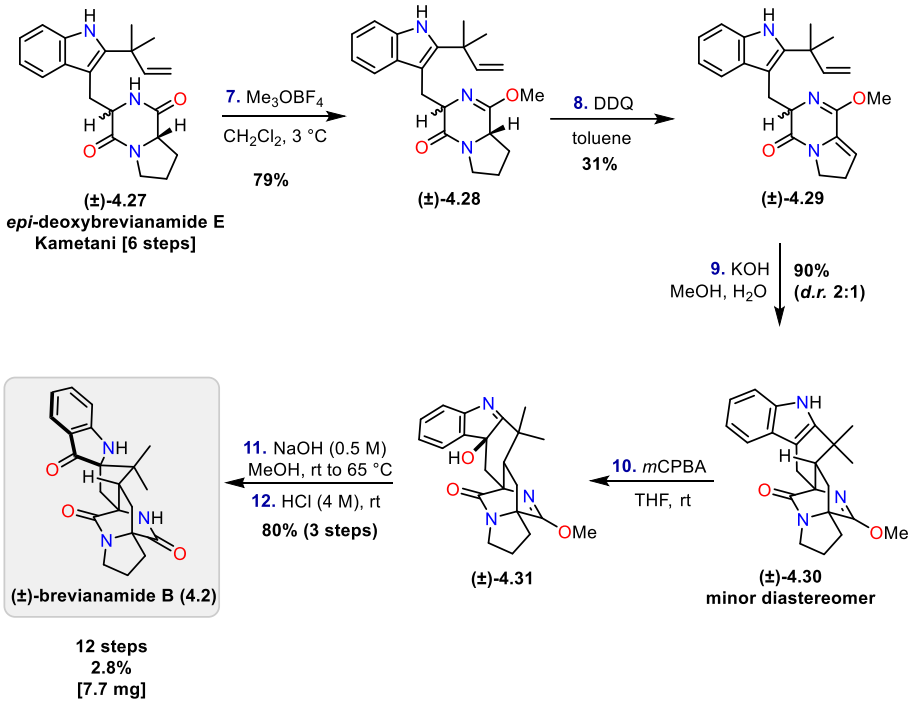

Scheme 4.9: Williams' 1998 biomimetic synthesis of (–)-brevianamide B (**4.2**)

Despite only managing the preparation of racemic material, this bioinspired approach dramatically reduced the previous longest linear step count by six steps. This approach also provided crucial experimental validation for Williams' first-generation biosynthetic proposal. Supporting Sammes' hypothesis that a hetero-Diels–Alder could be responsible for forging the core bicyclo[2.2.2]diazaoctane ring system in nature.[137] However, during the chemical synthesis it was unfortunately revealed that the proposed cycloaddition proceeds in favour of an unwanted diastereomer, therefore suggesting another pathway may be responsible for the biogenesis of brevianamide A (**4.1**). In addition, Williams conducted biosynthetic feeding in which cycloaddition adducts **4.23** and **4.24** were isotopically labelled (**Scheme 4.8**). These experiements failed to indicate incorporation into (+)-brevianamide A (**4.1**)[147] and based on these experimental findings, Williams reassessed his original biosynthetic proposal (*vide infra*).

4.3.3 Total Synthesis, (±)-Brevianamide B, Williams 2006

In 2006, Williams and co-workers published another synthesis of (±)-brevianamide B (**4.2**), again focusing on a bioinspired Sammes' type hetero-Diels–Alder reaction.[148] This was used in combination with a late stage Fischer indole synthesis to construct the indole moiety.

Intermediate **4.32**, which was synthesised in just 7 steps from commercially available 3-methyl-2-buten-1-ol, was heated with aluminium chloride to catalyse an intramolecular Diels–Alder reaction and afford (±)-**4.33** in 48% yield in high diastereoselectivity (**Scheme 4.10**). Fortunately, the Diels–Alder adduct possessed the required *anti*-configured bicyclo[2.2.2]diazaoctane motif, which was evidenced through its eventual conversion to (±)-brevianamide B (**4.2**). To install the indole ring, (±)-**4.33** was converted to the corresponding phenyl hydrazine (±)-**4.34** by heating with molecular sieves and phenylhydrazine. Compound (±)-**4.34** was then ready to undergo the late-stage Fischer indole rearrangement by heating with zinc chloride to afford the fused indole (±)-**4.24**. From here, Williams and co-workers were able to utilise the previously developed conditions of oxidation and subsequent semi-pinacol [1,2]-shift under basic conditions to afford (±)-brevianamide B (**4.2**). This synthesis matched the previous best step count of 12 steps and formed the product in an overall yield of 1.4%.

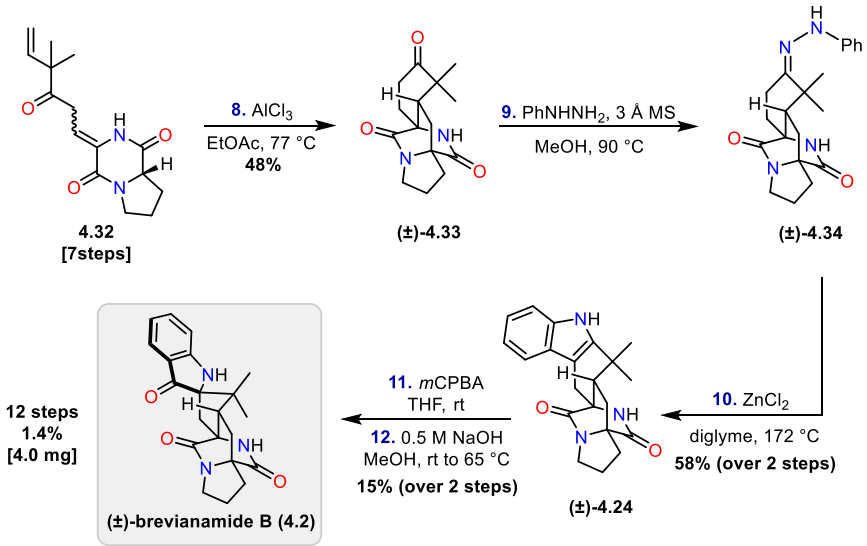

Scheme 4.10: Williams' 2006 synthesis of (±)-brevianamide B (**4.2**) in racemic form

This synthesis offered an innovative new approach for the addition of the indole ring in a late-stage fashion. Interestingly, Williams chose a bioinspired intramolecular Diels–Alder reaction, but opted against the use of the amino acid tryptophan.

4.3.4 Total Synthesis, (±)-Brevianamide B, Williams 2007

In 2007, Williams and co-workers re-examined their biomimetic approach in their fourth synthesis of (±)-brevianamide B (**4.2**).[149,150] This synthesis was based on Williams' modified second-generation biosynthetic proposal, which started from the same intermediate, deoxybrevianamide E (**4.5**) (**Scheme 4.11**). However, this time Williams suggested that an alternative stereoselective indole oxidation of deoxybrevianamide E (**4.5**) would generate hydroxyindolenine **4.35**.[147] This could be followed by a stereospecific semi-pinacol rearrangement of **4.35** to install the key indoxyl ring in intermediate **4.36**. Subsequent oxidation of the diketopiperazine moiety (**4.37**) and hetero Diels–Alder cycloaddition would result in the formation of brevianamide A (**4.1**) and B (**4.2**).

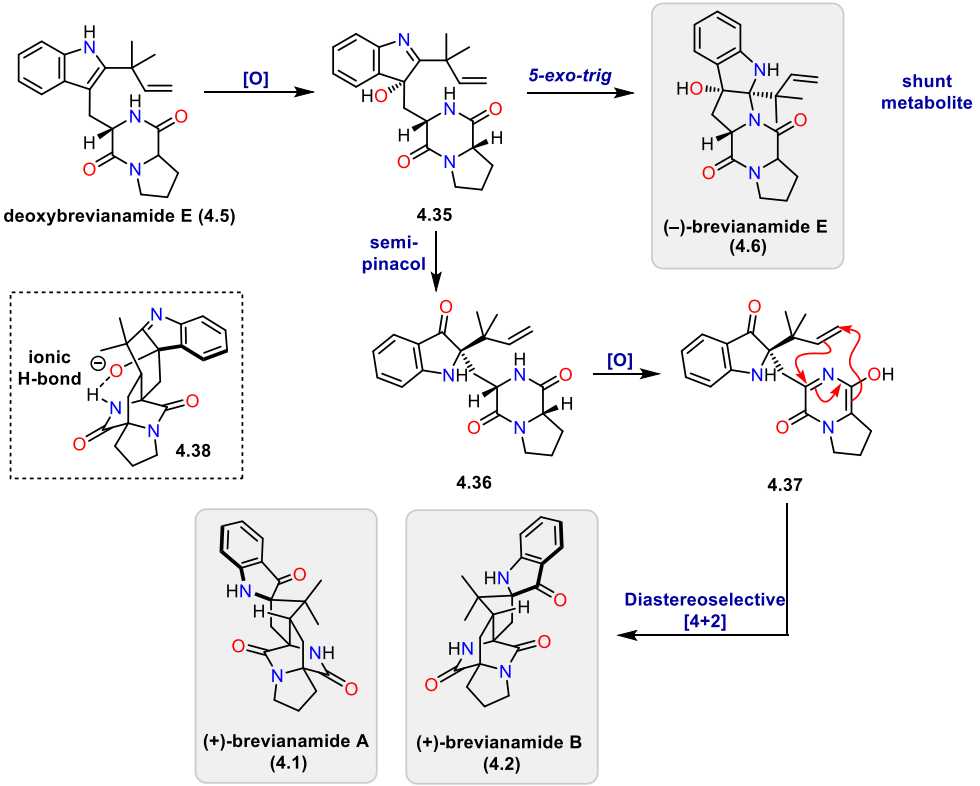

Scheme 4.11: Williams' second generation biosynthetic proposal of brevianamide A (**4.1**) and B (**4.2**), starting from deoxybrevianamide E (**4.5**)

This hypothesis was later supported by computational studies completed by their collaborator Domingo, which revealed the origin of the 90:10 *d.r.* of brevianamide A (**4.1**) to B (**4.2**).[151] Domingo's studies indicated that the assumed cycloaddition favours the formation of brevianamide A (**4.1**) over B (**4.2**) due to a stabilising hydrogen bond (**4.38**), between the indoxyl N–H and the proximal lactam C=O in the transition state towards brevianamide A (**4.1**). To achieve this chemically, Williams started with a coupling of a Boc protected tryptophan intermedaite (±)-**4.39**, accessed in 8 steps from a gramine derivative, with *cis*-3-hydroxyproline ethyl ester salt (**4.40**) in the presence of HATU (**Scheme 4.12**).[147,152] This afforded peptide (±)-**4.41** as a mixture of inseparable epimers in 97% yield. Peptide (±)-**4.41** was treated with acid to reveal the primary amine through Boc removal. Upon heating the primary amine with 2-hydroxypyridine, which is a known catalyst for amide coupling in non-polar solvents, it underwent a spontaneous cyclisation with the pendant ester to form the core diketopiperazine ring ((±)-**4.42**).[153] Warming (±)-**4.42** in the presence of DEAD and *n*-Bu_3P facilitated a Mitsunobu-type dehydration, which allows the key bioinspired intramolecular Diels–Alder reaction to occur. The cycloadducts (±)-**4.43** and (±)-**4.44**, are formed as a 2.1:1 mixture of diastereomers favouring the *syn* adduct ((±)-**4.43**). The minor *anti* configured diastereomer ((±)-**4.44**) was subjected to the well-established method of oxidation/semi-pinacol rearrangement reported by Williams and co-workers in their previous 2006 synthesis of (±)-brevianamide B (**4.2**).[148] Following this route they were able to complete their second biomimetic synthesis of (±)-brevianamide B (**4.2**) in 14 steps in 0.9% overall yield.

This route also facilitated the synthesis of a related natural product, isolated from various *Penicillium* and *Aspergillus* fungi, (±)-dehydrodeoxybrevianamide E (**4.45**).[133,154,155] When the Mitsunobu-type dehydration of indole (±)-**4.42** was performed at room temperature (±)-dehydrodeoxybrevianamide E (**4.45**) was formed in 12 steps with an overall 8% yield.

Manipulation of the Mitsunobu reaction allows for the formation of both (±)-dehydrodeoxybrevianamide E (**4.45**), and an azadiene intermediate capable of performing the subsequent bioinspired Diels–Alder reaction to produce (±)-**4.44**. This suggests that (±)-dehydrodeoxybrevianamide E (**4.45**) is an intermediate formed along the pathway at higher

temperatures. The hypothesis was probed mechanistically by adding LiOH base to (±)-dehydrodeoxybrevianamide E (**4.45**) to afford the cycloadducts in a 2.1:1 mixture of diastereomers (89%). Williams postulated that the zwitterionic complex formed by the nucleophilic addition of *n*-Bu_3P onto DEAD acts as a 'proton chaperone' to initiate the tautomerisation to the azadiene intermediate when the reaction is performed at higher temperatures.

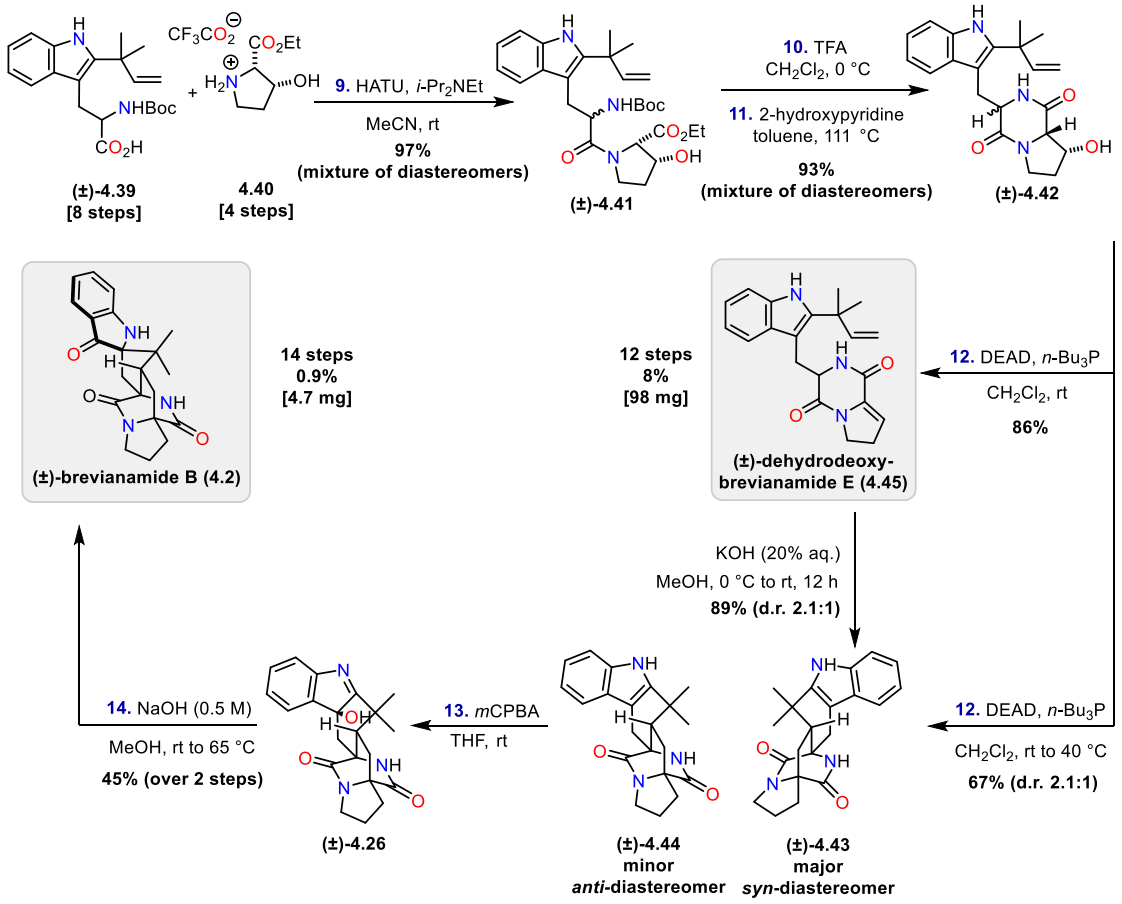

Scheme 4.12: Williams' 2007 biomimetic synthesis of (±)-brevianamide B (**4.2**) and (±)-dehydrodeoxybrevianamide E (**4.45**)

The final steps of Williams' second bioinspired route generate structures of high complexity through an innovative Mitsunobu dehydration/hetero-Diels–Alder domino reaction. However, due to the difficulties in forming the tryptophan coupling partner (8 steps) this synthesis has a larger step-count than Williams' first bioinspired route. This route also represented the first example of an intramolecular Diels–Alder reaction performed with a free hydroxyl group present on the

azadiene. This provides support for the azadiene being a plausible biosynthetic intermediate for the construction of these motifs in nature, without the need for prior conversion to a lactim ether.

However, with regards to Williams second-generation biosynthetic proposal, this synthesis was never able to provide the validation required synthetically, largely due to the inherent instability of the hydroxyindolenine intermediate **4.35**.[125] Experiments later eluded to the preference of hydroxyindolenine **4.35** to form the known shunt metabolite, (–)-brevianamide E (**4.7**), through a *5-exo-trig* cyclisation (**Scheme 4.13**).[156]

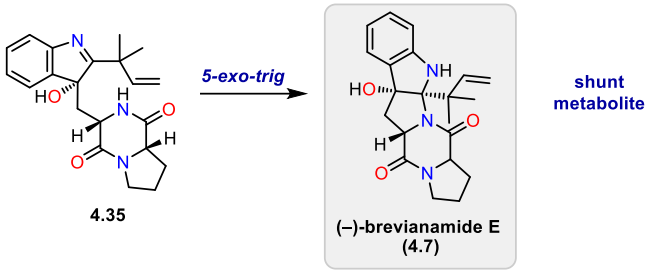

Scheme 4.13: The rearrangement of hydroxyindolenine **4.35** to form brevianamide E (**4.7**)

4.3.5 Total Synthesis, (–)-Brevianamide Y, Williams 2007/2012

The first synthesis of (±)-brevianamide Y (**4.4**) was completed in 14 steps by Williams and co-workers in 2007 (**Scheme 4.14**).[149,150] The synthesis of (±)-brevianamide Y (**4.4**) was a non-target orientated synthesis and was achieved serendipitously while investigating conditions to oxidise (±)-**4.44** to (±)-brevianamide B (**4.2**). Interestingly, Williams' total synthesis of brevianamide Y (**4.4**) was completed before the isolation of the natural product was reported 10 years later by Qi and co-workers in 2017.

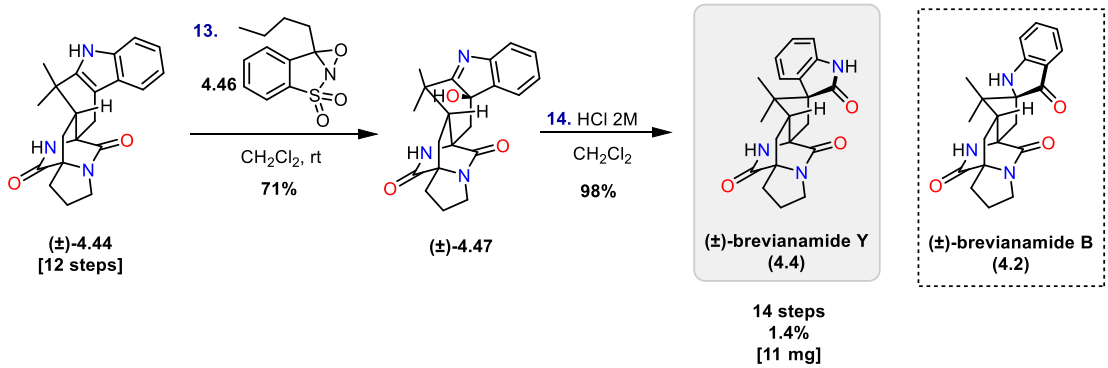

Scheme 4.14: Williams' 2007/2012 synthesis of (–)-brevianamide Y (**4.4**)

Williams used a divergent approach to oxidise indole (±)-**4.44**, which is a common intermediate in the synthesis of brevianamide B (**4.2**) and Y (**4.4**), which was mediated by Davis' oxaziridine (**4.46**) gave hydroxyl-indolenine (±)-**4.47**. This was initially misassigned as brevianamide Y (**4.4**), but later in 2012 this was found to undergo a semi-pinacol [1,2]-shift to give (±)-brevianamide Y (**4.4**) under acidic conditions.[150]

4.3.6 Total Synthesis, (–)-Brevianamide B, Simpkins 2010

The cationic cyclisation approach used in the first total synthesis of brevianamide B (**4.2**) was revisited by Simpkins and co-workers in their total synthesis of enantiopure (–)-brevianamide B (**4.2**).[157,158] Simpkins' synthesis of brevianamide B (**4.2**) was also reported alongside the synthesis of malbrancheamide B and intermediates towards the synthesis of stephacidin A, which are both

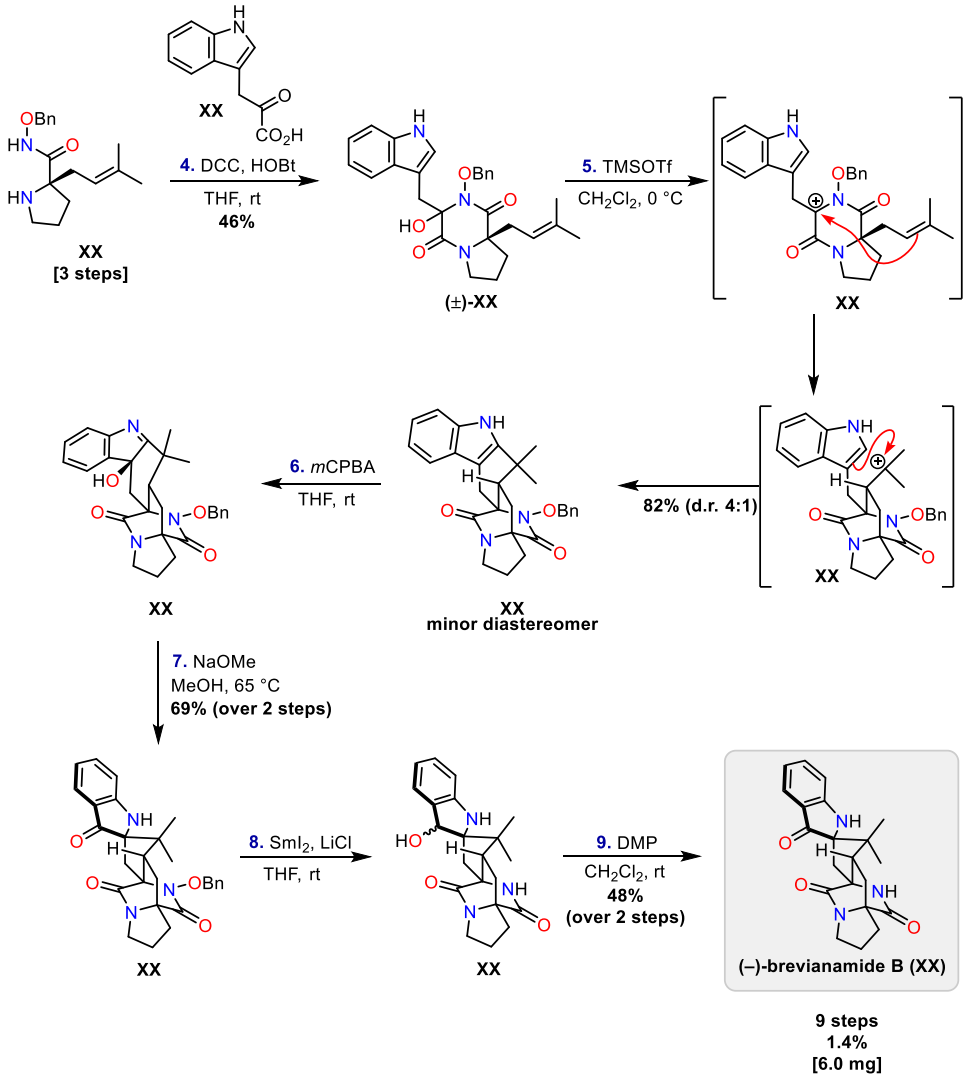

Scheme 4.15: Simpkins' 2010 synthesis of (–)-brevianamide B (**4.2**)

related bicyclo[2.2.2]diazaoctane containing natural products.

The key steps of Simpkins' synthesis commenced with an amide coupling of the commercially available indole pyruvic acid (**4.48**) and *O*-benzyl proline hydroxamic acid (**4.49**) using DCC and HOBt (**Scheme 4.15**). The direct coupling resulted in the core diketopiperazine ring being formed *in situ.* Treatment of the coupled adduct ((±)-**4.50**) with TMSOTf resulted in the desired doubly cyclised product **4.51**. Unfortunately, poor diastereoselectivity was observed in the cyclisation under these conditions, and the undesired C-6 epimer was formed as the major diastereomer in a 4:1 ratio. However, through the formation of the minor diastereomer (**4.51**) this enabled Simpkins to synthesise brevianamide B (**4.2**). Following the precedent established by Williams, they were able to perform the required oxidation and base-mediated semi-pinacol rearrangement to afford indoxyl **4.52**.[140–142] From here, they were able to cleave the N–O bond of the benzyl protecting group with using samarium iodide and lithium chloride. The lithium chloride additive proved vital for the success of the reaction as it activated compound **4.52**, as previously described by Flowers and co-workers.[159,160] Although successful in the deprotection, this protocol had the issue of a concomitant indoxyl reduction to afford compound **4.53**. Oxidation of **4.53** using Dess–Martin periodinane afforded the unnatural enantiomer of brevianamide B (**4.2**). This approach represented a significant improvement at the time, achieving the shortest total synthesis of enantiopure (–)-brevianamide B (4.2) in 9 steps and 1.4% overall yield. Simpkins was able to halve the step count of the previous enantioselective synthesis of Williams' in 1988 (18 steps). Like Williams' route, the inherent diastereoselectivity of the cyclisation (*d.r.* 4:1), ultimately leads to the favoured formation the unnatural enantiomer of brevianamide B (**4.2**). The only deficiency in the method is the need to re-oxidise compound **4.53**, due to chemoselectivity issue in the previous benzyl deprotection step. Simpkins' approach closely follows Williams' original synthesis.[15] The key one-step double cationic cyclisation cascade to form the bicyclo[2.2.2]diazaoctane system bears a high resemblance strategically to Williams S_N2' cyclisation/cationic cyclisation (**Scheme 4.7**). In addition, Williams' protocol to install the indoxyl through an oxidation and semi-pinacol rearrangement was also employed.[16] Throughout the paper, Simpkins' acknowledges and praises

Williams for the impact on this particular synthesis and his broader contributions to the field of brevianamide natural product synthesis.

4.3.7 Total Synthesis, (–)-Brevianamide Y, Qin 2015

In 2015, the unnatural enantiomer of brevianamide Y (**4.4**) was synthesised by Qin and co-workers in 18 steps (**Scheme 4.16**).[161] Once again, this synthesis pre-dated the isolation of brevianamide Y (**4.4**), and was discovered serendipitously while investigating a model study for the structurally related pyrano- natural product (–)-versicolamide B (**4.54**). Their strategy relied upon a late-stage hetero-Diels–Alder reaction and being able to install the carbonyl of the oxindole as the final step. The diastereoselectivity of this Sammes' type Diels–Alder reaction again favoured the formation of the unnatural analogue of (–)-brevianamide B (**4.2**) in 2.2% overall yield. Qin's synthesis also required a number of protecting group manipulations, en route to intermediate **4.55** which impacted the overall step economy of the route.

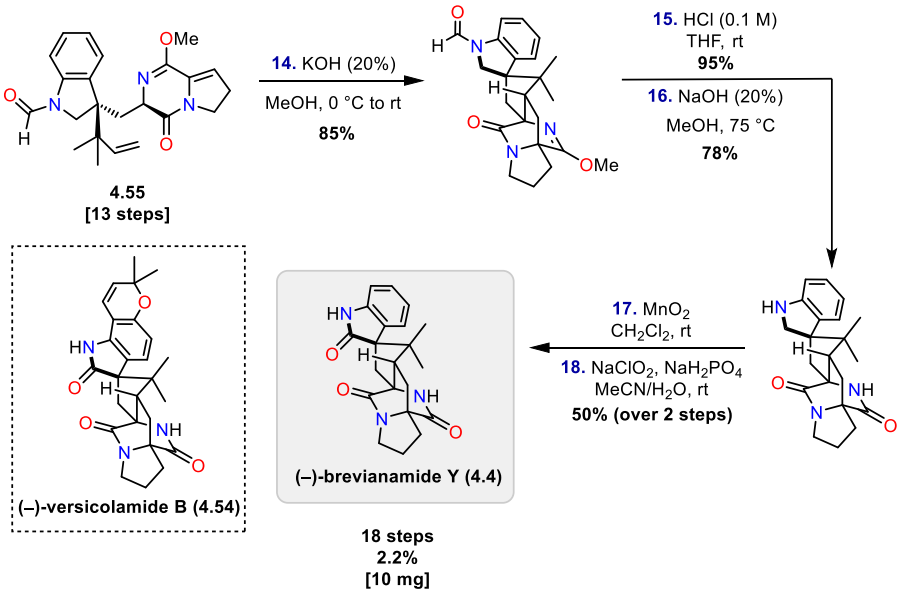

Scheme 4.16: Qin's 2015 synthesis of (–)-brevianamide Y(**4.4**)

4.3.8 Formal Synthesis, (±)-Brevianamide B, Scheerer 2016

In 2016, Scheerer and co-workers published a formal synthesis of (±)-brevianamide B (**4.2**).[162] Strategically, the route centred around an early stage intermolecular Diels–Alder reaction to construct the bicyclo[2.2.2]diazaoctane system. Using this strategy, Scheerer synthesised a well-

established intermediate (**4.44**) towards brevianamide B (**4.2**), to complete a 13 step formal synthesis (**Scheme 4.17**). The intermolecular Diels–Alder route offers a complimentary convergent approach to forming the key bicyclo[2.2.2]diazaoctane scaffold that is competitive in terms of number of steps compared to the traditional intramolecular Diels–Alder method.

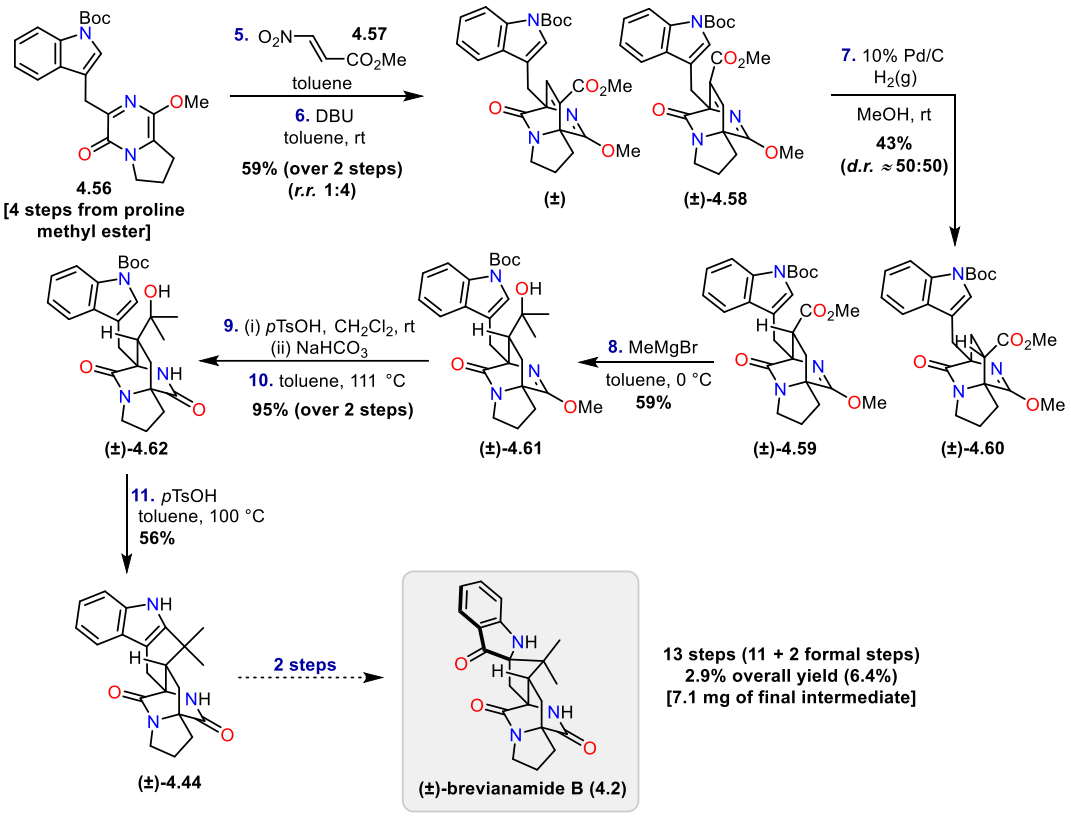

Scheme 4.17: Scheerer's 2016 total synthesis of (±)-brevianamide B (**4.2**)

Scheerer employed pyrazinone **4.56** as the azadiene in the key intermolecular Diels–Alder reaction. Pyrazinone **4.56** was synthesised in four steps from proline methyl ester using protocols previously reported by Scheerer.[163] Interestingly, methyl 2-nitroacrylate (**4.57**) was chosen as the dienophile due to its unique property of reversing the regioselectivity in cycloaddition reactions.[164] The *endo* selective intermolecular Diels–Alder reaction gave a mixture of regioisomers (4:1 isomeric ratio). The dominant cycloadduct possessed the desired regiochemistry, but due to both adducts being inseparable they were carried through to the next step. Elimination with DBU afforded compound (±)-**4.58** in a 59% yield over the two steps. Hydrogenation with palladium on carbon gave both the *anti* configured ester (±)-**4.59** and the corresponding *syn* configured ester in a near equal mixture.

Both diastereomers proved useful intermediates, with the *anti* fused compound ((±)-**4.59**) functioning as a precursor to brevianamide B and the *syn* fused compound (±)-**4.60** leading to an intermediate used by Baran in the total synthesis of other complex natural products.[165]

Towards this end, the *anti* fused ester (±)-**4.59,** was converted to tertiary alcohol (±)-**4.61** through double addition of methyl magnesium bromide. From here the acid hydrolysis of the lactim-ether was performed to afford (±)-**4.62**. Taking inspiration from Williams' first total synthesis of brevianamide B (**4.2**), an acid-mediated cationic cyclisation was performed on (±)-**4.44** as the final step in their synthesis.[140–142] The annulated product (±)-**4.44**, is a common intermediate in Williams' 2006 and 2007 syntheses of brevianamide B (**4.2**), thus completing a formal synthesis of (±)-brevianamide B (**4.2**) in 13 steps (11 steps + 2 formal steps) and a predicted formal yield of 2.9% (6.4% × 45% formal yield).

4.3.9 Formal Synthesis, (±)-Brevianamide B, Scheerer 2017

One year later, Scheerer and co-workers published a follow up paper with another formal synthesis of (±)-brevianamide B (**4.2**), again utilising an intermolecular Diels–Alder reaction to form the key bicyclo[2.2.2]diazoctane system.[166]

Continuing their investigation into the intermolecular Diels–Alder reactions of diketopiperazine diene **4.56**, maleic anhydride was used as an alternative dienophile (**Scheme 4.18**). This cycloaddition with maleic anhydride (**4.63**) proved to be more selective than the analogous reaction with methyl 2-nitroacrylate (**4.57**) featured in their previous synthesis (8:1 *endo vs. exo*) and formed adduct (±)-**4.64** in 58% yield.[162]

A regioselective anhydride ring opening was achieved using lithio benzyl alcohol, followed by an esterification with TMS-diazomethane to afford **(±)-(4.65)**. Selective hydrogenolysis of the benzyl ester on compound **(±)-(4.66)** was achieved using palladium on carbon. The carboxylic acid was then transformed into a new ester (**(±)-(4.67)**) capable of undergoing a radical decarboxylation. The radical decarboxylation was achieved using *N*-hydroxyphthaliminde (NHPI) to form ester **(±)-**(**4.68**) which was decarboxylated using thermally initiated conditions with *t*-butyl thiol and

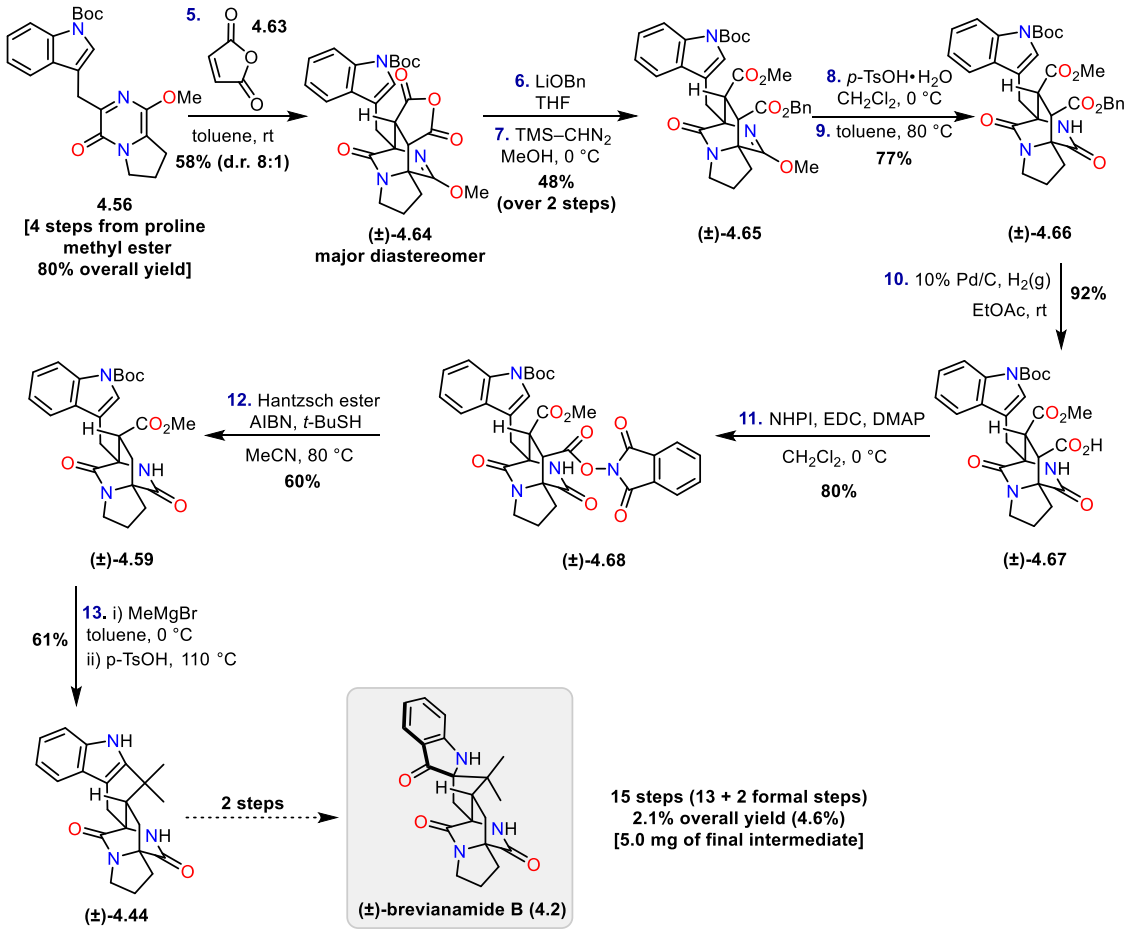

Scheme 4.18: Scheerer's 2017, second formal synthesis of (±)-brevianamide B (**4.2**)

Hantzsch ester.[167] The product of the decarboxylation **(±)-(4.59)** matched their previously synthesised intermediate. From here, Scheerer mirrored his previous synthesis of a Grignard addition and subsequent acidification to allow cationic cyclisation to form the bicyclo[2.2.2]diazaoctane motif (**(±)-4.44**).[162] This again led to the well-known intermediate (**(±)-4.44**) in the synthesis to (±)-brevianamide B (**4.2**), completing Scheerer's second formal synthesis in 15 steps (13 steps + 2 formal steps) and 2.1% (4.6% × 45% formal yield) calculated yield.

This route highlights the potential of another dienophile in the early stage intermolecular Diels–Alder reaction. Unfortunately, in this case there are additional steps required for the difficult anhydride decarboxylation, which resulted in a longer step count for Scheerer's second formal synthesis of (±)-brevianamide B (**4.2**).

4.3.10 Total Synthesis, (+)/(–)-Brevianamide A and B, Lawrence 2020

In 2020, the Lawrence group reported the first total synthesis of (+)-brevianamide A (**4.1**) and the shortest total synthesis of (+)-brevianamide B (**4.2**).[168] Lawrence's biomimetic route was inspired by a modified biosynthetic proposal (**Scheme 4.19**). The unique element of the proposal employed the synthetic intermediate (+)-dehydrodeoxybrevianamide E (**4.45**), which itself is a natural product isolated from *Pencillium* and *Aspergillus* fungi.[133,154,155] The modified hypothesis started with a diastereoselective indole oxidation of (+)-dehydrodeoxybrevianamide (**4.45**) to form dehydrobrevianamide E (**4.69**). As dehydrobrevianamide E (**4.69**) is not a known natural product it was anticipated that, unlike Williams' proposal, this would not represent a dead end.[149] Instead it would furnish hydroxyindolenine **4.70** through a reversible retro *5-exo-trig* ring opening. A stereospecific semi-pinacol rearrangement followed by tautomerisation would afford azadiene intermediate **4.37**, culminating with a substrate controlled *anti*-diastereoselective Sammes-type Diels–Alder reaction to form brevianamide A (**4.1**) and B (**4.2**). By invoking (+)-dehydrodeoxybrevianamide (**4.45**) in the biosynthesis of brevianamide A (**4.1**), it allows for the Sammes type Diels–Alder reaction of the diketopiperazine to occur without the need for any further redox manipulation.

To validate their biosynthetic hypothesis, Lawrence and co-workers began their synthesis with L-tryptophan methyl ester, which was converted to compound **4.72** in two steps (**Scheme 4.20**). Attempts were made to hydrolyse the ester (**4.72**) to form the corresponding carboxylic acid, but under classic base mediated conditions a diacid was formed from a simultaneous phthaloyl ring opening. To circumvent this issue of phthaloyl opening, ester **4.72** was instead converted to lithium carboxylate **4.73** at elevated temperatures in the presence of lithium chloride.[169–171] The lithium carboxylate **4.73** proved to be a suitable coupling partner for the amide coupling reaction with dehydroproline **4.74**. The strategic decision to use a lithium carboxylate as the coupling partner instead of the carboxylic acid also enabled a reduction in step count. As previous routes required the amine protecting group to be altered at this point.[140–142]

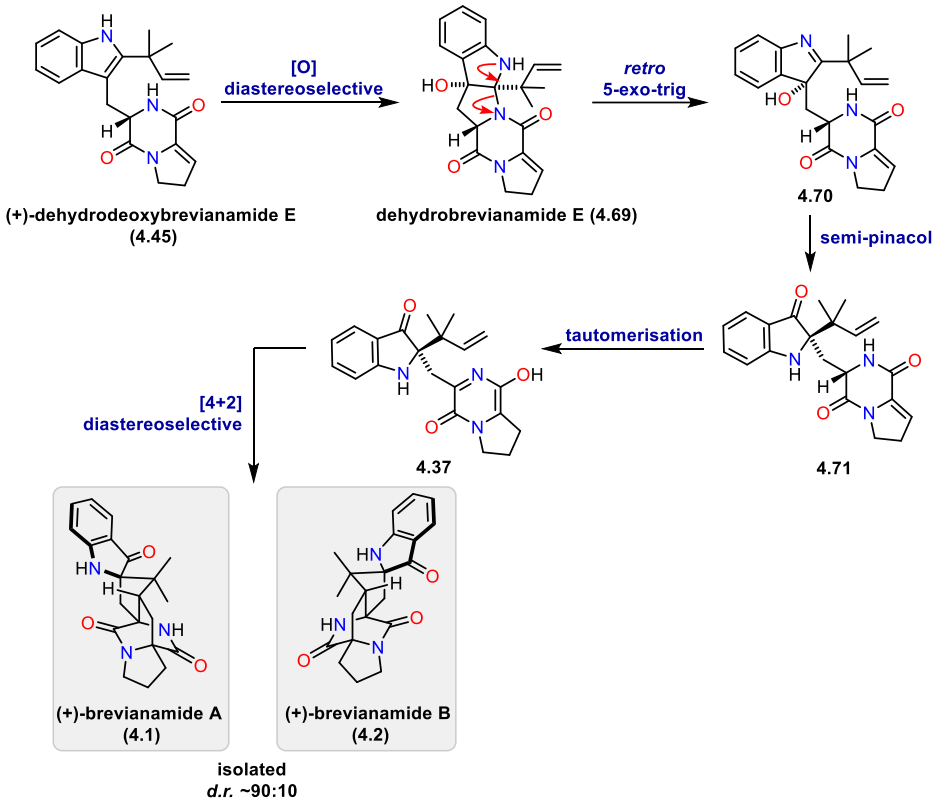

Scheme 4.19: Lawrence's 2020 modified biosynthetic proposal for brevianamide A (**4.1**) and brevianamide B (**4.2**)

The phathloyl group of compound **4.75** was removed with ammonia in methanol to reveal the free amine, which concomitantly condensed with the pendant ester on the five-membered ring to form the core diketopiperazine ring and complete the synthesis of (+)-dehydrodeoxybrevianamide E (**4.45**) in 5 steps. By developing a new imine acylation approach, and avoiding extraneous protecting group manipulations, the step count was less than half the previous step count achieved by Williams (12 steps) of (+)-dehydrodeoxybrevianamide E (**4.45**).[149] (+)-Dehydrodeoxybrevianamide E (**4.45**) was then oxidised in a moderately diastereoselective manner (63:37 *d.r.*) using *m*CPBA. Both diastereomers of dehydrobrevianamide E (**4.69**) were useful as they could be used to achieve the synthesis of both enantiomers of brevianamide A (**4.1**) and B (**4.2**). Dehydrobrevianamide E (**4.69**) was treated with aqueous lithium hydroxide triggering a complex cascade sequence. This concise route provides access to both enantiomers of brevianamide A (**4.1**) and brevianamide B (**4.2**) in 7 steps. The key bioinspired chemical cascade matched the

observed isolation *d.r.* (90:10), for brevianamide A (**4.1**) and B (**4.2**), indicating an enzyme-free substrate controlled Diels–Alder pathway may be responsible for the observed stereoselectivity in nature.[128,129] Lawrence's synthesis was also the first to be performed on a scale that allowed access to comparably large quantities of both brevianamide A (**4.2**) (750 mg) and B (**4.3**) (128 mg) for future biological testing.

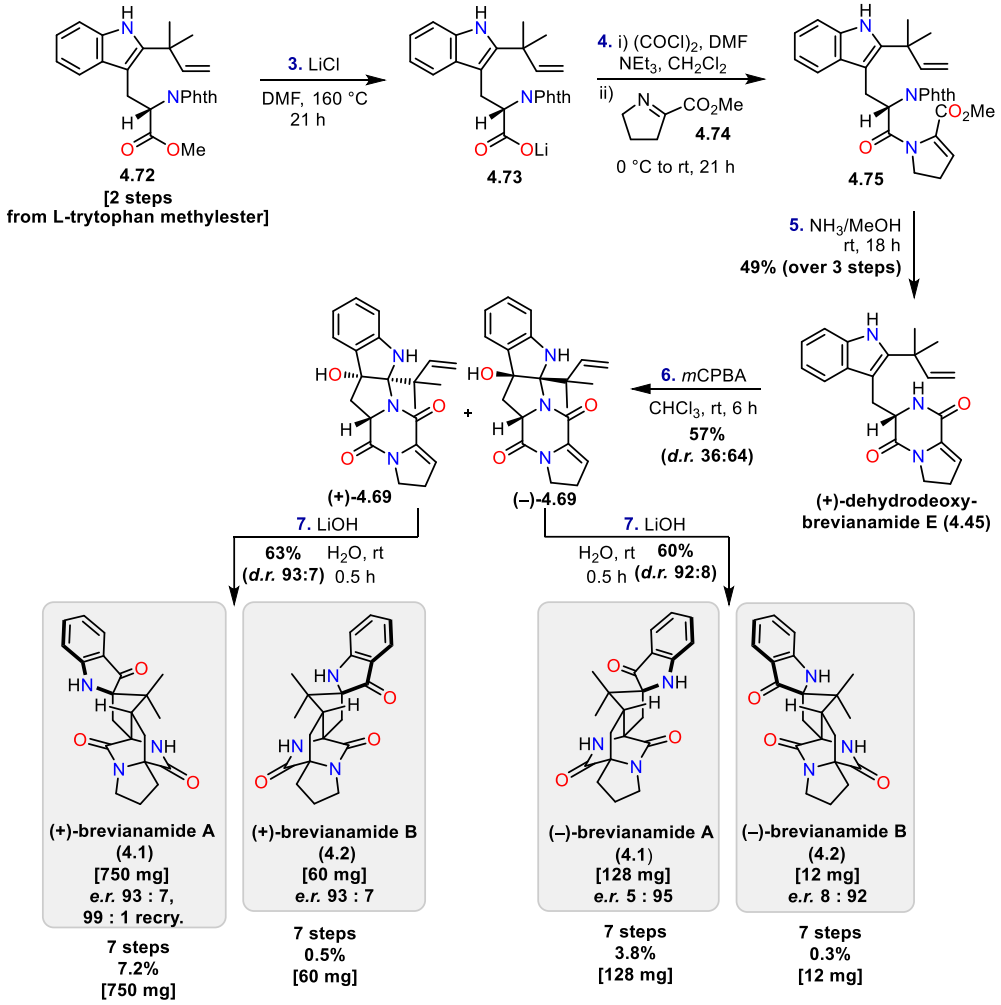

Scheme 4.20: Lawrence's 2020 total synthesis of (+)-dehydrodeoxybrevianamide (**4.45**), (+)/(–)-brevianamide A (**4.1**) and B (**4.2**)

4.3.11 Total Synthesis, (±)-Brevianamide A, Smith 2021

Most recently in 2021, Smith and co-workers developed novel methodology to form 2,2-disubstitued indoxyls from the corresponding C2-substituted indoles.[172] Smith showcases their methodology of a nucleophilic coupling with a 2-alkoxyinoxdyl on a broad range of substituted

indoles. The utility of their approach was highlighted in the synthesis of two natural products; brevianamide A (**4.1**) and trigonoliimine C.[124,173]

Smith's novel approach to brevianamide A (**4.1**), began with intermediate **4.76**, which is formed in four steps from the amino acid L-propargylglycine (**Scheme 4.21**). To form 2-alkoxyindoxyl intermediate **4.77**, indole **4.76** undergoes a MoOPH (oxodiperoxymolybdenum(pyridine) (hexamethylphosphoric triamide) mediated oxidation.[40] This was followed by subsequent treatment with the prenyltributyl stannane which acted as the nucleophilic partner, proceeding smoothly to form the desired 2,2-disubstitued indoxyl (**4.78**) in 45% yield over the two steps. It is important to note, that indoxyl **4.78** was formed as a mixture of diastereomers (*d.r.* 1.2:1) which Smith and co-workers elected not to separate. Therefore, resulting in brevianamide A (**4.2**) eventually being formed racemically, but in principle, separation of the diastereomers could lead to the formation of enatiopure brevianamide A (**4.2**). Using Lawrence's conditions, indoxyl **4.78** was treated with ammonia in methanol to remove the phthaloyl group to free the amine. This subsequently cyclised with the pendant ester to form the diketopiperazine ring (**4.79**). After removal of the solvent and excess ammonia, Smith elected again to follow Lawrence's conditions of aqueous lithium hydroxide to initiate the domino tautomerisation/hetero-Diels–Alder sequence to furnish (±)-brevianamide A (**4.1**) in a 6% overall yield in 7 steps.

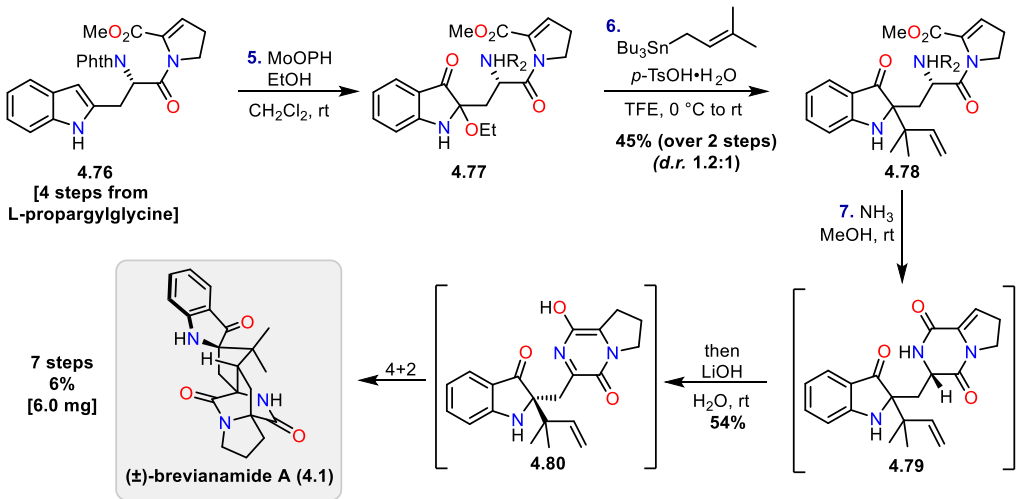

Scheme 4.21: Smith's 2021 total synthesis of (±)-brevianamide A (**4.1**) utilising novel rearrangement of C2 substituted indoles to the corresponding 2,2-disubstitued indoxyls

This impressive and concise total synthesis utilises different methods to not only install the indoxyl, but also the indole ring (JohnPhos cyclisation) and the reverse prenyl group, which are starkly to different the previous literature (See SI). Through this, Smith is able to achieve an impressive step count matching Lawrence and co-workers previous synthesis of enantiopure brevianamide A (**4.1**). However, upon closer inspection Smith and co-workers class going from compound **4.78** to brevianamide A (**4.1**) as a single step. During this process they remove methanolic solvent and excess ammonia through reduced pressure between reactions. The swapping of solvent and removal of excess reagent, could be potentially classed a one-pot two-step reaction.

4.4 Current Understanding of Biosynthesis

Shortly after Lawrence's modified biosynthetic proposal was published, Williams, Li and Sherman reported their identification of the biosynthetic gene cluster (NRRL 864) of brevianamide A (**4.1**).[174] They also discovered that an isomerase/semipinacolase catalysed the essential semi-pinacol rearrangement, which then directed the diastereoselective assembly of brevianamide A (**4.1**) in a spontaneous intramolecular Diels–Alder reaction. This idea of a spontaneous Diels–Aldersase-free cycloaddition supports Lawrence's observations of substrate-controlled stereoselectivity, through the closely matched *d.r.* observed in chemical synthesis and isolation.[168] (For the full synthesis of all the routes dicussed and the synthesis of intermediates see **Appendix 11.2-11.13**)

Chapter 5: Total Synthesis of Brevianamide Y and Brevianamide Z

5.1 Introduction

As introduced earlier (**Section 4.3.5, page 85**), brevianamide Y (**4.4**) was isolated in 2017 by Qi and co-workers from the deep sea fungal strain of *Penicillium brevicompactum*.[132] The first synthesis of (±)-brevianamide Y (**4.4**) was published, 10 years prior to its isolation, in 2007 by Williams and co-workers (**Scheme 5.1**).[149] The synthesis consisted of a longest linear sequence of 14 steps and was a non-targeted synthesis achieved serendipitously while investigating conditions to oxidise (±)-**4.44** to give (±)-brevianamide B (**4.2**). Oxidation of (±)-**4.44**, using Davis' oxaziridine (**4.46**), gave hydroxyindolenine (±)-**4.47**, which was initially misassigned as brevianamide Y (**4.2**). Subsequently, in 2012, indolenine (±)-**4.47** was found to undergo a semi-pinacol [1,2] rearrangement to give (±)-brevianamide Y (**4.2**).[150]

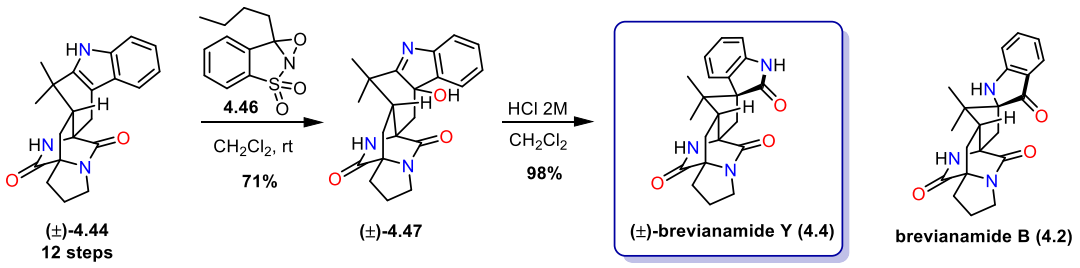

Scheme 5.1: Williams' non targeted synthesis of (±)-brevianamide Y (**4.4**) while trying to synthesise brevianamide B (**4.2**)

A second total synthesis, also published prior to isolation, was reported in 2015 by Qin and co-workers (**Scheme 5.2**).[161] While investigating a model study for the total synthesis of the structurally related natural product (–)-versicolamide B (**4.54**), Qin achieved an 18 step synthesis of (–)-brevianamide Y (**4.4**).

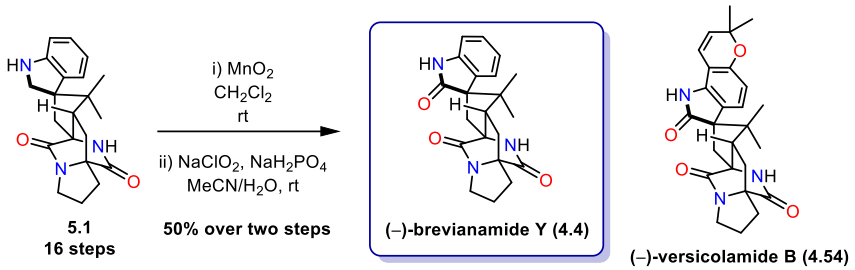

Scheme 5.2: Qin's synthesis of (–)-brevianamide Y (**4.4**) as a simplified analogue of (–)-versicolamide B (**4.54**)

Structurally, brevianamide Y (**4.4**) possess the archetypal bicyclo[2.2.2]diazaoctane system, but differs from brevianamide A (**4.1**) and B (**4.2**), through the inclusion of an oxindole ring instead of an indoxyl ring (**Figure 5.1**).

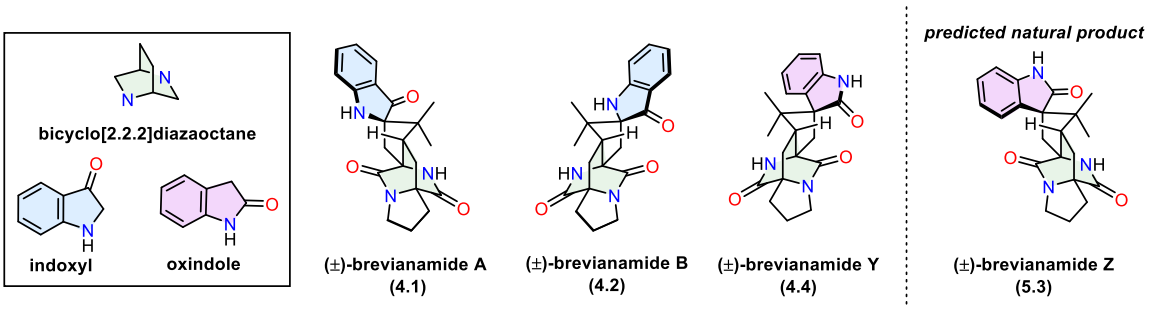

Figure 5.1: Key structural motifs of brevianamide A (**4.1**), B (**4.2**), Y (**4.4**) and Z (**5.3**)

Brevianamide A (**4.1**) and B (**4.2**) are diastereomers. Birch and co-workers confirmed this experimentally *via* chemical interconversion (**Scheme 5.3**).[175] (+)-Brevianamide A (**4.1**) was reduced using sodium borohydride to give deoxybrevianamide A (**5.2**), which spontaneously oxidises in air to afford (–)-brevianamide B (**4.2**), the antipode of the natural product, as confirmed spectroscopically and through polarimetry.[136] Biosynthetically, this relationship is believed to be derived from a late-stage diastereoselective hetero-Diels–Alder reaction, which forms both brevianamide A (**4.1**) and B (**4.2**) in a *d.r.* 90:10.[124,128,129] This diastereoselective hetero-Diels–Alder reaction to form the core bicyclo[2.2.2]diazaoctane system, was initially proposed by Sammes and Porter in 1970 in the biosynthesis of brevianamide A (**4.1**) and B (**4.2**),[137] but is now believed to

extend to the greater bicyclo[2.2.2]diazaoctane family of alkaloids.[176] Therefore, we anticipate that a yet undiscovered natural product exists, which we are naming, brevianamide Z (**5.3**), which is a diastereomer of brevianamide Y (**4.4**).

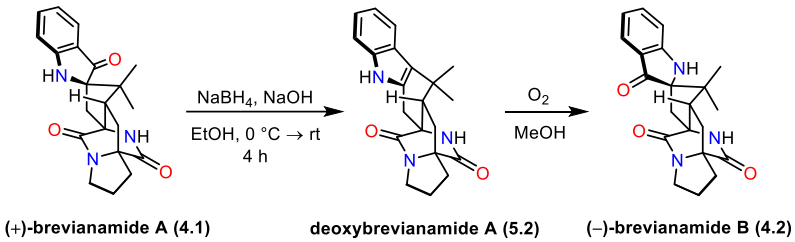

Scheme 5.3: Interconversion by Birch and co-workers between the diasteromers (+)-brevianamide A (**4.1**) and (–)-brevianamide B (**4.2**)

Brevianamide Y (**4.4**) and brevianamide Z (**5.3**) also have the same *anti*-relationship between the methine C–H and proximal piperazine N–H as seen in brevianamide A (**4.1**) and B (**4.2**) (**Figure 5.2**).

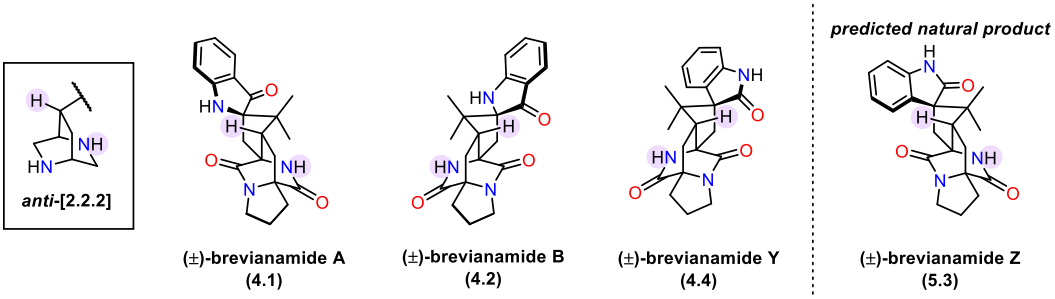

Figure 5.2: Relationship of [2.2.2] ring in brevianamide A (**4.1**), B (**4.2**), Y (**4.4**) and Z (**5.3**)

Recently, our group reported the first total synthesis of (+)-brevianamide A (**4.1**) and the shortest total synthesis to date of its diastereomer (+)-brevianamide B (**4.2**).[168] The unique element of the route employed the synthetic intermediate (+)-dehydrodeoxybrevianamide E (**4.45**), which itself is a natural product isolated from *Pencillium* fungi (**Scheme 5.4**).[154] No previous synthesis has involved the (+)-dehydrodeoxybrevianamide E (**4.45**) intermediate, which is at the correct oxidation level to perform a late-stage hetero-Diels–Alder reaction.

Our group postulated that oxidation of **4.45** to (+)-dehydrobrevianamide E (**4.69**), which when subjected to appropriate reaction conditions could initiate a biomimetic cascade to generate brevianamide A (**4.1**) and brevianamide B (**4.2**). The complex cascade sequence would start with a retro *5-exo-trig* ring opening reaction to form alkoxyindolenine intermediate **5.5**, which would then be followed by a stereospecific semi-pincaol rearrangement to install the required indoxyl ring (**4.71**). Subsequent deprotonation of the diketopiperazine moiety gives *aza* diene **5.6**, which is then set up for a Sammes-type hetero Diels–Alder reaction with the promixal reverse prenyl group to afford brevianamide A (**4.1**) and brevianamide B (**4.2**).

Synthetically, this biosynthetic proposal was achieved through a *m*CPBA mediated oxidation of (+)-dehydrodeoxybrevianamide E (**4.45**) to form (+)-dehydrobrevianamide E (**4.69**). Then treatment of (+)-dehydrobrevianamide E (**4.69**) with lithium hydroxide in water afforded both brevianamide A (**4.1**) and brevianamide B (**4.2**) with a *d.r.* 93:7.

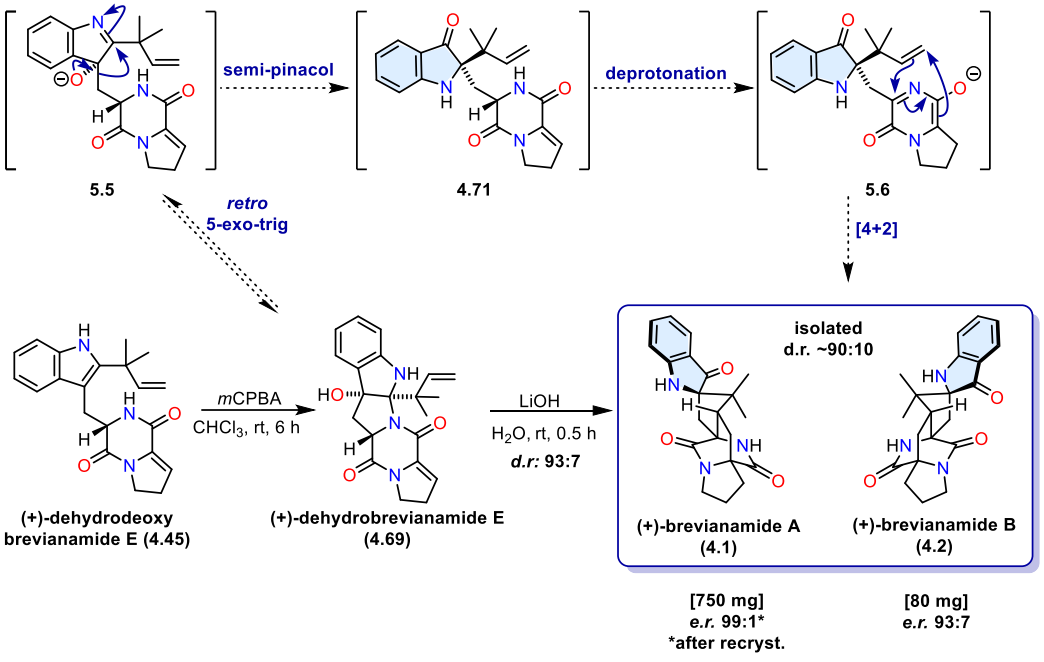

Scheme 5.4: Lawrence's route to (+)-brevianamide A (**4.1**) (+)-brevianamide B (**4.2**) from key intermediate (+)-dehydrodeoxybrevianamide E (**4.45**)

Using the chemistry our group developed for the bioinspired synthesis of brevianamide A (**4.1**) and B (**4.2**), we hoped to modify this to achieve the shortest synthesis of brevianamide Y (**4.4**) and first total synthesis of brevianamide Z (**5.3**). This could be achieved by adapting the oxidation conditions previously used in the transformation of (+)-dehydrodeoxybrevianamide E (**4.45**) to (+)-dehydrobrevianamide E (**4.69**), the use of alternative conditions would trigger a retro *5-exo-trig* ring opening to afford alkoxyindolenine **5.7** (**Scheme 5.5**), *via* a transient epoxide **5.8**. This can again undergo another semi-pinacol rearrangement to form the key oxindole ring (**5.9**). Finally, deprotonation to the *aza*-diene intermediate (**5.10**) would result in a hetero-Diels–Alder reaction with the promixal reverse prenyl group.

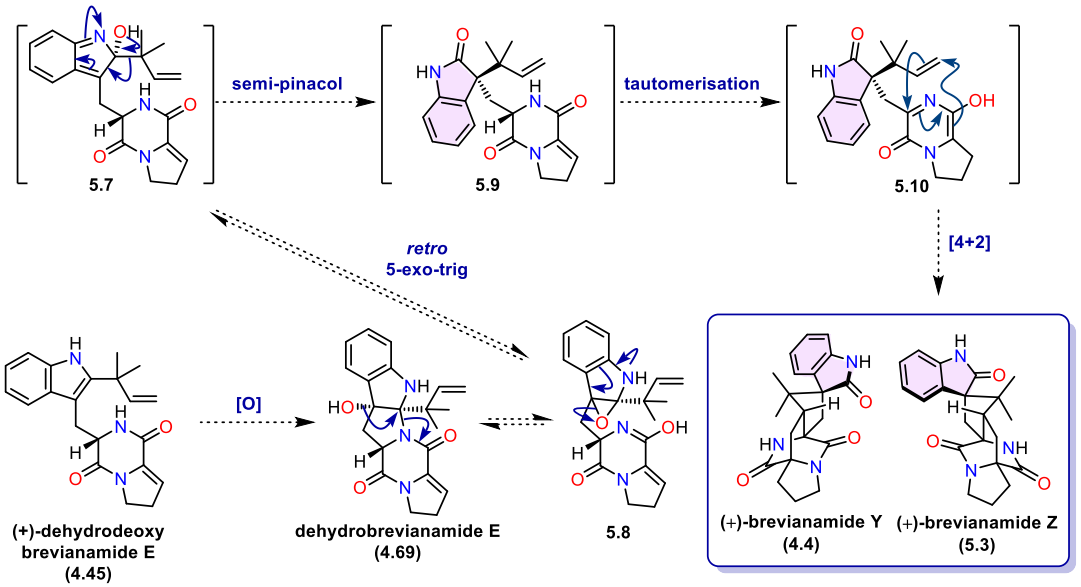

Scheme 5.5: Proposed route to brevianamide Y (**4.4**) brevianamide Z (**5.3**) from key intermediate (+)-dehydrodeoxybrevianamide E (**4.45**)

The key challenge would be favouring the formation of the oxindole moiety instead of the indoxyl ring. These types of transformations where a hydroxyindolenine is rearranged to give an oxindole or indoxyl are well known in the literature, and it is possible to tune the reaction outcome depending on the conditions used.[177] This was demonstrated by Brasholz and co-workers in 2017 by employing different acids in a reagent-controlled 1,2 rearrangement of 3-hydroyindolenines (**Scheme 5.6**).[178]

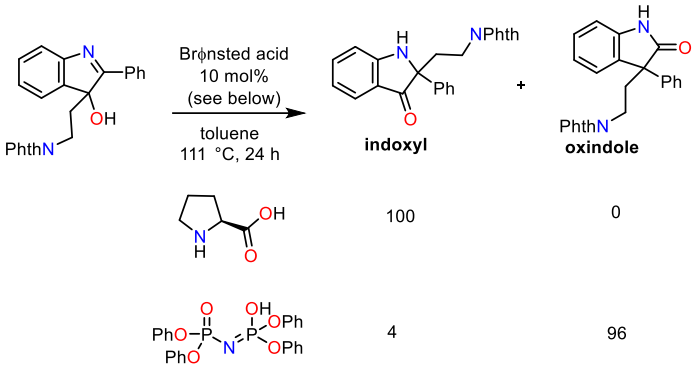

Scheme 5.6: Reagent-controlled 1,2-rearrangement of 3-hydroxoyindolenines to indoxyls and oxindoles

5.2 Results and Discussion: Total synthesis of Brevianamide Y and Z

5.2.1 Synthesis of (+)-Dehydrodeoxybrevianamide E (4.45)

The synthesis of the key (+)-dehydrodeoxybrevianamide E (**4.45**) intermediate in our synthetic strategy began by repeating work conducted by previous group members, Rob Godfrey and Dr Nick Green, during their total synthesis of brevianamide A (**4.1**) and B (**4.2**).[168] When describing this body of work, all yields and scales stated are of reactions I conducted myself. Within this section, I also include improvements I made and further optimisations found while synthesising the common intermediate, (+)-dehydrodeoxybrevianamide E (**4.45**).

The synthesis began with phthaloyl protection of commercially available L-tryptophan methyl ester (**5.11**) (**Scheme 5.7**).[179] This was completed by heating **5.11** to reflux with phthalic anhydride to give the protected compound (**5.12**), which was used without further purification. To install the reverse prenyl group at the C2 of the indole, the reverse prenylation procedure developed by Danishefsky and co-workers was employed.[180] This proceeds *via* oxidation of the indole with *t*--BuOCl to generate a chloro-indolenine intermediate **5.13**. Then freshly prepared *B*-prenyl-9-borabicyclo[3.3.1]nonane (**5.14**) was added slowly at low temperature to induce the transfer of the reverse prenyl group to the C2 position.

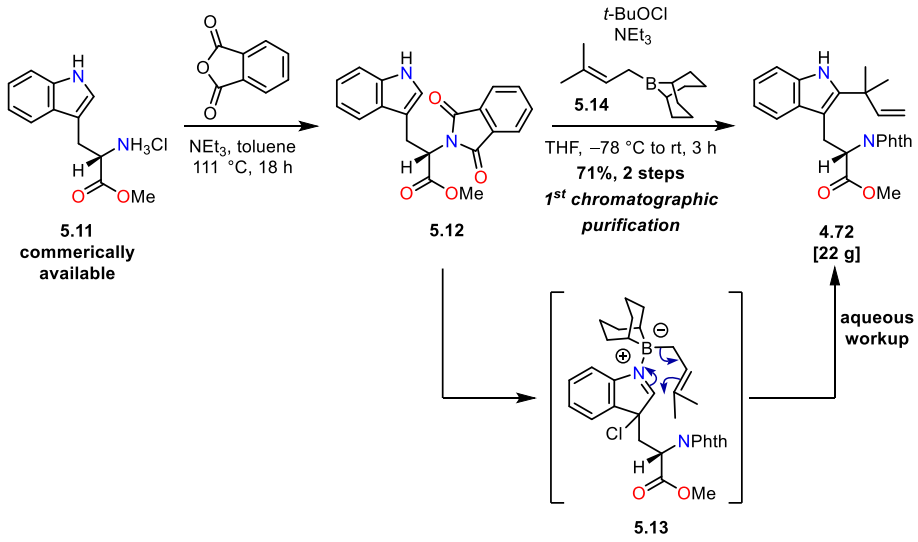

Scheme 5.7: Phthaloyl protection of tryptophan methyl ester **5.11** and then reverse prenylation of **5.12**

The reverse prenylation reaction required the synthesis of both the *B*-prenyl-9-borabicyclo[3.3.1]nonane compound (**5.14**) and *t*-butyl hypochlorite, as they are not commercially available. For the preparation *B*-prenyl-9-borabicyclo[3.3.1]nonane (**5.14**), propargyl alcohol (**5.15**) was added to a pre-cooled vessel of concentrated hydrochloric acid and small portions of anhydrous calcium chloride were added cautiously (**Scheme 5.8**).[181] Rigorous temperature control was found to be crucial for the success of this reaction to form propargyl chloride **5.16**, without it decomposition occurred. Propargyl chloride **5.16**, was then added carefully added to activated zinc to form an organozinc species *in situ*. Following protonation by the solvent, 1,1-dimethylallene (**5.17**) was collected through continuous distillation of the reaction.[181] This allene (**5.17**) was then subjected to hydroboration to give a solution of *B*-prenyl-9-borabicyclo[3.3.1]nonane (**5.14**), which was used directly in the reverse prenylation.[182] This reaction sequence was completed on a larger scale than previously published (123 g vs. 103 g) and through tighter temperature control the yields were improved (59% vs 49% and 82% vs 66%).[168]

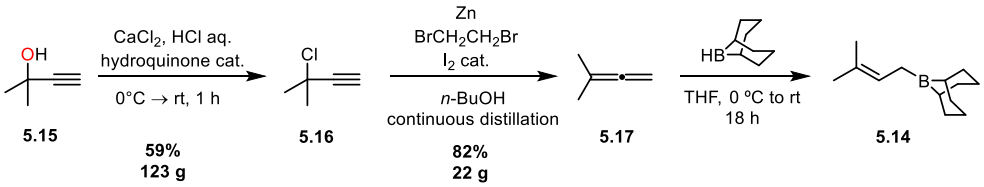

Scheme 5.8: Synthesis of *B*-prenyl-9-borabicyclo[3.3.1]nonane (**5.14**) from propargyl alcohol (**5.15**)

To synthesise *t*-butyl hypochlorite, *tert*-butanol (**5.18**) was added to an acidic solution of sodium hypochlorite (**Scheme 5.9**).[183] This afforded the light and moisture-sensitive hypochlorite, which was stored over calcium chloride in an amber flask and kept in the freezer before use.

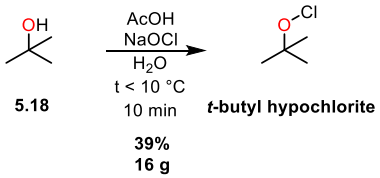

Scheme 5.9: Synthesis of *t*-butyl hypochlorite from *tert*-butanol (**5.18**)

During the initial studies completed by Rob Godfrey, in the synthesis of (+)-dehydrodeoxybrevianamide E (**4.45**), it was found that exposure of the protected tryptophan derivative (**4.72**) to alkaline lithium hydroxide solution resulted in the formation of di-carboxylic acid **5.19** (**Scheme 5.10**). This occurred through the anticipated hydrolysis of the methyl ester accompanied by the unexpected ring opening of the phthalimide ring.[184] Retrospectively, the susceptibility of the phthalimide to base-mediated ring opening explains why previous synthesises of related compounds required a change in amide protecting group at this stage.[185,186] With poor chemoselectivity exhibited under basic hydrolysis conditions, alternative dealkylation conditions were investigated. Fisher and co-workers demonstrated the utility of using lithium halides in the dealkylation of esters.[169,170,171] I was able to use the alternate demethylation approach, using LiCl in DMF, to access lithium carboxylate (**4.73**) in good yield and avoid unnecessary protecting group manipulation.

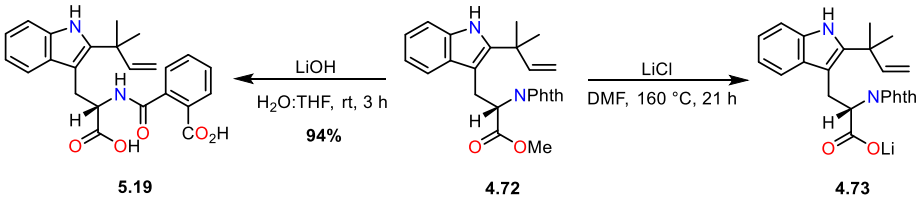

Scheme 5.10: Hydrolysis of ester **4.72** to give dicarboxylic acid **5.19** and demethylation of ester **4.72** to give lithium carboxylate **4.73**

Lithium carboxylate (**4.73**), was then converted to the corresponding acyl chloride (**5.20**) using catalytic dimethylformamide and oxalyl chloride (**Scheme 5.11**).[187,188] This was then coupled with imine **4.74** *in-situ* to give the desired *N*-acyl-enamine (**4.75**).

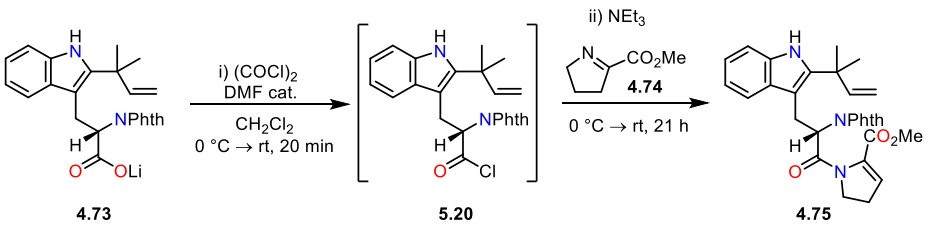

Scheme 5.11: Coupling of imine **4.74** with lithium carboxylate **4.73**

The imine (**4.74**) used in the condensation reaction was formed following a procedure by Schmalz and co-workers (**Scheme 5.12**),[188] using the commercially available proline methyl ester **5.21**, and *N*-chlorosuccinimide. Again, I was able to scale this reaction up and obtained a slightly improved yield compared to the original publication (82% vs 79%).[168]

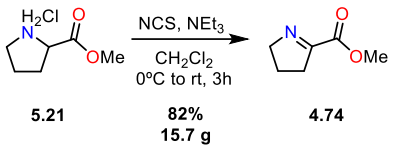

Scheme 5.12: Oxidation of proline methyl ester **5.21** to imine **4.74**

To perform the required deprotection of the amine, the group found the mild conditions of ammonia in methanol worked the best (**Scheme 5.13**). The free amine then concomitantly condensed with the pendant ester on the five membered ring to form the core diketopiperazine ring, which completed the synthesis of (+)-dehydrodeoxybrevianamide E (**4.45**).

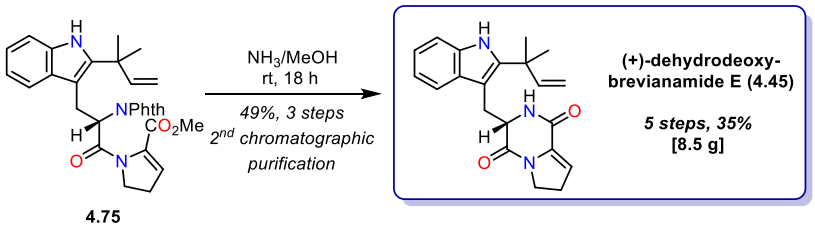

Scheme 5.13: Phthaloyl deprotection of compound **4.75** and subsequent cyclisation to form (+)-dehydrodeoxybrevianamide E (**4.45**)

The synthesis of the key synthetic intermediate (+)-dehydrodeoxybrevianamide E (**4.45**) was thus successfully completed starting from tryptophan methyl ester (**5.11**) in 5 steps with an overall yield of 35%. This procedure was amenable to being conducted on a large scale and only required two chromatographic purifications (**Scheme 5.14**). This total synthesis of (+)-dehydrodeoxybrevianamide E (**4.45**) represents a significant improvement on Williams' previous synthesis of 12 steps and 8% overall yield.[189]

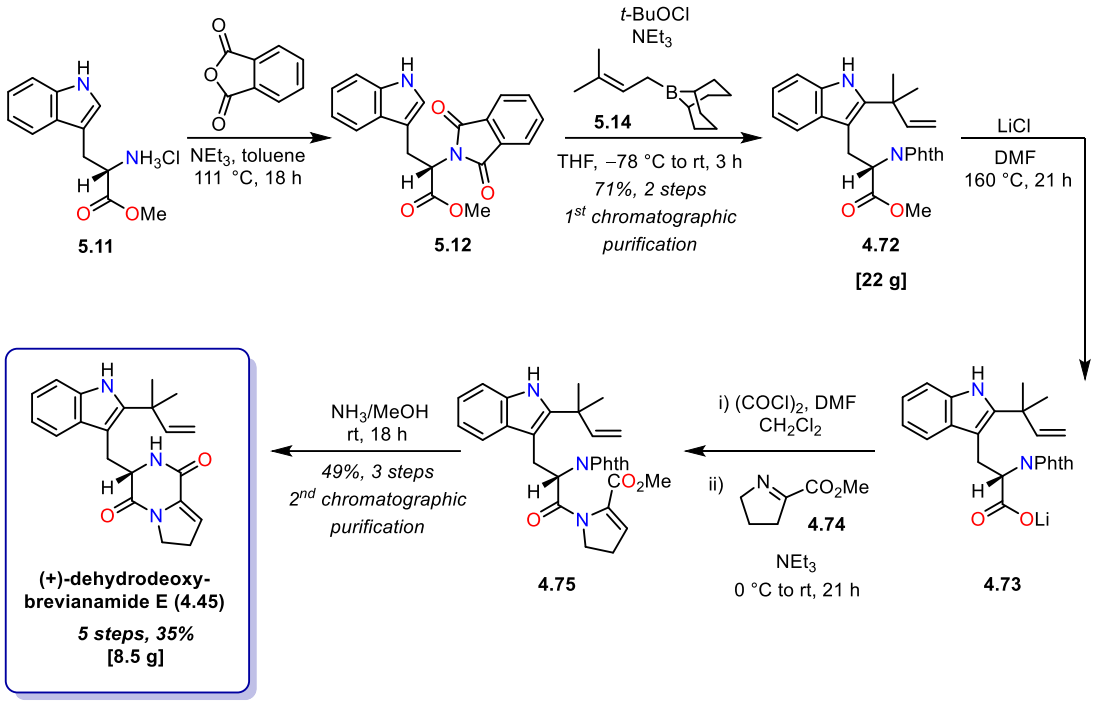

Scheme 5.14: Summary of (+)-dehydrodeoxybrevianamide E (**4.45**) synthesis starting from L-tryptophan methyl ester (**5.11**)

5.2.2 Synthesis of Brevianamide Y (4.4) and Brevianamide Z (5.3)

To test the chemical feasibility of our bioinspired cascade to form brevianamide Y (**4.4**) and brevianamide Z (**5.3**), investigations began with the oxidation of (+)-dehydrodeoxybrevianamide E (**4.45**) to form dehydrobrevianamide E (**4.69**). Using the conditions previously developed by the group in the synthesis of brevianamide A (**4.1**) and brevianamide B (**4.2**), an *m*CPBA oxidation of the indole ring was performed (**Scheme 5.15**).[168] This is believed to proceed through the corresponding transient epoxide (**5.22**), which ring opens through the diketopiperazine nitrogen adding to the C2 position of the indole ring. This successfully gave access to dehydrobrevianamide E (**4.69**) in moderate diastereoselectivity and yield. Sherman, Williams and Tsukamoto demonstrated that in nature the stereoselectivity is tightly controlled through the use of flavin-dependent monooxygenase enzymes.[176] However, having access to both diastereomers would be beneficial for attempting to synthesise both the natural and unnatural enantiomers of brevianamide Y (**4.4**) and brevianamide Z (**5.3**).

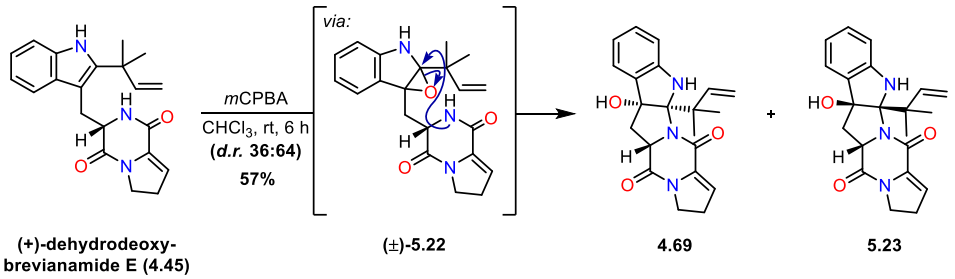

Scheme 5.15: Diastereoselective oxidation of (+)-dehydrodeoxybrevianamide E (**4.45**) to dehydrobrevianamide E **4.69** and **5.23**

As previously mentioned, the rearrangements of 3-hydroxyindolenines to form either oxindoles or indoxyls has been explored under different conditions.[178,190] In addition, the previous syntheses of brevianamide A (**4.1**) and B (**4.2**) by Green and Godfrey found that when dehydrobrevianamide E (**4.69**) and its minor diastereomer (**5.23**) was subjected to the basic conditions of lithium hydroxide this resulted in indoxyl formation (**Scheme 5.16**).[168]

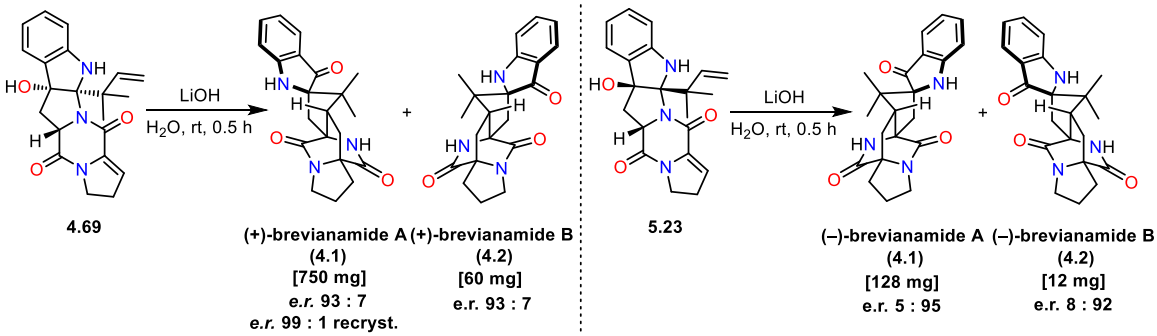

Scheme 5.16: Dehydrobrevianamide E (**4.69**) and its minor diastereomer (**5.23**) treated with lithium hydroxide to form brevianamide A (**4.1**) and brevianamide B (**4.2**)

Therefore, I investigated an alternative acid-mediated rearrangement of hydroxyindolenines **4.69** and **5.23**, in hope of forming the required oxdinoles. This was conducted on NMR scale using compound **4.69** under different conditions and the ratio of product to starting material was monitored (**Table 5.1**). Heating to 65 °C with trifluoroacetic acid in both deuterated methanol and water resulted in full conversion to the desired oxindole product (**5.24**) (**Table 5.1, Entries 1 and**

2). When using *p*-toluenesulfonic acid and hydrochloric acid (**Table 5.1, Entries 2 and 3**) full consumption of starting material was also observed, but the ^{1}H NMR spectrum was a lot more complex, therefore indicating the formation of unknown products through competitive side reactions. Reduced conversion was seen when conducting the reaction in *iso*-propanol (**Table 5.1**, **Entry 5**).

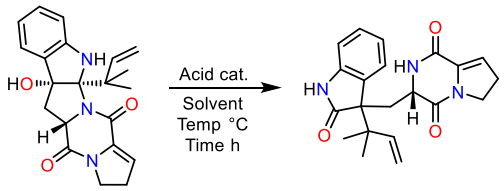

4.69 **5.24**

Entry	Solvent	Acid	Temp (°C)	Time (h)	SM : P ratio*
1	MeOD	TFA	65	72	0:100
2	MeOD	PTSA	65	24	0:100 ^
3	MeOD	HCl (2 M)	65	24	0:100 ^
4	H_2O	TFA	65	24	0:100
5	IPA	TFA	83	24	6:94

Table 5.1: Conditions screened for the acid mediated semi pinacol [1,2]-shift of hydroxyindolenine **4.69** to oxdinole **5.24**. *ratios calculated through ^{1}H NMR spectroscopy. ^Complex mixture of unidentified products

Using this information, both diastereomers of dehydrobrevianamide E (**4.69** and **5.23**) were heated with trifluoroacetic acid in water, which resulted in the formation of the desired oxindole products **5.24** and **5.25** respectively, albeit in low isolated yields (**Scheme 5.17**). The configuration of the oxindole products (**5.24-5.25**) was assumed at this stage, but we were able to indirectly confirm this later in the synthesis.

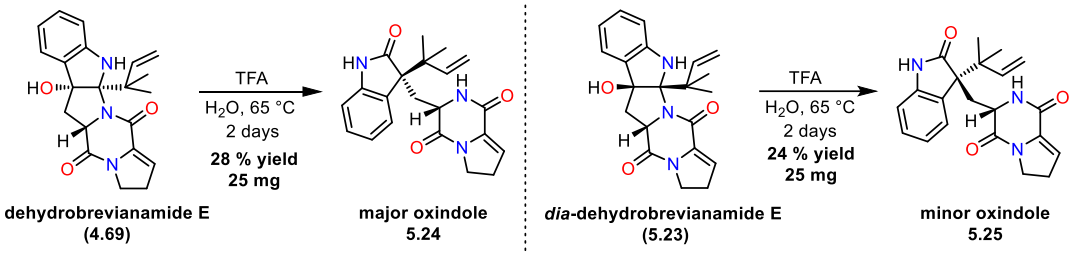

Scheme 5.17: Acid mediated rearrangement of both dehydrobrevianamide E (**4.69**) and *dia*-dehydrobrevianamide E (**5.23**) to the corresponding oxindoles (**5.24** and **5.25**)

After extensive experimentation it was later found by Dr Nick Green, that these two reactions could be telescoped together by employing an *N*-chlorosuccinimide oxidation with catalytic trifluoroacetic acid to (+)-dehydrodeoxybrevianamide E (**4.45**) (**Scheme 5.18**). To our delight, this was not only more step economic, but also greatly improved the yield of the transformation and slightly improved the diastereoselectivity of the reaction. When I conducted this reaction on a 500 mg scale I obtained and separated both diastereomers in 83% yield (combined yield of both diastereomers) with a *d.r.* 31:69.

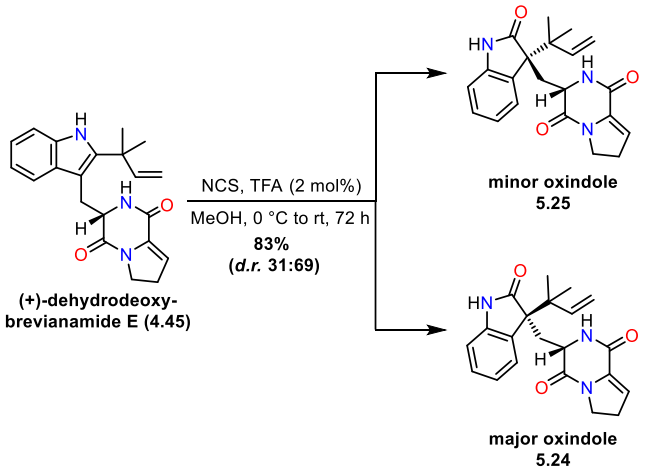

Scheme 5.18: One pot procedure for the diastereoselective oxidation and rearrangement of (+)-dehydrodeoxybrevianamide E (**4.45**) to oxindoles **5.24** and **5.25**

With access to both diasteromers of the oxindole intermediate (**5.24** and **5.25**) investigation began into conditions that could initiate the domino tautomerisation/hetero Diels–Alder reaction. Initially,

I attempted the rearrangement/hetero Diels–Alder reaction using Williams' base-mediated approach with potassium hydroxide (**Scheme 5.19**).[149] This reaction was performed on NMR scale and I noted the formation of peaks in the ^{1}H NMR spectrum corresponding to brevianamide Y (**4.4**). This was accompanied by lots of unknown peaks present in the ^{1}H NMR spectrum.

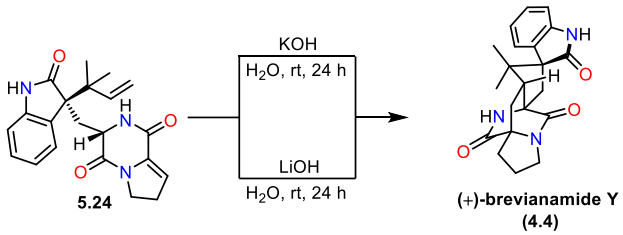

Scheme 5.19: Conditions trialled for rearrangement/hetero Diels–Alder of oxindole **5.24**

In the synthesis of brevianamide A (**4.1**) and brevianamide B (**4.2**) developed by the group, it was discovered that lithium hydroxide was able to induce a cascade that finished with a similar domino tautomerisation/hetero Diels–Alder (**Scheme 5.20**).[168] Subjecting oxindole **5.24** to the same lithium hydroxide conditions resulted in a cleaner ^{1}H NMR spectrum of brevianamide Y (**4.4**) being produced and full consumption of starting material (**5.24**).

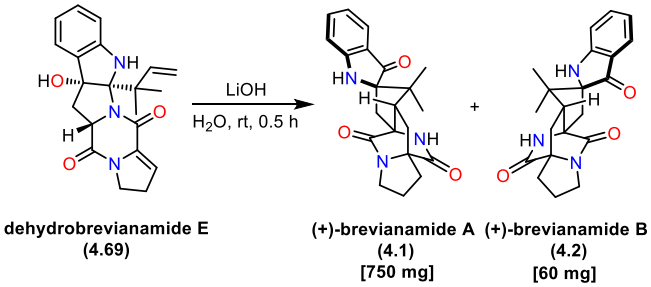

Scheme 5.20: Cascade reaction of dehydrobrevianamide E (**4.69**) under lithium hydroxide to form (+)-brevianamide A (**4.1**) and (+)-brevianamide B (**4.1**)

Finally, in order to determine the correct length of reaction, parallel reactions were run. Through use of ^{1}H NMR spectroscopy I was able to monitor the ratio of oxindole (**5.24**) starting material to (+)-brevianamide Y (**4.4**) product (**Figure 5.3**). The doublet at 7.42 ppm corresponds to (+)-brevianamide Y (**4.4**) and the doublet at 7.38 ppm corresponds oxindole (**5.24**). Reactions were run at two-hour intervals until consumption of starting material was observed. This occurred when the reaction was left to stir for eight hours at room temperature.

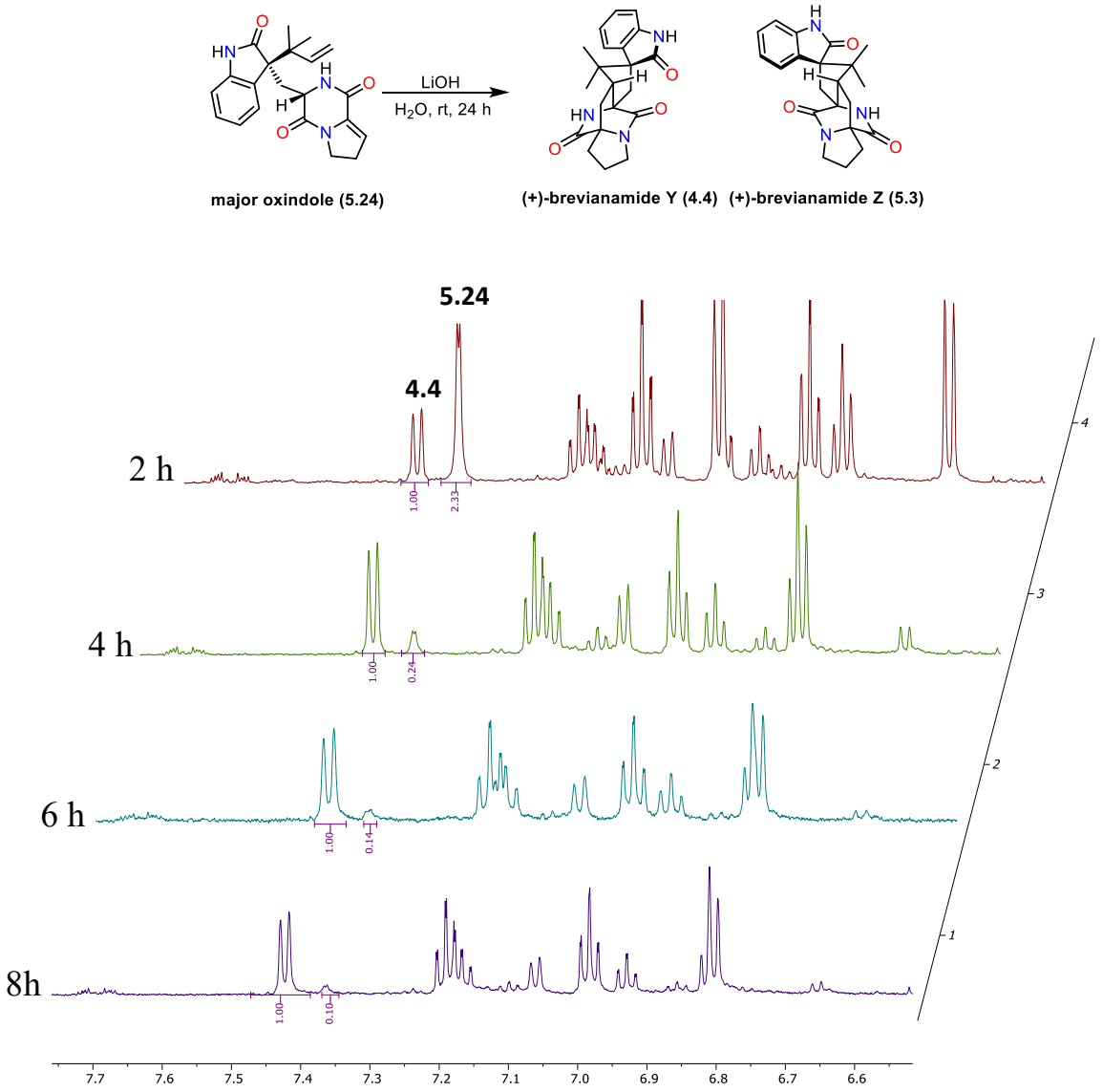

Figure 5.3: Effect of varying reaction length on the ratio of starting material (**5.24**) to product (+)-brevianamide Y (**4.4**) as observed by ^{1}H NMR spectroscopy (600 MHz, $CDCl_3$)

Using the knowledge acquired from this initial screen, we were able to scale up the domino tautomerisation and Diels–Alder reaction using the optimised conditions (**Scheme 5.21**). Oxindoles **5.24** and **5.25** were treated with aqueous lithium hydroxide at room temperature and left to stir for 8 hours. This resulted in the formation of (+)-brevianamide Y (**4.4**) and (+)-brevianamide Z (**5.3**)

from the major oxindole (**5.24**) and (–)-brevianamide Y (**4.4**) and (–)-brevianamide Z (**5.3**) from the minor oxindole (**5.25**).

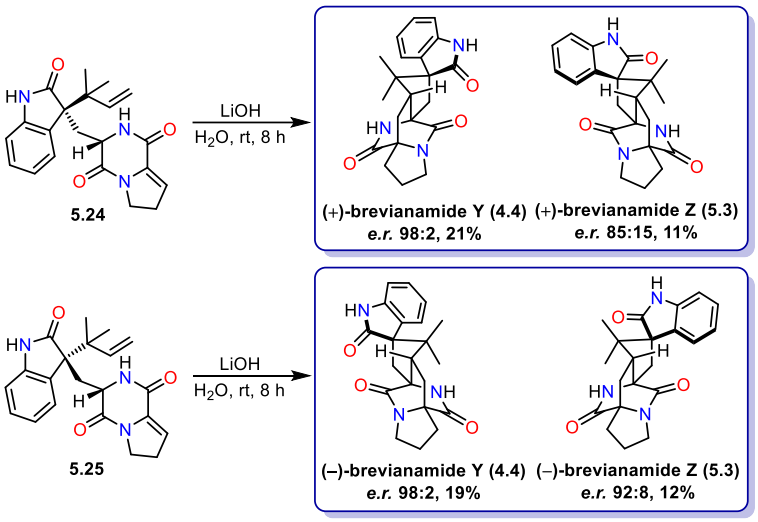

Scheme 5.21: Base mediated tautomerisation and hetero Diels–Alder of oxindoles **5.24** and **5.25** to form brevianamide Y (**4.4**) and brevianamide Z (**5.3**)

From this set of experiments I was able to get full characterisation data for each enantiomer of brevianamide Y (**4.4**) and brevianamide Z (**5.3**), including developing chiral HPLC assays. The optical rotations of each natural product were measured, which aided in the indirect assignment of the absolute stereochemistry of the major (**5.24**) and minor (**5.25**) oxindoles. The measured optical rotation and circular dichromism values were consistent with the isolation papers values and the recorded by Qi and co-workers.[132]

Through recrystalisation, an X-ray crystal structure of brevianamide Y (**4.4**) was acquired (**Figure 5.4**). The crystal structure of brevianamide Y (**4.4**) was found to be centrosymmetric suggesting the sample had somehow racemised upon crystallisation.

Further analysis of chiral HPLC samples were run of both the prism crystals and the mother liquor of the recrystallisation to determine the *e.r's.* Interestingly, it was found that upon crystallisation resulted in an increase in *e.r* of the sample remaining in the mother liquor (98:2 from 95:5), and the crystals were racemic (**Figure 5.5**). This is presumably a due to the original enantioenriched sample

not being entirely enantiopure, and the minor impurity co-crystallises out to yield the 1:1 racemic crystal.

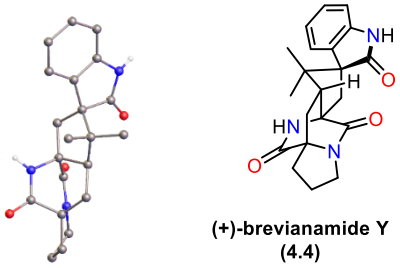

Figure 5.4: X-ray crystal structure of (±)-brevianamide Y (**4.4**)

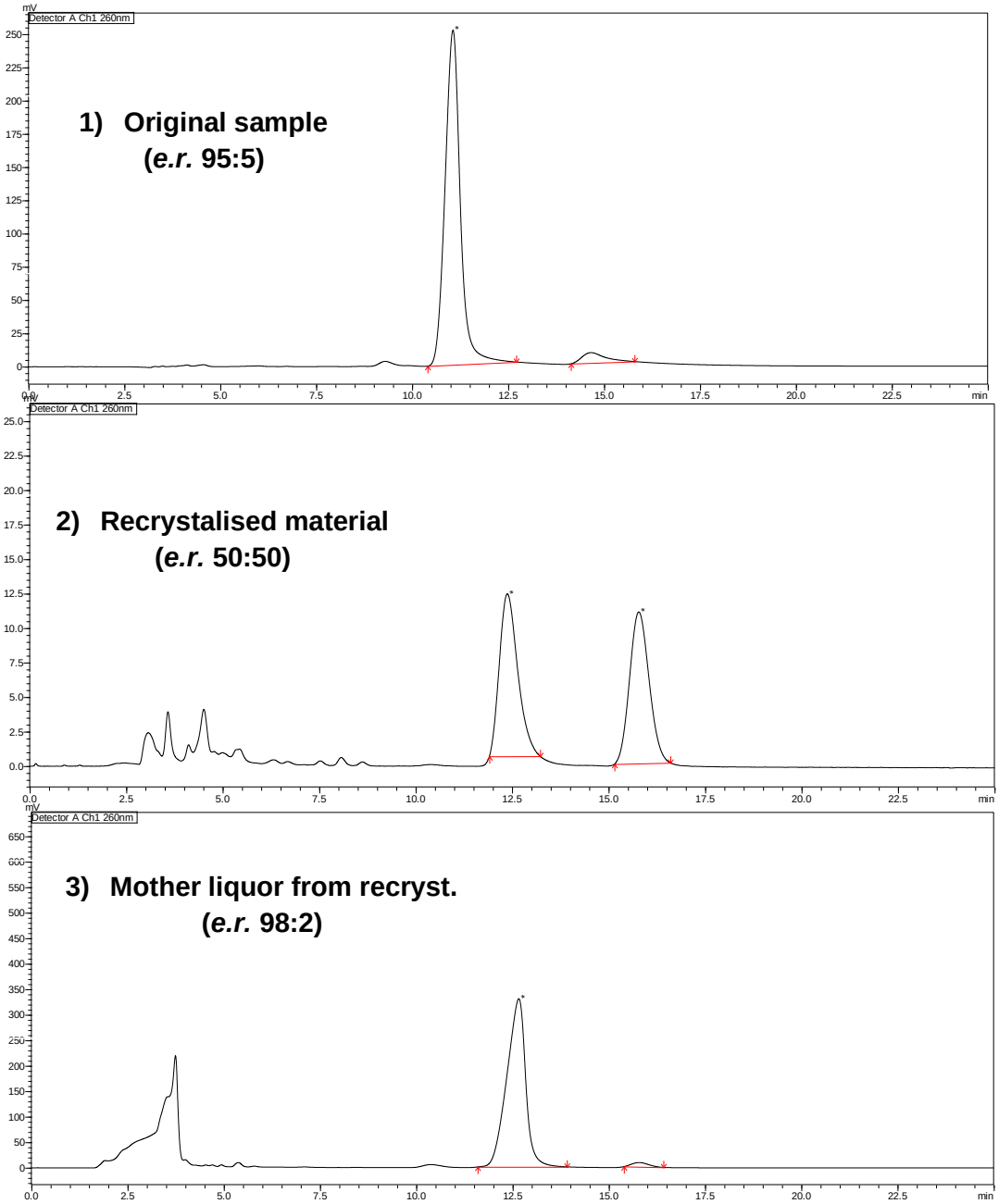

Figure 5.5: Chiral HPLC traces 1) (+)-brevianamide Y (**4.4**) before recrystallisation 2) mother liquor after recrystallisation 3) the crystals after recrystallisation. Chiralpak IC, 42:58 EtOH/hexane, 1.0 mL min^{-1}, λ 254 nm

Overall, this completed our synthesis of both enantiomers of brevianamide Y (**4.4**), with a longest linear sequence of seven steps, which was less than half the step count of Qin's previous targeted synthesis (18 steps) of (–)-brevianamide Y (**4.4**) (**Scheme 5.22**). [149,150] Alongside this, the first total synthesis of brevianamide Z (**5.3**) has been achieved in seven steps and a 2.1% overall yield.

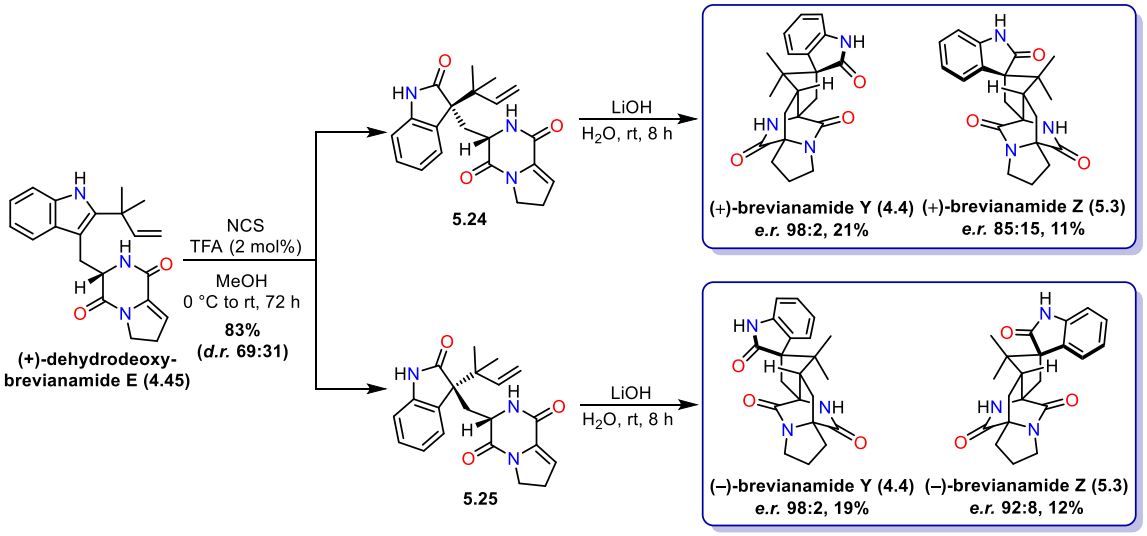

Scheme 5.22: Final steps in the synthesis of both enantiomers of brevianamide Y (**4.4**) and brevianamide Z (**5.3**) starting from (+)-dehydrodeoxybrevianamide E (**4.45**)

5.3 Conclusion

During the course of this project, the shortest total synthesis of both enantiomers of brevianamide Y (**4.4**) and the first total synthesis of both enantiomers of brevianamide Z (**5.3**) was successfully achieved (**Scheme 5.23**). This was accomplished through a bioinspired strategy starting from the commercially available L-tryptophan methyl ester (**5.11**), forming brevianamide Y (**4.4**) and brevianamide Z (**5.3**) in seven steps with just four chromatographic purifications. The key steps of the synthesis relied upon the selective rearrangements of an alkoxyindolenine intermediates to the corresponding oxindoles (**5.24** and **5.25**), followed by a base-mediated tautomerisation/hetero-Diels–Alder reaction sequence to form both enantiomers brevianamide Y (**4.4**) and brevianamide Z (**5.3**).

Brevianamide Z (**5.3**) is of interest as we believe it to be a natural product that is yet to be isolated. As it bares the same structural relationship to brevianamide Y (**4.4**) as brevianamide B (**4.2**) does to brevianamide A (**4.1**). With the full characterisation data now available from this synthesis, this may help direct future isolation studies to find brevianamide Z (**5.3**).

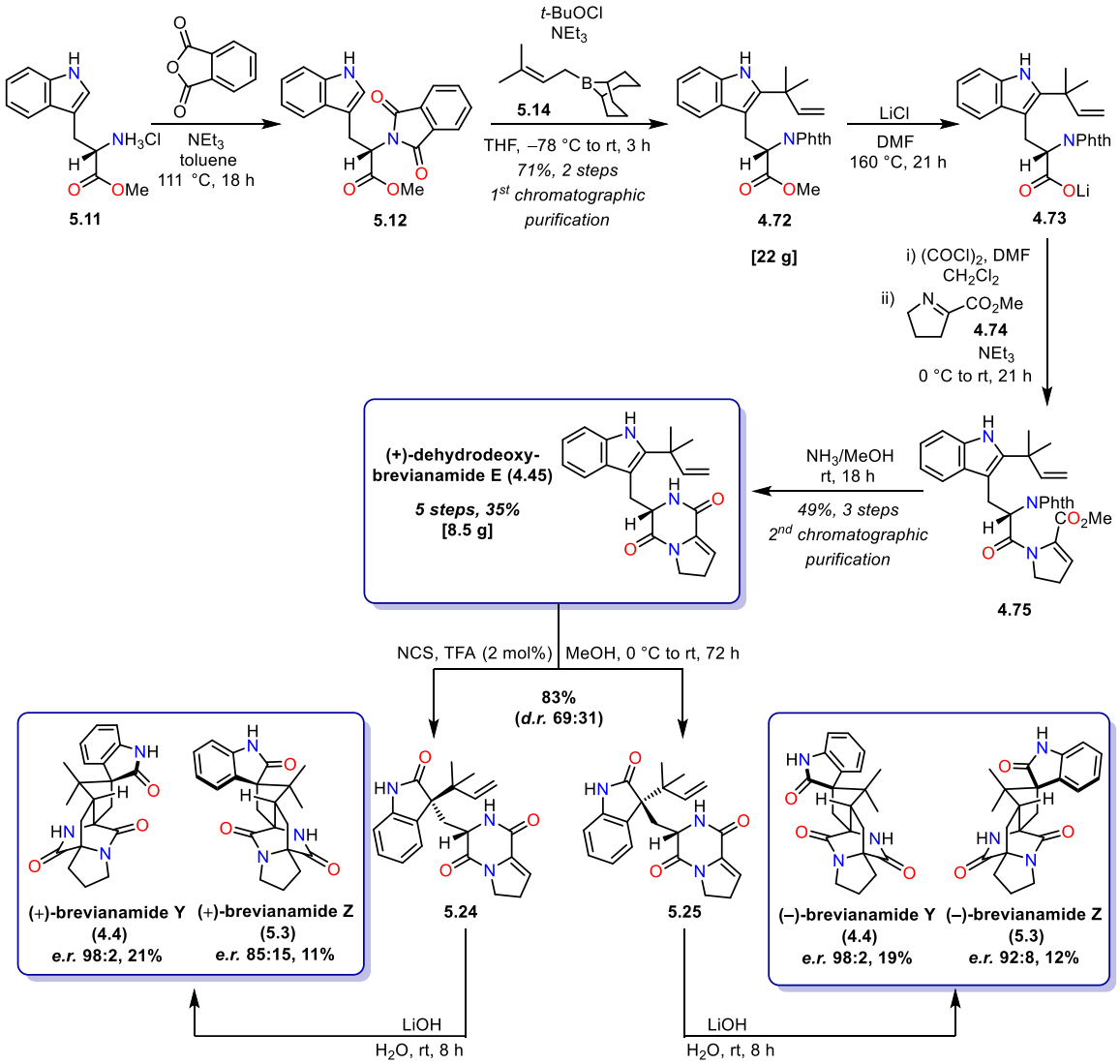

Scheme 5.23: Complete synthesis to brevianamide Y (**4.4**) and brevianamide Z (**5.3**) from L-tryptophan methyl ester (**5.11**)

5.4 Future Work

The future work on this project will be to investigate the synthesis of structurally related natural products (**Figure 5.6**). For example, (+)-versicolamide B (**4.54**) is structurally identical to (+)-brevianamide Y (**4.4**), bar the inclusion of a pyrano ring at the C6 – C7 position of the oxindole ring.

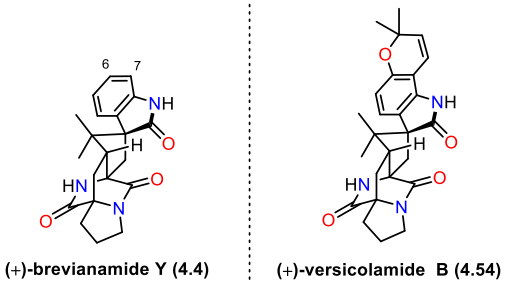

Figure 5.6: Structurally related natural product (+)-versicolamide B (**4.54**)

The synthesis of (+)-versicolamide B (**4.54**) could be achieved many ways, either through late stage functionalisation of (+)-brevianamide Y (**4.4**) with the introduction of a pyrano group (**Scheme 5.24, pathway 1**). Or, alternatively, the early installation of the pyrano group by functionalising the tryptophan starting material. The methodology developed throughout this project could then be used to carry the functionalised starting material through the synthesis (**Scheme 5.24, pathway 2**).

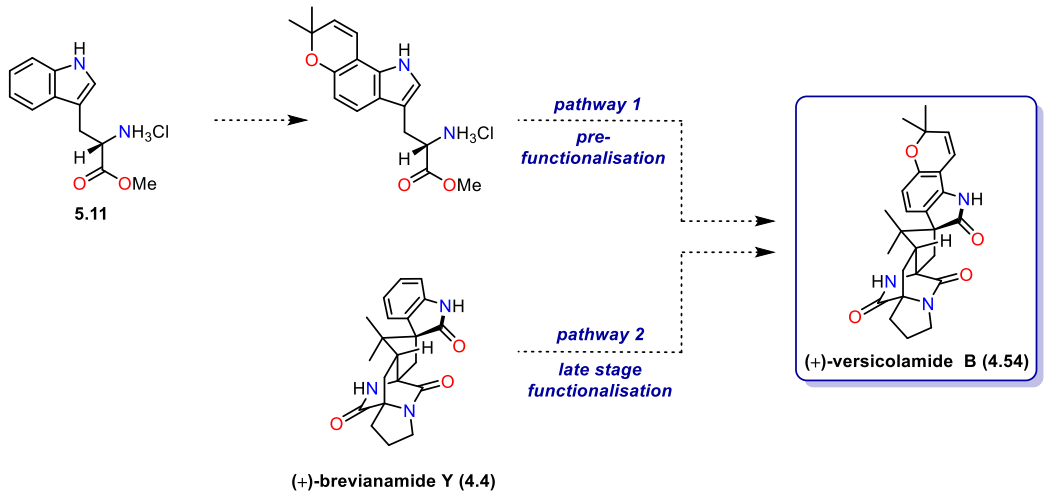

Scheme 5.24: Potential pathways towards the synthesis of (+)-versicolamide B (**4.54**)

Chapter 6: Mechanistic Studies into the Base-Catalysed Cascade in the Synthesis of Brevianamide A and B

6.1 Introduction

In parallel to the investigations in to the synthesis of brevianamide Y (**4.4**) and Z (**5.3**), mechanistic studies were performed to gain greater insight into the cascade reaction which features in the Lawrence Group's total synthesis of (+)-brevianamide A (**4.1**) and (+)-brevianamide B (**4.2**), published in 2020.[168]

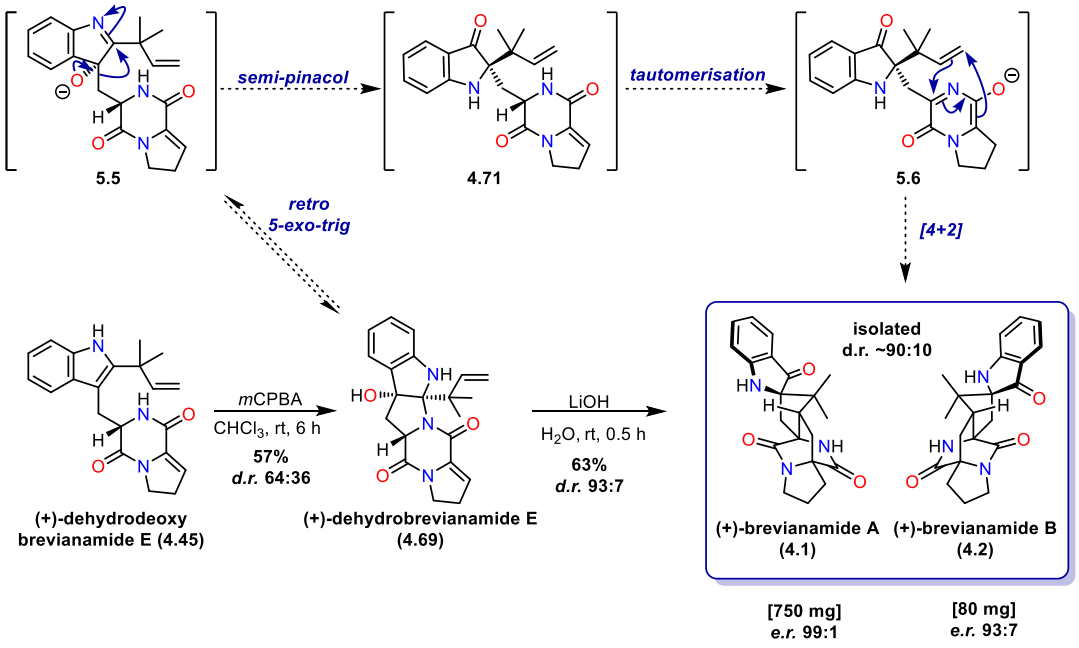

Scheme 6.1: Proposed cascade sequence for the formation of (+)-brevianamide A (**4.1**) and (+)-B (**4.2**) and chemical synthesis from (+)-dehydrodeoxybrevianamide E (**4.45**)

The key step in the group's synthesis of brevianamide A (**4.1**) and brevianamide B (**4.2**) was a complex cascade sequence starting from (+)-dehydrobrevianamide E (**4.69**) (**Scheme 6.1**). When (+)-dehydrodeoxybrevianamide E (**4.45**) was oxidised in a diastereoselective manner (63:37 *d.r.*) using *m*CPBA, two diastereomers of dehydrobrevianamide E (**4.69** and **5.23**) were obtained that

were crucial for the synthesis of both enantiomers of brevianamide A (**4.1**) and B (**4.2**). Dehydrobrevianamide E (**4.69**) was treated with aqueous lithium hydroxide, which triggered a cascade sequence that was proposed to start with a retro 5-*exo*-*trig* ring opening reaction to give the alkoxyindolenine intermediate **5.5**. Alkoxyindolenine **5.5**, would then be set up to undergo a semi-pinacol rearrangement to install the indoxyl ring (**4.71**). Deprotonation of the diketopiperazine moiety would allow for the formation of an *aza*-diene intermediate (**4.6**), which can undergo a final intramolecular hetro Diels–Alder reaction with the reverse prenyl fragment. This sequence proceeds to afford both (+)-brevianamide A (**4.1**) and (–)-brevianamide B (**4.2**).

While optimising the cascade reaction, Green and Godfrey found that using weaker carbonate bases and increasing the methanol content of the solvent, resulted in another product forming, suggesting a different reaction pathway was responsible. This project aimed to elucidate all products and possible pathways when the complex cascade sequence was performed under different conditions (**Scheme 6.2**).

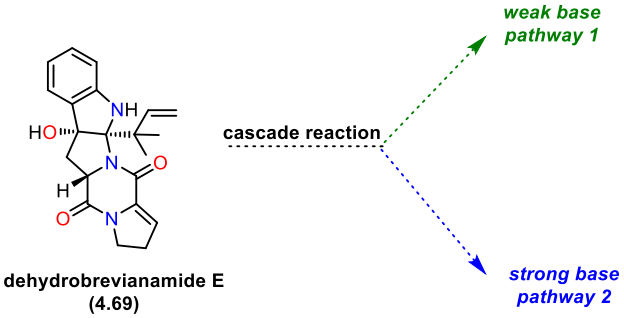

Scheme 6.2: Planned reactions for mechanistic studies, subjecting dehydrobrevianamide E (**4.69**) to different conditions

6.2 Results and Discussion: Mechanistic Investigation of the Cascade Sequence

To probe the mechanism of the cascade reaction from dehydrobrevianamide E (**4.69**) to form brevianamide A (**4.1**) and brevianamide B (**4.2**), NMR monitoring studies were conducted. Initially, *dia*-dehydrobrevianamide E (**5.23**) was subjected to the strongly basic conditions of lithium hydroxide, as used in the synthesis of the natural products.[168] This reaction was performed in various solvents and monitored for product formation *via* ^{1}H NMR spectroscopy (**Table 6.1**) (for raw NMR

data see **Section 8.5.1-8.5.5**, **pages 251-260**). The reaction was worked up after stirring for 30 minutes at room temperature and revealed the formation of (–)-brevianamide A (**4.1**) in all cases.

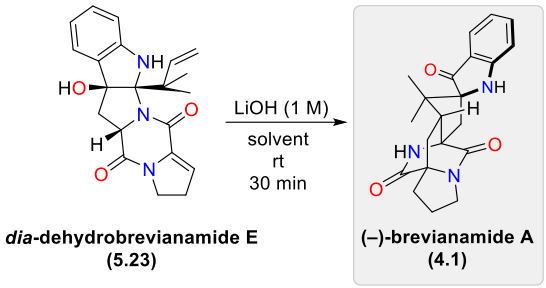

***dia*-dehydrobrevianamide E (5.23)** | **(–)-brevianamide A (4.1)**

Solvent		
H_2O	H_2O/MeOH (1:1)	MeOH
(–)-brevianamide A (**4.1**) formed	(–)-brevianamide A (**4.1**) formed	(–)-brevianamide A (**4.1**) formed

Table 6.1: The reaction of *dia*-dehydrobrevianamide E (**5.23**) with a 1 M LiOH solution. The 1 M LiOH solution was made up in different aqueous and methanolic solvents and the reaction was monitored by ^{1}H NMR (500 MHz, $CDCl_3$)

When the same set of reactions were performed with the weaker base, potassium carbonate, this resulted in a different product forming (**Table 6.2**).

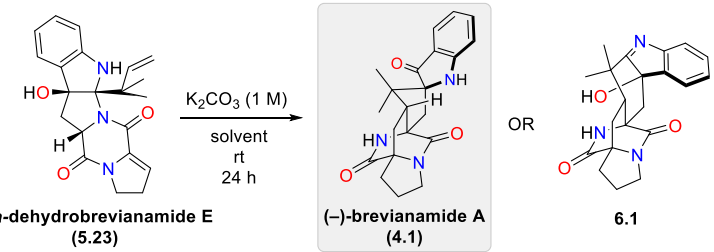

***dia*-dehydrobrevianamide E (5.23)** | **(–)-brevianamide A (4.1)** | **6.1**

Solvent		
H_2O	H_2O/MeOH (1:1)	MeOH
No reaction observed	**6.1** formed	**6.1** formed

Table 6.2: The reaction of *dia*-dehydrobrevianamide E (**5.23**) with a 1 M K_2CO_3 solution. The 1 M K_2CO_3 solution was made up in different aqueous and methanolic solvents and the reaction was monitored by ^{1}H NMR (500 MHz, $CDCl_3$)

This new product was isolated, fully characterised, and found to be consistent with the structure of hydroxyindolenine **6.1**.[174] However, conducting the reaction under aqueous conditions resulted in no reaction occurring, therefore indicating that the methanol content of the solvent of the reaction was also required for the formation of alkoxyindolenine **6.1**. It was postulated that the formation of **6.1** was the result of the *5-exo-trig* ring opening occurring to afford intermediate **6.2** (**Scheme 6.3**). Then, under weakly basic methanolic conditions, intermediate **6.2** undergoes a deprotonation to the *aza* diene intermediate **6.3**, which then undergoes a hetero-Diels–Alder reaction to give the alkoxyindolenine **6.4**. Work-up and proton transfer give hydroxyindolenine **6.1** as the sole product of the reaction. Therefore, suggesting under weakly basic conditions the hetero-Diels–Alder is faster than the semi-pinacol rearrangement.

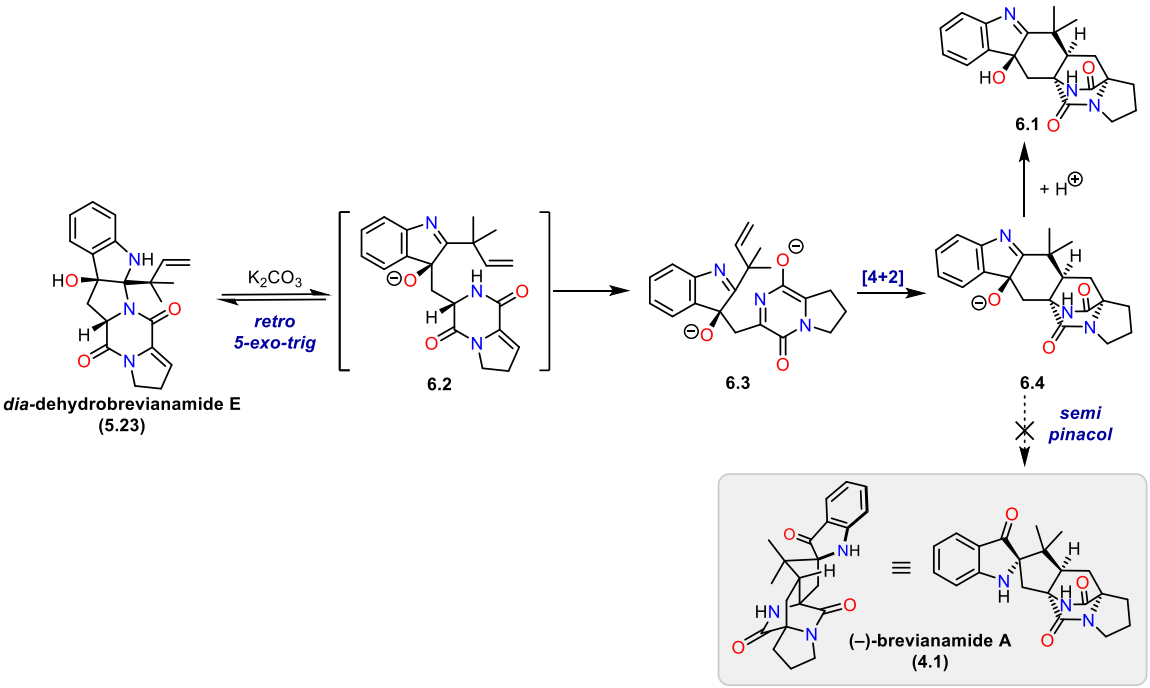

Scheme 6.3: Proposed cascade pathway of dehydrobrevianamide E (**5.23**) under weak base conditions to form hydroxyindolenine intermediate **6.1**

By repeating this reaction on a slightly larger scale we were able to isolate both diastereomers of the hydroxyindolenine intermediate (–)-(**6.1**) and (–)-(**6.5**) formed in the reaction (**Scheme 6.4**).

The relative stereochemistry of each hydroxyindolenine (**6.1** and **6.5**) was later assigned unambiguously by observing which diastereomer led to the formation of brevianamide B (**4.2**).

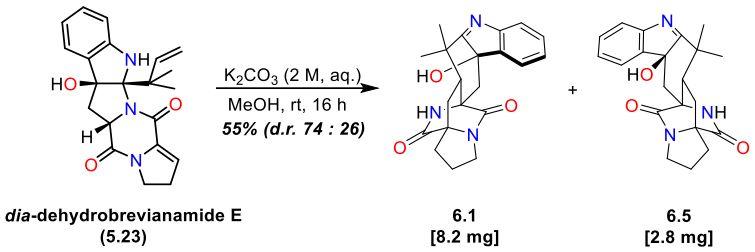

Scheme 6.4: Deprotonation and hetero Diels–Alder reaction of *dia*-dehydrodeoxybrevianamide E (**5.23**) to give hydroxyindolenines (–)-**6.1** and (–)-**6.5**

Further mechanistic studies were then undertaken using the authentic samples of the hydroxylindolenine diastereomers (**6.1** and **6.5**) isolated from the above reaction. As each hydroxyindolenine intermediate was a hypothetical precursor to either (–)-brevianamide A (**4.1**) or to (–)-brevianamide B (**4.2**) through a semi-pinacol rearrangement, both were subjected to conditions that attempted to initiate this transformation (**Table 6.3**). Hydroxyindolenine **6.1** was found not to undergo a semi-pinacol rearrangement to form (–)-brevianamide A (**4.1**) under strongly basic conditions.

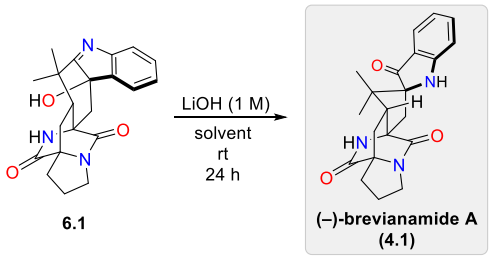

Solvent		
H_2O	H_2O/MeOH (1:1)	MeOH
no reaction	no reaction	no reaction

Table 6.3: The reaction of hydroxyindolenine **6.1** with a 1 M LiOH solution. The 1 M LiOH solution was made up in different aqueous and methanolic solvents and the reaction was monitored by ^{1}H NMR (500 MHz, $CDCl_3$)

In stark contrast to these results, when the other hydroxyindolenine diastereomer (**6.5**) was subjected to the strongly basic conditions of lithium hydroxide in a range of solvents, each reaction resulted in the formation of (–)-brevianamide B (**4.2**) (**Table 6.4**), confirming that a late-stage semi-pinacol rearrangement was possible in the synthesis of brevianamide B (**4.2**) under strongly basic conditions.

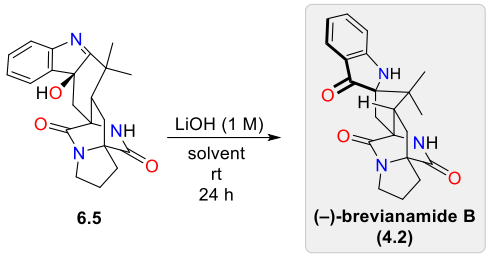

Solvent		
H_2O	H_2O/MeOH (1:1)	MeOH
(–)-brevianamide B (**4.2**) observed	(–)-brevianamide B (**4.2**) observed	(–)-brevianamide B (**4.2**) observed

Table 6.4: The reaction of hydroxyindolenine (**6.5**) with a 1 M LiOH solution. The 1 M LiOH solution was made up in different aqueous and methanolic solvents and the reaction was monitored by ^{1}H NMR (500 MHz, $CDCl_3$)

Finally, to ascertain if the semi-pinacol [1,2]-shift was reversible under strong bases, (–)-brevianamide A (**4.1**) was left to stir in different lithium hydroxide solutions (**Table 6.5**). No reaction was observed under each set of conditions, proving that a retro-semi-pinacol rearrangement back to hydroxyindolene **6.1** was not possible under these conditions.

These results indicated that there is only one pathway for the formation of brevianamide A (**4.1**), since our studies showed that a semi-pinacol rearrangement of the hydroxyindolenine intermediate **6.1** was not possible **(Scheme 6.5)**. Whereas for the formation of brevianamide B (**4.2**), the semi-pinacol rearrangement was possible from the corresponding hydroxyindolenine intermediate **6.5**.

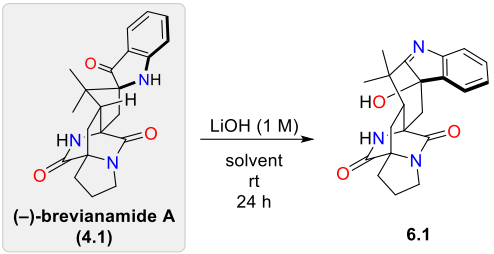

Solvent		
H_2O	H_2O/MeOH (1:1)	MeOH
no reaction observed	no reaction observed	no reaction observed

Table 6.5: The reaction of (–)-brevianamide A (**4.1**) with a 1 M LiOH solution. The 1 M LiOH solution was made up in different aqueous and methanolic solvents and the reaction was monitored by ^{1}H NMR (500 MHz, $CDCl_3$)

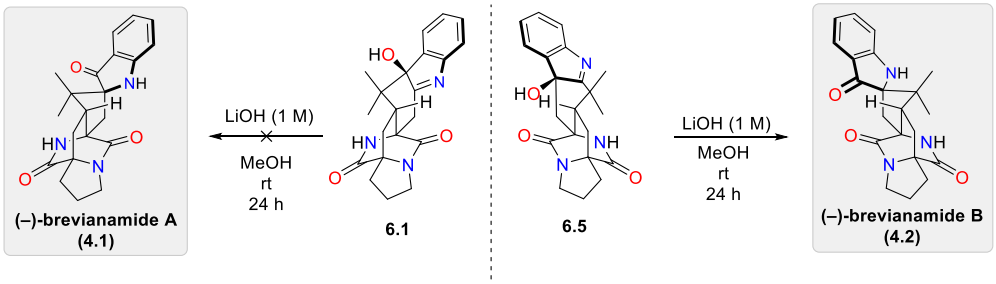

Scheme 6.5: Hydroxyindolenine intermediates **6.1** and **6.5** subjected to lithium hydroxide

These remarkable observations can be rationalised by invoking a stabilising interaction through an intramolecular ionic hydrogen bond (IHB) shown in **Figure 6.1**. IHBs form between ions and molecules and typically have bond strengths ranging from 5-35 kcal/mol.[191] Due to their incredible strength they play a vital role in protein folding, enzyme active sites, self-assembly in supramolecular chemistry and in many more systems.[192–194] In this case, an intramolecular IHB is only possible in the alkoxy indolenine intermediate **6.1** and would go on to form brevianamide A (**4.1**). As the negatively charged oxygen of the alkoxy group is in close proximity to the diketopiperazine N–H to form an ionic hydrogen bond. It is believed that this stabilising IHB

interaction is strong enough to prevent the corresponding semi-pinacol arrangement from occuring and therefore prevent the formation of brevianamide A (**4.1**) under basic conditions.

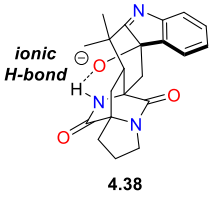

Figure 6.1: Proposed intramolecular ionic hydrogen bond that stabilises alkoxy indolenine intermediate **4.38**

Finally, to confirm the selectivity of the pathway did not correlate to the cation used, we also tried using strong bases with alternative metal cations. (+)-Dehydrodeoxybrevianamide E (**4.69**) was treated with sodium hydroxide and potassium hydroxide in water and methanol. Both reactions resulted in the clean formation (+)-brevianamide A (**4.1**) and (+)-brevianamide B (**4.2**) (**Scheme 6.6**). Unfortunately the equivalent weak base, lithium carbonate, was not soluble under the aqueous and the methanolic reaction conditions, so the reaction did not proceed.

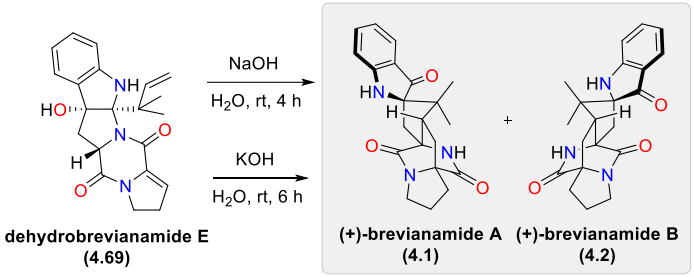

Scheme 6.6: Alternative strong bases used to synthesise brevianamide (+)-A (**4.1**) and (+)-B (**4.2**)

6.3 Conclusion

Through serveral control experiments I was able to gain greater insight into the complex bioinspired cascade, featured in the synthesis of brevianamide A (**4.1**) and brevianamide B (**4.2**).[168] For both brevianamide A (**4.1**) and brevianamide B (**4.2**) it was discovered that the order of steps in the cascade could be changed by tuning the reaction conditions.

The following conclusions can be drawn from the experiments conducted; a strong base is necessary to ensure the semi-pinacol [1,2]-shift occurs prior to the Diels–Alder reaction (**Scheme 6.7**). This is essential for the productive pathway in forming brevianamide A (**4.1**). However, under weakly basic conditions, such as in the presence of potassium carbonate the deprotonation to the *aza*-diene intermediate and subsequent Diels–Alder reaction occurs preferentially. This resulted in an unproductive pathway as it was found that the semi-pinacol shift cannot occur in the final step of the cascade sequence towards brevianamide A (**4.1**). This is believed to be due to an intramolecular ionic hydrogen bond that stabilises the hydroxyindolenine (**6.1**) formed and therefore prevents the rearrangement (**4.38, Figure 6.2**). In contrast, in the synthesis of brevianamide B (**4.2**) the diasteoromeric hydroxyindolenine (**6.5**) is in the wrong configuration to benefit from this stabilising interaction, and is therefore is able to undergo a semi-pinacol rearrangement in the final step of the cascade to form brevianamide B (**4.2**).

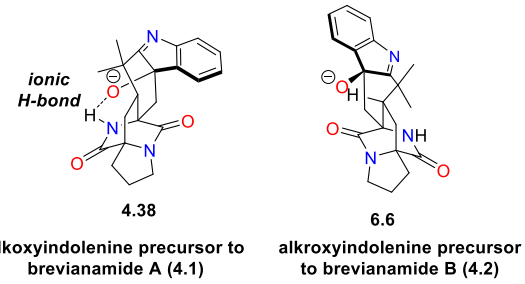

Figure 6.2: Proposed intramolecular ionic hydrogen bond that stabilises alkoxyindolenine intermediate **4.38**

This work demonstrates the importance of the final step of the cascade for forming brevianamide A (**4.1**) being a hetero Diels–Alder reaction. Many of the previous unsuccessful attempts at the synthesis of brevianamide A (**4.1**) have led to the synthesis of brevianamide B (**4.2**) as the sole product instead. These routes have previously relied upon installing the bicyclo[2.2.2]diazoctane ring before the indoxyl ring and therefore require a late-stage semi-pinacol rearrangement. These mechanistic studies help to understand why brevianamide A (**4.1**) has eluded synthetic chemists for so long.

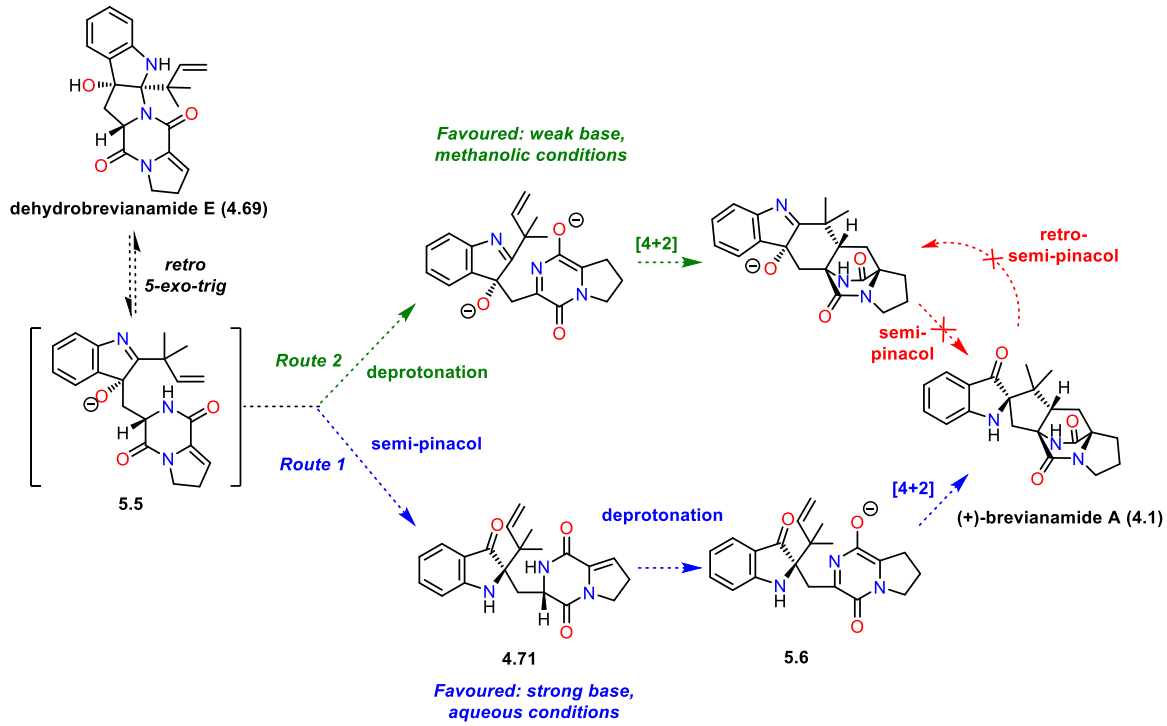

Scheme 6.7: Results of mechanistic investigation into the effect of base strength and solvent on the synthesis of brevianamide A (**4.1**)

Additionally, a recent collaboration between Williams, Sherman, Li and co-workers demonstrated the role of a *semi pinacolase* enzyme as the final enzyme in the biosynthesis of brevianamides A (**4.1**) and B (**4.2**).[174] Our new insights into the mechanistic detail of the synthetic cascade reaction indicate that the use of a strong base, like lithium hydroxide, provides the same function as the *semi pinacolase* enzyme in the biosynthesis.

6.4 Future Work

Future work on this project will be to back these experimental observations with computational studies to see the relevant energy barriers between the two distinct pathways. In addition, the stabilising interection in hydroxyindolenine **6.1** could also be modelled.

Chapter 7: Efforts Towards the Synthesis of Brevianamide S

7.1 Introduction

Alongside the total synthesis of brevianamide Y (**4.4**) and Z (**5.3**), the synthesis of another member of the brevianamide natural product family was investigated. Brevianamide S (**7.1**) is an achiral dimeric natural product isolated by Capon and co-workers from the deep sea fungi *Aspergillus versicolor* (**Figure 7.1**).[195] Capon found that brevianamide S (**7.1**) exhibited antibacterial properties against a screening surrogate for *Mycobacterium tuberculosis* (*Bacillus Calmette–Guérini*). Interestingly, he believed this occurred through a novel mechanism of action, which could represent a valuable new lead in the search for the next generation of antitubercular drugs.

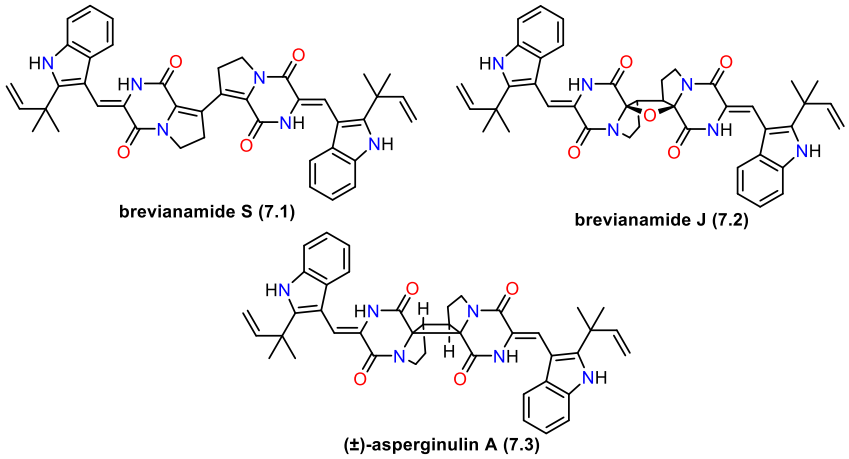

Figure 7.1: Dimeric diketopiperazine natural products; brevianamide S (**7.1**), brevianamide J (**7.2**) and asperginulin A (**7.3**)

Other compounds containing a dimeric diketopiperazine unit are rare, with only two other examples known; brevianamide J (**7.2**) and asperginulin A (**7.3**). Brevianamide J (**7.2**), which was also isolated from a strain of *Aspergillus versicolor* fungi by Zhang and co-workers in 2009, is structurally related to brevianamide S (**7.1**) although it is chiral.[196] Asperginulin A (**7.3**), isolated from mangrove endophytic fungus *Aspergillus* (*sp. SK-28*) in 2019 by She and Long, contains the structurally unique 6/5/4/5/6 fused ring system.[197]

7.2 Biominmetic Strategy Towards Brevianamide S (7.1)

The Lawrence group has had a long standing interest in the total synthesis of dimeric natural products.[198–200] Therefore, synthetic investigations into a brevianamide-derived dimeric natural product posed a fitting target. Biosynthetically, Zhang and Capon independently proposed that both brevianamide S (**7.1**) and J (**7.2**) were derived from the co-isolated natural product, brevianamide K (**7.4**) (**Scheme 7.1**). They both suggested that an oxidative coupling of brevianamide K (**7.4**) would afford brevianamide S (**7.1**). For the biosynthesis of brevianamide J (**7.2**), Zhang proposed this was then followed by an enzyme-mediated regio- and enantioselective hydration to form brevianamide J (**7.2**).

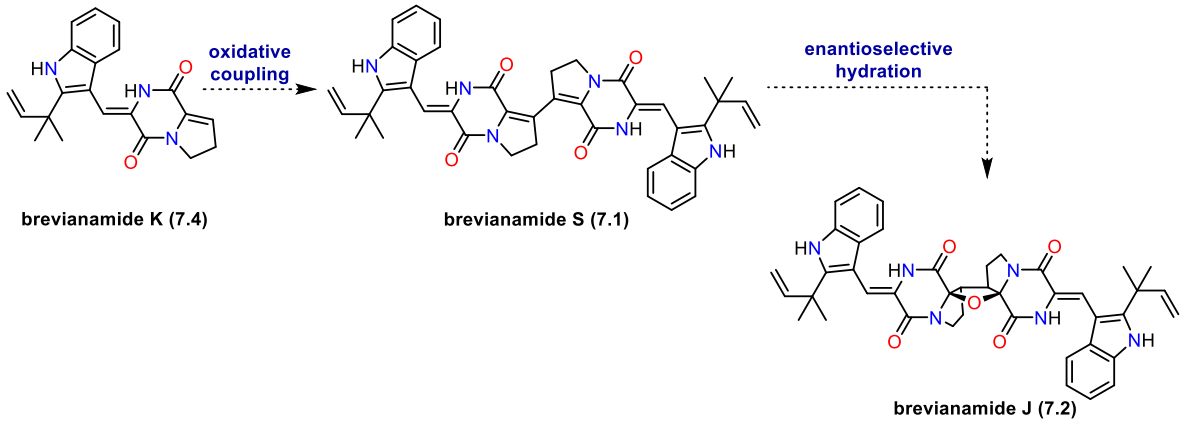

Scheme 7.1: Proposed biosynthesis of brevianamide J (**7.2**) and S (**7.1**) through oxidative coupling of brevianamide K (**7.4**)

In contrast, we proposed that (+)-dehydrodeoxybrevianamide E (**4.45**) could also be a plausible precursor for brevianamide S (**7.1**) and J (**7.2**) (**Scheme 7.2**). We hypothesised that a similar oxidative coupling reaction of two molecules of (+)-dehydrodeoxybrevianamide E (**4.45**) could form an unsaturated dimer, **7.5**. Compound **7.5** could undergo an oxidation to give brevianamide S (**7.1**) or be converted to brevianamide J (**7.2**) through a diastereoselective hydration and oxidation. Our route had the added benefit of using a known precursor, (+)-dehydrodeoxybrevianamide E (**4.45**), that the Lawrence group has previously synthesised.

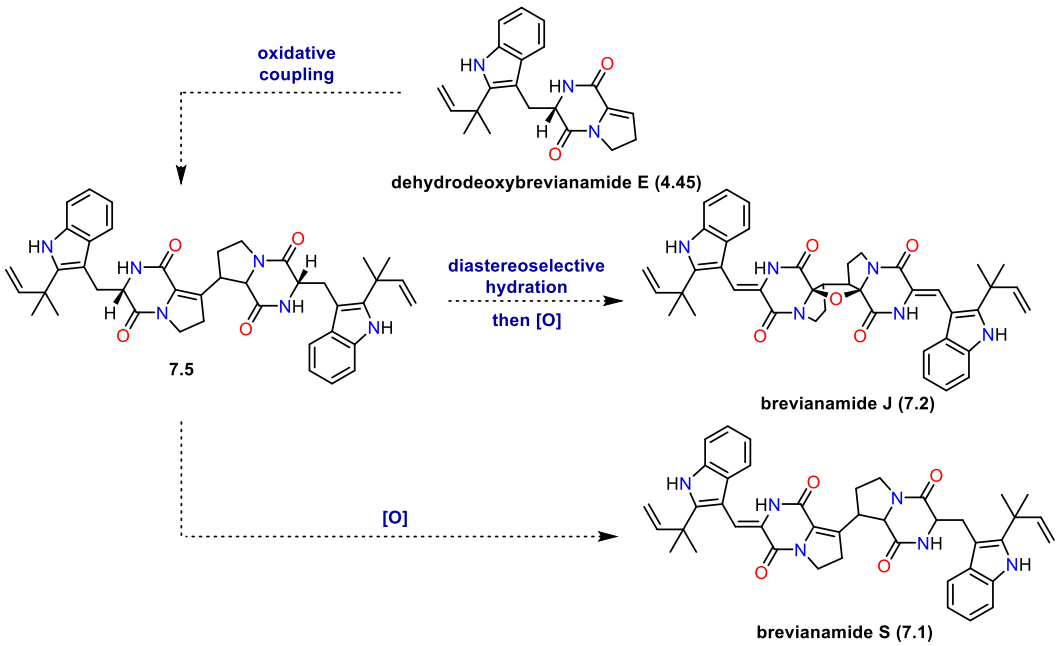

Scheme 7.2: Our proposed synthesis of brevianamide J (**7.2**) and S (**7.1**)

To investigate the chemical feasibility of our biosynthetic hypothesis, conditions for oxidation and subsequent coupling of (+)-dehydrodeoxybrevianamide E (**4.45**) were investigated (**Scheme 7.3**). This included a copper triflate-mediated single electron oxidation of (+)-dehydrodeoxybrevianamide E (**4.45**), which was performed by previous members of the Lawrence group. Interestingly, the dimeric structure **7.6** was tentatively assigned as the product. The structure is proposed to be the result of an unsymmetrical dimerisation between indole positions C3 and C6. Numerous other single electron oxidation and photo redox reactions were attemptted on (+)-dehydrodeoxybrevianamide E (**4.45**) with no success. Therefore, this led us to formulate a non-biomimetic route to synthesise brevianamide S (**7.1**).

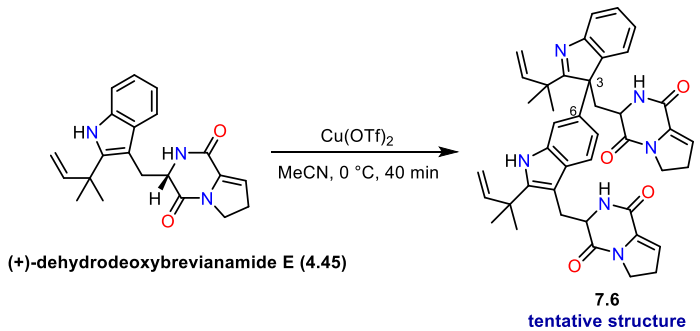

Scheme 7.3: Single electron oxidation of (+)-dehydrodeoxybrevianamide E (**4.45**)

7.3 Non-Biominmetic Strategy Towards Brevianamide S (7.1)

Our first non-biomimetic proposal adopted a two-directional synthesis approach, *via* the pre-coupling of the dehydroproline units (**7.7**) to form the key dimeric core (**7.8**) (**Scheme 7.4, route 1**).[201] Utilising this approach would allow for rapid elaboration around the dimeric core using the methodology previously developed in the synthesis of (+)-dehydrodeoxybrevianamide E (**4.45**). As the dimeric dehydroproline molecule would be added in a convergent manner, no extra steps in the longest linear sequence (LLS) would be incurred.

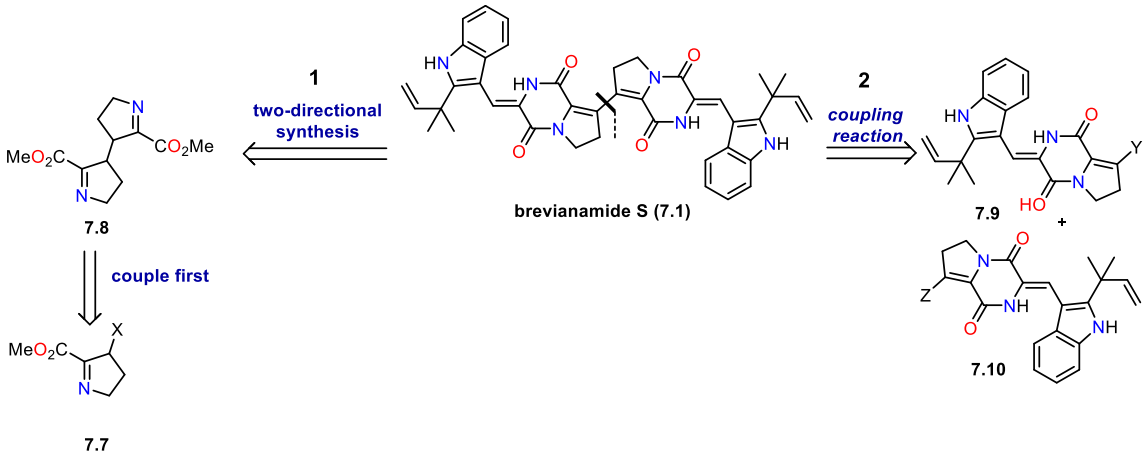

Scheme 7.4: Retrosynthesis plan of towards the synthesis of brevianamide S (**7.1**), Route one: coupling two dehydroproline units (**7.7**) to form key dimeric core (**7.8**) in a two-directional synthesis Route two: coupling reaction of two monomers

Alternatively, the second route focused on the C–C bond disconnection between the two monomeric subunits (**Scheme 7.4, route 2**), similar to Zhang's and Capon's initial biosynthetic proposals. However, a retrosynthetic disconnection could lead back to two functionalised monomers, **7.9** and **7.10**. By using similarly functionalised or differently functionalised monomers, this would enable us to investigate both homo-coupling and cross-coupling reactions to form brevianamide S (**7.1**).

Two alternative approaches could be investigated to install appropriate functional group handles for coupling the two monomers together (**Scheme 7.5**). The first could be a late-stage functionalisation approach (**Scheme 7.5, route 1a**). Strategically using (+)-dehydrodeoxybrevianamide E (**4.45**) as an intermediate in the route could enable the introduction

of functionality once the main diketopiperazine structure was in place.[168] Pursuing this approach would have the advantage of using the tried and tested methodology developed by the Lawrence group to synthesise (+)-dehydrodeoxybrevianamide E (**4.45**).

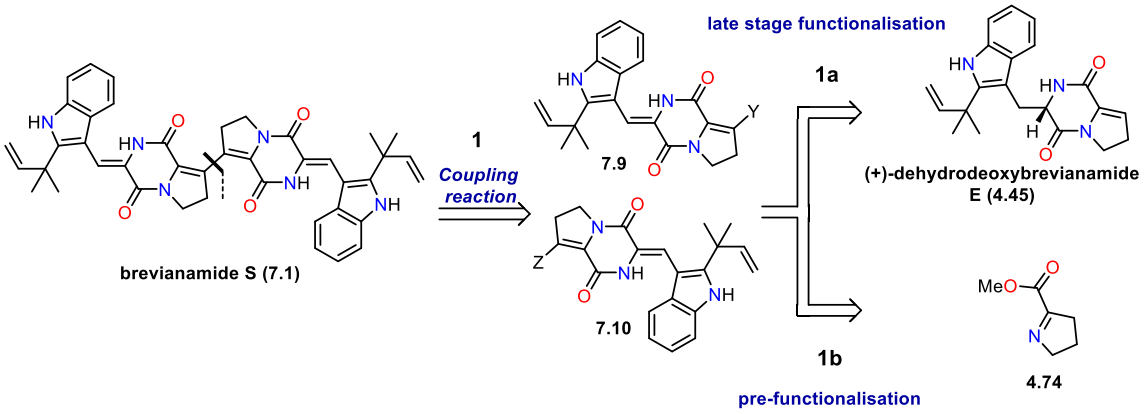

Scheme 7.5: Proposed synthesis of functionalised monomers (**7.9** and **7.10**) through late-stage functionalisation (**1a**) and pre functionalisation (**1b**)

Alternatively, we could look at adding a crucial functional group handle earlier in the synthesis in a pre-functionalisation approach (**Scheme 7.5, route 1b**). Pre-functionalising the dehydroproline unit (**4.74**), which is used to install the five membered ring featured in the final product, would reduce the total step count of the LLS in the synthesis, as this route would utilise a more convergent approach to synthesise brevianamide S (**7.1**). In addition, the dehydroproline unit could act as a model substrate for the late-stage functionalisation attempts and coupling reactions. With two different viable approaches available, this gave greater flexibility for contingency plans if required in the synthesis towards brevianamide S (**7.1**).

With no indication of which route would prove the most successful, significant experimentation was performed in parallel throughout this chapter of work. Successful results and progress in specific areas of this project directed the investigations and often caused other avenues to simultaneously be put on hold.

7.4 Results and Discussion: Mechanistic Investigation of the Cascade Sequence

7.4.1 Pre-Functionalisation of Dehydroproline Moiety

Initial investigations began with pre-functionalising the dehydroproline moiety (**Scheme 7.6**). Once more, this route offers many different opportunities for where to incorporate the functionalised intermediate into the overall synthetic route. One plausible route would involve using a functionalised dehydroproline ring (**7.7**) in the condensation with lithium carboxylate intermediate **4.73** to form compound **7.11**. The outcome of this would hinge on the condensation reaction being tolerant of the addition of this new functional group. From here, there are two viable pathways; either forming the diketopiperazine ring prior to coupling (**7.12**) (**Scheme 7.6, path 1**), or coupling immediately to install the key C–C bond (**7.13**) between the monomeric units (**Scheme 7.6, path 2**).

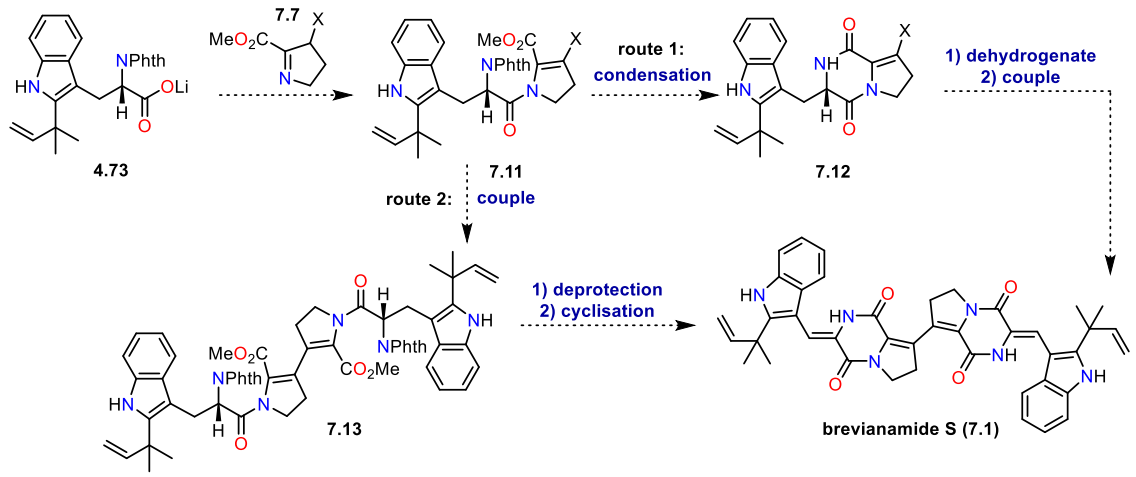

Scheme 7.6: Plausible route to incorporate pre-functionalised dehydroproline unit **7.7** into synthesis of (+)-dehydrodeoxybrevianamide E (**4.45**)

7.4.2 Halogenation of Imine 4.74

Investigations into the pre-functionalisation of the dehydroproline ring began with the installation of different halogens starting from imine **4.74**, the imine which was used in the original synthesis of (+)-dehydrodeoxybrevianamide E (**4.45**). Using methodology developed by Hausler, we were

able to synthesise the bromo- (**7.14**), chloro- (**7.15**) and a novel iodo- (**7.16**) derivatives (**Scheme 7.7**).[202] Surprisingly, these derivatives were found to be relatively stable, despite the three adjacent reactive sites (ester, imine, and allylic halide).

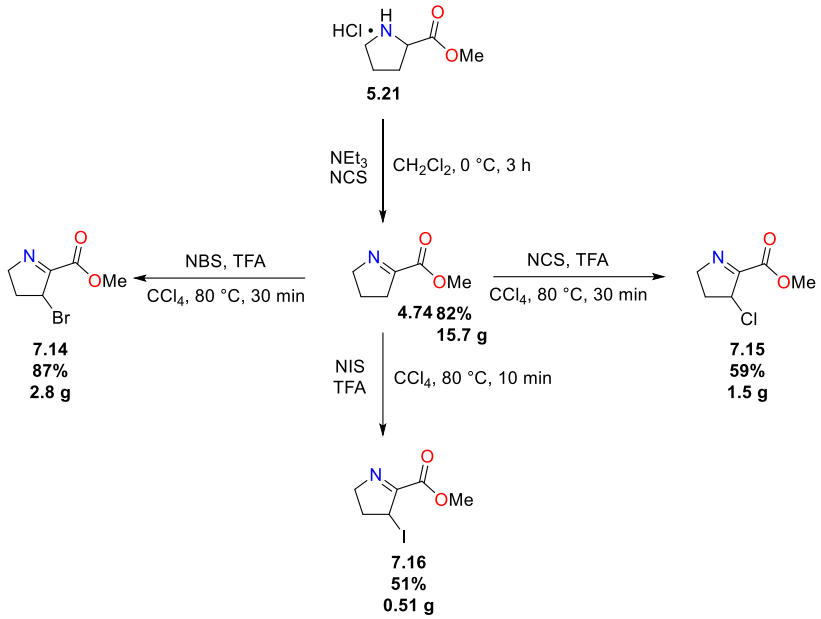

Scheme 7.7: Halogen functionalisation of imine **4.74**

7.4.3 Attempts at Homocoupling the Halogenated Derivatives

With the halogenated derivatives in hand, we first tried to adapt a reductive homo dimerisation protocol, inspired by the work of by Movassaghi and coworkers.[203] The authors used tris(triphenylphosphine)cobalt(I) to dimerise a tertiary benzylic bromide **7.17** in their total synthesis of (+)-11,11'-dideoxyverticillin A (**Scheme 7.8**).

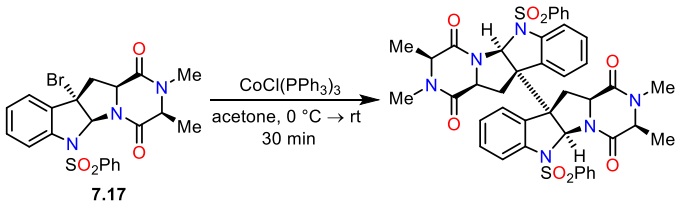

Scheme 7.8: Movassaghi's reductive dimerization of benzylic bromide **7.17**

Utilising a similar approach to Movassaghi on our dehydroproline system, the chloro derivative **7.15** was subjected to the reductive dimerisation conditions (**Scheme 7.9**). The chloro derivative (**7.15**) was used due to availability of material at the time. Regrettably, this resulted in mainly starting material being recovered.

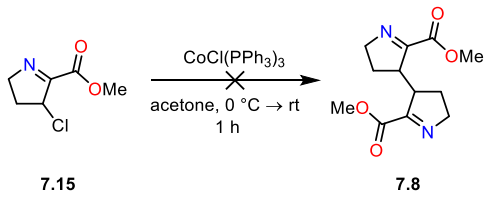

Scheme 7.9: Attempted reductive dimerisation of chloro imine **7.15** using tris(triphenylphosphine)cobalt(I)

7.4.4 Attempts at Condensation of Halogenated Derivatives

Unsuccessful in our attempts at a homo coupling, we briefly explored the possibility of using compounds **7.15** and **7.14** directly in the condensation reaction. To test the viability of using a halogenated dehydroproline unit in the *N*-acylation condensation reaction we performed a control reaction of chloro-derivate **7.15** and acetyl chloride (**Scheme 7.10**).[204] Using a very reactive unhindered acyl chloride to perform an *N*-acyl condensation would provide evidence of the feasibility of the reaction. To our delight, we observed formation of the novel *N*-acylated enamine product (**7.18**) through formation of a new carbonyl peak in the ^{13}C NMR spectrum, although it was decided not to purifty this test reaction.

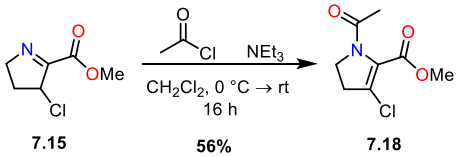

Scheme 7.10: *N*-acylation condensation reaction of acetyl chloride and imine (**7.15**)

In the hope that the positive result in the control reaction would translate into our actual system, we subjected the bromide (**7.14**) to the conditions normally used in the coupling reaction with lithium carboxylate **4.73** (**Scheme 7.11**). As before, bromide **7.14** was used due to availability of starting

material at the time. Unfortunately, there was no reaction between the two partners and only unreacted carboxylic acid **7.19** was recovered from the reaction.

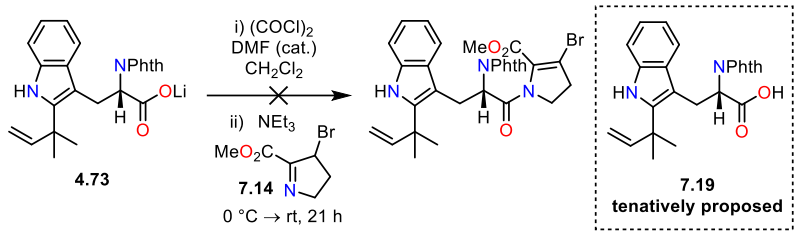

Scheme 7.11: Coupling of bromo dehydroproline **7.14** with lithium carboxylate **4.73**

Due to lack of success in the condensation attempts with the functionalised dehydroproline compounds, the focus moved to attempting to functionalise the 5-membered ring once attached to the tryptophan scaffold. Taking compound **4.75**, which was a known precursor in the synthesis of (+)-dehydrodeoxybrevianamide E (**4.45**), efforts were made to halogenate the 5-membered ring on the unsubstituted carbon of the C–C double bond (**Scheme 7.12**). Using the previously successful halogenation conditions of NIS and TFA with heating for the halogenation of proline derivatives (**Scheme 7.7**, **page 135**), we tried to install an iodo group. Disappointingly this resulted in recovered starting material. We also attempted the installation of a bromo group using alternative conditions, but again noted no reaction.[205] These results could be attributed to the C–C double bond becoming less electron rich when attached to the main tryptophan core. In the context of analogue **4.74**, donation of electron density into the alkene would have enhanced its nucleophilicity, therefore aiding the halogenation reaction. By contrast for amide **7.20**, competing delocalisation of the lone pair on nitrogen into the adjacent C=O leads to a less nucleophilic C=C bond, perhaps accounting for the decreased reactivity observed for this system.

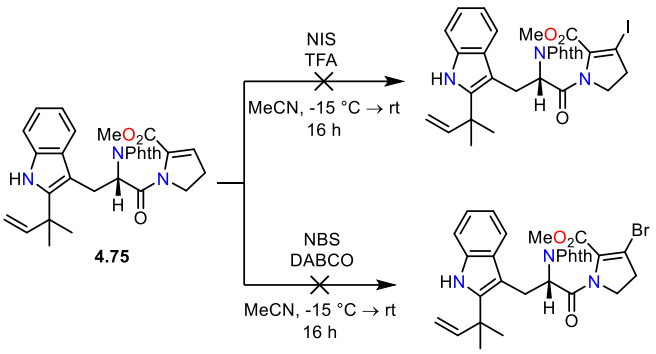

Scheme 7.12: Attempts of halogenating the 5-membered ring of compound **4.75**

7.4.5 Trapping the Dehydroproline Unit as The Enamine

Having encountered difficulties both coupling and introducing the pre-functionalised dehydroproline group (**7.7**) as an imine into our system, investigations moved on to attempt the incorporation of the dehydroproline moiety as an enamine. Protecting the nitrogen of the imine would translocate the double bond and hence form an enamine (**7.21**) (**Scheme 7.13**). The switching of functional groups would also allow alternative chemistry to be used in the functionalisation of the required position. The vital halogenation of compound **7.21** would now be an alkenyl halogenation as opposed to the previous allylic halogenation. Furthermore, if we were able to introduce a halogen into this motif, the halogen would now be connected to a sp^2 carbon (**7.22**). Thus the prospect of using a Pd-catalysed cross-coupling reaction could now be investigated.

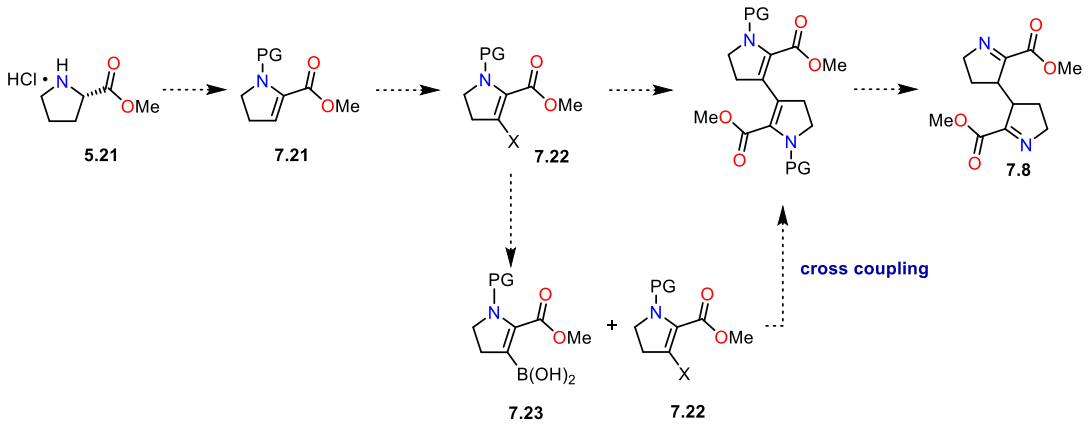

Scheme 7.13: Planned route for coupling of functionalised enamines **7.22** and **7.23**

Work began towards this new route by following the work of Bunch and co-workers, which enabled us to oxidise and protect proline methyl ester (**5.21**) in a one-pot procedure (**Scheme 7.14**).[205] From here, the enamine (**7.24**) was brominated using DABCO and NBS to afford the bromo analogue (**7.25**) in good yield.

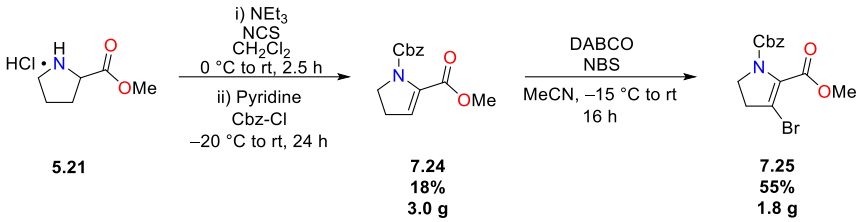

Scheme 7.14: Route to bromo enamine analogue **7.25** from proline methyl estser **7.24**

7.4.6 Attempts at Homocoupling of the Enamine Derivative 7.25

Having synthesised the key halogenated enamine intermediate (**7.25**), initial investigations began into the potential of a homo-coupling reaction to form the key dimeric core (**7.26**). Previously, Pei and co-workers developed an iron-catalysed homo-coupling of bromide compounds in combination with metallic magnesium in a one-pot procedure (**Scheme 7.15a**).[206] The benefit of this procedure was that no prior preparation of a Grignard reagent was required. Pei was able to apply this methodology to a broad range of different sp^2 and sp^3 hybridised C–Br bonds. Disappointingly, no reactivity was observed when the conditions were applied to our system (**Scheme 7.15b**).

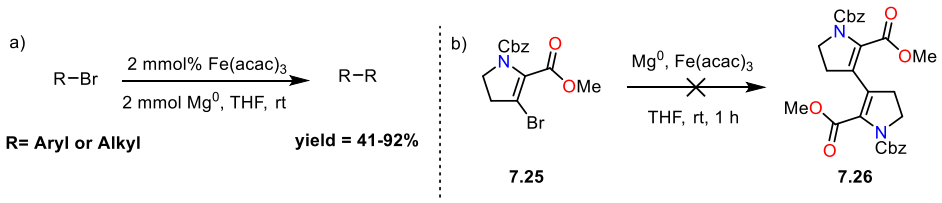

Scheme 7.15: a) Pei and co-worker's generic scheme of homo-coupling conditions b) conditions applied to homo-coupling of vinylic bromide **7.25**

Following this result, we also investigated the use of a traditional Gringard reaction. Self dimerisations of Grignard reagents (i.e., Wurtz coupling) are often an unwanted side product, which

can be minimised by using lower temperatures and slow addition of reagents.[207] Trying to leverage this property of Grignard reagents to our advantage, attempts were made to form the corresponding Grignard reagent from compound **7.25** *in situ* through magnesiation of the the C–Br bond (**Scheme 7.16a**). Another equivalent of vinylic bromide was added, but no evidence from NMR spectra of a self dimerision was observed. To prove if the formation of the Grignard was occurring, we planned to trap the Grignard out *via* addition to acetyl chloride (**Scheme 7.16b**). Using methodology developed by Knochel and co-workers, we opted for the formation of a Turbo Grignard using an *iso*-propylmagnesium chloride complex, as it had been shown to be tolerant to a wide range of functional groups including esters.[208] Yet again we unfortunately did not see any evidence of the desired product the ^{13}C NMR spectrum. Instead, it resulted in an inseparable mixture of decomposition products. The failures of these reactions could potentially be attributed to the generation of a Grignard nucleophile in the presence of an ester or Michael acceptor.

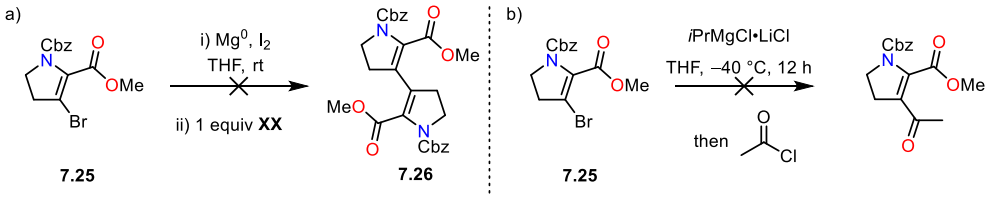

Scheme 7.16: a) Attempt at homocoupling *via* Grignard reaction b) attempt at turbo Gringard formation and condensation with acetyl chloride

Another classical reaction used to couple two alkenyl halides together is an Ullman-type coupling. Discovered by Ullman in 1901, it was the first reaction to utilise copper as a reducing agent in the coupling of brominated nitrobenzene derivatives at elevated temperatures.[209] Although the mechanism has been extensively researched, there is still no resounding proof for how the reaction works. Further developments have been made to the reaction; for example, extending it to alkenyl substituted systems with milder conditions of copper thiophene carboxylate conducted at room temperature.[210] These modern conditions established by Liebeskind and co-workers were investigated on our systems, but only a complex NMR spectrum of inseparable compounds was found (**Scheme 7.17**). In 2016, Ploypradith and co-workers reported the benefit of adding copper

(0) to mediate a copper (0)-copper (I) Ullman coupling.[211] These conditions were also applied to our system in hope of forming the dimeric unit (**7.26**) (**Scheme 7.17**), but this had no effect on the outcome of the reaction.

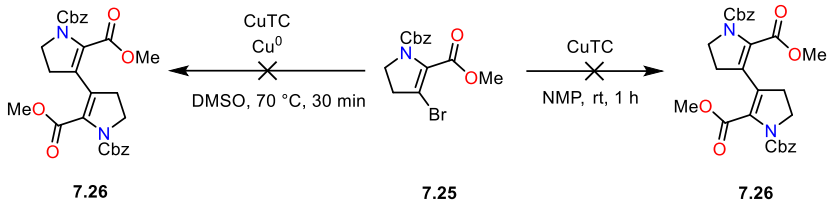

Scheme 7.17: Attempts to dimerise vinylic bromide **7.25** through reductive-type Ullman couplings

Using palladium on carbon to induce another metal-catalysed reductive coupling was also trialled (**Scheme 7.18**), but unfortunately resulted in an unidentifiable mixture.

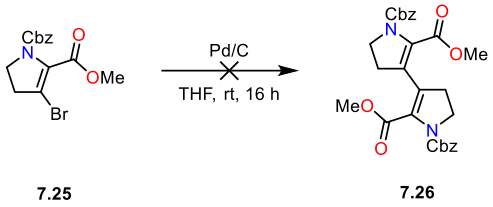

Scheme 7.18: Attempt to dimerise vinylic bromide **7.25** through a reductive coupling with palladium

Another method to perform a homocoupling would be to use a lithium-halogen exchange strategy followed by dimerisation of the resultant lithiate. This type of transformation has been shown to occur on similar pyrrole-derived bromides by Wasserman's Group.[212] By using *n*-butyllithium in combination with copper (II) bromide they were able to couple bromo pyrrole **7.27** in a symmetrical dimerisation to afford the bipyrrole product **7.28** (**Scheme 7.19**).

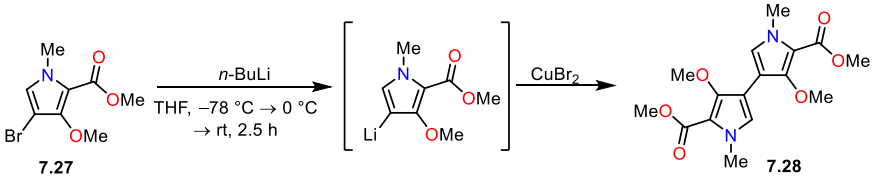

Scheme 7.19: Wasserman's homocoupling of bromomethoxy pyrrole **7.17** *via* halogen lithium exchange then addition of copper (II) bromide

When applying this methodology to our own system, the reaction resulted in the cleavage of the carbamate protecting group (**7.29**) and no homo-coupling (**7.26**) (**Scheme 7.20**).

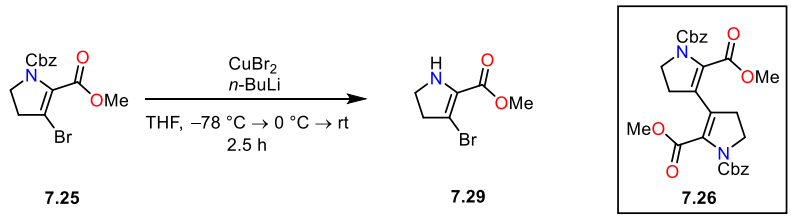

Scheme 7.20: Attempted homo coupling of **7.25** *via* halogen lithium exchange then addition of copper (II) bromide

To discover if the required lithium salt was formed during the reaction, we employed a D_2O quench to try and trap the lithiate. Monitoring the reaction through using ^2H NMR spectroscopy would enable us to ascertain if any deuterated product had formed during the quench of the lithium cation. We performed the reaction and varied the type of butyllithium base (**Scheme 7.21**). Conducting the reaction with *n*-butyllithium resulted in no deuteration of **7.25**. Instead, we observed cleavage of the carbamate protecting group, which was evident by the formation of benzyl alcohol. This is presumably a result of the butyl anion adding to the amide of the carbamate protecting group and eliminating benzyl alcohol. This observation matched the result seen earlier in the coupling of **7.25** using *n*-butyllithium and copper (II) bromide (**Scheme 7.20**). Moving to a more hindered alkyllithium, we performed the reaction with *sec*-butyllithium. Again no deuteration or nitrogen deprotection was observed, but starting material was recovered instead. As a last resort we moved on to using the most hindered and basic member of the butyllithium family; *tert*-butyllithium. This final reaction led to no deuteration or deprotection and hence efforts to perform a lithium halogen exchange reaction on substrate **7.25** ended here.

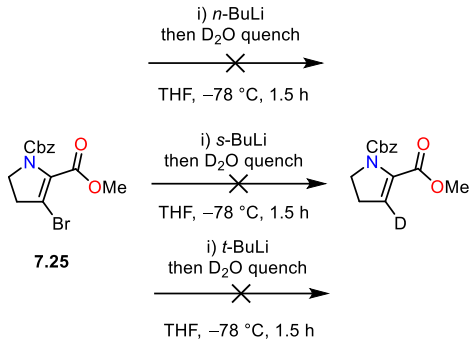

Scheme 7.21: Attempts at lithium halogen exchange reactions with a D_2O quench

7.4.7 Attempts at Cross Coupling of Enamine Derivative 7.25

Due to being unable to perform a lithium halogen exchange with vinyl bromide **7.25**, attempts were made to synthesise the vinyl iodide equivalent (**7.30**). The iodo derivative (**7.30**) was thought to be a superior coupling partner for the cross-coupling reactions due to the weaker C–I bond, and therefore allowed a more facile oxidative addition across the bond. By adapting the conditions used for synthesising the bromo equivalent (**7.25**), NIS in combination with DABCO were mixed with **7.24** to try and synthesise the iodo derivative. Unfortunately, this resulted in recovered starting material (**Scheme 7.22**). Halogen exchange was also attempted through a Finkelstein reaction on vinyl bromide **7.25** mediated by sodium iodide and tosic acid.[213] This again proved unsuccessful and resulted in decomposition of the starting material (**7.25**).

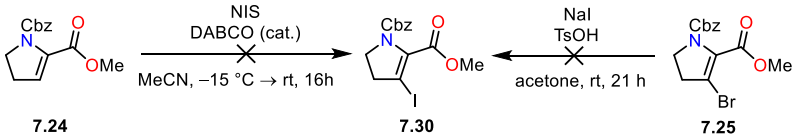

Scheme 7.22: Effort to synthesis vinyl iodide **7.30**

After this set back in synthesising the iodo derivative (**7.30**), the focus moved back to the functionalisation of the alkenyl bromide **7.25**. Specifically we sought an alternate method to substitute the halogen with functional groups suitable for cross-coupling reactions. One route to form a suitable cross-coupling partner would be borylation chemistry. If we gained access to a

boronic ester, or equivalent coupling partner, this would enable us to perform a Suzuki–Miyaura cross-coupling reaction to form the key dimeric core. To achieve this transformation, we first tried a one pot Miyaura borylation and Suzuki–Miyaura cross coupling reaction to form dimeric product **7.26** (**Scheme 7.23**).[214] Sadly, no reaction occurred with the borylating reagent or palladium source. We next tried to isolate the boronic ester to confirm whether it was being formed during the Miyaura borylation reaction.[215] Unfortunately, we never saw any incorporation of boron, which was confirmed using ^{11}B NMR spectroscopy.

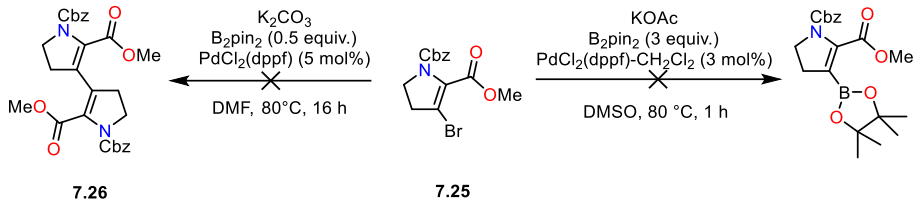

Scheme 7.23: Attempts at one-pot Miyaura borylation/Suzuki coupling and a single Miyaura borylation

Due to being unable to find conditions suitable for introducing boron, we sought for conditions to add a different metal in to the C3 position. Paterson and co-workers reported the use of modified Wulff–Stille conditions for a stannylation of a vinyl bromide with a methyl ester group (**7.31**) (**Scheme 7.24a**). [216,217] They employed the milder conditions of hexamethylditin ($(SnMe_3)_2$) as the source of tin, in combination with a palladium source ($Pd(PPh_3)_2Cl_2$), and Li_2CO_3 for the stannylation. To see if these conditions would be tolerated by our system, we performed the reaction with our vinyl bromide **7.25** (**Scheme 7.24b**). To our delight the stannylation worked, albeit with poor conversion to the product (**7.32**).

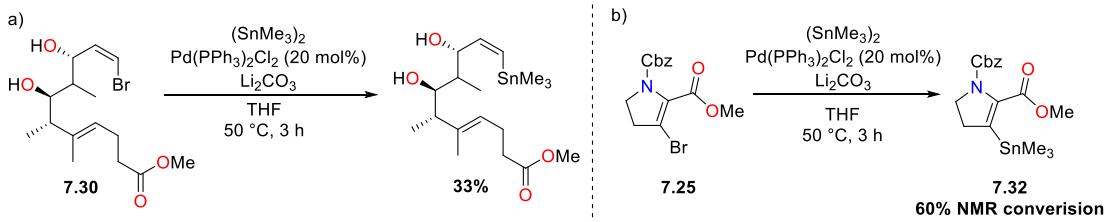

Scheme 7.24: a) Paterson's use of Wulff–Stille conditions on an intermediate (**7.30**) towards the total synthesis of leiodermatolide b) Wulff–Stille conditions applied to vinyl bromide **7.25**

To improve the efficiency of the reaction, we investigated running the reactions in different solvents in order to heat the reaction to higher temperatures (**Scheme 7.25**). These elevated-temperature stannylations were run in 2-MeTHF at 80 °C and in 1,4-dioxane at 100 °C. We saw comparable improved conversions at both conditions, but obtained slightly better yields when using 1,4-dioxane as the solvent. Therefore, the decision was made to scale up the reaction using 1,4-dioxane and we were able to form the novel stannane **7.32**, in an optimised 80% yield (100 mg).

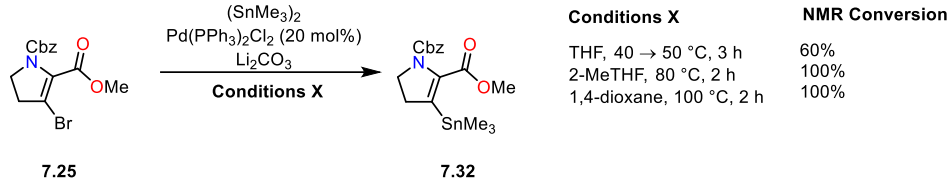

Scheme 7.25: Optimisation of the stannylation reaction at different temperatures

This represents the second functional group to be successfully inserted into this position on the 5-membered ring other than a halogen. With vinyl stannane **7.32** and vinyl bromide **7.25** in hand, we now had access to both partners required for a Stille cross-coupling reaction.

This part of the investigation began with using catalytic amounts of palladium-tetrakis(triphenylphosphine) in DMF in the presence of $Ph_2PO_2NBu_4$ as a tin halide scavenger (**Scheme 7.26**).[218] Copper thiophene carboxylate was added because copper salts are well known to accelerate Stille reactions.[219] It was hard to determine *via* NMR spectroscopy whether the reaction was successful, as the difference in proton and carbon chemical shift between the bromo monomer (**7.25**) and the symmetrical dimer (**7.26**) was likely to be small. However, we could see consumption of the stannylated monomer (**7.32**) through disappearance of the diagnostic peak at 0.2 ppm in the ^{1}H NMR spectrum, corresponding to the nine hydrogens on the $SnMe_3$ group. It was hypothesised that compound **7.32** undergoes proto-destannylation under these conditions and hence forms compound **7.24** (**Scheme 7.26**). This was later confirmed by the identification of the molecular ion peak corresponding to compound **7.24**. The mass spectrum also showed peaks that could relate to both **7.26** and **7.25**, but both fell outside the acceptable range of ppm (± 5.0 ppm).

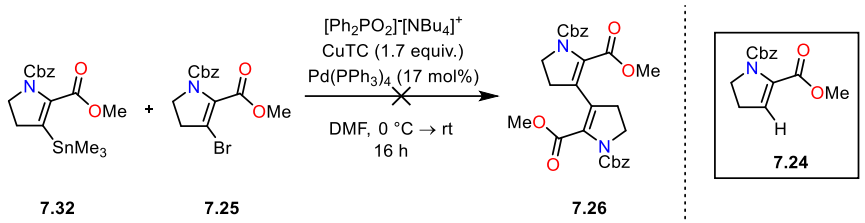

Scheme 7.26: Attempted Stille cross-coupling reaction between stannane **7.32** and bromide **7.25**

Due to the Stille cross-coupling reaction providing inconclusive results, we next tried to perform the reaction with a simpler aryl halide. Iodobenzene (**7.33**) would provide a suitable cross-coupling partner as well as forming a non-symmetrical cross-coupled product that would aid in product identification. By subjecting stannane **7.32** and iodobenzene (**7.33**) to the same reaction conditions previously trialled we were able to confirm product formation (**Scheme 7.27**). Although successful, the residual tin halide scavenger proved impossible to separate from product **7.34** and had to be prepared fresh each time it was used.[220] Therefore alternative Stille conditions developed by Baldwin using caesium fluoride were investigated (**Scheme 7.27**).[221] This resulted in a much cleaner reaction and simpler purification of product **7.34**.

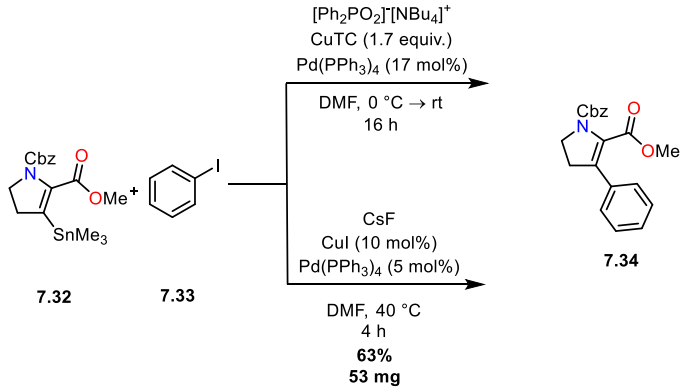

Scheme 7.27: Stille cross-coupling reactions between stannane **7.32** and iodobenzene (**7.33**)

Conducting Stille reactions on these model dehydroproline units (**7.32**) enabled us to develop workable conditions for performing a Stille cross-coupling reaction later in the synthesis.

7.4.8 Late-Stage Functionalisation of (+)-Dehydrodeoxybrevianamide E (4.45)

Alongside the pre-functionalisation approach, another route was investigated towards the total synthesis of brevianamide S (**7.1**). This focused on a late-stage functionalisation and coupling two monomeric units (**7.9** and **7.10**) derived from (+)-dehydrodeoxybrevianamide E (**4.45**) (**Scheme 7.28**). The key challenges faced in this route would first be the synthesis of the two monomeric units (**7.9** and **7.10**) and then finding suitable conditions to form the central C–C bond between the two.

Investigations into the first challenge began with trying to install a versatile functional group into the required position on the ring. This would then be followed by finding conditions for a dehydrogenation to form the exo-cyclic double bond present in monomers **7.9** and **7.10**.

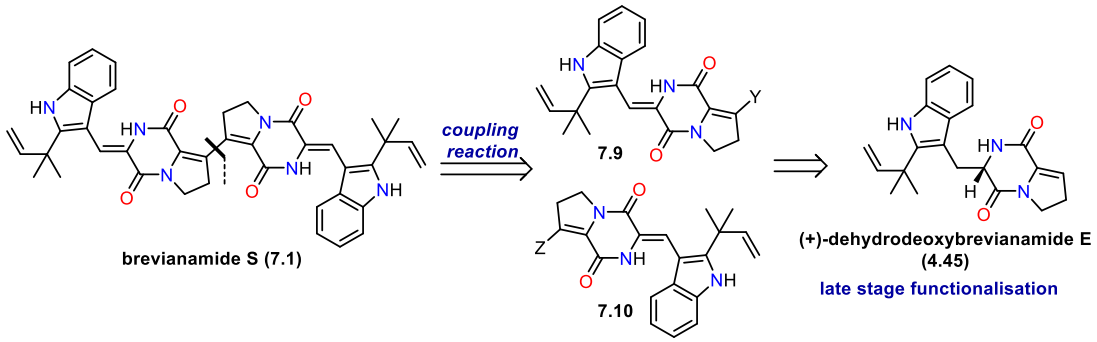

Scheme 7.28: Retrosynthetic plan for synthesis of brevianamide S through late-stage functionalisation of (+)-dehydrodeoxybrevianamide E (**4.45**)

7.4.9 Halogenation of (+)-Dehydrodeoxybrevianamide E (4.45)

A versatile synthetic handle to achieve this transformation would be the installation of a halogen. Previously, while working on this project, Dr Nick Green developed conditions for the functionalisation of (+)-dehydrodeoxybrevianamide E (**4.45**) through a facile iodination procedure. This proceeded through initial indole oxidation to form halo-indolenine intermediate **7.35** (**Scheme 7.29**). When subjected to polar conditions, such as performing the reaction in DMF, the halo-

indolenine intermediate undergoes an isomerisation to form the desired product with the halogen positioned on the 5-membered ring (**7.36**). I was able to repeat this reaction on larger scale than previously performed to gain access to a key synthetic intermediate in our retrosynthetic plan.

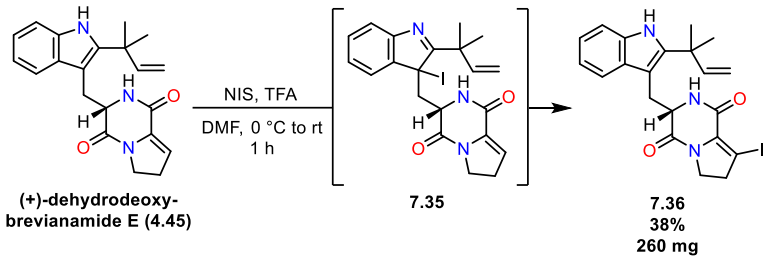

Scheme 7.29: Iodination of (+)-dehydrodeoxybrevianamide E (**4.45**) *via* halo-indolenine intermediate **7.35** to form compound **7.36**

7.4.10 Dehydrogenation of Iodo Derivative 7.36 and Brevianamide K (7.4) Synthesis

To install the exo-cyclic double bond, several dehydrogenation approaches were investigated. In 2000, Mukaiyama and co-workers developed methodology to perform a range of dehydrogenations using a new sulfur reagent, *N*-*tert*-butyl phenylsulfinimidoyl chloride (**7.37**) (TBPSC).[222] This strategy has been applied to the dehydrogenation of a wide a range of compounds including ketones[223] and carbamates.[224] The one-pot procedure proceeds through a non-isolatable sulfimide intermediate (**7.38**) that collapses through a pericyclic *ene*-type reaction (**Scheme 7.30**).

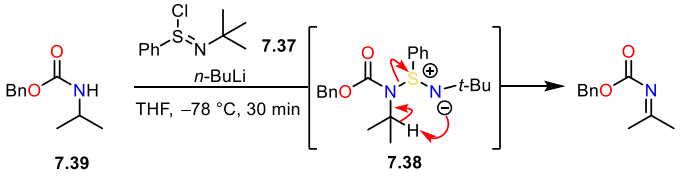

Scheme 7.30: Dehydrogenation of carbamate **7.39** using Mukaiyama's reagent

Mukaiyama's reagent (**7.37**) is synthesised in two steps from *tert*-butylamine (**7.40**) and proceeds through a dichloroamine intermediate **7.41** (**Scheme 7.31**). Due to the high instability of the chloro sulfinimidoyl intermediate it was necessary to freshly prepare it before each use and for it to be stored in the freezer.

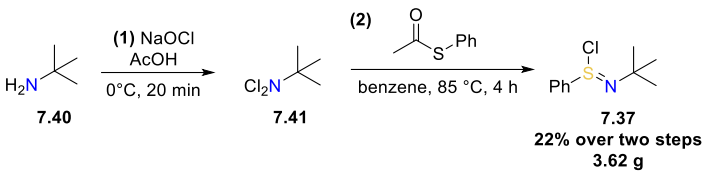

Scheme 7.31: Two step synthesis of Mukaiyama's reagent (**7.37**) from *tert*-butylamine (**7.40**)

Dehydrogenation using Mukaiyama's reagent (**7.37**) in combination with Barton's base (**7.43**), were first successfully applied to our system by Dr Robert Godfrey in a test reaction to form 2 mg of **7.42** in a 13% yield. Following this initial hit, I was able to perform the dehydrogenation to synthesise compound **7.42** in an improved yield of 32% yield (**Scheme 7.32**).

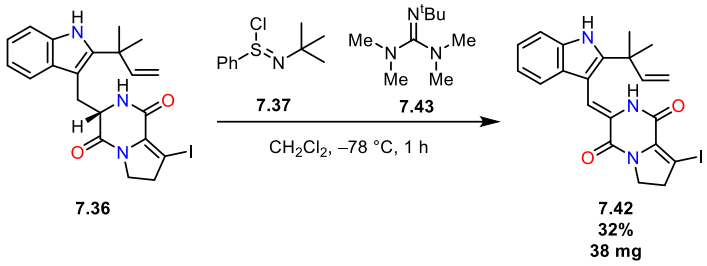

Scheme 7.33: Dehydrogenation of **7.36** using Mukaiyama's reagent and Barton's base

In parallel to these reactions, this newly developed methodology was used to form another member of the brevianamide natural product family. Brevianamide K (**7.4**) was first isolated from the fungus *Aspergillus versicolor* in 2009 by Zhang and co-workers, and contains the key diketopiperzine ring motif found in brevianamide type natural products.[196] Structurally, it is related to (+)-dehydrodeoxybrevianamide E (**4.45**) through a dehydrogenation α to the amide. For that reason we subjected (+)-dehydrodeoxybrevianamide E (**4.45**) to the conditions developed earlier for the dehydrogenation (**Scheme 7.34**). Gratifyingly this was successful and completed the first total synthesis of brevianamide K (**7.4**) in 6 steps. When I repeated this, I was able to improve the dehydrogenation yield slightly to 62% yield from 55%.

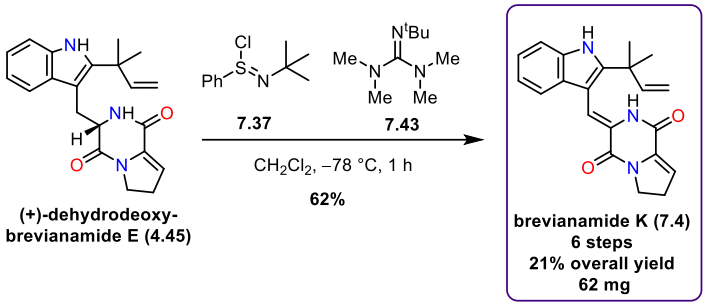

Scheme 7.34: Synthesis of brevianamide K (**7.4**) through dehydrogenation of (+)-dehydrodeoxybrevianamide E (**4.45**)

7.4.11 Attempts at Cross Coupling of Iodo Derivative 7.42

Returning to the main aim of this project; namely the synthesis of brevianamide S (**7.1**), with access to the dehydrogenated halogenated precursor (**7.42**) now achieved, we concentrated on installing a functional group that could function as a cross-coupling handle. Using this promising halogenated intermediate (**7.42**) we looked into methods for further functionalisation. Again we investigated the possibility of performing a lithium-halogen exchange followed by a sequential quench with different electrophiles. We chose electrophiles that would lead to compounds that could be utilised

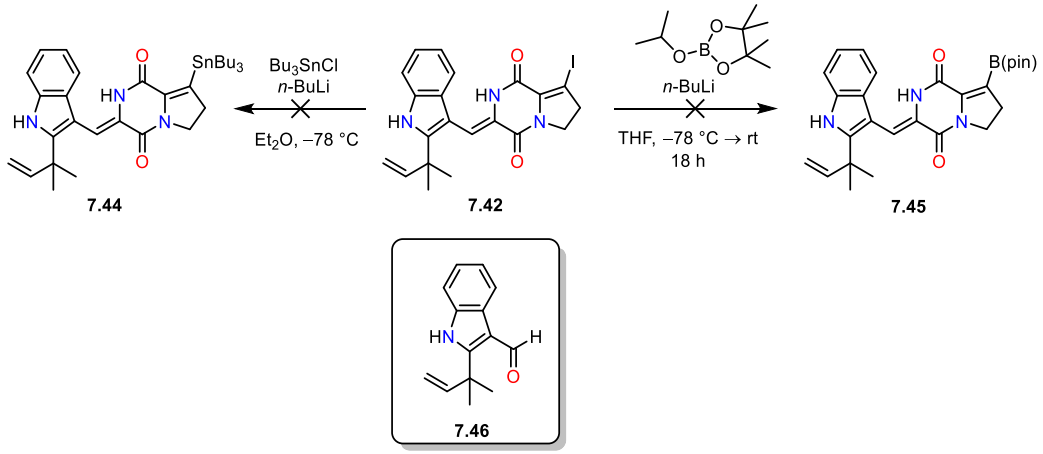

Scheme 7.35: Attempted stannylation and borylation of **7.42** *via* lithium halogen exchange and electrophilic quench strategy and formylated product **7.46**

in cross-coupling reactions. Therefore, we performed the reaction with tributyltin chloride[225] to permit stannane formation (**7.44**), and isopropoxy-tetramethyl-dioxaborolane[226] to form the boronic ester (**7.45**) (**Scheme 7.35**). Unfortunately, yet again we were unable to apply this lithium-halogen

exchange methodology to our system and saw no formation of the desired functionalised products (**7.44** or **7.45**). In both reactions we saw the formation of the same formylated indole **7.46**, although we were unable to isolate the diketopiperazine fragment.

This formylated indole product (**7.46**) is hypothesised to form *via* a retro-aldol type mechanism during the work-up under aqueous conditions (**Scheme 7.36**).

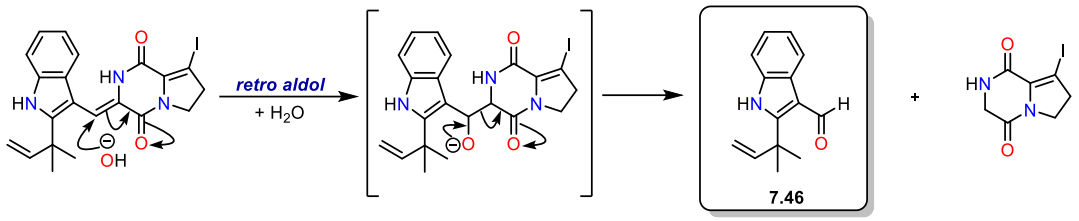

Scheme 7.36: Potential retro aldol mechanism for the formation of **7.46**

This type of reactivity is not dissimilar to the retro aldol reaction observed for the natural product neoechinulin B (**7.47**).[227] Neoechinulin B (**7.47**) was isolated in 1973 by Casanati and co-workers and is a structurally related natural product containing both an indole and diketopiperazine moieties.[228] It was found that under basic conditions neoechinulin B underwent a retro aldol to fragment into two products (**Scheme 7.37**).

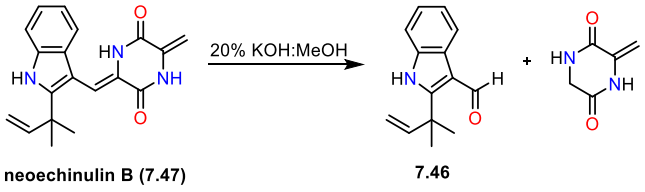

Scheme 7.37: Retro aldol of neoechinulin B (**7.47**) under mildly basic conditions

Since compound **7.42** was potentially unstable under basic conditions, we returned to the chemistry performed previously on the model dehydroproline unit (**7.25**, **Scheme 7.25**, **page 145**). This involved an alternative method for stannylation using palladium insertion into the C–I bond. This enabled us to insert a tin group into the required position to form novel stannane **7.48**, in 63% yield (**Scheme 7.38**).

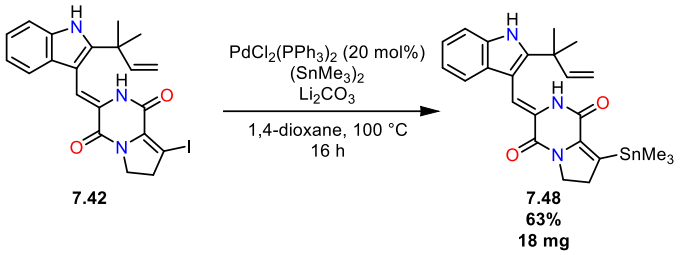

Scheme 7.38: Stannylation of iodo derivative **7.42** using palladium chemistry

With access to this promising intermediate (**7.48**), we now had both partners required for a Stille cross-coupling reaction. Using the previous knowledge gained from performing Stille cross-couplings on the model dehyrdoproline system (**Scheme 7.27**, **page 146**), we opted for Baldwin's Stille conditions (**Scheme 7.39**). [221] Full consumption of the stannylated compound (**7.48**) was again evident from the diagnostic $SnMe_3$ peak disappearing in the ^1H NMR spectrum (0.2 ppm). The major product matched the NMR spectrum of brevianamide K (**7.4**), which could be either a result of protodehalogenation or protodestanylation.

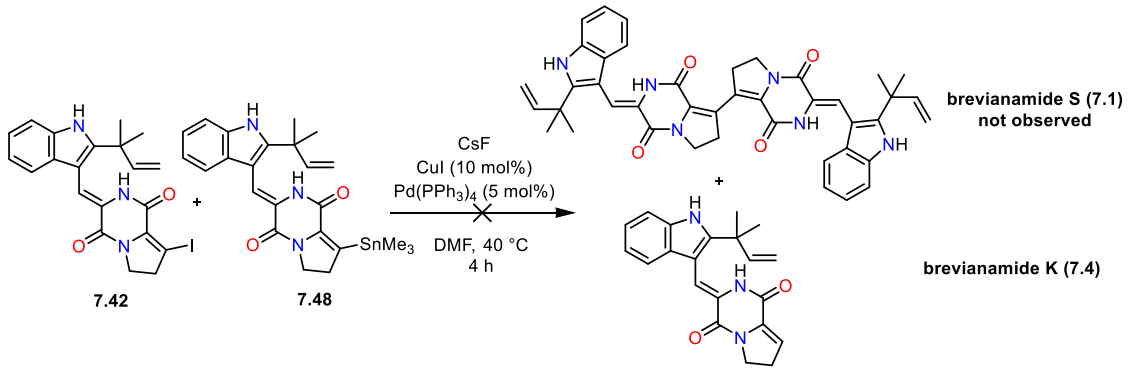

Scheme 7.39: Attempts at a Stille cross-coupling reaction with **7.42** and **7.48**

Further Stille cross-coupling conditions were tested, including performing the reaction at higher temperatures, the removal of the copper iodide, and an alternative palladium source. However, with limited time and access to material it was not viable to investigate this Stille cross-coupling reaction further. A full summary of the route investigated is shown below (**Scheme 7.40**).

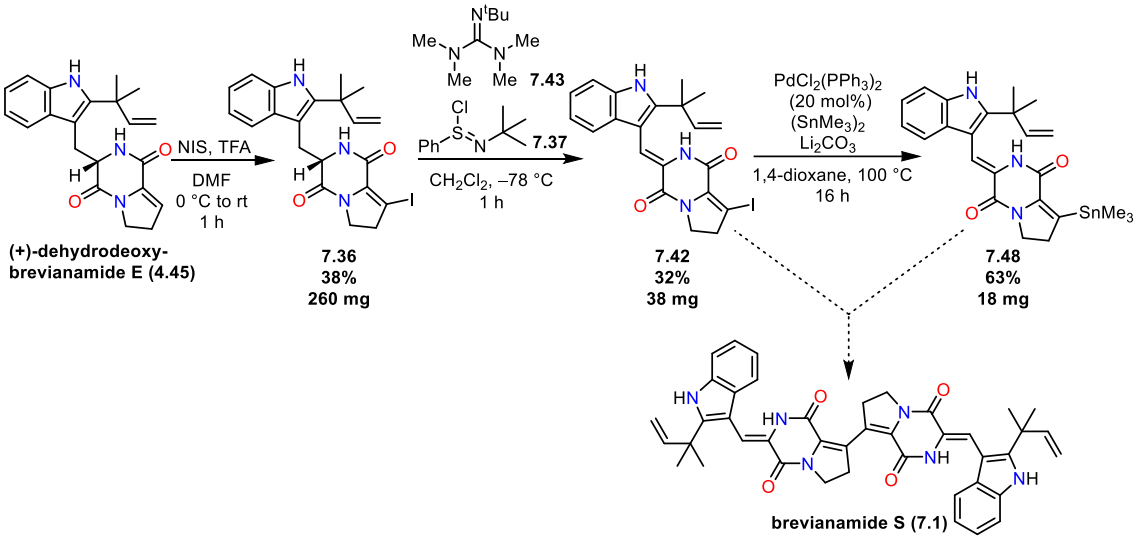

Scheme 7.40: Summary of route through stannylated intermediate **7.48** towards brevianamide S (**7.1**)

7.4.12 Homo Coupling of (+)-Dehydrodeoxybrevianamide E (4.45) and 7.36

Having failed to perform a successful cross-coupling reaction between the two monomeric units (**7.42** and **7.48**), we explored the possibility of conducting a homo coupling instead. In 1992, Gribble and co-workers demonstrated the dimerisation of keto lactams under using simple conjugate addition chemistry (**Scheme 7.41**).[229]

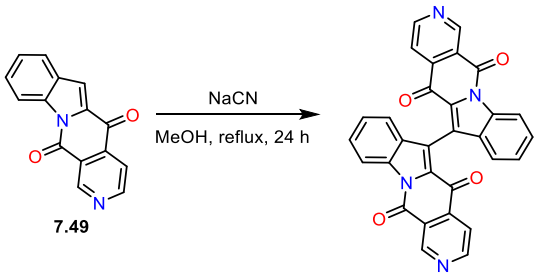

Scheme 7.41: Gribble's dimerisation of keto lactam **7.49** through C3 of indole ring

Extending this approach to our system (+)-dehydrodeoxybrevianamide E (**4.45**) was treated with sodium cyanide under reflux for 24 h (**Scheme 7.42**). Unfortunately, under these conditions we saw no evidence of any reaction occurring. Even if the cyanide anion added to the double bond of the

α,β-unsaturated system successfully, we have the added complication of having two potential nucleophiles within molecule **4.45**. One nucleophilic site could be the C3 position of the indole, which would result in an unwanted dimeric product. The other would be through the C19 position on the fused 5-membered ring, which would lead to the desired dimeric product **7.5**.

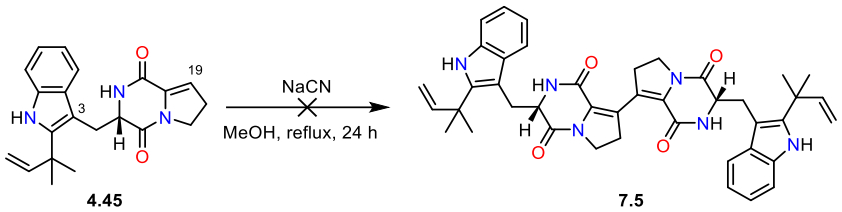

Scheme 7.42: Bioinspired dimerisation attempts to form ddE_2 (**7.5**) dimer

Due to lack of success in applying a conjugate addition coupling strategy for the homo-coupling, we returned to the iodinated derivative (**7.42**) of (+)-dehydrodeoxybrevianamide E (**4.45**) to explore its chemistry further. Ullman-type reductive coupling reactions are usually confined to the coupling of aryl halide substrates, but there have been limited examples of using alkenyl halides.[210] In 1997 Liebeskind and coworkers reported mild conditions using copper thiophene carboxylate as the reductant for room temperature coupling of alkenyl iodides (**Scheme 7.43**).

Initially the Ullman coupling reaction was performed the original reaction on substrate **7.50** from the paper. This was performed on both the scale of the paper (2.4 mmol), and at the scale planned for the dimerization of **7.42** (0.16 mmol) (**Scheme 7.43**).

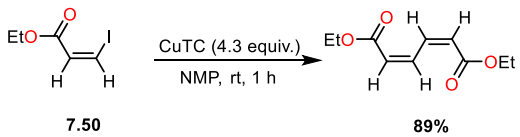

Scheme 7.43: Original Ullman coupling of alkenyl iodide **7.50**

Once confident with performing the reaction on a small scale I applied it to our own system. We heated the iodo-substituted (+)-dehydrodeoxybrevianamide E (**4.45**) in NMP with copper thiophene

carboxylate to afford the (+)-dehydrodeoxybrevianamide E dimer (ddE$_2$, **7.5**) in a yield of 66% (**Scheme 7.44**).

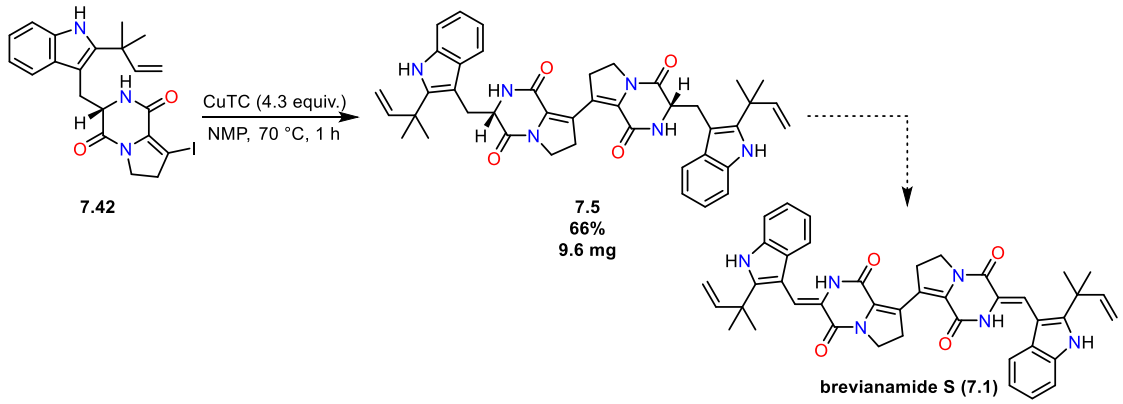

Scheme 7.44: Ullman coupling of **7.42** to form dimer **7.5**

To the best of our knowledge, this represents the first linkage between two diketopiperazine units at this position. This unique dimer scaffold presents a viable route towards the dimeric members of the brevianamide natural product family. Synthetically, dimer product **7.5** is a double dehydrogenation away from completing the first total synthesis of the dimeric natural product brevianamide S (**7.1**).

7.4.13 Attempts at Dehydrogenation of Dimer 7.5

We initially looked to use the conditions developed earlier in the synthesis of brevianamide K (**7.4**), using Mukaiyama's reagent (**7.37**) in combination with Barton's base (**7.43**), to perform the desired double dehydrogenation. Unfortunately, under these conditions we saw no evidence of reaction (**Scheme 7.45**). This indicated that a stronger base than Barton's (**7.43**) was required for the dehydrogenation of dimer **7.5**.

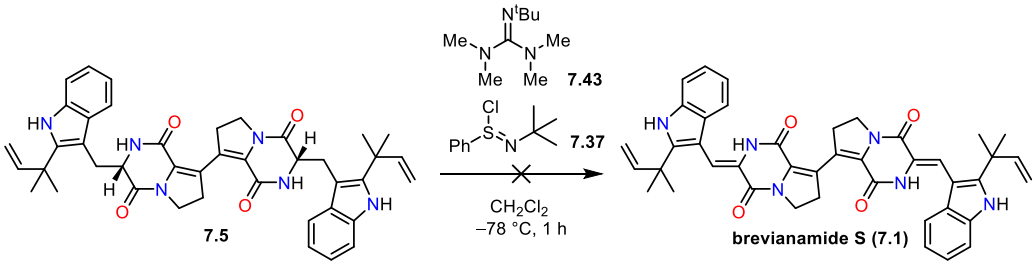

Scheme 7.45: Attempt at dehydrogenation of dimer **7.5** to form brevianamide S (**7.1**)

Typical dehydrogenations using Mukaiyama's reagent in the literature utilise LDA as the basic partner in the reaction.[230] The use of even under more basic conditions (LDA) for the dehydrogenation, we still saw no reaction with Mukaiyama's reagent (**Scheme 7.46**). As a final attempt to dehydrogenate the dimer (**7.5**) we used DDQ as it has previously been shown to oxidise certain indolic enamides derived from tryptophan.[231] This resulted in a mixture of inseparable compounds with no indication of brevianamide S (**7.1**) or starting material (**7.5**).

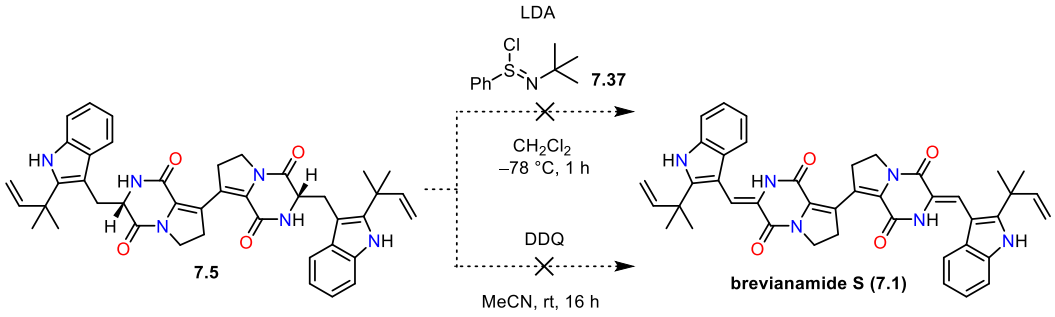

Scheme 7.46: Dehydrogenation attempts of ddE_2 (**7.5**) to form brevianamide S (**7.1**)

With limited dimer available for more test reactions, we used the earlier intermediate **7.36** to develop conditions for the dehydrogenation.

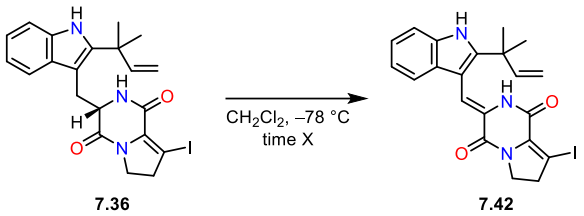

Entry	Conditions	Time	Outcome
1	Barton's base/Mukaiyama's reagent	1 h	32%
2	Barton's base/Mukaiyama's reagent	16 h	28%
3	P_1-*t*-Bu/Mukaiyama'sreagent	15 min	RSM
4	PhNO/$ZrCl_4$	16 h	RSM

Table 7.1: Conditions tested for dehydrogenation of iodo derivative **7.36**

We left the reaction stirring overnight to ascertain if longer reactions times using Barton's base would improve the reaction. This resulted in a small decrease in isolated yields of **7.42** (**Table 7.1,**

Entry 2), which indicated that increasing the time of the reaction would not help. Due to no reactivity being observed with LDA and Mukaiyama's reagent we instead used an organic superbase, phosphazene P_1-*t*-Bu, (**Table 7.1, Entry 3**). Once more, we saw no reaction with this stronger base.

Moving away from using Mukaiyama's reagent for the dehydrogenation, Baran and co-workers have developed conditions to perform direct dehydrogenation on a range of tryptophan derivatives.[165] One of the tryptophan derivatives used bears a strong resemblance to our iodinated derivative (**7.36**) (**Scheme 7.47**). Repeating Baran's conditions using nitrosobenzene and zirconium tetrachloride for the dehydrogenation of **7.36**, regrettably resulted in recovered starting material (**Table 7.1, Entry 4**). In Baran's screen of related tryptophan derivatives none of them possessed a group at the C2 position of the indole ring. Instead, they opted for the installation of groups at C2 after the dehydrogenation. This suggests that the reaction may not be compatible with indoles bearing a group at C2.

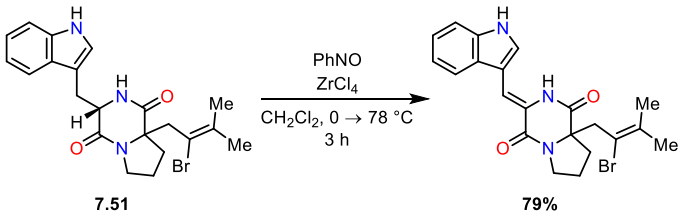

Scheme 7.47: Baran's direct dehydrogenation of a tryptophan derivative with a diketopiperazine ring (**7.51**)

Due to the inability to dehydrogenate dimer **7.5** or find any promising conditions for an alternative dehydrogenation methods in **Table 7.1**, the investigations towards the total synthesis of brevianamide S (**7.1**) paused here.

7.4.14 Derivative Synthesis

Having been able to synthesise an iodo derivative (**7.36**) of (+)-dehydrodeoxybrevianamide E (**4.45**), we wanted to test the feasibility of a cross-coupling reaction. To prove that palladium insertion into the C–I bond of the five-membered ring was possible, iodo derivative (**7.36**) was

reacted with a less hindered and more reactive coupling partner; phenyl boronic acid. Using classic Suzuki–Miyaura conditions we performed the cross-coupling reaction which resulted in the phenylated product (**7.52**) in 65% yield (**Scheme 7.48a**).[205]

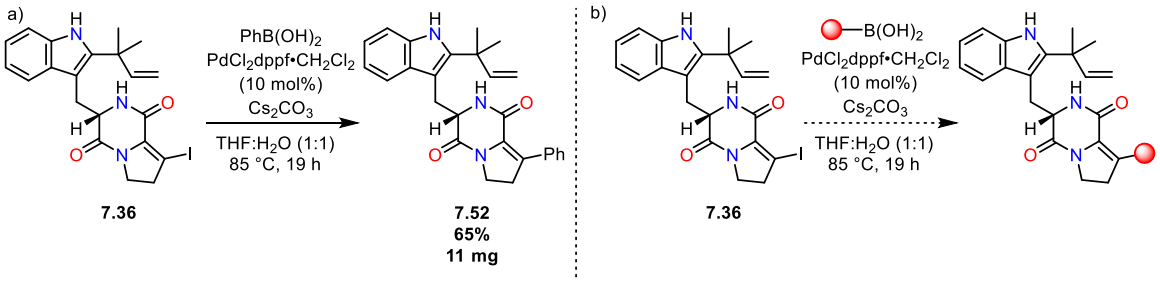

Scheme 7.48: a) Suzuki–Miyaura cross-coupling of iodo derivative **7.36** with phenyl boronic acid b) Route for potential derivative synthesis of (+)-dehydrodeoxybrevianamide E

Achieving this cross-coupling highlights an entry point for divergency in our synthesis. A range of different aryl and alkenyl groups could be coupled into this system, giving the opportunity to synthesise a small library of potentially biologically active derivatives of the natural product (+)-dehydrodeoxybrevianamide E (**4.45**) (**Scheme 7.48b**).

The Suzuki–Miyaura reaction developed for iodide **7.36** was simultaneously successful for the bromide (**7.25**) (**Scheme 7.49a**). Additionally, stannane **7.32** may also constitute a viable entryway into derivatives, as it successfully underwent a Stille coupling with iodobenzene (**7.33**) to form **7.34** (**Scheme 7.49b**). Again, this highlights a potential entry for derivative synthesis. This reaction should be possible with a wide range of boronic acids/esters and aryl halides, which should provide accesss to various substituted dehydroproline compounds. This is notable because it demonstrates that the proline unit can act as both a nucleophile and an electrophile at this position and therefore is synthetically versatile.

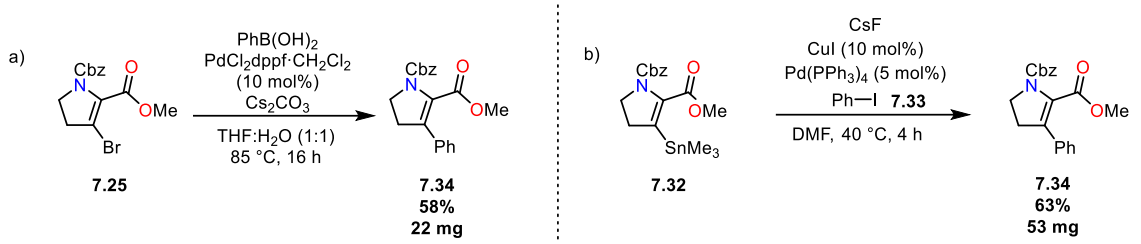

Scheme 7.49: a) Suzuki–Miyaura cross-coupling reaction of **7.25** and phenyl boronic acid b) Stille cross-coupling reaction of **7.32** and iodobenzene

7.5 Conclusion

Although unsuccessful in our goal to complete the first total synthesis of brevianamide S (**7.1**) we have made significant progress with two distinct routes towards the natural product. Both routes are currently a single transformation away from the natural product (**Scheme 7.50**). The first route was centred around performing a late-stage coupling reaction on functionalised intermediates. We synthesised two distinct coupling partners **7.42** and **7.48** during this investigation. This involved developing conditions to perform an alkenyl oxidation of the 5-membered ring to install a halogen, followed by optimising a crucial stannylation reaction to yield stannane **7.48**. Finally, protocols were developed for a dehydrogenation reaction using Mukaiyama's reagent (**7.37**) to install the core *exo*-cyclic double bond.

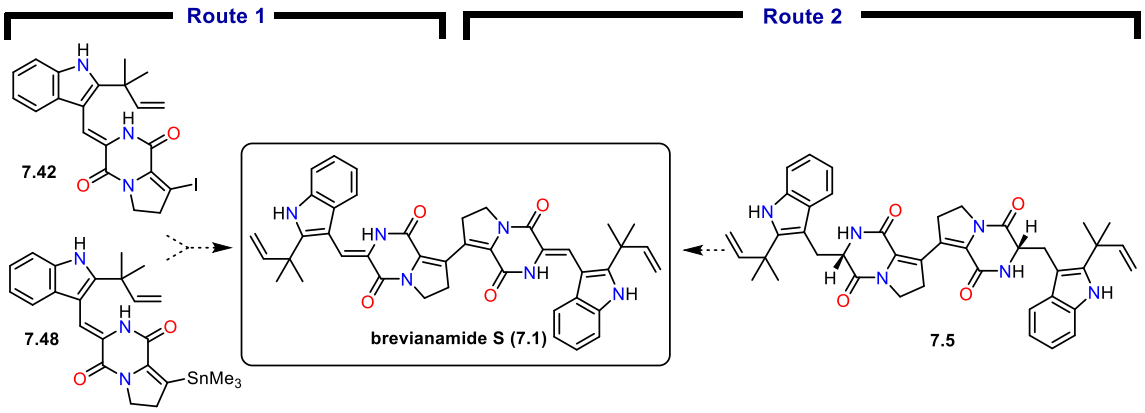

Scheme 7.50: Routes trialled towards brevianamide S (**7.1**)

Studies into the second route allowed the development of the core dimeric structure of brevianamide S (**7.1**) *via* a key reductive Ullman-type coupling, which is just a single dehydrogenation reaction away from the product. This unique C–C bond between the two monomeric units is the first linkage at this position in the literature.

Novel derivatives of (+)-dehydrodeoxybrevianamide E (**4.45**) and the dehydroproline moiety (**4.74**) have been successfully synthesised (**Scheme 7.51**). By using the halogenated and stannylated compounds, synthesised during the course of the project, we were able to make derivatives through cross-coupling reactions. These cross-coupling reactions provide potential for the synthesis of libraries of derivatives in the future.

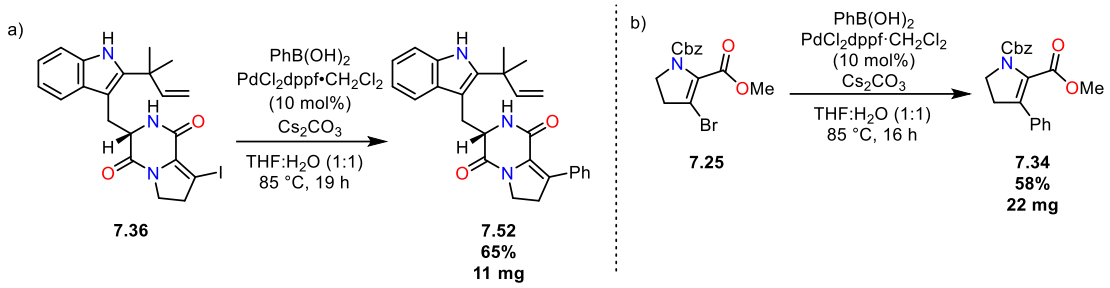

Scheme 7.51: Derivatives synthesised through Suzuki-Miyaura and Stille cross-coupling reactions

7.6 Future work

Future work in this project would involve investigating alternative dehydrogenation conditions for the final step in the total synthesis of brevianamide S (**7.1**) (**Scheme 7.52**).

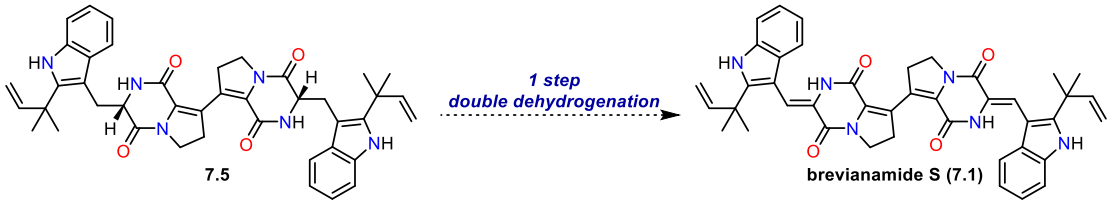

Scheme 7.52: Final double dehydrogenation step towards the synthesis of brevianamide S (**7.1**)

Enamides are synthetically useful building blocks and this is highlighted by their board spectrum of reactivity.[232] Consequently, there has been long standing interest in the chemical community to develop more methods to synthesise enamides. Most recently, Maulide and co-workers have developed a novel strategy towards enamides *via* *N*-dehydrogenation of amides using LiHMDS and

triflic anhydride in a one-step protocol with a broad substrate scope and good yields (**Scheme 7.53**).[233] This interesting combination of LiHMDS and triflic anhydride, functions as both the oxidant and the electrophilic activator in the reaction. This new methodology could be applied to the double dehydrogenation required in our brevianamide S (**7.1**) synthesis (**Scheme 7.52**).

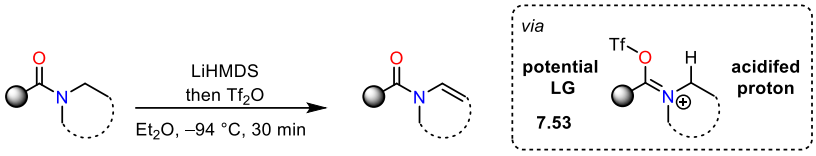

Scheme 7.53: Enamide formation through N-dehydrogenation of amides *via* activated intermediate **7.53**

If unsuccessful in performing the crucial double dehydrogenation, new routes could be investigated towards the synthesis of brevianamide S (**7.1**). During this project we saw first-hand evidence of a potential retro-aldol fragmentation occurring in our systems. Inspired by this, further investigations could lead to a constructive aldol condensation reaction, such as that seen in the reversible aldol reaction of neoechinulin B (**7.47**), which is a structurally related indole-fused diketopiperazine natural product (**Scheme 7.54**).[182,234–236]

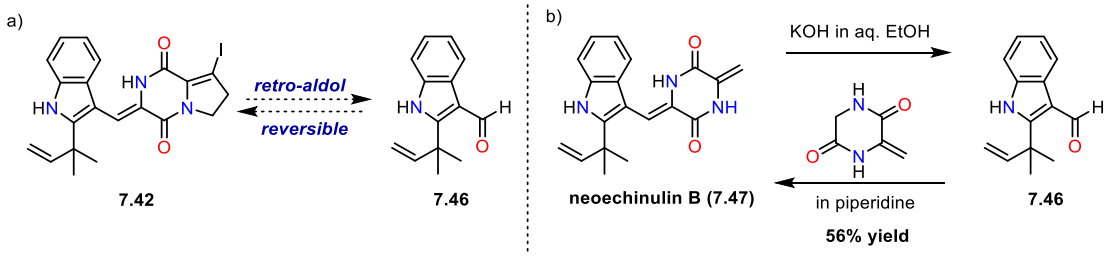

Scheme 7.54: a) Potential retro aldol of **7.42** to form formaulated product **7.46** b) Reversible retro aldol/aldol reaction of the related diketopiperzine natural product neoechinulin B (**7.47**)

By harnessing the inherent reactivity of these indolic diketopiperzine molecules to our advantage, an alternative synthesis of brevianamide S (**7.1**) can be envisaged. The key step of this convergent synthesis would be a "*three component"* double aldol condensation of the dimeric diketopiperazine

unit (**5.54**) with two molecules of the formylated indole (**7.46**) (**Scheme 7.55**). For example, indole **7.46** has previously been synthesised by Trauner and co-workers in 3 steps from indole.[182] This would diverge from the developed chemistry surrounding the synthesis of (+)-dehydrodeoxybrevianamide E (**4.45**) and could allow for a more elegant approach to the synthesis of brevianamide S (**7.1**). This route circumvents the previous problem of finding suitable dehydrogenation conditions.

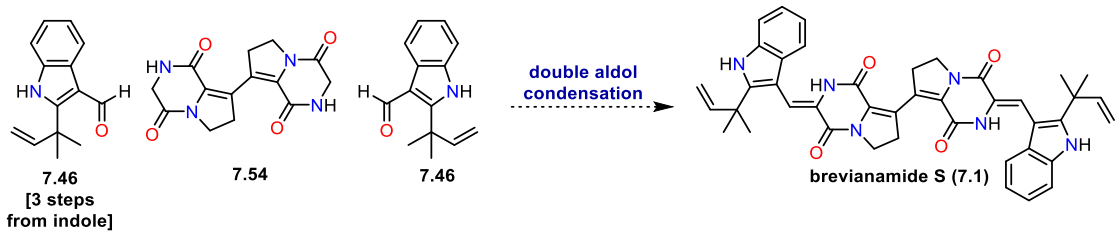

Scheme 7.55: "3 component" double aldol condensation to form brevianamide S (**7.1**)

The main challenges of this route would be developing conditions for the double aldol condensation, and formation of the fused diketopiperazine unit (**7.54**). A logical starting point for this route would be from diketopiperazine intermediate **7.55**, which is a known compound formed in 2 steps from the commercially dipeptide; cyclo-glycyl-L-proline.[237] We could then hopefully use chemistry developed during this project to achieve the synthesis of the core dimeric diketopiperazine scaffold (**7.54**) (**Scheme 7.56**).

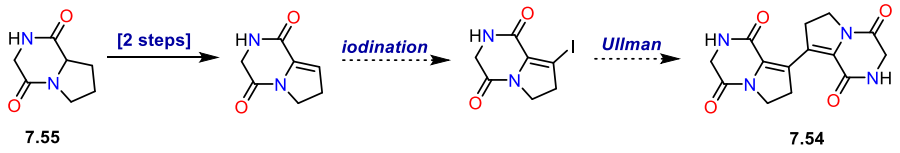

Scheme 7.56: Proposed synthesis of key fused diketopiperazine unit (**7.54**)

Further investigations into derivative synthesis could also be undertaken. Boronic coupling partners could be synthesised for use in Suzuki–Miyaura cross coupling reactions (**Scheme 7.57a**). As well as sourcing a range of commercially available aryl and alkenyl halides for use in Stille cross-coupling reactions (**Scheme 7.57b**). A small library of derivatives of (+)-

dehydrodeoxybrevianamide E (**4.45**) could be quickly synthesised, which could allow access to derivatives of brevianamide A (**4.1**) and B (**4.2**). Such derivatives have the potential for biological activity, which could be tested once access is gained to these compounds.

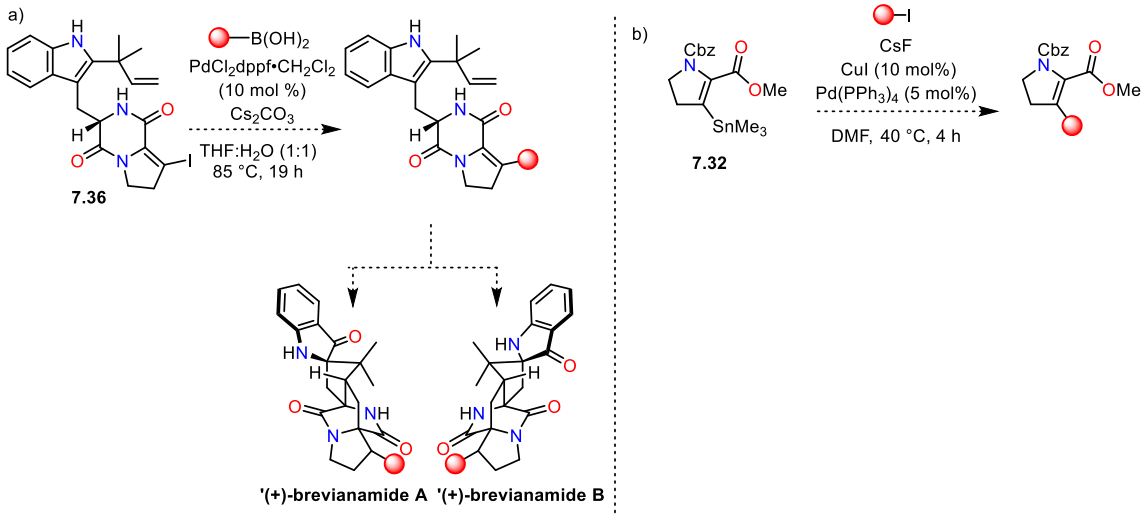

Scheme 5.57: a) Derivative synthesis of (+)-dehydrodeoxybrevianamide E (**4.45**) *via* a Suzuki–Miyaura leading to derivative of brevianamide A (**4.1**) and B (**4.2**) b) Derivative synthesis of dehydroproline unit *via* a Stille coupling

Chapter 8: Experimental Conditions

8.1 General Experimental

NMR Spectroscopy: ^{1}H and ^{13}C NMR Spectra were recorded in the deuterated solvent stated using an internal deuterium lock. ^{1}H NMR spectra were recorded at 600 MHz, 500 MHz, and 400 MHz using a Bruker AVANCE 600, Bruker AVANCE 500, Bruker PRO 500, Varian INOVA 500 or Bruker AVANCE 400 spectrometer and referenced to residual solvent proton resonance ($CDCl_3$ δ 7.26 ppm, DMSO δ 2.5 ppm, CD_2Cl_2 δ 5.3 ppm). Chemical shifts are given in ppm on a δ scale, and coupling constants (*J*) are reported to nearest 0.1 Hz. Peak multiplicities are defined as: s = singlet, d = doublet, t = triplet, q = quartet, qu = quintet, sxt = sextet, m = multiplet, app. = apparent, br. = broad. Assignment of proton signals was assisted by ^{1}H-^{1}H COSY, HSQC, HMBC and NOESY experiments. ^{13}C NMR spectra were recorded at 151 MHz, 126 MHz or 100 MHz using a Bruker AVANCE 600, Bruker AVANCE 500, Bruker PRO 500, Varian INOVA 500 or Bruker AVANCE 400 spectrometer and referenced to the solvent resonance ($CDCl_3$ δ 77.0 ppm, DMSO δ 39.5 ppm, CD_2Cl_2 δ 53.8 ppm). Assignment of carbon signals was assisted by HSQC, HMBC and NOESY experiments.

Infrared Spectroscopy: Infrared spectra of solids and liquids were recorded as neat samples on a Bruker Tensor 27 FT-IR spectrometer fitted with an ATR attachment.

Melting Point: Melting points were measured on a Gallenkamp Melting Point System or a Stanford Research Systems OptiMelt MPA100.

Mass Spectrometry: Accurate mass (HRMS) data was acquired on a Bruker MicroTOF instrument using electrospray ionisation (ESI+). High resolution values are calculated to 4 decimal places from the molecular formula, and all values are within a tolerance of 5 ppm.

Reagents, solvents and techniques: All reagents, obtained from Acros, Aldrich and Fluorochem fine chemicals suppliers, were used directly as supplied. Reactions were conducted under a positive pressure of dry nitrogen and the glassware was dried with a heat gun. Anhydrous solvents were

used and reaction were conducted at room temperature unless stated otherwise. The yields reported are shown as isolated yields unless otherwise stated. Reactions were monitored by thin layer chromatography on pre-coated aluminium-backed plates (Merck Kieselgel 60 with fluorescent indicator UV254, 0.2 mm). Spots were visualised by quenching of UV fluorescence fluorescence (λ_{max}= 254 nm) or by staining with potassium permanganate or vanillin. Flash column chromatography was performed according to the method described by Still, Kahn and Mitra[238] with silica gel obtained from Macherey Nagel (MN 60, 230–400 mesh) under positive nitrogen pressure. THF, toluene, and acetonitrile were purified using an inert technology PureSolv MD5 Solvent Purification Systems. DMSO was used as supplied without distillation. Anhydrous DMF was obtained by first stirring overnight over 4 Å molecular sieves, then refluxing under reduced pressure for 2 h, followed by distillation and was stored over 4 Å molecular sieves.

8.2 Experimental Conditions Chapter 2

8.2.1 General Procedure 1 – Epoxidation

Adapted from literature[37]

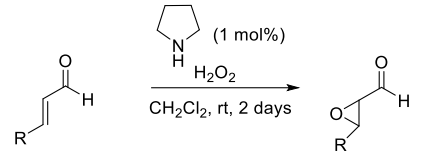

26, R = Me
40, R = C_3H_7

(±)-**33**, R = Me
(±)-**41**, R = C_3H_7

Pyrrolidine (1 mol%) was added to a solution of enal **X** (1.0 equiv.) in dichloromethane and stirred until the reaction turned slightly yellow. H_2O_2 (30 w/v%, 1.35 equiv.) was added dropwise and after 30 minutes of stirring at rt the reaction vessel was sealed and left to stir at ambient temperature for 2 days to achieve full conversion to the epoxy aldehyde. Solvent was removed *via* carefully controlled distillation (45 °C/600 mbar - 400 mbar).

8.2.2 General Procedure 2 - Imine formation

Adapted from literature [17]

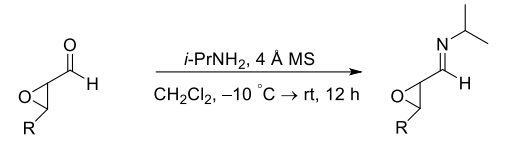

(±)-33, R = Me
(±)-41, R = C_3H_7

(±)-20, R = Me
(±)-42, R = C_3H_7

4 Å MS was added to a solution of epoxy aldehyde **X** (1.0 equiv.) in CH_2Cl_2. *Iso*propylamine (1.1 equiv.) was added dropwise to the mixture at −10 °C and left to stir at rt for 12 h. When complete the the reaction mixture was filtered by vacuum and the resulting cake washed copiously with CH_2Cl_2. The crude product was purified *via* vacuum distillation.

8.2.3 Experimental Procedure for Compound (±)-2.1

Compound **(±)-2.1** was prepared according to general procedure**1**.

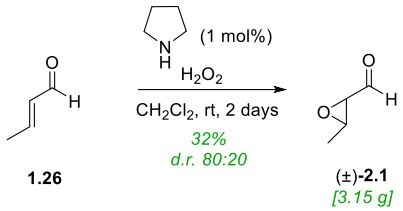

Crotonaldehyde (**1.26**) (10.0 mL, 1.0 equiv., 113 mmol) in CH_2Cl_2 (330 mL), pyrrolidine (0.95 mL, 0.01 equiv., 1.13 mmol) and H_2O_2 (15.6 mL, 30% w/w aq., 1.35 equiv., 153 mmol). Purified *via* vacuum distillation (28 ˚C/1 mbar) to give the title compound as a colourless oil (3.15 g, 36.6 mmol, 32%, *d.r.* 80:20).

R_f = 0.33 (petroleum ether 40/60:ethyl acetate, 7:3), [$KMnO_4$];

^{1}H NMR (600 MHz, $CDCl_3$) δ 9.47 (1H, dd, *J* = 5.1, 1.1 Hz)‡, 9.00 (1H, dd, *J* = 6.3, 1.1 Hz)†, 3.40 – 3.34 (2H, m)‡, 3.31 (1H, m)†, 3.09 (1H, dd, *J* = 6.3, 1.6 Hz)†, 1.47 (3H, dd, *J* = 5.5, 1.1 Hz)‡, 1.44 (3H, dd, *J* = 5.1, 1.1 Hz)† ppm;

^{13}C NMR (150 MHz, $CDCl_3$) δ 199.1‡, 198.4†, 60.1†, 57.8‡, 54.8‡, 52.8†, 16.9†, 13.6‡ ppm;

†Major diastereoisomer (*trans*), ‡ minor diastereoisomer (*cis*);

HRMS (ESI^+) calc. for $C_4H_6O_2$ ($[M+H]^+$): 87.0441; found: 87.0256;

IR (film) ν_{max}/cm^{-1} 3682, 3641, 3009, 2989, 2895, 1063, 1031, 1016;

Data consistent with literature.[26]

8.2.4 Experimental Procedure for Compound (±)-2.9

Compound **(±)-2.9** was prepared according to general procedure **1**.

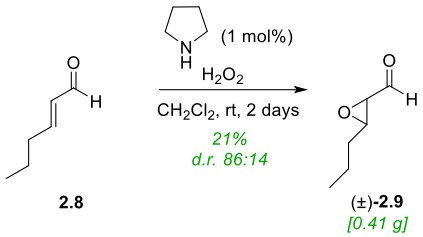

trans-2-Hexenal (**2.8**) (2.0 mL, 1.0 equiv., 17 mmol) in CH_2Cl_2 (60 mL), pyrrolidine (0.14 mL, 0.01 equiv., 1.7 mmol) and H_2O_2 (2.35 mL, 30% w/w aq., 1.35 equiv., 23 mmol). Purified *via* vacuum distillation (58 ˚C/10 mbar) to give the title compound as a colourless oil (0.41 g, 3.6 mmol, 21%, *d.r.* 86:14).

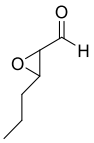

R_f = 0.37 (petroleum ether 40/60:ethyl acetate, 9:1), [$KMnO_4$];

^{1}H NMR (500 MHz, $CDCl_3$) δ 9.45 (1H, dd, *J* = 5.2, 2.0 Hz)‡, 9.00 (1H, ddd, *J* = 6.4, 2.8, 1.1 Hz)†, 3.32 (1H, td, *J* = 4.9, 1.8 Hz)‡, 3.27 – 3.24 (1H, m)‡, 3.22 (1H, td, *J* = 5.1, 2.0 Hz)†, 3.12 (1H, dt, *J* = 6.4, 2.1 Hz)†, 1.63 (4H, dddd, *J* = 14.1, 8.3, 6.7, 1.9 Hz)‡, 1.63 (2H, dddd, *J* = 14.1, 8.3, 6.7, 1.9 Hz)†, 1.55 – 1.44 (2H, m)†, 1.55 – 1.44 (3H, m)‡, 0.97 (3H, td, *J* = 7.4, 2.0 Hz)† ppm;

^{13}C NMR (125 MHz, $CDCl_3$) δ 199.1‡, 198.5†, 59.1†, 57.8‡, 56.6†,‡, 33.2†, 30.0‡, 19.9‡, 19.1†, 13.7†,‡ ppm;

HRMS (ESI$^+$) calc. for $C_6H_{10}O_2$ ($[M+H]^+$): 115.0762; found: 115.0753;

IR (film) ν_{max}/cm^{-1} 2963, 2936, 2876, 1726, 1464, 1435, 1157, 1121, 1047, 1003, 970, 912, 881, 851, 800, 781, 741, 723;

†Major diastereoisomer (*trans*), ‡ minor diastereoisomer (*cis*);

Data consistent with literature.[239]

8.2.5 Experimental Procedure for Compound (±)-2.13

Compound **(±)-2.13** was prepared according to literature.[45]

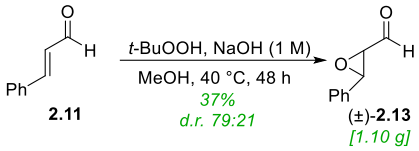

Cinnamaldehyde (**2.11**) (2.52 mL, 1.0 equiv., 20 mmol) in methanol (10 mL) was added dropwise to a 40 ˚C solution, of *t*-butyl hydroperoxide (3.1 mL, 70% w/v aq., 1.2 equiv., 24 mmol) in methanol (8 mL). NaOH (1 mL, 1 M aq.). After stirring at this temperature for a further 48 h water (10 mL) was added to quench the reaction. The two phases were separated and the aqueous layer was extracted with CH_2Cl_2 (3 × 10 mL). The combined organics were dried ($MgSO_4$) and the solvent was removed *via* carefully controlled distillation (45 °C/600 400 mbar). Flash column chromatography (95:5 petroleum ether 40/60:ethyl acetate) afforded epoxide **(±)-2.13** as a yellow oil (1.1 g, 7.4 mmol, 37%, *d.r.* 79:21).

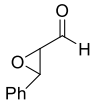

R_f = 0.42 (petroleum ether 40/60:ethyl acetate, 9:1), [UV, $KMnO_4$];

^{1}H NMR (600 MHz, $CDCl_3$) δ 9.20 (1H, d, *J* = 6.0 Hz)†, 9.09 (1H, d, *J* = 6.0 Hz)‡, 7.48 – 7.27 (10H, m)†‡*, 4.40 (1H, d, *J* = 4.6 Hz)‡, 4.17 (1H, d, *J* = 1.8 Hz)†, 3.54 (1H, dd, *J* = 6.1, 4.6 Hz)‡, 3.45 (1H, dd, *J* = 6.0, 1.8 Hz)† ppm *major and minor diastereomer peaks overlapped;

HRMS (ESI^+) calc. for $C_9H_8O_2$ ($[M+H]^+$):149.0597; found:149.0623;

†Major diastereoisomer (*trans*), ‡ minor diastereoisomer (*cis*);

Data consistent with literature.[240]

8.2.6 Experimental Procedure for Compound (±)-1.20

Compound **(±)-1.20** was prepared according to general procedure **2**.

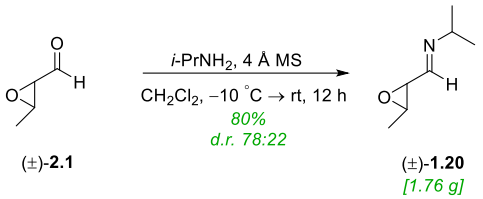

(±)-2,3-Epoxybutanal (**(±)-2.1**) (1.5 mL, 1.0 equiv., 17.4 mmol) in CH_2Cl_2 (6.5 mL), *iso*propylamine (1.65 mL, 1.1 equiv., 19.2 mmol) and 4 Å MS (2 g). Purified *via* vacuum distillation (36 ˚C/1 mbar) to give the title compound as a colourless oil (1.76 g, 13.8 mmol, 80%, *d.r.* 78:22).

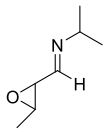

R_f = 0.39 (petroleum ether 40/60:ethyl acetate, 7:3), [$KMnO_4$];

^{1}H NMR (500 MHz, $CDCl_3$) δ 7.43 (1H, dd, *J* = 6.7, 0.8 Hz)‡, 7.14 (1H, dd, *J* = 7.2, 0.8 Hz)†, 3.45 – 3.35 (2H, m)†‡*, 3.28 – 3.22 (1H, m)‡, 3.19 (1H, dd, *J* = 7.3, 2.1 Hz)†, 3.08 (1H, qd, *J* = 5.2, 2.1 Hz)†, 1.38 **–** 1.32 (3H, dd, *J* = 5.2, 1.1 Hz)†‡, 1.19 – 1.15 (6H, m)†‡ ppm*major and minor diastereomer peaks overlapped;

^{13}C NMR (125 MHz, $CDCl_3$) δ 159.5†, 157.8‡, 61.6‡, 61.1†, 59.0†, 56.3‡, 54.0†,‡, 24.1‡, 24.0‡ 23.9†, 23.8†, 17.1†, 13.8‡ ppm;

HRMS (ESI^+) calc. for $C_7H_{13}NO$ ($[M+H]^+$): 128.1070; found:128.1094;

IR (film) ν_{max}/cm^{-1} 2975, 2896, 2968, 2342, 2324, 1665, 663, 640, 621, 602, 586, 562;

†Major diastereoisomer (*trans*), ‡ minor diastereoisomer (*cis*);

Data consistent with literature.[17]

8.2.7 Experimental Procedure for Compound (±)-2.10

Compound **(±)-2.10** was prepared according to general procedure **2**.

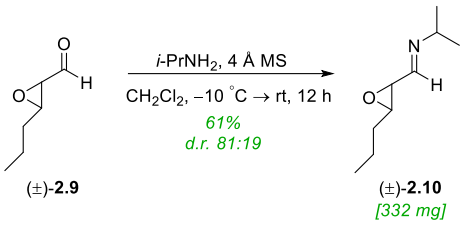

2,3-Epoxyhexanal (**(±)-2.9**) (0.4 g, 1.0 equiv., 3.5 mmol) in CH_2Cl_2 (2.0 mL), *iso*propylamine (0.33 mL, 1.1 equiv., 3.9 mmol) and 4 Å MS (600 mg). Purified *via* vacuum distillation (78 ˚C/10 mbar) to give the title compound as a colourless oil (332 mg, 2.1 mmol 61%, *d.r*. 81:19).

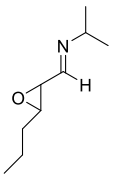

R_f = 0.36 (petroleum ether 40/60:ethyl acetate, 9:1), [$KMnO_4$];

^{1}H NMR (500 MHz, $CDCl_3$) δ 7.41 (1H, dd, *J* = 6.8, 0.7 Hz)‡, 7.13 (1H, dd, *J* = 7.2, 0.7 Hz)†, 3.44 (1H, dd, *J* = 6.8, 4.4 Hz)‡, 3.36 (1H, dd, *J* = 6.4, 0.8 Hz)†, 3.21 – 3.18 (1H, m)†‡, 2.99 (1H, ddd, *J* = 6.3, 4.8, 2.1 Hz)†, (1H, ddd, *J* = 6.9, 5.4, 4.4 Hz)‡, 1.64 – 1.44 (4H, m)†‡, 1.16 (6H, ddd, *J* = 10.4, 6.3, 4.1 Hz)†‡, 0.95 – 0.88 (3H, m)†‡ ppm;

^{13}C NMR (125 MHz, $CDCl_3$) δ 159.6†, 158.0‡, 61.5‡, 61.1†, 59.7‡, 58.1‡, 57.9†, 57.8†, 56.2‡, 33.5†, 30.3‡, 24.0‡, 23.9†, 23.8†, 19.8‡, 19.1†, 13.9†,‡ ppm;

HRMS (ESI^+) calc. for $C_9H_{17}NO$ ($[M+H]^+$): 156.1383; found: 156.1397;

IR (film) ν_{max}/cm^{-1} 3004, 2934, 2870, 1665, 1466, 1443, 1381, 1362, 1161.15 1132, 957, 941, 889, 862;

†Major diastereoisomer (*trans*), ‡ minor diastereoisomer (*cis*).

8.2.8 Experimental Procedure for Compound (±)-2.14

Compound **(±)-2.14** was prepared according to literature.[241]

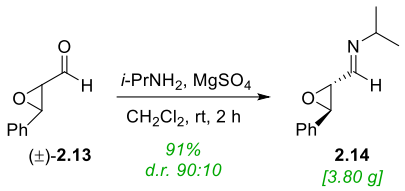

$MgSO_4$ (5.3 g, 2.0 equiv., 44 mmol) was added to a solution of epoxide **(±)-2.13** (3.3 g, 1.0 equiv., 22 mmol) in CH_2Cl_2 (4.4 mL). This mixture *iso*propylamine (1.89 mL, 1.0 equiv., 22 mmol) was added dropwise at rt. After addition the reaction was left to stir for a further 2 h. The $MgSO_4$ was filtered off and washed thoroughly with CH_2Cl_2 (20 mL). The crude filtrate was concentrated *in vacuo* and then purified *via* column chromatography (silica gel, diethyl ether: petroleum ether 40/60, 8:2) afforded the title compound as a yellow oil (3.80 g, 20.1 mmol, 91%).

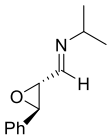

R_f = 0.38 (petroleum ether 40/60:ethyl acetate, 8:2), [UV, $KMnO_4$];

^{1}H NMR (500 MHz, $CDCl_3$) δ 7.38 – 7.26 (5H, m), 3.96 (1H, d, *J* = 2.0 Hz), 3.56 (1H, dd, *J* = 7.1, 2.0 Hz), 3.44 (1H, pd, *J* = 6.3, 0.7 Hz), 1.20 – 1.15 (7H, m) ppm;

^{13}C NMR (125 MHz, $CDCl_3$) δ 158.4, 135.8, 128.6, 128.6, 125.7, 61.9, 61.2, 57.9, 23.8, 23.8 ppm;

HRMS (ESI^+) calc. for $C_{12}H_{15}NO$ ($[M+H]^+$): 190.1227; found:190.1228;

IR (film) ν_{max}/cm^{-1} 2968, 2932, 2857, 1665, 1497, 1458, 1379, 1364, 1275, 1157, 1126, 959, 945, 854, 791, 752, 696, 617, 573;

Data consistent with literature.[241]

8.2.9 Experimental Procedure for Compound (±)-2.17

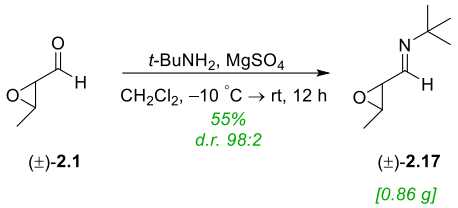

$MgSO_4$ (2.65 g, 2.0 equiv., 22.0 mmol) was added to a solution of epoxide **(±)-2.1** (0.95 g, 1.0 equiv., 11.0 mmol) in CH_2Cl_2 (15 mL). This mixture was cooled to –10 °C and *tert*-butylamine (1.4 mL, 1.2 equiv., 13.2 mmol) was added dropwise. After addition the reaction was left to warm to rt and allowed to stir for a further 2 h. The $MgSO_4$ was filtered off and washed thoroughly with CH_2Cl_2 (50 mL). The filtrate was concentrated *in vacuo*, then passed through a silica plug eluted with diethyl ether (20 mL). This was concentrated *in vacuo* to afford the title compound as a light brown oil (0.86 g, 6.1 mmol, 55%, *d.r.* 98:2), which was used without further purification.

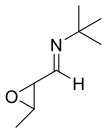

R_f = 0.40 (diethyl ether), [very faint UV, $KMnO_4$];

^{1}H NMR (400 MHz, $CDCl_3$) δ 7.07 (1H, d, *J* = 7.1 Hz), 3.23 (1H, dd, *J* = 7.1, 2.1 Hz), 3.10 (1H, qd, *J* = 5.2, 2.1 Hz), 1.39 (3H, d, *J* = 5.2 Hz), 1.19 (9H, s) ppm; *only major diastereomer peaks are listed as not all minor diastereomer peaks can be identified;

^{13}C NMR (100 MHz, $CDCl_3$) δ 156.8, 59.7, 57.6, 54.0, 29.3, 17.2 ppm *only major diastereomer peaks are listed as not all minor diastereomer peaks can be identified;

HRMS (ESI^+) calc. for $C_8H_{15}NO$ ($[M+H]^+$):142.1227; found:142.1219;

IR (film) ν_{max}/cm^{-1} 29690, 2931, 2871, 1670, 1431, 1366, 1229, 1008, 958, 894, 841.

8.2.10 Experimental Procedure for Compound (±)-1.24

Compound **(±)-1.24** was prepared by adapting literature.[17]

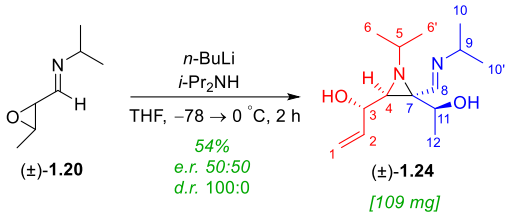

To diisopropylamine (0.48 mL, 2.00 equiv., 1.58 mmol) in anhydrous THF (1.0 mL) was added *n*-butyllithium (1.96 mL, 1.6 M, 2.00 equiv., 1.58 mmol) at –78 °C under an inert atmosphere. This was left to stir at this temperature for 1 h, then imino epoxide **(±)-1.20** (200 mg, 1.00 equiv., 1.58 mmol) in anhydrous THF (1.0 mL) was added dropwise at –78 °C. After 10 minutes this mixture was warmed to 0 °C over 90 min and stirred at this temperature for 1 h. The reaction mixture was quenched with water (5 mL) and the two phases were separated. The aqueous layer was extracted with CH_2Cl_2 (5 × 5 mL). The combined organics were dried ($MgSO_4$) and concentrated *in vacuo*. The crude residue was purified *via* column chromatography (silica gel diethyl ether: petroleum ether 40/60, 8:2) to give the title compound as a white crystalline solid (109 mg, 0.86 mmol, 54%, *d.r.* 100:0, *e.r.* 50:50).

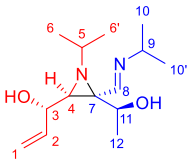

^{1}H NMR (600 MHz, $CDCl_3$) δ 7.47 (1H, d, *J* = 1.7 Hz, C8H), 6.04 (1H, ddd, *J* = 17.2, 10.6, 5.0 Hz, C2H), 5.41 (1H, apt dt, *J* = 17.3, 1.6 Hz, C1H$_{trans}$), 5.20 (1H, apt dt, *J* = 10.6, 1.5 Hz, C1H*cis*), 4.22 (1H, apt ddt, *J* = 6.6, 5.0, 1.6 Hz, C3H), 3.66 (1H, qd, *J* = 6.6, 1.7 Hz, C11H), 3.43 – 3.19 (1H, m, C9H), 2.56 (1H, sept, *J* = 6.2 Hz, C5H), 2.13 (1H, d, *J* = 6.4 Hz, C4H) 1.41 (3H, d, *J* = 6.5 Hz, C12H$_3$), 1.20 (3H, d, *J* = 3.8 Hz, C10H3 or C10′H3), 1.19 (3H, d, *J* = 4.0 Hz,

C10H3 or C10′H_3), 1.17 (3H, d, *J* = 6.3 Hz, C6H_3 or C6'H_3), 1.05 (3H, d, *J* = 6.2 Hz, C6H_3 or C6′H_3) ppm;

^{13}C NMR (125 MHz, $CDCl_3$) 158.7 (C8), 138.6 (C2), 115.4 (C1), 69.1 (C11), 69.0 (C3), 61.9 (C9), 54.9 (C4), 52.1 (C5), 50.0 (C7), 24.1 (C10 or C10′), 23.9 (C10 or C10′), 22.9 (C6 or C6′), 22.0 (C6 or C6′), 19.9 (C12) ppm;

HRMS (ESI$^+$) calc. for $C_{14}H_{26}N_2O_2$ ([M+H]$^+$): 255.2067; found: 255.2072.

***e.r.* 50:50** (Chiralpak ID, 100 hexane, 0.8 mL min^{-1}, λ 210 nm) t_{R1} = 8.18 min, t_{R2} = 9.08 min. See page **291** for chiral HPLC traces.

Data consistent with literature.[17]

8.2.11 Experimental Procedure for Compound (±)-2.19

Compound **(±)-2.19** was prepared by adapting literature.

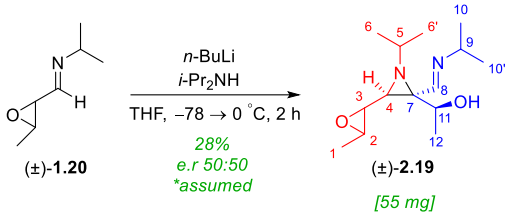

To di*iso*propylamine (0.23 mL, 0.95 equiv., 1.50 mmol) in anhydrous THF (1.0 mL) was added *n*-butyllithium (0.93 mL, 1.6 M, 0.95 equiv., 1.50 mmol) at –78 °C under an inert atmosphere. This was left to stir at this temperature for 1 h, then imine epoxide **(±)-1.20** (200 mg, 1.00 equiv., 1.58 mmol) in anhydrous THF (1.0 mL) was added dropwise at –78 °C. After 10 minutes this mixture was warmed to 0 °C over 90 min and stirred at this temperature for 1 h. The reaction mixture was quenched with water (5 mL) the two phases were separated. The aqueous layer was extracted with CH_2Cl_2 (5 × 5 mL). The combined organics were dried ($MgSO_4$) and concentrated *in vacuo*. The crude residue was purified via column chromatography (silica gel diethyl ether: petroleum ether 40/60, 8:2) to give the title compound as a white crystalline solid (55 mg, 0.22 mmol, 28%, *e.r* 50:50*).

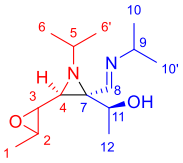

^{1}H NMR (400 MHz, $CDCl_3$) δ 7.45 (1H, t, *J* = 0.8 Hz, C8H), 4.25 (1H, s, OH), 3.92 (1H, d, *J* = 6.8 Hz, C11H), 3.32 (1H, sept, *J* = 6.4 Hz, C9H), 3.01 (1H, qd, *J* = 5.2, 2.3 Hz, C2H), 2.83 (1H, dd, *J* = 6.6, 2.3 Hz, C3H), 2.47 (1H, sept, *J* = 6.2 Hz, C5H), 1.85 (1H, d, *J* = 6.6 Hz, 1H, C4H), 1.32 (6H, dd, *J* = 6.5, 5.8 Hz, C1H_3 and C12H_3), 1.20 – 1.13 (9H, m, C6′H_3, C10H_3 and C10′H_3), 1.00 (3H, d, *J* = 6.2 Hz, C6H_3) ppm;

^{13}C NMR (100 MHz, $CDCl_3$) δ 158.0 (C8), 67.5 (C11), 62.0 (C9), 57.3 (C2), 53.6 (C4), 52.1 (C5), 50.13 (C3), 50.05 (C7), 24.1 (C10 or C10′), 23.9 (C10 or C10′), 22.7 (C6 or C6′), 21.9 (C6 or C6′), 19.7 (C12), 17.2 (C1) ppm;

^{13}C NMR (125 MHz, $CDCl_3$) 158.7 (C8), 138.6 (C2), 115.4 (C1), 69.1 (C11), 69.0 (C3), 61.9 (C9), 54.9 (C4), 52.1 (C5), 50.0 (C7), 24.1 (C10 or C10′), 23.9 (C6 or C10′), 22.9 (C6 or C6′), 22.0 (C6 or C6′), 19.9 (C12) ppm;

HRMS (ESI^+) calc. for $C_{14}H_{26}N_2O_2$ ($[M+H]^+$): 255.2067; found: 255.2076.

*A chiral HPLC chromatogram could not be acquired due to the poor chromophore of the compound, but due to the use of a nature of the reaction it is assumed to proceed with an *e.r* 50:50.

8.2.12 Experimental Procedure for Compound (±)-2.20

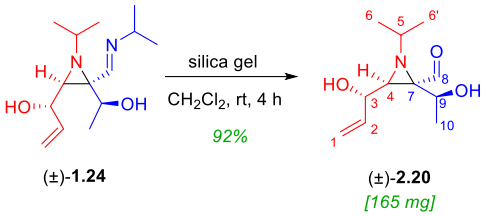

Silica gel (1.0 g) was added to dimer **(±)-1.24** (200 mg, 1.0 equiv., 0.84 mmol) in CH_2Cl_2 (2.0 mL). The reaction was stirred for 4 h at rt after which the silica was filtered off and washed with CH_2Cl_2 (10.0 mL). The mixture was concentrated *in vacuo* to afford the title compound as a colourless oil (165 mg, 0.77 mmol, 92%), without need for further purification.

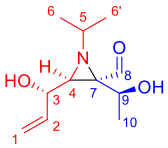

^{1}H NMR (500 MHz, $CDCl_3$) δ 9.51 (1H, d, *J* = 1.0 Hz, C8H), 6.01 (1H, ddd, *J* = 17.3, 10.6, 5.3 Hz, C2H), 5.41 (1H, apt dt, *J* = 17.3, 1.5 Hz, C1H$_{trans}$), 5.25 (1H, apt dt, *J* = 10.6, 1.4 Hz, C1H*cis*), 4.24 (1H, apt ddt, *J* = 6.9, 5.4, 1.6 Hz, C3H), 3.88 (1H, q, *J* = 6.6 Hz, C9H), 2.86 (1H, sept, *J* = 6.2 Hz, C5H), 2.64 (1H, d, *J* = 6.9 Hz, C4H), 1.45 (3H, d, *J* = 6.6 Hz, C10H$_3$), 1.23 (3H, d, *J* = 6.2 Hz, C6H$_3$ or C6′H$_3$), 1.04 (3H, d, *J* = 6.2 Hz, C6H$_3$ or C6′H$_3$) ppm;

^{13}C NMR (125 MHz, $CDCl_3$) δ 200 (C8), 137.7 (C2), 116.4 (C1), 69.6 (C3), 66.8 (C9), 55.6 (C4), 54.2 (C7), 51.9 (C5), 22.8 (C10), 22.1 (C6 or C6′), 19.8 (C6 or C6′) ppm;

HRMS (ESI$^+$) calc. for $C_{11}H_{19}NO_3$ ([M+H]$^+$): 214.1438; found: 214.1438;

IR (film) ν_{max}/cm^{-1} 2967, 2924, 2855, 2360, 2342, 1706, 1455, 1372, 1055, 1033, 1013, 689.

8.2.13 Experimental Procedure for Compound (±)-2.3

Compound **(±)-2.3** was prepared according to literature.[46]

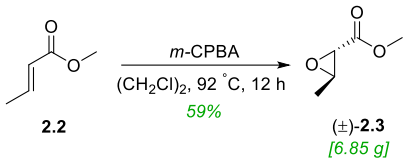

A solution of methyl crotonate (**2.2**) (10.6 mL, 1.0 equiv., 0.1 mol) and *m*-CPBA (25.0 g, 70% w/w, 1.0 equiv., 0.1 mol) in dichloroethane (125 mL) was refluxed at 92 ˚C overnight. The reaction mixture was filtered and the white precipitate formed was washed thoroughly with *n*-hexane (200 mL). The filtrate was concentrated *in vacuo* to half volume. The residue was washed with $NaHCO_3$ (50 mL, (7% aq.)), Na_2CO_3 (50 mL, (15% aq.)) and $Na_2S_2O_3$ (50 mL, (3% aq.)). The combined organics were dried ($MgSO_4$) and concentrated *in vacuo* to afford the title compound as a pale yellow oil (6.85 g, 59 mmol, 59%), which was used without further purification.

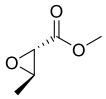

R_f = 0.05 (ethyl acetate), [UV];

^{1}H NMR (500 MHz, $CDCl_3$) δ 3.77 (3H, s), 3.23 (1H, qd, *J* = 5.2, 1.9 Hz), 3.19 (1H, d, *J* = 1.9 Hz), 1.40 (3H, d, *J* = 5.1 Hz) ppm;

^{13}C NMR (100 MHz, $CDCl_3$) δ 169.7, 54.5, 53.8, 52.4, 17.1 ppm;

HRMS (ESI$^+$) calc. for $C_5H_8O_2$ ($[M+H]^+$): 117.0545; found:117.0552;

IR (film) ν_{max}/cm^{-1} 2985 (br), 1738, 1441, 1426, 1379, 1339, 1292, 1254, 1203, 1146, 1034, 1009, 951, 908, 862, 779, 725, 719, 696;

Data consistent with literature.[242]

8.2.14 Experimental Procedure for Compound (±)-2.4

Compound **(±)-2.4** was prepared according to literature. [33]

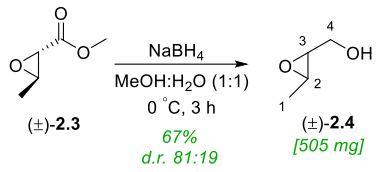

$NaBH_4$ (0.49 g, 1.5 equiv., 12.9 mmol) in MeOH and H_2O (1:1, 10 mL) was added dropwise to a solution of **(±)-**methyl-*trans*-(2,3)-epoxybutanoate **(±)-2.3** (1.0 g, 1.0 equiv., 8.6 mmol) in MeOH and H_2O (1:1, 2 mL) at 0 ˚C. The mixture was stirred at this temperature for 3 h then H_2O (15 mL) was added. The mixture was saturated with NaCl and then extracted with diethyl ether (8 × 20 mL). The combined organics were dried ($MgSO_4$) and concentrated *in vacuo*. The crude was purified *via* vacuum distillation (59 ˚C/12 mbar) to give the title compound as a colourless oil (505 mg, 5.7 mmol, 67%, *d.r.* 81:19).

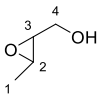

R_f = 0.27 (petroleum ether 40/60:ethyl acetate, 3:7), [$KMnO_4$];

^{1}H NMR (400 MHz, $CDCl_3$) δ 3.94 – 3.82 (1H, m, C2H†), 3.59 (1H, dddq, *J* = 11.4, 5.6, 4.6, 1.2 Hz, C3H†), 3.24 – 3.19 (1H, m, C2H‡), 3.18 ─ 3.10 (1H, m, C3H‡), 3.07 – 2.87 (2H, m, C4H† and C4'H†, C4H‡ and C4'H‡), 1.38 (3H, dd, *J* = 5.2, 1.0 Hz, C1H$_3^\ddagger$), 1.32 (dt, *J* = 5.2, 0.8 Hz, C1H$_3^\dagger$) ppm;

^{13}C NMR (100 MHz, $CDCl_3$) δ 61.7†, 59.5†, 54.6‡, 53.9‡, 52.4‡, 52.0†, 17.2†, 17.1‡ ppm;

HRMS (ESI$^+$) calc. for $C_4H_8O_2$ ([M+H]$^+$): 89.0597; found:89.0602;

IR (film) ν_{max}/cm^{-1} 3414 (br), 3000, 2944, 1481, 1450, 1406, 1379, 1346, 1391, 1244, 1146, 1099, 988, 718;

†Major diastereoisomer (*trans*), ‡ minor diastereoisomer (*cis*);

Data consistent with literature.[243]

8.2.15 Experimental Procedure for Compound 2.25

Compound **2.25** was prepared according to literature.[59]

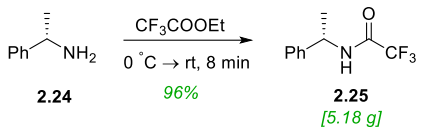

2.24 **2.25** *[5.18 g]*

To neat (*R*)-(+)-α-methylphenylamine (**2.24**) (3.18 mL, 1.0 equiv., 24.8 mmol), ethyl trifluoroacetate (4.41 mL, 1.5 equiv., 37.2 mmol) was added dropwise at 0 ˚C and stirred for 8 min at rt. Ethanol was removed by repeated azeotropic distillation with toluene (3 × 30 mL). The crude residue was recrystallized from hexane to afford the title compound as a white crystalline solid (5.18 g, 23.9 mmol, 96%).

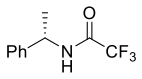

R_f = 0.18 (petroleum ether 40/60:ethyl acetate, 95:5), [UV, $KMnO_4$];

MP = 85-88 ˚C recrystallized from hexane, lit.[244] 88 ˚C;

^{1}H NMR (600 MHz, $CDCl_3$) δ 7.41 – 7.37 (2H, m, Ph), 7.36 – 7.31 (3H, m, Ph), 6.42 (1H, br, NH), 5.15 (1H, d, *J* = 7.1 Hz, C1H), 1.60 (3H, d, *J* = 6.9 Hz, $C2H_3$) ppm;

^{13}C NMR (125 MHz, $CDCl_3$) δ 156.3 (q, $^2J_{CF}$ = 37.1 Hz), 140.9, 129.1, 128.3, 126.2, 115.8 (q, $^1J_{CF}$ = 288.2 Hz), 114.7, 49.8, 21.1 ppm;

IR (film) ν_{max}/cm^{-1} 3333, 1697, 1545, 1454, 1342, 1223, 1190, 1110, 1092, 1074, 1011, 881,760, 723, 698, 658;

Data consistent with literature.[59]

8.2.16 Experimental Procedure for Compound 2.26

Compound **2.26** was prepared according to literature.[59]

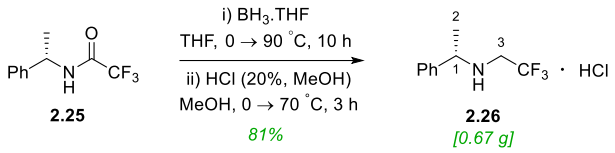

A solution of borane·THF (13.8 mL, 1 M, 4.0 equiv., 13.8 mmol) was added to a stirred solution of (*R*)-*N*-trifluoroacetyl-1-phenylethylamine (**2.25**) (0.75 g, 1.0 equiv., 3.46 mmol) in THF (4.3 mL) at 0 ˚C. The resulting mixture was refluxed with the heating block at 90 ˚C for 10 h, then cooled down to rt and MeOH (3.5 mL) was added to the reaction mixture and concentrated *in vacuo*. The residue was then dissolved in MeOH (3.5 mL) and a solution of HCl (20% in MeOH, 3.5 mL) was added at 0 ˚C. The mixture was then refluxed with the heating block at 70 ˚C for 3 h, cooled and then concentrated *in vacuo*. The residue was suspended in toluene (8 mL) and concentrated *in vacuo*. This process was repeated a further 3 times to afford a white solid. The crude residue was recrystallized from hot *iso*-propyl alcohol to afford the title compound as a white crystalline solid (0.67 g, 2.8 mmol, 81%).

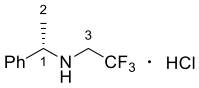

R_f = 0.35 (petroleum ether 40/60:ethyl acetate, 95:5), [UV, $KMnO_4$];

^{1}H NMR (500 MHz, $CDCl_3$) δ 7.67 – 7.63 (2H, m, Ph), 7.54 – 7.38 (3H, m, Ph), 4.47 (1H, q, *J* = 6.8 Hz, C1H), 3.77 – 3.65 (1H, br, NH), 3.42 (1H, dq, *J* = 14.6, 9.0 Hz, C3H′ or C3H) 3.28 (1H, dq, *J* = 14.6, 8.5 Hz, C3H′ or C3H) , 2.01 (3H, d, *J* = 6.8 Hz, $C2H_3$) ppm;

^{13}C NMR (125 MHz, $CDCl_3$) δ 134.7, 130.0, 130.0, 128.1, 121.4 (q, $^1J_{CF}$ = 279.0 Hz), 60.0, 44.8 (q, $^2J_{CF}$ = 31.0 Hz), 20.3 ppm;

IR (film) ν_{max}/cm^{-1} 2956 (br), 2656 (br), 2585 (br), 2542 (br), 2426 (br), 1593, 1576, 1402, 1335, 1263, 1213, 1136, 1125, 1088, 1045, 1022;

Data consistent with literature.[59]

8.2.17 Experimental Procedure for Chiral Amine B

Chiral amine **B** was prepared according to literature.[59]

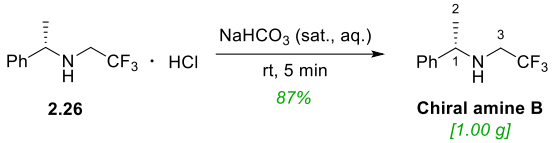

2.26

Chiral amine B
[1.00 g]

Salt **2.26** (1.4 g, 5.68 mmol) was then dissolved in $NaHCO_3$ (sat., aq., 15 mL) and was extracted with hexane (3 × 15 mL). The combined organics were washed with brine (20 mL) dried ($NaSO_4$) and concentrated *in vacuo* to give a colourless oil (1.00 g, 4.9 mmol, 87%), which was used without further purification.

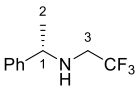

R_f = 0.32 (petroleum ether 40/60:ethyl acetate, 95:5), [UV, $KMnO_4$];

^{1}H NMR (600 MHz, $CDCl_3$) δ 7.38 – 7.30 (4H, m, Ph), 7.29 – 7.24 (1H, m, Ph), 3.92 (1H, q, *J* = 6.6 Hz, C1H), 3.02 (2H, d, *J* = 9.5 Hz, $C3H_2$), 1.59 (1H, br, NH), 1.38 (3H, d, *J* = 6.6 Hz, $C2H_3$) ppm;

^{13}C NMR (150 MHz, $CDCl_3$) δ 144.2, 128.7, 127.4, 126.6, 57.3, 48.1 (q, $^2J_{CF}$ = 31.0 Hz), 24.4 ppm;*

*CF_3 q, cannot be peak picked;

IR (film) ν_{max}/cm^{-1} 2968 (br), 1493, 1450, 1402, 1373, 1263, 1146, 1097, 1078, 1028, 968, 953, 914, 869, 822, 762, 700, 664;

Data consistent with literature.[59]

8.2.18 Experimental Procedure for Chiral Amine C

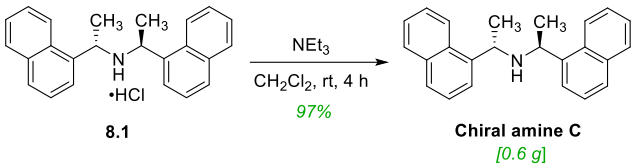

Triethylamine (0.5 mL, 2.1 equiv., 4.0 mmol) was added to a solution of amine salt **8.1** (0.60 g, 1.0 equiv., 1.9 mmol) in CH_2Cl_2 (10 mL) at rt. This mixture was left to stir for 2 h, then the reaction was quenched with HCl (1M aq., 1 mL) and diluted with water (10 mL). The organics were separated and the aqueous was extracted with CH_2Cl_2 (2 × 10 mL). The combined organics were dried (Na_2SO_4) and concentrated *in vacuo* to afford the title compound as a colourless oil (0.6 g, 1.85 mmol, 97%), which was used without further purification.

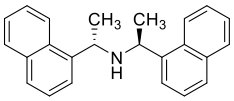

^{1}H NMR (600 MHz, $CDCl_3$) δ 7.84 (2H, dd, *J* = 8.2, 1.3 Hz), 7.79 – 7.74 (4H, m), 7.73 (2H, d, *J* = 7.2 Hz), 7.52 (2H, dd, *J* = 8.1, 7.1 Hz, 2H), 7.38 (2H, ddd, *J* = 8.0, 6.7, 1.1 Hz), 7.22 (2H, ddd, *J* = 8.4, 6.7, 1.4 Hz), 4.51 (2H, q, *J* = 6.7 Hz), 1.46 (6H, d, *J* = 6.7 Hz, 6H) ppm *residual triethylamine couldn't be fully removed. (2.55 (2H, q, *J* = 7.2 Hz) 1.05 (3H, t, *J* = 7.2 Hz);

^{13}C NMR (150 MHz, $CDCl_3$) δ 142.0, 133.9, 131.5, 128.7, 127.1, 125.7, 125.4, 125.2, 123.1, 122.7, 46.3, 24.5 ppm;

HRMS (ESI^+) calc. for $C_{24}H_{23}N$ ($[M+H]^+$): 326.1903; found: 326.1911;

IR (film) ν_{max}/cm^{-1} 3048, 2968, 2360, 2342, 1595, 1510, 1448, 1393, 1369, 1174, 799, 777.

8.2.19 Experimental Procedure for Chiral Amine D

Chiral amine **D** was prepared according to literature.[245]

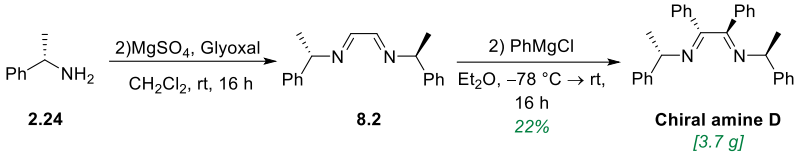

(**Step 1**) To a solution of glyoxal (8.8 M, w/w 40%, 47.0 mL, 1.0 equiv., 41.3 mmol) in CH_2Cl_2 (90 mL) was added $MgSO_4$ (20 g) in 2.0 g portions over 20 mins at rt. After the addition to mixture was allowed to stir for a further 10 mins, after which (*R*)-(+)-α-methylphenylamine (**2.24**) (10.5 mL, 2 equiv., 83 mmol) was added over 5 minutes at room temp. The mixture was left to stir overnight. The crude reaction mixture was then passed through a sinter funnel to remove the $MgSO_4$ and the filter cake was washed thoroughly with CH_2Cl_2 (200 mL). The organics were concentrated *in vacuo* and the crude orange oil was used directly in the next step.

(**Step 2**) A solution of crude **8.2** in Et_2O (100 mL) was cooled to –78 °C and phenylmagnesium chloride solution (2 M in THF, 81 mL, 4.0 equiv., 163 mmol) was added dropwise *via* syringe pump over 2 h. Once complete the reaction mixture was left to warm to rt overnight. Then the mixture was cooled to 4 °C and carefully quenched with NH_4Cl (100 mL (sat., aq.)) over 30 mins. The resultant solid is dissolved in H_2O (100 mL) and this is then extracted with ethyl acetate (3 × 50 mL). The combined organics were washed with brine (100 mL (sat., aq.)) and dried ($MgSO_4$) and concentrated *in vacuo.* The crude residue was recrystallized from hot petroleum ether 40/60 and CH_2Cl_2, to afford the title compound as large colourless needles (3.7 g, 8.9 mmol, 22% over two steps).

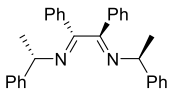

^{1}H NMR (500 MHz, $CDCl_3$) δ 7.29 – 7.24 (2H, m), 7.27 – 7.18 (4H, m), 7.16 – 7.08 (6H, m), 7.06 – 7.00 (4H, m), 6.96 – 6.89 (2H, m), 3.43 (1H, q, *J* = 6.7 Hz), 3.37 (2H, s), 1.26 (6H, d, *J* = 6.7 Hz);

^{13}C NMR (125 MHz, $CDCl_3$) δ 145.6, 141.6, 128.3, 127.9, 127.8, 126.65, 126.59, 65.8, 55.0, 25.3;

HRMS (ESI^+) calc. for $C_{30}H_{33}N_2$ ($[M+H]^+$): 421.2638; found: 421.2642;

IR (film) ν_{max}/cm^{-1} 3326, 2925, 2860, 1598, 1492, 1456, 1363, 1106, 921, 862.

Data consistent with literature.[245]

8.2.20 General Procedure 3 – Dimerisation 2 Equivalents of Chiral Base

2 equivalents of base (**Entries 1-17, 19-22 and 24, Table 8.1, page 193**)

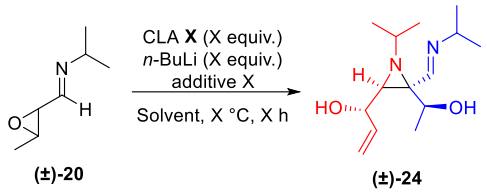

In to an oven dried schlenk flask chiral amine **X** (**Column 1, Table 8.1**) (2.00 equiv., 1.58 mmol) and solvent **X** (**Column 2, Table 8.1**) (0.50 mL) were added under an inert atmosphere. The external temperature of the solution was cooled down to –78 °C using a cryostat. *n*-Butyllithium (0.98 mL, 1.6 M in hexanes, 2.00 equiv., 1.58 mmol) was then added dropwise. After 15 min stirring at –78 °C, additive **X** (**Column 3, Table 8.1**) (2.00 equiv., 1.58 mmol) was added dropwise and the mixture was left to stir for a further 45 min. The reaction was cooled/warmed to the stated temperature (**Column 4, Table 8.1**) and (±)-*N*-*iso*propyl-3,4-epoxy-1-aza-pent-1-ene (**(±)-1.20**) (100 mg, 1.00 equiv., 0.79 mmol) in solvent **X** (0.50 mL) (**Column 2, Table 8.1**) was added dropwise. The temperature was maintained for 15 minutes and then the crystostat was set to 0 °C to gradually warm up to rt (typically –78 °C to 0 °C took 80 min). Once it had reached 0 °C it was left to stir for a further 50 min. The reaction was then quenched with H_2O (1.00 mL) and diluted with CH_2Cl_2 (1.00 mL). The organics were separated and the aqueous layer was extracted with CH_2Cl_2 (2 × 3.00 mL). The combined organics were dried (Na_2SO_4) and concentrated *in vacuo*. Purification via column chromatography (silica gel diethyl ether: petroleum ether 40/60 (8:2)) afforded the title compound as a white crystalline solid.

8.2.21 General Procedure 4 – Dimerisation 1 Equivalent of Chiral Base

1 equivalent of base (**Entries 18, 23 and 25, Table 8.1, page 191**)

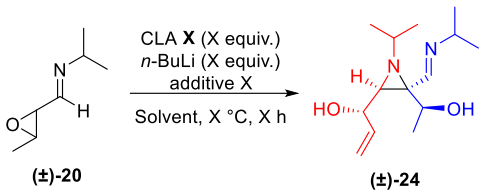

In to an oven dried schlenk flask chiral amine **X** (**Column 1, Table 8.1**) (1.00 equiv., 0.79 mmol) and solvent **X** (**Column 2, Table 8.1**) (0.50 mL) were added under an inert atmosphere. The external temperature of the solution was cooled down to –78 °C using a cryostat. *n*-Butyllithium (0.98 mL, 1.6 M in hexanes, 1.00 equiv., 0.79 mmol) was then added dropwise. After 15 min stirring at –78 °C additive **X** (**Column 3, Table 8.1**) (1.00 equiv., 0.79 mmol) was added dropwise and the mixture was left to stir for a further 45 min. The reaction was cooled/warmed to the stated temperature (**Column 4 Table 8.1**) and (±)-*N*-isopropyl-3,4-epoxy-1-aza-pent-1-ene (**(±)-1.20**) (100 mg, 1.00 equiv., 0.79 mmol) in solvent **X** (0.50 mL) (**Column 2, Table 8.1**) was added dropwise. The temperature was maintained for 15 minutes and then the crystostat was set to 0 °C to gradually warm up to rt (typically –78 °C to 0 °C took 80 min). Once it had reached 0 °C it was left to stir for a further 50 min. The reaction was then quenched with H_2O (1.00 mL) and diluted with CH_2Cl_2 (1.00 mL). The organics were separated and the aqueous layer was extracted with CH_2Cl_2 (2 × 3.00 mL). The combined organics were dried (Na_2SO_4) and concentrated *in vacuo*. Purification via column chromatography (silica gel diethyl ether: petroleum ether 40/60 (8:2)) afforded the title compound as a white crystalline solid.

Table 8.1: Conditions screen for enantioconvergent aza-Darzens reaction

8.2.22 Table of Chiral Lithium Amines Used for *aza*-Darzens Reaction

	1	2	3	4	5		
Entry	**CLA (2 equiv.)**	**Solvent**	**Additives**	**Temp (˚C)**	**Time (h)**	***e.r***	**Yield**
1	**A**	THF	-	–78	4	82:18	57%
2	**B**	THF	-	–78	4	76:24	40%
3	**E**	THF	-	–78	4	72:28	46%
4	**F**	THF	-	–78	4	no dimer	n/a
5	**G**	THF	-	–78	4	no dimer	n/a
6	**D**	THF	-	–78	4	no dimer	n/a
7	**H**	THF	-	–78	4	no dimer	n/a
8	**C**	THF	-	–78	4	trace amount	-
9	**A**	toluene	-	–78	4	trace amount	-
10	**A**	MTBE	-	–78	4	no dimer	n/a
11	**A**	Et_2O	-	–78	4	77:23	39%
12	**A**	2-M-THF	-	–78	4	83:17	51%
13	**A**	THF	HMPA	–78	4	no dimer	n/a
14	**A**	THF	TMEDA	–78	4	80:20	47%
15	**A**	THF	LiCl	–78	4	86:14	51%
16	**A**	THF	12-crown-4	–78	4	80:20	49%
17	**A**	THF	-	–78	16	75:25	51%
18	**A** (1 equiv.)	THF	-	–78	4	85:15	44%
19	**A**	THF	-	–40	4	61:39	52%
20	**A**	THF	-	–90	4	86:14	52%
21	**A**	THF	-	–95	4	90:10	56%
22	**A**	THF	-	–100	4	80:20	52%
23	**A** (1 equiv.)	THF	-	–95	4	no dimer	n/a
24	**A**	THF	LiCl	–95	4	no dimer	n/a
25	**A** (1 equiv.)	THF	LiCl	–95	4	84:16	42%

Table 8.1: Conditions screen for enantioconvergent aza-Darzens reaction

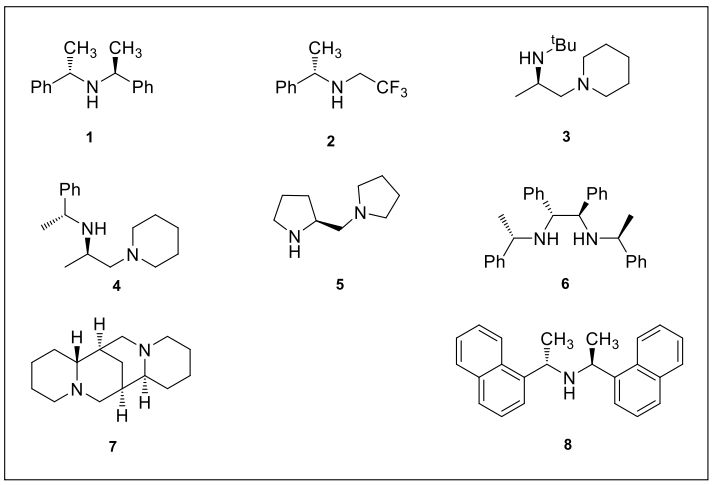

Figure 8.1: Chiral amines used in screen for enantioconvergencry

8 3 Experimental Conditions Chapter 3

8.3.1 Route Summary 1 – Pivaloyloxymethyl protected

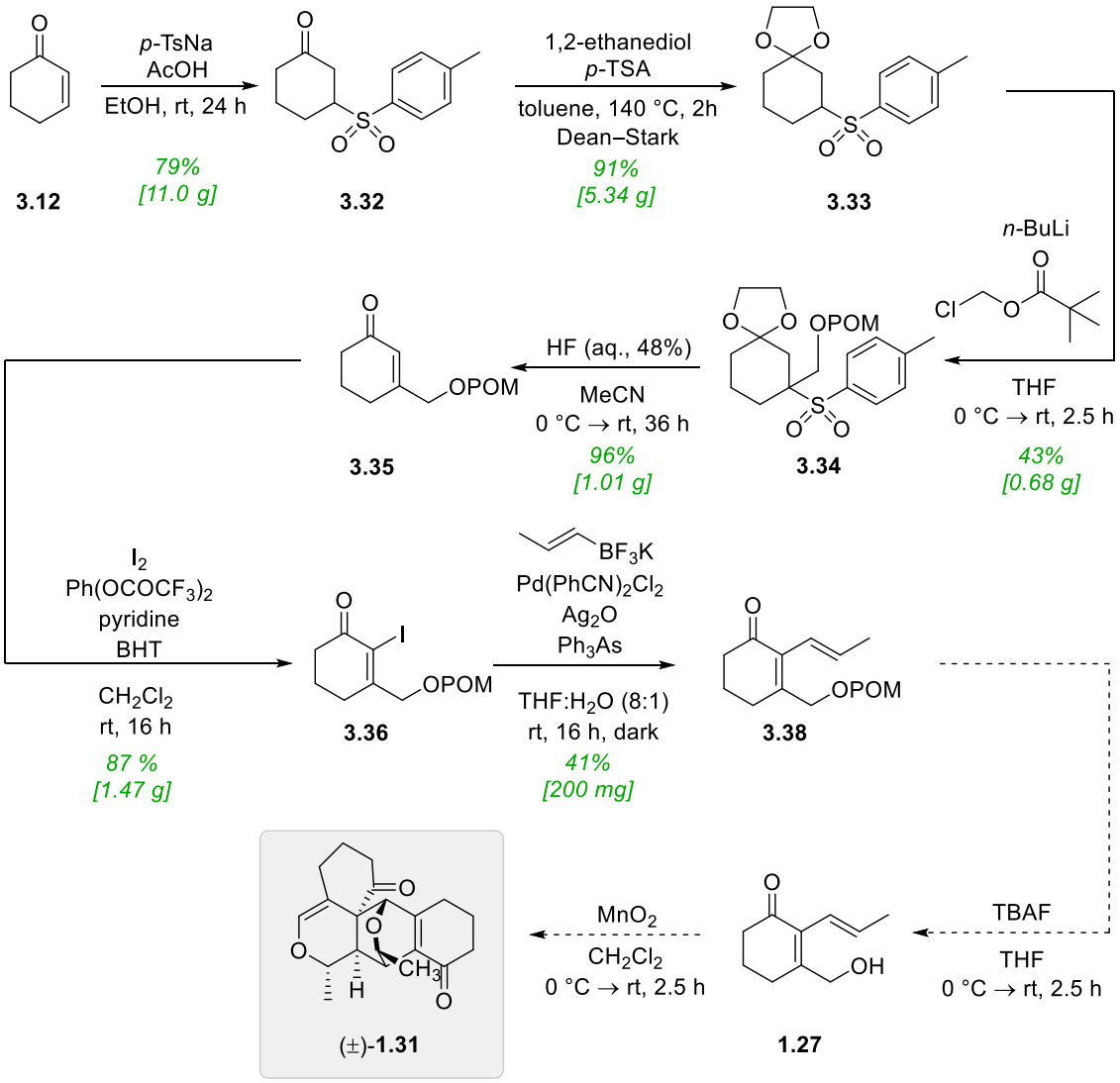

8.3.2 Route Summary 2 – TBS protected

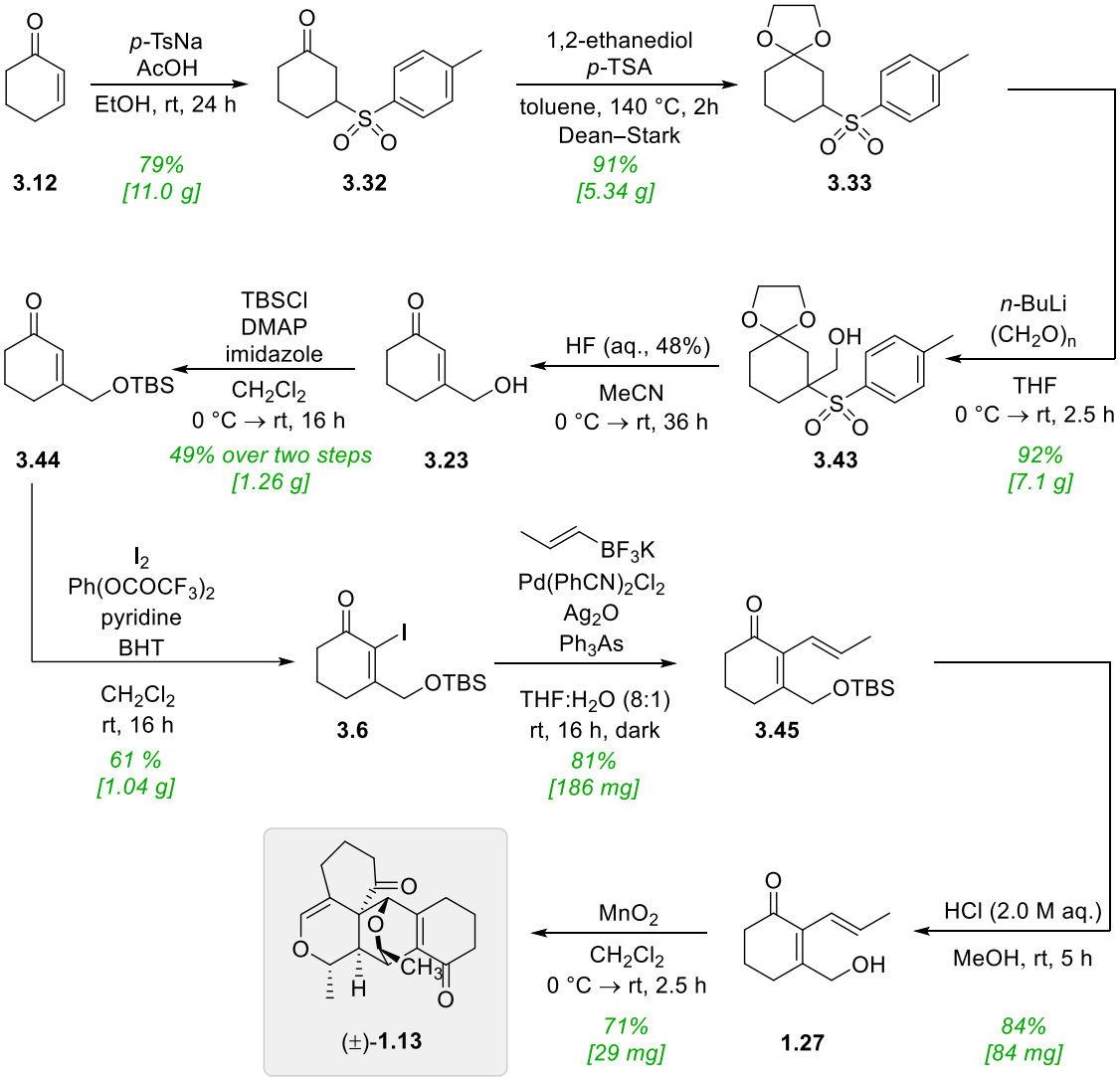

8.3.3 Experimental Procedure for Compound 3.1

Compound **3.1** was prepared according to literature.[67]

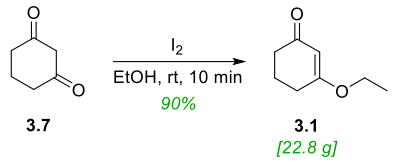

To a stirred solution of 1,3-cyclohexanedione (**3.7**) (20.2 g, 1.0 equiv., 180 mmol) in ethanol (400 mL) was added iodine (1.38 g, 0.03 equiv., 5.4 mmol). After 10 mins the reaction mixture was concentrated *in vacuo*. The residue was extracted with CH_2Cl_2 (3 × 100 mL) and washed with $Na_2S_2O_3$ (sat. aq., 100 mL), brine (100 mL) and H_2O (100 mL). The combined organics were then dried ($MgSO_4$) filtered and concentrated *in vacuo*, to afford the title compound as a yellow oil (22.8 g, 0.163 mmol, 90%), which was used without further purification.

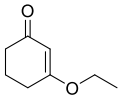

R_f = 0.26 (petroleum ether 40/60:ethyl acetate, 2:8), [UV, $KMnO_4$];

^{1}H NMR (400 MHz, $CDCl_3$) δ 5.33 (1H, s), 3.89 (2H, q, *J* = 7.0 Hz), 2.42 – 2.37 (2H, m), 2.33 (2H, dd, *J* = 7.2, 6.0 Hz), 2.01 – 1.92 (2H, m), 1.35 **–** 1.30 (3H, m) ppm;

^{13}C NMR (100 MHz, $CDCl_3$) δ 199.8, 177.9, 102.7, 64.2, 36.8, 29.1, 21.3, 14.1 ppm;

IR (film) ν_{max}/cm^{-1} 2982, 2943, 1647, 1600, 1476, 1456, 1429, 1377, 1346, 1327, 1215, 1182, 1134, 1111, 1059, 1028, 966, 930, 903, 868, 814, 758, 658, 606;

Data consistent with literature.[20]

8.3.4 Experimental Procedure for Compound 3.8

Compound **3.8** was prepared according to literature.[246]

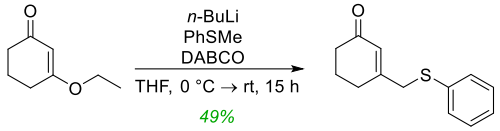

To a solution of thioanisole (3.31 mL, 1.0 equiv., 32.0 mmol) and DABCO (3.59 g, 1.0 equiv., 32.0 mmol) in THF (25 mL) at 0 ˚C was added dropwise *n*-butyllithium (1.6 M in hexanes, 20 mL, 1.0 equiv., 32.0 mmol) and the mixture was stirred at 0 ˚C for 45 mins. Compound **3.1** (4.50 g, 1.0 equiv., 32 mmol) in THF (12 mL) was added dropwise at 0 ˚C, the mixture was stirred at rt for 15 h, after which H_2O (25 mL) was added. The resulting mixture was acidified (pH 3) with HCl (conc.) and stirred at rt for 1 h. The mixture was neutralised with $NaHCO_3$ (sat. aq.) and extracted with Et_2O (3 × 40 mL). The combined organics were washed with H_2O (2 × 40 mL), dried ($MgSO_4$), and concentrated *in vacuo*. Purification *via* column chromatography (silica gel hexane:ethyl acetate (9:1)) afforded the title compound as a yellow oil (3.43 g, 15.7 mmol, 49%).

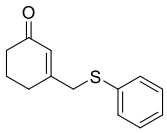

R_f = 0.24 (petroleum ether 40/60:ethyl acetate, 7:3), [UV, $KMnO_4$];

^{1}H NMR (500 MHz, $CDCl_3$) δ 7.35 – 7.20 (5H, m), 5.76 (1H, s), 3.60 (2H, app. q, *J* = 0.8 Hz), 2.52 (2H, t, *J* = 7.1), 2.32 (2H, t, *J* = 7.1), 2.01 – 1.94 (2H, m) ppm;

^{13}C NMR (125 MHz, $CDCl_3$) δ 199.4, 160.0, 134.5, 131.3, 129.1, 127.6, 127.4, 41.9, 37.3, 28.3, 22.6 ppm;

IR (film) ν_{max}/cm^{-1} 2945, 2927, 1663, 1620, 1582, 1479, 1454, 1439, 1425, 1369, 1346, 1323, 1254, 1190, 1155, 1136, 1123, 1086, 1047, 1024, 966, 885, 739, 691;

Data consistent with literature.[20]

8.3.5 Experimental Procedure for Compound 3.65

Compound **3.65** was obtained when attempting to synthesise the corresponding sulfoxide (**3.2**) based on a literature procedure. [20]

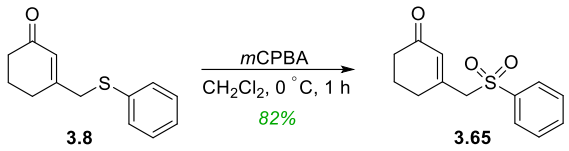

To a solution of compound **3.8** (2.50 g, 1.0 equiv., 11 mmol) in anhydrous CH_2Cl_2 (21 mL) was added *m*-CPBA (2.97 g, 1.5 equiv., 17 mmol) at 0 ˚C and stirred for 1 h under an inert atmosphere. The mixture was quenched with $NaHCO_3$ (sat., aq., 20 mL) and extracted with $CHCl_3$ (2 × 20 mL). The combined organics were washed with brine (20 mL) and dried (Na_2SO_4) and concentrated *in vacuo*. Purification *via* hot recrystallisation (MeOH:hexane, 8:2) afforded the title compound as a white powder (2.12 g, 9.1 mmol, 82%).

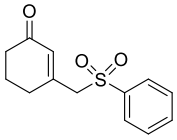

R_f = 0.24 (petroleum ether 40/60:ethyl acetate, 7:3), [UV, $KMnO_4$];

M.p = 124-126 ˚C; no literature value;

^{1}H NMR (400 MHz, $CDCl_3$) δ 7.90 – 7.83 (2H, m), 7.72 – 7.65 (1H, m), 7.62 – 7.54 (2H, m), 5.60 (1H, tt, = 1.7, 0.8 Hz), 3.93 (2H, s), 2.55 – 2.47 (2H, m), 2.39 – 2.31 (2H, m), 2.06 – 1.93 (2H, m) ppm;

^{13}C NMR (150 MHz, $CDCl_3$) δ 198.3, 150.7, 137.8, 134.4, 132.7, 129.4, 128.4, 64.3, 37.0, 29.9, 22.6 ppm;

IR (film) ν_{max}/cm^{-1} 2986, 2947, 1753, 1657, 1624, 1584, 1477, 1449, 1414, 1377, 1350, 1331, 1306, 1290, 1250, 1198, 1138, 1082, 1024, 995, 895, 849, 835, 764, 739, 687, 667.

8.3.6 Experimental Procedure for Compound 3.32

Compound **3.32** was prepared according to literature.[90]

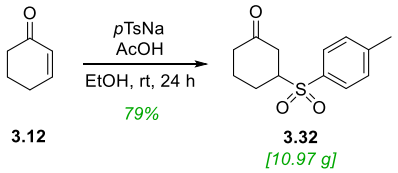

Glacial acetic acid (4.45 mL, 78 mmol, 1.5 equiv.) was added in one portion to a stirred suspension of sodium *para*-toluenesulfinate (10.39 g, 78 mmol, 1.5 equiv.) in ethanol (100 mL). To this mixture cyclohex-1-en-2-one (**3.12**) (5.54 mL, 54 mmol 1.0 equiv.) was added dropwise and the reaction was left to stir for 24 h at rt. The reaction was then diluted with $NaHCO_3$ (75 mL) and extracted with ethyl acetate (3 × 100 mL). The combined organics were dried (Na_2SO_4) filtered and concentrated *in vacuo*. The crude residue was purified *via* column chromatography (silica gel, petroleum ether 40/60:ethyl acetate, 7:3) to afford the titled compound as a white solid (10.97 g, 43.5 mmol, 79%).

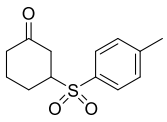

R_f = 0.37 (petroleum ether 40/60:ethyl acetate, 7:3), [UV, vanillin];

^{1}H NMR (500 MHz, $CDCl_3$) δ 7.75 (2H, d, *J* = 8.0 Hz), 7.37 (2H, d, *J* = 8.0 Hz), 3.25 (1H, tdd, *J* = 11.5, 5.8, 3.7 Hz), 2.61 – 2.49 (2H, m), 2.46 (3H, s), 2.43 – 2.18 (4H, m), 1.91 (1H, tdd, *J* = 13.1, 11.7, 3.7 Hz), 1.68 – 1.61 (1H, m) ppm;

^{13}C NMR (125 MHz, $CDCl_3$) δ 206.6, 145.3, 133.6, 130.1, 129.0, 62.4, 40.5, 40.5, 23.7, 23.5, 21.7 ppm;

HRMS (ESI^+) calc. for $C_{13}H_{16}O_3S$ ($[M+H]^+$): 253.0893; found: 253.0892;

Data consistent with literature.[90]

8.3.7 Experimental Procedure for Compound 3.33

Compound **3.33** was prepared adapting literature.[90]

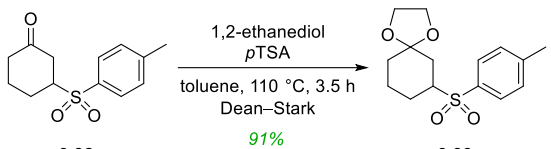

1,2-Ethanediol (1.30 mL, 23.31 mmol, 5.4 equiv.) and *para*-toluenesulfonic acid monohydrate (10.0 mg, 0.10 mmol, 0.01 equiv.) was added to a stirred solution of 3-tosylcyclohexan-1-one (**3.32**) (5.01 g, 19.85 mmol, 1.0 equiv.) in toluene (50 mL). The reaction flask was attached to a Dean–Stark apparatus under a reflux condenser. The reaction was heated to reflux at 110 ˚C for 3.5 h and then allowed to cool to rt and the volatiles were removed. The resulting residue was then partitioned between ethyl acetate (50 mL) and water (50 mL) and the organics were separated. The aqueous layer was extracted with ethyl acetate (2 × 50 mL) and the combined organics were washed with brine (100 mL), dried (Na_2SO_4) and concentrated *in vacuo*. The crude residue was purified via hot recrystallisation (MeOH:petroleum ether 40/60, 1:5). To afford the tile compound as white crystals (5.34 g, 18.00 mmol 91%).

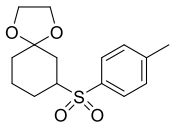

R_f = 0.16 (petroleum ether 40/60:ethyl acetate, 8:2), [UV, $KMnO_4$];

^{1}H NMR (600 MHz, $CDCl_3$) δ 7.72 (2H, d, *J* = 8.2 Hz), 7.34 (2H, d, *J* = 8.0 Hz), 3.96 – 3.85 (4H, m), 3.18 (1H, tt, *J* = 12.7, 3.5 Hz), 2.45 (3H, s), 2.15 – 2.08 (2H, m), 1.85 – 1.76 (1H, m), 1.17 – 1.64 (1H, m), 1.63 – 1.56 (2H, m), 1.55 – 1.45 (1H, m), 1.41 (1H, td, *J* = 13.1, 4.2 Hz), 1.33 (1H, qd, *J* = 12.8, 4.0 Hz) ppm;

^{13}C NMR (150 MHz, $CDCl_3$) δ 144.7, 134.0, 129.8, 129.1, 108.1, 64.6, 64.5, 61.5, 34.3, 34.0, 24.7, 21.9, 21.6 ppm;

Data consistent with literature.[90]

8.3.8 Experimental Procedure for Compound 3.43

Compound **3.43** was prepared according to literature.[90]

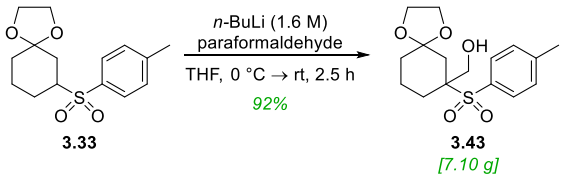

n-Butyllithium (1.6 M in hexanes, 16.1 mL, 1.6 M, 26.9 mmol, 1.1 equiv.) was added dropwise to cooled (0 ˚C) solution of dioxolane (**3.33**) (7.00 g, 23.6 mmol, 1.0 equiv.) in THF (115 mL). After stirring for 30 min at this temperature, paraformaldehyde (2.80 g, 94.4 mmol, 4.0 equiv.) dried in a desiccator over P_2O_5 was added in one portion and the reaction was warmed up to rt to stir for a further 2 h. After this the reaction was diluted with NH_4Cl (100 mL) then the aqueous layer was extracted with ethyl acetate (3 × 125 mL) and the combined organics washed with brine (250 mL), dried (Na_2SO_4) and concentrated *in vacuo* to give a yellowish gel as the crude product. The crude residue was purified *via* column chromatography (silica gel, petroleum ether 40/60:ethyl acetate, 6:4) to afford the titled compound as a white crystalline solid (7.10 g, 21.8 mmol, 92%).

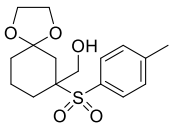

R_f = 0.13 (petroleum ether 40/60:ethyl acetate, 6:4), [UV, vanillin];

^{1}H NMR (600 MHz, $CDCl_3$) δ 7.74 (2H, d, *J* = 8.3 Hz), 7.37 (2H, d, *J* = 7.6 Hz), 4.12 (1H, dd, *J* = 13.5, 8.0 Hz), 3.98 – 3.87 (5H, m), 3.06 (1H, dd, *J* = 8.0, 6.0 Hz), 2.46 (3H, s), 1.99 – 1.90 (3H, m), 1.80 – 1.62 (4H, m), 1.56 (1H, s), 1.43 (1H, td, *J* = 13.1, 4.3 Hz) ppm;

^{13}C NMR (150 MHz, $CDCl_3$) δ 145.2, 131.7, 130.5, 129.7, 108.1, 67.4, 64.8, 64.1, 60.9, 34.7, 33.7, 24.5, 21.7, 19.0 ppm;

Data consistent with literature.[90]

8.3.9 Experimental Procedure for Compound 3.34

Compound **3.34** was prepared according to literature.[90]

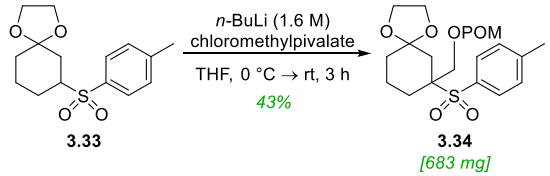

n-Butyllithium (1.6 M in hexanes, 2.40 mL, 1.6 M, 3.8 mmol, 1.1 equiv.) was added dropwise to cooled 0 ˚C solution of dioxolane (**3.33**) (1.00 g, 3.4 mmol, 1.0 equiv.) in THF (25 mL). After stirring for 30 min at this temperature chloromethylpivalate (0.60 mL, 4.2 mmol, 1.3 equiv.) was added in one portion and the reaction was warmed up to rt to stir for a further 2 h. After this the reaction was diluted with NH_4Cl (30 mL) then the aqueous layer was extracted with ethyl acetate (3 × 25 mL) and the combined organics washed with brine (25 mL), dried (Na_2SO_4) and concentrated *in vacuo* to give a yellowish gel as the crude product. The crude residue was purified *via* column chromatography (silica gel, petroleum ether 40/60:ethyl acetate, 3:1) to afford the titled compound as a white crystalline solid (683 mg, 1.45 mmol, 43%).

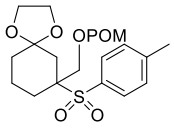

R_f = 0.17 (petroleum ether 40/60:ethyl acetate, 8:2), [UV, $KMnO_4$];

^{1}H NMR (600 MHz, $CDCl_3$) 7.72 (2H, d, *J* = 8.3 Hz), 7.33 (2H, d, *J* = 7.8 Hz), 4.62 (1H, d, *J* = 13.3 Hz), 4.34 (1H, d, *J* = 13.3 Hz), 3.95 – 3.80 (4H, m), 2.44 (3H, s), 2.20 (1H, d, *J* = 13.6 Hz), 1.99 (1H, dt, *J* = 13.5, 2.1 Hz), 1.96 – 1.88 (2H, m), 1.79 (1H, dtd, *J* = 11.2, 4.1, 2.0 Hz), 1.76 – 1.71 (1H, m), 1.64 – 1.56 (1H, m), 1.54 – 1.46 (1H, m), 1.06 (9H, s) ppm;

^{13}C NMR (150 MHz, $CDCl_3$) δ 177.6, 144.8, 133.3, 130.3, 129.7, 108.1, 67.0, 64.9, 64.1, 61.2, 38.7, 34.2, 34.0, 26.9, 25.0, 21.6, 19.1 ppm;

Data consistent with literature.[90]

8.3.10 Experimental Procedure for Compound 3.23

Compound **3.23** was prepared adapting literature.[90]

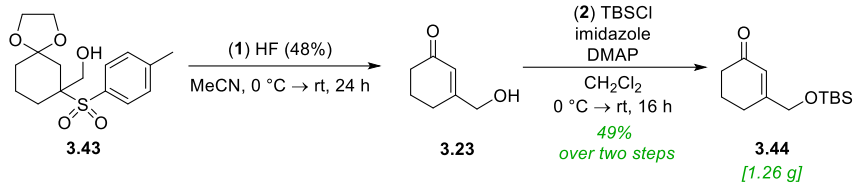

(**Step 1**) Dioxolane **3.43** (3.5 g, 10.7 mmol, 1.0 equiv.) was dissolved in MeCN (94 mL) and stirred for 10 min at rt. The reaction mixture was then cooled to 0 °C and HF (48%, aq., 14 mL, 230 mmol, 21.5 equiv.) was added in one portion and the reaction was left to stir at this temperature for 1 h, and then 24 h at rt. The reaction was quenched slowly with $NaHCO_3$ (aq., sat., 400 mL). The aqueous layer was extracted with CH_2Cl_2 (3 × 200 mL) and the combined organics were washed with brine (300 mL), dried (Na_2SO_4) and concentrated *in vacuo* to give a slight yellow oil. The crude residue was used directly in the next step without further purification.

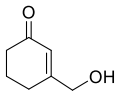

R_f = 0.23 (petroleum ether 40/60:ethyl acetate, 7:3), [UV, vanillin];

8.3.11 Experimental Procedure for Compound 3.44

Compound **3.44** was prepared adapting literature.[90]

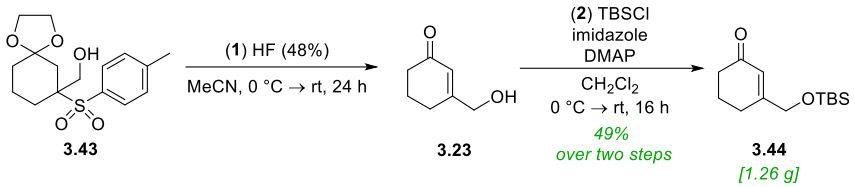

(**Step 2**) To a solution of *tert*-butyldimethylsilyl chloride (1.75 g, 11.6 mmol, 1.1 equiv.) in CH_2Cl_2 (12 mL) was added dropwise to a solution of alcohol **3.23** (1.40 g, 11.1 mmol, 1.0 equiv.), imidazole (1.21 mL, 17.8 mmol, 1.6 equiv.) and DMAP (134 mg, 1.1 mmol, 0.1 equiv.) in CH_2Cl_2 (2.5 mL) at 0 ˚C. The reaction mixture was immediately warmed to rt and left to stir for 10 h. The reaction was then quenched with H_2O (15 mL) and extracted with ethyl acetate (3 × 20 mL). The combined organics were dried (Na_2SO_4) and concentrated *in vacuo* to afford an off white solid. The crude residue was purified *via* column chromatography (silica gel, petroleum ether 40/60:ethyl acetate, 8:2) to afford the titled compound as a white solid (1.26 g, 5.25 mmol, 49%, over two steps).

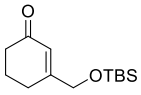

R_f = 0.37 (petroleum ether 40/60:ethyl acetate, 8:2), [UV, $KMnO_4$];

^{1}H NMR (500 MHz, $CDCl_3$) δ 6.15 (1H, p, *J* = 1.7 Hz), 4.22 (2H, dt, *J* = 1.6, 0.8 Hz), 2.40 (2H, dd, *J* = 7.3, 6.0 Hz), 2.21 (2H, t, *J* = 6.0 Hz), 2.01 (1H, dt, *J* = 12.2, 6.3 Hz), 0.92 (9H, s), 0.08 (6H, s) ppm;

^{13}C NMR (125 MHz, $CDCl_3$) δ 199.8, 164.4, 123.3, 65.2, 38.1, 26.1, 26.0, 22.7, 18.5, –5.3 ppm;

Data consistent with literature.[20]

8.3.12 Experimental Procedure for Compound 3.35

Compound **3.35** was prepared according to literature.[90]

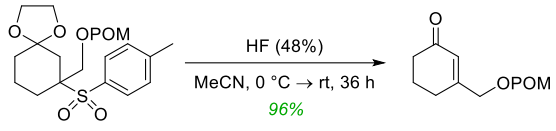

3.34 **3.35** *[1.01 g]*

Dioxolane **3.34** (1.86 g, 4.23 mmol, 1.0 equiv.) was dissolved in MeCN (13 mL) and stirred for 10 min at rt. The reaction mixture was then cooled to 0 °C and HF (48% aq., 4.00 mL, 97.0 mmol, 23.0 equiv.) was added in one portion and the reaction was left to stir at this temperature for 1 h, and then 24 h at rt. The reaction was quenched slowly with $NaHCO_3$ (aq., sat., 50 mL). The aqueous layer was extracted with CH_2Cl_2 (3 × 25 mL) and the combined organics were washed with brine (25 mL), dried ((Na_2SO_4) and concentrated *in vacuo* to give a slight yellow oil. The crude residue was purified *via* column chromatography (silica gel, petroleum ether 40/60:ethyl acetate, 8:2) to afford the titled compound as a yellow oil (1.01 g, 4.21 mmol, 96%).

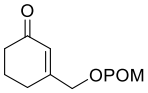

R_f = 0.38 (petroleum ether 40/60:ethyl acetate, 8:2), [UV, $KMnO_4$];

^{1}H NMR (600 MHz, $CDCl_3$) δ 6.03 (1H, s), 4.66 (2H, s), 2.42 (2H, t, *J* = 6.7 Hz), 2.28 (2H, t, *J* = 6.2 Hz), 2.04 (2H, p, *J* = 6.3 Hz), 1.24 (9H, s) ppm;

^{13}C NMR (150 MHz, $CDCl_3$) δ 199.0, 177.8, 158.7, 124.3, 64.9, 38.9, 37.6, 27.2, 26.3, 22.3 ppm;

Data consistent with literature.[90]

8.3.13 Experimental Procedure for Compound 3.6

Compound **3.6** was prepared according to literature.[21]

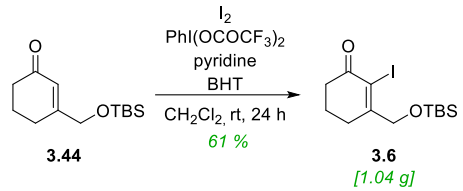

To a solution of I_2 (1.17 g, 4.62 mmol, 1.0 equiv.) and pyridine (0.80 mL, 9.70 mmol, 2.1 equiv.) in anhydrous CH_2Cl_2 (8.6 mL) was added $PhI(OCOCF_3)_2$ (1.99 g, 4.62 mmol, 1.0 equiv.) and BHT (11.0 mg, 0.05 mmol, 1.0 equiv.) and stirred at rt for 20 min. To the reaction mixture, cyclohexenone **3.44** (1.11 g, 4.62 mmol, 1.0 equiv.) in CH_2Cl_2 (8.6 mL) was added and stirred in the absence of light for 24 h. The reaction was quenched with $NaHCO_3$ (aq., sat., 20 mL) and diluted with ethyl acetate (25 mL). The organic phase was washed with $Na_2S_2O_3$ (aq., sat., 20 mL) and extracted with ethyl acetate (2 × 25 mL) and then washed with brine (25 mL) and extracted with ethyl acetate (2 × 25 mL). The combined organics were dried (Na_2SO_4) and concentrated *in vacuo* while protecting the compound from light. The crude residue was purified *via* column chromatography (silica gel, petroleum ether 40/60:ethyl acetate, 9:1) to afford the titled compound as a yellow oil (1.04 g, 2.84 mmol, 61%).

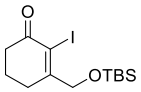

R_f = 0.44 (petroleum ether 40/60:ethyl acetate 9:1), [UV, $KMnO_4$];

^{1}H NMR (500 MHz, $CDCl_3$) δ 4.44 (2H, s), 2.69 – 2.56 (4H, m), 2.01 (2H, q, *J* = 6.1 Hz), 0.93 (9H, s), 0.12 (6H, s) ppm;

^{13}C NMR (125 MHz, $CDCl_3$) δ 191.7, 168.8, 102.5, 72.2, 37.2, 29.7, 25.8, 22.2, 18.3, –5.4 ppm;

Data consistent with literature.[20]

8.3.14 Experimental Procedure for Compound 3.36

Compound **3.36** was prepared according to literature.[90]

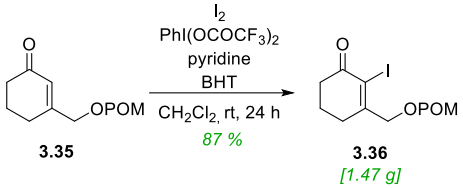

To a solution of I_2 (1.14 g, 4.5 mmol, 1.0 equiv.) and pyridine (0.77 mL, 9.70 mmol, 2.1 equiv.) in anhydrous CH_2Cl_2 (6.0 mL) was added $PhI(OCOCF_3)_2$ (1.94 g, 4.62 mmol, 1.0 equiv.) and BHT (20.0 mg, 0.05 mmol, 1.0 equiv.) and stirred at rt for 20 min. To the reaction mixture, cyclohexenone **3.35** (1.11 g, 4.62 mmol, 1.0 equiv.) in CH_2Cl_2 (6.0 mL) was added and stirred in the absence of light for 24 h. The reaction was quenched with $NaHCO_3$ (aq., sat., 25 mL) and diluted with ethyl acetate (25 mL). The organic phase was washed with $Na_2S_2O_3$ (aq., sat., 25 mL) and extracted with ethyl acetate (2 × 25 mL) and then washed with brine (25 mL) and extracted with ethyl acetate (2 × 25 mL). The combined organics were dried (Na_2SO_4) and concentrated *in vacuo* while protecting the compound from light. The crude residue was purified *via* column chromatography (silica gel, petroleum ether 40/60:ethyl acetate, 9:1) to afford the titled compound as a yellow oil (1.47 g, 4.02 mmol, 87%).

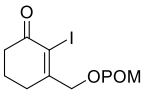

R_f = 0.20 (petroleum ether 40/60:ethyl acetate 8:2), [UV, $KMnO_4$];

^{1}H NMR (500 MHz, $CDCl_3$) δ 4.90 (2H, t, *J* = 1.3 Hz), 2.67 (2H, t, *J* = 6.1 Hz), 2.48 (2H, t, *J* = 6.1 Hz), 2.04 (2H, m), 1.25 (9H, t, *J* = 1.0 Hz) ppm;

^{13}C NMR (150 MHz, $CDCl_3$) δ ^{13}C 191.4 177.8, 162.9, 105.4, 72.0, 39.0, 36.8, 29.6, 27.2, 22.1 ppm;

Data consistent with literature.[90]

8.3.15 Experimental Procedure for Compound 3.45

Compound **3.45** was prepared according to literature.[21]

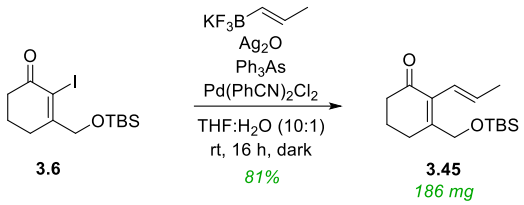

To a solution of compound **3.6** (300 mg, 0.82 mmol, 1.0 equiv.), potassium *trans*-propenyltrifluoroborate (372 mg, 2.52 mmol, 3.1 equiv.), Ag_2O (600 mg, 2.59 mmol, 3.2 equiv.), Ph_3As (50 mg, 0.16 mmol, 0.2 equiv.) in THF/H_2O (10:1, 16.5 mL) was added $Pd(PhCN)_2Cl_2$ (315 mg, 0.82 mmol, 1.0 equiv.) under an inert atmosphere and stirred for 16 h in the dark. The reaction was quenched with NH_4Cl (aq., sat., 25 mL) and stirred for 30 min at rt. The reaction mixture was filtered through Celite© and washed with $CHCl_3$ (40 ml). The organics were then extracted with $CHCl_3$ (20 mL) and washed with brine (50 mL), dried (Na_2SO_4) and concentrated *in vacuo.* The crude residue was passed through a pad of silica (petroleum ether 40/60:ethyl acetate, 10:1) to afford the titled compound as a yellow oil (186 mg, 0.66 mmol, 81%).

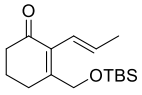

R_f = 0.17 (petroleum ether 40/60:ethyl acetate, 8:2), [UV,vanillin];

^{1}H NMR (600 MHz, $CDCl_3$) δ 6.06 (1H, dq, *J* = 15.9, 1.7 Hz), 5.69 (1H, dq, *J* = 15.9, 6.6 Hz), 4.43 (2H, d, *J* = 1.2 Hz), 2.51 (2H, t, *J* = 6.2 Hz), 2.44 – 2.36 (2H, m), 1.99 – 1.90 (2H, m), 1.82 (3H, dd, *J* = 6.6, 1.8 Hz), 0.90 (9H, s), 0.07 (6H, s) ppm;

^{13}C NMR (125 MHz, $CDCl_3$) δ 199.3, 157.4, 132.8, 132.2, 123.3, 63.5, 38.3, 27.3, 25.8, 21.9, 19.0, 18.3, –5.4 ppm;

Data consistent with literature.[20]

8.3.16 Experimental Procedure for Compound 3.38

Compound **3.38** was prepared adapting literature.[20]

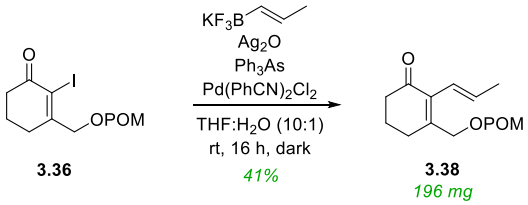

To a solution of **3.36** (620 mg, 1.69 mmol, 1.0 equiv.), *trans*-1-propen-1-ylboronic acid (700 mg, 8.26 mmol, 4.9 equiv.), Ag_2O (1.96 g, 8.45 mmol, 5.0 equiv.), Ph_3As (52.0 mg, 0.17 mmol, 0.1 equiv.) in THF/H_2O (8:1, 26 mL) was added $Pd(PhCN)_2Cl_2$ (32.0 mg, 0.085 mmol, 0.05 equiv.) under an inert atmosphere and stirred for 16 h in the dark. The reaction was quenched with NH_4Cl (aq., sat., 40 mL) and stirred for 30 min at rt. The reaction mixture was filtered through Celite and washed with $CHCl_3$ (50 ml). The organics were then extracted with $CHCl_3$ (30 mL) and washed with brine (50 mL), dried (Na_2SO_4) and concentrated *in vacuo.* The crude residue was passed through a pad of silica (petroleum ether 40/60:ethyl acetate, 10:1) to afford the titled compound as a yellow oil (196 mg, 41%).

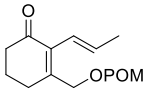

R_f = 0.22 (petroleum ether 40/60:ethyl acetate 8:2), [UV, vanillin];

^{1}H NMR (500 MHz, $CDCl_3$) δ 6.11 (1H, dt, *J* = 16.0, 1.8 Hz), 5.74 (1H, dqd, *J* = 14.7, 6.5, 1.4 Hz), 4.87 (2H, s), 2.59 – 2.32 (4H, m), 1.97 (2H, pd, *J* = 6.3, 1.3 Hz), 1.83 (3H, dt, *J* = 6.4, 1.7 Hz), 1.23 (9H, d, *J* = 1.6 Hz) ppm;

^{13}C NMR (125 MHz, $CDCl_3$) δ 198.8, 178.1, 151.2, 135.2, 133.1, 123.2, 64.5, 39.0, 38.1, 27.7, 27.2, 21.8, 19.0 ppm.

8.3.17 Experimental Procedure for Compound 1.27

Compound **1.27** was prepared according to literature.[20]

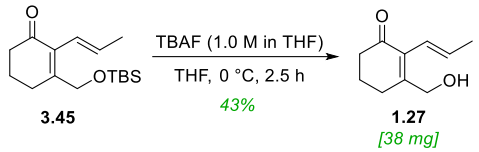

3.45 **1.27** *[38 mg]*

To a solution of compound **3.45** (150 mg, 0.53 mmol, 1.0 equiv.) in THF (1.2 mL) was added TBAF (1.0 M in THF, 0.58 mL) at 0 °C and stirred for 2.5 h at that temperature. The reaction mixture was then concentrated *in vacuo*. The crude residue was purified *via* column chromatography (silica gel, petroleum ether 40/60:ethyl acetate, 8:2) to afford the titled compound a yellow oil (38 mg, 0.23 mmol, 43%).

Alternatively

3.45 **1.27** *[84 mg]*

To a solution of compound **3.45** (170 mg, 0.6 mmol, 1.0 equiv.) in MeOH (7.5 mL) was added HCl (2.0 M, aq., 3.5 mL) at rt and stirred for 5 h at that temperature. The reaction mixture was then quenched with $NaHCO_3$ (5 mL) and the extracted with CH_2Cl_2 (3 × 10 mL), dried (Na_2SO_4) and concentrated *invacuo*. The crude residue was purified *via* column chromatography (silica gel, petroleum ether 40/60:ethyl acetate, 7:3) to afford the titled compound a yellow oil (84 mg, 0.505 mmol, 84%).

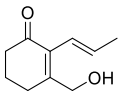

R_f = 0.20 (petroleum ether 40/60:ethyl acetate 8:2), [UV, vanillin (stains blue)];

^{1}H NMR (600 MHz, $CDCl_3$) δ 6.10 (1H, dq, *J* = 16.0, 1.7 Hz), 5.74 (1H, dq, *J* = 15.9, 6.6 Hz), 4.45 (2H, s), 2.56 (2H, t, *J* = 6.1 Hz), 2.46 – 2.41 (2H, m), 2.01 – 1.96 (2H, m), 1.83 (3H, dd, *J* = 6.6, 1.8 Hz) ppm;

^{13}C NMR (125 MHz, $CDCl_3$) 199.3, 155.9, 133.8, 132.9, 123.3, 63.5, 38.2, 27.8, 21.9, 19.0 ppm;

Data consistent with literature.[20]

8.3.18 Experimental Procedure for Compound (±)-1.31

Compound **(±)-1.31** was prepared according to literature.[20]

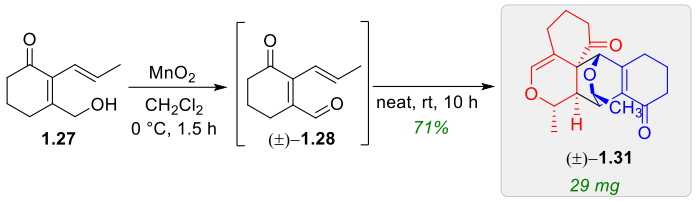

To a solution of alcohol **1.27** (40 mg, 1.0 equiv., 0.24 mmol) in CH_2Cl_2 (5.4 mL) was added activated MnO_2 (1.3 g, 63.0 equiv., 15.0 mmol) at 0 °C under inert atmosphere and stirred for 1.5 h at that temperature. The reaction mixture was then filtered through a pad of Celite© which was washed thoroughly with CH_2Cl_2 (50 mL) and then concentrated *in vacuo* to afford the aldehyde. The crude residue was then left to stand neat overnight at room temperature. The crude residue was purified *via* column chromatography (silica gel, petroleum ether 40/60:ethyl acetate, 1:1) to afford the titled compound a white solid (29 mg, 0.18 mmol, 71%).

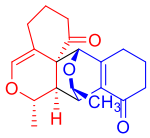

R_f = 0.60 (petroleum ether 40/60:ethyl acetate 1:1), [UV, $KMnO_4$];

Separation of the two dimers was performed by repetitive HPLC chiral column iterations Shimazdu fraction collector (Chiralpak OD-H, 87:13 Hexane/IPA, 0.5 mL min^{-1}, 100 µL injection volume, run time 30 min, λ = 265 nm). This enabled clean spectra and assignment of major dimer but for the minor dimer not enough sample was collected to gain full 2D spectra to assign product.

Major (Hetero chiral dimer);

^{1}H NMR (800 MHz, $CDCl_3$) δ 6.38 (1H, d, *J* = 1.6 Hz), 4.60 (1H, s), 4.44 (1H, qd, *J* = 6.3, 1.3 Hz), 4.34 (1H, q, *J* = 6.7 Hz), 3.17 (1H, t, *J* = 1.7 Hz), 2.59 – 2.41 (7H, m), 2.27 (1H, ddt, *J* = 14.2, 4.5, 2.2 Hz), 2.20 (1H, dddt, *J* = 13.0, 6.6, 4.6, 2.6 Hz), 2.01 (3H, tddd, *J* = 14.2, 11.2, 5.9, 3.5 Hz), 1.78 (1H, tdt, *J* = 13.4, 8.8, 4.5 Hz), 1.07 (3H, d, *J* = 6.7 Hz), 0.83 (3H, d, *J* = 6.3 Hz) ppm;

^{13}C NMR (150 MHz, $CDCl_3$) δ 207.2, 195.3, 157.8, 138.9, 136.2, 112.9, 74.7, 73.0, 67.8, 53.3, 39.9, 39.1, 37.4, 37.2, 29.7, 27.7, 27.5, 26.1, 22.8, 20.8, 19.6 ppm;

HRMS (FAB) calc. for $C_{20}H_{24}O_4$ ($[M+H]^+$): 328.1675; found: 328.1669;

IR (film, cm^{-1}) 2924, 2852, 2359, 2340, 1706, 1670, 1456, 1399, 1376, 1229, 1211, 1194, 1164, 1112, 1095, 1043, 1024, 1007, 899, 834;

Data consistent with literature.[20]

8.3.19 General Procedure 5 – For Chiral Additives Screen

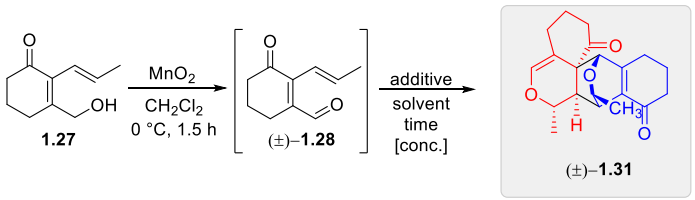

To a solution of alcohol **1.27** (40 mg, 1.0 equiv., 0.24 mmol) in CH_2Cl_2 (5.4 mL) was added activated MnO_2 (1.3 g, 63.0 equiv., 15.0 mmol) at 0 °C under inert atmosphere and stirred for 1.5 h at that temperature. The reaction mixture was then filtered through a pad of Celite which was washed thoroughly with CH_2Cl_2 (25 mL) and then concentrate *in vacuo* at 0 °C to afford the aldehyde. The crude residue was dissolved in a solvent (X mL) and left to stir at the rt temperature. NMR aliquots were taken at specified time points to measure conversion of the crude aldehyde into product. The hetero:homo chiral dimer ratio and e.r. was measure of the product *via* chiral HPLC (Chiralpak OD-H, 87:13 Hexane/IPA, 0.5 mL min^{-1}, 5 µL injection volume, run time 30 min, λ = 265 nm).

8.3.20 Experimental Procedure for Compound 3.42

Compound **3.42** was prepared according to literature.[95]

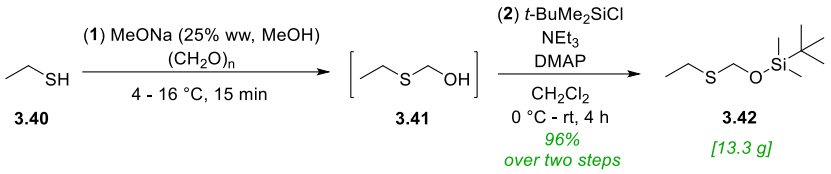

(Step 1): To a solution of ethanethiol (**3.40**) (6.4 mL, 1.0 equiv., 67 mmol) and paraformaldehyde (2.8 g, 1.1 equiv., 93 mmol) in a three necked flask under an inert atmosphere at 4 °C was added a solution of MeONa (25% w/w in MeOH, 35 µL, 0.002 equiv.) was added slowly. Once the solid paraformaldehyde was fully dissolved the cooling bath was removed and the reaction mixture was stirred for 15 mins to afford the crude intermediate **3.41** as a yellow liquid which was used immediately in the next reaction.

(Step 2): To the same reaction flask CH_2Cl_2 (60 mL) was added and the solution was cooled to 3 °C. DMAP (0.45 g, 0.04 equiv., 3.7 mmol), NEt_3 (15 mL, 1.3 equiv., 0.11 mol) was added and *t* $BuMe_2SiCl$ (15 g, 1.2 equiv., 0.1 mol) added in 3 portions over 10 min. After the addition, the cooling bath was removed and replaced with a water bath and the reaction was stirred for a further 4 h. The reaction was diluted with CH_2Cl_2 (30 mL) and the organic layer was washed with water (2 × 50 mL) and NH_4Cl (aq. sat., 50 mL). The combined organics were dried (Na_2SO_4) and concentrated *in vacuo*. The crude residue was diluted with hexanes (50 mL) and washed with water (2 × 50 ml) and brine (aq. sat., 50 ml). The combined organics were dried (Na_2SO_4) and concentrated *in vacuo*. The crude residue was purified *via* vacuum distillation (93 mbar, 125-128 °C) to afford the title compound as a colourless oil (13.3 g, 96% over two steps).

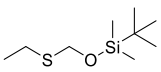

^{1}H NMR (500 MHz, $CDCl_3$) δ 4.81 (2H, s), 2.67 (2H, q, *J* = 7.4 Hz), 1.29 (3H, t, *J* = 7.5 Hz), 0.90 (9H, d, *J* = 0.5 Hz), 0.12 (6H, s) ppm;

^{13}C NMR (125 MHz, $CDCl_3$) δ 66.0, 25.8, 24.6, 18.2, 14.9, –5.0 ppm;

Data consistent with literature.[95]

8.3.21 Experimental Procedure for Compound 3.37

Compound **3.37** was prepared adapting literature.[89]

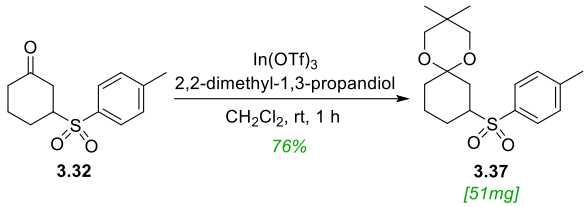

To a solution of 3-tosylcyclohexan-1-one (**3.32**) (50 mg, 1.0 equiv., 0.2 mmol) and 2,2-dimethyl-1,3-propandiol (52 mg, 2.0 equiv., 0.4 mmol) in CH_2Cl_2 (3 mL) was added $In(OTf)_3$ (0.6 mg, 0.5 mol%, 1.0 µmol) at rt and left to stir. After 10 min another portion of $In(OTf)_3$ (0.6 mg, 0.5 mol%, 1.0 µmol) was added and left to stir at this temperature for 1 h. The reaction was then passed through a short plug of neutral alumina and washed with CH_2Cl_2 (5 mL) and concentrated *in vacuo* to afforded the title compound as an off white solid (51 mg, 0.15 mmol, 76%).

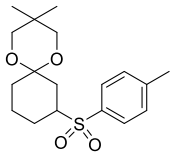

R_f = 0.32 (petroleum ether 40/60:CH_2Cl_2, 8:2)), [UV, $KMnO_4$];

^{1}H NMR (400 MHz, $CDCl_3$) δ 7.77 (2H, d, *J* = 8.3 Hz), 7.37 (1H, d, *J* = 7.7 Hz), 3.56 (1H, d, *J* = 11.4 Hz), 3.50 (1H, dd, *J* = 11.4, 0.9 Hz), 3.47 – 3.36 (2H, m), 3.13 (1H, tt, *J* = 12.6, 3.4 Hz), 2.81 – 2.71 (1H, m), 2.47 (3H, s), 2.20 (1H, dd, *J* = 13.5, 2.7 Hz), 2.00 (1H, ddt, *J* = 12.7, 3.4, 1.8 Hz), 1.73 (1H, dq, *J* = 13.2, 3.2 Hz), 1.55 – 1.15 (4H, m), 0.98 (3H, s), 0.93 (3H, s) ppm;

^{13}C NMR (150 MHz, $CDCl_3$) δ 144.7, 134.0, 129.7, 129.1, 97.2, 70.1, 69.9, 60.5, 32.1, 30.9, 30.1, 25.3, 22.7, 22.6, 21.6, 20.7 ppm.

8.3.22 General Procedure 6 – TADDOL formation from aryl bromide

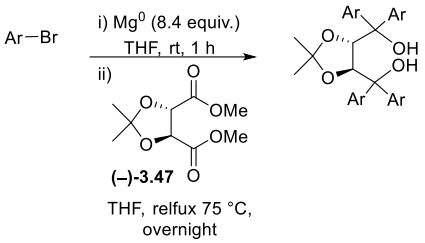

To a suspension of magnesium turnings (8.4 equiv.) in anhydrous THF and a single crystal of iodine was added aryl bromide (8.4 equiv.) dropwise and this was left to stir for 1 hour at rt. (4*R*,5*R*)-dimethyl 2,2-dimethyl-1,3-dioxolane-4,5-dicarboxylate **(–)-**(**3.47**) (1.0 equiv.) in anhydrous THF was added dropwise and then the reaction was heated to reflux (heating block set to 75 °C) overnight. The reaction was quenched with NH_4Cl (sat., aq.) and extracted with EtOAc (3 × X mL). The combined organics were dried (Na_2SO_4) and concentrated *in vacuo* to afford the crude product.

8.3.23 General Procedure 7 – TADDOL formation from Grignard

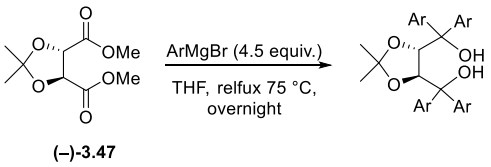

Grignard (4.5 equiv.) was added dropwise to a solution of (4*R*,5*R*)-dimethyl 2,2-dimethyl-1,3-dioxolane-4,5-dicarboxylate **(–)-**(**3.47**) (1.0 equiv.) in anhydrous THF at 0 °C. The reaction was then heated to reflux (heating block set to 75 °C) and left to stir overnight. The reaction was quenched with NH_4Cl (sat., aq.) and extracted with EtOAc (3 × X mL). The combined organics were dried (Na_2SO_4) and concentrated *in vacuo* to afford the crude product.

8.3.24 Experimental Procedure for Compound (–)-3.51

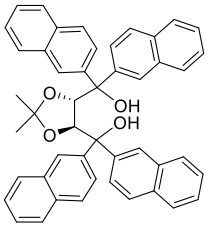

(–)-3.51
79%
[0.85 g]

Compound (–)-**3.51** was prepared according to general procedure **6**. Magnesium turnings (0.29 g, 8.4 equiv., 12 mmol), 1 crystal of iodine in anhydrous THF (3.4 mL), 2-bromonaphthalene (2.37 g, 8.4 equiv., 12.0 mmol) in anhydrous THF (11.4 mL) and (4*R*,5*R*)-dimethyl 2,2-dimethyl-1,3-dioxolane-4,5-dicarboxylate **(–)-(3.47)** (0.29 mL, 1.0 equiv., 1.6 mmol) in anhydrous THF (7.1 mL). Purified *via* column chromatography (silica gel, toluene, 100%) to afford the titled compound as fine yellow crystals (0.85 g, 1.27 mmol, 79%).

R_f = 0.1 (toluene), [UV, vanillin];

Mp = 213-215 °C, Lit. 213-216 °C (Sigma)

^{1}H NMR (600 MHz, $CDCl_3$) δ 8.25 – 7.21 (aromatic 28H, m), 4.99 (2H, s), 4.36 – 4.23 (2H, m), 1.19 (6H, s) ppm;

^{13}C NMR (150 MHz, $CDCl_3$) δ 142.5, 140.6, 132.8, 132.72, 132.69, 132.6, 128.61, 128.60, 127.9, 127.5, 127.4, 127.2, 127.1, 126.9, 126.2, 126.12, 126.10, 125.99, 125.97, 125.8, 110.0, 81.5, 78.7, 27.5 ppm;

HRMS (ESI^+) calc. for $C_{47}H_{38}O_4$ ($[M+Na]^+$): 689.2692; found 689.2647;

IR (film) ν_{max}/cm^{-1} 3290 (broad), 3058, 2987, 2931, 2837, 2360, 2342, 2246, 1773, 1734, 1717, 1706, 1702, 1684, 1653, 1647, 1632, 1600, 1577, 1559, 1540, 1533, 1505, 1456, 1436, 1381, 1371, 1355, 1335, 1274, 1238, 1221, 1165,1125, 1061, 1038, 1028, 1018;

Data consistent with literature.[247]

8.3.25 Experimental Procedure for Compound (–)-3.50

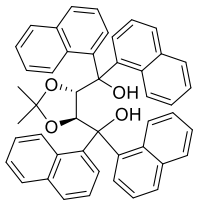

(–)-3.50
88%
[0.93 g]

Compound **(–)-3.50** was prepared according to general procedure **6**. Magnesium turnings (0.29 g, 8.4 equiv., 12 mmol), 1 crystal of iodine in anhydrous THF (3.4 mL), 1-bromonaphthalene (1.60 mL, 8.4 equiv., 12.0 mmol) in anhydrous THF (11.4 mL) and (4*R*,5*R*)-dimethyl 2,2-dimethyl-1,3-dioxolane-4,5-dicarboxylate (**(–)-3.47**) (0.29 mL, 1.0 equiv., 1.6 mmol) in anhydrous THF (7.1 mL). Purified *via* column chromatography (silica gel, toluene, 100) to afford the titled compound as off white fine crystals (0.93 g, 1.4 mmol, 88%).

R_f = 0.27 (toluene), [UV, vanillin];

Mp = 204-207 °C Lit. 200 °C (Sigma)

^{1}H NMR (600 MHz, CDCl3) δ 8.52-6.56 (28H, br, m), 3.22 (2H, s), 1.19 (6H, s) ppm;

NMR spectra is poorly resolved due to restricted conformation;

IR (film) ν_{max}/cm^{-1} 3310 (broad), 3089, 3048, 2987, 1599, 1509, 1436, 1395, 1381, 1371, 1344, 1309, 1235, 1217, 1170, 1061, 1037, 1027;

HRMS (ESI$^+$) calc. for $C_{47}H_{38}O_4$ ([M+Na]$^+$): 689.2692; found 689.2649;

Data consistent with a sample purchased from Sigma.[248]

8.3.26 Experimental Procedure for Compound (–)-3.56

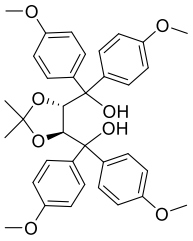

(–)-3.56
88%
[0.83 g]

Compound **(–)-3.56** was prepared according to general procedure **6**. Magnesium turnings (0.29 g, 8.4 equiv., 12 mmol), 1 crystal of iodine in anhydrous THF (3.4 mL), 4-bromoanisole (1.50 mL, 8.4 equiv., 12.0 mmol) in anhydrous THF (11.4 mL) and (4*R*,5*R*)-dimethyl 2,2-dimethyl-1,3-dioxolane-4,5-dicarboxylate (**(–)-3.47**) (0.29 mL, 1.0 equiv., 1.6 mmol) in anhydrous THF (7.1 mL). Purified *via* column chromatography (silica gel, diethyl ether:petroleum ether 40/60, 2:1) to afford the titled compound as off white fine crystals (0.83 g, 1.40 mmol, 88%).

R_f = 0.38 (diethyl ether:petroleum ether 40/60, 2:1), [UV, vanillin stains red];

^{1}H NMR (600 MHz, $CDCl_3$) δ 7.50 – 7.41 (4H, m), 7.26 – 7.23 (4H, m), 6.88 – 6.84 (4H, m), 6.80 – 6.76 (4H, m), 4.49 (2H, s), 3.99 (2H, s), 3.83 (6H, s), 3.76 (6H, s), 1.07 (6H, s) ppm;

^{13}C NMR (150 MHz, $CDCl_3$) δ 158.8, 158.6, 138.5, 135.1, 129.7, 128.9, 113.4, 112.6, 109.2, 81.1, 77.6, 55.2, 27.2 ppm;

HRMS (ESI^+) calc. for $C_{35}H_{38}O_8$ ($[M+Na]^+$): 609.2492; found 609.2446;

IR (film) ν_{max}/cm^{-1} 3340 (broad), 2987, 2955, 2934, 2905, 2837, 1609, 1583, 1509, 1463, 1442, 1415, 1381, 1371, 1335, 1301, 1175, 1122, 1085, 1053, 1035, 1030;

Data consistent with literature.[249]

8.3.27 Experimental Procedure for Compound (–)-3.52

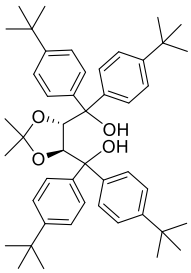

(–)-3.52
64%
[0.70 g]

Compound **(–)-3.52** was prepared according to general procedure **6**. Magnesium turnings (0.29 g, 8.4 equiv., 12 mmol), 1 crystal of iodine in anhydrous THF (3.4 mL), 4-*tert*-butylbenzyl bromide (2.08 mL, 8.4 equiv., 12.0 mmol) in anhydrous THF (11.4 mL) and (4*R*,5*R*)-dimethyl 2,2-dimethyl-1,3-dioxolane-4,5-dicarboxylate (**(–)- 3.47**)(0.29 mL, 1.0 equiv., 1.6 mmol) in anhydrous THF (7.1 mL). Purified *via* column chromatography (silica gel, diethyl ether:petroleum ether 40/60, 1:10) to afford the titled compound as off white foam (0.70 g, 1.02 mmol, 64%).

R_f = 0.14 (diethyl ether:petroleum ether 40/60, 1:10), [UV, vanillin];

^{1}H NMR (600 MHz, $CDCl_3$) δ 7.46 – 7.28 (16H, m), 4.57 (2H, s), 3.92 (2H, s), 1.33 (18H, s), 1.28 (18H s), 1.01 (6H, s) ppm;

^{13}C NMR (150 MHz, $CDCl_3$) δ 149.8, 143.3, 139.7, 128.1, 127.3, 125.0, 124.1, 109.3, 81.2, 77.8, 34.5, 34.4, 31.4, 31.3, 27.0 ppm;

HRMS (ESI^+) calc. for $C_{47}H_{62}O_4$ ($[M+Na]^+$): 713.4492; found 713.4510;

IR (film) ν_{max}/cm^{-1} 3250 (broad), 2962, 2904, 2868, 2360, 2341, 1653, 1609, 1559, 1512, 1475, 1459, 1405, 1395, 1379, 1363, 1335, 1269, 1244, 1218, 1204, 1170, 1110, 1087, 1053, 1038, 1018;

Data consistent with literature.[249]

8.3.28 Experimental Procedure for Compound (–)-3.48

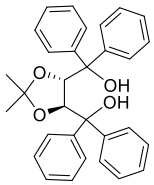

(–)-3.48
22%
[0.61 g]

Compound **(–)-3.48** was prepared according to general procedure **7**. (4*R*,5*R*)-Dimethyl 2,2-dimethyl-1,3-dioxolane-4,5-dicarboxylate (1.1 mL, 1.0 equiv., 6.0 mmol) in anhydrous THF (12.0 mL) and phenylmagnesium bromide (**(–)-3.47**) (9.0 mL, 3 M in diethyl ether, 4.5 equiv., 27 mmol). Purified *via* hot recrystalisation (petroleum ether 40/60 and minimum amount of methanol) to afford the titled compound as colourless crystals (0.61 g, 1.31 mmol, 22%).

R_f = 0.19 (cyclohexane:ethyl acetate, 10:1), [UV, vanillin];

^{1}H NMR (500 MHz, $CDCl_3$) δ 7.55 – 7.51 (4H, m), 7.37 – 7.22 (16H, m), 4.61 (2H, s), 3.87 (2H, s), 1.04 (6H, s) ppm;

^{13}C NMR (125 MHz, $CDCl_3$) δ 145.9, 142.7, 128.6, 128.1, 127.6, 127.3, 109.6, 81.0, 78.2, 27.2 ppm;

HRMS (ESI^+) calc. for $C_{31}H_{30}O_4$ ($[M+NH_4]^+$): 484.2438; found 484.2436;

IR (film) ν_{max}/cm^{-1} 3325 (broad), 3058, 3031, 2987, 2360, 1495, 1448, 1381, 1371, 1241, 1219, 1170, 1081, 1047;

Data consistent with literature.[250]

8.3.29 Experimental Procedure for Compound (–)-3.55

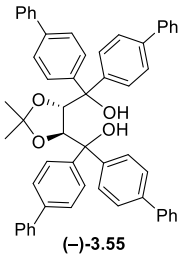

(–)-3.55
87%
[1.07 g]

Compound **(–)-3.55** was prepared according to general procedure **6**. Magnesium turnings (0.29 g, 8.4 equiv., 12 mmol), 1 crystal of iodine in anhydrous THF (3.4 mL), 4-bromobiphenyl (2.08 mL, 8.4 equiv., 12.0 mmol) in anhydrous THF (11.4 mL) and (4*R*,5*R*)-dimethyl 2,2-dimethyl-1,3-dioxolane-4,5-dicarboxylate (**(–)-3.47**) (0.29 mL, 1.0 equiv., 1.6 mmol) in anhydrous THF (7.1 mL). Purified *via* hot recrystalisation (CH_2Cl_2 and minimum amount of MeOH) to afford the titled compound as a white solid (1.07 g, 1.4 mmol, 87%).

R_f = 0.15 (toluene), [UV, vanillin];

^{1}H NMR (500 MHz, $CDCl_3$) δ 7.70 – 7.61 (12H, m), 7.55 – 7.32 (24H, m), 4.75 (2H, s), 4.13 (2H, s), 1.18 (6H, s) ppm;

^{13}C NMR (125 MHz, $CDCl_3$) δ 144.6, 141.9, 140.7, 140.6, 140.4, 140.0, 129.0, 128.8, 128.8, 128.0, 127.4, 127.3, 127.1, 127.1, 126.9, 126.1, 109.8, 81.2, 78.1, 27.4 ppm;

HRMS (ESI^+) calc. for $C_{55}H_{46}O_4$ ($[M+NH_4]^+$): 788.3738; found 788.3729;

IR (film) ν_{max}/cm^{-1} 3250 (broad), 3058, 3031, 2987, 2360, 1600, 1519, 1486, 1402, 1381, 1371, 1336, 1241, 1218, 1170, 1054, 1007;

Data consistent with literature.[251]

8.3.30 Experimental Procedure for Compound (–)-3.57

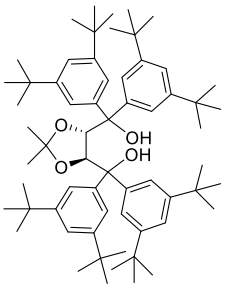

(–)-3.57
76%
[1.11 g]

Compound **(–)-3.57** was prepared according to general procedure **6**. Magnesium turnings (0.29 g, 8.4 equiv., 12 mmol), 1 crystal of iodine in anhydrous THF (3.4 mL), 3,5-di-*tert*-butylbenzyl bromide (2.08 mL, 8.4 equiv., 12.0 mmol) in anhydrous THF (11.4 mL) and (4*R*,5*R*)-dimethyl 2,2-dimethyl-1,3-dioxolane-4,5-dicarboxylate (**(–)-3.47**) (0.29 mL, 1.0 equiv., 1.6 mmol) in anhydrous THF (7.1 mL). Purified *via* hot recrystalisation (petroleum ether 40/60 and minimum amount of CH_2Cl_2) to afford the titled compound as a crystalline white solid (1.11 g, 1.21 mmol, 76%).

R_f = 0.14 (toluene), [UV, vanillin];

^{1}H NMR (500 MHz, $CDCl_3$) δ 7.46 (4H, q, *J* = 2.0 Hz), 7.34 (2H, q, *J* = 2.0 Hz), 7.28 (2H, q, *J* = 2.0 Hz), 7.22 (4H, q, *J* = 2.0 Hz), 4.79 – 4.68 (2H, m), 3.85 – 3.64 (2H, m), 1.35 – 1.32 (36H, m), 1.25 – 1.20 (36H, m), 0.99 – 0.94 (6H, m) ppm;

^{13}C NMR (125 MHz, $CDCl_3$) δ 149.7, 149.1, 145.2, 141.8, 123.0, 122.2, 120.9, 120.5, 108.3, 81.9, 78.9, 34.9, 34.9, 31.7, 31.4, 26.9 ppm;

HRMS (ESI^+) calc. for $C_{63}H_{94}O_4$ ($[M+NH_4]^+$): 932.7538; found 932.7455;

IR (film) ν_{max}/cm^{-1} 3330 (broad), 2964, 2905, 2868, 1597, 1478, 1393, 1362, 1248, 1201, 1170;

Data consistent with literature.[249]

8.4 Experimental Conditions Chapter 5

8.4.1 Experimental Procedure for Compound 5.12

Compound **5.12** was prepared adapting literature.[179]

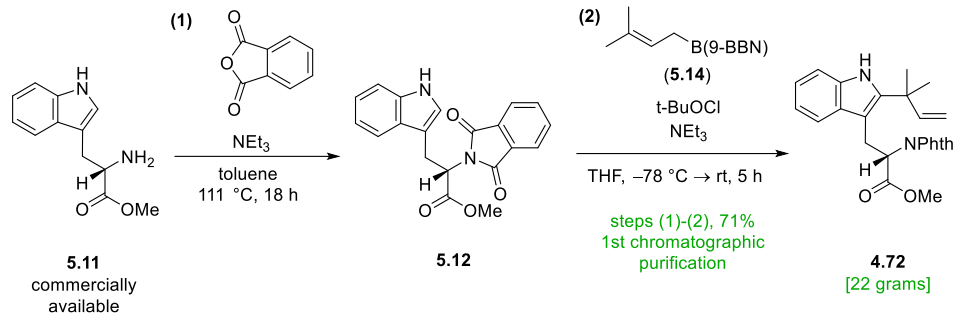

Step (1) To a stirred suspension of L-tryptophan methyl ester hydrochloride (**5.11**) (25.0 g, 1.0 equiv., 98.2 mmol) and phthalic anhydride (14.5 g, 1.0 equiv., 98.2 mmol) in toluene (1000 mL) was added NEt_3 (27.4 mL, 2.0 equiv., 196 mmol) and the mixture heated at reflux (111 °C) for 18 h. The reaction was allowed to cool to room temperature and a mixture of saturated aq. NH_4Cl (150 mL) and water (150 mL) was added. The organic phase was separated, washed with brine (300 mL), dried (Na_2SO_4) and concentrated under reduced pressure to give crude **5.12** (33.4 g, 98% crude mass recovery), which was used without further purification in the next step. A small sample was purified by flash chromatography (2:3 EtOAc/petroleum spirit) to give compound **5.12** as a pale-yellow foam suitable for characterisation.

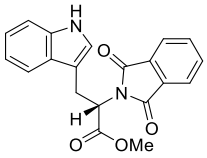

R_f 0.24 (2:3 EtOAc/petroleum spirit);

^{1}H NMR (500 MHz, $CDCl_3$) δ 7.97 (1H, br. s), 7.74 (2H, dd, *J* = 5.5, 3.1 Hz), 7.65 (2H, dd, *J* = 5.5, 3.0 Hz), 7.60 (1H, app. dt, *J* = 7.9, 0.9 Hz), 7.25 (1H, app. dt, *J* = 7.3, 0.9, 0.9 Hz), 7.12 (1H,

ddd, *J* = 8.1, 7.0, 1.2 Hz), 7.05 (1H, ddd, *J* = 8.0, 7.0, 1.1 Hz), 6.99 (1H, d, *J* = 2.3 Hz), 5.28 (1H, dd, *J* = 9.9, 6.1 Hz), 3.79 (3H, s), 3.77 – 3.71 (2H, m) ppm;

^{13}C NMR (125 MHz, $CDCl_3$) δ 169.8, 167.7, 136.2, 134.1, 131.8, 127.3, 123.5, 122.7, 122.2, 119.6, 118.6, 111.24, 111.21, 53.0, 52.7, 24.9 ppm;

IR (film, cm^{-1}) 3404, 3057, 3013, 2953, 2924, 2849, 1775, 1740, 1705, 1612, 1555;

HRMS (ESI^+) calc. for $C_{20}H_{16}N_2O_4$ ($[M + H]^+$): 349.1183; found: 349.1191), ($[M + Na]^+$): 371.1003; found: 371.1002;

$[\boldsymbol{\alpha}]_{\boldsymbol{D}}^{\boldsymbol{23.3}}$ −201.1° (*c* 1.07, $CHCl_3$);

Data consistent with literature.[123]

8.4.2 Experimental Procedure for Compound 4.72

Compound **4.72** was prepared according to literature.[180]

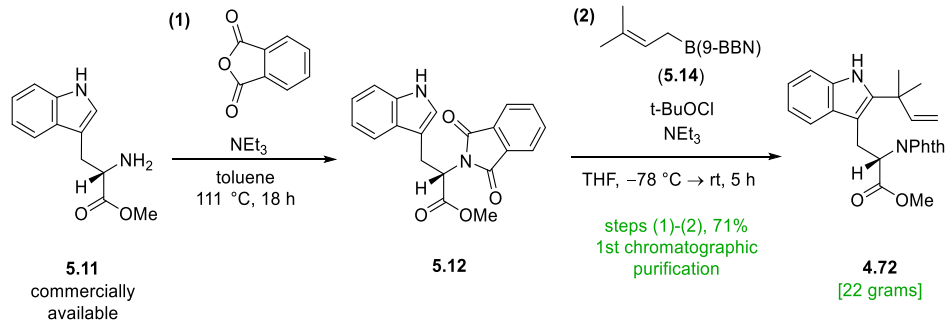

Step (2) Reaction performed under anhydrous reaction conditions. A solution of crude compound **5.12** (25.0 g, 1.0 equiv., 71.8 mmol) and dry NEt_3 (12.0 mL, 1.2 equiv., 86.1 mmol) in THF (250 mL) was cooled to −78 °C in the absence of light. *t*-BuOCl (9.7 mL, 1.2 equiv., 86.1 mmol, see **page 238** for preparation) was added dropwise *via* a syringe pump over 30 minutes and the reaction stirred for 30 minutes at −78 °C. A solution of *B*-prenyl-9-BBN (**5.14**) (360 mL, 2.5 equiv., 180 mmol, 0.5 M in THF, see pages **236**-**237** for preparation) was added dropwise at −78 °C, over 50 min *via* a cannula. After stirring for 1 h at −78 °C the cooling bath was removed and the reaction allowed to slowly warm to room temperature. Reaction progress was monitored by TLC analysis; starting material **5.12**, R_f 0.24 (1:1 EtOAc/petroleum spirit), intermediate, R_f 0.63 (1:1 EtOAc/petroleum spirit). After stirring for 2 h saturated aq. K_2CO_3 (75 mL) was added. The layers were separated and the aqueous layer extracted with EtOAc (3 × 125 mL). The combined organic layers were dried ($MgSO_4$) and concentrated under reduced pressure. The crude product was filtered through silica with CH_2Cl_2, concentrated and purified by flash chromatography (1:9 to 3:7 EtOAc/petroleum spirit) to give compound **4.72** (21.6 g, 51.9 mmol, 71% over 2 steps) as a pale-yellow foam.

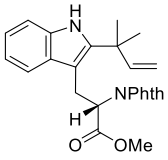

R_f 0.55 (1:1 EtOAc/petroleum spirit), 0.24 (1:4 EtOAc/petroleum spirit);

^{1}H NMR (600 MHz, $CDCl_3$) δ 7.86 (1H, br. s), 7.69 (2H, dd, *J* = 5.5, 3.0 Hz), 7.62 (2H, dd, *J* = 5.5, 3.0 Hz), 7.28 (1H, app. dt, *J* = 7.9, 0.9 Hz), 7.13 (1H, app. dt, *J* = 8.0, 0.8 Hz), 6.90 (1H, ddd, *J* = 8.1, 7.0, 1.1 Hz), 6.71 (1H, ddd, *J* = 8.0, 7.0, 1.0 Hz), 6.19 (1H, dd, *J* = 17.5, 10.5 Hz), 5.23 – 5.17 (2H, m), 5.15 (1H, dd, *J* = 10.5, 1.0 Hz), 3.86 (1H, dd, *J* = 15.4, 3.9 Hz), 3.78 (3H, s), 3.67 (1H, dd, *J* = 15.4, 11.3 Hz), 1.58 (3H, s), 1.57 (3H, s) ppm;

^{13}C NMR (150 MHz, $CDCl_3$) δ 169.7, 167.8, 146.0, 140.3, 134.0, 134.0, 132.0, 129.9, 123.3, 121.3, 119.3, 117.9, 112.3, 110.3, 106.4, 53.6, 52.9, 39.3, 27.8, 27.7, 24.6 ppm;

$[\boldsymbol{\alpha}]_{\boldsymbol{D}}^{\mathbf{23.7}}$ −221.6° (*c* 3.97, $CHCl_3$), literature: $[\boldsymbol{\alpha}]_{\boldsymbol{D}}^{\mathbf{25}}$ −180.8° (*c* 3.9, $CHCl_3$);[180]

Data consistent with literature.[180]

8.4.3 Experimental Procedure for Compound 4.73

Compound **4.73** was prepared adapting literature by the work of Hell,[170,171] and Fisher.[169]

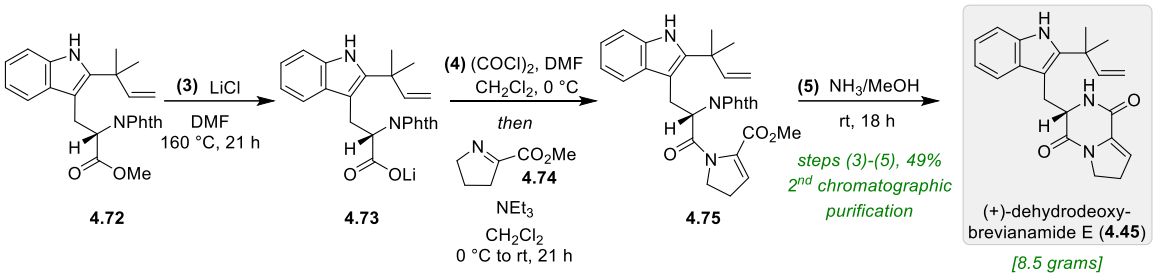

Step (3) Compound **4.72** (24.6 g, 1.0 equiv., 59.0 mmol) and LiCl (50.0 g, 20.0 equiv., 1180 mmol) were suspended in DMF (125 mL) and the resulting mixture refluxed (heating block set to 160 °C) for 21 h under a flow of nitrogen. The thick brown suspension was diluted with CH_2Cl_2 (300 mL) and the solid was washed with CH_2Cl_2 (100 mL) and removed by filtration. The residual solid was broken up, suspended in CH_2Cl_2 (300 mL), stirred vigorously for 30 minutes. The solution was then filtered and the solid was again washed with CH_2Cl_2 (100 mL). The combined filtrates were concentrated under reduced pressure, then dried at 160 °C under reduced pressure. The crude product was re-dissolved in CH_2Cl_2 (200 mL), filtered and concentrated. This process was repeated until there was no residual LiCl solid remaining, before being dried at 160 °C under reduced pressure to give crude lithium carboxylate **4.73** (23.6 g) as a brown foam, which was used without further purification in the next step.

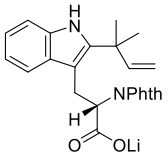

^{1}H NMR (500 MHz, CD_3OD) δ 7.62 (4H, app. s), 7.21 (1H, app. dt, *J* = 8.1, 0.9 Hz), 7.11 (1H, app. t, *J* = 8.0, 0.9 Hz), 6.75 (1H, ddd, *J* = 8.1, 7.0, 1.1 Hz), 6.53 (1H, ddd, *J* = 8.0, 7.0, 1.0 Hz), 6.26 (1H, dd, *J* = 17.4, 10.6 Hz), 5.13 (1H, dd, *J* = 17.4, 1.2 Hz), 5.04 (1H, dd, *J* = 10.6, 1.2 Hz), 4.95 (1H, dd, *J* = 12.0, 3.3 Hz), 3.84 (1H, dd, *J* = 15.3, 3.3 Hz), 3.58 (1H, dd, *J* = 15.3, 12.0 Hz), 1.59 (3H, s), 1.54 (3H, s) ppm;

^{13}C NMR (125 MHz, CD_3OD) δ 176.1, 170.1, 147.8, 141.3, 136.2, 134.6, 133.7, 131.1, 123.5, 121.2, 118.9, 118.5, 111.7, 111.3, 108.4, 57.8, 40.4, 28.6, 28.3, 26.0 ppm;

IR (film, cm^{-1}) 2924, 2365, 1773, 1701, 1611, 1466, 1396, 1350;

HRMS (ESI^-) calc. for $C_{24}H_{21}N_2O_4$ ($[M - Li]^-$): 401.1507; found: 401.1496);

$[\boldsymbol{\alpha}]_{\boldsymbol{D}}^{\mathbf{22.9}}$ −226.0° (*c* 0.20, MeOH).

8.4.4 Experimental Procedure for Compound 4.75

Compound **4.75** was prepared adapting literature by the work of Schmalz,[188] and Soai.[187]

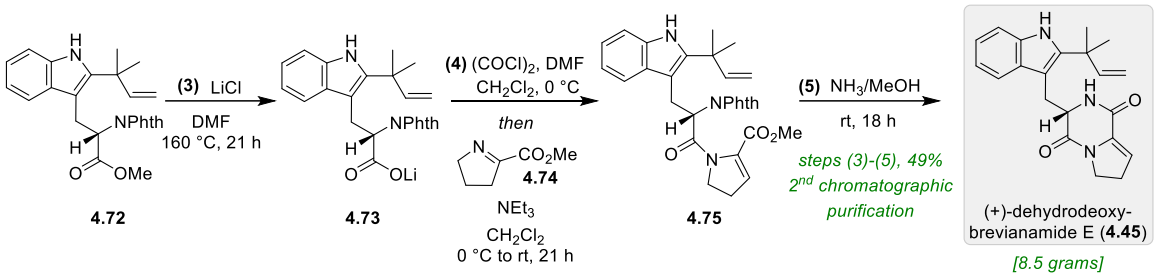

Step (4) Reaction performed under anhydrous reaction conditions. DMF (1.90 mL, 1.0 equiv., 24.6 mmol) was added dropwise to a solution of oxalyl chloride (6.24 mL, 3.0 equiv., 73.8 mmol) in CH_2Cl_2 (200 mL) at 0 °C. A suspension of crude compound **4.73** from **Step (3)** (20.1 g) in CH_2Cl_2 (250 mL) was then added *via* a cannula dropwise over 30 min at 0 °C and the resulting mixture was stirred at 0 °C for 30 min. A solution of compound **4.74** (5.84 mL, 2.0 equiv., 49.2 mmol, see **page 235** for preparation) and NEt_3 (10.3 mL, 3.0 equiv., 73.8 mmol) in CH_2Cl_2 (200 mL) was added *via* a cannula over 20 min at 0 °C. The cooling bath was then removed and the reaction stirred for 21 h at rt. The reaction was quenched by the addition of 1 M aq. HCl (80 mL), the phases separated and the aqueous phase extracted with CH_2Cl_2 (3 × 50 mL). The combined organics were washed with saturated aq. $NaHCO_3$ (80 mL), and the aqueous layer then back extracted with CH_2Cl_2 (50 mL). The combined organics were washed with brine (120 mL), dried (Na_2SO_4) and concentrated under reduced pressure to give crude compound **4.75** (23.9 g) which was used without further purification in the next step. A small sample could be purified by flash chromatography (1:1 EtOAc/petroleum spirit) to give compound **4.75** as a lemon-yellow foam suitable for characterisation.

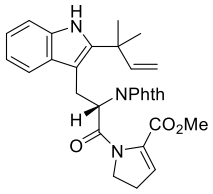

R_f 0.28 (1:1 EtOAc/petroleum spirit);

^{1}H NMR (500 MHz, CD_2Cl_2) δ 7.99 (1H, s), 7.63 (4H, app. s), 7.17 – 7.13 (2H, m), 6.86 (1H, dd, *J* = 8.2, 7.1 Hz), 6.61 (1H, app. t, *J* = 7.4 Hz), 6.20 (1H, dd, *J* = 17.4, 10.5 Hz), 5.87 (1H, dd, *J* = 3.5, 2.5 Hz), 5.24 (1H, dd, *J* = 10.4, 4.4 Hz), 5.20 (1H, dd, *J* = 17.5, 1.1 Hz), 5.13 (1H, dd, *J* = 10.6, 1.1 Hz), 3.94 (1H, br. s,), 3.83 (1H, dd, *J* = 15.4, 4.4 Hz), 3.72 (3H, s), 3.62 (1H, app. q, *J* = 10.5 Hz), 3.46 (1H, dd, *J* = 15.4, 10.4 Hz), 2.62 (1H, app. dtd, *J* = 17.6, 10.0, 2.5 Hz), 2.39 (1H, app. ddt, *J* = 17.5, 10.6, 3.4 Hz), 1.55 (6H, s), ppm;

^{13}C NMR (150 MHz, CD_2Cl_2) δ 167.8, 167.7, 162.1, 146.6, 140.9, 137.0, 134.52, 134.48, 131.9, 130.3, 123.6, 123.5, 121.5, 119.4, 118.1, 112.3, 110.6, 106.6, 54.2 (beneath CD_2Cl_2 solvent peak), 52.6, 50.4 (br.), 39.7, 29.6, 27.91, 27.98, 25.4 ppm;

IR (film, cm^{-1}) 1775, 1713, 1655, 1639, 1611, 1437, 1381;

HRMS (ESI^+) calc. for $C_{30}H_{29}N_3O_5$ ($[M + H]^+$): 512.2180; found: 512.2202); ($[M + Na]^+$): 534.1999; found: 534.2016;

$[\boldsymbol{\alpha}]_{\boldsymbol{D}}^{\mathbf{23.0}}$ −130.1° (*c* 0.38, MeOH).

8.4.5 Experimental Procedure for Compound (+)-Dehydrodeoxybrevianamide E (4.45)

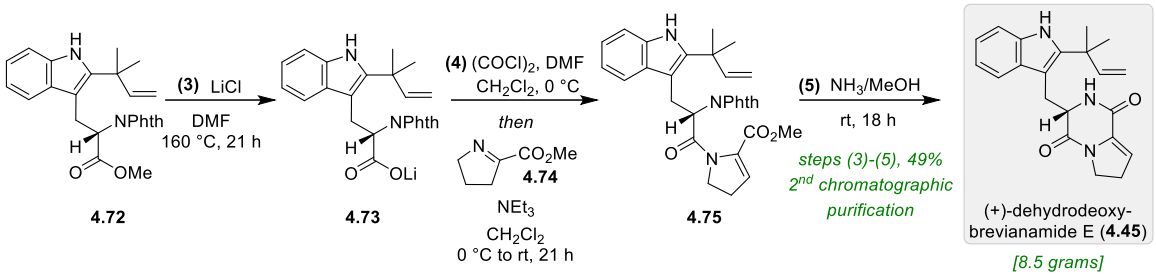

Step (5) The crude product **4.75** (23.9 g, 65.4 mmol) from **Step (4)** was dissolved in a solution of NH_3 in MeOH (7 M, 1200 mL, 128 equiv., 8.4 mol) and stirred at room temperature for 18 h. The crude reaction mixture was concentrated under reduced pressure until approximately 25 mL of solvent was left. This was directly purified by flash chromatography (7:3 to 8:2 EtOAc/petroleum spirit) to give (+)-dehydrodeoxybrevianamide E (**4.45**) (8.51 g, 24.4 mmol, 49% over 3 steps) as a pale-yellow foam.

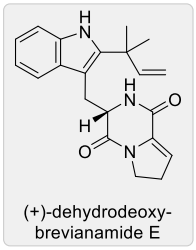

R_f 0.19 (8:2 EtOAc/petroleum spirit);

^{1}H NMR (500 MHz, $CDCl_3$) δ 8.07 (1H, br. s), 7.53 (1H, d, *J* = 7.9 Hz), 7.32 (1H, app. dt, *J* = 8.1, 0.9 Hz), 7.17 (1H, ddd, *J* = 8.1, 7.1, 1.2 Hz), 7.11 (1H, ddd, *J* = 8.1, 7.1, 1.1 Hz), 6.14 (1H, app. t, *J* = 3.1 Hz), 6.12 (1H, dd, *J* = 17.2, 10.4 Hz), 5.66 (1H, br. s), 5.20 – 5.15 (2H, m), 4.52 (1H, ddd, *J* = 11.3, 3.5, 1.8 Hz), 4.14 – 4.02 (2H, m), 3.73 (1H, dd, *J* = 14.7, 3.7 Hz), 3.23 (1H, dd, *J* = 14.6, 11.3 Hz), 2.78 (2H, app. td, *J* = 9.1, 3.1 Hz), 1.55 (3H, s), 1.55 (3H, s) ppm;

^{13}C NMR (125 MHz, $CDCl_3$) δ 162.7, 156.6, 145.8, 141.8, 134.4, 133.2, 128.9, 122.3, 120.2, 118.9, 118.3, 112.6, 110.9, 104.7, 57.6, 45.7, 39.2, 30.9, 28.1, 28.0, 27.9 ppm;

IR (film, cm^{-1}) 3331 (br.), 2967, 2926, 1672, 1639, 1435;

HRMS (ESI^+) calc. for $C_{21}H_{23}N_3O_2$ ($[M + H]^+$): 350.1863; found: 350.1875); ($[M + Na]^+$): 372.1682; found: 372.1689;

$[\boldsymbol{\alpha}]_{\boldsymbol{D}}^{\mathbf{23.1}}$ −33.2° (*c* 1.30, $CHCl_3$), literature: $[\boldsymbol{\alpha}]_{\boldsymbol{D}}^{\mathbf{22}}$ −38° (*c* 1.3, $CHCl_3$);[133]

Data consistent with literature.[149]

8.4.6 Experimental Procedure for Compound 4.74

Compound **4.74** was prepared according to literature adapted by the work of Schmalz.[188]

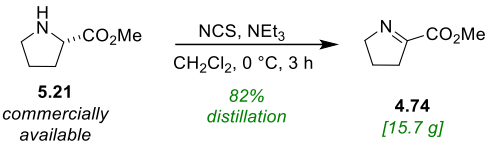

To a rapidly stirred suspension of L-proline methyl ester hydrochloride (**5.21**) (25.0 g, 1.0 equiv., 151 mmol) and NEt_3 (48.3 mL, 2.3 equiv., 347 mmol) in CH_2Cl_2 (450 mL) at 0 °C was added slowly, in 2.5 g portions, solid *N*-chlorosuccinimide (22.2 g, 1.1 equiv., 166 mmol). The mixture was stirred at room temperature for 3 h and then diluted with CH_2Cl_2 (350 mL). A mixture of saturated aq. NH_4Cl (150 mL) and water (150 mL) was added, the organic phase was separated and the aqueous phase was extracted with CH_2Cl_2 (2 × 150 mL). The combined organics were washed with a mixture of saturated aq. NH_4Cl (100 mL) and water (100 mL), saturated aq. $NaHCO_3$ (150 mL), brine (150 mL), dried (Na_2SO_4) and concentrated under reduced pressure. Vacuum distillation with a 15 cm vigreux column under reduced pressure (5 mbar) with vigorous heating gave imine **4.74** (15.7 g, 123 mmol, 82%) as a pale-yellow liquid.

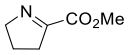

BP 65–69 °C (5 mbar);

^{1}H NMR (500 MHz, $CDCl_3$) δ 4.04 (2H, app. tt, *J* = 7.6, 2.6 Hz), 3.80 (3H, s), 2.76 (2H, app. ddt, *J* = 8.5, 7.6, 2.6 Hz), 1.96 – 1.89 (2H, m) ppm;

^{13}C NMR (125 MHz, $CDCl_3$) δ 168.2, 163.2, 62.5, 52.5, 35.3, 22.1 ppm;

Data consistent with literature.[255]

8.4.7 Experimental Procedure for B-Prenyl-9-BBN (5.14)

(**Steps 1-2**) 1,1-Dimethylallene (**5.17**) is a commercially available reagent, but was prepared on large scale based on a procedure reported by Pfeffer and co-workers.[181]

(**Steps 3**) A solution of *B*-Prenyl-9-BBN (**5.14**) was prepared under anhydrous conditions, based on a procedure reported by Trauner and co-workers.[182]

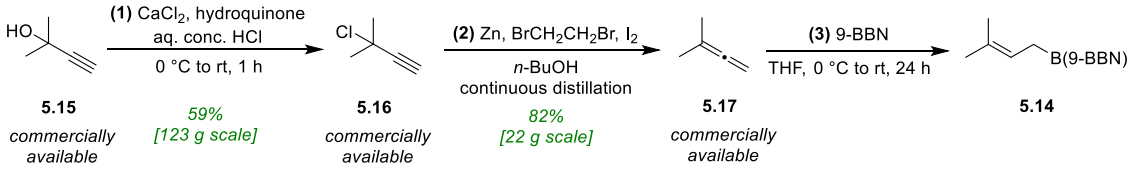

Step (1) Concentrated hydrochloric acid (800 mL) was cooled to 0 °C and stirred for 10 minute. To this solution was added 2-methyl-3-butyn-2-ol (**5.15**) (200 mL, 1.0 equiv., 2.06 mol) and hydroquinone (1.82 g, 0.008 equiv., 16.5 mmol). Anhydrous $CaCl_2$ (229 g, 1.0 equiv., 2.06 mol) was added in 20 g portions to the stirred mixture at 0 °C over 7 minutes and the reaction was stirred for 1 h at room temperature. The layers were separated and solid K_2CO_3 added cautiously to the upper organic phase until effervescence ceased. The organic phase was then distilled under reduced pressure, collected up to 50 °C at 147 mbar. The crude distillate was redistilled under reduced pressure (147 mbar) to give 3-chloro-3-methyl-1-butyne (**5.16**) (123 g, 1.00 mol, 59%) as a colourless oil.

BP 32–36 °C (147 mbar);

^{1}H NMR (500 MHz, $CDCl_3$) δ 2.62 (1H, s), 1.87 (6 H,s) ppm;

^{13}C NMR (100 MHz, $CDCl_3$) δ 86.7, 72.0, 57.1, 34.7 ppm;

All spectroscopic data matched a comercially available sample.

Step (2) Zinc powder (52.0 g, 1.95 equiv., 760 mmol) was washed with 3% aq. HCl (4 × 40 mL), 2% aq. $CuSO_4$ (2 × 60 mL), ethanol (2 × 60 mL) and *n*-butanol (2 × 60 mL). The treated zinc was suspended in *n*-butanol (110 mL) in a 3 neck RBF with a dropping funnel, magnetic stirrer bar and a distillation head fitted with a 30 cm Vigreux column. 3-Chloro-3-methyl-1-butyne (**5.16**) (44.4 mL, 1.0 equiv., 390 mmol) was placed in the dropping funnel along with 1,2-dibromoethane (2.50 mL, 0.074 equiv., 29.0 mmol). To the zinc butanol slurry was added a few crystals of iodine and 1,2-dibromoethane (2.50 mL, 0.074 equiv., 29.0 mmol). Then a portion of the alkyne mixture (3 mL) was added dropwise to the slurry. The mixture was then heated cautiously (using a temperature controlled heat gun set slowly raised to 290 °C with stirring until the reaction initiated (signalled by rapid expansion of the zinc slurry up the Vigreux column and then back into the reaction flask). The mixture was then kept under a controlled reflux from external heating with heat gun, while slow addition of the remaining alkyne mixture. The crude product was collected by distillation from the reaction mixture during the course of the reaction, and external heat applied to continue collection up to a temperature of 60 °C. The crude distillate was redistilled to give 1,1-dimethylallene (**5.17**) (21.7 g, 319 mmol, 81.2%) as a colourless liquid.

BP 40–42 °C;

^{1}H NMR (500 MHz, $CDCl_3$) δ 4.52 (2H, hept, *J* = 3.1 Hz), 1.69 (6H, t, *J* = 3.2 Hz) ppm;

^{13}C NMR (150 MHz, $CDCl_3$) δ 206.8, 94.2, 72.7, 20.3 ppm;

Data consistent with literature.[181]

Step (3) A solution of 9-BBN in THF (360 mL, 1.0 equiv., 179 mmol, 0.5 M in THF) was cooled to 0 °C and stirred for 20 minutes. Once the solution was observed to go cloudy, 1,1-dimethylallene (**5.17**) (20.5 mL, 1.16 equiv., 208 mmol) was added dropwise *via* a syringe pump over 30 minutes with stirring. The reaction was warmed to room temperature and stirred for 18 h before being used directly in the reverse prenylation procedure described on page **227**.

8.4.8 Experimental Procedure for *t*-BuOCl

t-BuOCl was prepared based on a procedure reported by Mintz and co-workers.[183] For safety reasons exposure of the reaction and product to light was minimised.

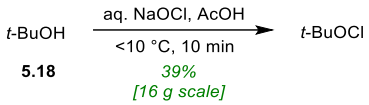

An aqueous solution of bleach (500 mL, 0.767 M, 1.0 equiv., 384 mmol)* was cooled below 10 °C with stirring. A pre mixed solution of *t*-BuOH (**5.18**) (43.3 mL, 1.0 equiv., 383 mmol) and glacial acetic acid (24.1 mL, 1.1 equiv., 421 mmol) was added in a single portion to the rapidly stirred bleach and the stirring continued for 10 min in the absence of light. The entire reaction mixture was transferred to a separating funnel, the aqueous layer discarded, the yellow organic layer washed with and water (50 mL). The product was dried ($CaCl_2$ approximately 3 g) and decanted into its final container via pipette. The *t*-BuOCl (16.4 g, 151 mmol, 39%) was stored in a fridge over $CaCl_2$ in an amber glass bottle as a yellow liquid.

*Bleach solution was titrated to a concentration of 0.767 M by iodometric titration using sodium thiosulfate prior to use.

^{1}H NMR (500 MHz, $CDCl_3$) δ 1.33 (9H, s) ppm;

^{13}C NMR (125 MHz, $CDCl_3$) δ 84.1, 27.0 ppm;

Data consistent with literature.[183]

8.4.9 Experimental Procedure for Compounds 4.69 and 5.23

Compound **4.69** and **5.23** was prepared according to literature adapted from the work of Kametani[256] and Wolff.[257]

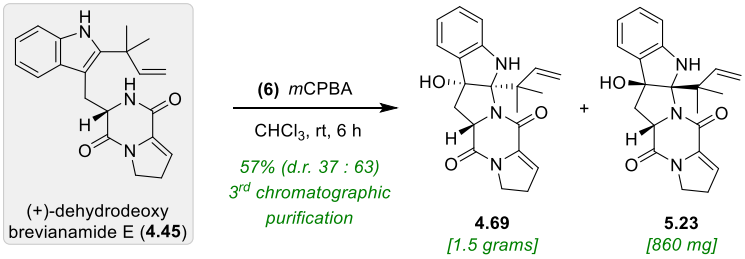

Step (6) To a rapidly stirred solution of (+)-dehydrodeoxybrevianamide E (**4.45**) (4.00 g, 1.0 equiv., 11.5 mmol) in $CHCl_3$ (80 mL) at room temperature was added dropwise over 4 h a solution of *m*CPBA in $CHCl_3$ (0.29 M, 40 mL, 1.02 equiv., 11.7 mmol).* The reaction was stirred for 2 h at room temperature and quenched by the addition of saturated aq. $Na_2S_2O_3$ (20 mL) and saturated aq. $NaHCO_3$ (20 mL). The reaction mixture was diluted with EtOAc (200 mL) and $CHCl_3$ (150 mL) and the phases separated. The aqueous phase was back-extracted with $CHCl_3$ (50 mL) and the combined organics washed with saturated aq. $NaHCO_3$ (80 mL), brine (80 mL), dried (Na_2SO_4) and concentrated under reduced pressure. A diastereomeric ratio of 63:37 for **4.69**:**5.23** was determined by analysis of the ^1H NMR spectrum of this crude reaction product. Three round of flash column chromatography were peformed (1st = 1.5:7:3 petroleum spirit/CH_2Cl_2/*i*-Pr_2O 2nd = 7:3 CH_2Cl_2/*i*-Pr_2O 3rd = EtOAc to *i*-PrOH) Overall, purification by column chromatography gave dehydrobrevianamide E (**4.69**) (1.54 g, 4.21 mmol, 37%), compound **5.23** (0.859 g, 2.35 mmol, 20%), and recovered dehydrodeoxybrevianamide E (**4.45**) (0.270 g, 0.774 mmol, 7%).

* *m*CPBA (69% w/w by iodometric titration, 4.38 g, 17.5 mmol) was added to $CHCl_3$ (60 mL) and dried over Na_2SO_4 (27.5 g) with stirring for 40 mins.

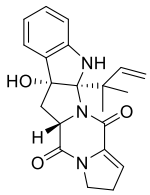

R_f 0.15 (7:3 CH_2Cl_2/*i*-Pr_2O);

^{1}H NMR (500 MHz, $CDCl_3$) δ 7.24 (1H, dd, *J* = 7.5, 1.2 Hz), 7.18 (1H, app. td, *J* = 7.7, 1.3 Hz), 6.81 (1H, td, *J* = 7.4, 1.0 Hz), 6.74 (1H, app. dt, *J* = 7.9, 0.8 Hz), 6.40 – 6.34 (2H, m), 6.16 (1H, app. t, *J* = 3.1 Hz), 5.15 (1H, dd, *J* = 17.7, 1.4 Hz), 5.07 (1H, dd, *J* = 10.9, 1.3 Hz), 4.06 (1H, ddd, *J* = 12.0, 8.7, 7.3 Hz), 3.93 – 3.83 (1H, m), 3.81 (1H, dd, *J* = 11.5, 7.3 Hz), 2.79 – 2.69 (4H, m), 2.43 (1H, br. s), 1.34 (3H, s), 1.27 (3H, s) ppm;

^{13}C NMR (125 MHz, $CDCl_3$) δ 163.7, 162.1, 149.4, 144.7, 136.4, 131.0, 129.8, 123.8, 120.6, 120.2, 113.4, 111.2, 91.5, 89.3, 60.3, 45.8, 45.0, 36.7, 29.0, 27.6, 23.2 ppm;

IR (film, cm^{-1}) 3362, 2967, 2926, 1670, 1634, 1609, 1485, 1468, 1437, 1393, 1360;

HRMS (ESI$^+$) calc. for $C_{21}H_{23}N_3O_3$ ([M + H]$^+$): 366.1812; found: 366.1814); ([M + Na]$^+$): 388.1632; found: 388.1629;

$[\boldsymbol{\alpha}]_{\boldsymbol{D}}^{\boldsymbol{20.9}}$−208° (*c* 0.23, EtOH).

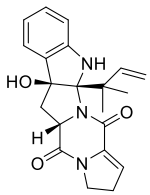

R_f 0.09 (7:3 CH_2Cl_2/*i*-Pr_2O);

^{1}H NMR (500 MHz, $CDCl_3$) δ 7.22 (1H, d, *J* = 7.5 Hz), 7.13 (1H, app. td, *J* = 7.7, 1.3 Hz), 6.76 (1H, app. td, *J* = 7.4, 0.9 Hz), 6.62 (1H, app. dt, *J* = 7.9, 0.8 Hz), 6.47 (1H, br. s), 6.34 (1H, dd, *J* = 17.7, 10.8 Hz), 6.06 (1H, app. t, *J* = 3.0 Hz), 5.22 (1H, dd, *J* = 17.7, 1.3 Hz), 5.10 (1H, dd, *J* = 10.9, 1.3 Hz), 4.73 (1H, app. t, *J* = 8.8 Hz), 4.00 (1H, ddd, *J* = 12.4, 11.1, 6.1 Hz), 3.82 (1H, dddd, *J* = 12.3, 11.4, 8.3, 0.8 Hz), 2.86 (1H, ddd, *J* = 13.6, 8.6, 0.7 Hz), 2.80 – 2.62 (3H, m), 2.57 (1H, br. s), 1.45 (3H, s), 1.35 (3H, s) ppm;

^{1}H NMR (500 MHz, $(CD_3)_2SO$) δ 7.16 (1H, dd, *J* = 7.4, 1.4 Hz), 7.02 (1H, td, *J* = 7.6, 1.3 Hz), 6.74 (1H, s), 6.70 – 6.62 (2H, m), 6.49 (1H, dd, *J* = 17.6, 10.8 Hz), 5.90 (1H, t, *J* = 3.0 Hz), 5.73 (1H, s), 5.10 (1H, dd, *J* = 17.6, 1.6 Hz), 5.00 (1H, dd, *J* = 10.7, 1.6 Hz), 4.67 (1H, dd, *J* = 10.2, 6.8 Hz), 3.86 – 3.76 (1H, m), 3.63 (1H, td, *J* = 11.6, 8.2 Hz), 2.74 (1H, dd, *J* = 13.5, 6.8 Hz), 2.66 – 2.52 (3H, m), 1.30 (6H, d, *J* = 2.4 Hz) ppm;

^{13}C NMR (125 MHz, $CDCl_3$) δ 161.9, 156.2, 147.0, 144.8, 134.7, 131.5, 130.4, 123.8, 119.5, 119.3, 114.1, 109.9, 95.3, 89.6, 60.5, 46.6, 45.4, 43.4, 28.2, 27.2, 22.5 ppm;

^{13}C NMR (125 MHz, $(CD_3)_2SO$) δ 162.5, 155.5, 148.1, 145.5, 134.9, 133.0, 129.6, 124.1, 118.8, 118.7, 112.9, 110.1, 96.0, 87.4, 59.6, 45.5, 41.1, 31.2, 28.0, 25.3, 24.7 ppm;

IR (film, cm^{-1}) 3360, 2965, 2924, 2854, 1665, 1632, 1611, 1487, 1466, 1439, 1414, 1371;

HRMS (ESI^+) calc. for $C_{21}H_{23}N_3O_3$ ($[M + H]^+$): 366.1812; found: 366.1807;

$[\boldsymbol{\alpha}]_{\boldsymbol{D}}^{\boldsymbol{22.3}}$ +86.3° (*c* 0.19, EtOH).

8.4.10 Experimental Procedure for Compounds 5.24 and 5.25

Experimental procedure A

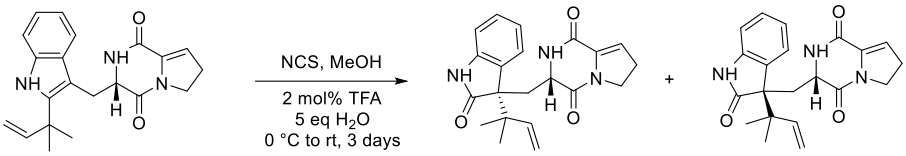

To a solution of dehydrodeoxy-brevianamide E (**4.45**) (500 mg, 1.0 equiv., 1.43 mmol) in MeOH (30 mL) at 0 °C was added a solution of trifluoroacetic acid (2.2 µL, 0.02 equiv., 0.029 mmol) in water (130 µL) with stirring, followed by addition of *N*-chlorosuccinimide (200 mg, 1.05 equiv., 1.50 mmol). The reaction was allowed to warm slowly to room temperature and stirred for 3 days. The entire mixture was concentrated under reduced pressure. Flash column chromatography (2:8 to 13:7 MeCN/$CHCl_3$) gave major oxindole **5.24** (300 mg, 0.82 mmol, 57%) as an off white foam and minor oxindole **5.25** (134 mg, 0.37 mmol, 26%) as a white foam.

Experimental procedure B

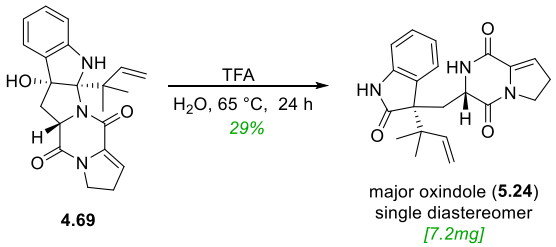

To a solution of dehydrobrevianamide E (**4.69**) (25 mg, 1.0 equiv., 0.068 mmol) in H_2O (3.0 mL) was added trifluoroacetic acid (0.21 mL, 4.0 equiv., 0.275 mmol). The reaction was heat to 65 °C and left to stir at this temperature for 24 h. The mixture was allowed to cool down and quenched with $NaHCO_3$ (5 mL, sat., aq.) and extracted with $CHCl_3$ (5 × 10 mL), dried (Na_2SO_4) and concentrated under reduced pressure. Preparative TLC (7:3 $CHCl_3$/MeCN) gave major oxindole **5.24** (7.2 mg, 0.020 mmol, 29%) as an off white foam.

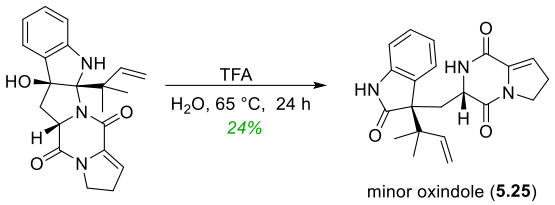

5.23

minor oxindole (**5.25**)
single diastereomer
[6.1mg]

To a solution of dia-dehydrobrevianamide E (**5.23**) (25 mg, 1.0 equiv., 0.068 mmol) in H_2O (3.0 mL) was added trifluoroacetic acid (0.21 mL, 4.0 equiv., 0.275 mmol). The reaction was heat to 65 °C and left to stir at this temperature for 24 h. The mixture was allowed to cool down and quenched with $NaHCO_3$ (5 mL, sat., aq.) and extracted with $CHCl_3$ (5 × 10 mL), dried (Na_2SO_4) and concentrated. Preparative TLC (7:3 $CHCl_3$/MeCN) gave minor oxindole **5.25** (6.1 mg, 0.017 mmol, 24%) as a white foam.

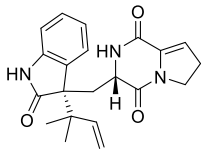

major oxindole

R_f 0.11 (1:1 MeCN/$CHCl_3$);

^{1}H NMR (500 MHz, $CDCl_3$) δ 10.94 (1H, br. s), 8.75 (1H, br. s), 7.18 (1H, dd, *J* = 7.6, 1.2 Hz), 7.11 (1H, td, *J* = 7.7, 1.2 Hz), 6.94 – 6.85 (2H, m), 6.08 (1H, dd, *J* = 17.4, 10.8 Hz), 5.55 (1H, app. t, *J* = 3.0 Hz), 5.10 (1H, dd, *J* = 10.9, 1.2 Hz), 4.97 (1H, dd, *J* = 17.4, 1.2 Hz), 4.31 (1H, d, *J* = 7.2 Hz), 3.71 (2H, app. t, *J* = 9.1 Hz), 3.03 (1H, dd, *J* = 14.8, 1.5 Hz), 2.75 (1H, dd, *J* = 14.8, 7.4 Hz), 2.51 – 2.43 (2H, m), 1.11 (3H, s), 0.97 (3H, s) ppm;

^{13}C NMR (125 MHz, $CDCl_3$) δ 183.1, 162.6, 157.6, 143.1, 143.1, 132.1, 128.4, 128.0, 127.9, 120.5, 118.3, 114.2, 111.1, 56.3, 55.8, 45.2, 42.6, 33.7, 27.5, 22.2, 21.6 ppm;

IR (film, cm^{-1}) 3200, 3084, 2963, 2930, 1676, 1643, 1618, 1470, 1449;

HRMS (ESI$^+$) calc. for $C_{21}H_{23}N_3O_3$ ([M + H]$^+$): 366.1812; found: 366.1811; ([M + Na]$^+$): 388.1632; found: 388.1627;

$[\boldsymbol{\alpha}]_{\boldsymbol{D}}^{\boldsymbol{21.5}}$ +18.0 (c 0.20, MeOH).

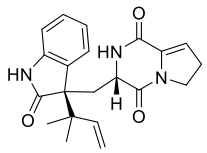

minor oxindole

R_f 0.25 (1:1 MeCN/$CHCl_3$);

^{1}H NMR (500 MHz, $CDCl_3$) δ 10.42 (1H, br. s), 7.58 (1H, br. d, *J* = 3.7 Hz), 7.29 – 7.22 (2H, m), 7.05 (1H, td, *J* = 7.6, 1.1 Hz), 6.97 (1H, dd, *J* = 8.2, 1.1 Hz), 6.06 (1H, dd, *J* = 17.5, 10.8 Hz), 5.95 (1H, app. t, *J* = 3.0 Hz), 5.13 (1H, dd, *J* = 10.7, 1.1 Hz), 5.02 (1H, dd, *J* = 17.4, 1.2 Hz), 4.05 (1H, ddd, *J* = 12.3, 11.2, 5.4 Hz), 3.83 (1H, ddd, *J* = 11.9, 11.8, 8.3 Hz), 3.56 (1H, dt, *J* = 11.3, 3.2 Hz), 2.80 (1H, dddd, *J* = 18.4, 11.2, 8.3, 2.8 Hz), 2.72 – 2.61 (2H, m), 2.41 (1H, dd, *J* = 14.0, 11.7 Hz), 1.15 (3H, s), 1.05 (3H, s) ppm;

^{13}C NMR (125 MHz, $CDCl_3$) δ 182.9, 163.6, 157.9, 142.7, 142.3, 133.3, 128.2, 127.9, 126.3, 121.9, 119.0, 114.6, 112.0, 56.7, 55.9, 45.7, 42.6, 38.9, 28.0, 22.0, 21.9 ppm;

IR (film, cm^{-1}) 3211, 2957, 2926, 1703, 1676, 1643, 1618, 1470, 1441;

HRMS (ESI$^+$) calc. for $C_{21}H_{23}N_3O_3$ ([M + H]$^+$): 366.1812; found: 366.1819; ([M + Na]$^+$): 388.1632; found: 388.1628;

$[\boldsymbol{\alpha}]_{\boldsymbol{D}}^{\boldsymbol{23.1}}$ −89.1 (c 0.19, MeOH).

8.4.11 Experimental Procedure for (+)-Brevianamide Y (4.4) and (+)-Brevianamide Z (5.3)

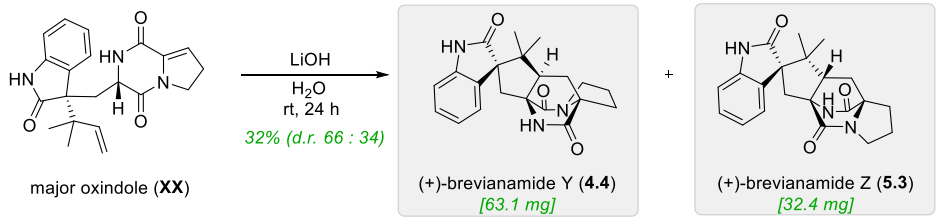

Oxindole **5.24** (300 mg, 1.0 equiv., 0.82 mmol) was added to 1 M aq. LiOH (120 mL) at rt and the reaction was stirred for 24 h. The reaction was quenched with saturated aq. 1 M HCl (150 mL) and extracted with $CHCl_3$ (3 × 200 mL). The combined organics were dried (Na_2SO_4) and concentrated under reduced pressure. Preparative TLC (2:3 1,2-dimethoxyethane/MTBE) gave (+)-brevianamide Z (**5.3**) (32.4 mg, 0.089 mmol, 10.8%) as a white amorphous solid and (+)-brevianamide Y (**4.4**) (63.1 mg, 0.099 mmol, 21%) as a white amorphous solid.

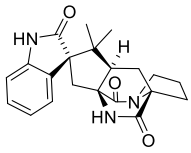

(+)-brevianamide Y

R_f 0.15 (2:3 1,2-dimethoxyethane/MTBE);

^{1}H NMR (600 MHz, $(CD_3)_2SO$) δ 10.30 (1H, br. s), 8.79 (1H, br. s), 7.42 (1H, dd, *J* = 7.6, 1.2 Hz), 7.19 (1H, td, *J* = 7.7, 1.2 Hz), 6.98 (1H, td, *J* = 7.6, 1.1 Hz), 6.81 (1H, dd, *J* = 7.7, 1.0 Hz), 3.36 – 3.22 (2H, m), 3.17 (1H, dd, *J* = 10.4, 7.2 Hz), 2.82 (1H, d, *J* = 15.1 Hz), 2.46 (1H, dd, *J* = 12.3, 6.6 Hz), 2.13 (1H, d, *J* = 15.2 Hz), 2.02 – 1.96 (1H, m), 1.93 (1H, dd, *J* = 13.1, 10.4 Hz), 1.85 – 1.75 (2H, m), 1.65* (1H, dd, *J* = 13.0, 7.2 Hz), 0.99 (3H, s), 0.69 (3H, d, *J* = 2.1 Hz) ppm;

*A literature table of NMR data doesn't report this peak. However a printout of the literature ^{1}H NMR spectrum shows a peak at δ = 1.639, which integrates for 1.11, appears to be a dd and wasn't reported in the table. Instead the table reports 'δ = 2.47, dd (6.4, 12.1)' twice, which is presumably a typographical error.

^{13}C NMR (125 MHz, $(CD_3)_2SO$) δ 181.8, 172.5, 169.0, 142.4, 129.8, 128.1, 126.3, 120.8, 109.0, 68.6, 67.1, 62.1, 50.0, 46.8, 43.2, 33.6, 28.4, 28.0, 24.4, 23.0, 20.4 ppm;

IR (film, cm^{-1}) 3225, 2970, 2928, 2872, 2359, 2324, 1719, 1694, 1668, 1595, 1470, 1445, 1404;

HRMS (ESI^+) calc. for $C_{21}H_{23}N_3O_3$ ($[M + H]^+$): 366.1812; found: 366.1813; ($[M + Na]^+$): 388.1632; found: 388.1624;

$[\boldsymbol{\alpha}]_{\boldsymbol{D}}^{\boldsymbol{26}}$ +27.1 (*saturated*, MeOH) *attempts to prepare a solution of (c 0.2) resulted in a saturated solution*, literature: $[\boldsymbol{\alpha}]_{\boldsymbol{D}}^{\boldsymbol{25}}$ +11.5 (*c* 0.2, MeOH);[132]

$[\boldsymbol{\alpha}]_{\boldsymbol{D}}^{\boldsymbol{23.3}}$+10.9 (*c* 0.44, DMSO), literature: $[\boldsymbol{\alpha}]_{\boldsymbol{D}}^{\boldsymbol{25}}$ +255.2 (*c* 0.37, DMSO);[174]

***e.r.* 95:5** (Chiralpak IC, 42:58 EtOH/hexane, 1.0 mL min^{-1}, λ 254 nm) t_{Rmajor}= 11.06 min, t_{Rminor} = 14.66 min. See **pages 311-314** for chiral HPLC traces.

Data consistent with literature.[132]

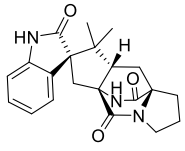

(+)-brevianamide Z

R_f 0.26 (2:3 1,2-dimethoxyethane/MTBE);

^{1}H NMR (500 MHz, $(CD_3)_2SO$) δ 10.27 (1H, br. s), 8.69 (1H, br. s), 7.17 (1H, td, *J* = 7.6, 1.2 Hz), 7.06 (1H, d, *J* = 7.4 Hz), 6.93 (1H, td, *J* = 7.6, 1.1 Hz), 6.81 (1H, dd, *J* = 7.7, 1.1 Hz), 3.40 (1H, dt, *J* = 10.7, 6.8 Hz), 3.30 – 3.22 (1H, m), 2.63 (1H, dd, *J* = 10.1, 7.5 Hz), 2.59 (1H, d, *J* = 14.9 Hz),

2.49 – 2.43 (2H, m), 2.05 – 1.98 (1H, m), 1.94 (1H, dd, *J* = 13.0, 10.1 Hz), 1.89 – 1.75 (2H, m), 1.66 (1H, dd, *J* = 13.0, 7.4 Hz), 1.05 (3H, s), 0.41 (3H, s) ppm;

^{13}C NMR (125 MHz, $(CD_3)_2SO$) δ 178.6, 172.2, 169.4, 141.5, 134.3, 127.8, 124.0, 121.0, 109.1, 68.5, 67.5, 62.4, 53.0, 47.7, 43.3, 33.1, 28.4, 27.3, 24.4, 23.1, 19.5 ppm;

IR (film, cm^{-1}) 3235, 2961, 2930, 2880, 1686, 1678, 1618, 1470, 1395;

HRMS (ESI^+) calc. for $C_{21}H_{23}N_3O_3$ ($[M + H]^+$): 366.1812; found: 366.1816;

$[\alpha]_D^{24.1}$ +40.0 (*c* 0.13, DMSO);

e.r. 85:15 (Chiralpak IC, 25:75 EtOH/hexane, 1.0 mL min^{-1}, λ 254 nm) t_{Rmajor}= 19.73 min t_{Rminor} = 22.94 min See **page 317** for chiral HPLC traces.

8.4.12 Experimental Procedure for (–)-Brevianamide Y (4.4) and (–)-Brevianamide Z (5.3)

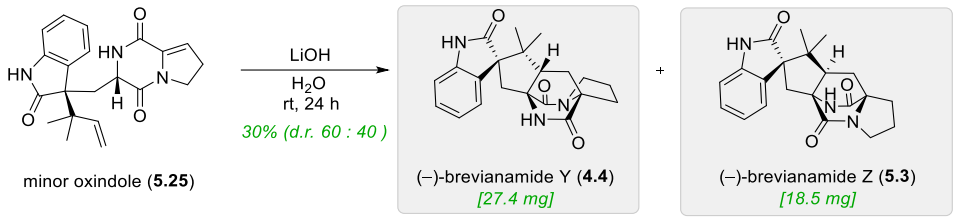

To a solution of compound **5.25** (150 mg, 1.0 equiv., 0.41 mmol) at rt was added 1 M aq. LiOH (60 mL), the reaction stirred for 24 h. The reaction was quenched with saturated aq. 1 M HCl (75 mL) and extracted with $CHCl_3$ (3 × 100 mL). The combined organics were dried (Na_2SO_4) and concentrated under reduced pressure. Preparative TLC (2:3 1,2-dimethoxyethane/MTBE) gave compound (–)-brevianamide Z (*ent*-**4.4)** (18.5 mg, 0.051 mmol, 12.0%) as a white amorphous solid and (–)-brevianamide Y (*ent*-**5.3**) (27.4 mg, 0.075 mmol, 18.2%) as a white amorphous solid.

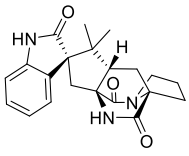

(–)-brevianamide Y

$[\alpha]_D^{23.0}$ –10.3 (*c* 0.39, DMSO);

e.r. 98:2 (Chiralpak IC, 42:58 EtOH/hexane, 1.0 mL min^{-1}, λ 254 nm) t_{Rmajor} = 11.59 min, t_{Rminor} = 14.42 min. See **page 315** for chiral HPLC traces.

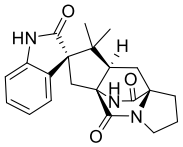

(–)-brevianamide Z

$[\alpha]_D^{24.2}$ –12.6 (*c* 0.19, DMSO);

e.r. 92:8 (Chiralpak IC, 25:75 EtOH/hexane, 1.0 mL min^{-1}, λ 254 nm) t_{Rmajor} = 20.01 min, t_{Rminor} = 22.98 min. See **page 318** for chiral HPLC traces.

8.4.13 Comparison of the ^{1}H and ^{13}C NMR Data for Synthetic and Natural (+)-Brevianamide Y (4.4)

Provided below is a tabulated comparison of the NMR data collected for (+)-brevianamide Y (**4.4**) vs the NMR data reported by the isolation chemist.[1]

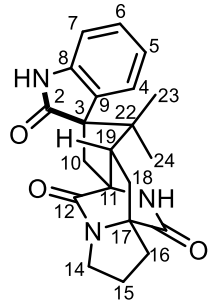

(–)-brevianamide Y

Atom	Synthetic brevianamide Y (4.4) $(CD_3)_2SO$			Natural brevianamide Y (4.4) $(CD_3)_2SO$				
	^{1}H δ (601 MHz)	**m, *J* (Hz)**	**^{13}C δ (126 MHz)**	**^{1}H δ (500 MHz)**	**m, *J* (Hz)**	**^{13}C δ (125 MHz)**	**Δ ^{1}H δ**	**Δ ^{13}C δ**
1	10.30	s	-	10.31	-	-	0.01	-
2	-	-	181.8	-	-	182.3	-	0.5
3	-	-	62.2	-	-	62.6	-	0.4
4	7.42	dd, 7.6, 1.2	126.3	7.43	d, 17	126.8	0.01	0.5
5	6.98	td apt., 7.6, 1.1	120.8	6.99	dd, 7.5, 7.6	121.3	0.01	0.5
6	7.19	dd, 7.7, 1.2	128.1	7.20	dd, 7.6, 7.6	128.6	0.01	0.5
7	6.81	dd, 7.7,1.0	109	6.81	d, 7.6	109.5	0.00	0.5
8	-	-	142.4	-	-	142.9	-	0.5
9	-	-	129.8	-	-	130.2	-	0.5
10	2.13	d, 15.2	33.6	2.14	d, 15.2	34.1	0.01	0.5
	2.82	d, 15.1	-	2.83	d, 15.2	-	0.01	-
11	-	-	67.1	-	-	67.6	-	0.5
12	-	-	169	-	-	169.5	-	0.5
14	3.36-3.22	m	43.2	3.30	m	43.7	0.01	0.5
15	1.85-1.75*	m	24.4	1.83	m	24.9	0.03	0.5
	2.02-1.96	m	-	2.00	dd, 5.9, 12.1	-	0.01	-

16	1.85-1.75*	m	28.4	1.79	m	28.9	0.01	0.5
	2.46	dd, 12.3, 6.6	-	2.47	dd, 6.4, 12.1	-	0.01	-
17	-	-	68.6	-	-	69.1	-	0.5
18	1.65†	dd, 13.0, 7.2	28	1.79	m	28.4	0.14	0.5
	1.93†	dd, 13.1, 10.4	-	2.47	dd, 6.4, 12.1	-	0.54	-
19	3.17	dd, 7.2, 10.1	50	3.18	dd, 5.0, 10.0	50.5	0.01	0.5
20	-	-	172.5	-	-	173.0	-	0.5
21	8.79	s	-	8.81	s	-	0.02	-
22	-	-	46.8	-	-	47.3	-	0.5
23	0.99	s	20.2	1.00	s	20.9	0.01	0.7
24	0.69	s	23	0.69	s	23.5	0.00	0.5

* For the synthetic data the peak in the ^{1}H NMR at 1.85-1.75 ppm is a complex multiple, which integrates for 3 hydrogen atoms.

†A literature table of NMR data doesn't report the peak at 1.65 ppm or 1.93 ppm. Instead the table reports 'δ = 2.47, dd (6.4, 12.1)' and 'δ = 1.79, m' twice, which is presumably a typographical error. Otherwise ^{1}H NMR data is in good agreement with all peaks found to be within ± 0.03 ppm.

For the ^{13}C data all peaks consistently vary by ± 0.5 ppm.

8.5 Experimental Conditions Chapter 6

8.5.1 Solvent Screen with LiOH and Compound 5.23

The following reactions show qualitatively that treating compound **5.23** with LiOH in different solvent systems favours the formation of (–)-brevianamide A (**4.1**).

To compound **5.23** (5.0 mg, 1.0 equiv., 14 µmol) was added LiOH (2 mL, 1 M, solution see table for solvent) at rt. The reaction mixture was left to stir for 24 h. The reaction was then acidified with 1 M aq. HCl (2 mL), extracted with $CHCl_3$ (3 × 5 mL), dried (Na_2SO_4) and concentrated under reduced pressure. The residue was transferred to an NMR tube with $CHCl_3$ (1.5 mL) and concentrated under reduced pressure. To the NMR tube was then added ethylene carbonate internal standard (400 µL, in $(CD_3)_2SO$) and a ^1H NMR Spectrum (500 MHz, in $(CD_3)_2SO$) was recorded.

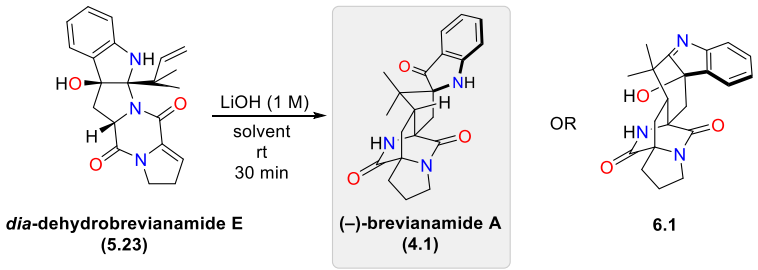

***dia*-dehydrobrevianamide E (5.23)** | **(–)-brevianamide A (4.1)** | **6.1**

Solvent		
Experiment 1	Experiment 2	Experiment 3
H_2O	H_2O/MeOH (1:1)	MeOH
(–)-brevianamide A (**4.1**) formed	(–)-brevianamide A (**4.1**) formed	(–)-brevianamide A (**4.1**) formed

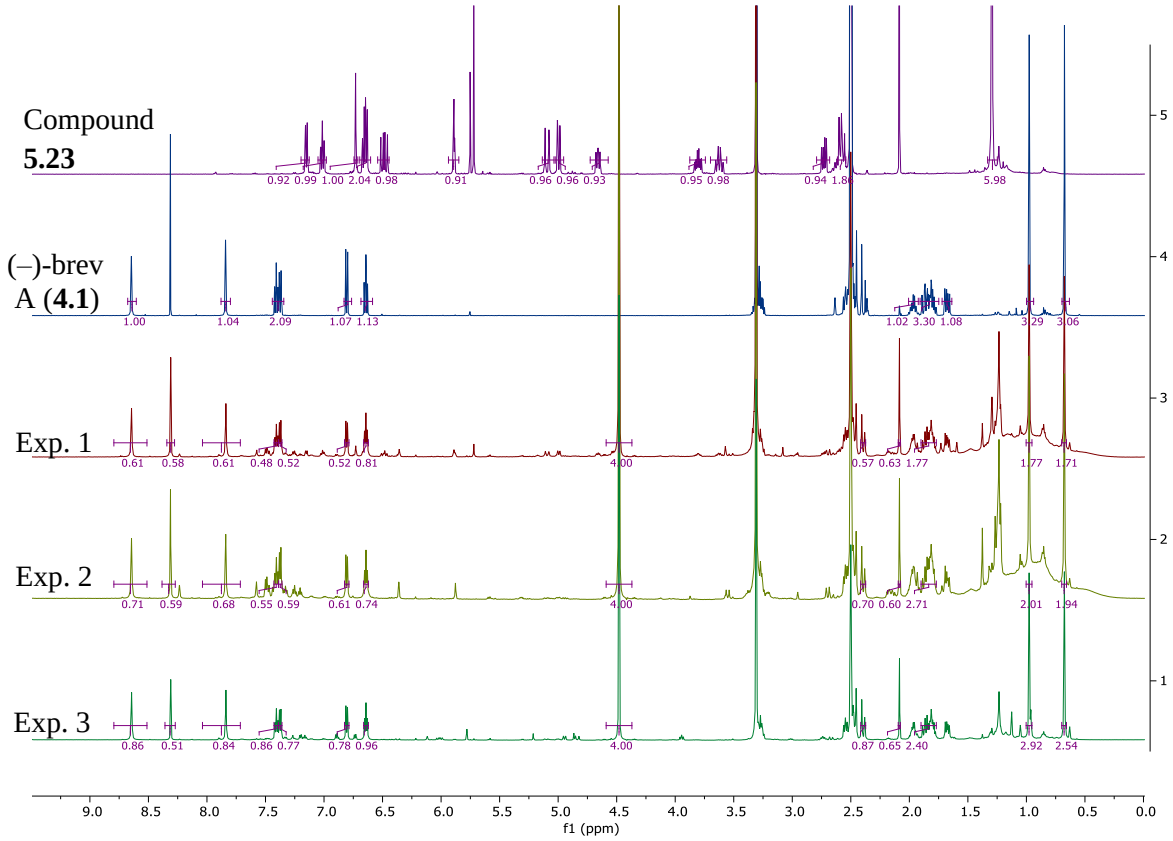

*Peak at 4.50 ppm (Internal Standard ethylene carbonate) at 8.31 ppm $CHCl_3$ and at 3.30 ppm water

^{1}H NMR Spectrum (500 MHz, in $(CD_3)_2SO$)

8.5.2 Solvent Screen with K_2CO_3 and Compound 5.23

The following reactions show qualitatively that compound **6.1** is formed when compound **5.23** is treated K_2CO_3 with in a solvent system containing methanol.

To compound **5.23** (5.0 mg, 1.0 equiv., 14 µmol) was added K_2CO_3 (2 mL, 1 M, solution see table for solvent) at rt. The reaction mixture was left to stir for 24 h. The reaction was then acidified with 1 M aq. HCl (2 mL), extracted with $CHCl_3$ (3 × 5 mL), dried (Na_2SO_4) and concentrated under reduced pressure. The residue was transferred to an NMR tube with $CHCl_3$ (1.5 mL) and concentrated under reduced pressure. To the NMR tube was then added ethylene carbonate internal standard (400 µL, in $(CD_3)_2SO$) and a ^1H NMR Spectrum (500 MHz, in $(CD_3)_2SO$) was recorded.

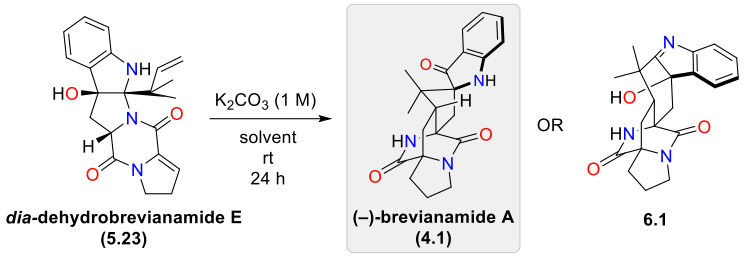

Solvent		
Experiment 1	Experiment 2	Experiment 3
H_2O	H_2O/MeOH (1:1)	MeOH
No reaction observed	Compound **6.1** formed	Compound **6.1** formed

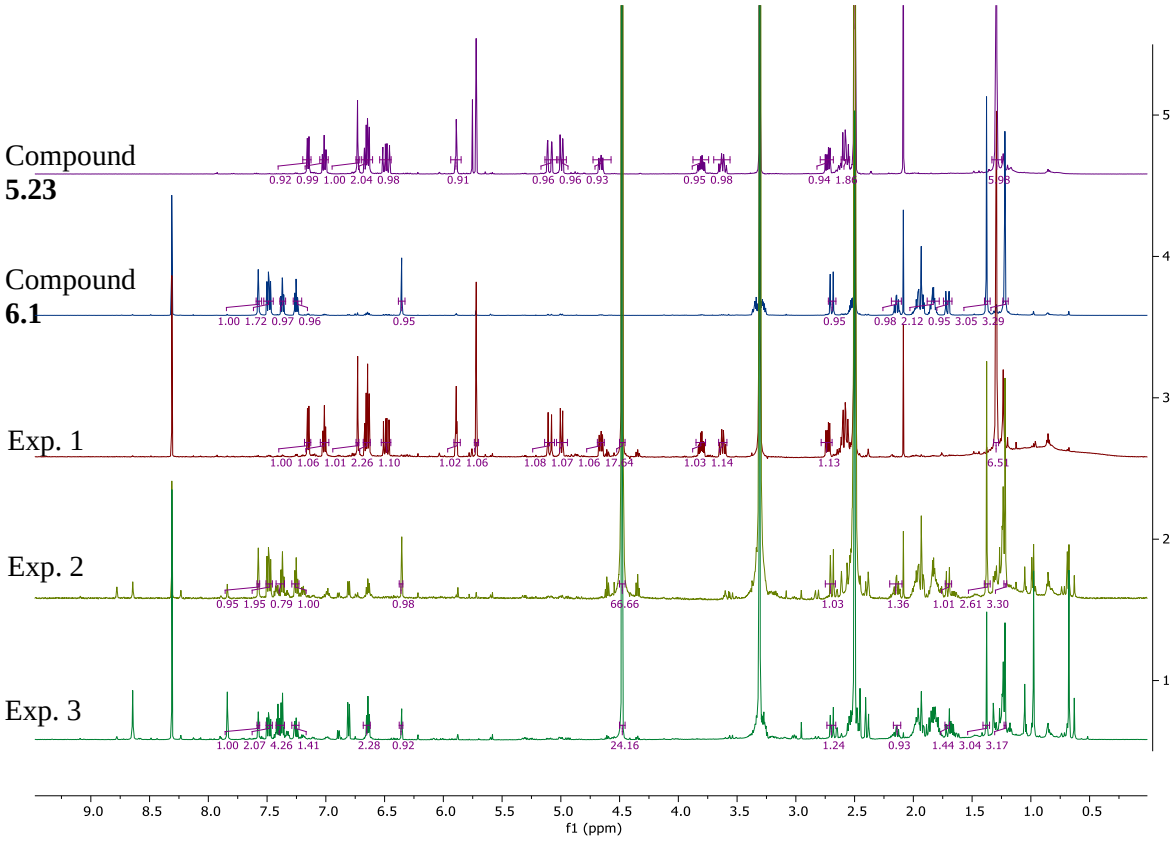

*Peak at 4.50 ppm (Internal Standard ethylene carbonate) at 8.31 ppm $CHCl_3$ and at 3.30 ppm water

^1H NMR Spectrum (500 MHz, in $(CD_3)_2SO$)

8.5.3 Solvent Screen with LiOH and Compound 6.1

The following reactions show qualitatively that treating compound **6.1** to LiOH, in different solvent systems, does not promote the semi-pinacol rearrangement to give (–)-brevianamide A (**4.1**).

To compound **6.1** (5.0 mg, 1.0 equiv., 14 µmol) was added LiOH (2 mL, 1 M, solution see table for solvent) at rt. The reaction mixture was left to stir for 24 h. The reaction was then acidified with 1 M aq. HCl (2 mL), extracted with $CHCl_3$ (3 × 5 mL), dried (Na_2SO_4) and concentrated under reduced pressure. The residue was transferred to an NMR tube with $CHCl_3$ (1.5 mL) and concentrated under reduced pressure. To the NMR tube was then added ethylene carbonate internal standard (400 µL, in $(CD_3)_2SO$) and a ^1H NMR Spectrum (500 MHz, in $(CD_3)_2SO$) was recorded.

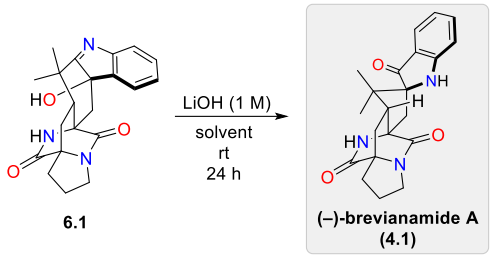

Solvent		
Experiment 1	Experiment 2	Experiment 3
H_2O	H_2O/MeOH (1:1)	MeOH
no reaction	no reaction	no reaction

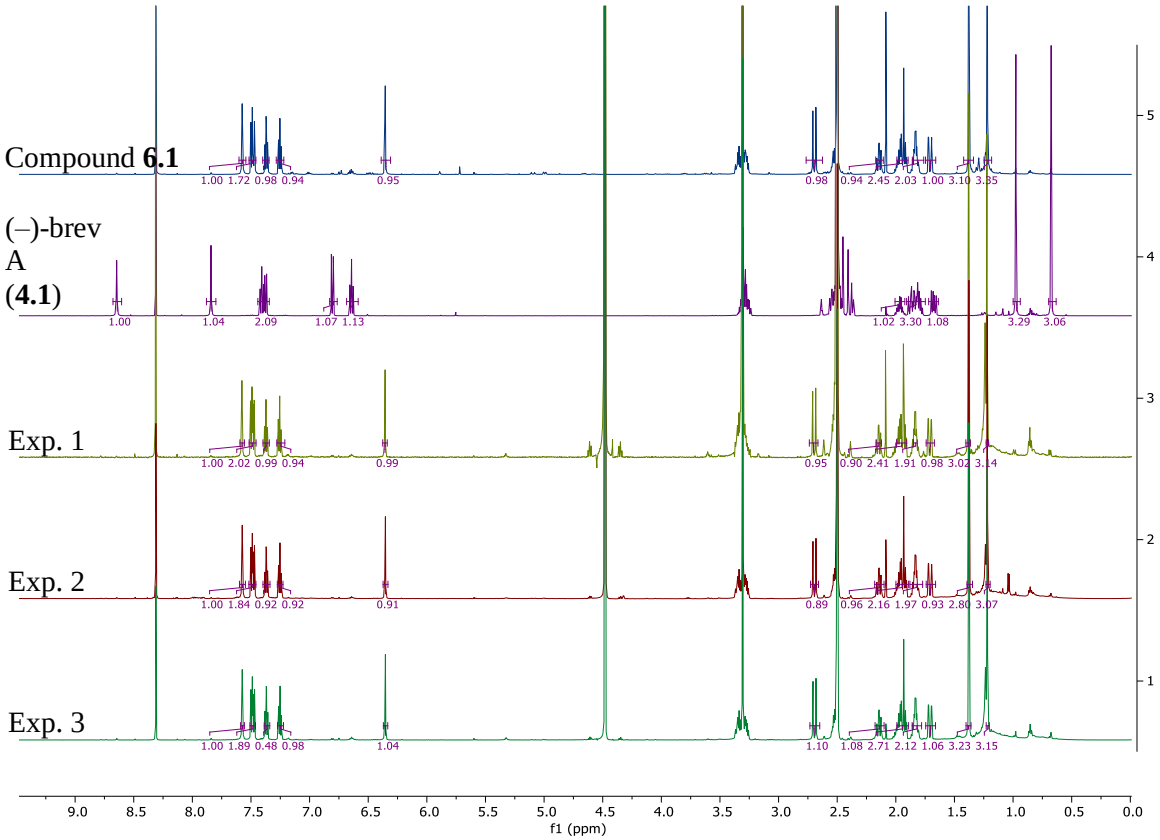

*Peak at 4.50 ppm (Internal Standard ethylene carbonate) at 8.31 ppm $CHCl_3$ and at 3.30 ppm water

^{1}H NMR Spectrum (500 MHz, in $(CD_3)_2SO$)

8.5.4 Solvent Screen with LiOH and Compound 6.5

The following reactions show qualitatively that treating compound **6.5** to LiOH, in different solvent systems, results in the formation of (–)-brevianamide B (**4.2**) through a base induced semi-pinacol rearrangement.

To compound **6.5** (5.0 mg, 1.0 equiv., 14 µmol) was added LiOH (2 mL, 1 M, solution see table for solvent) at rt. The reaction mixture was left to stir for 24 h. The reaction was then acidified with 1 M aq. HCl (2 mL), extracted with $CHCl_3$ (3 × 5 mL), dried (Na_2SO_4) and concentrated under reduced pressure. The residue was transferred to an NMR tube with $CHCl_3$ (1.5 mL) and concentrated under reduced pressure. To the NMR tube was then added ethylene carbonate internal standard (400 µL, in $(CD_3)_2SO$) and a ^1H NMR Spectrum (500 MHz, in $(CD_3)_2SO$) was recorded.

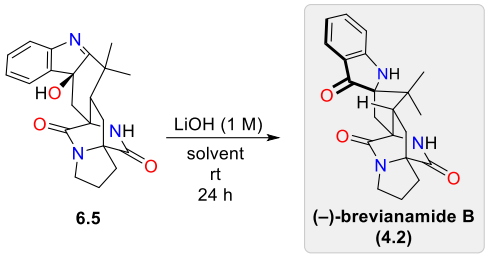

Solvent		
Experiment 1	Experiment 2	Experiment 3
H_2O	H_2O/MeOH (1:1)	MeOH
(–)-brevianamide B (**4.2**) observed	(–)-brevianamide B (**4.2**) observed	(–)-brevianamide B (**4.2**) observed

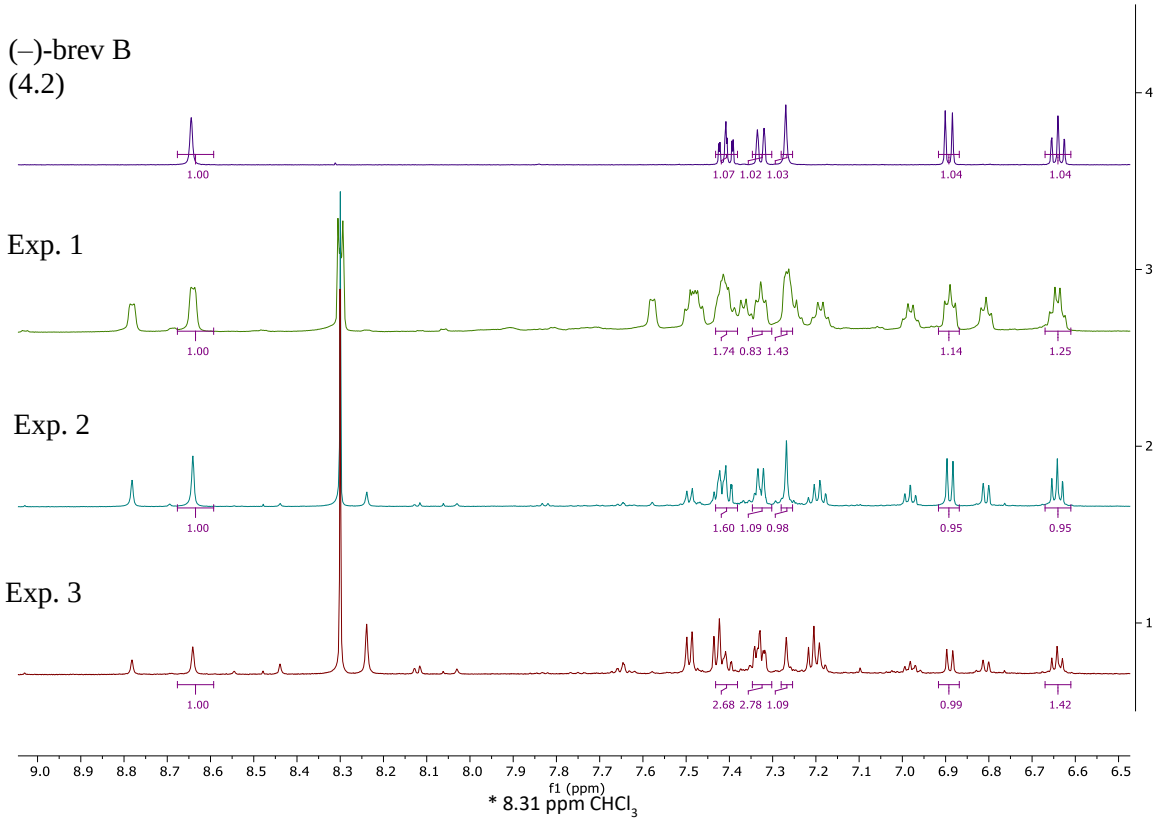

* 8.31 ppm $CHCl_3$

^1H NMR Spectrum (500 MHz, in $(CD_3)_2SO$)

8.5.5 Solvent Screen with LiOH and (–)-brevianamide A (4.1)

The following reactions show qualitatively that (–)-brevianamide A (**4.1**) is relatively stable to LiOH in different solvent systems and does not, for example, result in the formation of compound **6.1**, through a base induced retro-semi-pinacol rearrangement.

To (–)-brevianamide A (**4.1**) (5.0 mg, 1.0 equiv., 14 µmol) was added LiOH (2 mL, 1 M, solution see table for solvent) at rt. The reaction mixture was left to stir for 24 h. The reaction was then acidified with 1 M aq. HCl (2 mL), extracted with $CHCl_3$ (3 × 5 mL), dried (Na_2SO_4) and concentrated under reduced pressure. The residue was transferred to an NMR tube with $CHCl_3$ (1.5 mL) and concentrated under reduced pressure. To the NMR tube was then added ethylene carbonate internal standard (400 µL, in $(CD_3)_2SO$) and a ^1H NMR Spectrum (500 MHz, in $(CD_3)_2SO$) was recorded.

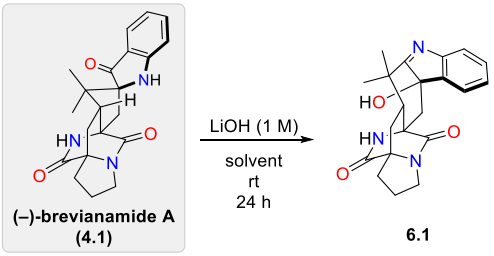

Solvent		
Experiment 1	Experiment 2	Experiment 3
H_2O	H_2O/MeOH (1:1)	MeOH
no reaction observed	no reaction observed	no reaction observed

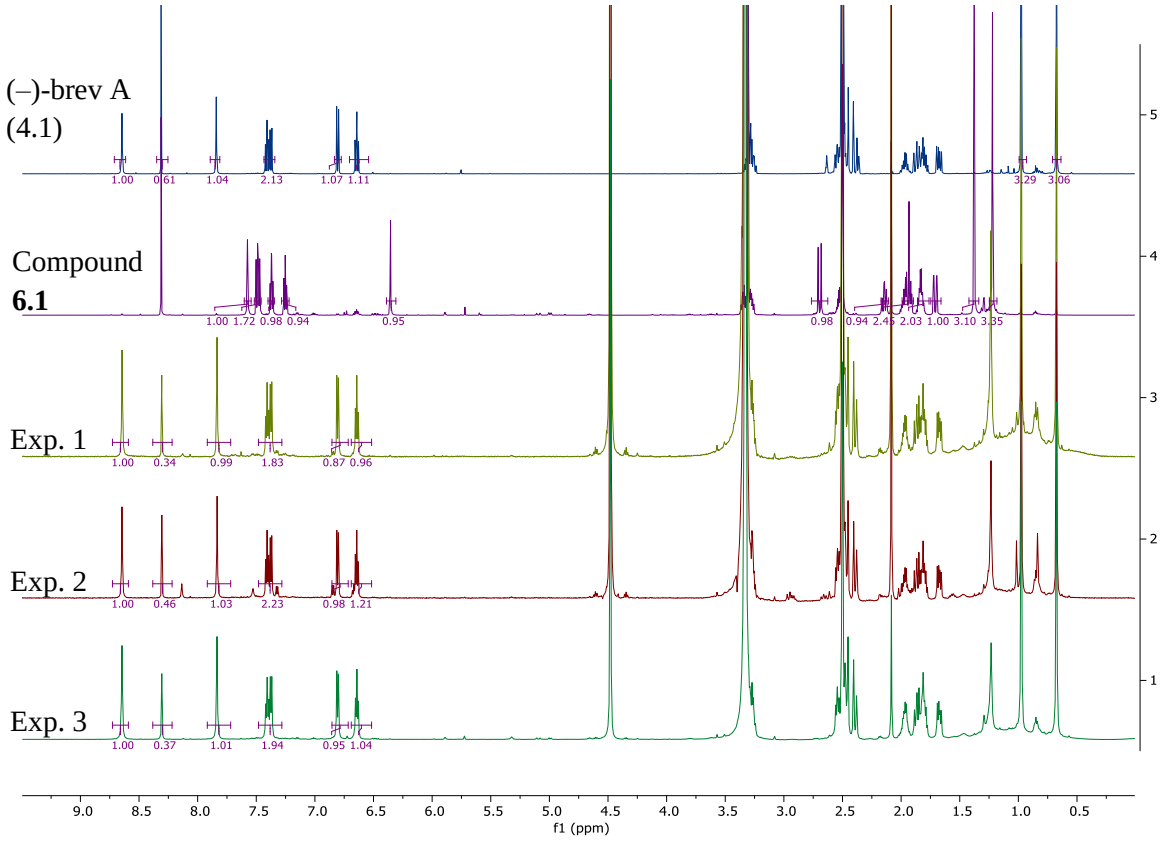

*Peak at 4.50 ppm (Internal Standard ethylene carbonate) at 8.31 ppm $CHCl_3$ and at 3.30 ppm water^{1}H NMR Spectrum (500 MHz, in $(CD_3)_2SO$)

8.5.6 Experimental Procedure for Compound 6.1 and 6.5

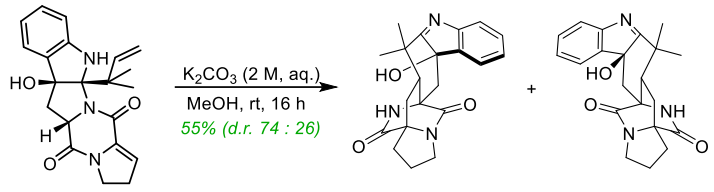

5.23 | *ent*-**5.24** [8.2 mg] | *ent*-**5.25** [2.8 mg]

To a solution of compound **5.23** (20 mg, 54.7 µmol) in MeOH (1 mL) was added a solution of 2 M K_2CO_3 (1 mL) and the reaction stirred at room temperature16 h. The reaction was acidified with 1 M aq. HCl (3 mL), extracted with CH_2Cl_2 (3 × 5 mL), dried (Na_2SO_4) and concentrated under reduced pressure. Preparative TLC (1:9 *i*-PrOH/$CHCl_3$) gave **6.1** (8.2 mg, 22.0 µmol, 41%) as a white glass and **6.5** (2.8 mg, 7.7 µmol, 14%) as a white glass.

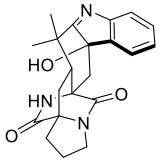

R_f 0.33 (1:9 *i*-PrOH/$CHCl_3$), 0.32 (3:7 THF/$CHCl_3$);

^{1}H NMR (500 MHz, $CDCl_3$) δ 7.51 – 7.46 (1H, m), 7.38 (1H, ddd, *J* = 7.3, 2.4, 1.4 Hz), 7.32 (1H, td apt., *J* = 7.6, 1.2 Hz), 7.21 – 7.13 (2H, m), 3.95 (1H, hept apt., *J* = 6.1 Hz), 3.36 (2H, tt, *J* = 6.5, 1.8 Hz), 2.75 (1H, d, *J* = 15.8 Hz), 2.71 – 2.64 (1H, m), 2.06 – 1.86 (4H, m), 1.78 (1H, dt, *J* = 13.0, 7.4 Hz), 1.39 (3H, s), 1.29 (3H, s) ppm;

^{1}H NMR (500 MHz, $(CD_3)_2SO$) δ 7.58 (1H, s), 7.53 – 7.43 (2H, m), 7.37 (1H, td, *J* = 7.6, 1.3 Hz), 7.25 (1H, td, *J* = 7.4, 1.0 Hz), 6.36 (1H, d, *J* = 2.1 Hz), 3.34 (1H, dt, *J* = 8.0, 5.5 Hz), 3.28 (1H, ddd, *J* = 11.1, 5.6, 2.2 Hz), 2.69 (1H, d, *J* = 15.4 Hz), 2.55 – 2.51 (1H, m), 2.17 – 2.11 (1H, m), 2.02 – 1.89 (3H, m), 1.87 – 1.78 (2H, m), 1.71 (1H, dd, *J* = 15.4, 2.2 Hz), 1.38 (3H, s), 1.22 (3H, s) ppm;

^{13}C NMR (126 MHz, $CDCl_3$) δ 188.3, 172.4, 168.3, 151.9, 140.7, 129.9, 126.4, 122.3, 121.0, 82.2, 67.1, 62.0, 50.3, 44.0, 40.4, 37.9, 32.5, 29.0, 27.3, 24.3, 20.0 ppm;

IR (film, cm^{-1}) 3362, 2968, 2882, 1730, 1674, 1580, 1458, 1390;

HRMS (ESI^+) calc. for $C_{21}H_{23}N_3O_3$ ($[M + H]^+$): 366.1812; found: 366.1809;

$[\boldsymbol{\alpha}]_{\boldsymbol{D}}^{\mathbf{21.9}}$ +89.0 (*c* 0.53, MeOH).

Data consistent with literature.[174]

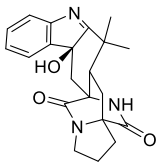

R_f 0.29 (1:9 *i*-PrOH/$CHCl_3$);

^{1}H NMR (500 MHz, $CDCl_3$) δ 7.50 (2H, dddd, *J* = 6.4, 4.9, 1.5, 0.7 Hz), 7.37 (1H, apt. td, *J* = 7.7, 1.3 Hz), 7.24 (1H, dd, *J* = 7.5, 0.9 Hz), 6.28 (1H, s), 3.80 – 3.70 (1H, m), 3.56 – 3.33 (4H, m), 2.80 – 2.68 (1H, m), 2.14 (1H, dd, *J* = 13.1, 10.2 Hz), 2.06 – 1.98 (2H, m), 1.95 (1H, dd, *J* = 13.2, 7.0 Hz), 1.87 (1H, dt, *J* = 13.1, 7.1 Hz), 1.39 (3H, s), 1.35 (4H, app. s) ppm;

^{1}H NMR (500 MHz, $(CD_3)_2SO$) δ 8.24 (1H, s), 7.54 – 7.47 (1H, m), 7.43 (1H, dd, *J* = 7.6, 0.9 Hz), 7.33 (1H, app. td, *J* = 7.6, 1.3 Hz), 7.21 (1H, app. td, *J* = 7.4, 1.0 Hz), 5.88 (1H, d, *J* = 1.6 Hz), 3.55 (1H, d, *J* = 15.0 Hz), 3.42 – 3.32 (2H, m), 3.21 (1H, dd, *J* = 10.5, 5.6 Hz), 2.17 (1H, dd, *J* = 13.3, 10.5 Hz), 2.02 – 1.93 (1H, m), 1.88 – 1.73 (3H, m), 1.27 (3H, s), 1.25 (3H, s) ppm;

^{13}C NMR (126 MHz, $CDCl_3$) δ 189.3, 173.0, 170.5, 153.4, 139.4, 130.0, 126.5, 122.4, 120.8, 81.9, 67.1, 60.1, 44.4, 43.3, 39.0, 34.8, 30.5, 29.0, 28.1, 24.6, 23.4 ppm;

^{13}C NMR (126 MHz, $(CD_3)_2SO$) δ 192.1, 173.0, 169.2, 153.8, 142.0, 129.4, 126.1, 123.0, 120.4, 81.7, 66.8, 60.0, 44.3, 42.8, 38.9, 33.6, 30.7, 29.3, 29.1, 24.5, 23.0 ppm;

IR (film, cm^{-1}) 3269, 2970, 2879, 1694, 1674, 1578, 1456, 1404;

HRMS (ESI^+) calc. for $C_{21}H_{23}N_3O_3$ ($[M + H]^+$): 366.1812; found: 366.1821; ($[M + Na]^+$): 388.1632; found: 388.1635;

$[\boldsymbol{\alpha}]_{\boldsymbol{D}}^{\boldsymbol{23.3}}$ +80.8 (*c* 0.24, MeOH).

Data consistent with literature.[174]

8.6 Experimental Conditions Chapter 6

8.6.1 General Experimental Procedure 8 – Halogenation of Dehydroproline Derivative

Compounds **7.14** and **7.15** were prepared by following literature and compounds **7.16** was prepared by adapting literature.[202]

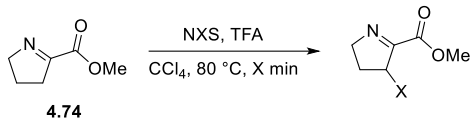

4.74

To a stirred solution of dehydroproline methyl ester **4.74** (synthesis see page **235)** (1.0 equiv.) in CCl_4 (X mL) was added NXS (1.0 equiv.). The reaction mixture was heated at 80 °C for a set amount of time and then cooled to rt, then quenched with water and diluted with $CHCl_3$. The layers were then separated and the aqueous phase was extracted with $CHCl_3$ (3 × X mL). The combined organics were then washed with $Na_2S_2O_3$ (sat., aq.), dried (Na_2SO_4) and concentrated *in vacuo*. The crude residue was then purified by flash column chromatography on silica gel to give the halogenated product.

8.6.2 Experimental Procedure for Compound 7.15

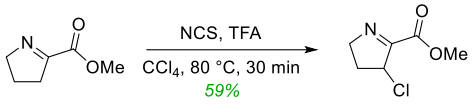

4.74 **7.15** *[1.5 g]*

Compound **7.15** was synthesised according the General Procedure **8**, using compound **4.74** (2.0 g, 1.0 equiv., 15.7 mmol), NCS (2.1 g, 1.0 equiv., 15.7 mmol), TFA (120 µL, 0.1 equiv., 1.6 mmol) in CCl_4 (20 mL) and heated for 30 min. The crude residue was purified *via* column chromatography (silica gel, petroleum ether 40/60:ethyl acetate, 8:2) to give compound **7.15** (1.5 g, 9.32 mmol, 59%) as a colourless oil.

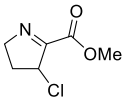

R_f = 0.25 (petroleum ether 40/60:ethyl acetate, 8:2), [UV, $KMnO_4$];

^{1}H NMR (500 MHz, $CDCl_3$) δ 5.10 (1H, dtd, *J* = 7.8, 1.9, 0.5 Hz), 4.32 – 4.21 (2H, m), 3.93 (3H, s), 2.46 (1H, apt. dq, *J* = 14.7, 7.9 Hz), 2.31 (1H, dddd, *J* = 14.7, 6.3, 2.7, 1.8 Hz) ppm;

^{13}C NMR (125 MHz, $CDCl_3$) δ 165.8, 161.5, 60.9, 58.8, 53.2, 34.8 ppm;

IR (film, cm^{-1}) 2956, 2361, 2341, 1750, 1730, 1626, 1441, 1350, 1294, 1245, 1109;

HRMS (ESI$^+$) calc. for $C_6H_8ClNO_2$ ($[M+H]^+$): 162.0317; found: 162.0323; and ($[M+Na]^+$): 184.0136; found: 184.0136;

Data consistent with literature.[252]

8.6.3 Experimental Procedure for Compound 7.14

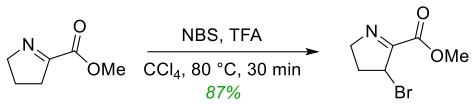

4.74 **7.14** *[2.78 g]*

Compound **7.14** was synthesised according the General Procedure **8**, using compound **4.74** (2.0 g, 1.0 equiv., 15.7 mmol), NBS (2.8 g, 1.0 equiv., 15.7 mmol), TFA (120 µL, 0.1 equiv., 1.6 mmol) in CCl_4 (20 mL) and heated for 30 min. The crude residue was purified *via* column chromatography (silica gel, petroleum ether 40/60:ethyl acetate, 8:2) to give compound **7.14** (2.78 g, 13.6 mmol, 87%) as a colourless oil.

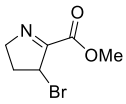

R_f = 0.44 (petroleum ether 40/60:ethyl acetate, 8:2), [UV, $KMnO_4$];

^{1}H NMR (500 MHz, $CDCl_3$) δ 5.11 (1H, apt. dt, *J* = 7.1, 1.7 Hz), 4.29 (1H, ddd, *J* = 18.0, 7.5, 1.8 Hz), 4.21 – 4.13 (1H, m), 3.93 (3H, s), 2.50 (1H, ddd, *J* = 14.9, 7.5, 0.8 Hz), 2.46 – 2.41 (1H, m) ppm;

IR (film, cm^{-1}) 2955, 1726, 1619, 1440, 1354, 1324, 1290, 1238, 1202, 1145, 1104, 947, 918, 883, 834;

HRMS (ESI^+) calc. for $C_6H_8{}^{79}BrNO_2$ ($[M+H]^+$): 205.9824; found: 205.9811;

Data consistent with literature.[252]

8.6.3 Experimental Procedure for Compound 7.16

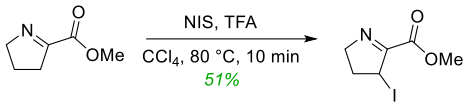

4.74 **7.16** *[0.51 g]*

Compound **7.16** was synthesised according the General Procedure **8,** using compound **4.74** (0.5 g, 1.0 equiv., 3.94 mmol), NIS (885 mg, 1.0 equiv., 3.94 mmol), TFA (30 µL, 0.1 equiv., 0.39 mmol) in CCl_4 (5.6 mL) and heated for 10 min at 80 °C. The crude residue was purified *via* column chromatography (silica gel, CH_2Cl_2:MeOH, 99:1) to give compound **7.16** (0.51 g, 2.02 mmol, 51%) as a brown oil.

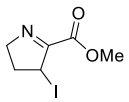

R_f = 0.22 (CH_2Cl_2:MeOH, 99:1), [UV, $KMnO_4$];

^{1}H NMR (500 MHz, $CDCl_3$) δ 5.17 (1H, ddd, *J* = 7.4, 1.9, 1.2 Hz), 4.15 (1H, ddd, *J* = 17.8, 7.4, 1.2 Hz), 3.93 (3H, s), 3.97 – 3.88 (1H, m), 2.44 (1H, apt. ddt, *J* = 14.9, 6.4, 1.2 Hz), 2.36 (1H, ddt, *J* = 14.9, 9.0, 7.4 Hz) ppm;

^{13}C NMR (126 MHz, $CDCl_3$) δ 167.9, 161.2, 60.5, 53.0, 37.8, 22.2 ppm;

IR (film, cm^{-1}) 2955, 1744, 1438, 1340, 1300, 1212, 1025;

HRMS (ESI^+) calc. for $C_6H_8INO_2$ ($[M+H]^+$): 253.9673; found: 253.9677.

8.6.4 Experimental Procedure for Compound 7.24

Compound **7.24** was prepared according to literature.[250]

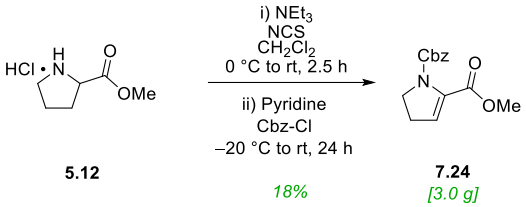

5.12 — *18%* — **7.24** *[3.0 g]*

To a solution of **5.12** (10.5 g, 1.0 equiv., 64 mmol) in CH_2Cl_2 (160 mL) was added NEt_3 (19.5 mL, 2.2 equiv., 140 mmol) and NCS (9.4 g, 1.1 equiv., 70.4 mmol) in small portions at 0 °C. The reaction was then warmed to rt and stirred for a further 2.5 h. Pyridine (11.9 mL, 2.3 equiv., 147 mmol) was then added over 30 mins using a syringe pump at rt. Then the reaction was cooled to –20 °C and Cbz-Cl (20.0 mL, 2.2 equiv., 140 mmol) was added slowly using a syringe pump over 30 minutes, after which time the reaction was allowed to warm to rt slowly and stirred at this temperature for a further 24 h. The reaction was then transferred to a separating funnel and washed with HCl (1M aq., 150 mL × 2), $NaHCO_3$ (sat., aq., 150 mL) and brine (sat., aq., 150 mL). The combined organics were then dried ($MgSO_4$) and concentrated *in vacuo*. The crude residue was purified *via* column chromatography (silica gel, cyclohexane:ethyl acetate, 5:2) to give the titled compound (**7.24**) (3.0 g, 11.5 mmol, 18%) as slightly yellow oil.

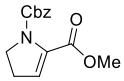

R_f = 0.28 (petroleum ether 40/60:ethyl acetate, 8:2), [UV, $KMnO_4$];

^{1}H NMR (500 MHz, $CDCl_3$) δ 7.39 – 7.28 (5H, m), 5.84 (1H, t, *J* = 2.9 Hz), 5.14 (2H, s), 4.00 (2H, dd, *J* = 9.3, 8.6 Hz), 3.65 (3H, s), 2.66 (2H, ddd, *J* = 9.5, 8.5, 2.9 Hz) ppm;

^{13}C NMR (125 MHz, $CDCl_3$) δ 162.5, 153.6, 136.3, 135.9, 128.5, 128.24, 128.22, 120.1, 67.8, 52.1, 48.5, 28.7 ppm;

IR (film, cm^{-1}) 2554, 1736, 1709, 1630, 1410, 1340, 1320, 1247, 1197, 1168, 1128, 1038, 1028, 910, 730;

HRMS (ESI^+) calc. for $C_{14}H_{15}NO_4$ ($[M+H]^+$): 262.1074; found: 262.1081;

Data consistent with literature.[250]

8.6.5 Experimental Procedure for Compound 7.25

Compound **7.25** was prepared according to literature.[205]

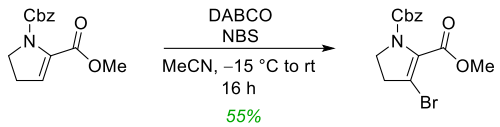

7.24 **7.25** *[1.8 g]*

DABCO (2.2 g, 2.0 equiv., 19.4 mmol) was added to a stirred solution of **7.24** (2.55 g, 1.0 equiv., 9.7 mmol) in anhydrous MeCN (19.0 mL) at rt. The reaction was then cooled to –15 °C and a solution of NBS (1.94 g, 1.1 equiv., 9.7 mmol) in anhydrous MeCN (29.0 mL) was added slowly over 30 min *via* syringe pump. This was left to stir for a further 16 h at rt. The reaction mixture was then concentrated *in vacuo* until 1-2 mL of solvent remained. The crude residue was purified directly *via* column chromatography (silica gel, petroleum ether 40/60:ethyl acetate, 8:2) to give the titled compound (**7.25**) (1.8 g, 5.3 mmol, 55%) as slightly yellow oil.

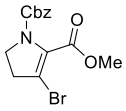

R_f = 0.44 (petroleum ether 40/60:ethyl acetate, 8:2), [UV, $KMnO_4$];

^{1}H NMR (500 MHz, $CDCl_3$) δ 7.39 – 7.31 (5H, m), 5.13 (2H, s), 3.99 (2H, dd, *J* = 9.7, 8.7 Hz), 3.72 – 3.56 (3H, m), 2.94 (2H, dd, *J* = 9.8, 8.7 Hz) ppm;

^{13}C NMR (125 MHz, $CDCl_3$) δ 161.6, 152.4, 135.5, 133.5, 128.6, 128.45, 128.45, 128.4, 68.2, 52.5, 47.3, 36.3 ppm;

IR (film, cm^{-1}) 2953, 2361, 2342, 1740, 1711, 1643, 1498, 1438, 1410, 1337, 1314, 1206, 1176, 1145, 1028, 981, 752, 699;

HRMS (ESI^+) calc. for $C_{14}H_{14}{}^{79}BrNO_4$ ($[M+H]^+$): 340.0179; found: 340.0196;

Data consistent with literature.[205]

8.6.6 Experimental Procedure for Compound 7.32

Compound **7.32** was prepared by adapting literature.[217]

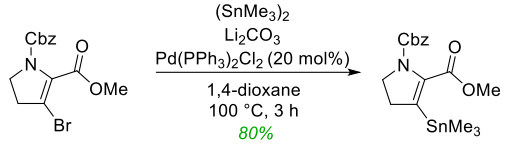

7.25 **7.32** *[100 mg]*

To solution of **7.25** (100 mg, 1.0 equiv., 0.30 mmol), Li_2CO_3 (56 mg, 2.6 equiv., 0.76 mmol) and $(SnMe_3)_2$ (250 µL, 4.0 equiv., 1.2 mmol) in 1,4-dioxane (10.0 mL) sparged with nitrogen gas, was added $Pd(PPh_3)_2Cl_2$ (40 mg, 0.19 equiv., 0.057 mmol) at rt. The reaction was stirred for 3 h at 100 °C. Then the reaction was cooled and concentrated *in vacuo*. The crude residue was purified *via* column chromatography (silica gel, petroleum ether 40/60:ethyl acetate, 8:2) to give the title compound (**7.32**) (100 mg, 0.24 mmol, 80%) as slightly yellow oil.

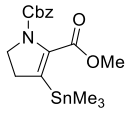

R_f = 0.18 (petroleum ether 40/60:ethyl acetate, 7:3), [UV, $KMnO_4$];

^{1}H NMR (600 MHz, $CDCl_3$) δ 7.37 – 7.29 (5H, m), 5.14 (2H, s), 3.94 (2H, dd, *J* = 9.0, 8.3 Hz), 3.62 (3H, s), 2.70 (2H, dd, *J* = 9.1, 8.4 Hz), 0.20 (9H, s) ppm;

*Sn satellites observable at peak at 0.2 which corresponds to $SnMe_3$;

^{13}C NMR (150 MHz, $CDCl_3$) δ 163.7, 153.2, 140.5, 136.1, 135.4, 128.5, 128.20, 128.16, 67.6, 51.9, 48.9, 35.2, 30.3, –9.0 ppm;

*peak at –9.0 corresponds to the methyl groups from $SnMe_3$ with Sn satellites also observable;

IR (film, cm^{-1}) 2922, 1741, 1709, 1438, 1403, 1363, 1337, 1311, 1232, 1196, 1168, 1031, 1054, 762;

HRMS (ESI^+) calc. for $C_{17}H_{23}NO_4{}^{120}Sn$ ($[M+H]^+$): 426.0723; found: 426.0722.

8.6.7 Experimental Procedure for Compound 7.56

Compound **7.56** was prepared according to literature.[253]

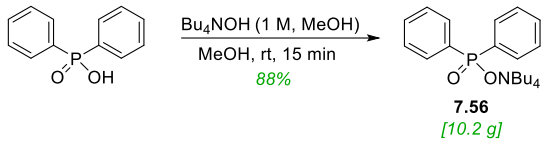

7.56
[10.2 g]

To a suspension of diphenylphosphinic acid (5.5 g, 1.0 equiv., 25.2 mmol) in anhydrous MeOH (28 mL) tetrabutylammonium hydroxide (1M in MeOH, 25.2 mL, 1.0 equiv., 25.2 mmol) was added at rt. The resulting solution was left to stir for 15 min and then filtered through a short pad of celite, eluting with MeOH. The combined filtrates were concentrated *in vacuo*. The resulting residue was dried under vacuum overnight to afford a yellow waxy solid. The crude residue was purified *via* recrystalisation by refluxing in 1:4 ethyl acetate/diethyl ether and then cooling to –20 °C to afford compound **7.56** as white, deliquescent crystalline needles (10.2 g, 22.2 mmol, 88%).

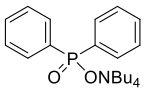

^{1}H NMR (500 MHz, $CDCl_3$) δ 7.94 – 7.84 (5H, m), 7.25 – 7.20 (5H, m), 3.34 – 3.24 (9H, m), 1.57 (8H, dq, *J* = 11.9, 8.1, 7.6 Hz), 1.35 (8H, sextet, *J* = 7.4 Hz), 0.93 (12 H, t, *J* = 7.3 Hz) ppm;

^{13}C NMR (150 MHz, $CDCl_3$) δ 131.7 (d, *J* = 8.6 Hz), 128.5 (d, *J* = 2.6 Hz), 127.6 (d, *J* = 11.3 Hz), 58.9, 24.1, 19.7, 13.7 ppm, *ipso* quaternary centre on the aromatic ring not observed;

^{31}P NMR (200 MHz, $CDCl_3$) δ 13.75 ppm;

Data consistent with literature.[253]

8.6.8 Experimental Procedure for Compound 7.41

Mukaiyama's *N*-*t*-butylbenzenesulfinimidoyl chloride reagent (**7.37**) and compound **7.41** were prepared according to a procedure reported by Trost and co-workers.[254]

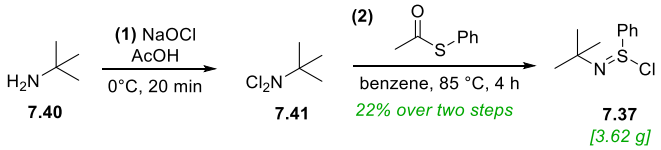

Step 1: NaOCl (200 mL, 38.0 equiv., 3.0 mol) was cooled to 0 °C shielded from light. Glacial acetic acid (9.8 mL, 2.2 equiv., 170.0 mmol) was added dropwise, followed by the dropwise cautious addition of tertbutylamine (**7.40**) (8.2 mL, 1.0 equiv., 78.0 mmol) over a period of 15 min. The reaction mixture was stirred for a further 15 minutes at this temperature. After this time the reaction was diluted with CH_2Cl_2 (200 mL) and the aqueous layer is separated and discarded. The organic layer was washed with $NaHCO_3$ (sat. aq., 150 mL), H_2O (150 mL), dried ($MgSO_4$) and then concentrated under reduced pressure (>200 mbar at 20 °C). This crude residue was used directly in the next step without purification.

^{1}H NMR (500 MHz, $CDCl_3$) δ 1.37 (9H, s) ppm;

^{13}C NMR (125 MHz, $CDCl_3$) δ 72.6, 25.9 ppm;

Data consistent with literature.[254]

8.6.9 Experimental Procedure for Compound 7.37

Mukaiyama's *N*-*t*-butylbenzenesulfinimidoyl chloride reagent (**7.37**) was prepared according to a procedure reported by Trost and co-workers.[254]

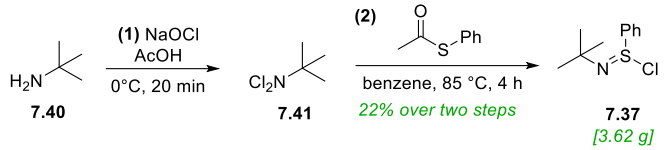

Step 2: To crude **7.41** (5.8 g, 1.2 equiv., 41 mmol) in benzene (35 mL) was added 5-phenylthioacetate (4.63 mL, 1.0 equiv., 34 mmol). The reactions was heated in a sealed system under reflux and monitored by TLC. After 4 h the volatiles were removed azeotropically with benzene (2 × 30 mL). The crude residue was passed through a short plug of sand and washed with CH_2Cl_2 (50 mL), to afford the titled compound (**7.37**) as an orange oil (3.62 g, 17 mmol, 22% over two steps).

*This compound was made fresh and stored under nitrogen in the freezer for no more than a week before use.

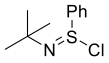

^{1}H NMR (500 MHz, $CDCl_3$) δ 8.15 – 8.11 (2H, m), 7.65 – 7.56 (3H, m), 1.58 (9H, s) ppm;

Data consistent with literature.[254]

8.6.10 Experimental Procedure for Compound 7.36

Compound **7.36** was prepared under anhydrous conditions. After the addition of I_2, effort was made to limit exposure of the material to light.

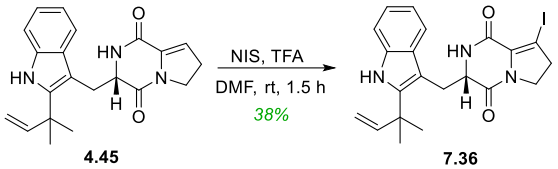

4.45 **7.36** *[261 mg]*

To a stirred solution of (+)-dehydrodeoxybrevianamide E (**4.45**) (500 mg, 1.0 equiv., 1.43 mmol) in anhydrous DMF* (25.0 mL) was added a solution of a TFA* (3.2 µL, 0.03 equiv., 0.042 mmol) in anhydrous DMF (100 µL). The reaction mixture was cooled to 0 °C and NIS* (322 mg, 1.0 equiv., 1.43 mmol) was added in a single portion. The reaction was stirred at 0 °C for 5 minutes, the cooling bath was removed and the reaction was stirred at room temperature for 1.5 h. The reaction was cooled to 0 °C and NEt_3 (1.5 mL, 7.15 equiv., 10.76 mmol) was added. The reaction mixture was poured onto a stirred mixture of ethyl acetate (200 mL) and 10% aq. $Na_2S_2O_3$ (100 mL). The organic layer was separated, washed with brine (5 × 200 mL) and concentrated under reduced pressure. Flash column chromatography (silica gel, petroleum ether 40/60:ethyl acetate, 7:13 to 13:7) gave compound **7.36** (261 mg, 0.55 mmol, 38%) as a cream foam.

*Anhydrous DMF was dried over activated 4 Å molecular sieves. Commercial TFA was distilled under inert atmosphere before use and a stock solution was prepared in DMF. NIS was recrystallised from 1,4-dioxane/diethyl ether.

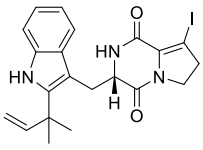

R_f = 0.50 (petroleum ether 40/60:ethyl acetate, 3:7), [UV, $KMnO_4$];

^{1}H NMR (500 MHz, $CDCl_3$) δ 8.16 (br. s, 1H), 7.50 (1H, d, *J* = 7.9 Hz), 7.31 (1H, dd, *J* = 8.0, 1.0 Hz), 7.15 (1H, ddd, *J* = 8.1, 7.0, 1.1 Hz), 7.09 (1H, ddd, *J* = 8.0, 7.0, 1.1 Hz), 6.13 (1H, dd, *J* = 17.5, 10.6 Hz), 5.79 (1H, br. s), 5.19 – 5.14 (2H, m), 4.46 (1H, ddd, *J* = 10.7, 3.5, 2.1 Hz), 4.07 – 3.93 (2H, m), 3.69 (1H, dd, *J* = 14.6, 3.6 Hz), 3.23 (1H, dd, *J* = 14.6, 10.8 Hz), 3.05 – 2.89 (2H, m), 1.55 (3H, s), 1.54 (3H, s) ppm;

^{13}C NMR (125 MHz, $CDCl_3$) δ 162.0, 156.0, 145.9, 141.9, 134.4, 130.9, 128.9, 122.2, 120.1, 118.3, 112.5, 110.9, 104.4, 80.3, 57.7, 45.8, 40.3, 39.2, 30.9, 28.1, 27.9 ppm;

IR (film, cm^{-1}) 3340, 2967, 2924, 1654, 1620;

HRMS (ESI^+) calc. for $C_{21}H_{22}IN_3O_2$ ($[M+H]^+$): 476.0830; found: 476.0844; ($[M+Na]^+$): 498.0649; found: 498.0665;

$[\boldsymbol{\alpha}]_{\boldsymbol{D}}^{\mathbf{20.9}}$ +9.7 (*c* 1.57, MeOH).

8.6.11 Experimental Procedure for Compound 7.57

Compound **7.57** was prepared by adapting literature.[217]

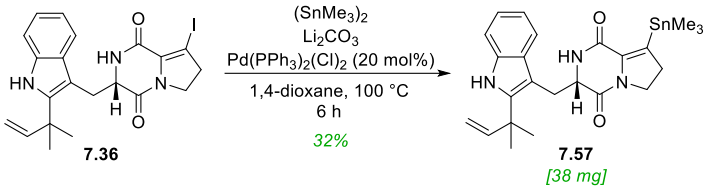

To a solution of **7.36** (110 mg, 1.0 equiv., 0.23 mmol), Li_2CO_3 (45 mg, 2.6 equiv., 0.60 mmol) and $(SnMe_3)_2$ (193 µL, 4.0 equiv., 0.93 mmol) in 1,4-dioxane (7.8 mL) sparged with nitrogen gas, was added $Pd(PPh_3)_2Cl_2$ (31 mg, 0.19 equiv., 0.044 mmol) at rt. The reaction was stirred for 6 h at 100 °C. Then the reaction was cooled then passed through a small pad of Celite and washed with CH_2Cl_2 (15 mL). This was diluted with water (15 mL) and the layers were separated. The aqueous was washed with CH_2Cl_2 (15 mL × 2) and the combined organics were dried (Na_2SO_4) and concentrated *in vacuo*. The crude residue was purified *via* column chromatography (silica gel, petroleum ether 40/60:ethyl acetate, 1:1) to give the title compound (**7.57**) (38 mg, 0.074 mmol, 32%) as yellow solid.

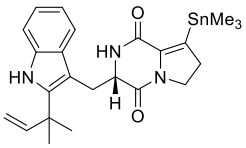

R_f = 0.11 (petroleum ether 40/60:ethyl acetate, 1:1), [UV, $KMnO_4$];

^{1}H NMR (600 MHz, $CDCl_3$) δ 8.09 (1H, d, *J* = 6.2 Hz), 7.53 (1H, d, *J* = 7.8 Hz), 7.30 (1H, d, *J* = 8.0 Hz), 7.16 (1H, t, *J* = 7.5 Hz), 7.10 (1H, t, *J* = 7.5 Hz), 6.12 (1H, ddd, *J* = 17.6, 10.5, 2.0 Hz), 5.57 (1H, s), 5.15 (2H, dd, *J* = 13.9, 10.3 Hz), 4.56 – 4.47 (1H, m), 4.18 – 3.93 (2H, m), 3.71 (1H, dd, *J* = 14.7, 3.6 Hz), 3.31 – 3.18 (1H, m), 2.81 (2H, t, *J* = 8.9 Hz), 1.54 (6H, d, *J* = 3.0 Hz), 0.21 (9H, d, *J* = 2.2 Hz,) ppm;

*Sn satellites observable at peak at 0.21 which corresponds to $SnMe_3$;

^{13}C NMR (150 MHz, $CDCl_3$) δ 162.1, 157.8, 145.8, 141.7, 137.4, 136.5, 134.3, 128.8, 122.0, 120.0, 118.2, 112.3, 110.7, 104.7, 57.5, 46.5, 39.0, 34.2, 30.9, 27.9, 27.8, –8.4 ppm;

*satellites observable at peak at 46.5 beta to the tin peak at –9.0 corresponds to the methyl groups from $SnMe_3$ with Sn satellites also observable;

IR (film, cm^{-1}) 3355, 2967, 2923, 1667, 1618, 1438, 1316, 1253, 1054, 913, 770, 743;

HRMS (ESI^+) calc. for $C_{24}H_{31}N_3O_2{}^{120}Sn$ ($[M+H]^+$): 514.1512; found: 514.1501; ($[M+Na]^+$): 536.1332; found: 536.1330.

8.6.12 Experimental Procedure for Compound 7.42

Compound **7.42** was prepared under anhydrous conditions, by adapting the work of Matsuo[224] and Mukaiyama.[222]

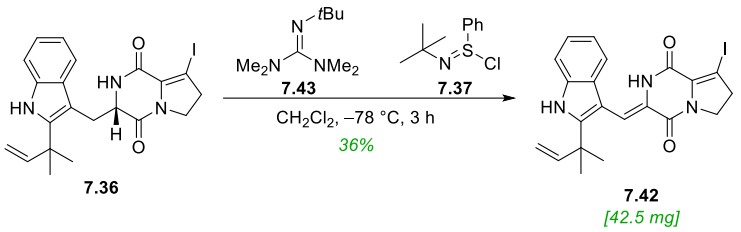

To a solution of compound **7.36** (120 mg, 1.0 equiv., 0.25 mmol) in CH_2Cl_2 (6 mL) was added 2-*t*-butyl-1,1,3,3-tetramethylguanidine (**7.43**) (0.10 mL, 2.0 equiv., 0.50 mmol) and the reaction cooled to −78 °C with stirring. A solution of *N*-*t*-butylbenzenesulfinimidoyl chloride **7.37*** (107 mg, 2.0 equiv., 0.50 mmol) in CH_2Cl_2 (2.6 mL) was added dropwise over 10 minutes at −78 °C. After stirring for 3 h at −78 °C the reaction was quenched by the addition of saturated aq. $NaHCO_3$ (10 mL) and the reaction was left to warm to room temperature over 1 h. The reaction mixture was diluted with water (10 mL) and CH_2Cl_2 (10 mL). The phases were separated and the aqueous layer was back-extracted with CH_2Cl_2 (3 × 10 mL). The combined organics were dried (Na_2SO_4) and concentrated under reduced pressure. Two rounds of flash column chromatography (silica gel, petroleum ether 40/60:ethyl acetate, 3:7) gave **7.42** contaminated with *N*-(phenylsulfinyl)-*N*-(*tert*-butyl)amine. Flash column chromatography (silica gel, CH_2Cl_2 to ethyl acetate/CH_2Cl_2, 1:9) gave compound **7.42** (42.5 mg, 0.09 mmol, 36%) as a yellow glass.

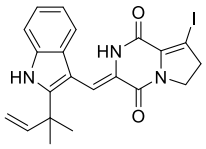

R_f = 0.33 (ethyl acetate:CH_2Cl_2, 1:9), [UV, $KMnO_4$];

^{1}H NMR (500 MHz, $CDCl_3$) δ 8.30 (1H, s), 7.61 (1H, s), 7.36 (1H, dt, *J* = 8.0, 0.9 Hz), 7.28 (1H, ddt, *J* = 7.9, 1.6, 0.8 Hz), 7.20 (1H, ddd, *J* = 8.2, 7.1, 1.3 Hz), 7.19 (1H, s), 7.15 (1H, ddd, *J* = 8.1,

7.1, 1.2 Hz), 6.07 (1H, dd, *J* = 17.4, 10.6 Hz), 5.23 (1H, dd, *J* = 10.5, 0.9 Hz), 5.19 (1H, dd, *J* = 17.5, 0.9 Hz), 4.17 (2H, dd, *J* = 10.1, 8.6 Hz), 3.15 (2H, dd, *J* = 10.0, 8.7 Hz), 1.52 (6H, s) ppm;

^{13}C NMR (126 MHz, $CDCl_3$) δ 154.5, 153.6, 144.3, 144.1, 134.4, 131.9, 126.1, 126.0, 122.6, 121.4, 119.2, 113.6, 111.4, 111.3, 103.4, 81.4, 46.1, 40.6, 39.4, 27.5 ppm;

IR (film, cm^{-1}) 2925, 2359, 1740, 1712, 1435, 1410, 1338, 1316, 1205, 1032, 749, 698;

HRMS (ESI^+) calc. for $C_{21}H_{20}IN_3O_2$ ($[M+H]^+$): 474.0673; found: 474.0678; ($[M+Na]^+$): 496.0492; found: 496.0476.

8.6.13 Experimental Procedure for Compound 7.5

Compound **7.5** was prepared under anhydrous conditions, by adapting the work of Zhang and coworkers.[210]

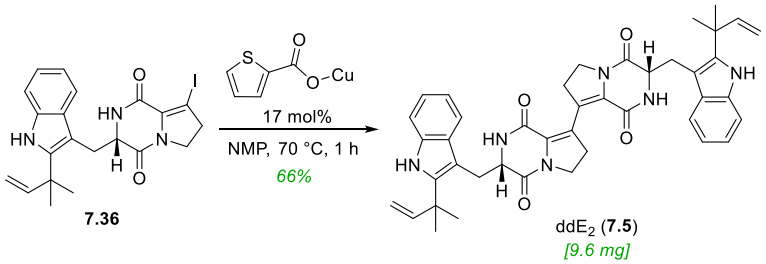

To a stirred solution of compound **7.36** (20 mg, 1.0 equiv., 42 µmol) in anhydrous NMP (0.4 mL) at 70 °C was added copper(I) thiophene-2-carboyxlate (32 mg, 0.4 equiv., 170 µmol). After 50 minutes the reaction was cooled to rt. The reaction mixture was diluted with ethyl acetate, washed through a small plug of neutralised silica (silica was neutralised by passing through eluent of ethyl acetate with 1% NEt_3) with ethyl acetate and the filtrate was concentrated *in vacuo*. The crude residue was purified *via* flash chromatography on neutralised silica (silica gel, ethyl acetate, 100 to MeOH/ethyl acetate, 6:100) gave dimer **7.5** (9.6 mg, 18 µmol, 66%) alongside dehydrodeoxy-brevianamide E (**4.45**) (2.4 mg, 6.9 µmol, 16%).

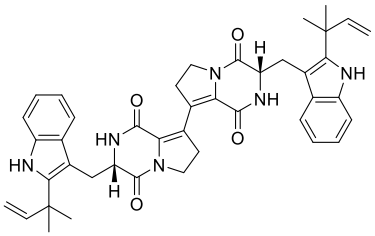

R_f = 0.11 (ethyl acetate, 100), [UV, $KMnO_4$];

Mp 158-162 °C;

^{1}H NMR (500 MHz, $CDCl_3$) δ 8.04 (1H, s), 7.52 (1H, d, *J* = 7.9 Hz), 7.31 (1H, d, *J* = 8.0 Hz), 7.16 (1H, ddd, *J* = 8.0, 7.0, 1.2 Hz), 7.13 – 7.07 (1H, m), 6.11 (1H, dd, *J* = 17.6, 10.5 Hz), 5.62 (1H, d, *J* = 1.9 Hz), 5.26 – 5.04 (2H, m), 4.45 (1H, dt, *J* = 11.1, 3.0 Hz), 4.01 (2H, tq, *J* = 10.2, 3.2 Hz),

3.72 (1H, dd, *J* = 14.6, 3.5 Hz), 3.22 (1H, dd, *J* = 14.6, 11.1 Hz), 3.03 (2H, t, *J* = 9.4 Hz), 1.54 (6H, s), 1.53 (6H, s) ppm;

^{13}C NMR (125 MHz, $CDCl_3$) δ 162.7, 156.4, 145.8, 141.8, 134.4, 129.0, 128.0, 127.1, 122.2, 120.3, 118.4, 112.7, 110.9, 104.8, 57.3, 44.3, 39.2, 31.5, 30.7, 28.1, 28.0 ppm;

IR (film, cm^{-1}) 3345, 2958, 2924, 1669, 1432, 669;

HRMS (ESI^+) calc. for $C_{42}H_{44}N_6O_4$ ($[M+H]^+$): 697.3497; found: 697.3495.

8.6.14 Experimental Procedure for Compound 7.52

Compound **7.52** was prepared by adapting literature.[205]

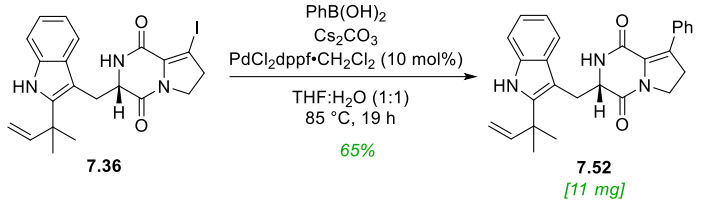

Compound **7.36** (19 mg, 1.0 equiv., 40 µmol), $PhB(OH)_2$ (7.3 mg, 1.5 equiv., 60 µmol), Cs_2CO_3 (18 mg, 1.4 equiv., 56 µmol) and $PdCl_2dppf{\cdot}CH_2Cl_2$ (3.3 mg, 0.1 equiv., 4.0 µmol) was cycled under N_2 three times in a Schleck flask. Then THF:H_2O (1:1, 1 mL:1 mL) was added and the reactions was heated to 85 °C and stirred for 19 h. The reaction was then cooled to rt and the solvent was concentrated under reduced pressure. The aqueous phase was extracted with ethyl acetate (5 mL × 3), dried ($MgSO_4$) and concentrated *in vacuo*. The crude residue was purified *via* preparative TLC (silica gel, petroleum ether 40/60:ethyl acetate, 8:2) to afford the titled compound (11 mg, 26 µmol, 65%) as slightly yellow oil.

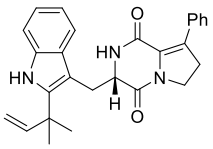

R_f = 0.37 (petroleum ether 40/60: ethyl acetate, 8:2), [UV, $KMnO_4$];

^{1}H NMR (500 MHz, $CDCl_3$) δ 8.02 (1H, s), 7.57 (3H, ddd, *J* = 7.3, 4.7, 1.4 Hz), 7.36 – 7.28 (4H, m), 7.17 (1H, ddd, *J* = 8.1, 7.0, 1.2 Hz), 7.11 (1H, ddd, *J* = 8.2, 7.1, 1.1 Hz), 6.15 (1H, dd, *J* = 17.4, 10.5 Hz), 5.66 – 5.60 (1H, m), 5.21 – 5.18 (1H, m), 5.17 (1H, d, *J* = 1.2 Hz), 4.53 (1H, ddd, *J* = 10.8, 3.7, 2.1 Hz), 4.09 – 3.99 (2H, m), 3.74 (1H, dd, *J* = 14.6, 3.6 Hz), 3.29 (1H, dd, *J* = 14.6, 10.6 Hz), 3.05 (2H, ddd, *J* = 10.1, 8.2, 1.8 Hz), 1.56 (6H, d, *J* = 1.7 Hz) ppm;

^{13}C NMR (125 MHz, $CDCl_3$) δ 163.2, 157.0, 145.8, 141.7, 134.3, 134.2, 132.9, 129.0, 128.9, 128.8, 127.8, 122.1, 120.1, 118.3, 112.5, 110.7, 104.7, 56.9, 43.2, 39.1, 33.0, 30.8, 30.3, 28.0, 27.9 ppm;

HRMS (ESI^+) calc. for $C_{27}H_{27}N_3O_3$ ($[M+H]^+$): 426.2178; found: 426.2180.

8.6.15 Experimental Procedure for Brevianamide K (7.4)

Brevianamide K (**7.4**) was prepared under anhydrous conditions, by adapting the work of Matsuo[224] and Mukaiyama.[222]

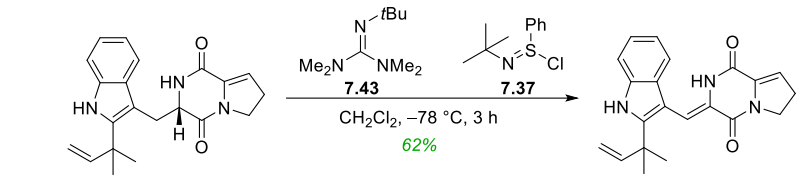

To a solution of (+)-dehydrodeoxybrevianamide E (**4.45**) (100 mg, 1.0.equiv., 0.286 mmol) in CH_2Cl_2 (5.0 mL) was added 2-*t*-butyl-1,1,3,3-tetramethylguanidine (**7.43**) (115 µL, 2.0 equiv., 0.572 mmol) and the reaction cooled to −78 °C with stirring. A solution of *N*-*t*-butylbenzenesulfinimidoyl chloride (**7.37**) (123 mg, 2.0 equiv., 0.572 mmol) in CH_2Cl_2 (4.1 mL) was added dropwise over 5 minutes at −78 °C. After stirring for 3 h at −78 °C the reaction was quenched by the addition of saturated aq. $NaHCO_3$ (15 mL) and the reaction was allowed to warm to room temperature. The phases were separated and the aqueous layer was extracted with CH_2Cl_2 (3 × 15 mL). The combined organics were washed with brine (15 mL), dried (Na_2SO_4) and concentrated under reduced pressure. Flash column chromatography (silica gel, petroleum ether 40/60:ethyl acetate, 3:7 to 1:1 to ethyl acetate) gave brevianamide K (**7.4**) (61.8 mg, 0.178 mmol 62%) as a pale brown glass.

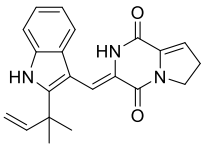

R_f = 0.13 (petroleum ether 40/60: ethyl acetate, 1:1), [UV, $KMnO_4$];

^{1}H NMR (500 MHz, $CHCl_3$) δ 8.47 (1H, s), 7.58 (1H, s), 7.35 (1H, dt, *J* = 8.0, 1.0 Hz), 7.29 – 7.26 (1H, m), 7.20 (1H, s), 7.17 (1H, dd, *J* = 8.0, 1.3 Hz), 7.13 (1H, td, *J* = 7.5, 1.2 Hz), 6.23 (1H, t, *J* =

3.2 Hz), 6.05 (1H, dd, *J* = 17.4, 10.5 Hz), 5.20 (1H, dd, *J* = 10.6, 1.0 Hz), 5.21 – 5.13 (1H, dd, *J* = 10.6, 1.0 Hz), 4.19 (2H, dd, *J* = 9.8, 8.6 Hz), 2.87 (2H, ddd, *J* = 9.8, 8.5, 3.2 Hz), 1.51 (6H, s) ppm;

^{13}C NMR (126 MHz, $CDCl_3$) δ 155.2, 154.4, 144.4, 144.0, 134.5, 134.0, 126.4, 126.1, 122.5, 121.2, 119.8, 119.1, 113.5, 111.4, 111.2, 103.3, 45.9, 39.4, 28.3, 27.5 ppm;

IR (film, cm^{-1}) 3312, 2963, 2922, 2853, 1668, 1636, 1616, 1409, 1350;

HRMS (ESI^+) calc. for $C_{21}H_{21}N_3O_2$ ($[M+H]^+$): 348.1707; found: 348.1697; ($[M+Na]^+$): 370.1526; found: 370.1516;

Spectroscopic data matched literature values.[196]

8.6.16 Experimental Procedure for Compound 7.48

Compound **7.48** was prepared by adapting literature.[217]

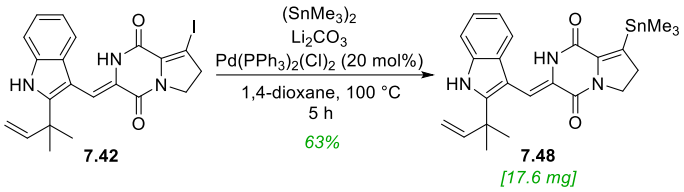

To a solution of **7.42** (26 mg, 1.0 equiv., 55 µmol), Li_2CO_3 (11 mg, 2.6 equiv., 140 µmol) and $(SnMe_3)_2$ (46 µL, 4.0 equiv., 22 µmol) in 1,4-dioxane (1.8 mL) sparged with nitrogen gas, was added $Pd(PPh_3)_2Cl_2$ (2 mg, 0.19 equiv., 2.7 µmol) at rt. The reaction was stirred for 5 h at 100 °C. Then the reaction was cooled, then passed through a small pad of Celite and washed with CH_2Cl_2 (5 mL). This was diluted with water (5 mL) and the layers were separated. The aqueous was washed with CH_2Cl_2 (10 mL × 2) and the combined organics were dried (Na_2SO_4) and concentrated *in vacuo*. The crude residue was purified *via* column chromatography (silica gel, petroleum ether 40/60:ethyl acetate, 8:2) to give the titled compound (**7.48**) (17.6 mg, 34.3 µmol, 63%) as slightly yellow oil.

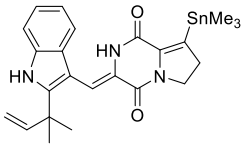

R_f = 0.17 (petroleum ether 40/60: ethyl acetate, 8:2), [UV, $KMnO_4$];

^{1}H NMR (600 MHz, $CDCl_3$) δ 8.26 (1H, s), 7.53 (1H, s), 7.33 (1H, dt, *J* = 8.1, 0.9 Hz), 7.30 (1H, ddd, *J* = 7.4, 1.6, 0.7 Hz), 7.19 – 7.16 (2H, m), 7.15 (1H, d, *J* = 1.6 Hz), 6.11 – 6.05 (1H, m), 5.22 (1H, dd, *J* = 10.6, 0.9 Hz), 5.19 (1H, dd, *J* = 17.4, 0.9 Hz), 4.14 (2H, dd, *J* = 9.5, 8.3 Hz), 2.96 – 2.89 (2H, m), 1.57 – 1.56 (6H, m), 0.23 (9H, s) ppm;

*Sn satellites observable at peak at 0.23 which corresponds to $SnMe_3$;

^{13}C NMR (150 MHz, $CDCl_3$) δ 155.5, 154.5, 144.4, 143.5, 139.3, 137.3, 134.3, 126.9, 126.1, 122.3, 121.1, 119.0, 113.3, 111.1, 110.2, 103.5, 46.7, 40.9, 39.2, 34.5, 32.0, 30.3, 27.4, –8.5 ppm;

*satellites observable at peak at 46.7 beta to the tin and peak at –8.44 corresponds to the Sn atom with satellites also observable;

IR (film, cm^{-1}) 3298, 2969, 2928, 1674, 1619, 1441, 1316, 1054, 743;

HRMS (ESI^+) calc. for $C_{24}H_{29}N_3O_2{}^{120}Sn$ ($[M+Na]^+$): 534.1174; found: 534.1173.

Chapter 9: Chiral HPLC Data

9.1 Chiral HPLC Chapter 2

9.1.1 Chromatograms of Compound (±)-1.24

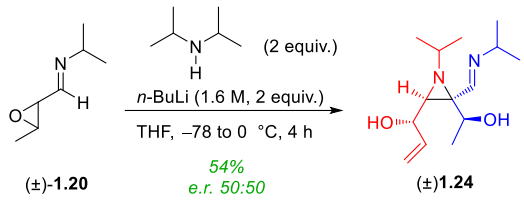

e.r. 50:50

Chiralpak ID, 100 hexane, 0.8 mL min^{-1}, λ 210 nm

t_{R1} = 8.18 min, t_{R2} = 9.08 min.

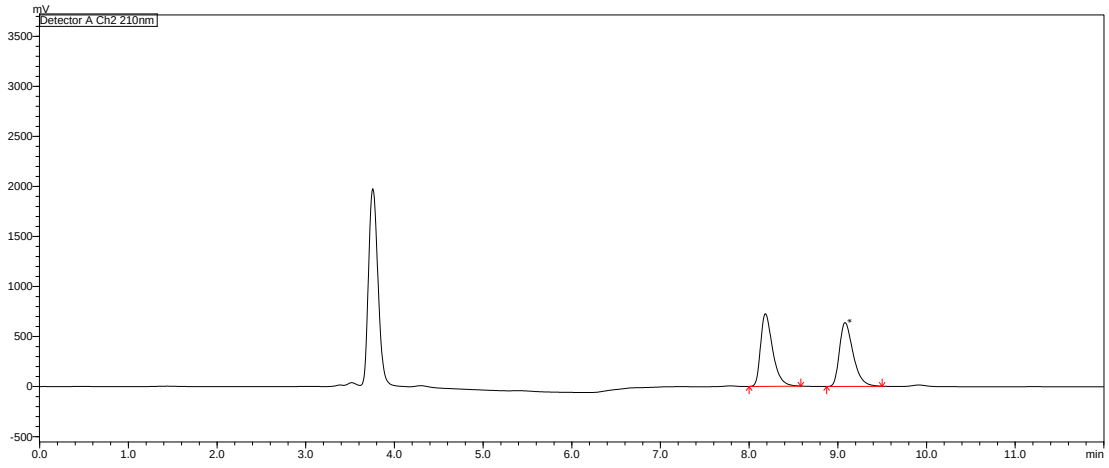

Peak #	Ret. Time	Area	Height	Conc.	Area %
1	8.184	6883960	726032	50.131	50.131
2	9.082	6847906	638392	49.869	49.869
Total		13731866	1364424	100.000	100.000

9.1.2 Chromatograms of Dimerisation Using Chiral Amine A

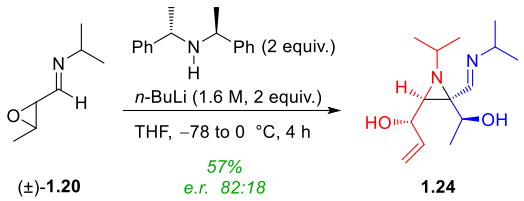

e.r. 82:18

Chiralpak ID, 100 hexane, 0.8 mL min^{-1}, λ 210 nm

t_{R1} = 9.21 min, t_{R2} = 10.10 min.

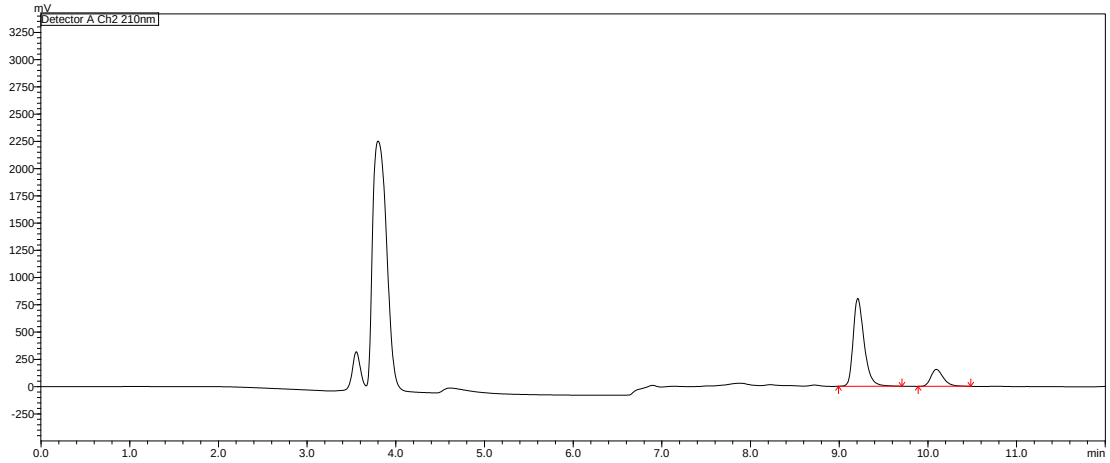

Peak #	Ret. Time	Area	Height	Conc.	Area %
1	9.210	6943327	807282	81.828	81.828
2	10.096	1541929	155899	18.172	18.172
Total		8485256	963181	100.000	100.000

9.1.3 Chromatograms of Dimerisation Using Chiral Amine B

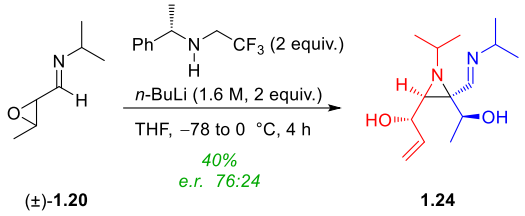

e.r. 76:24

Chiralpak ID, 100 hexane, 0.8 mL min^{-1}, λ 210 nm

t_{R1} = 9.54 min, t_{R2} = 10.41 min

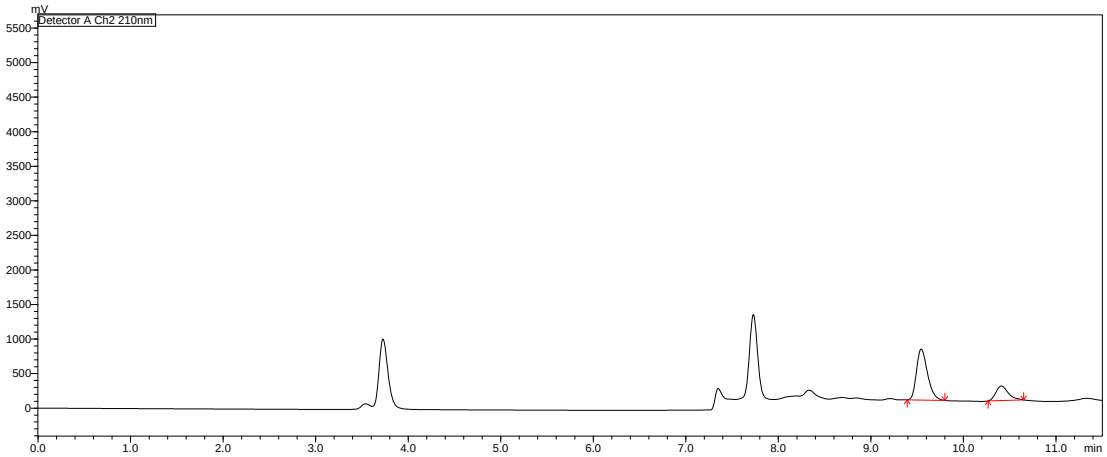

Peak #	Ret. Time	Area	Height	Conc.	Area %
1	9.544	6103268	739599	75.762	75.762
2	10.409	1952544	209722	24.238	24.238
Total		8055812	949321	100.000	100.000

9.1.4 Chromatograms of Dimerisation Using Chiral Amine E

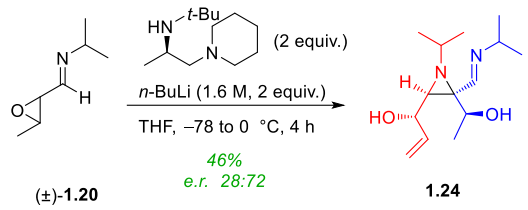

e.r. 28:72

Chiralpak ID, 100 hexane, 0.8 mL min^{-1}, λ 210 nm

t_{R1} = 8.49 min, t_{R2} = 9.34 min.

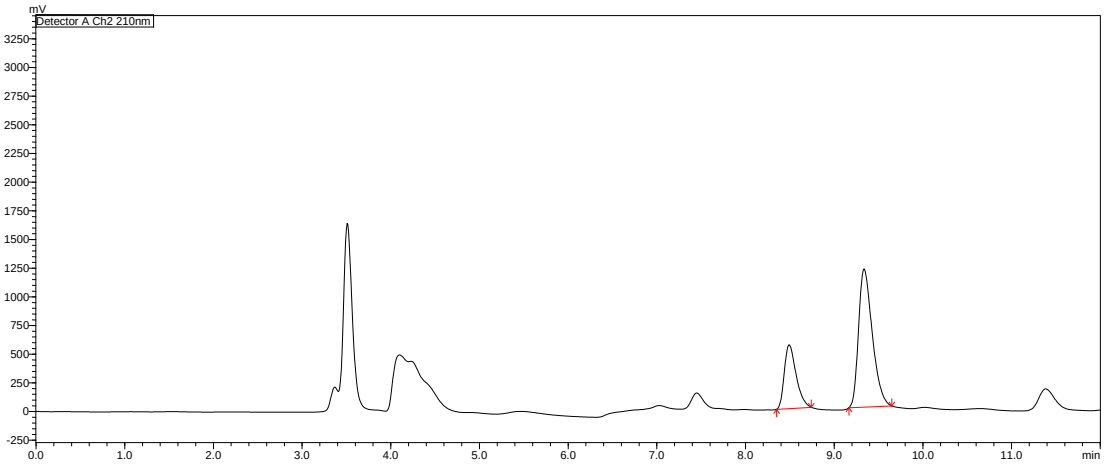

Peak #	Ret. Time	Area	Height	Conc.	Area %
1	8.493	5153323	556021	28.409	28.409
2	9.338	12986377	1203557	71.591	71.591
Total		18139700	1759578	100.000	100.000

9.1.5 Chromatograms of Dimerisation Using Chiral Amine A

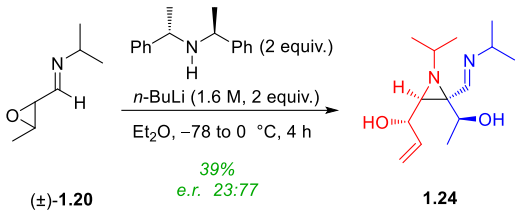

e.r. 23:73

Chiralpak ID, 100 hexane, 0.8 mL min^{-1}, λ 210 nm

t_{R1} = 9.66 min, t_{R2} = 10.47 min.

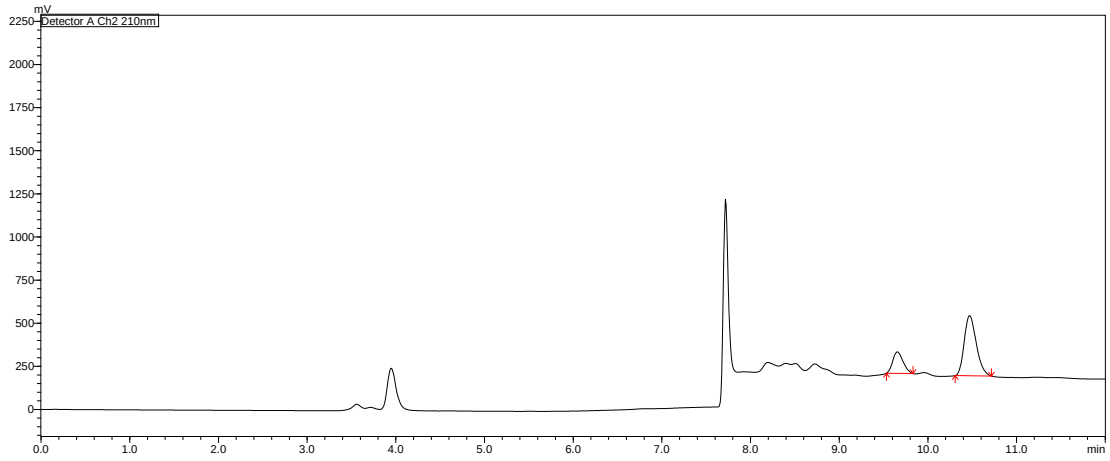

Peak #	Ret. Time	Area	Height	Conc.	Area %
1	9.656	1004700	4307783	23.323	23.323
2	10.471	3303082	348054	76.677	76.677
Total		4307783	472338	100.000	100.000

9.1.6 Chromatograms of Dimerisation Using Chiral Amine A

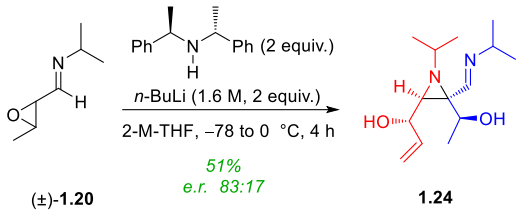

e.r. 83:17

Chiralpak ID, 100 hexane, 0.8 mL min^{-1}, λ 210 nm

t_{R1} = 9.24 min, t_{R2} = 10.13 min.

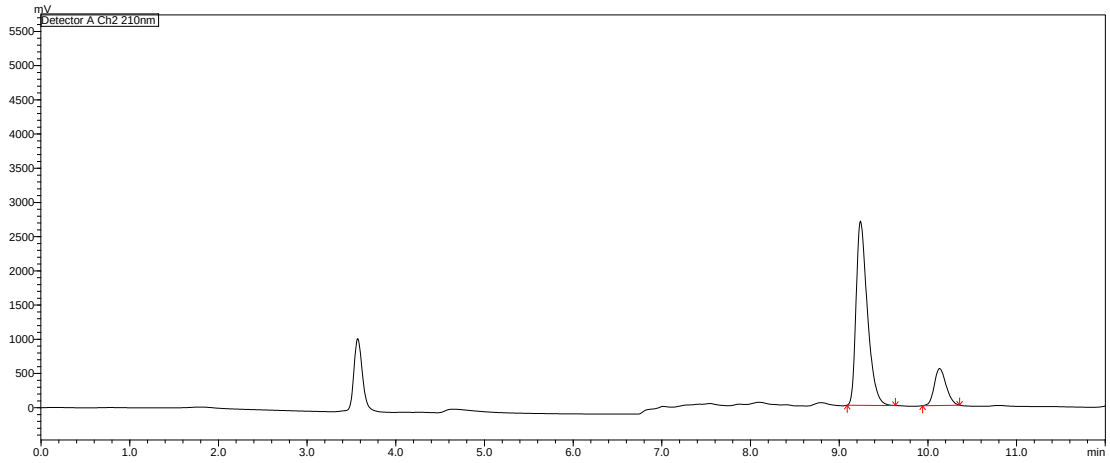

Peak #	Ret. Time	Area	Height	Conc.	Area %
1	9.241	23788766	2691757	83.060	83.060
2	10.133	4851552	532601	16.940	16.940
Total		28640318	3224358	100.000	100.000

9.1.7 Chromatograms of Dimerisation Using Chiral Amine A

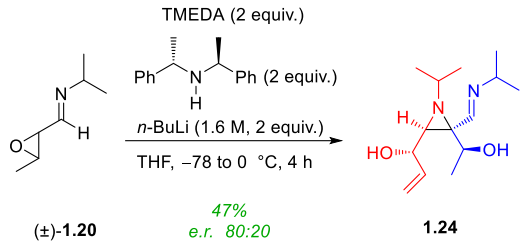

e.r. 80:20

Chiralpak ID, 100 hexane, 0.8 mL min^{-1}, λ 210 nm

t_{R1} = 9.57 min, t_{R2} = 10.44 min.

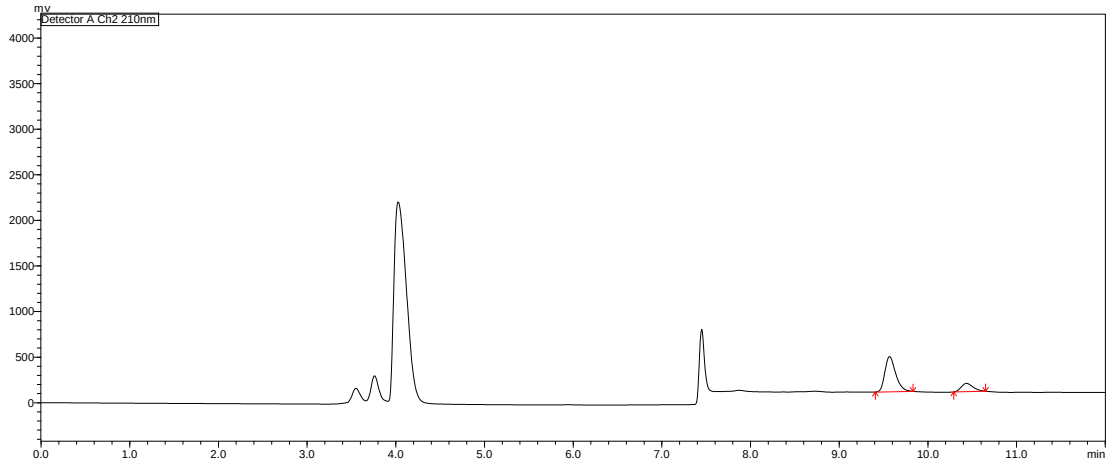

Peak #	Ret. Time	Area	Height	Conc.	Area %
1	9.568	3269672	386133	79.544	79.544
2	10.437	840854	90075	20.456	20.456
Total		4110526	476208	100.000	100.000

9.1.8 Chromatograms of Dimerisation Using Chiral Amine A

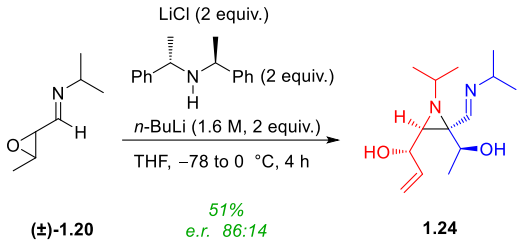

e.r. 86:14

Chiralpak ID, 100 hexane, 0.8 mL min^{-1}, λ 210 nm

t_{R1} = 9.48 min, t_{R2} = 10.36 min.

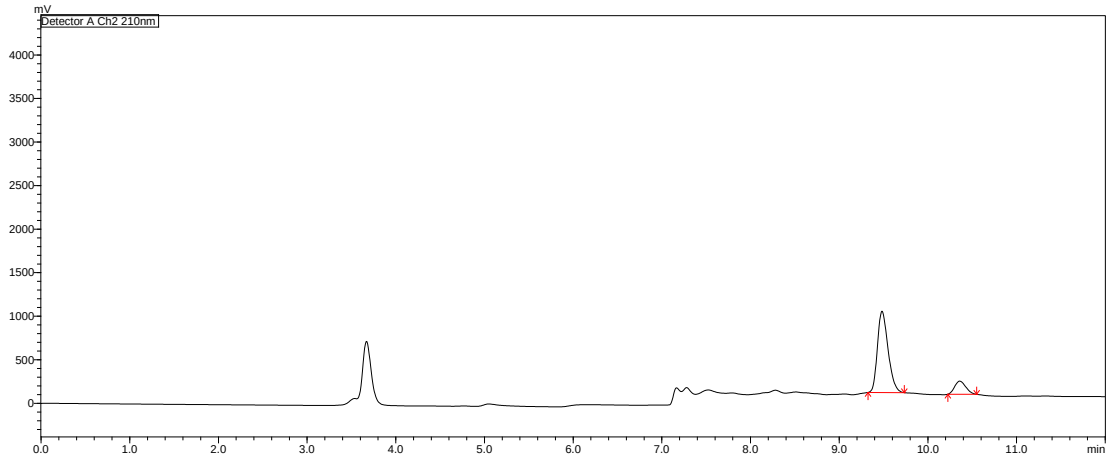

Peak #	Ret. Time	Area	Height	Conc.	Area %
1	9.483	7805790	934049	85.539	85.539
2	10.360	1319661	150945	14.461	14.461
Total		9125452	1084993	100.000	100.000

9.1.9 Chromatograms of Dimerisation Using Chiral Amine A

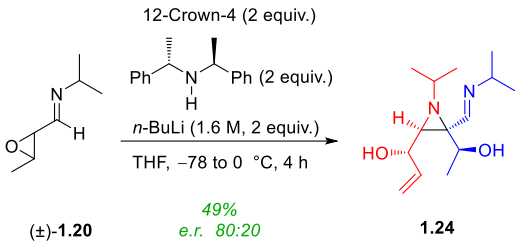

e.r. 80:20

Chiralpak ID, 100 hexane, 0.8 mL min^{-1}, λ 210 nm

t_{R1} = 9.49 min, t_{R2} = 10.39 min.

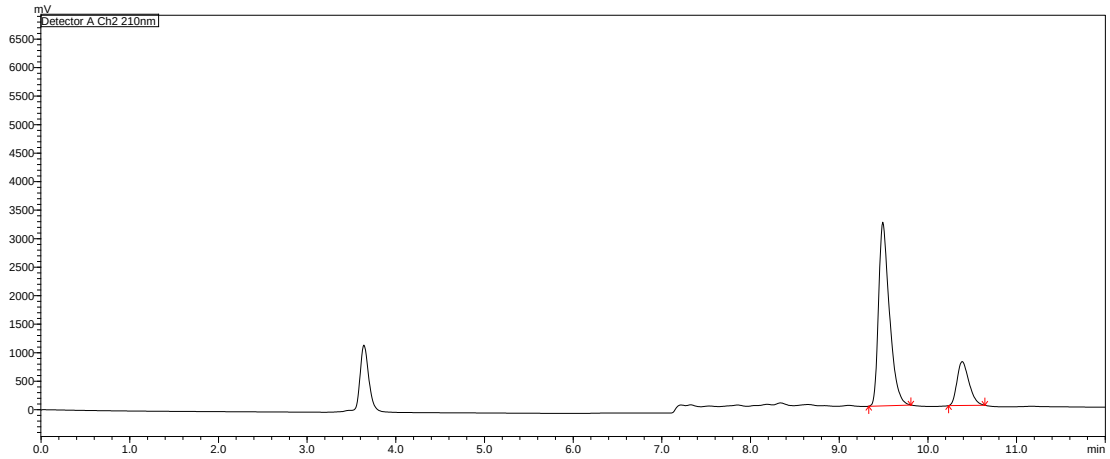

Peak #	Ret. Time	Area	Height	Conc.	Area %
1	9.492	26973537	3208853	80.160	80.160
2	10.387	6675943	747773	19.840	19.840
Total		33649480	3956626	100.000	100.000

9.1.10 Chromatograms of Dimerisation Using Chiral Amine A

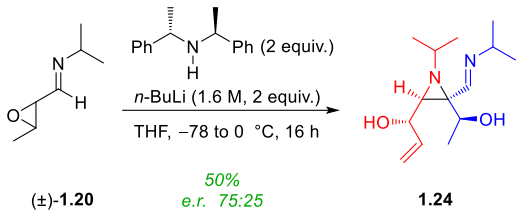

(±)-**1.20** — *50%* *e.r. 75:25* — **1.24**

e.r. 75:25

Chiralpak ID, 100 hexane, 0.8 mL min^{-1}, λ 210 nm

t_{R1} = 9.48 min, t_{R2} = 10.35 min.

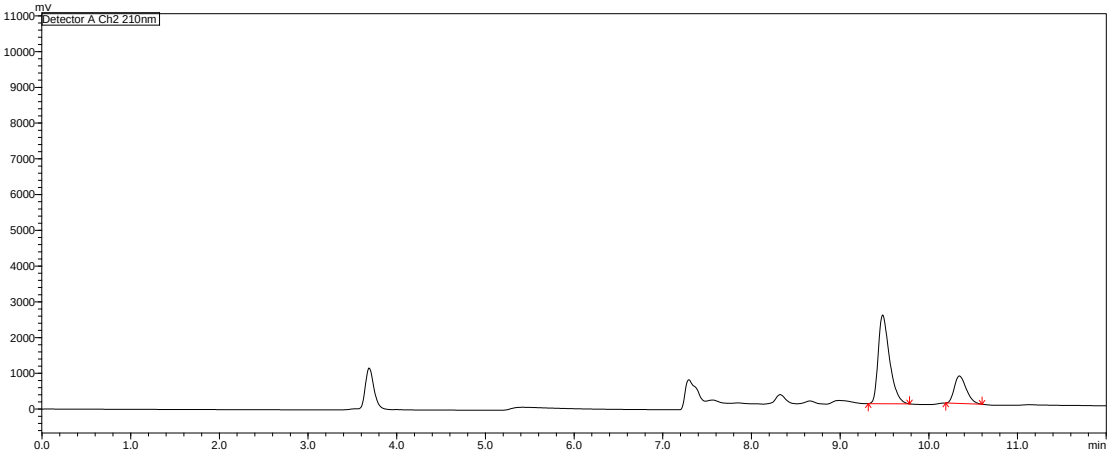

Peak #	Ret. Time	Area	Height	Conc.	Area %
1	9.480	22060560	2480690	75.414	75.414
2	10.345	7191911	769043	24.586	24.586
Total		29252470	3249733	100.000	100.000

9.1.11 Chromatograms of Dimerisation Using Chiral Amine A

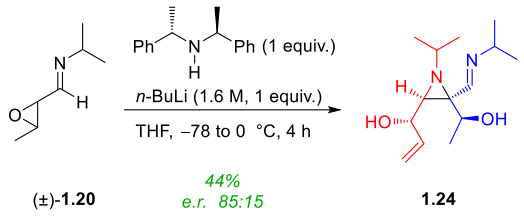

(±)-**1.20** *44%* *e.r. 85:15* **1.24**

e.r. 85:15

Chiralpak ID, 100 hexane, 0.8 mL min^{-1}, λ 210 nm

t_{R1} = 9.32 min, t_{R2} = 10.19 min.

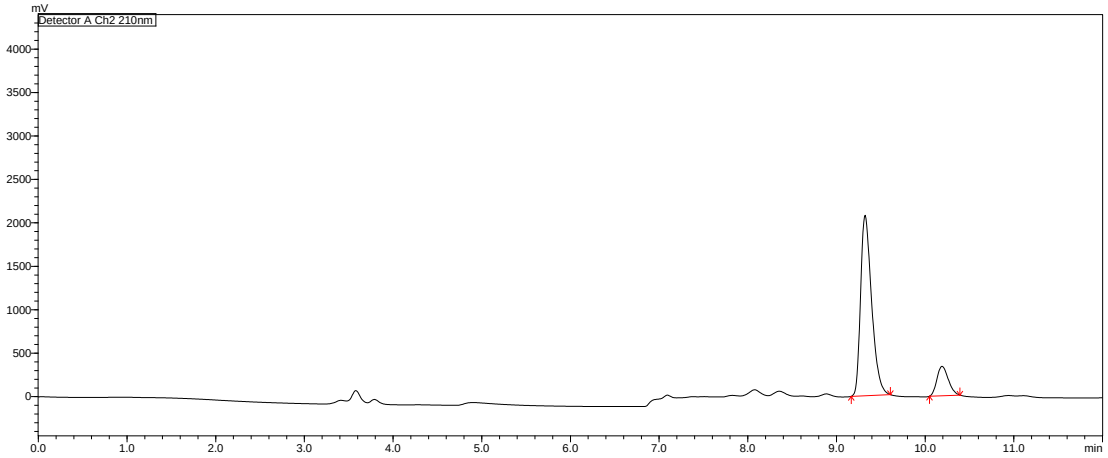

Peak #	Ret. Time	Area	Height	Conc.	Area %
1	9.323	17974557	2076631	85.642	85.642
2	10.191	3013487	339597	14.358	14.358
Total		20988043	2416228	100.000	100.000

9.1.12 Chromatograms of Dimerisation Using Chiral Amine A

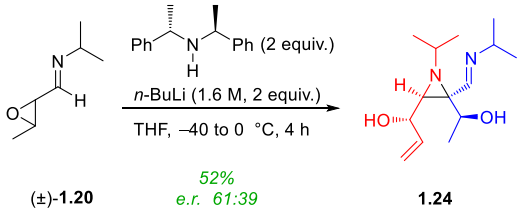

(±)-**1.20** *52%* *e.r. 61:39* **1.24**

e.r. 61:39

Chiralpak ID, 100 hexane, 0.8 mL min^{-1}, λ 210 nm

t_{R1} = 8.94 min, t_{R2} = 9.80 min.

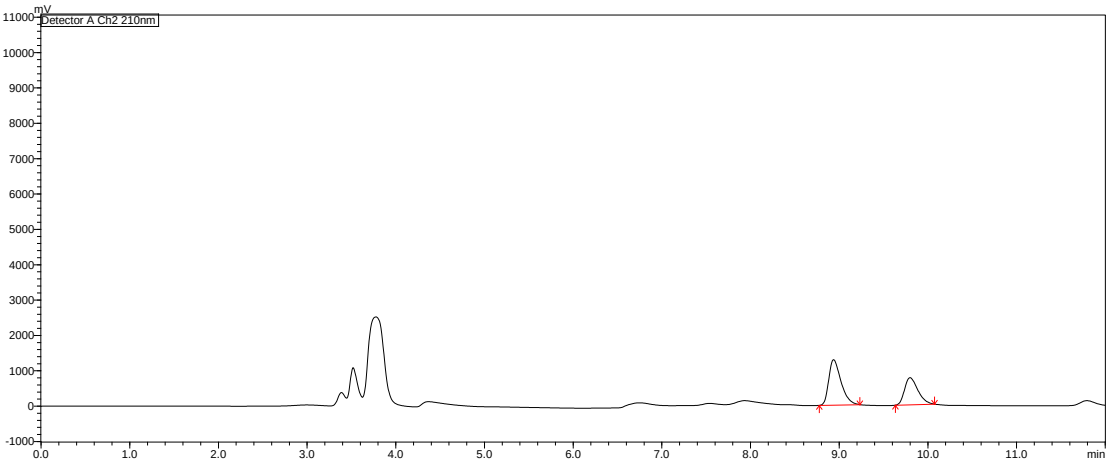

Peak #	Ret. Time	Area	Height	Conc.	Area %
1	8.937	12312365	1283461	60.557	60.557
2	9.800	8019575	767003	39.443	39.443
Total		20331940	2050464	100.000	100.000

9.1.13 Chromatograms of Dimerisation Using Chiral Amine A

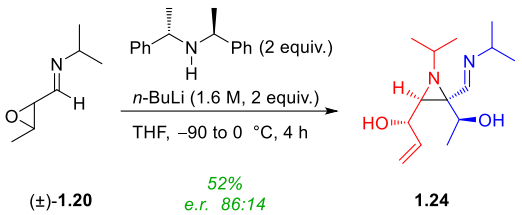

e.r. 86:14

Chiralpak ID, 100 hexane, 0.8 mL min^{-1}, λ 210 nm

t_{R1} = 9.40 min, t_{R2} = 10.31 min.

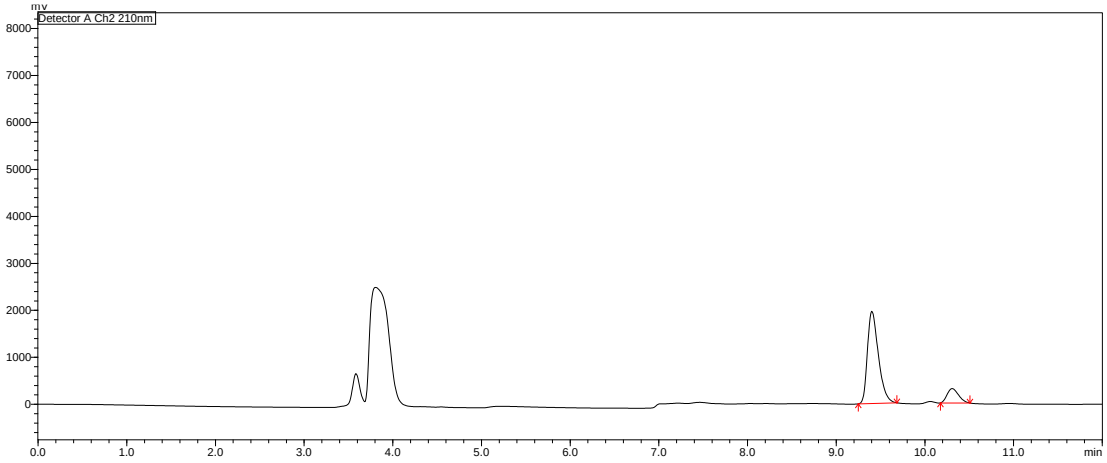

Peak #	Ret. Time	Area	Height	Conc.	Area %
1	9.402	16889822	1962576	86.041	86.041
2	10.308	2740069	306088	13.959	13.959
Total		19629891	2268663	100.000	100.000

9.1.14 Chromatograms of Dimerisation Using Chiral Amine A

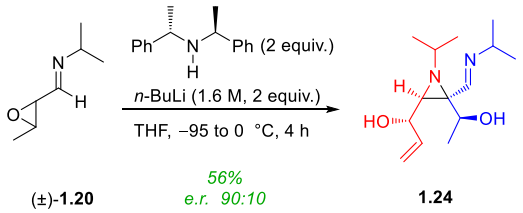

(±)-**1.20** — *56%* *e.r. 90:10* — **1.24**

e.r. 90:10

Chiralpak ID, 100 hexane, 0.8 mL min^{-1}, λ 210 nm

t_{R1} = 9.13 min, t_{R2} = 10.04 min

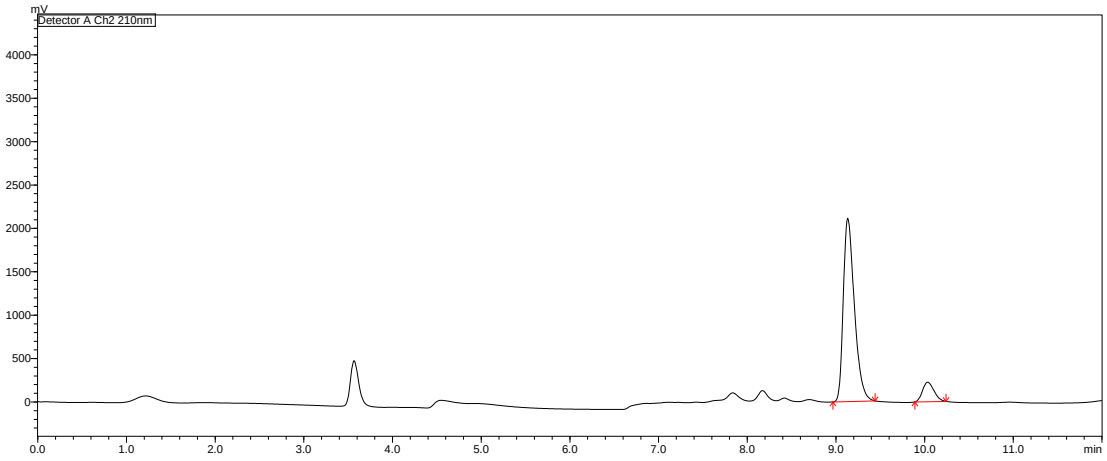

Peak #	Ret. Time	Area	Height	Conc.	Area %
1	9.134	18347236	2113152	90.061	90.061
2	10.035	2024787	225584	9.939	9.939
Total		20372023	2338735	100.000	100.000

9.1.15 Chromatograms of Dimerisation Using Chiral Amine A

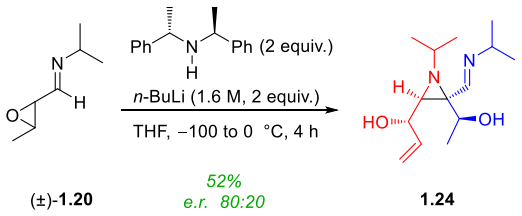

e.r. 80:20

Chiralpak ID, 100 hexane, 0.8 mL min^{-1}, λ 210 nm

t_{R1} = 7.79 min, t_{R2} = 8.71 min.

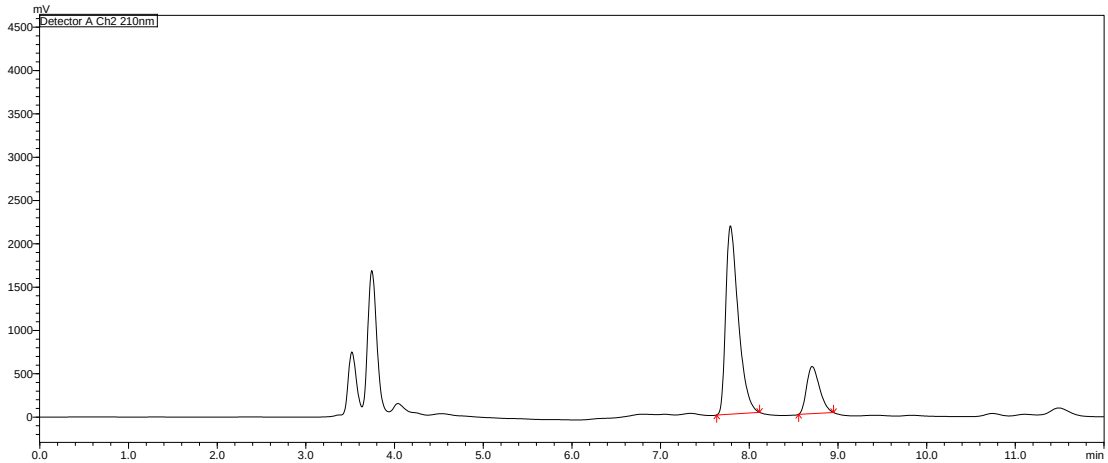

Peak #	Ret. Time	Area	Height	Conc.	Area %
1	7.788	21420484	2171085	79.557	79.557
2	8.709	5504162	2715422	20.443	20.443
Total		26924646	2715422	100.000	100.000

9.1.16 Chromatograms of Dimerisation Using Chiral Amine A

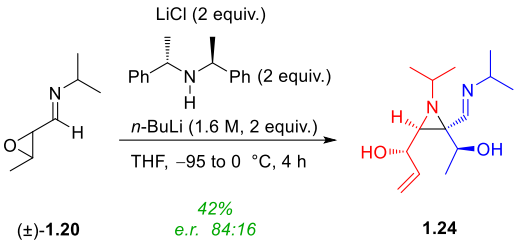

e.r. 84:16

Chiralpak ID, 100 hexane, 0.8 mL min^{-1}, λ 210 nm

t_{R1} = 9.51 min, t_{R2} = 10.38 min.

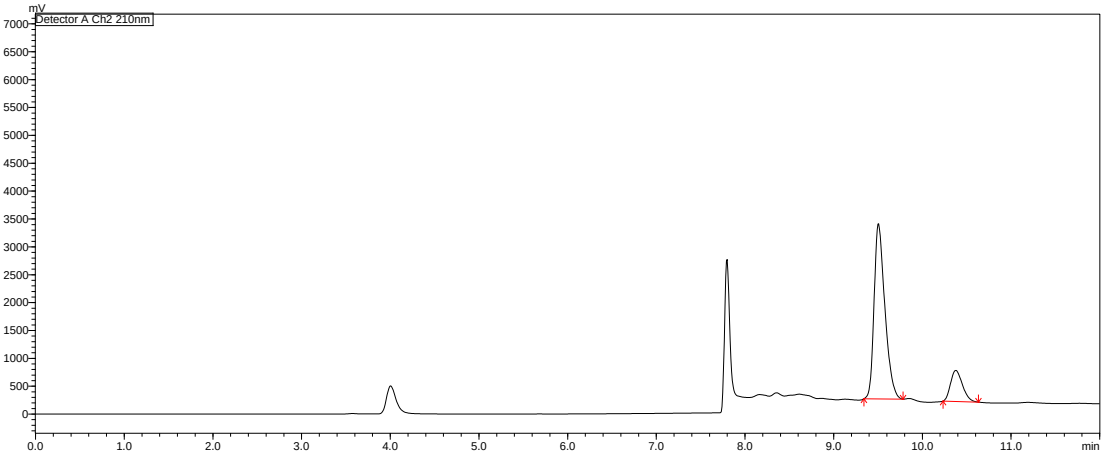

Peak #	Ret. Time	Area	Height	Conc.	Area %
1	9.505	26609729	3143213	83.665	83.665
2	10.377	5195264	557188	16.335	16.335
Total		31804993	3700401	100.000	100.000

9.1.17 Chromatograms of Compound 2.20

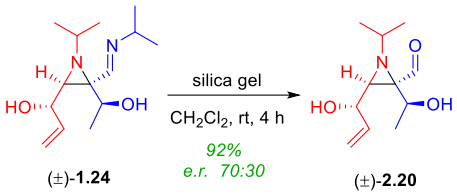

e.r. 30:70

Chiralpak ID, 100 hexane, 0.8 mL min^{-1}, λ 210 nm

t_{R1} = 10.12 min, t_{R2} = 10.76 min.

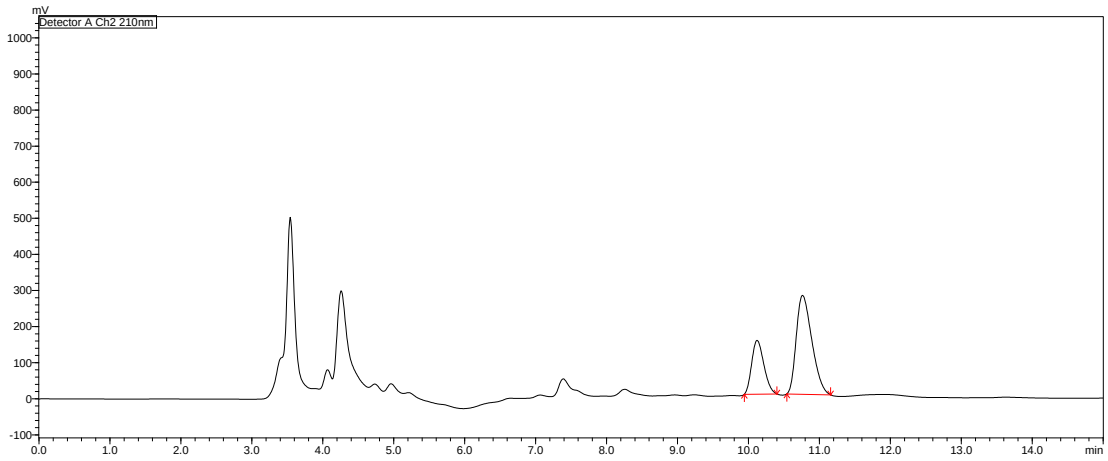

Peak #	Ret. Time	Area	Height	Conc.	Area %
1	10.122	1775199	148899	29.763	29.763
2	10.762	4189163	273896	70.237	70.237
Total		5964362	422795	100.000	100.000

9.2 Chiral HPLC Chromatograms Chapter 4

9.2.1 Chromatograms of Compound (±)-1.31 and (±)-3.46

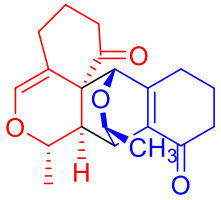

(±)-major
1.31

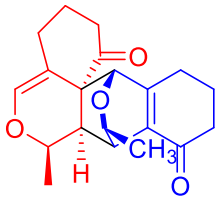

tentatively proposed
structure of
minor (±)-3.46

Chiralpak OD-H, 87:13 hexane/IPA, 0.5 mL min^{-1}, injection volume 2 µL, run time 30 min, λ = 265 nm, t_1 = 15.59 min (minor), t_2 = 18.30 min (minor), t_3 = 21.02 min (hetero), t_4 = 23.27 min (hetero).

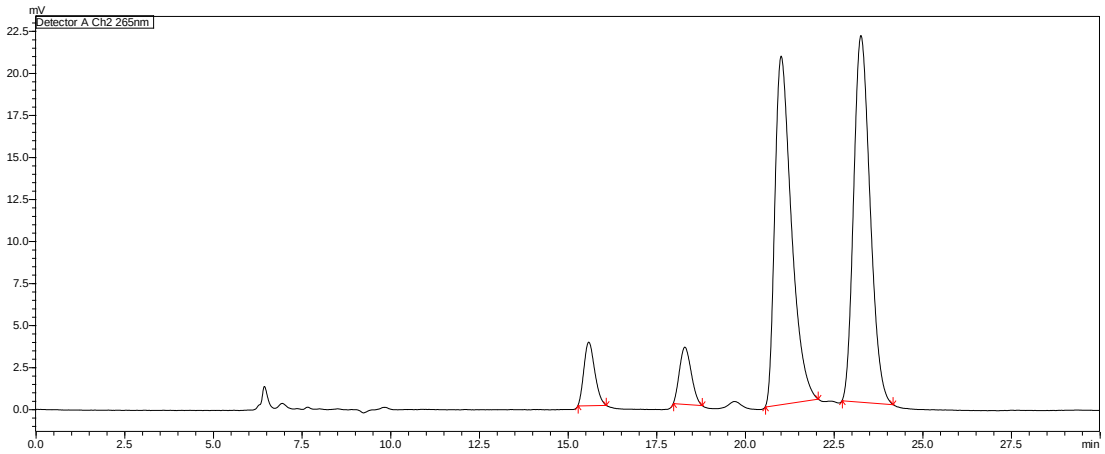

Peak #	Ret. Time	Area	Height	Conc.	Area %
1 (minor)	15.590	86861	3880	5.617	5.617
2 (minor)	18.299	87716	3583	5.672	5.672
3 (major)	21.015	679232	20719	43.922	43.922
4 (major)	23.265	692643	21729	44.789	44.789
Total		1546452	49911	100.000	100.00

9.3 Chiral HPLC Chromatograms Chapter 5

9.3.1 Chromatograms of (+)/(–)-Brevianamide Y (4.4)

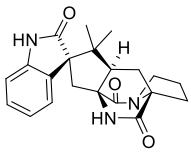

(+)-brevianamide Y (**4.4**)

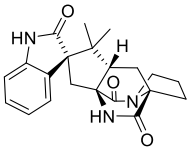

(–)-brevianamide Y (**4.4**)

e.r 40:60

Chiralpak IC, 42:58 EtOH/hexane, 1.0 mL min^{-1}, λ 254 nm

t_{R1} = 11.26 min, t_{R2} = 14.52 min.

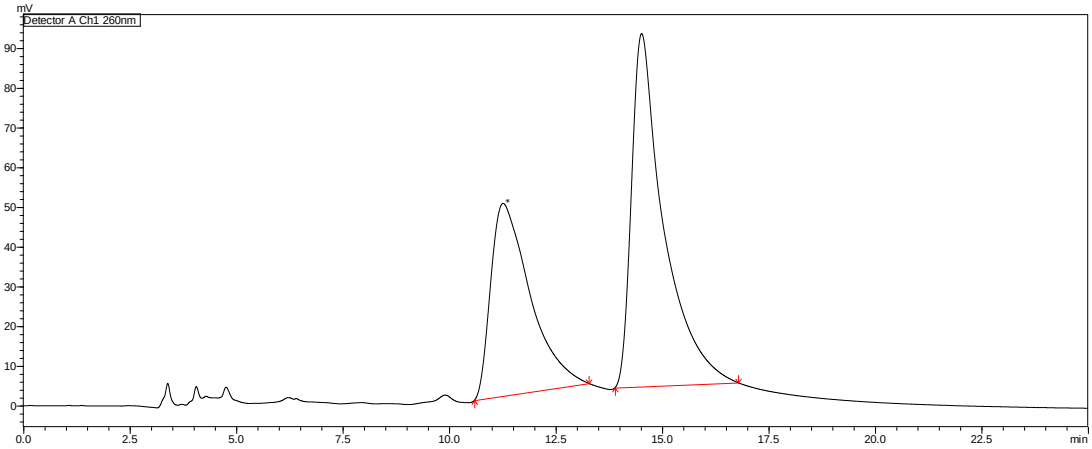

Peak #	Ret. Time	Area	Height	Conc.	Area %
1	11.264	3110505	48513	39.948	39.948
2	14.516	4675856	88917	60.052	60.052
Total		7786361	137430	100.000	100.000

9.3.2 Chromatograms of (+)-Brevianamide Y (4.4)

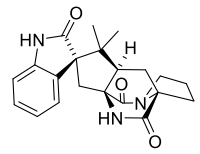

(+)-brevianamide Y (**4.4**)

e.r. 95:5

Chiralpak IC, 42:58 EtOH/hexane, 1.0 mL min^{-1}, λ 254 nm

t_{Rmajor} = 11.06 min, t_{Rminor} = 14.66 min.

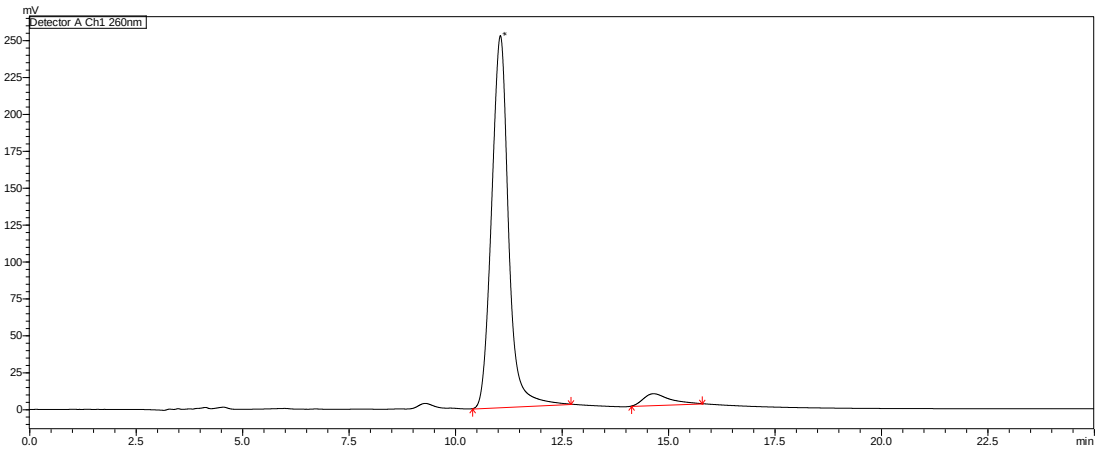

Peak #	Ret. Time	Area	Height	Conc.	Area %
1	11.059	6961488	251749	95.367	95.367
2	14.657	338197	7868	4.633	4.633
Total		7299684	259617	100.000	100.000

9.3.3 Chromatograms of (+)-Brevianamide Y (4.4)

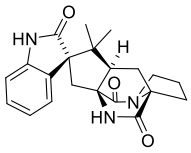

(+)-brevianamide Y (**4.4**)

e.r. 98:2* liquor after recrystalisation

Chiralpak IC, 42:58 EtOH/hexane, 1.0 mL min^{-1}, λ 254 nm

t_{Rmajor} = 12.66 min, t_{Rminor} = 15.78 min.

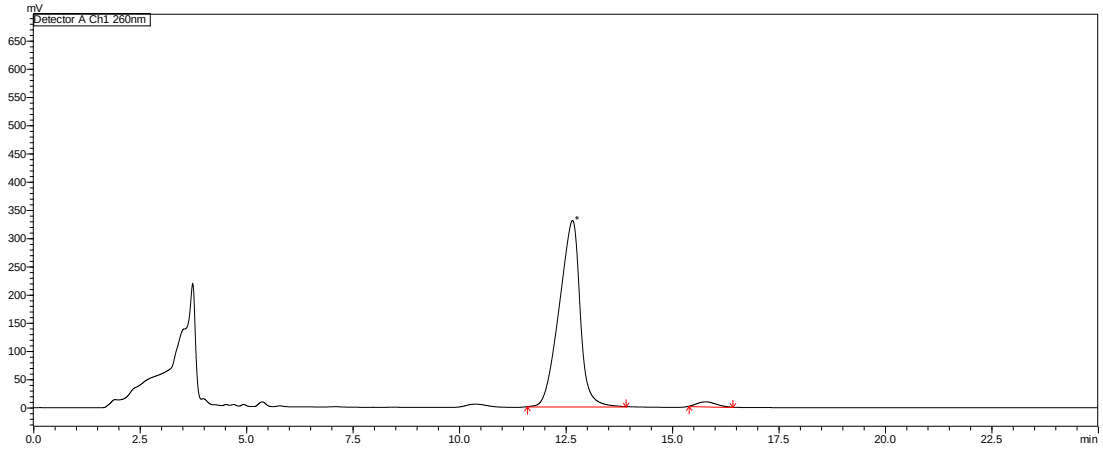

Peak #	Ret. Time	Area	Height	Conc.	Area %
1	12.658	11230063	329769	97.732	97.732
2	15.781	260570	8559	2.268	2.268
Total		11490633	338327	100.000	100.000

9.3.4 Chromatograms of Brevianamide Y (4.4)

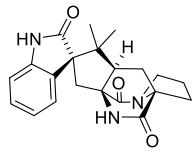

(+)-brevianamide Y (**4.4**)

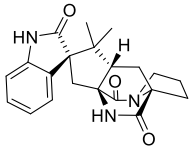

(–)-brevianamide Y (**4.4**)

e.r. 50:50* prism crystals used for X-ray crystallography

Chiralpak IC, 50:50 EtOH/hexane, 1.0 mL min^{-1}, λ 254 nm

t_{R2} = 12.37 min, t_{R2} = 15.78 min.

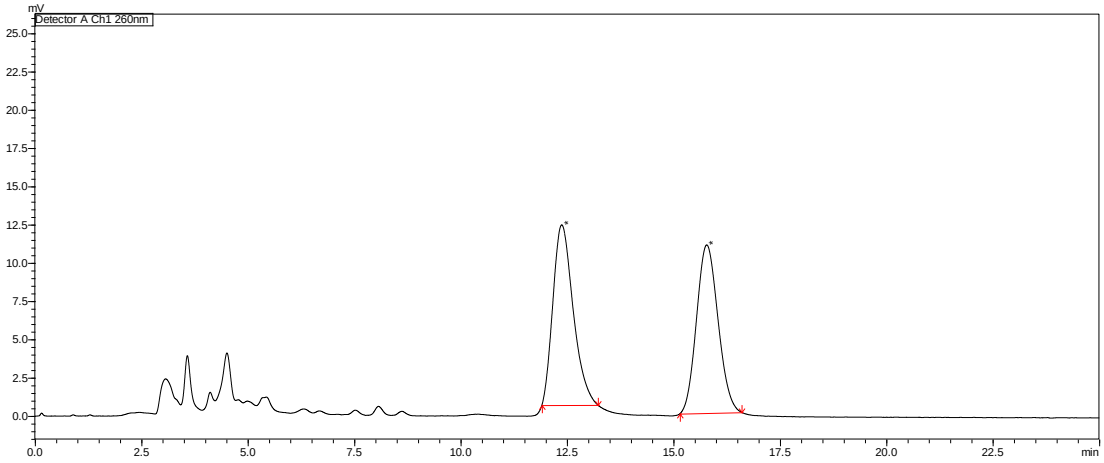

Peak #	Ret. Time	Area	Height	Conc.	Area %
1	12.372	390639	11786	50.286	50.286
2	15.778	386190	10996	49.714	49.714
Total		776829	22782	100.000	100.000

9.3.5 Chromatograms of (–)-Brevianamide Y (4.4)

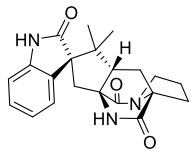

(–)-brevianamide Y (**4.4**)

e.r. 98:2

Chiralpak IC, 42:58 EtOH/hexane, 1.0 mL min^{-1}, λ 254 nm

t_{Rminor} = 11.59 min, t_{Rmajor} = 14.42 min.

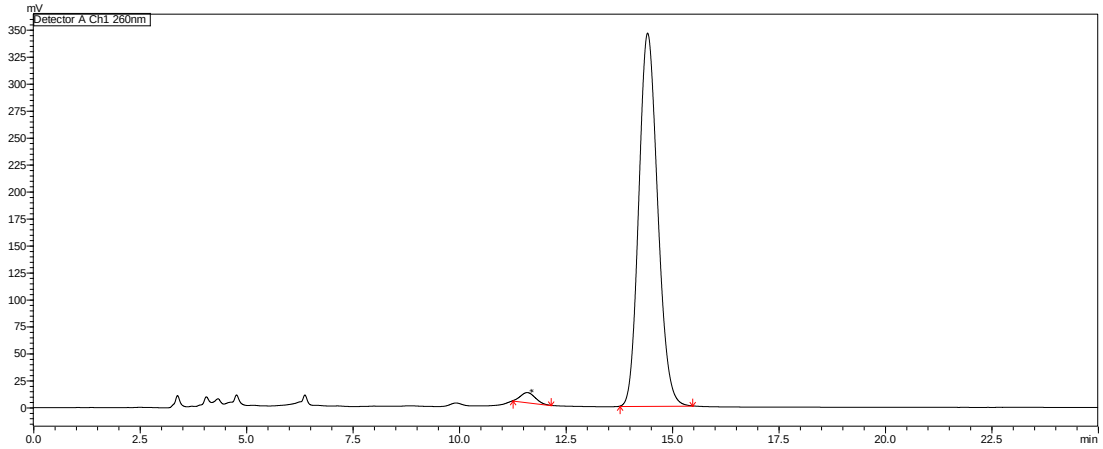

Peak #	Ret. Time	Area	Height	Conc.	Area %
1	11.594	217087	9163	1.997	1.997
2	14.422	10654930	345601	98.003	98.003
Total		10872017	354764	100.000	100.000

9.3.6 Chromatograms of (+)/(–)-Brevianamide Z (5.3)

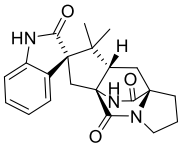

(+)-brevianamide Z (**5.3**)

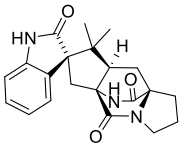

(–)-brevianamide Z (**5.3**)

e.r. 60:40

Chiralpak IC, 25:75 EtOH/hexane, 1.0 mL min^{-1}, λ 254 nm

t_{R1} = 20.13 min, t_{R2} = 22.87 min.

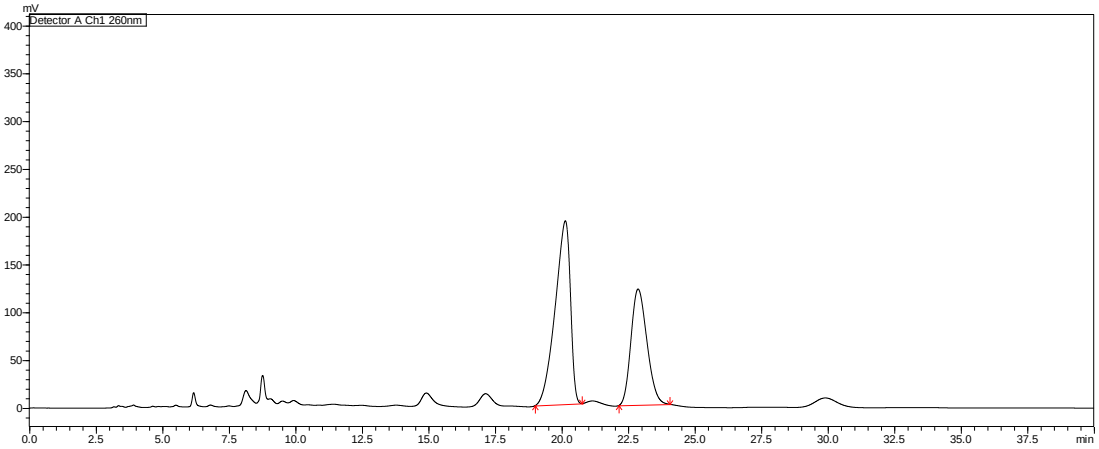

Peak #	Ret. Time	Area	Height	Conc.	Area %
1	20.134	7655394	192056	60.169	60.169
2	22.868	5067767	121468	39.831	39.831
Total		12723161	313524	100.000	100.000

9.3.7 Chromatograms of (+)-Brevianamide Z (5.3)

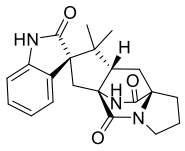

(+)-brevianamide Z (**5.3**)

e.r. 85:15

Chiralpak IC, 25:75 EtOH/hexane, 1.0 mL min^{-1}, λ 254 nm

t_{Rminor} = 19.73 min, t_{Rmajor} = 22.94 min.

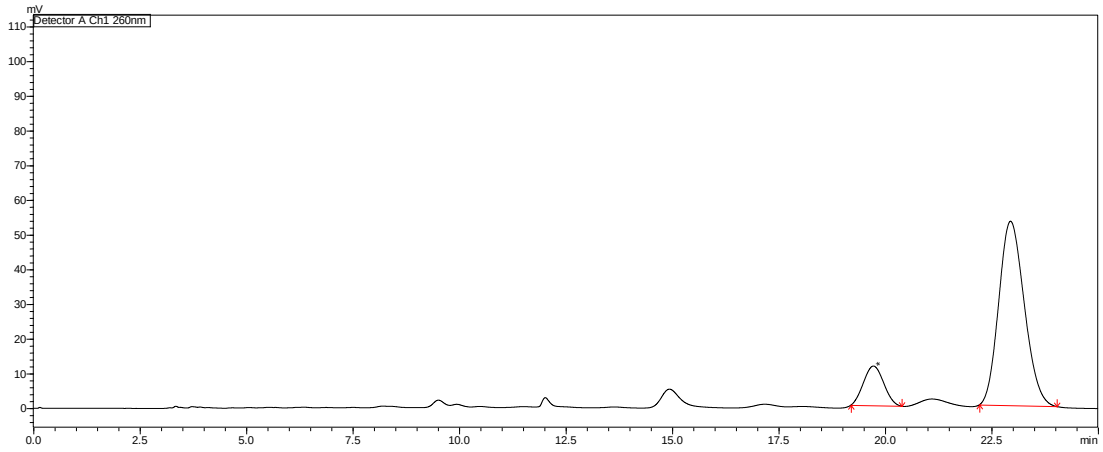

Peak #	Ret. Time	Area	Height	Conc.	Area %
1	19.726	376405	11409	14.516	14.516
2	22.944	2216619	53113	85.484	85.484
Total		2593024	64522	100.000	100.000

9.3.8 Chromatograms of (–)-Brevianamide Z (5.3)

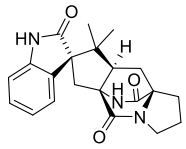

(–)-brevianamide Z (**5.3**)

e.r. 92:8

Chiralpak IC, 25:75 EtOH/hexane, 1.0 mL min^{-1}, λ 254 nm

t_{Rmajor} = 20.01 min, t_{Rminor} = 22.98 min.

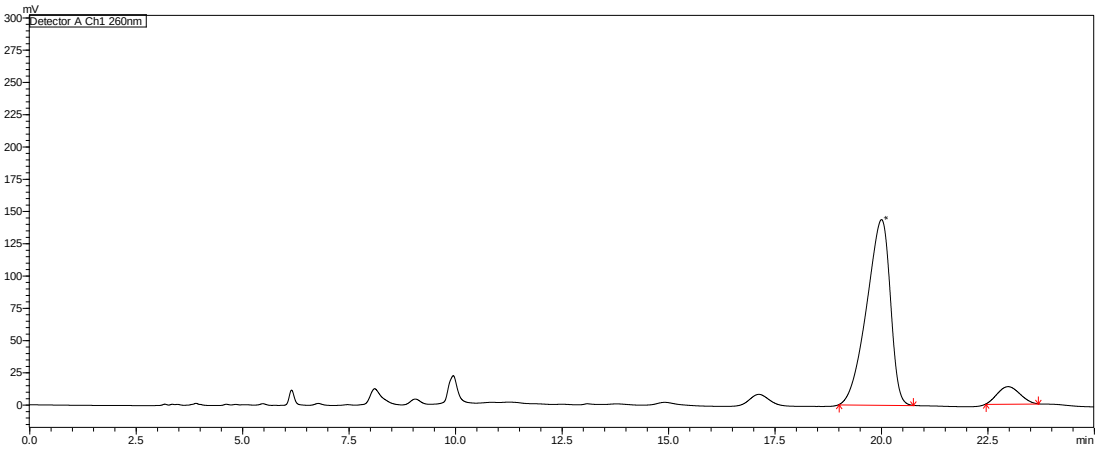

Peak #	Ret. Time	Area	Height	Conc.	Area %
1	20.009	5538964	143716	91.868	91.868
2	22.981	490327	13398	8.132	8.132
Total		6029291	157114	100.000	100.000

10.1 NMR Spectra Chapter 2

10.1.1 ^{1}H NMR Spectrum of Compound (±)-2.1 (600 MHz, $CDCl_3$)

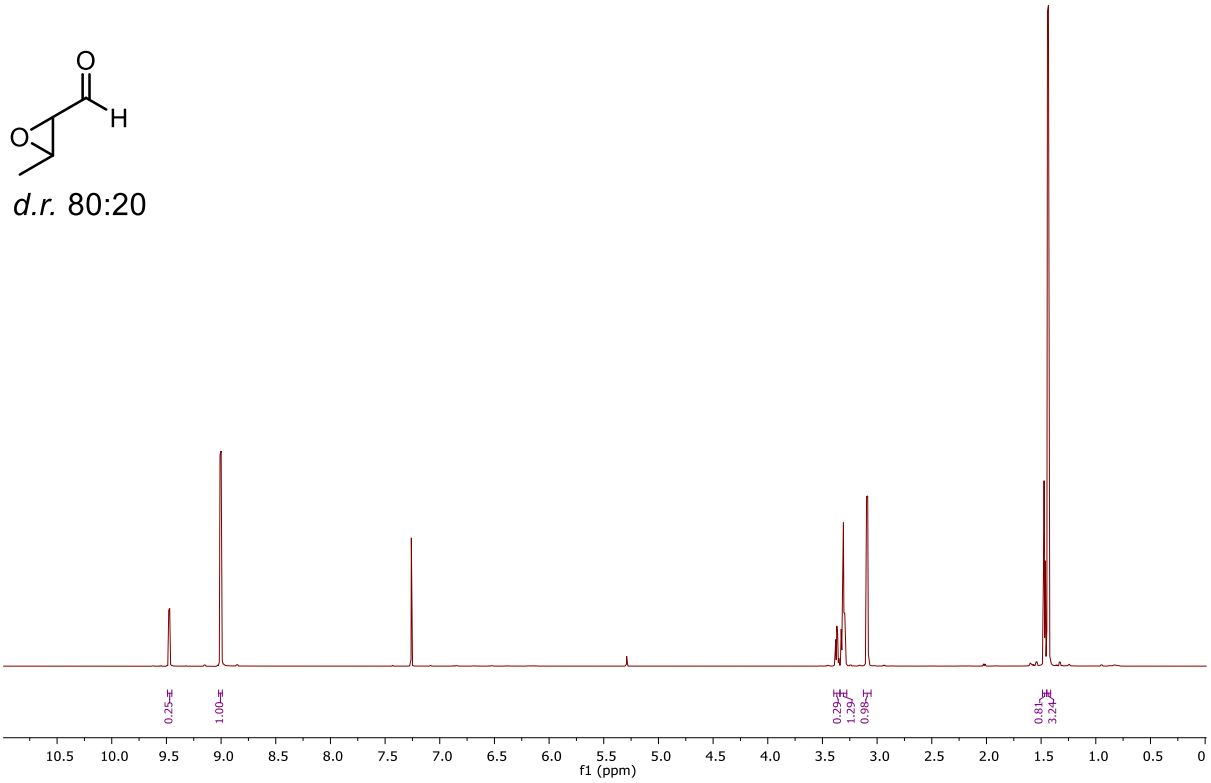

10.1.2 ^{13}C NMR Spectrum of Compound (±)-2.1 (150 MHz, $CDCl_3$)

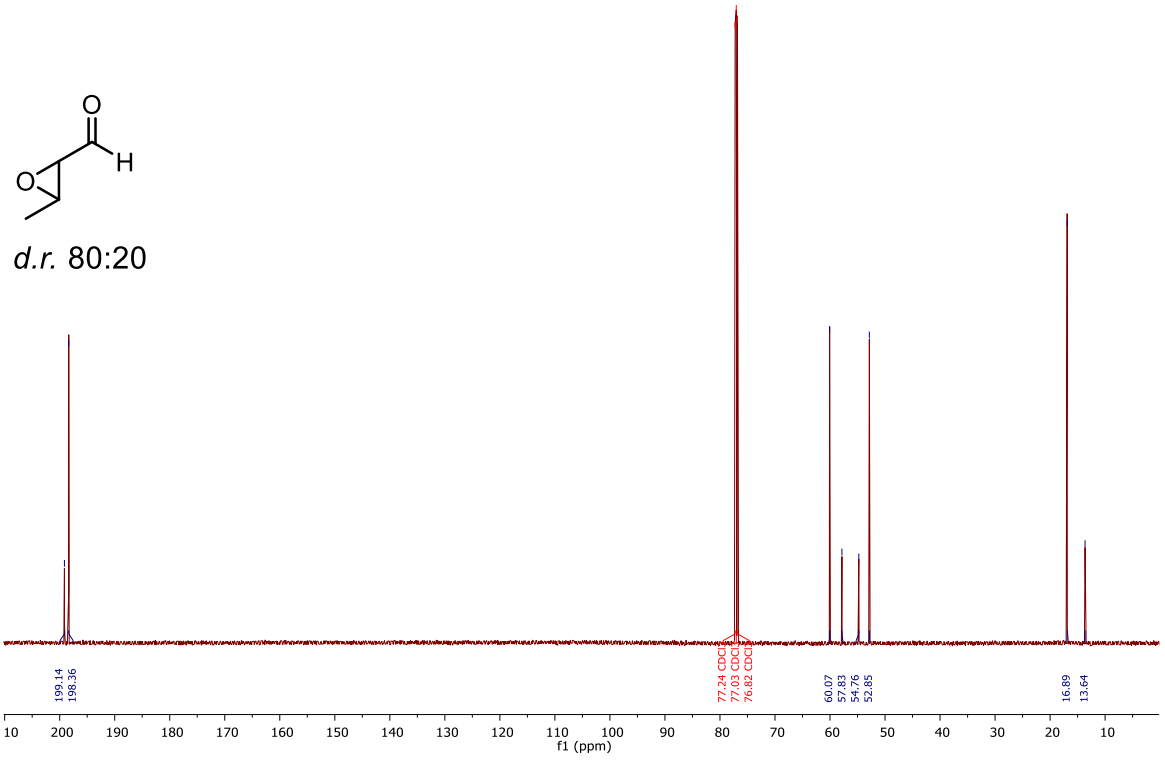

10.1.3 ^{1}H NMR Spectrum of Compound (±)-2.9 (500 MHz, $CDCl_3$)

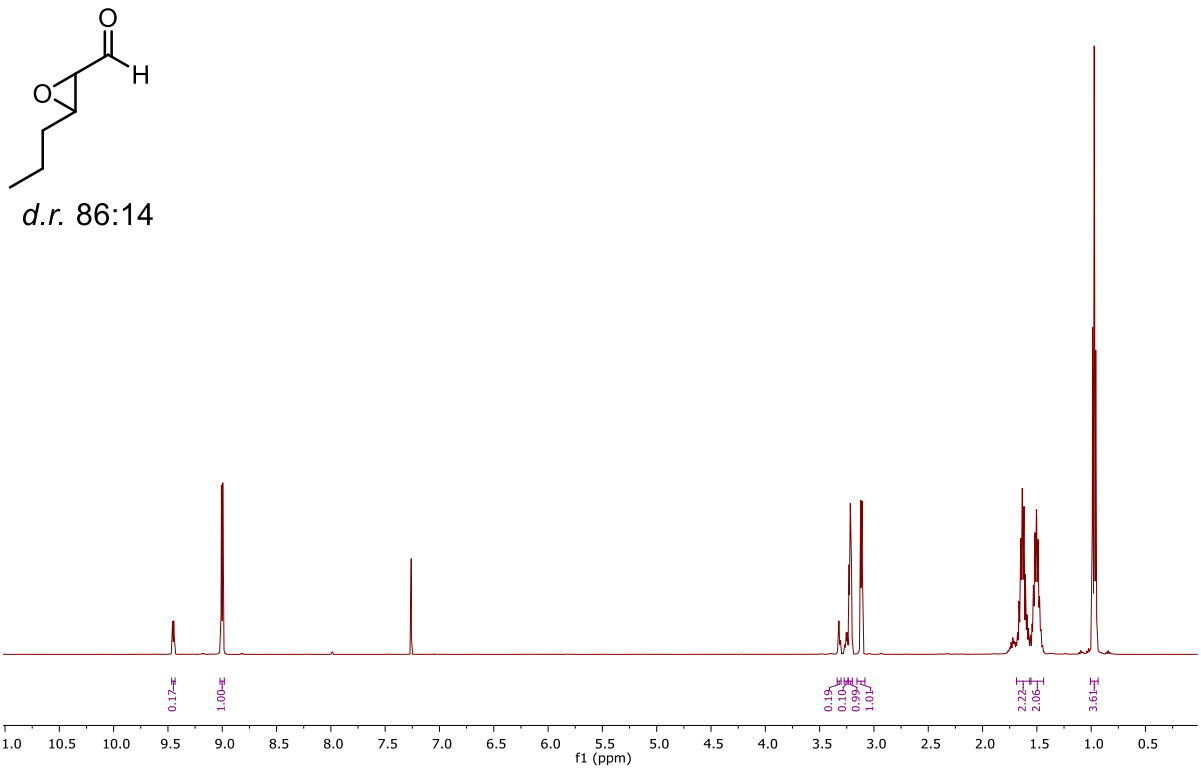

10.1.4 ^{13}C NMR Spectrum of Compound (±)-2.9 (125 MHz, $CDCl_3$)

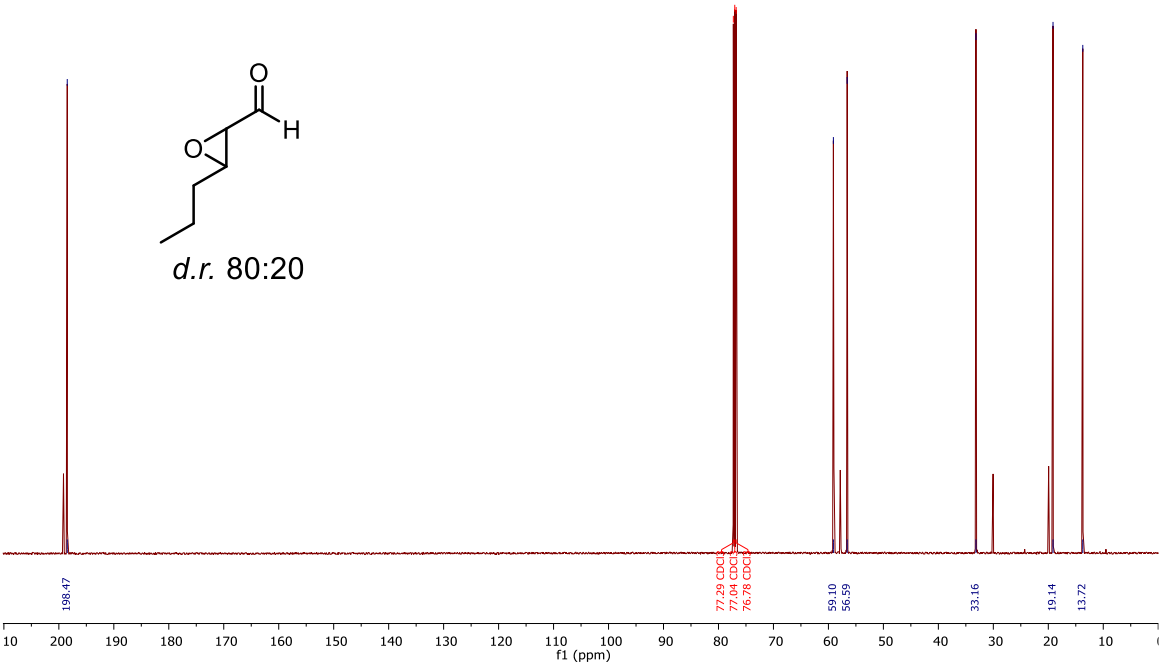

10.1.5 ^{1}H NMR Spectrum of Compound (±)-2.13 (600 MHz, $CDCl_3$)

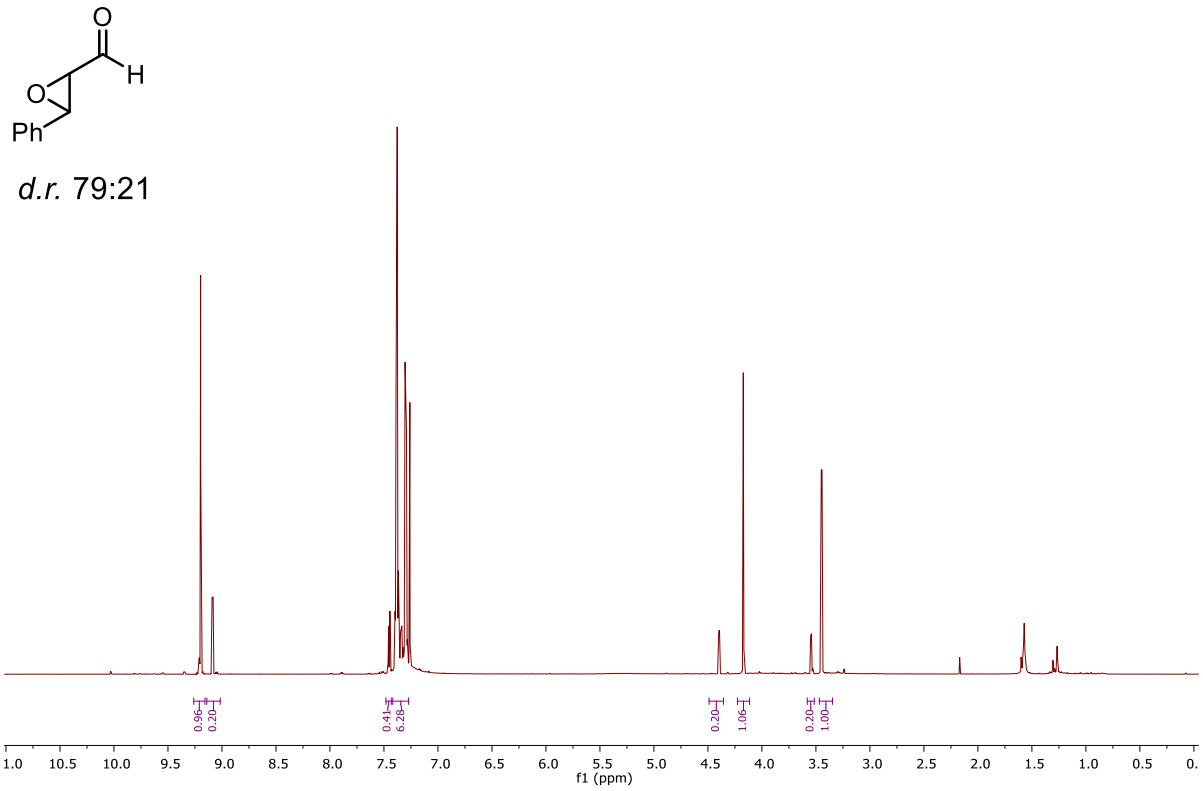

10.1.6 ^{1}H NMR Spectrum of Compound (±)-1.20 (500 MHz, $CDCl_3$)

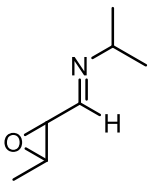

d.r. 78:22

10.1.7 ^{13}C NMR Spectrum of Compound (±)-1.20 (125 MHz, $CDCl_3$)

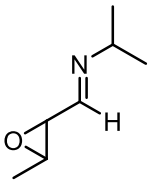

d.r. 78:22

10.1.8 ^{1}H NMR Spectrum of Compound (±)-2.10 (500 MHz, $CDCl_3$)

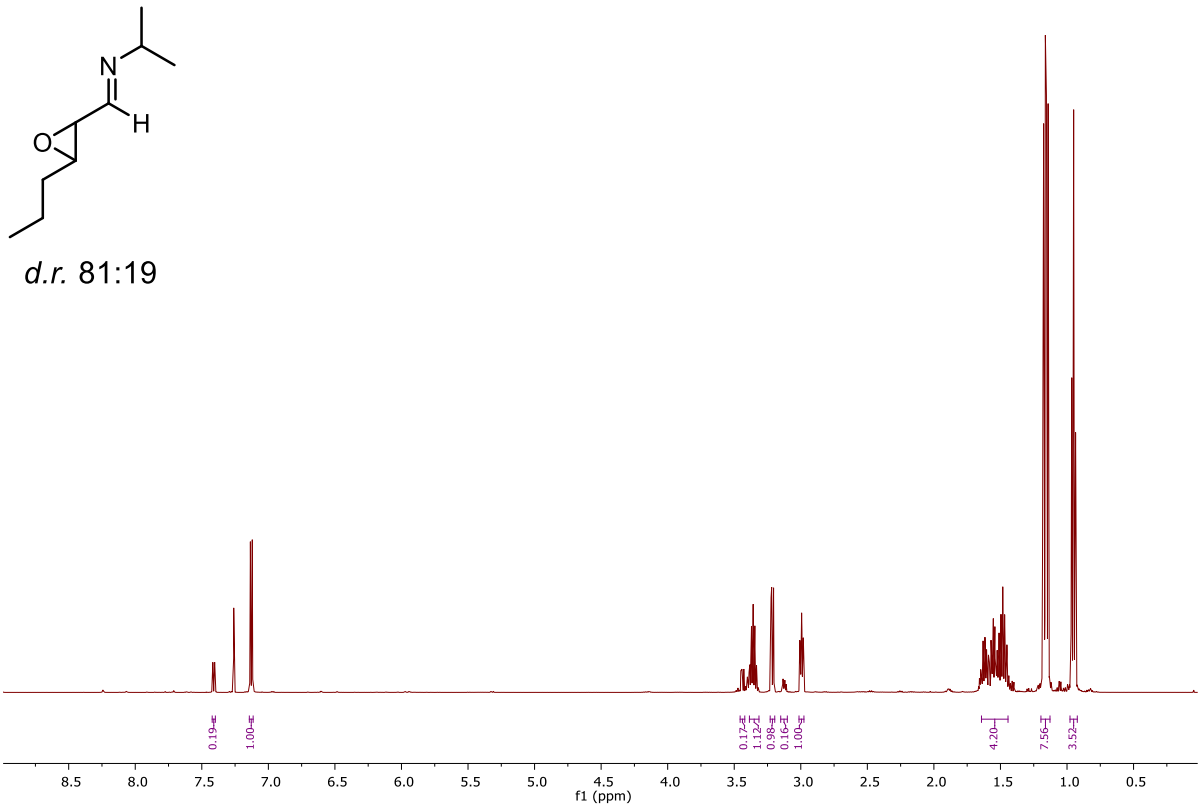

10.1.9 ^{13}C NMR Spectrum of Compound (±)-2.10 (125 MHz, $CDCl_3$)

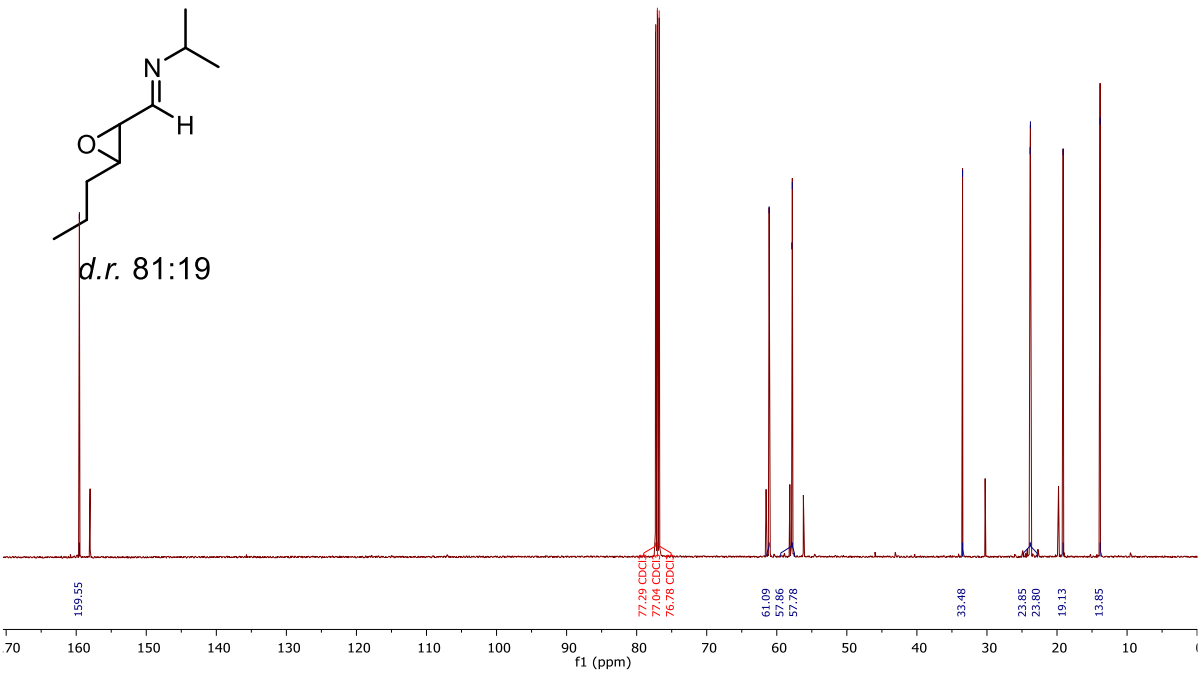

10.1.10 ^{1}H NMR Spectrum of Compound (±)-2.14 (500 MHz, $CDCl_3$)

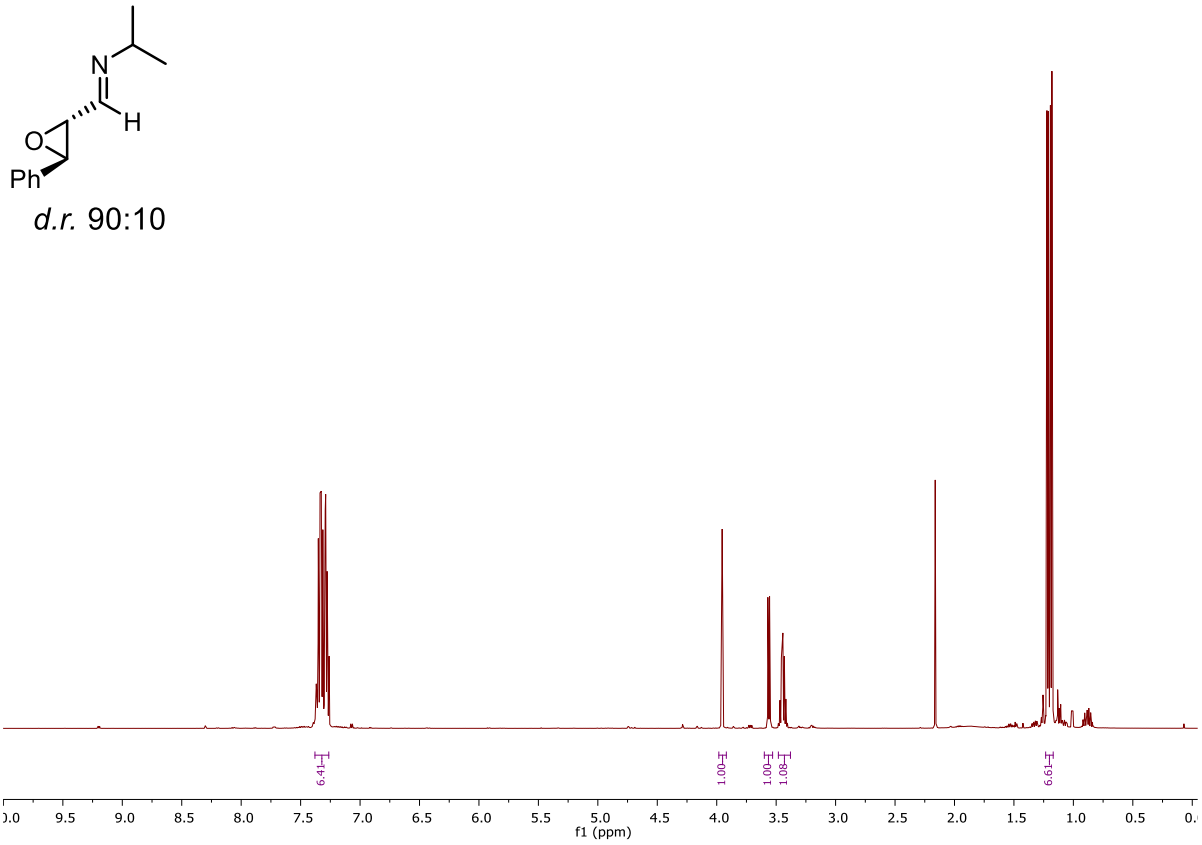

10.1.11 ^{13}C NMR Spectrum of Compound (±)-2.14 (125 MHz, $CDCl_3$)

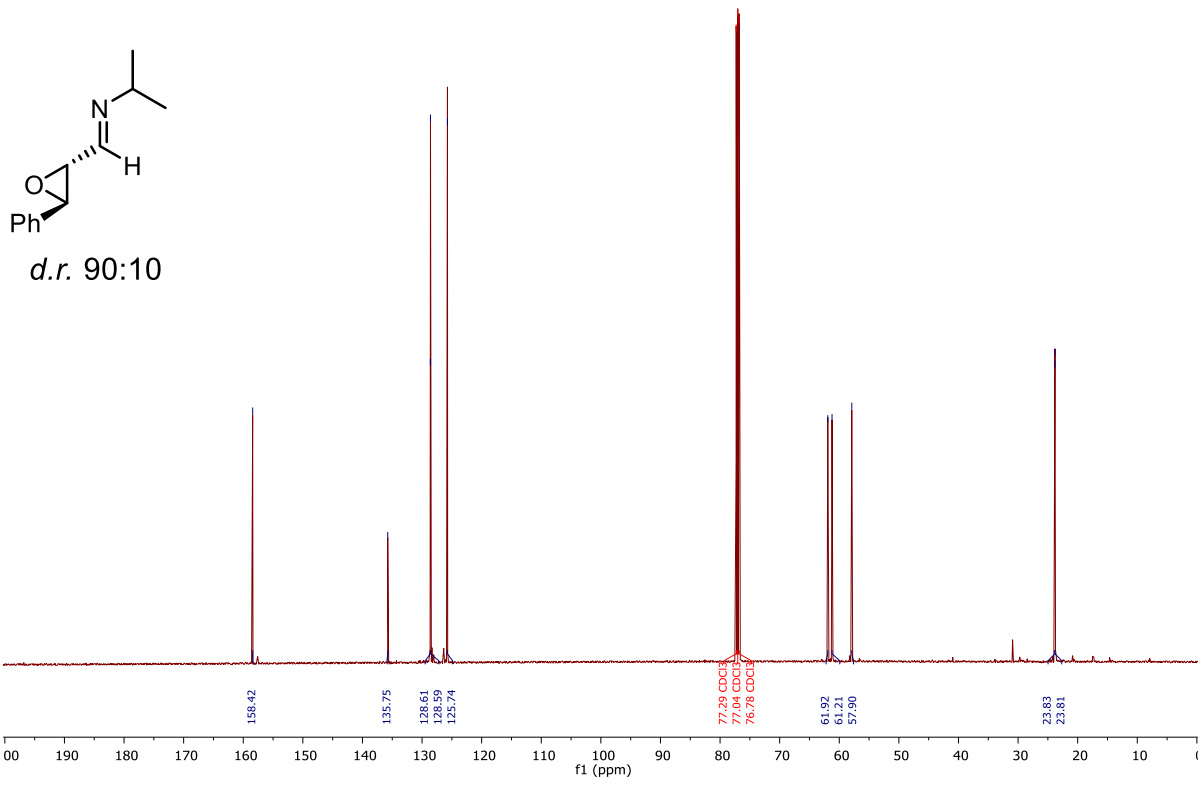

10.1.12 ^{1}H NMR Spectrum of Compound (±)-2.17 (400 MHz, $CDCl_3$)

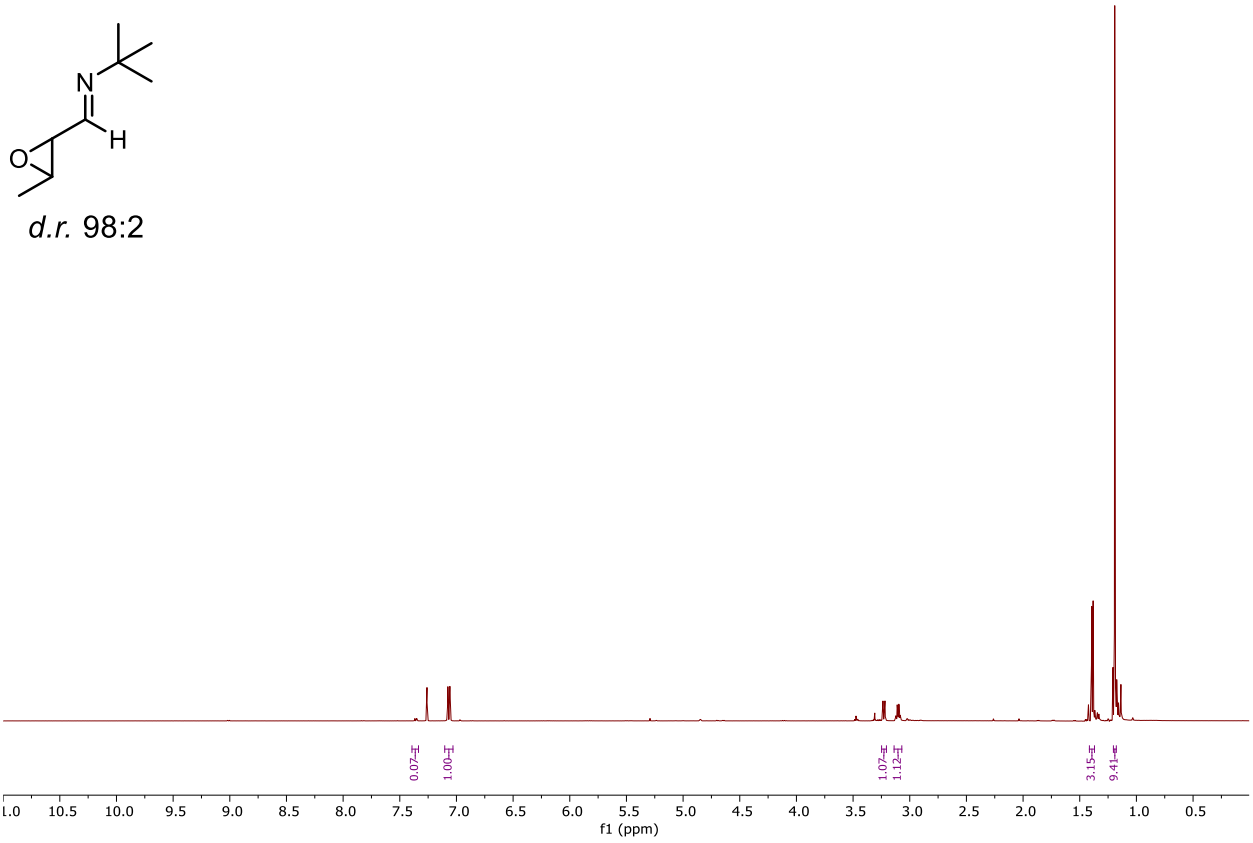

10.1.13 ^{13}C NMR Spectrum of Compound (±)-2.17 (100 MHz, $CDCl_3$)

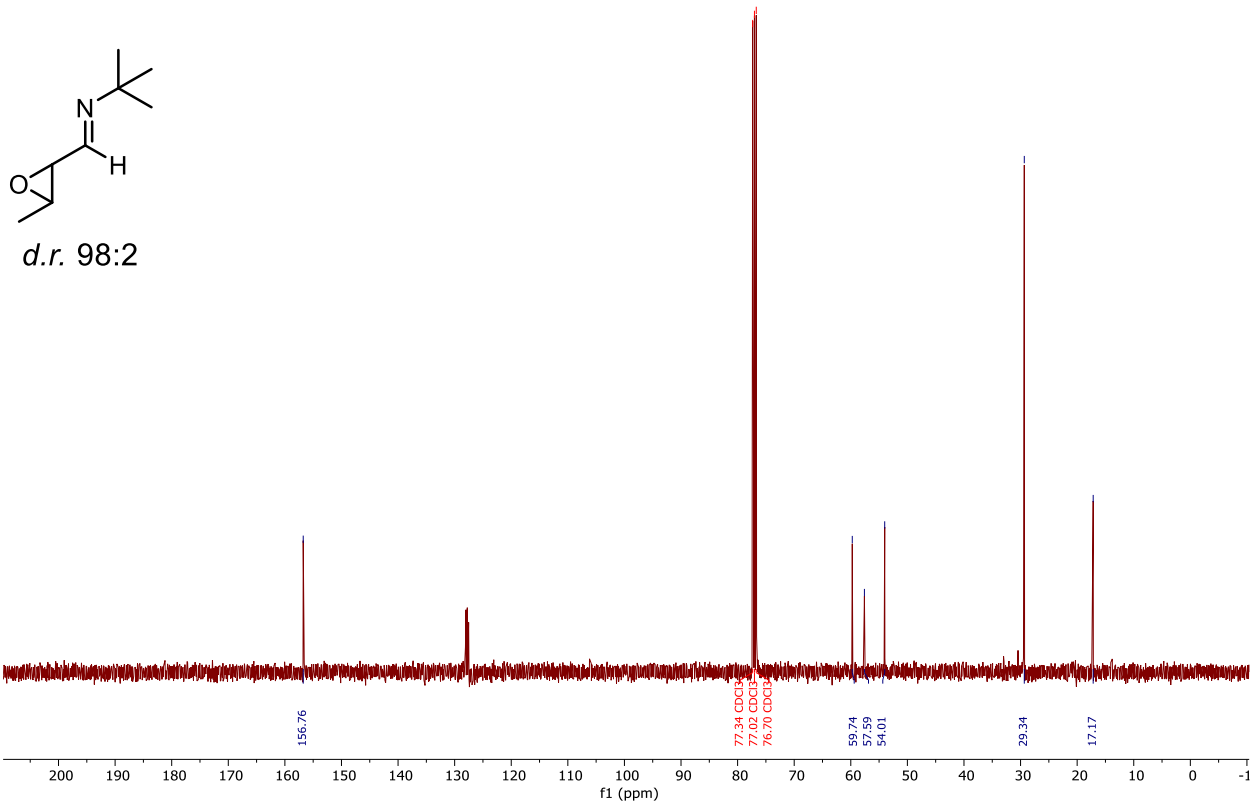

10.1.14 ^{1}H NMR Spectrum of Compound (±)-1.24 (600 MHz, $CDCl_3$)

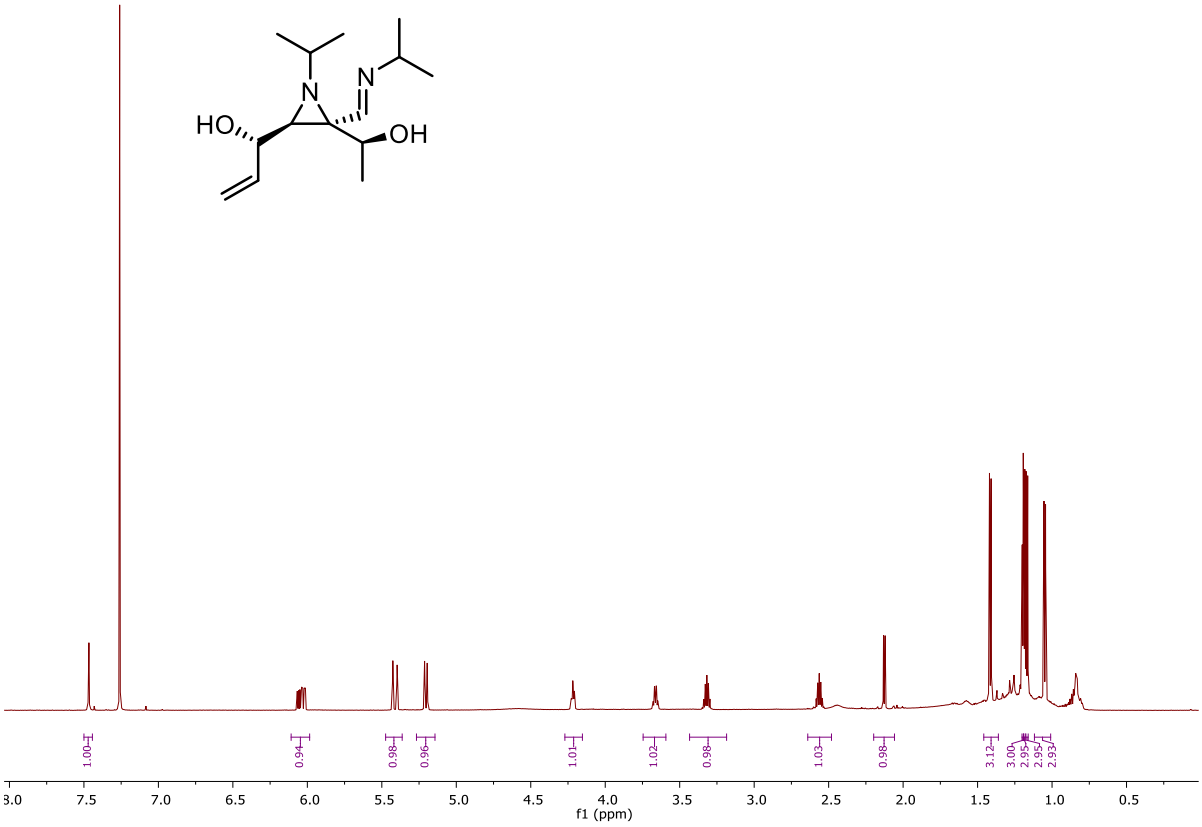

10.1.15 ^{13}C NMR Spectrum of Compound (±)-1.24 (125 MHz, $CDCl_3$)

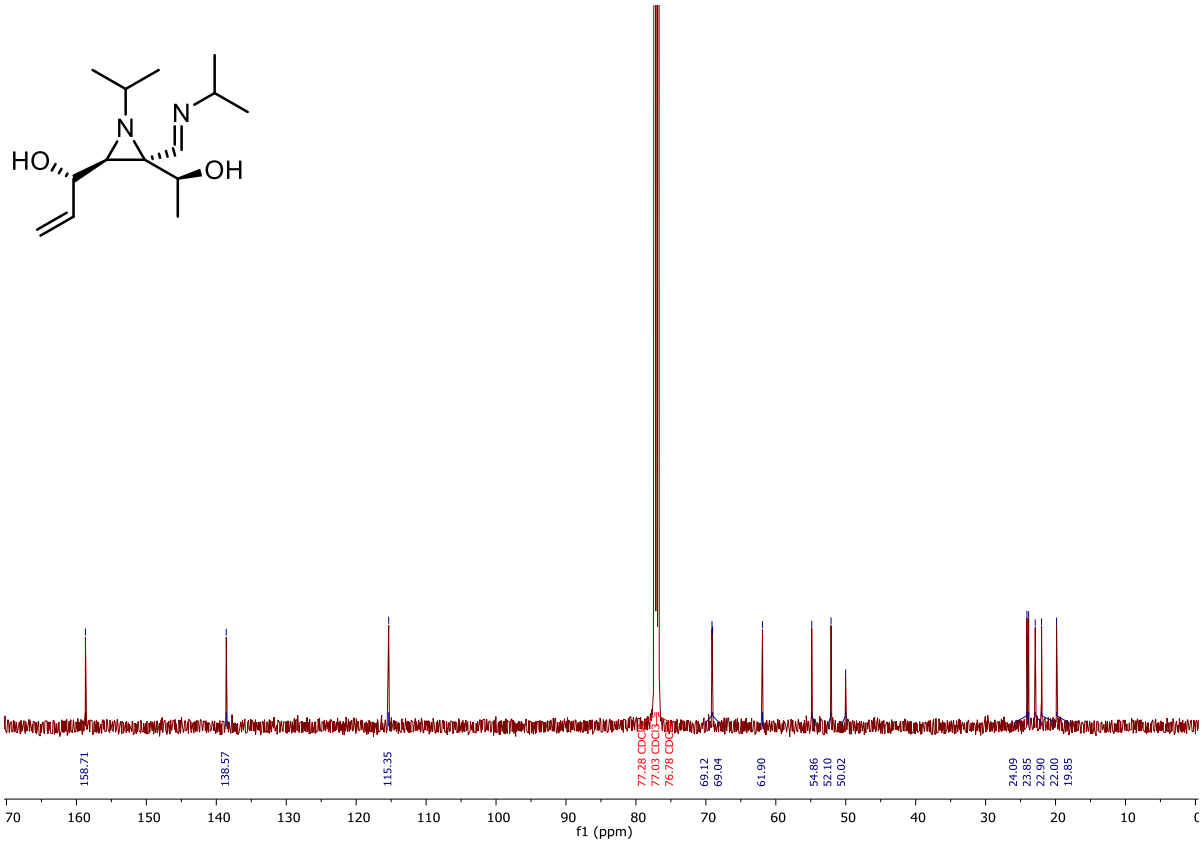

10.1.16 ^{1}H-^{1}H COSY Spectrum of Compound (±)-1.24 ($CDCl_3$)

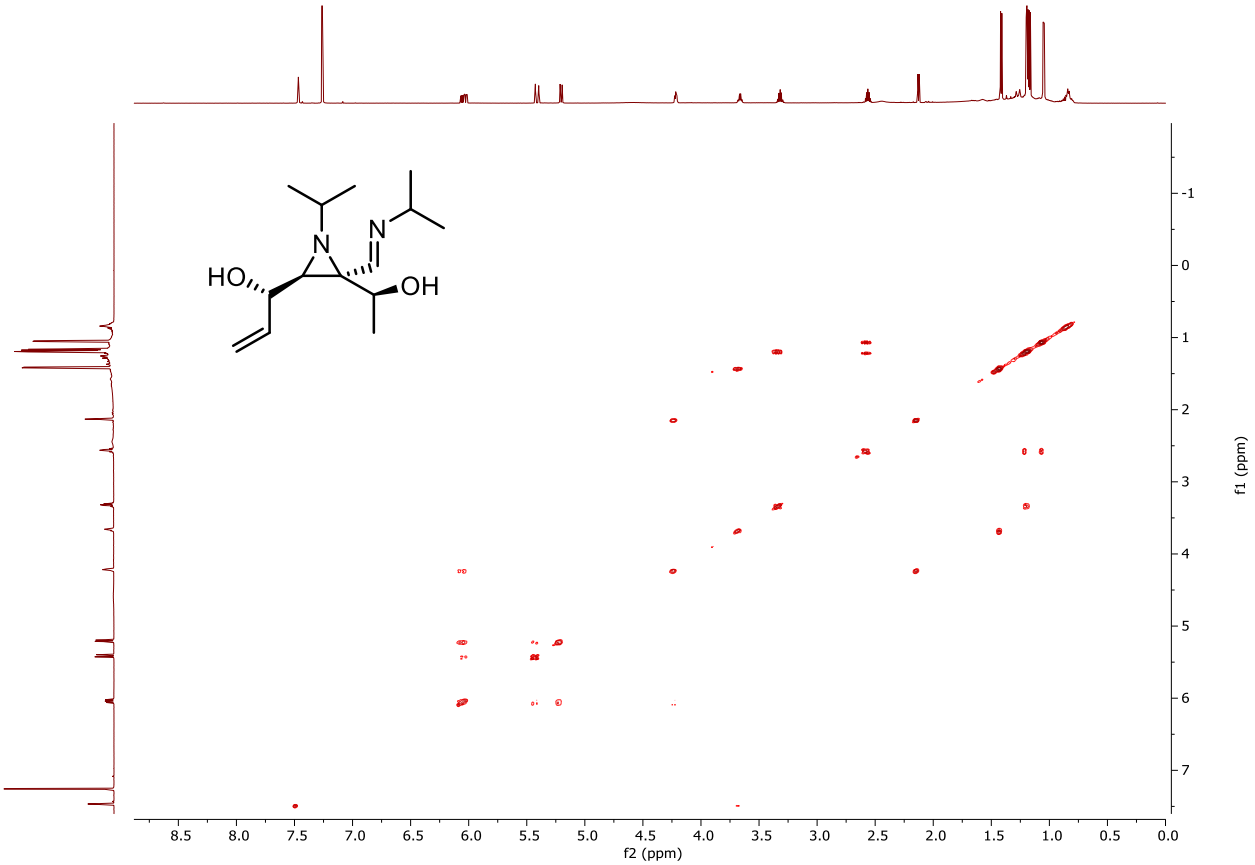

10.1.17 ^{1}H-^{13}C HSQC Spectrum of Compound (±)-1.24 ($CDCl_3$)

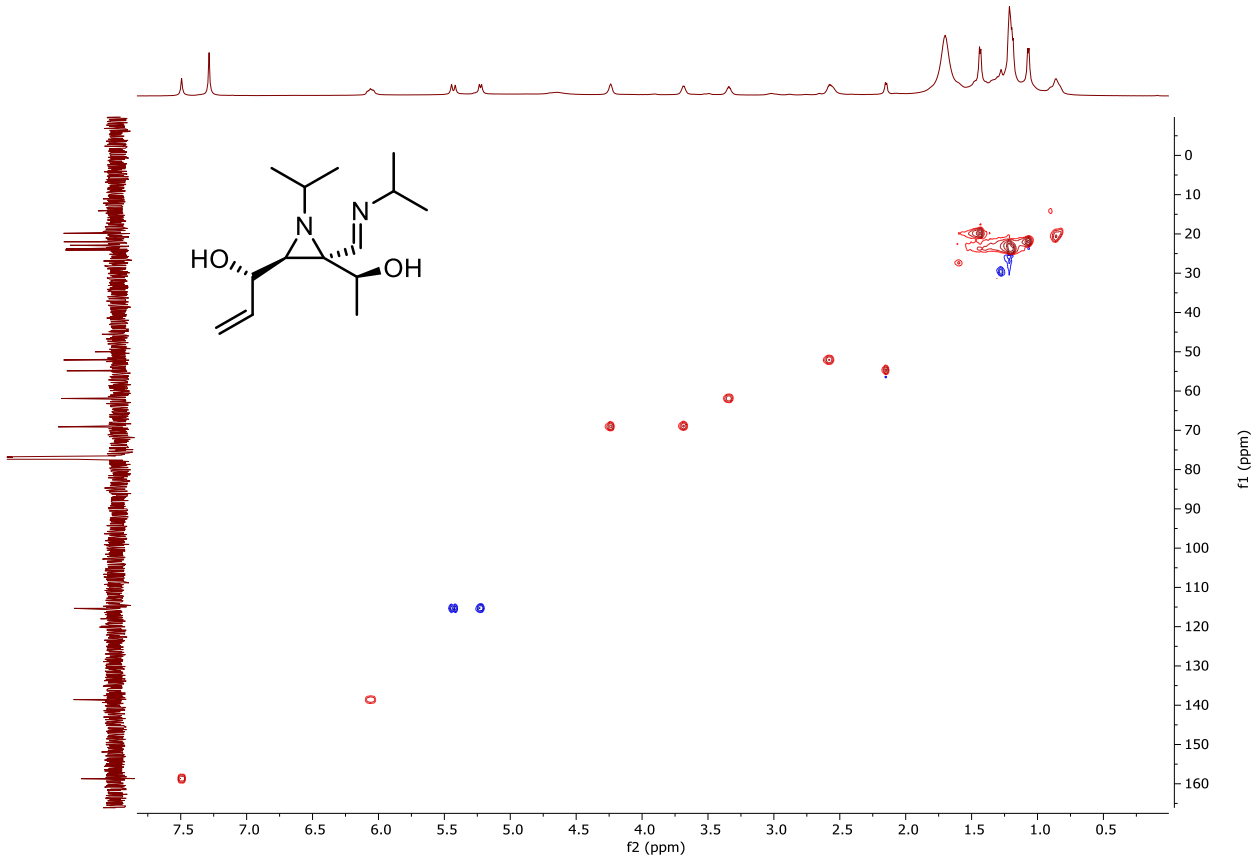

10.1.18 ^{13}C DEPT Spectrum of Compound (±)-1.24 ($CDCl_3$)

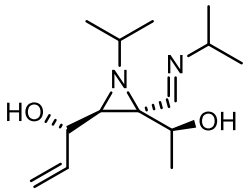

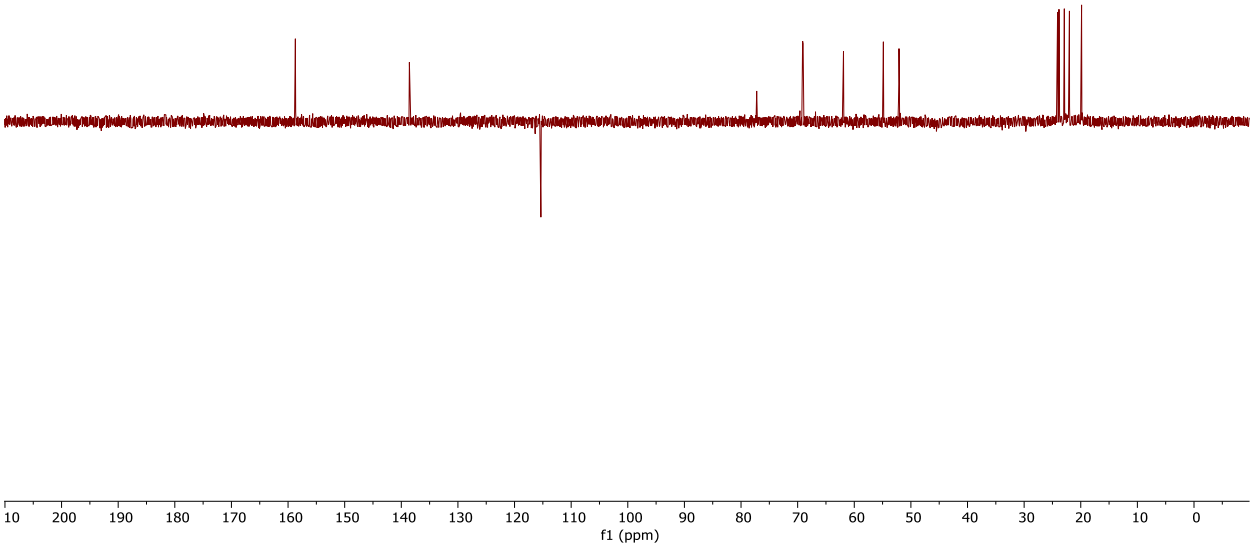

10.1.19 ^{1}H NMR Spectrum of Compound (±)-2.19 (400 MHz, $CDCl_3$)

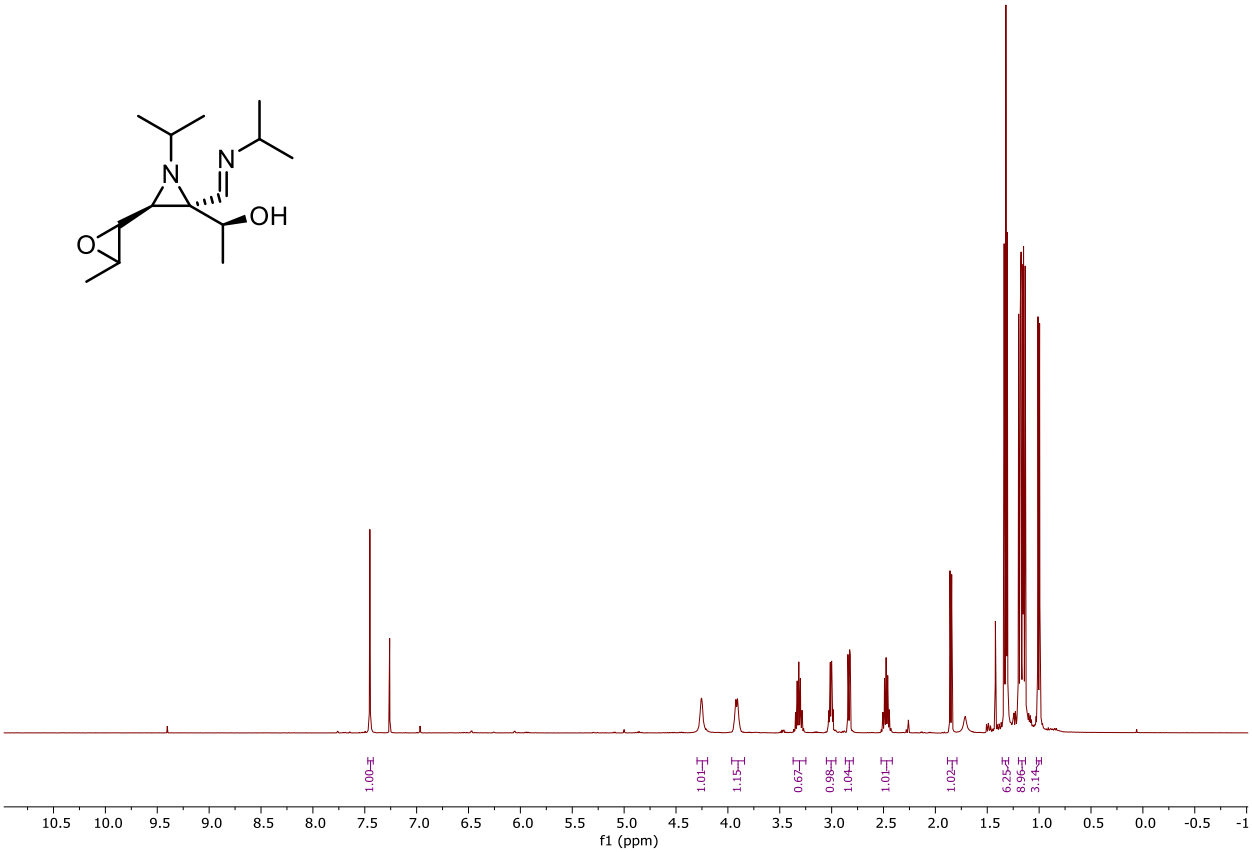

10.1.20 ^{13}C NMR Spectrum of Compound (±)-2.19 (100 MHz, $CDCl_3$)

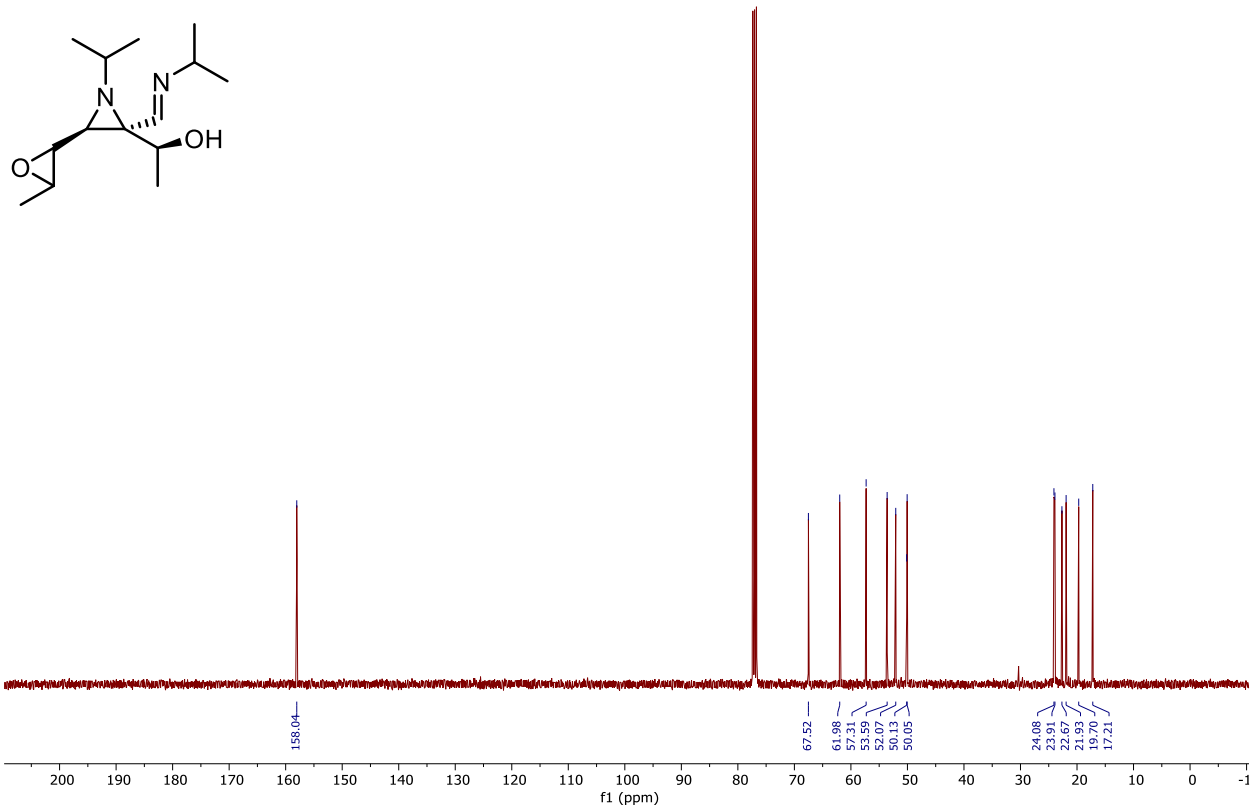

10.1.21 ^{1}H NMR Spectrum of Compound (±)-2.20 (500 MHz, $CDCl_3$)

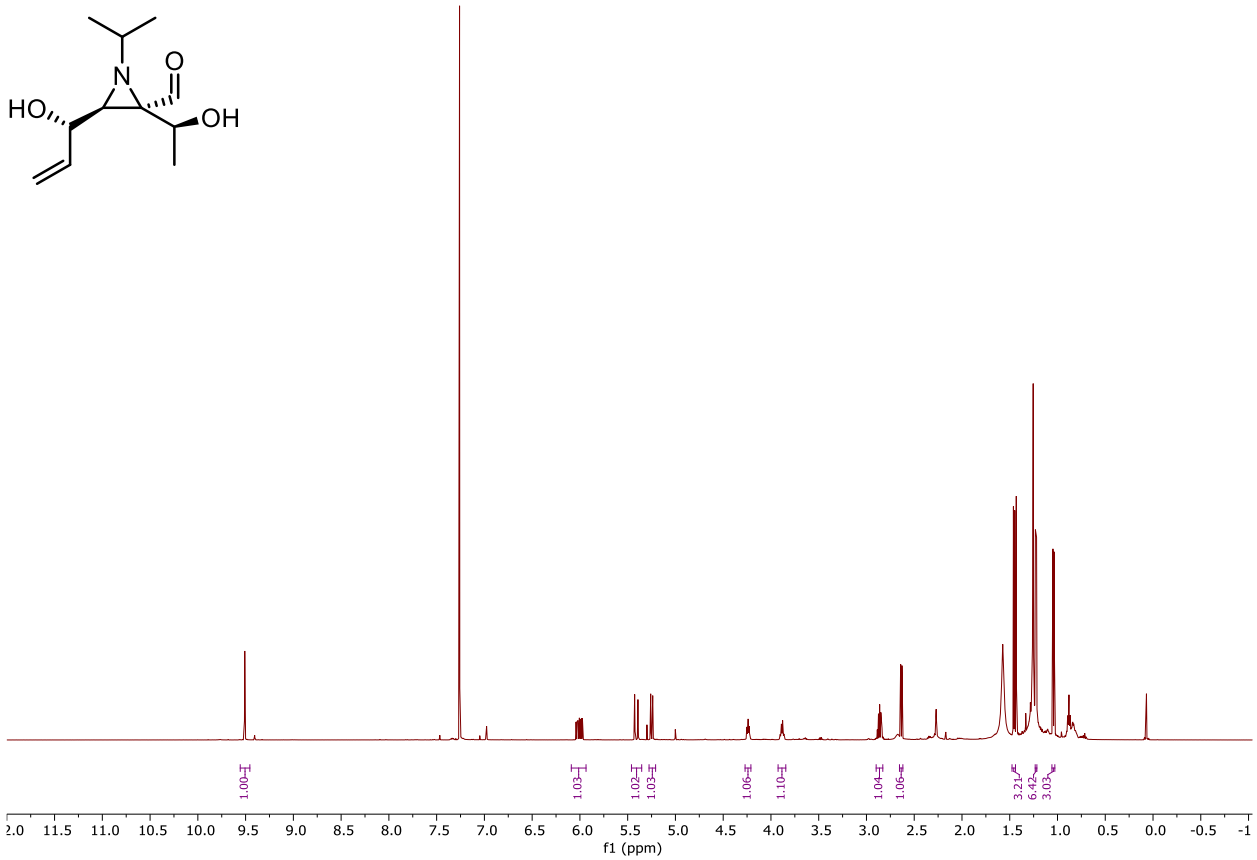

10.1.22 ^{13}C NMR Spectrum of Compound (±)-2.20 (125 MHz, $CDCl_3$)

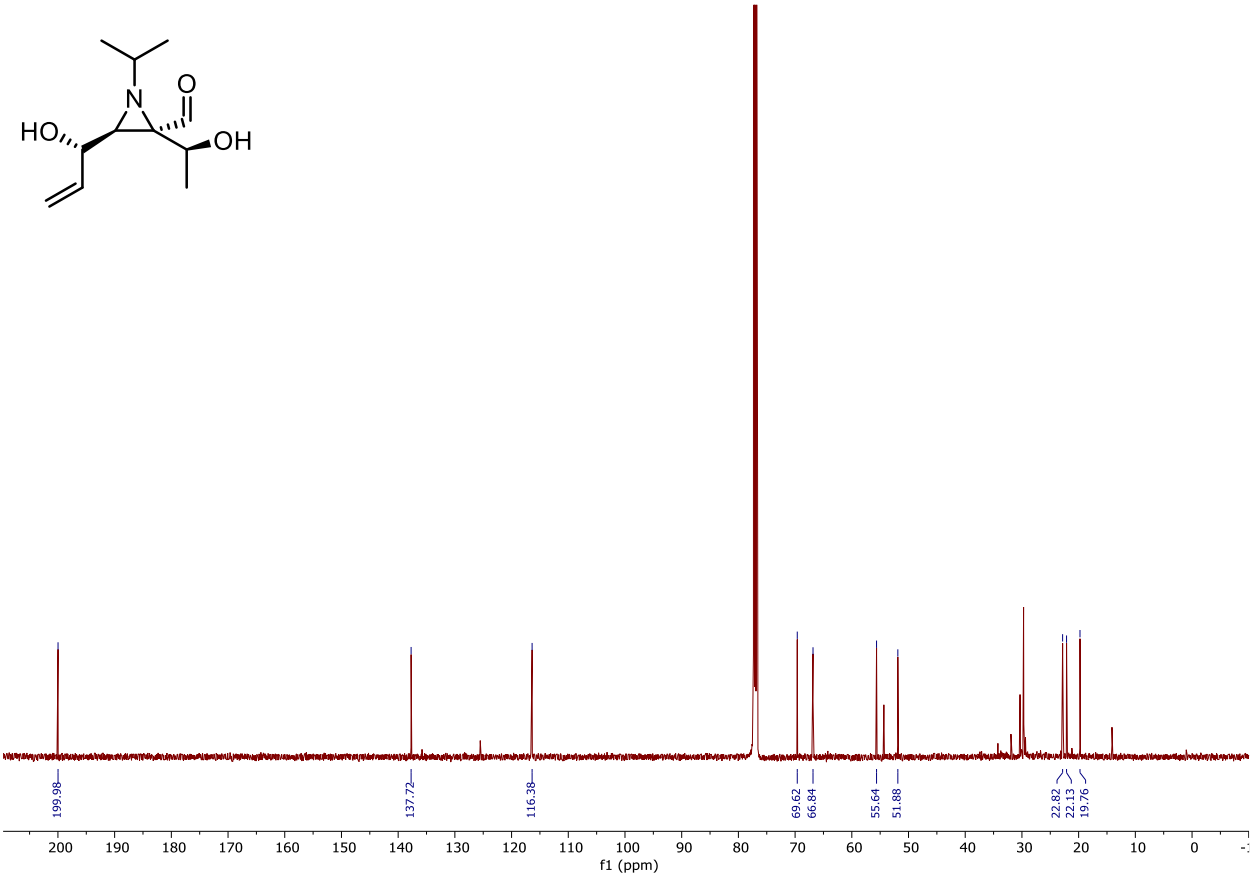

10.1.23 ^{1}H-^{1}H COSY Spectrum of Compound (±)-2.20 ($CDCl_3$)

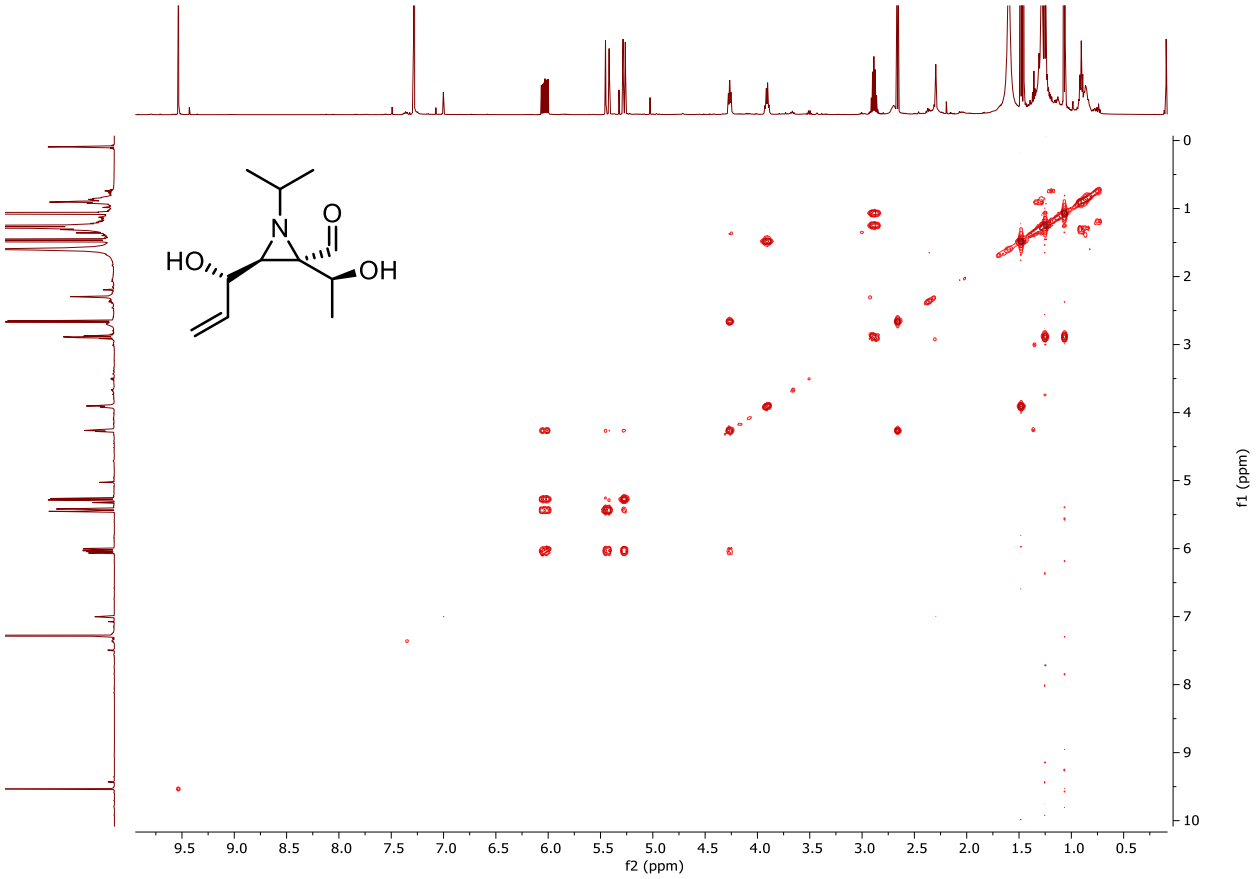

10.1.24 ^{1}H-^{13}C HSQC Spectrum of Compound (±)-2.20 ($CDCl_3$)

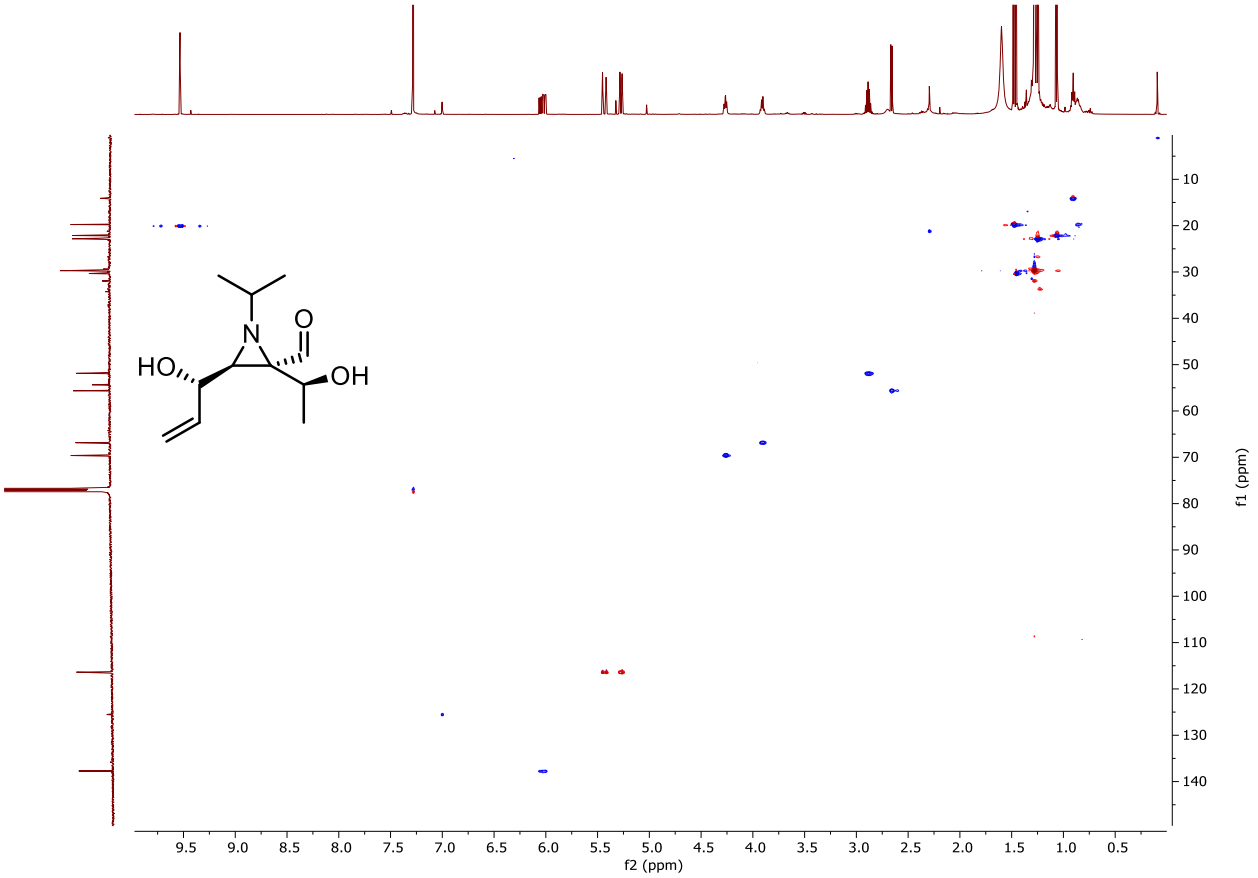

10.1.25 ^{1}H-^{13}C HMBC Spectrum of Compound (±)-2.20 ($CDCl_3$)

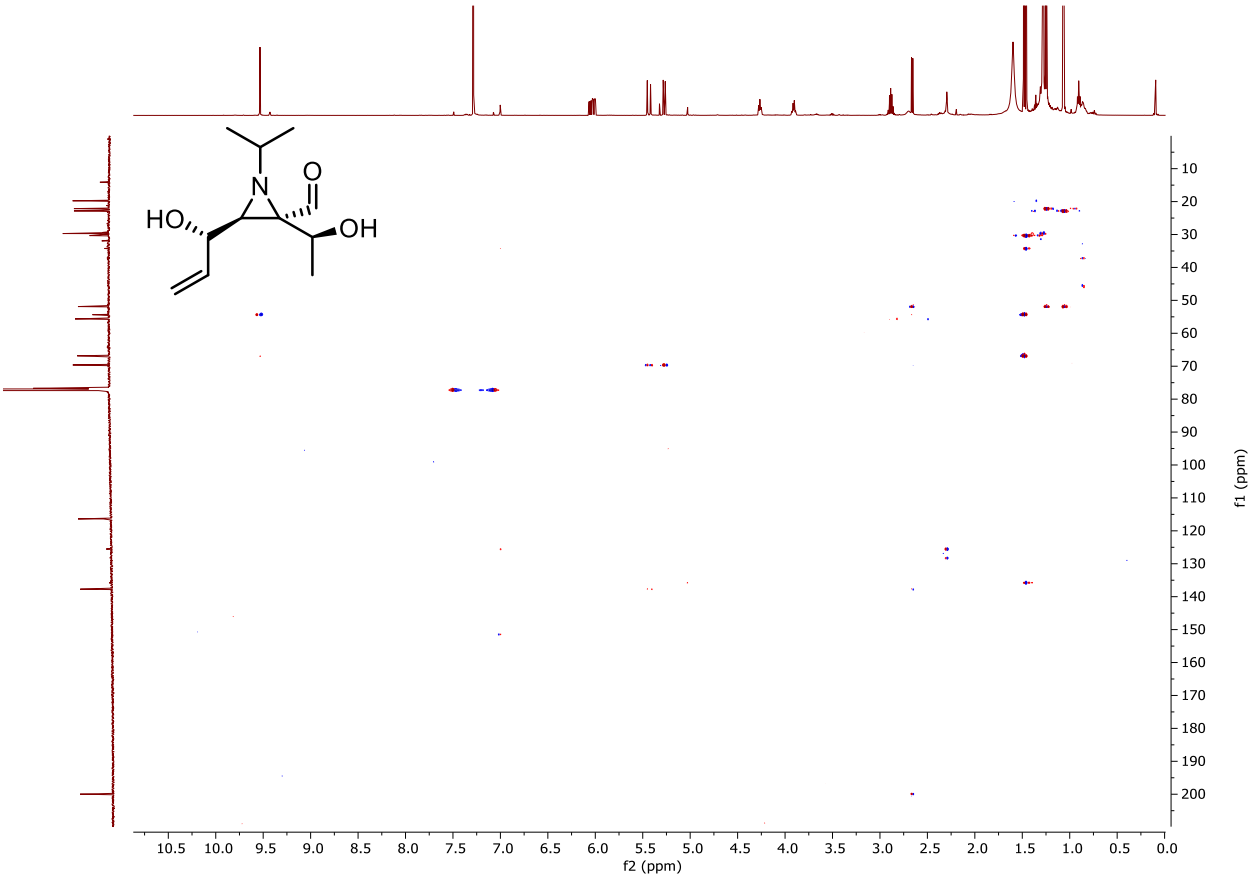

10.1.26 ^{13}C DEPT Spectrum of Compound (±)-2.20 ($CDCl_3$)

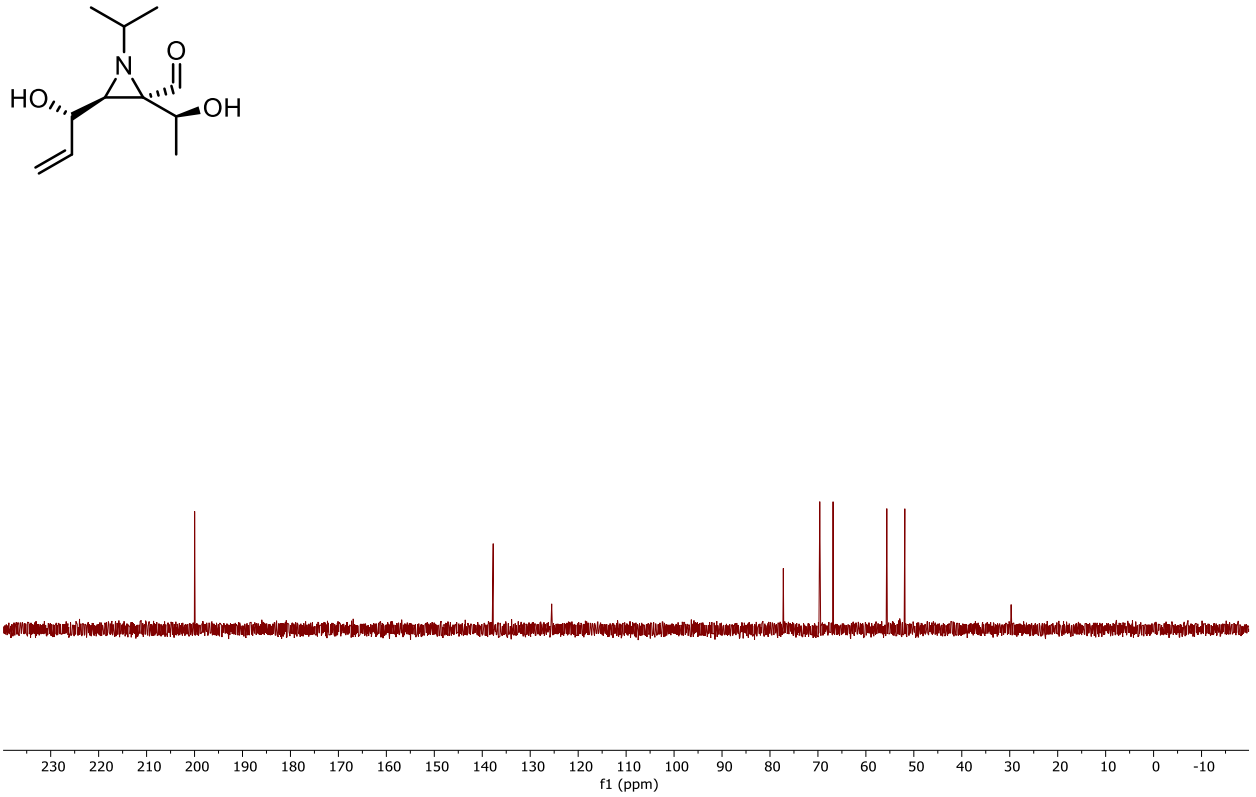

10.1.27 ^{1}H NMR Spectrum of Compound (±)-2.3 (500 MHz, $CDCl_3$)

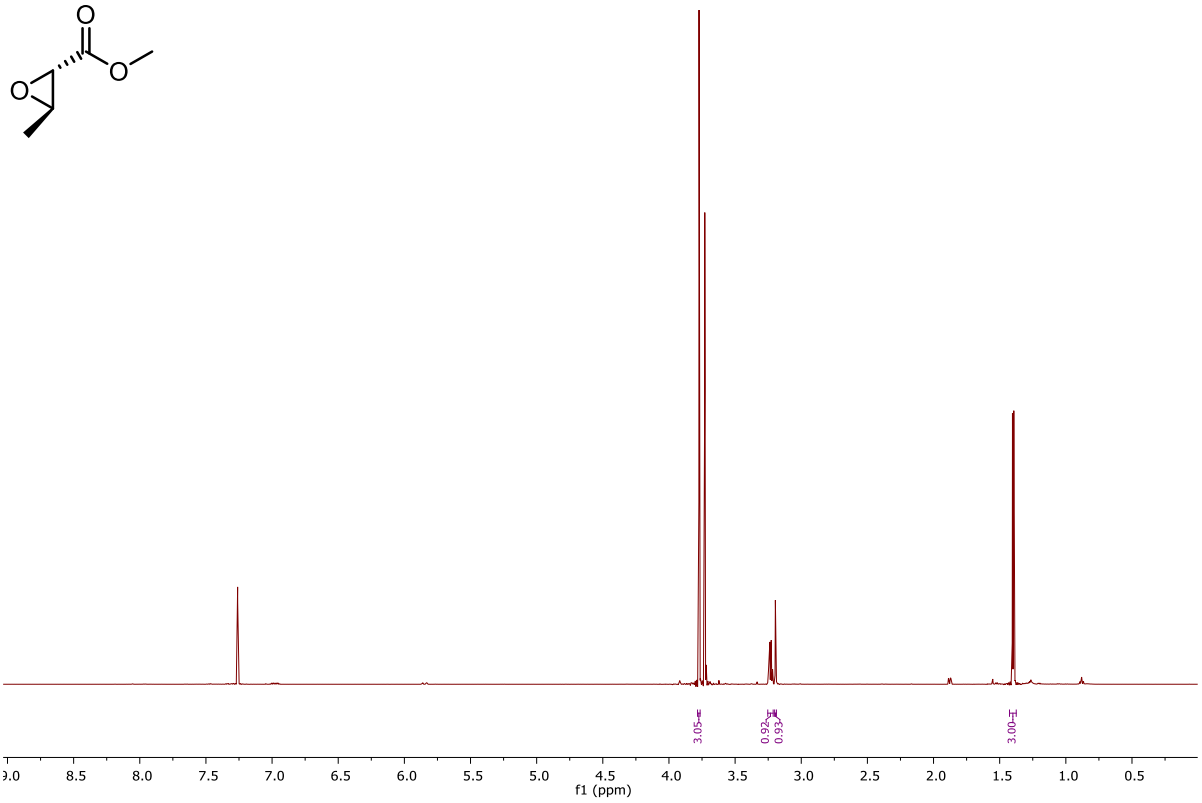

10.1.28 ^{13}C NMR Spectrum of Compound (±)-2.3 (100 MHz, $CDCl_3$)

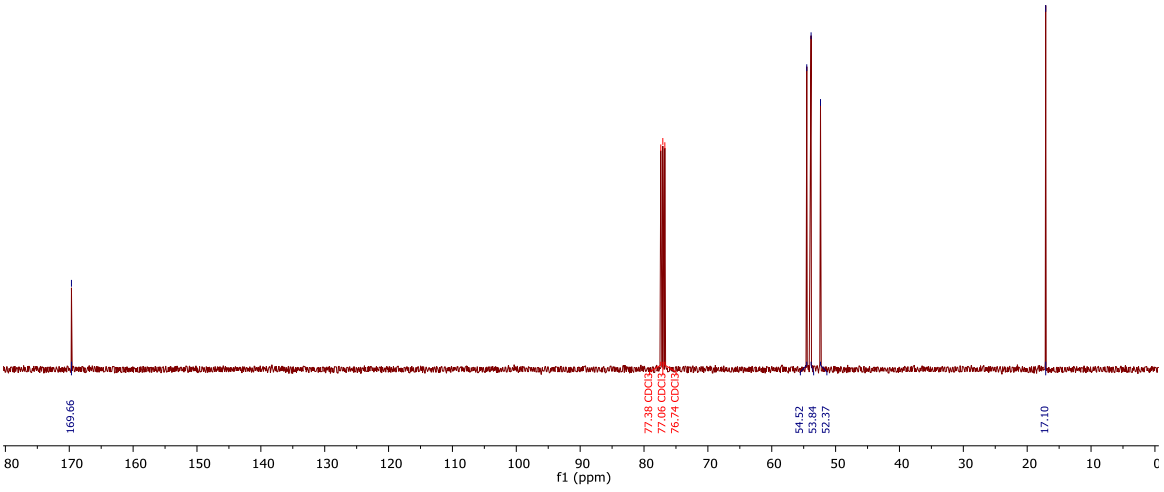

10.1.29 ^{1}H NMR Spectrum of Compound (±)-2.4 (400 MHz, $CDCl_3$)

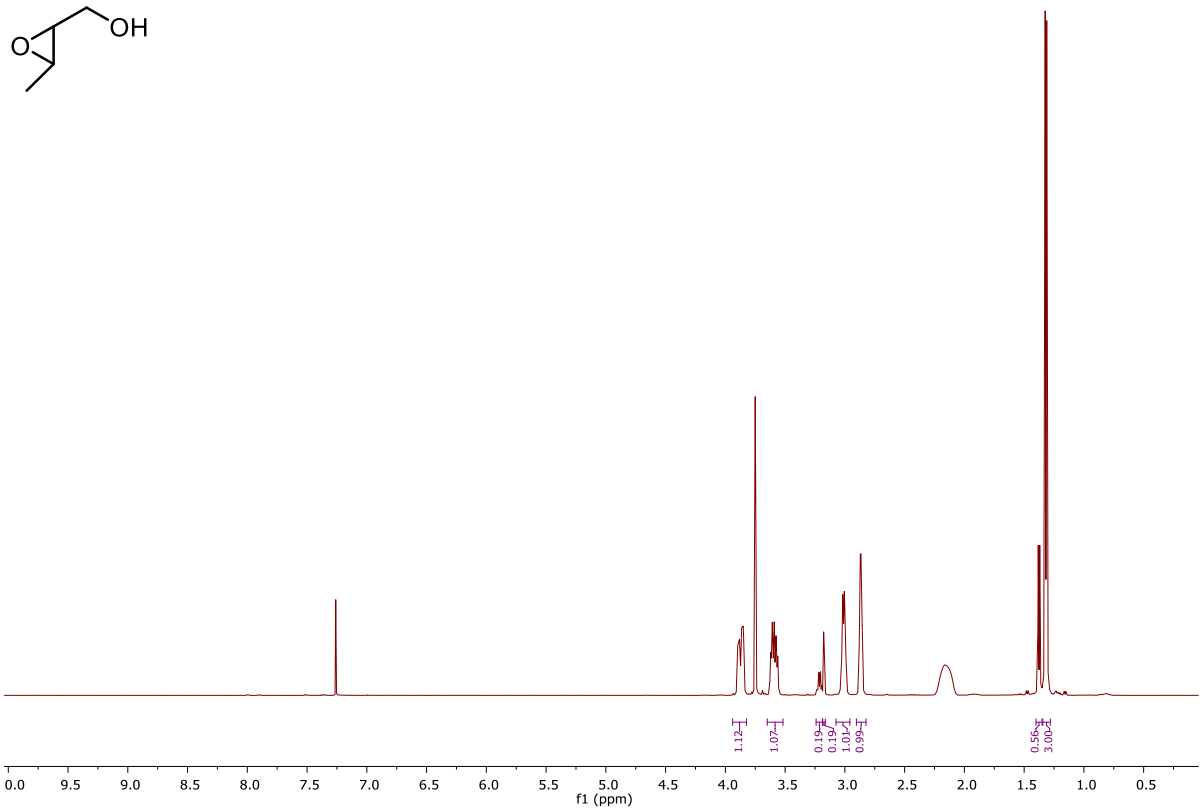

10.1.30 ^{13}C NMR Spectrum of Compound (±)-2.4 (100 MHz, $CDCl_3$)

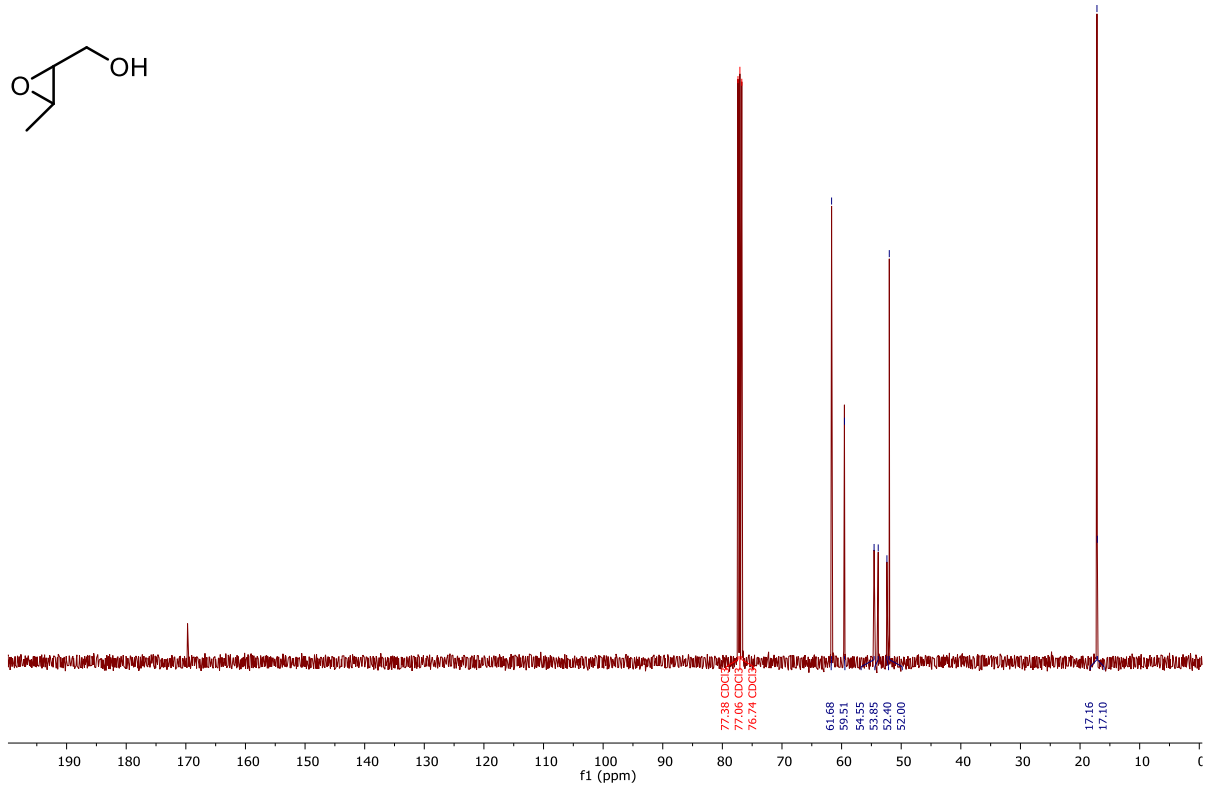

10.1.31 ^{1}H NMR Spectrum of Compound 2.25 (600 MHz, $CDCl_3$)

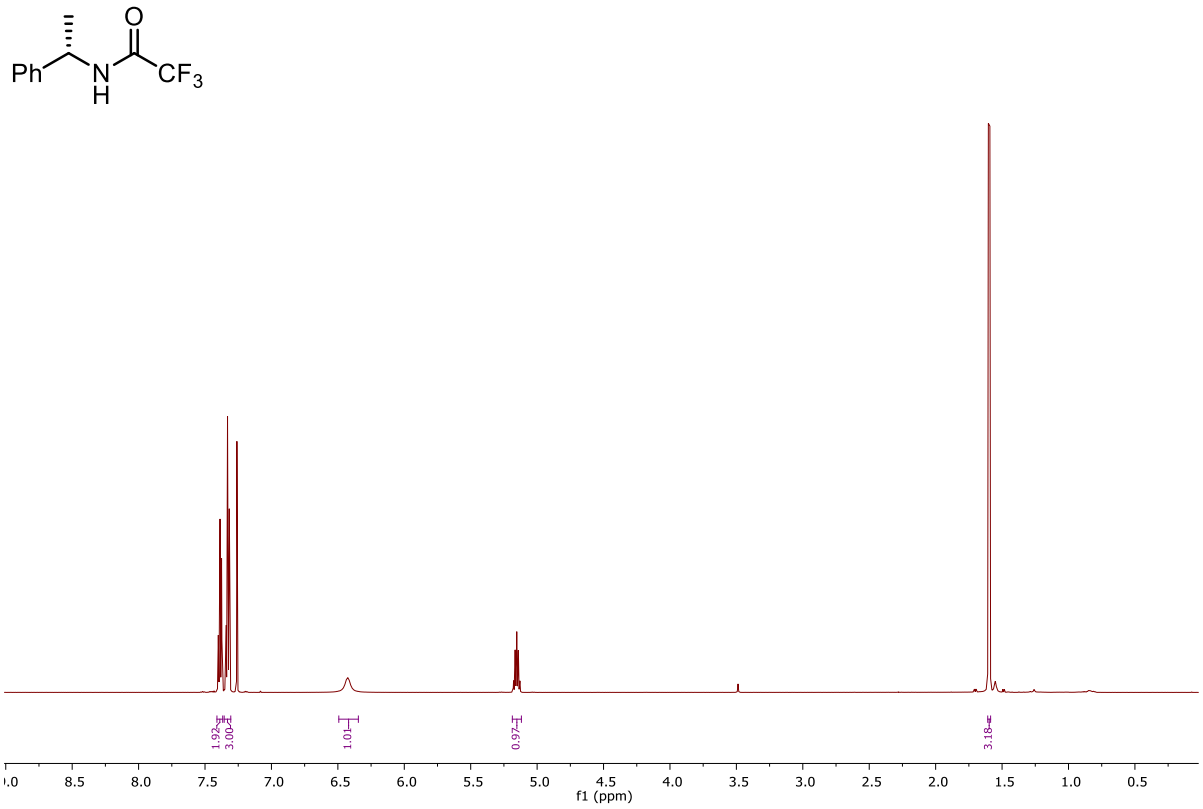

10.1.32 ^{13}C NMR Spectrum of Compound 2.25 (125 MHz, $CDCl_3$)

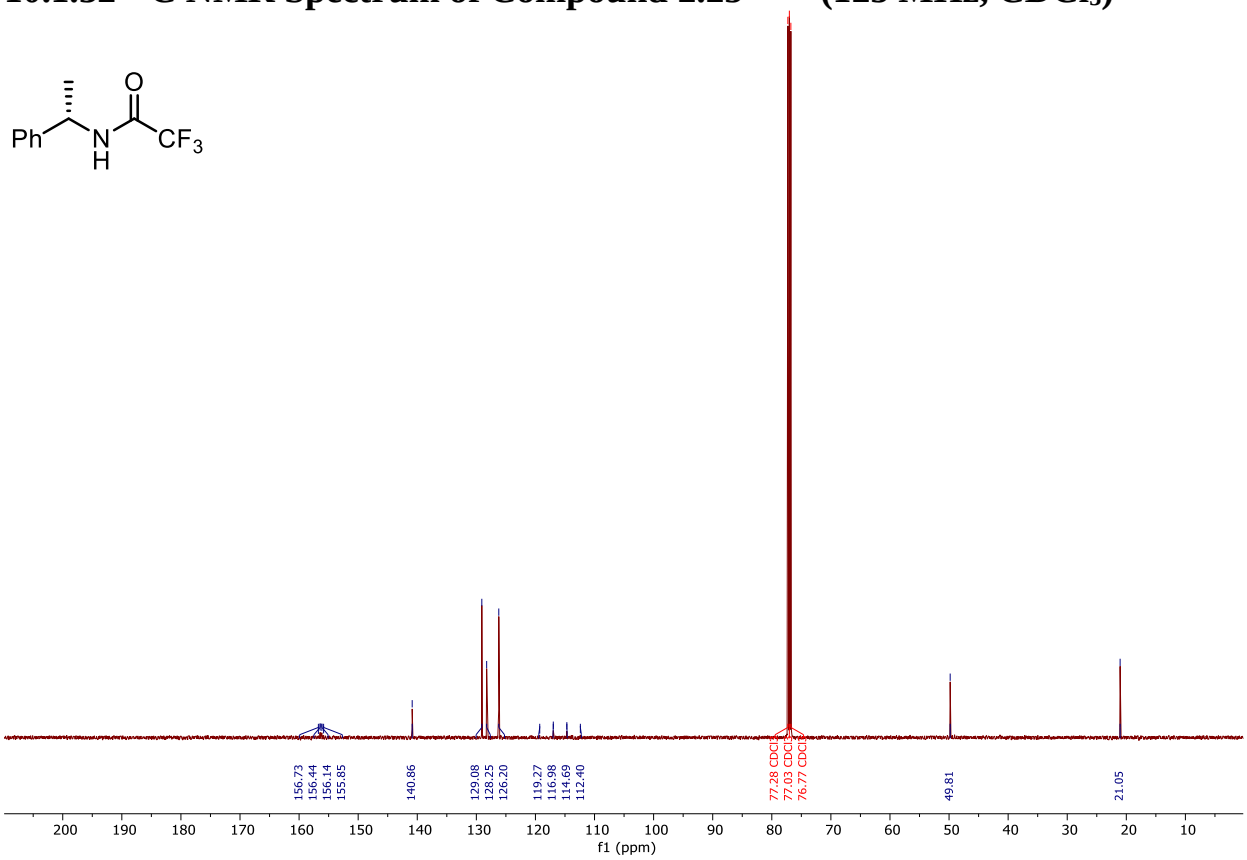

10.1.33 ^{1}H NMR Spectrum of Compound 2.26 (500 MHz, $CDCl_3$)

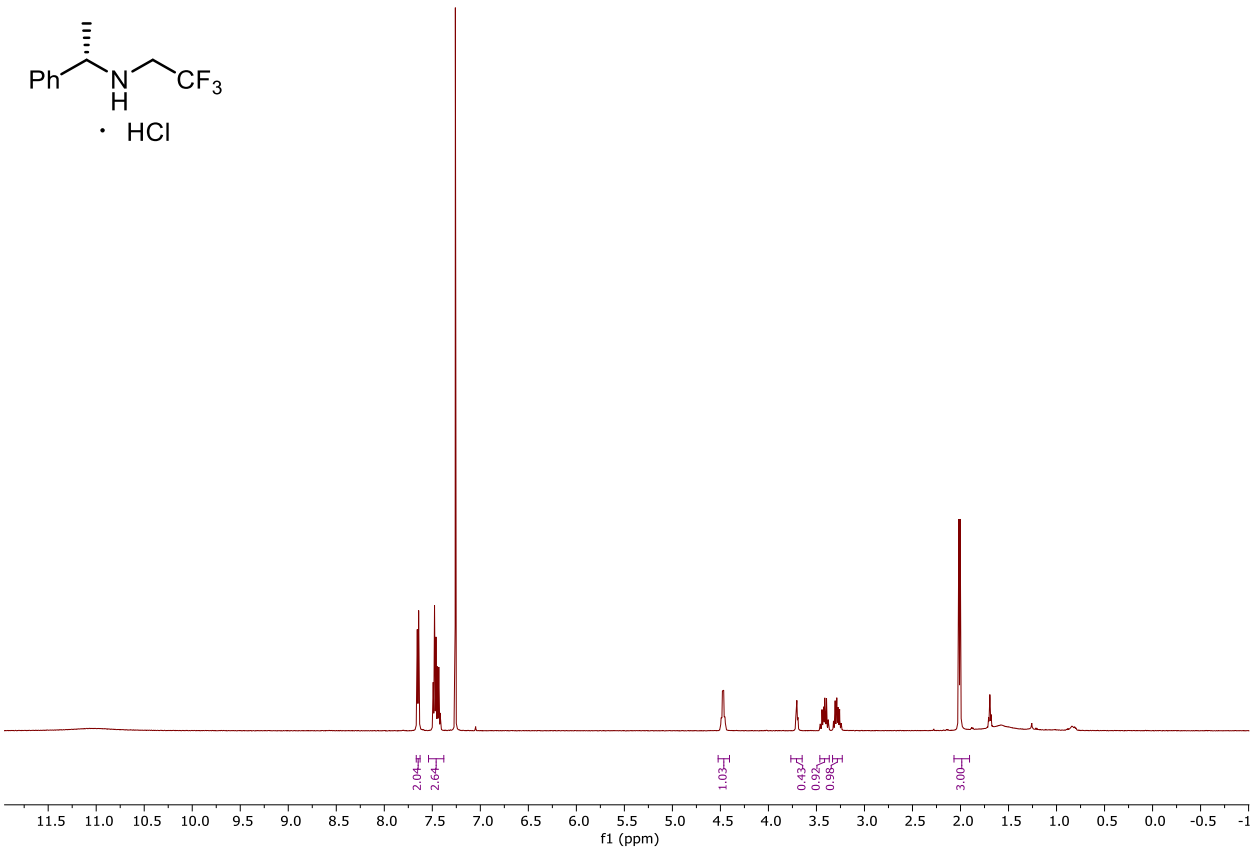

10.1.34 ^{13}C NMR Spectrum of Compound 2.26 (125 MHz, $CDCl_3$)

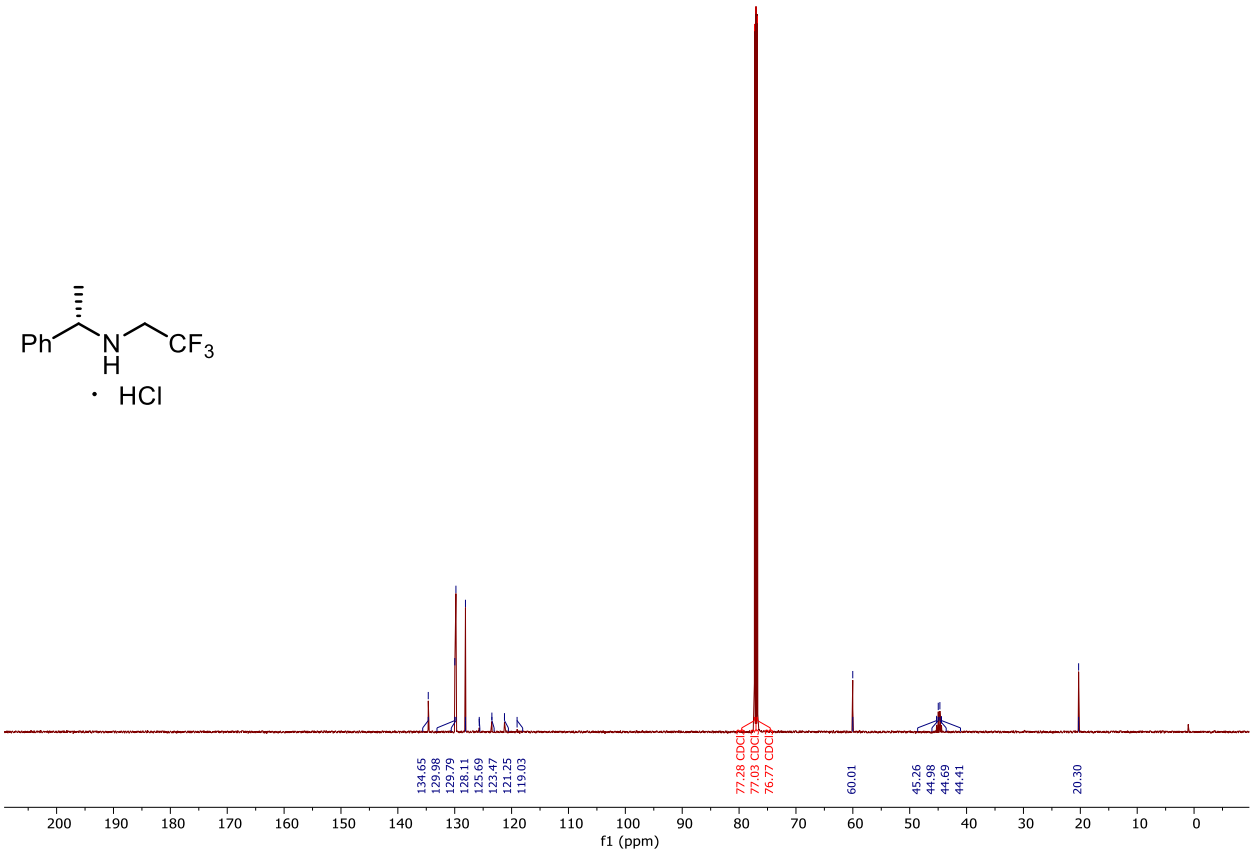

10.1.35 ^{1}H NMR Spectrum of Chiral Amine B (600 MHz, $CDCl_3$)

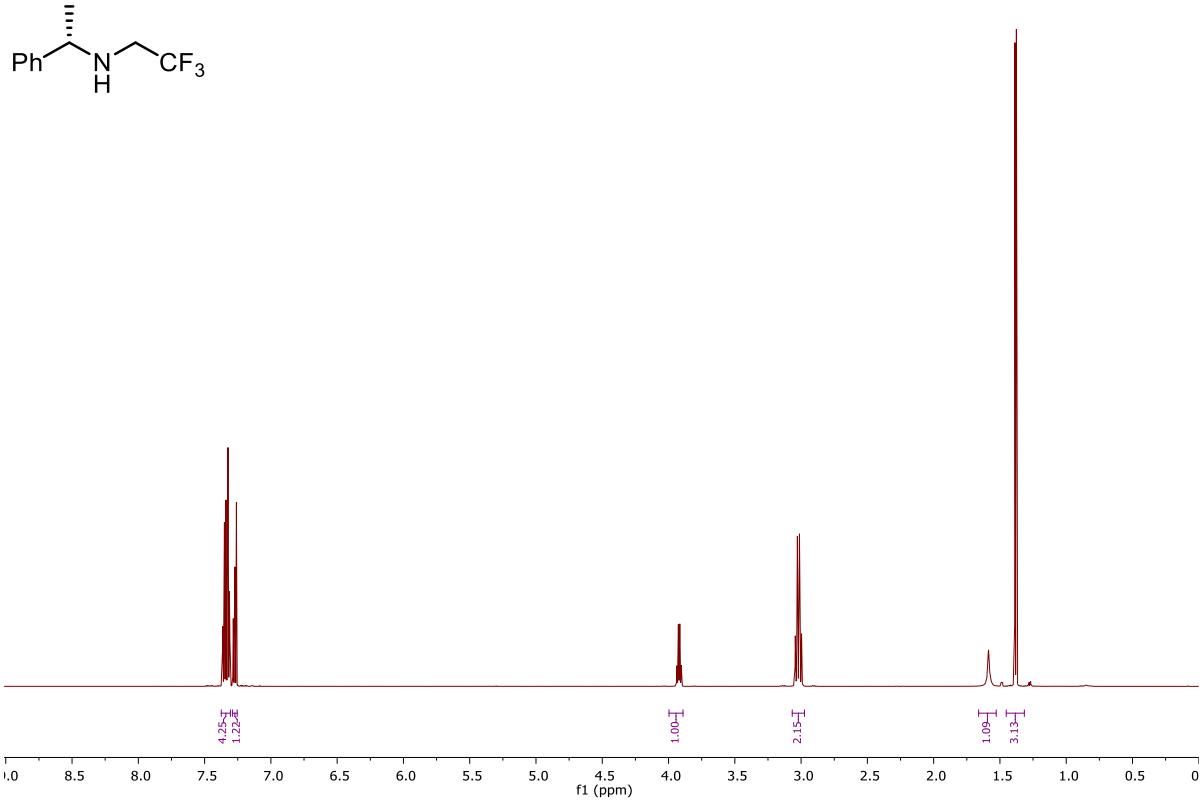

10.1.36 ^{13}C NMR Spectrum of Chiral Amine B (150 MHz, $CDCl_3$)

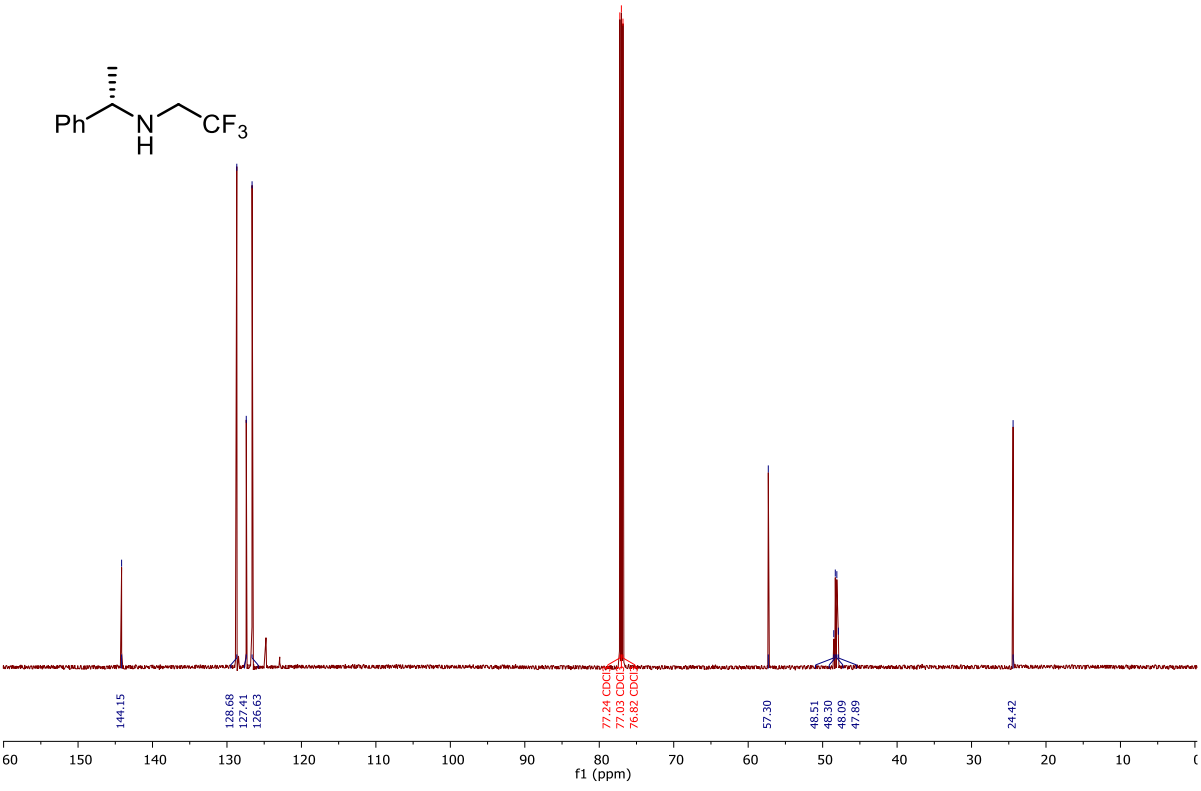

10.1.37 ^{1}H NMR Spectrum of Chiral Amine C (600 MHz, $CDCl_3$)

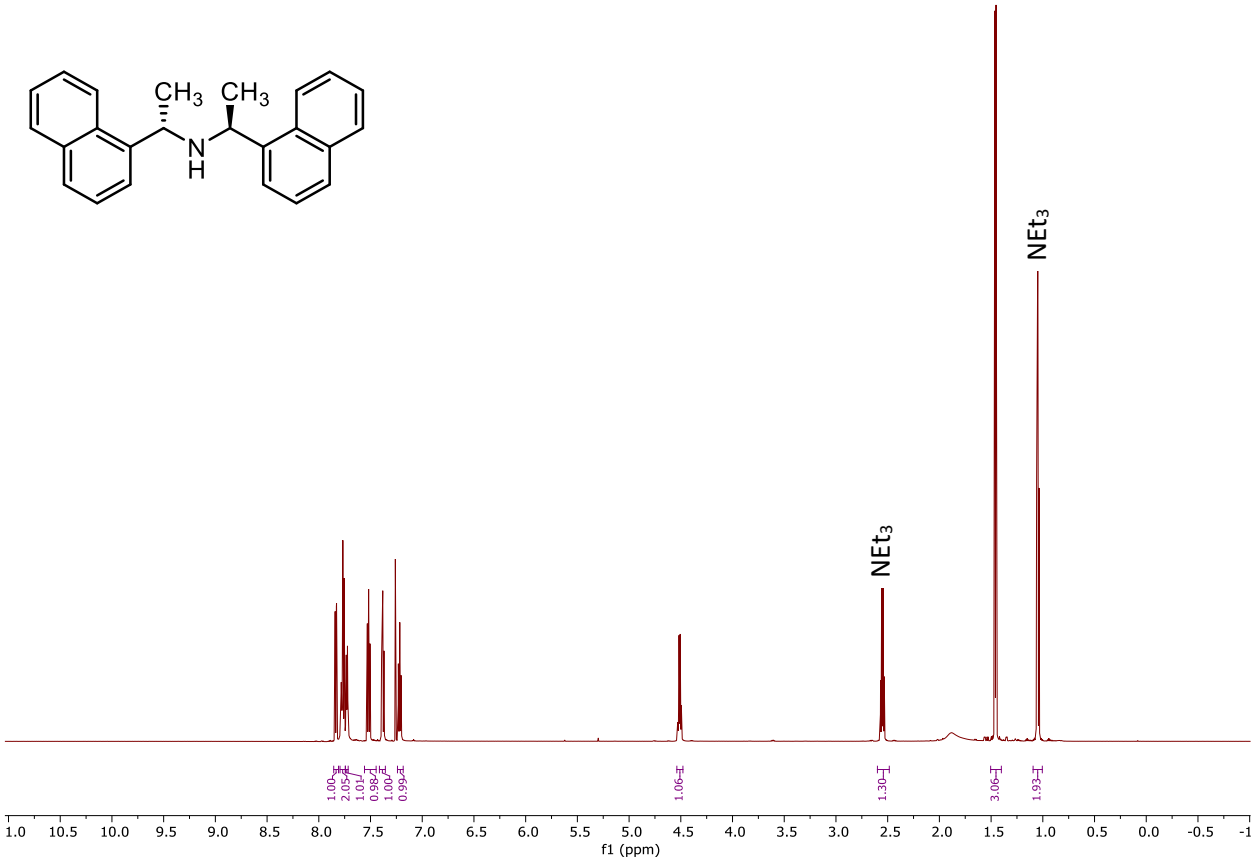

10.1.38 ^{13}C NMR Spectrum of Chiral Amine C (150 MHz, $CDCl_3$)

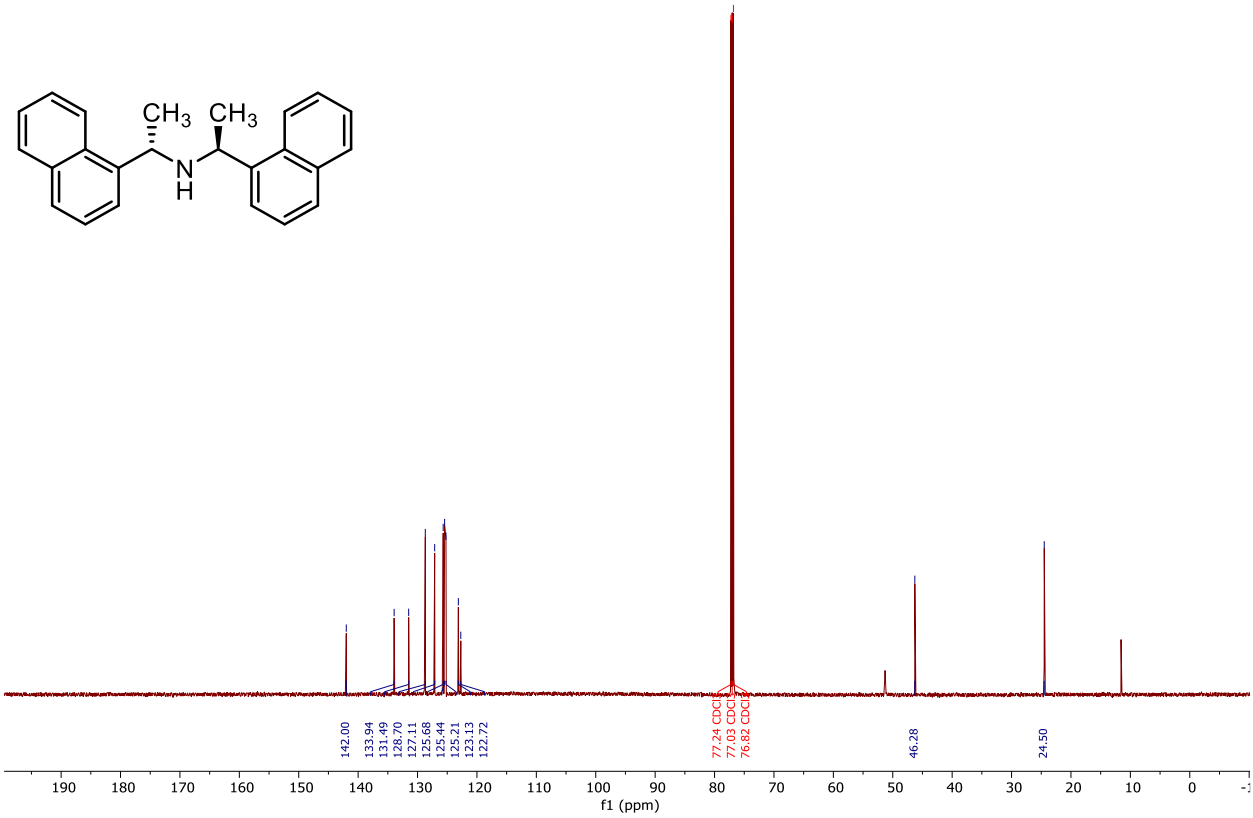

10.1.39 ^{1}H NMR Spectrum of Chiral Amine D (500 MHz, $CDCl_3$)

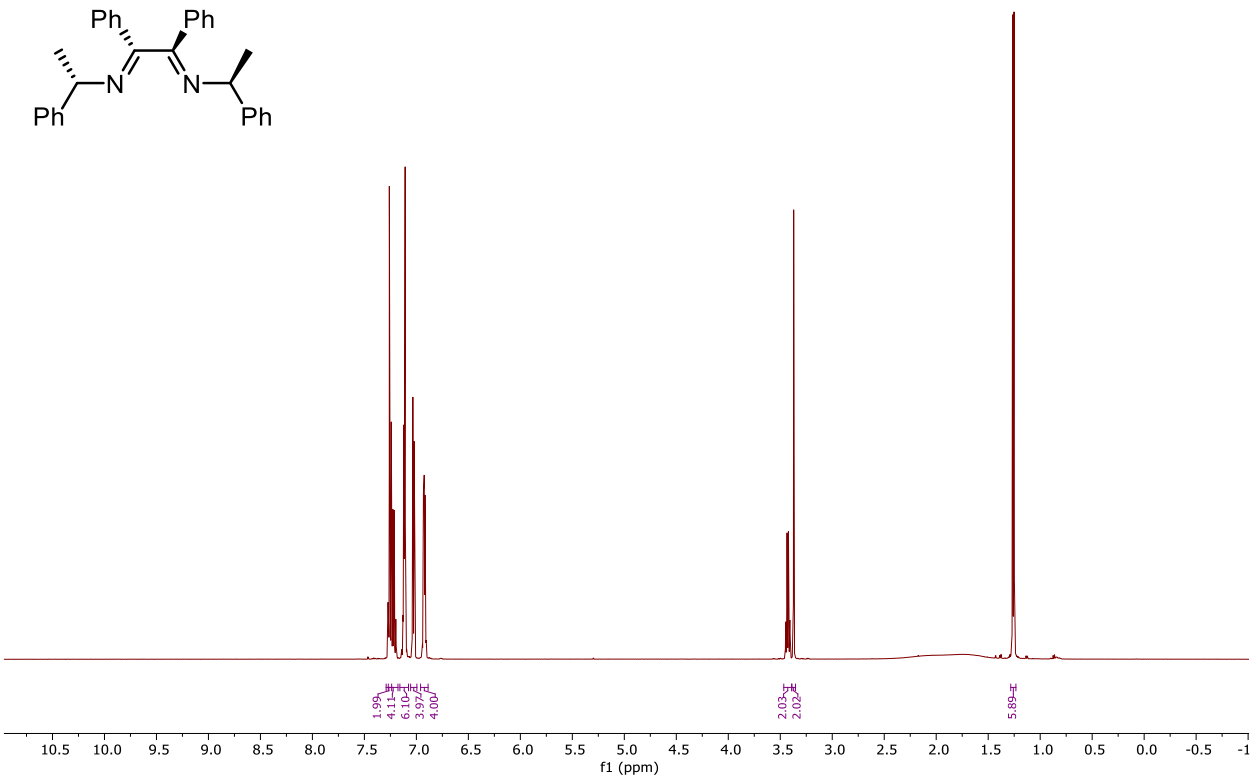

10.1.40 ^{13}C NMR Spectrum of Chiral Amine D (125 MHz, $CDCl_3$)

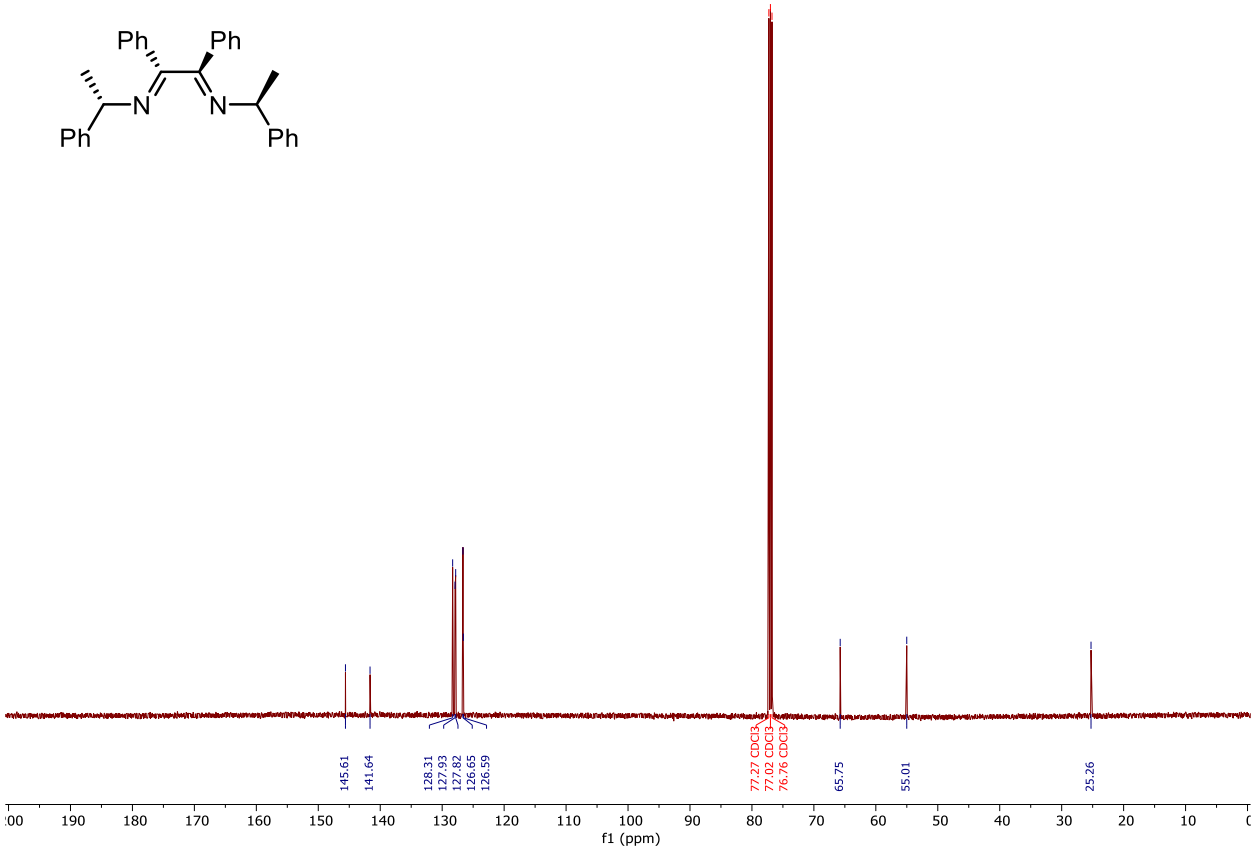

10.2 NMR Spectra Chapter 3

10.2.1 ^{1}H NMR Spectrum of Compound 3.1 (400 MHz, $CDCl_3$)

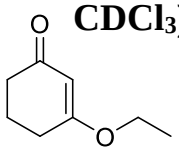

10.2.2 ^{13}C NMR Spectrum of Compound 3.1 (100 MHz, $CDCl_3$)

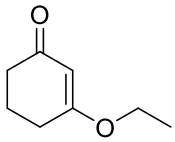

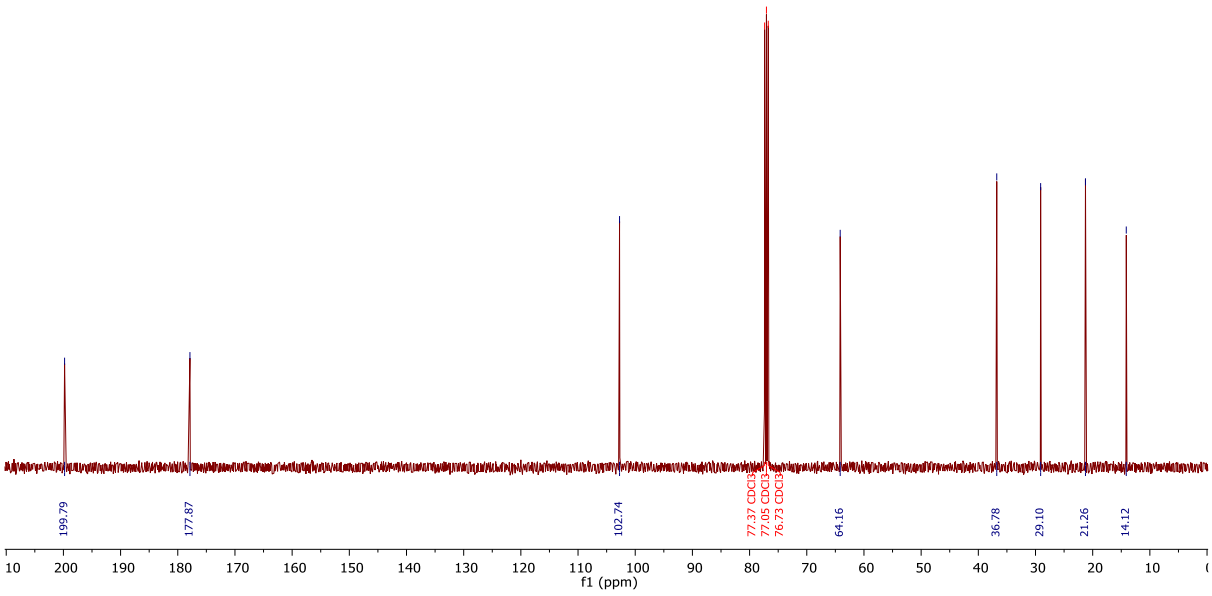

10.2.3 ^{1}H NMR Spectrum of Compound 3.8 (400 MHz, $CDCl_3$)

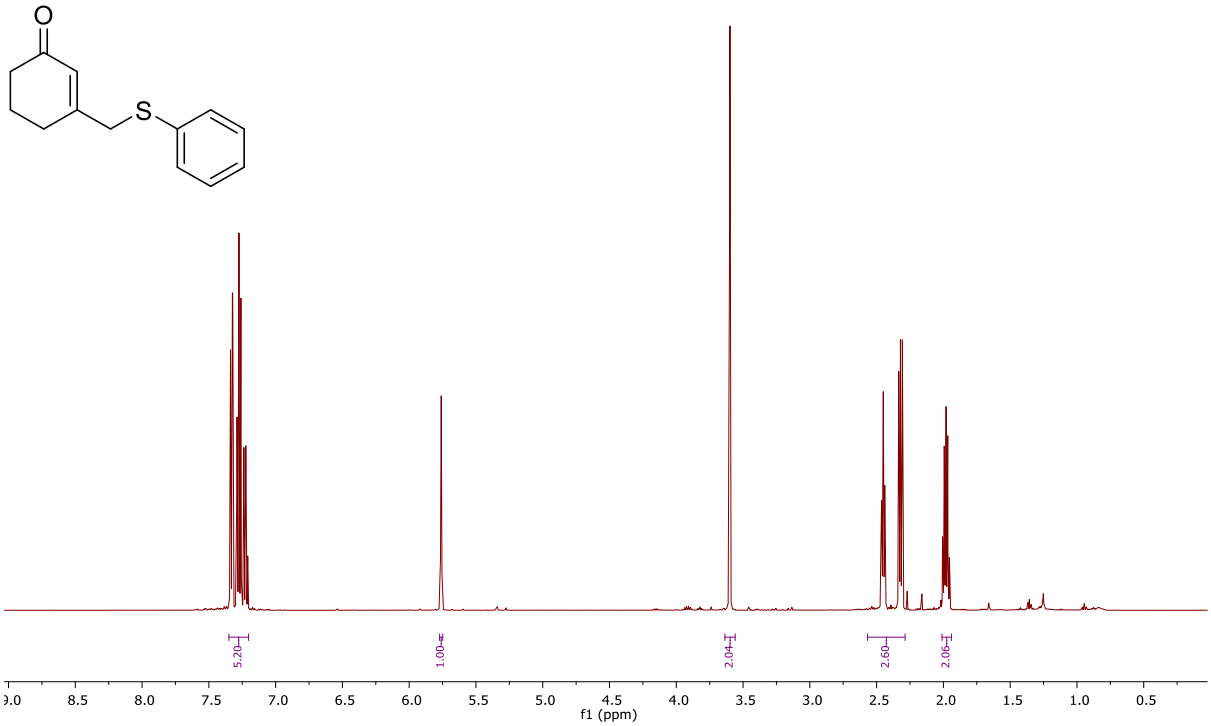

10.2.4 ^{13}C NMR Spectrum of Compound 3.8 (150 MHz, $CDCl_3$)

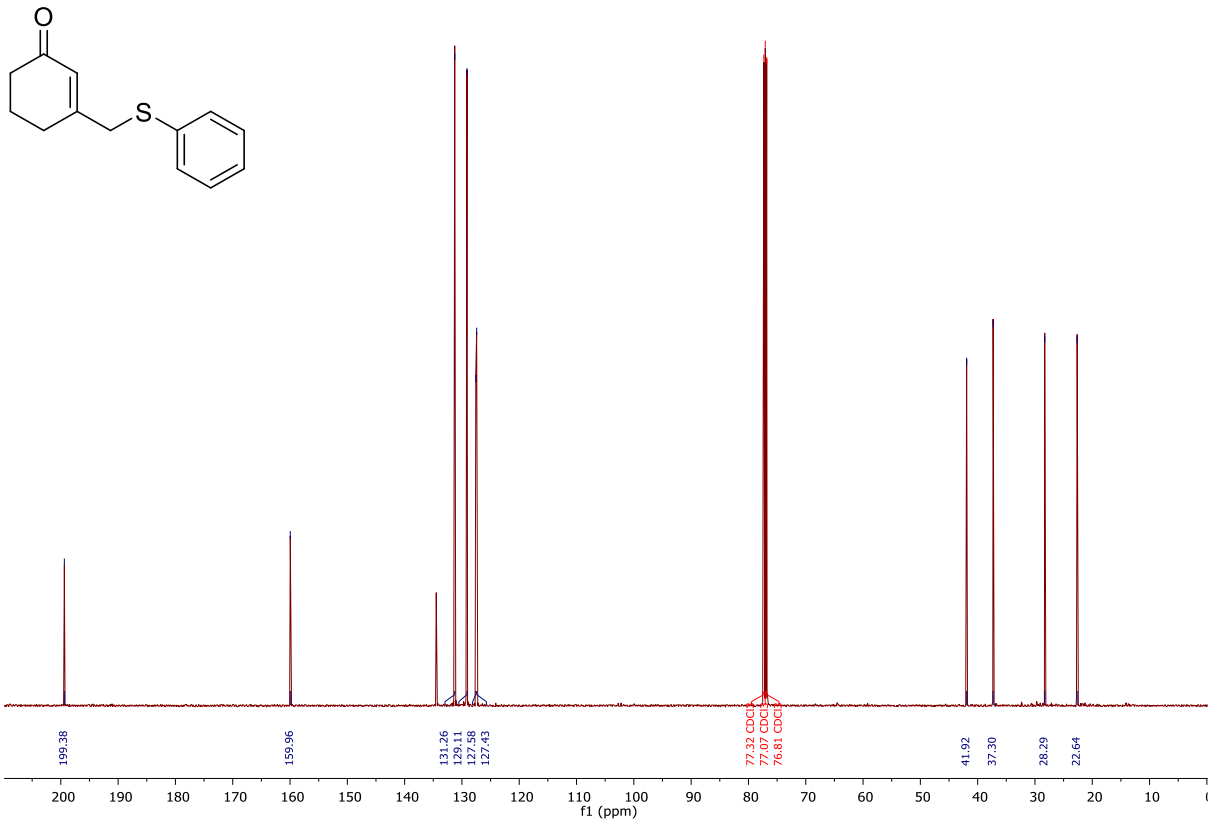

10.2.5 ^{1}H NMR Spectrum of Compound 3.65 (500 MHz, $CDCl_3$)

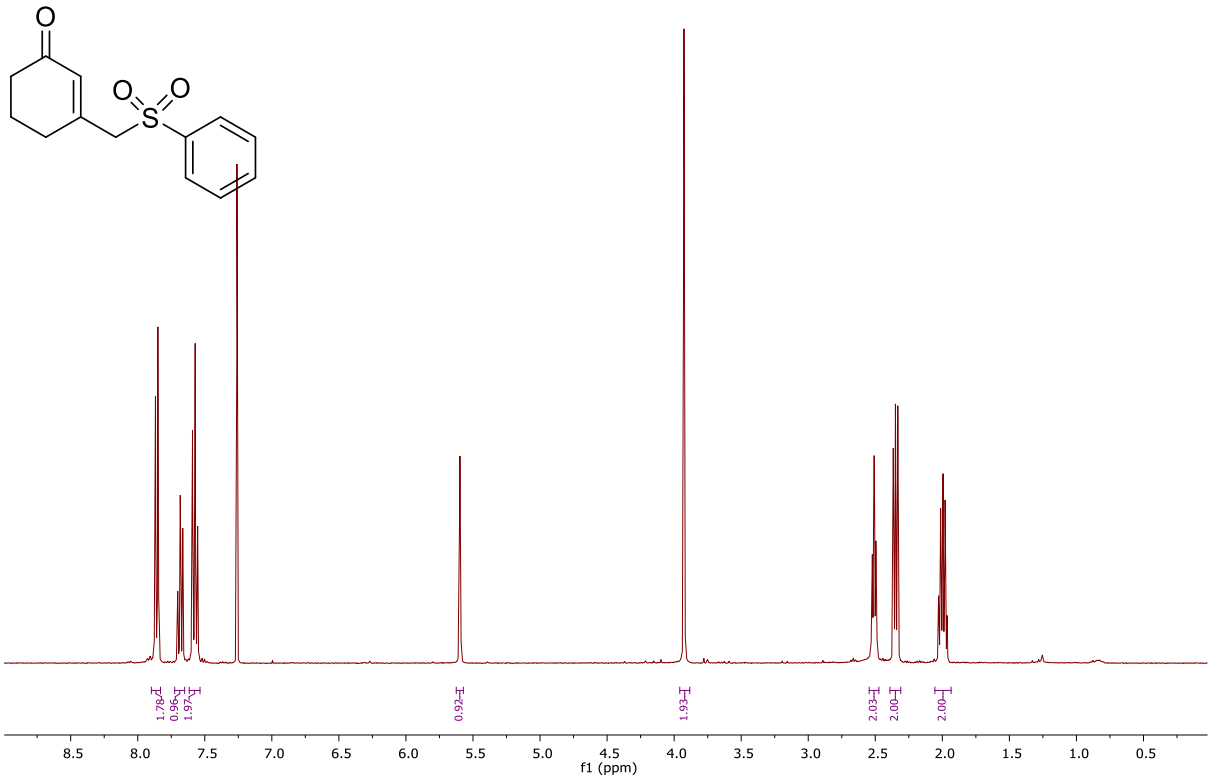

10.2.6 ^{13}C NMR Spectrum of Compound 3.65 (125 MHz, $CDCl_3$)

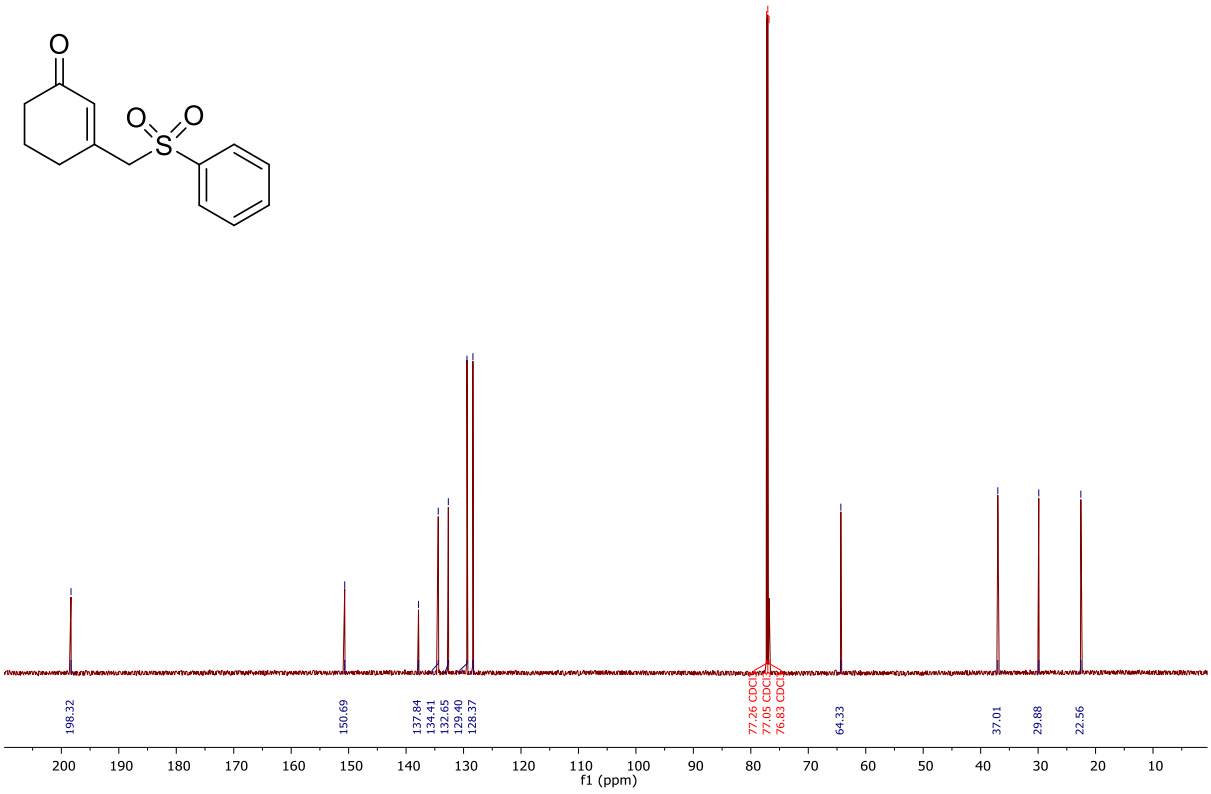

10.2.7 ^{1}H NMR Spectrum of Compound 3.32 (500 MHz, $CDCl_3$)

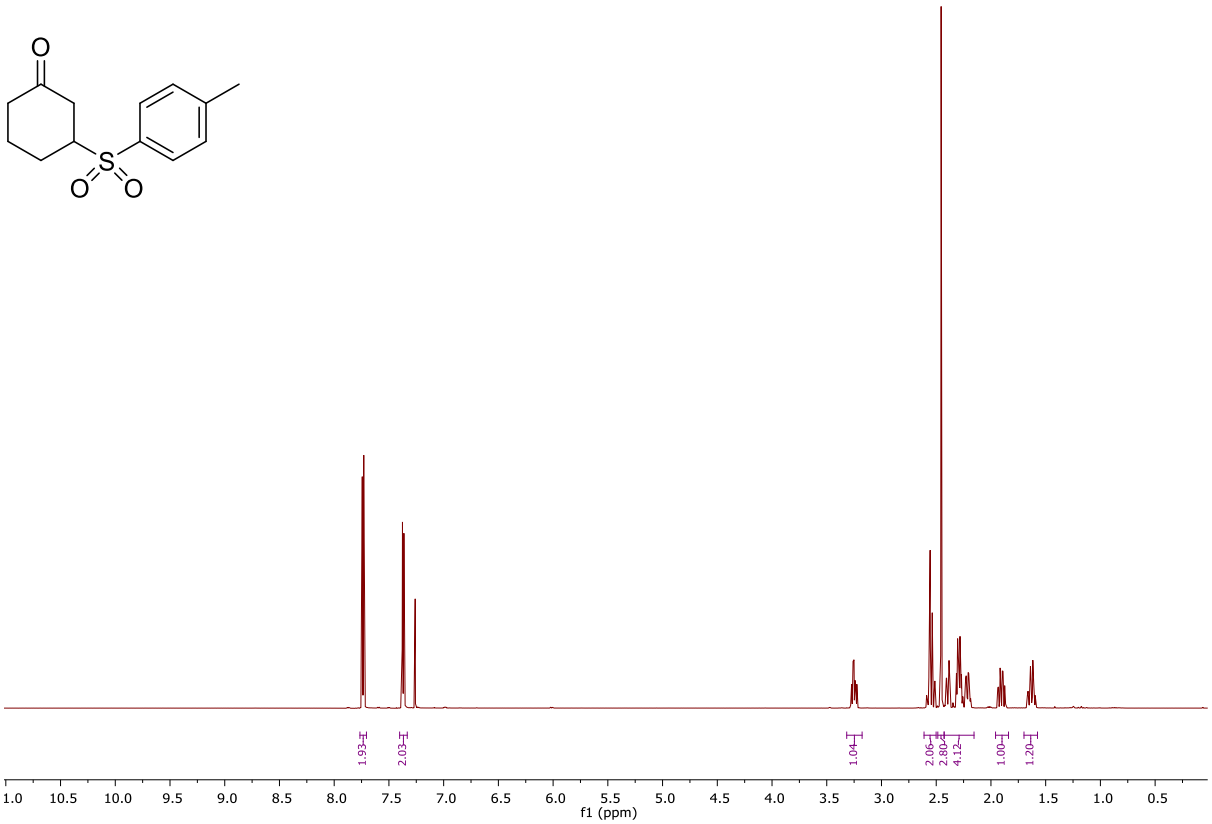

10.2.8 ^{13}C NMR Spectrum of Compound 3.32 (150 MHz, $CDCl_3$)

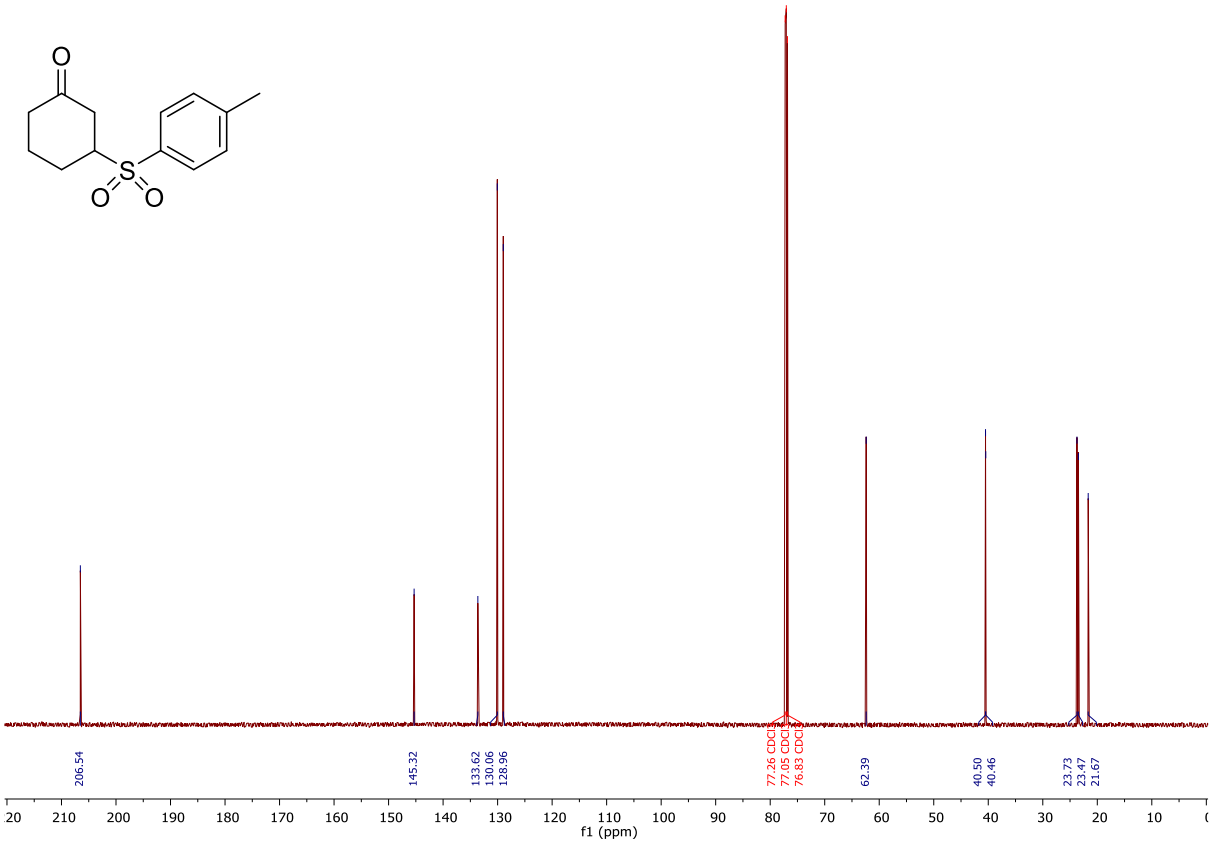

10.2.9 ^{1}H NMR Spectrum of Compound 3.33 (600 MHz, $CDCl_3$)

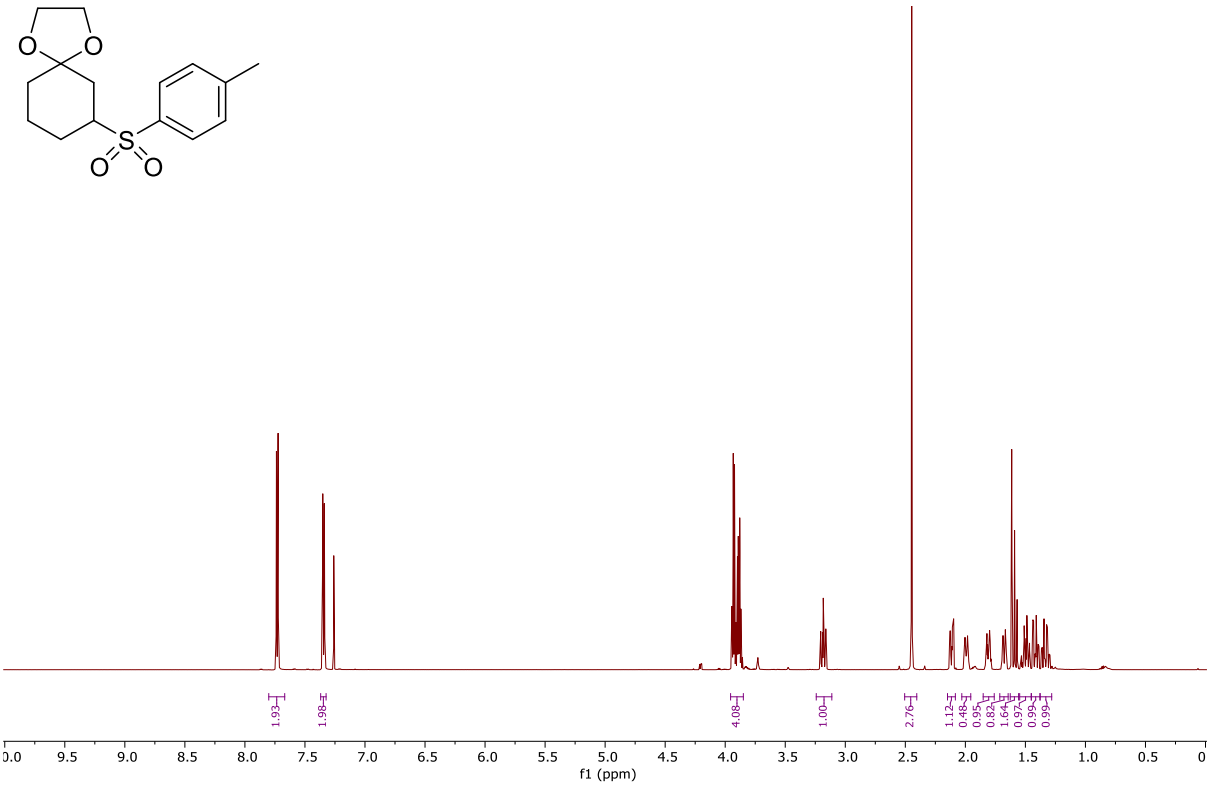

10.2.10 ^{13}C NMR Spectrum of Compound 3.33 (150 MHz, $CDCl_3$)

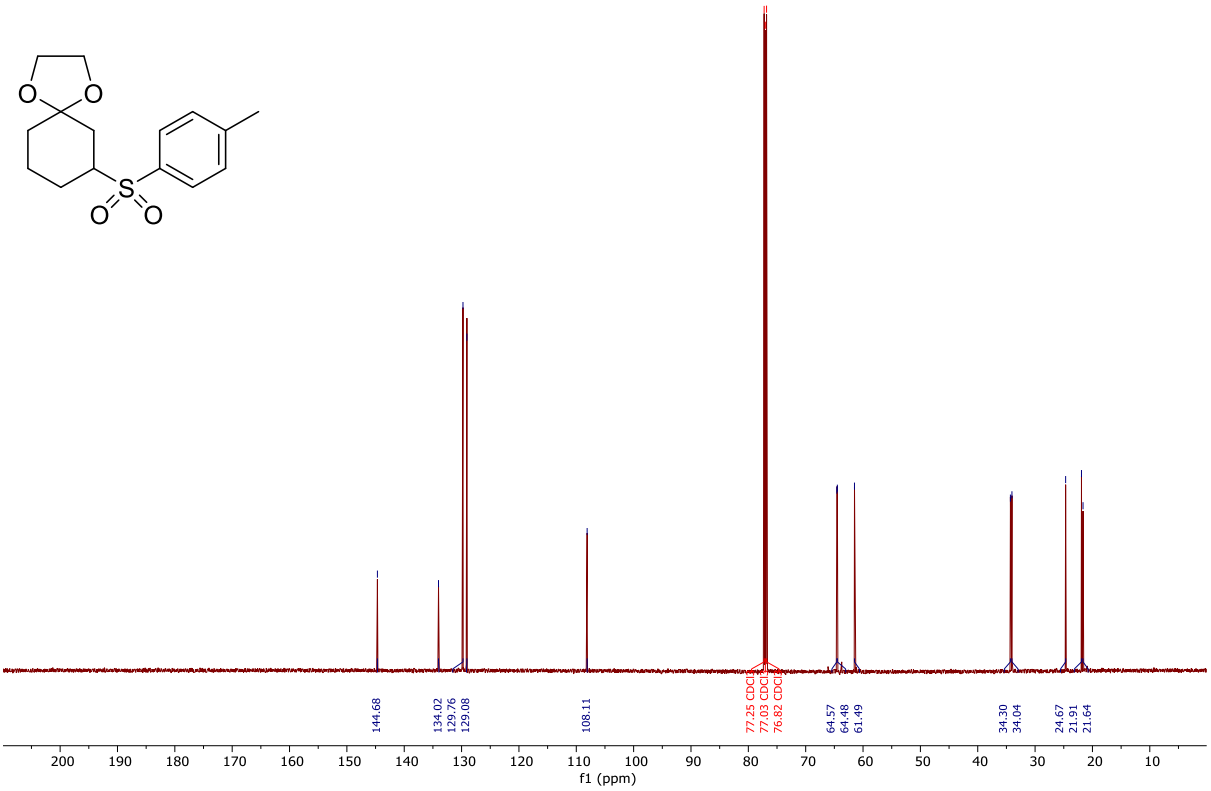

10.2.11 ^{1}H NMR Spectrum of Compound 3.43 (600 MHz, $CDCl_3$)

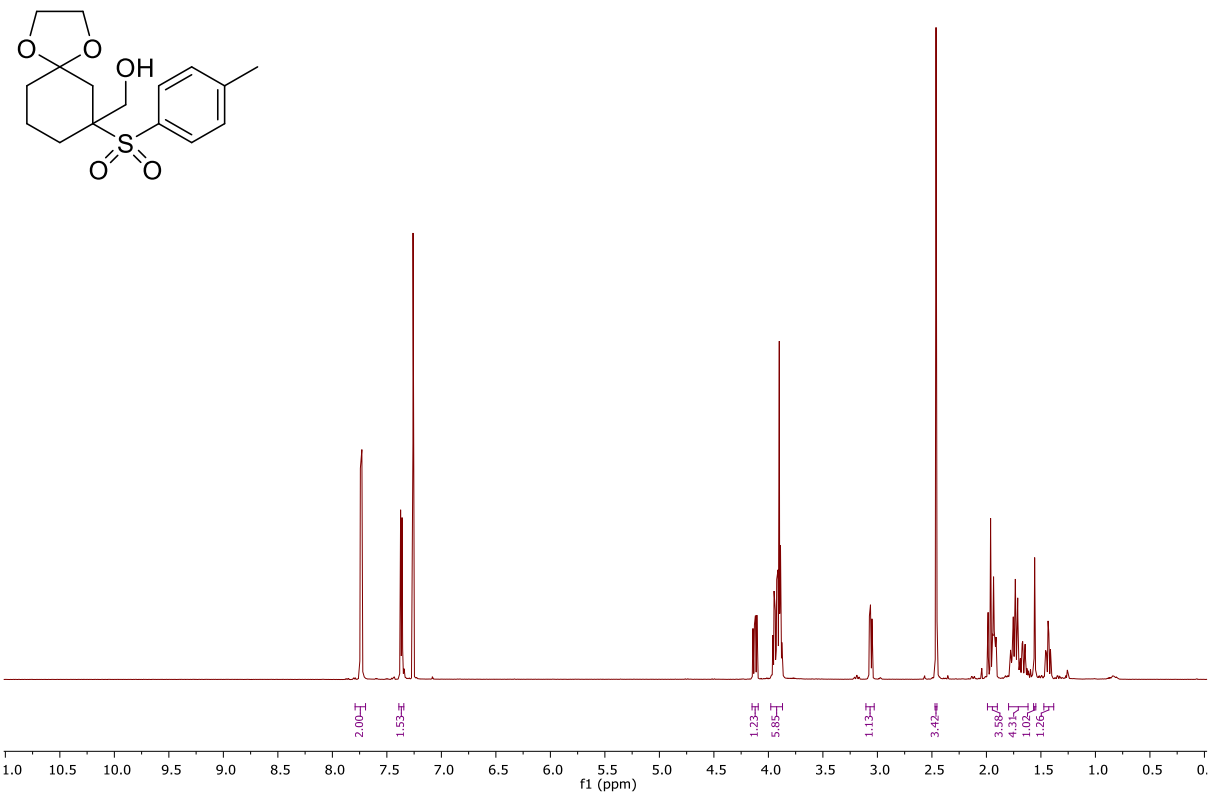

10.2.12 ^{13}C NMR Spectrum of Compound 3.43 (150 MHz, $CDCl_3$)

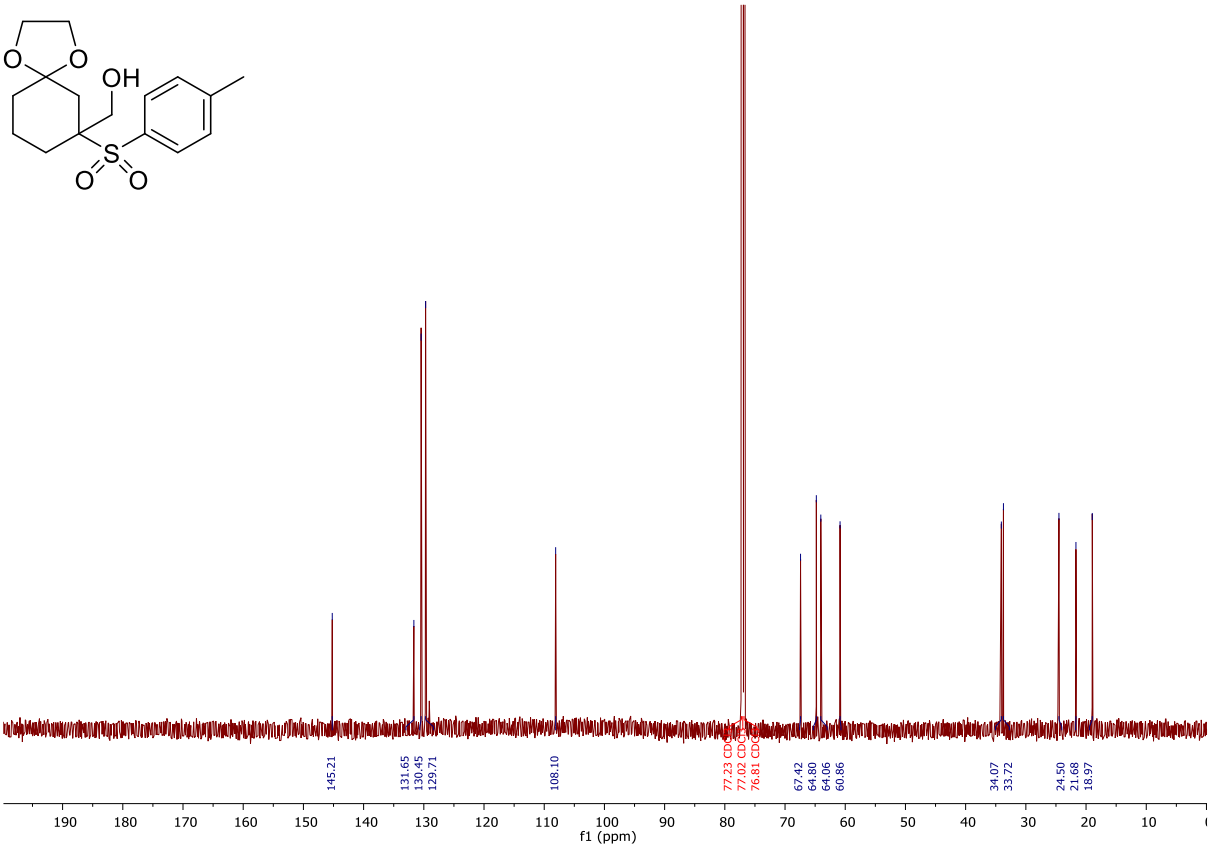

10.2.13 ^{1}H NMR Spectrum of Compound 3.34 (600 MHz, $CDCl_3$)

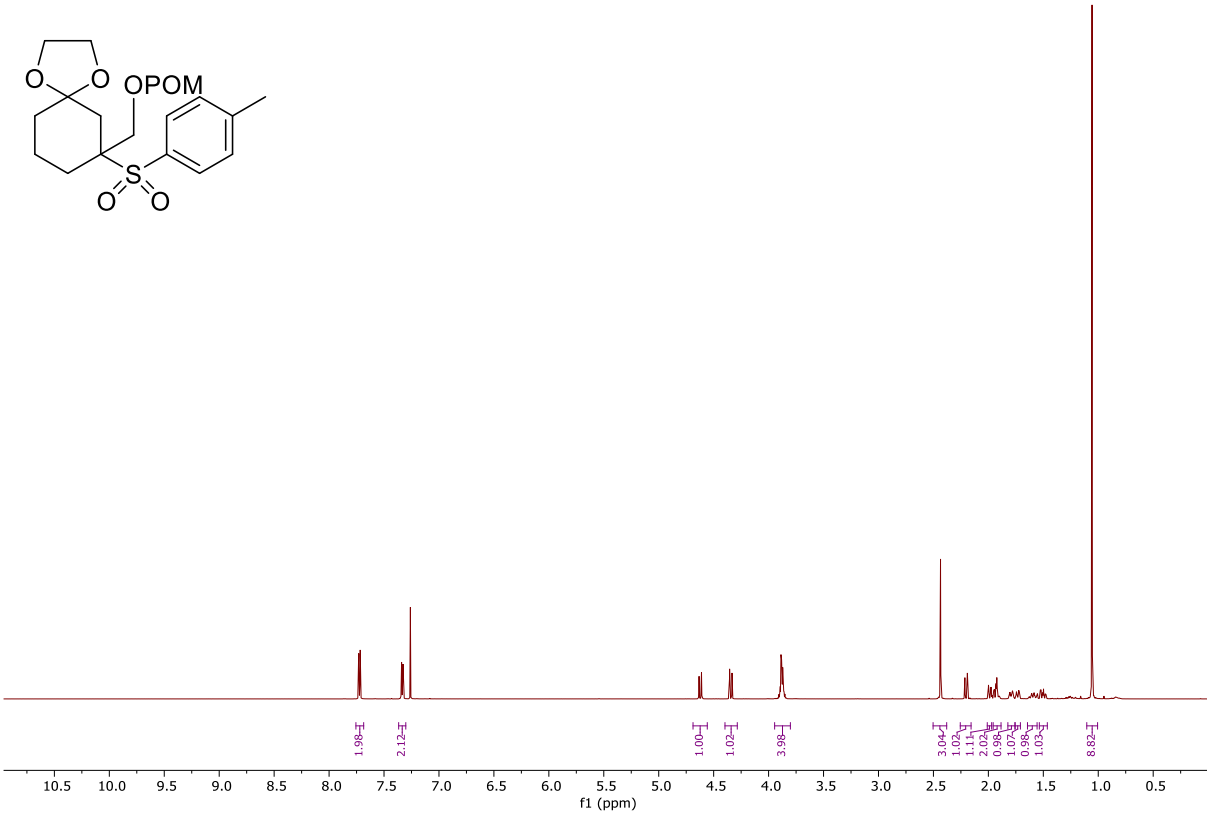

10.2.14 ^{13}C NMR Spectrum of Compound 3.34 (150 MHz, $CDCl_3$)

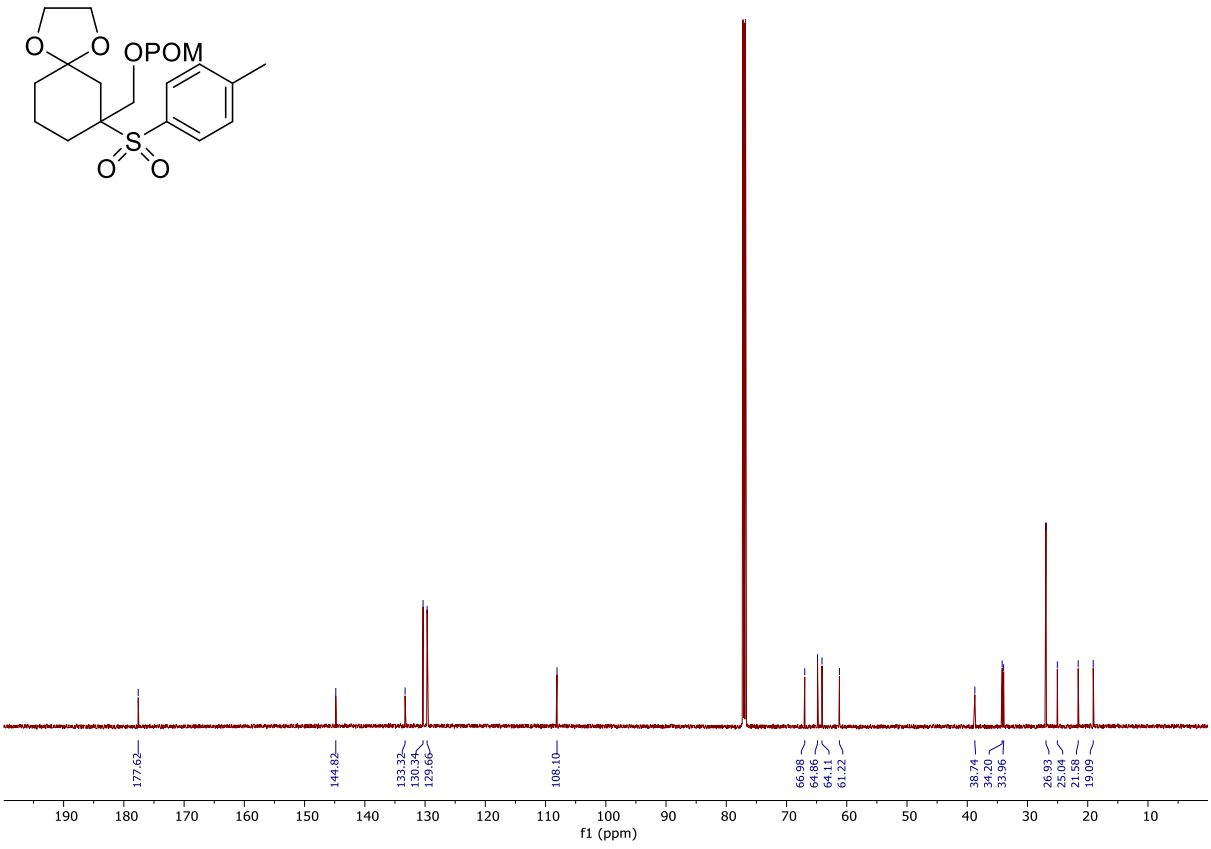

10.2.15 ^{1}H NMR Spectrum of Compound 3.44 (600 MHz, $CDCl_3$)

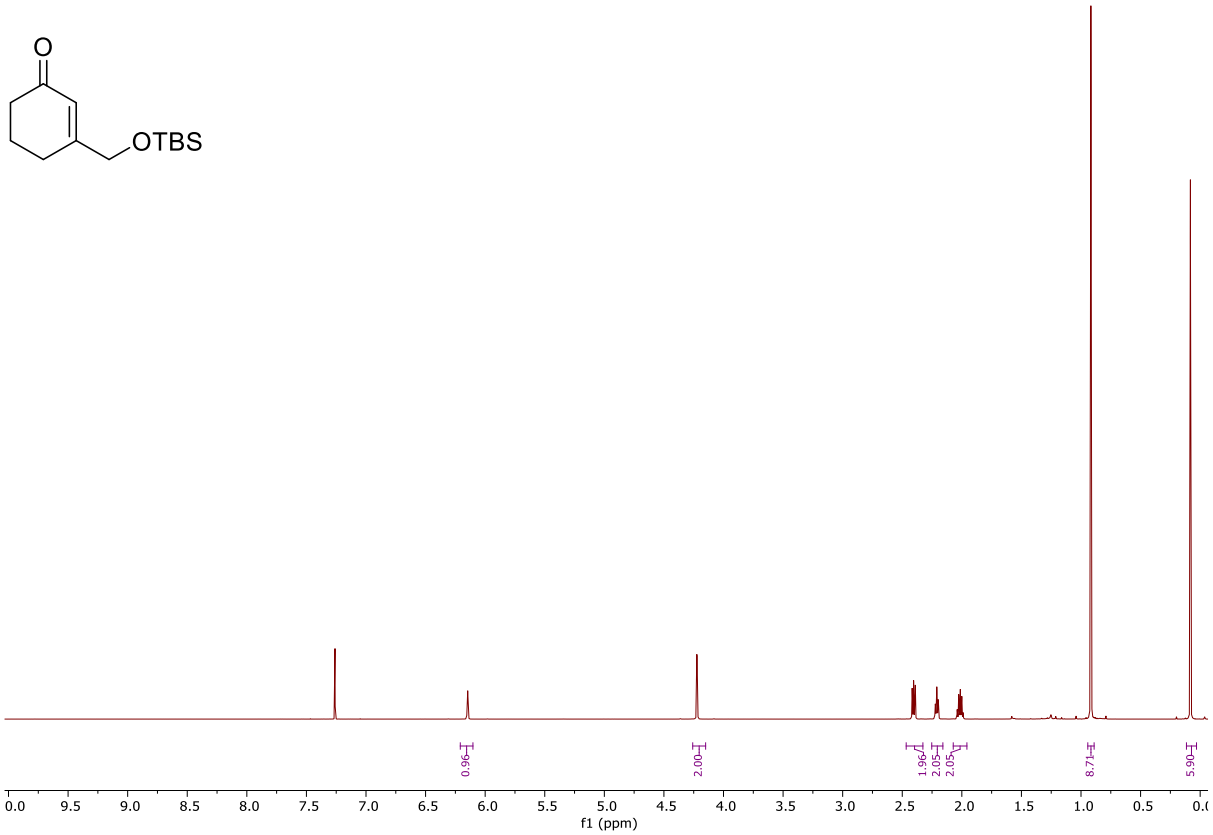

10.2.16 ^{13}C NMR Spectrum of Compound 3.44 (150 MHz, $CDCl_3$)

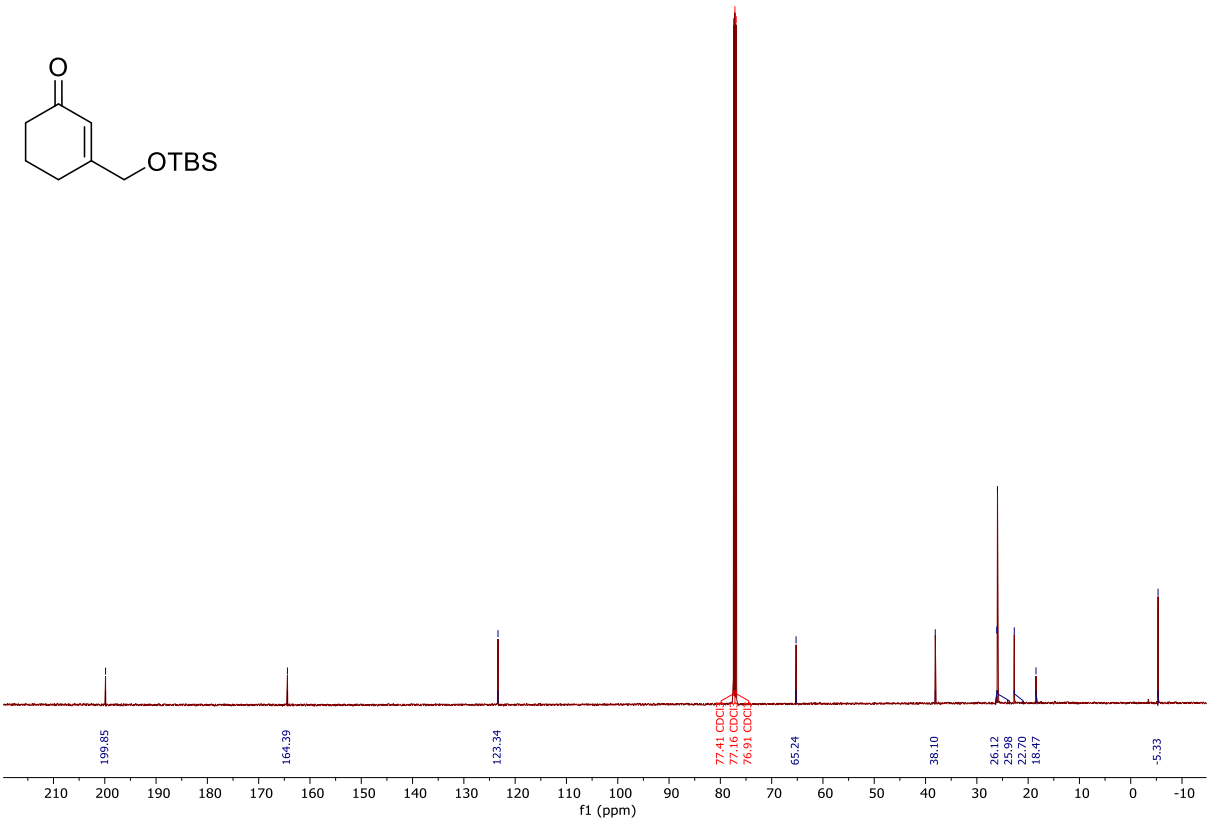

10.2.17 ^{1}H NMR Spectrum of Compound 3.35 (600 MHz, $CDCl_3$)

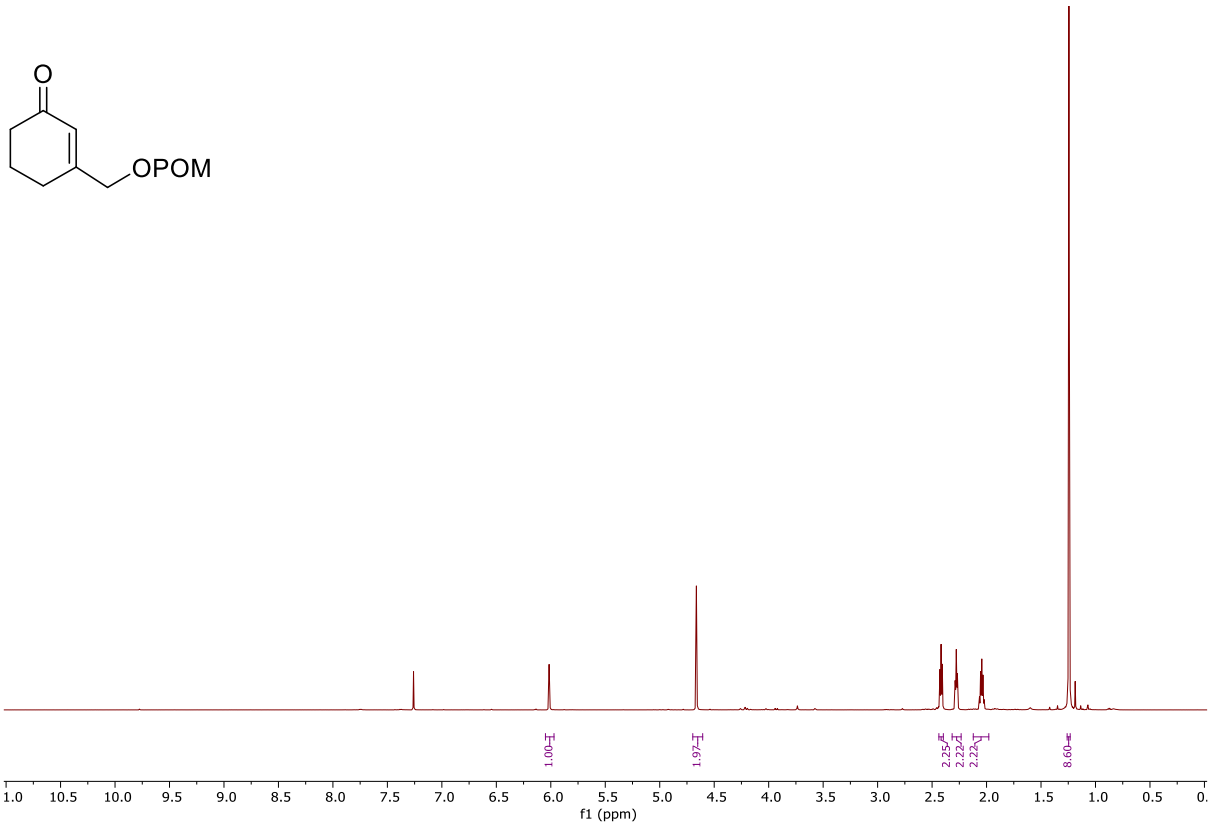

10.2.18 ^{13}C NMR Spectrum of Compound 3.35 (150 MHz, $CDCl_3$)

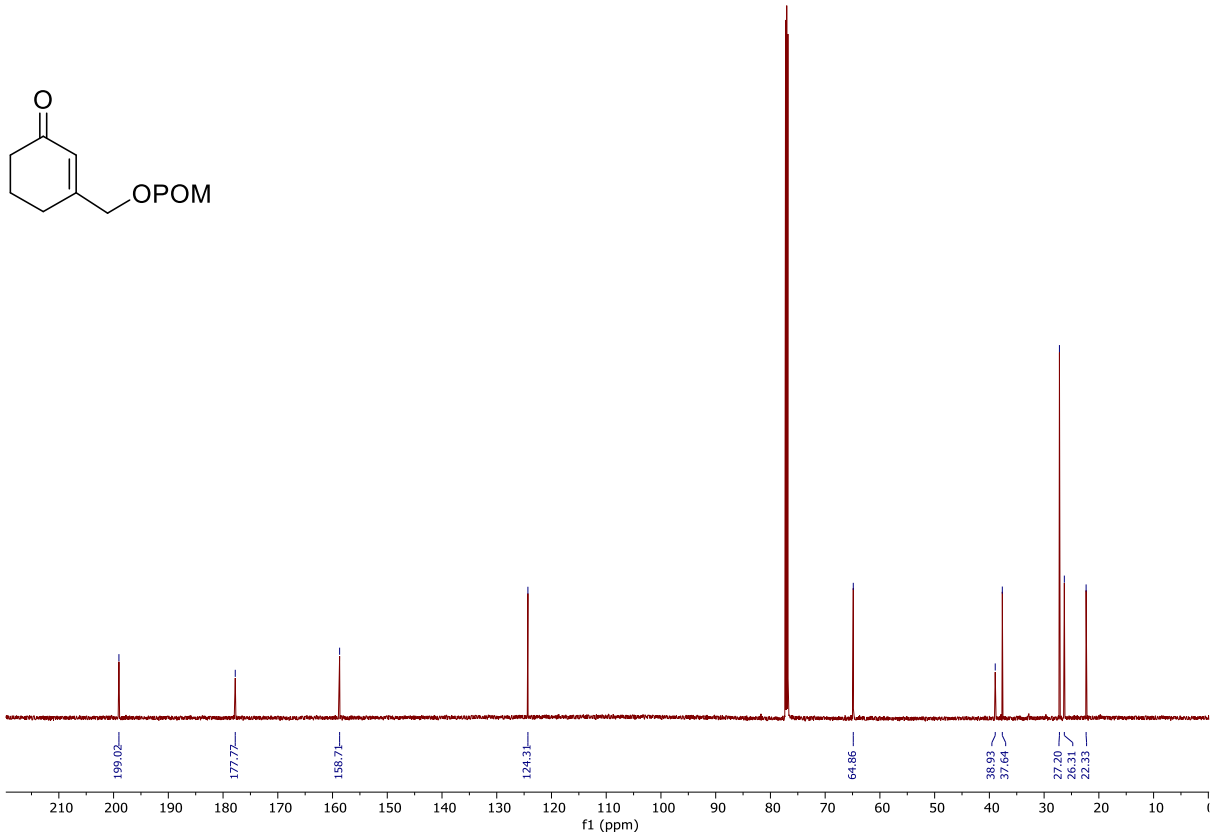

10.2.19 ^{1}H NMR Spectrum of Compound 3.6 (500 MHz, $CDCl_3$)

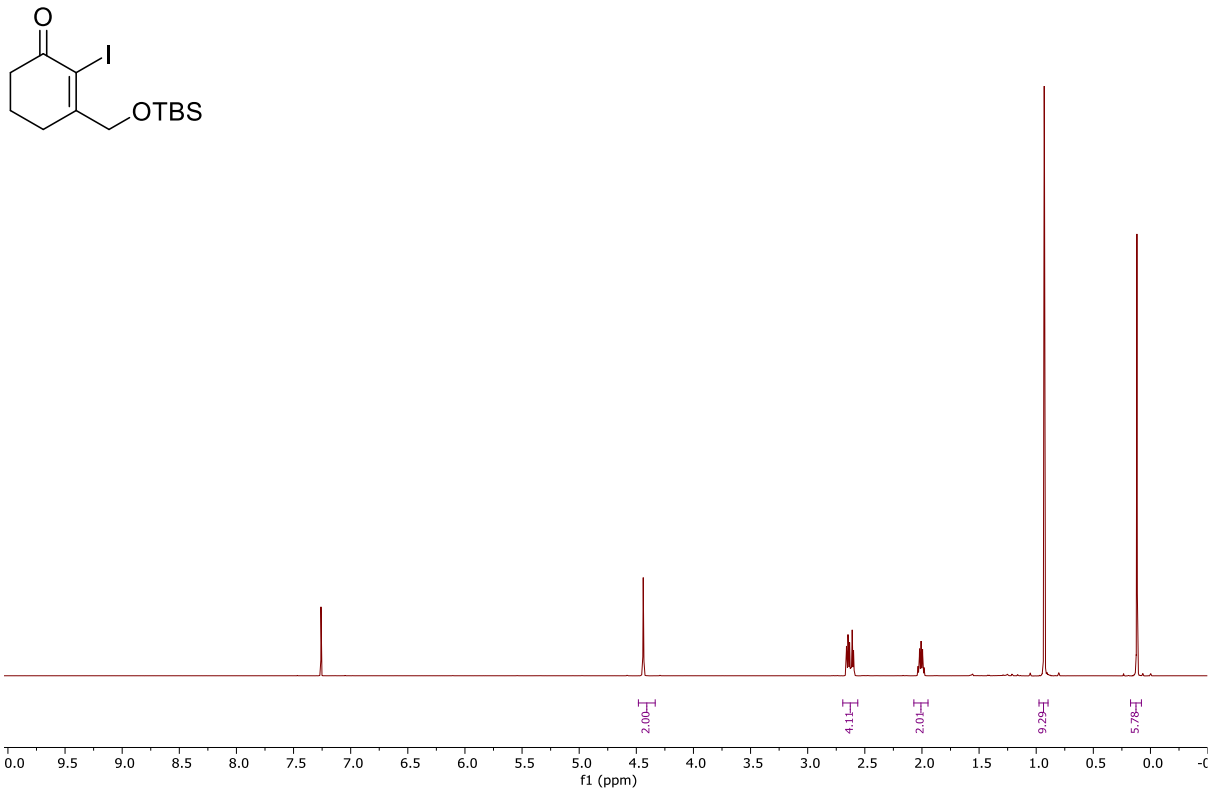

10.2.20 ^{13}C NMR Spectrum of Compound 3.6 (150 MHz, $CDCl_3$)

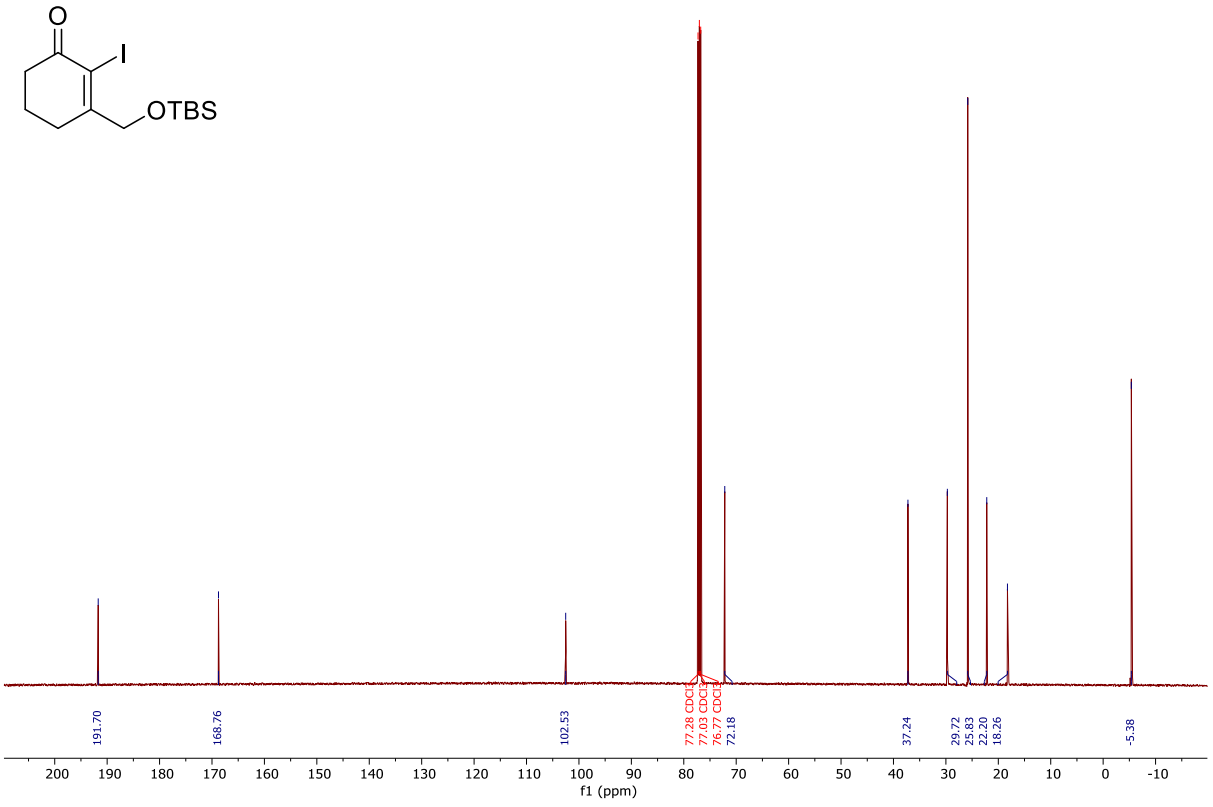

10.2.21 ^{1}H NMR Spectrum of Compound 3.36 (500 MHz, $CDCl_3$)

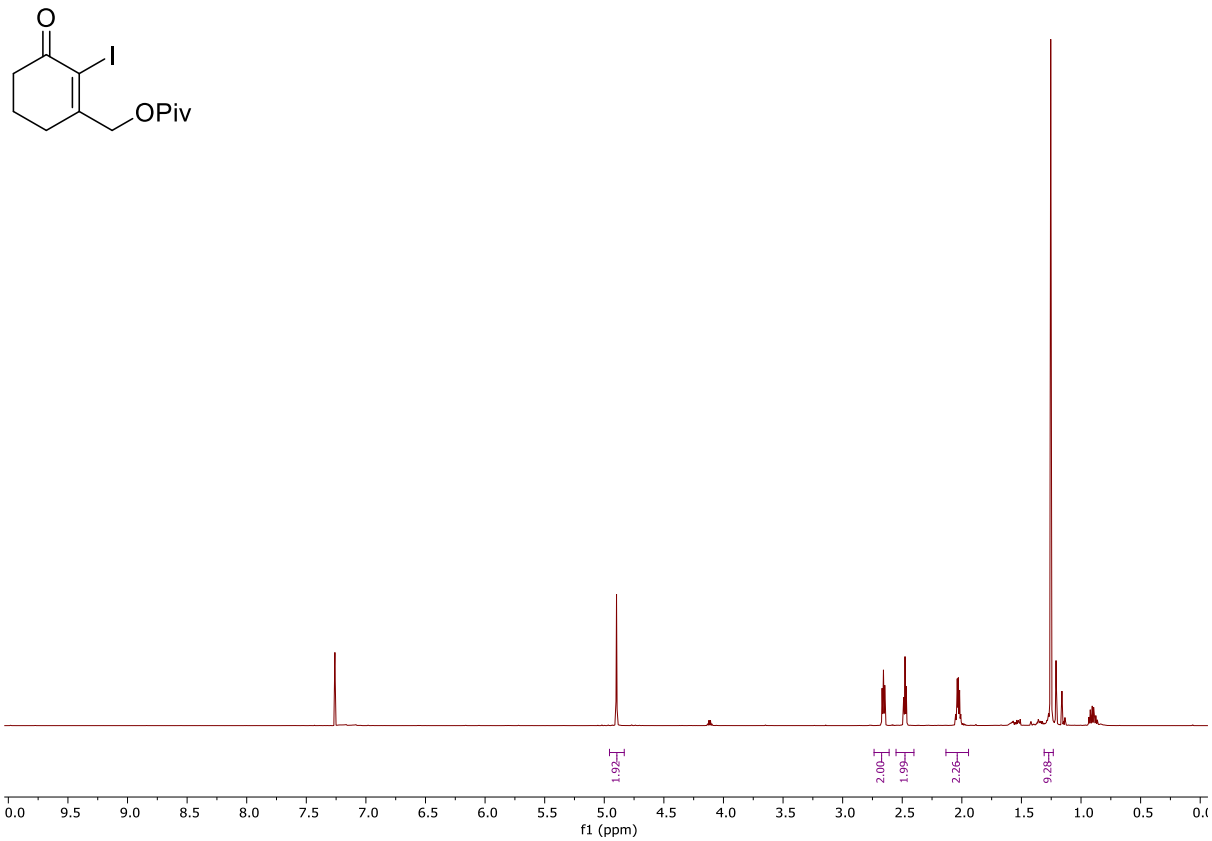

10.2.22 ^{13}C NMR Spectrum of Compound 3.36 (150 MHz, $CDCl_3$)

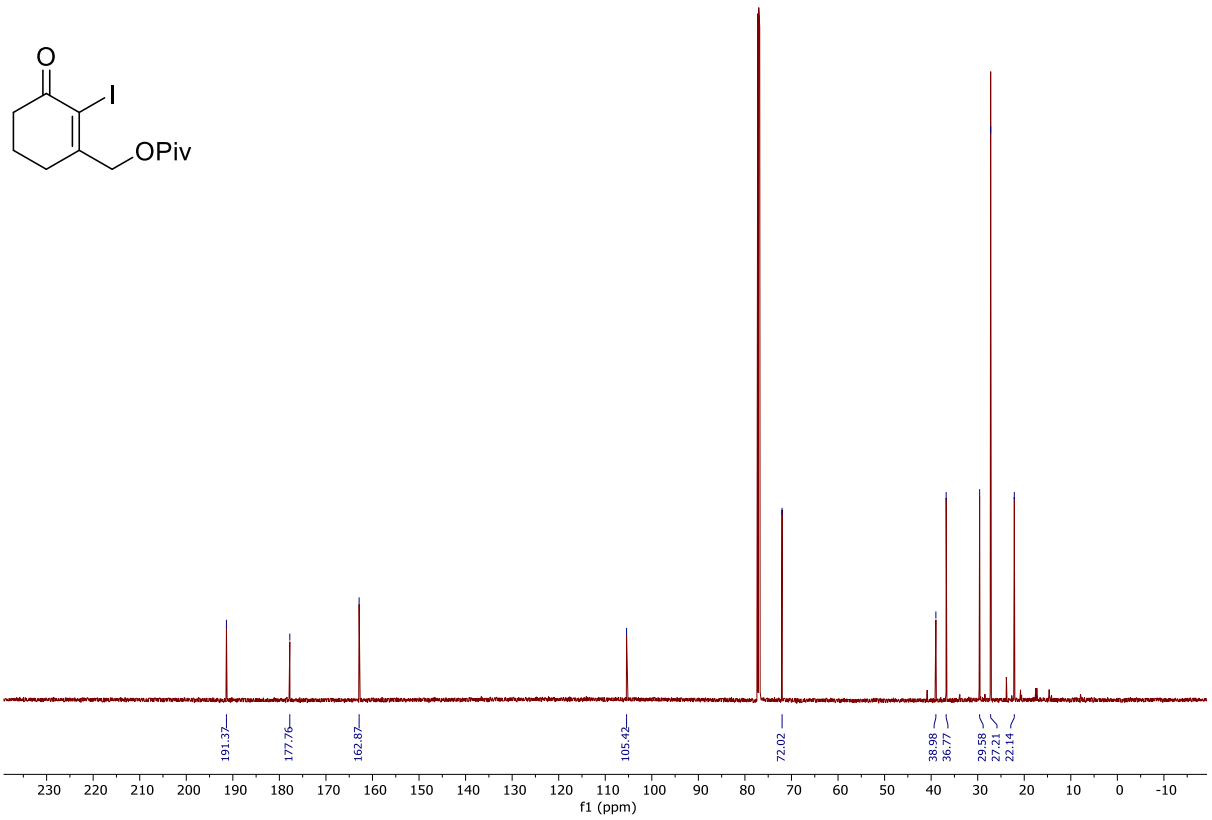

10.2.23 ^{1}H NMR Spectrum of Compound 3.45 (500 MHz, $CDCl_3$)

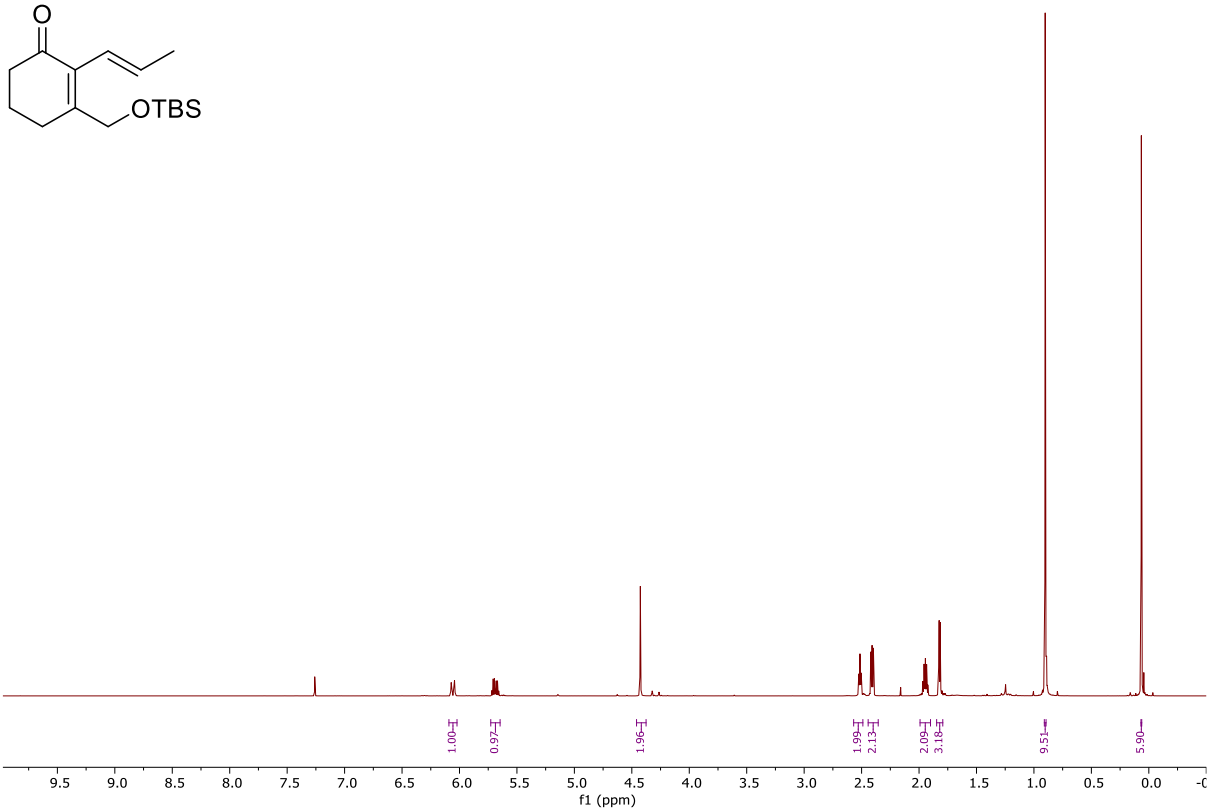

10.2.24 ^{13}C NMR Spectrum of Compound 3.45 (150 MHz, $CDCl_3$)

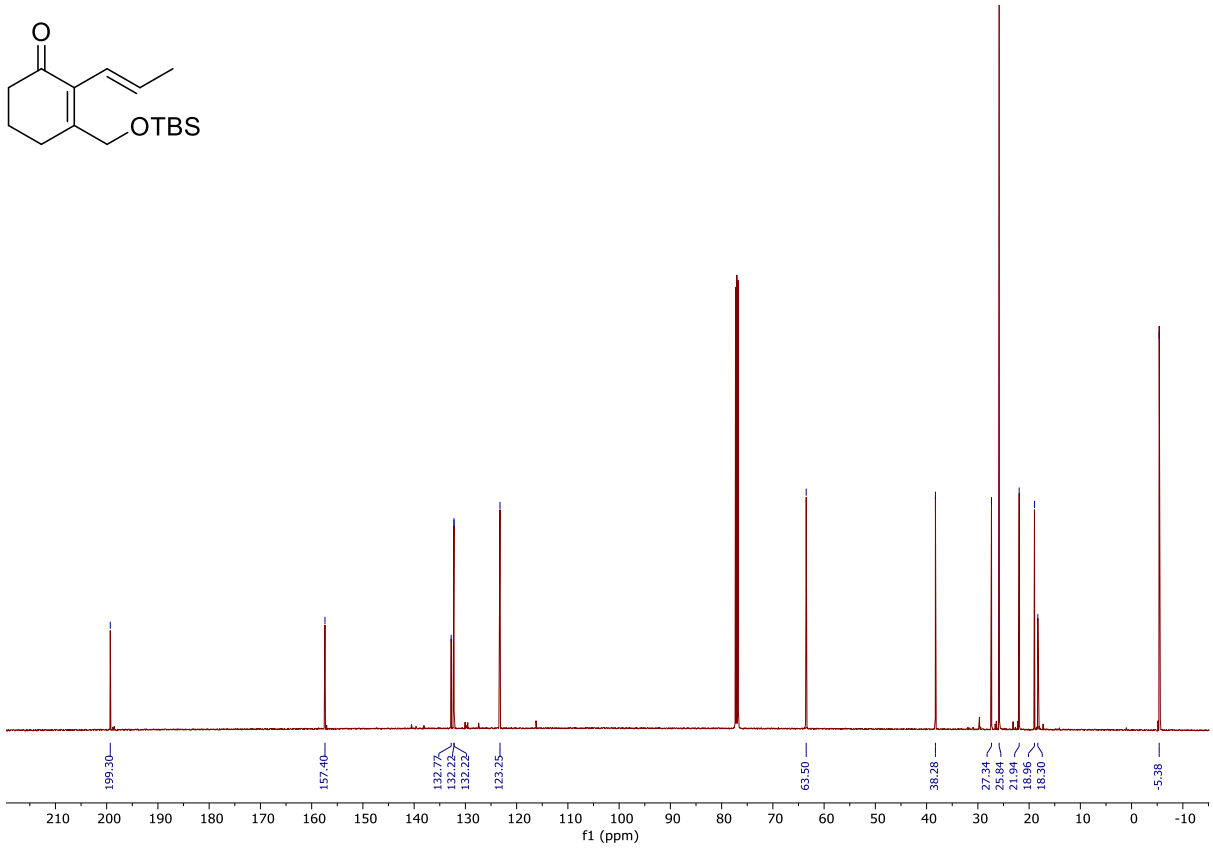

10.2.25 ^{1}H NMR Spectrum of Compound 3.38 (500 MHz, $CDCl_3$)

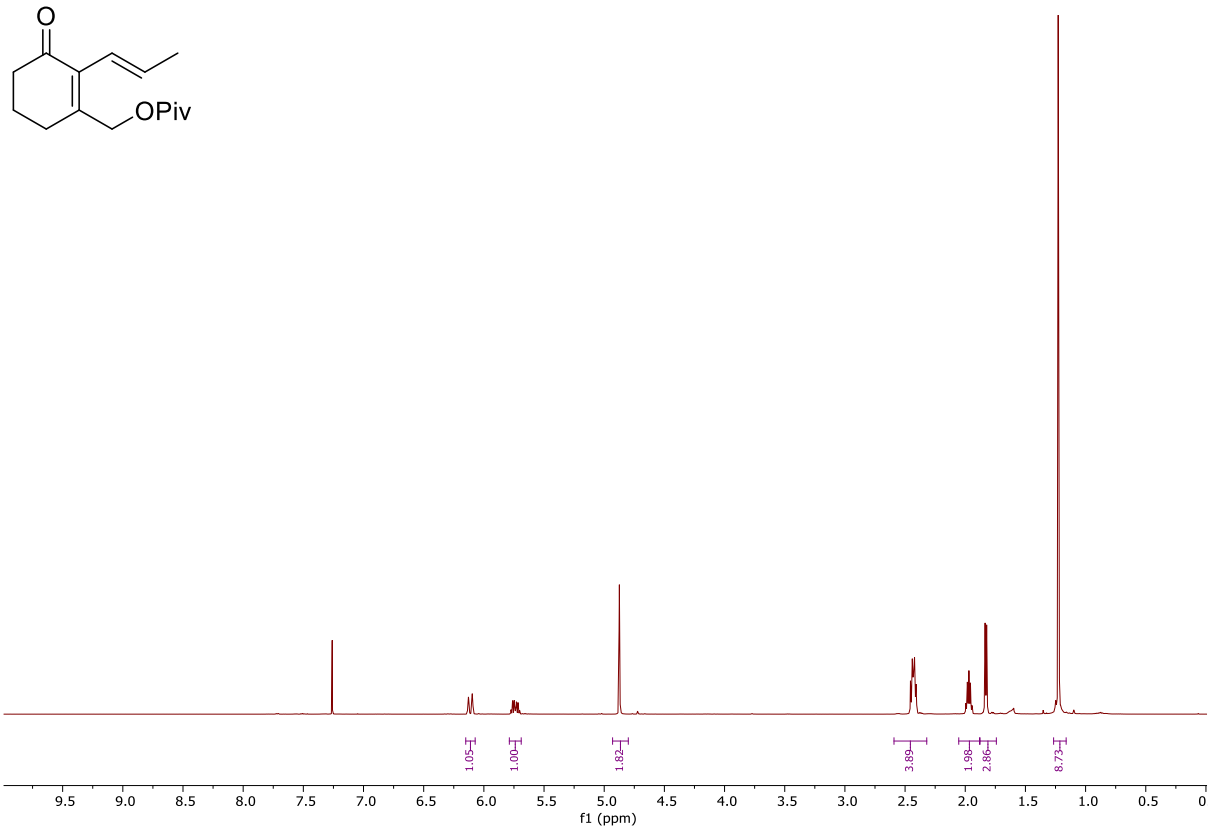

10.2.26 ^{13}C NMR Spectrum of Compound 3.38 (150 MHz, $CDCl_3$)

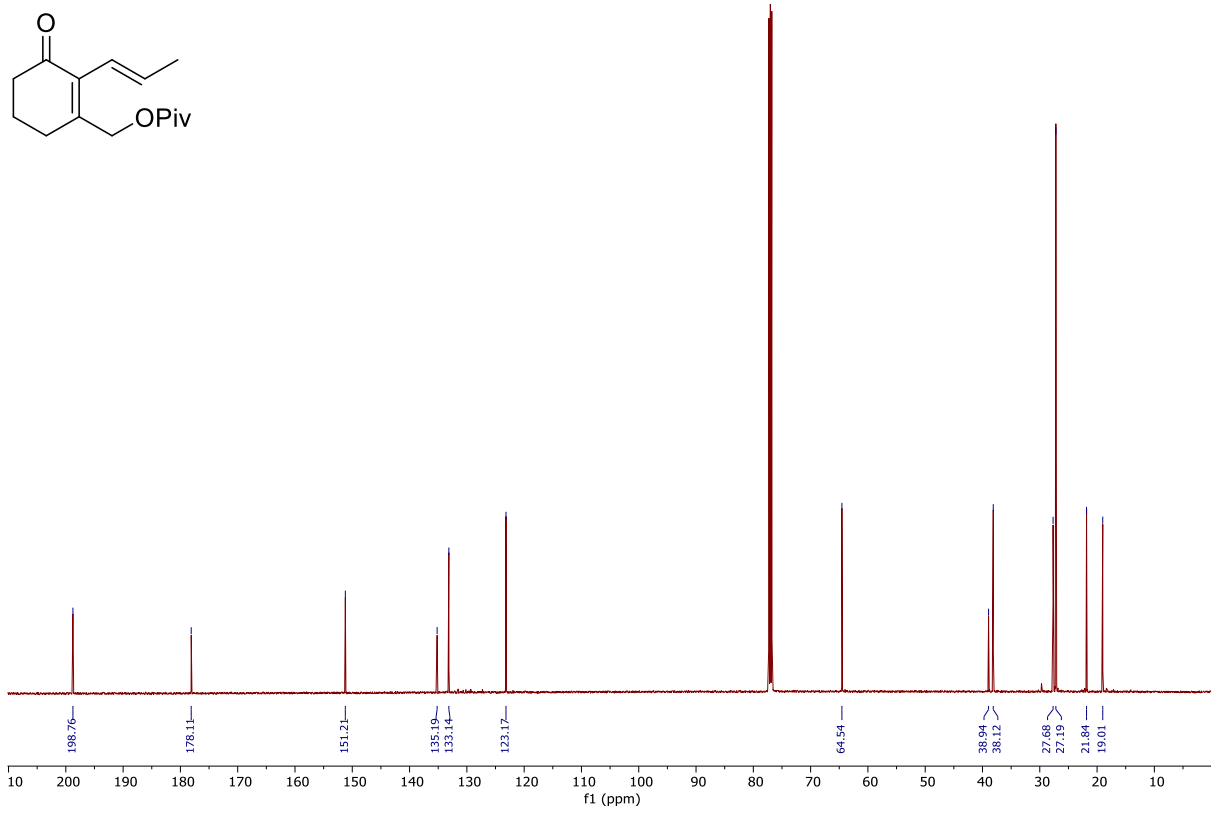

10.2.27 ^{1}H NMR Spectrum of Compound 1.27 (800 MHz, $CDCl_3$)

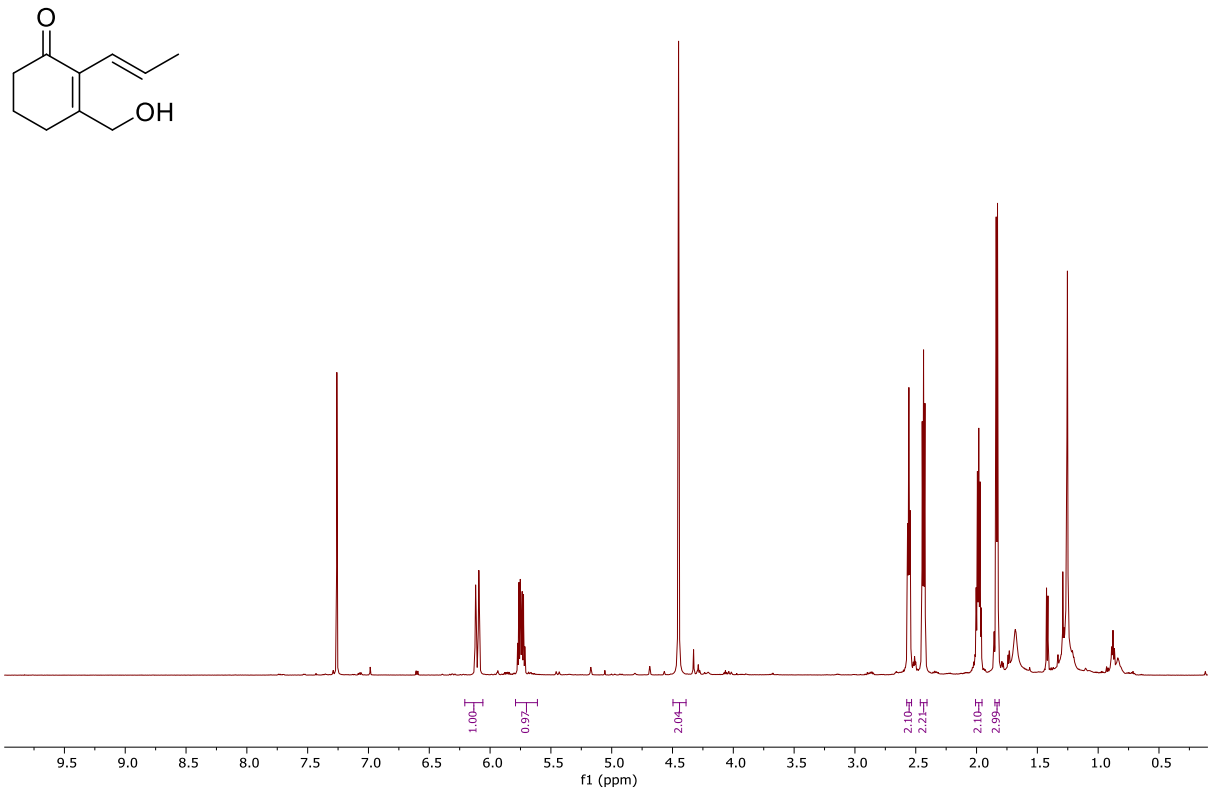

10.2.28 ^{13}C NMR Spectrum of Compound 1.27 (150 MHz, $CDCl_3$)

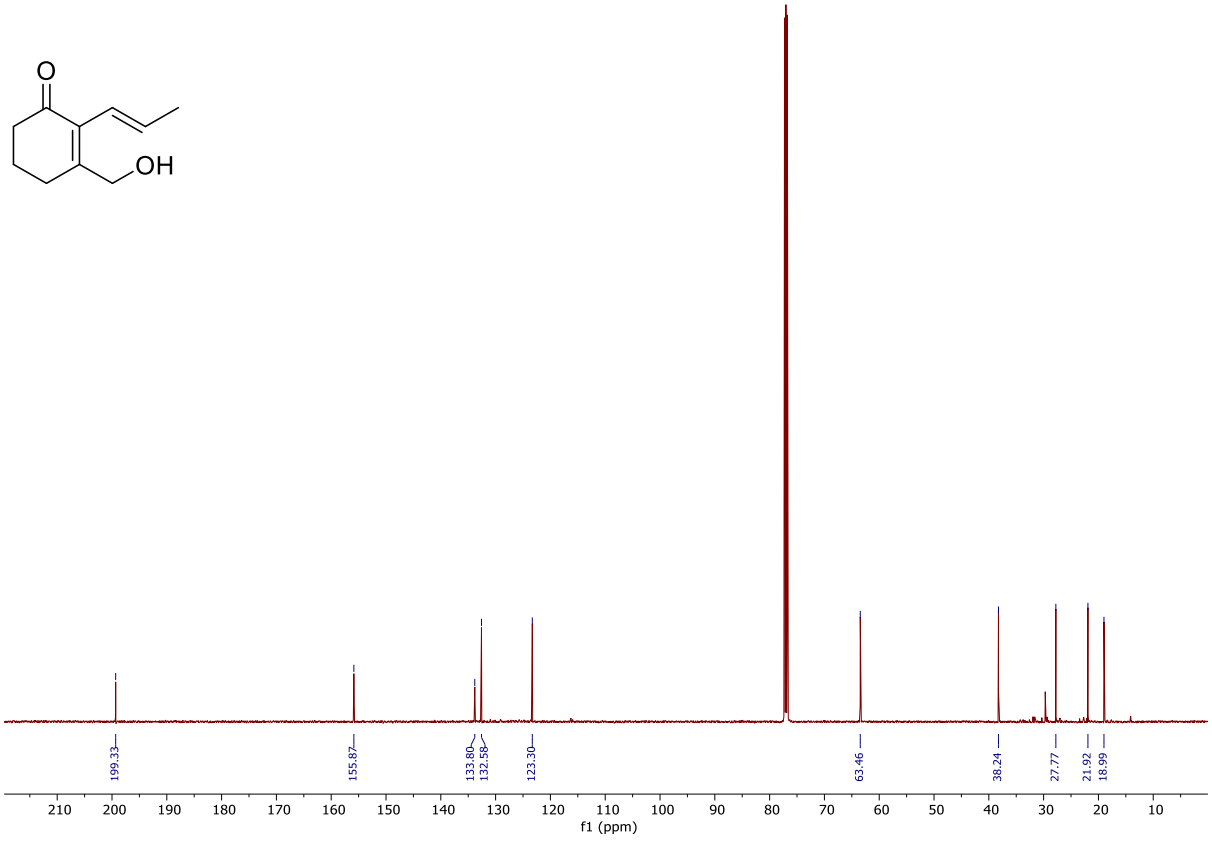

10.2.29 ^{1}H NMR Spectrum of Compound (±)-1.31 (800 MHz, $CDCl_3$)

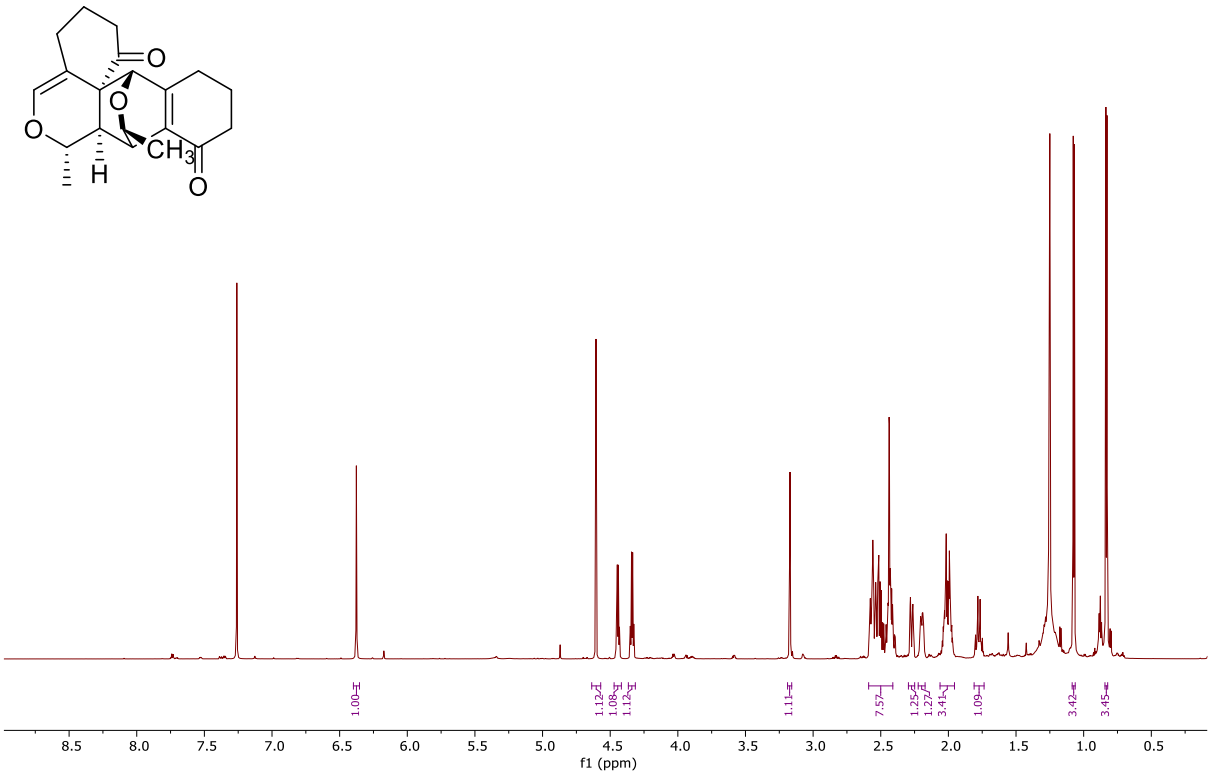

10.2.30 ^{13}C NMR Spectrum of Compound (±)-1.31 (150 MHz, $CDCl_3$)

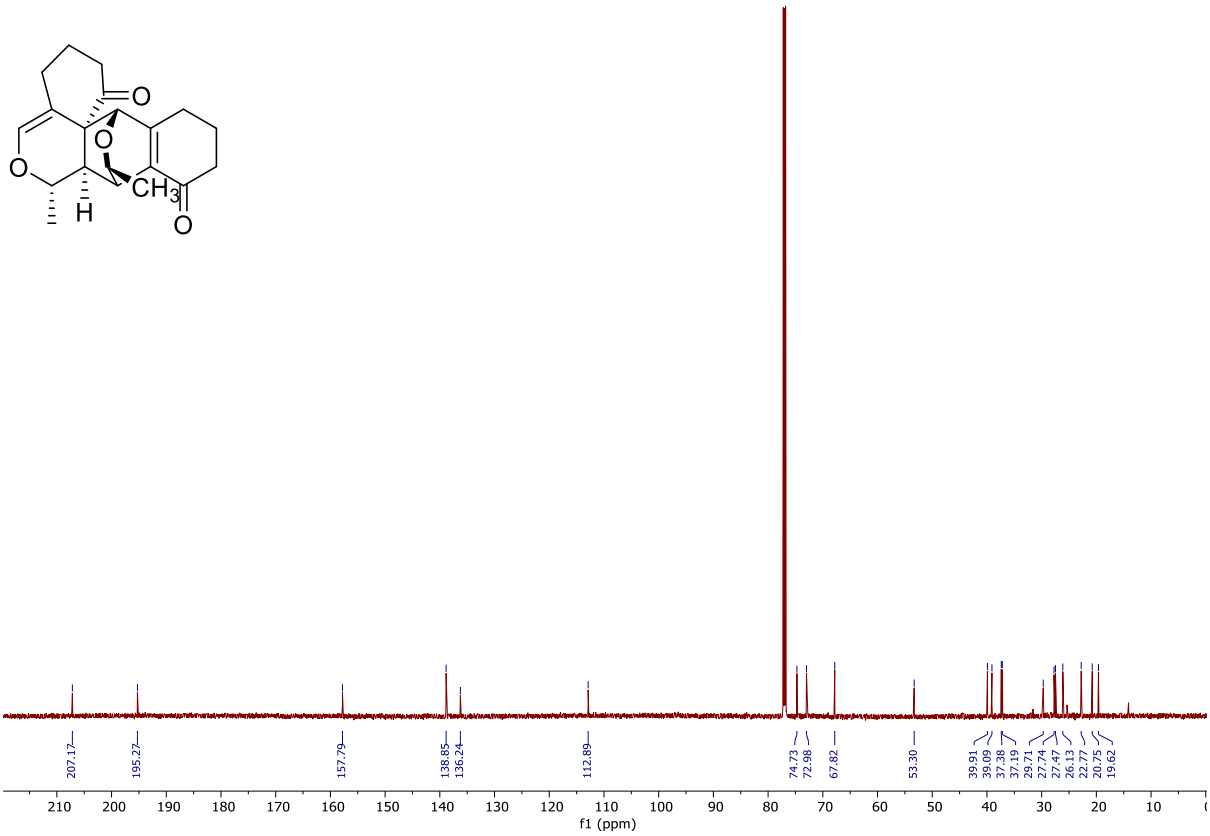

10.2.31 ^{1}H-^{1}H COSY Spectrum of Compound (±)-1.31 ($CDCl_3$)

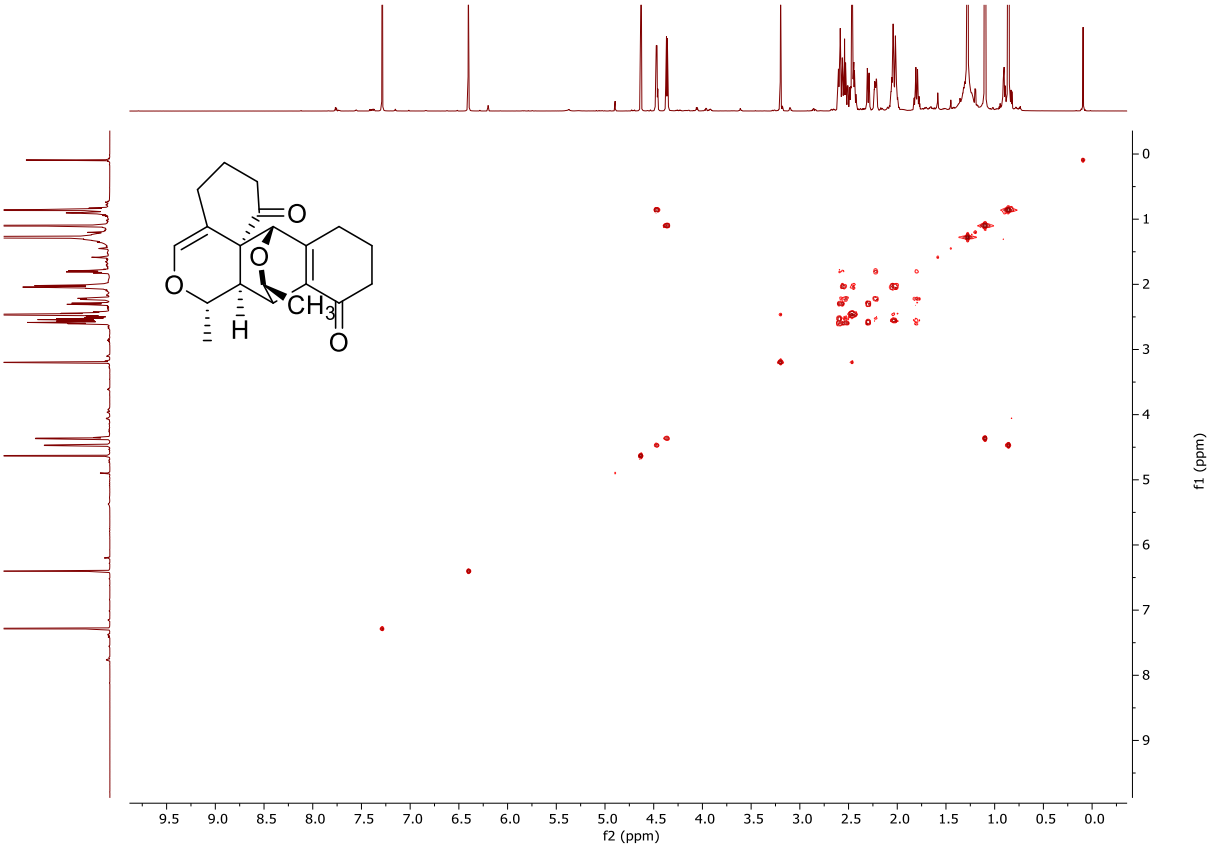

10.2.32 ^{1}H-^{13}C HSQC Spectrum of Compound (±)-1.31 ($CDCl_3$)

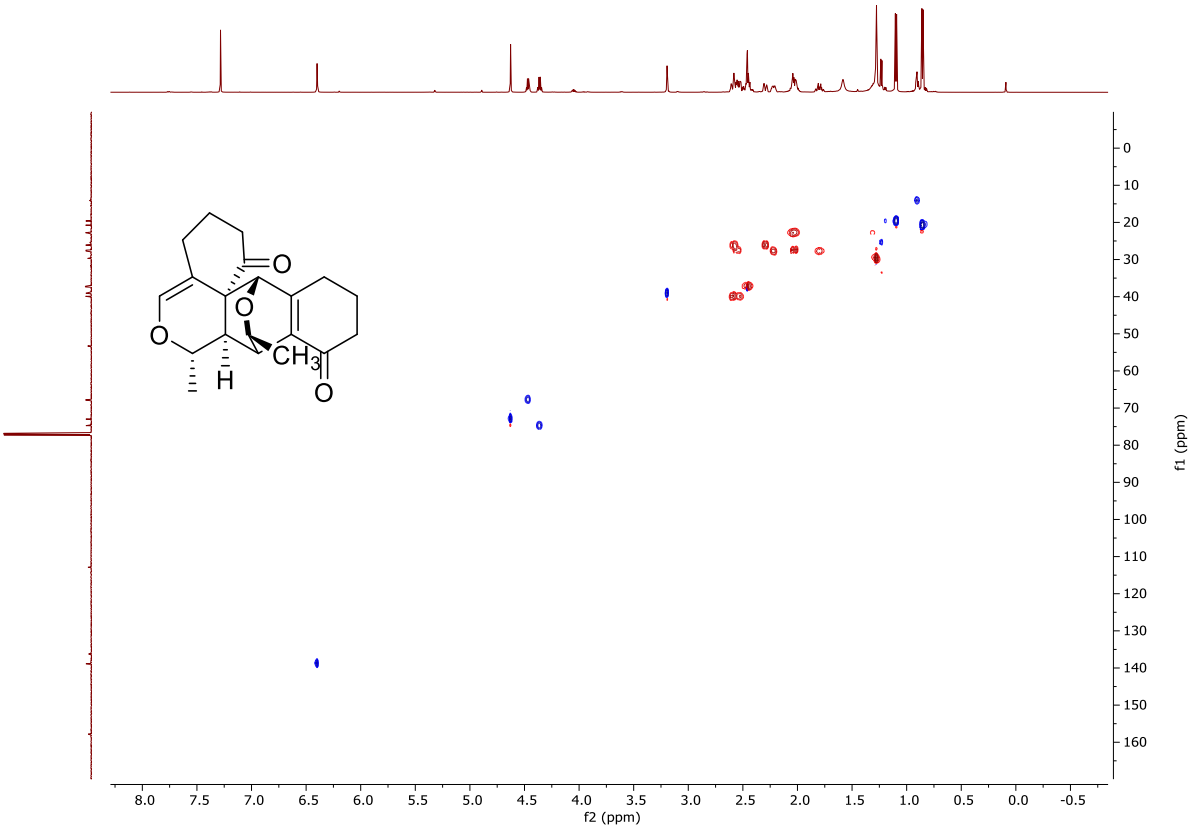

10.2.33 ^{1}H-^{13}C HMBC Spectrum of Compound (±)-1.31 ($CDCl_3$)

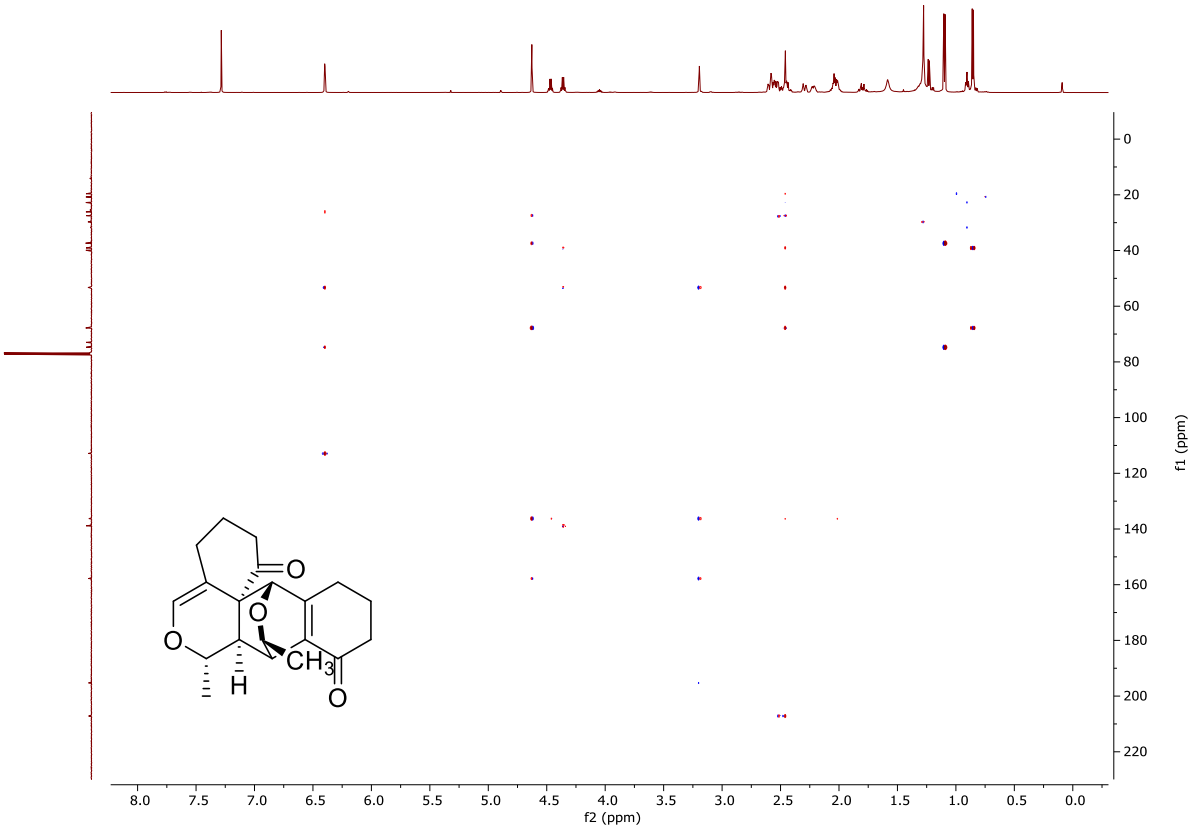

10.2.34 ^{13}C DEPT Spectrum of Compound (±)-1.31 ($CDCl_3$)

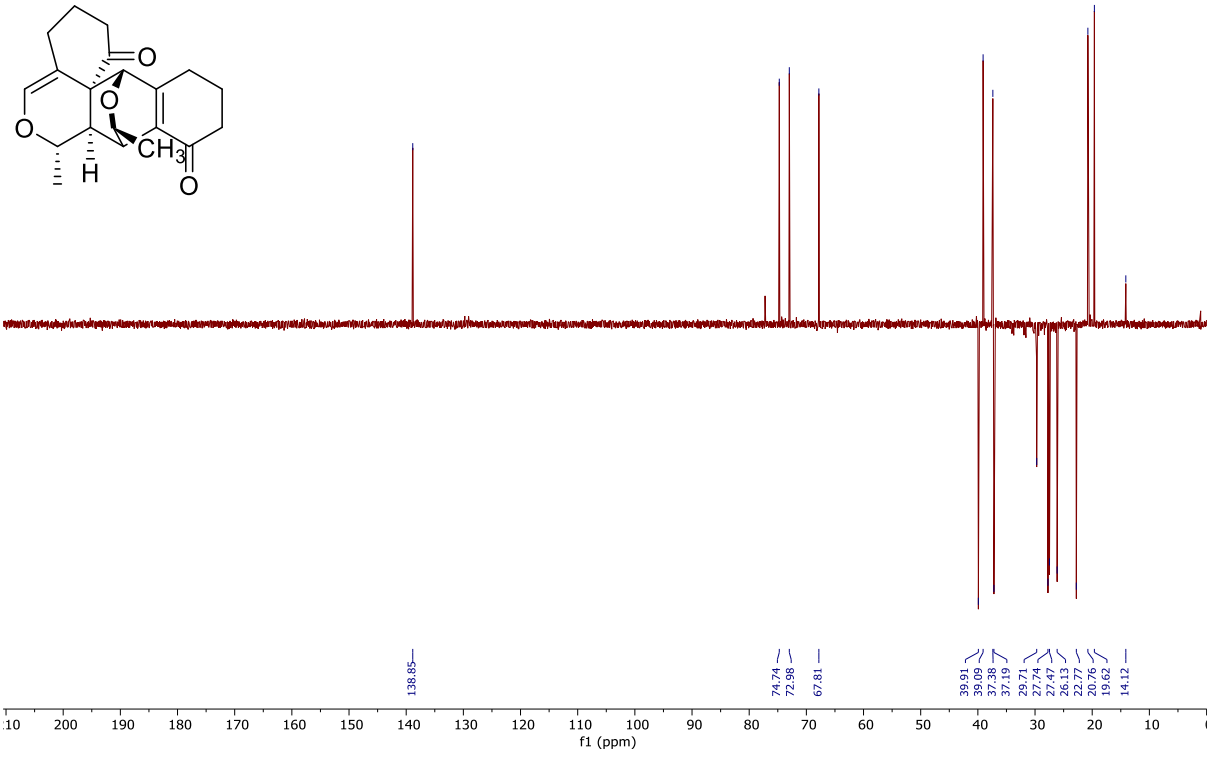

10.2.35 1H NMR Spectrum of Compound (±)-3.46 (800 MHz $CDCl_3$)

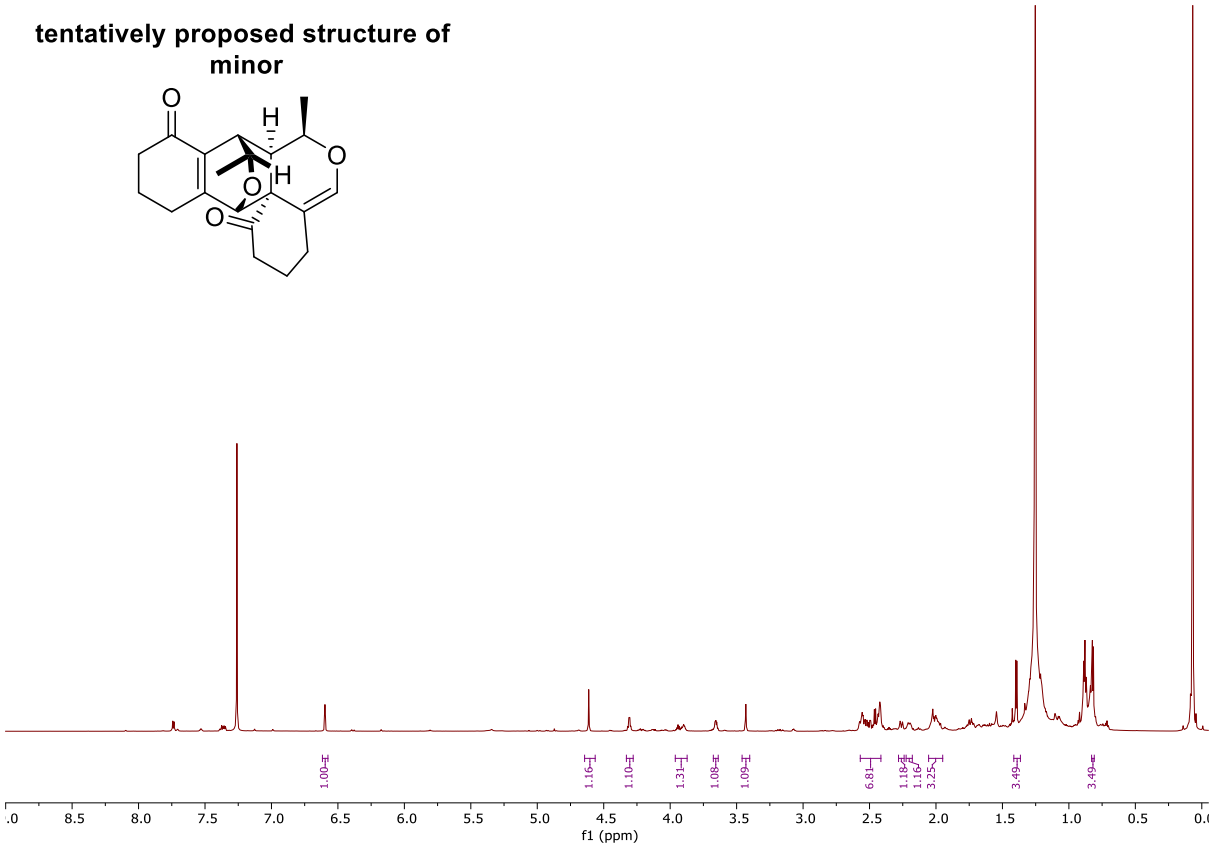

10.2.36 ^{1}H NMR Spectrum of Compound 3.42 (500 MHz, $CDCl_3$)

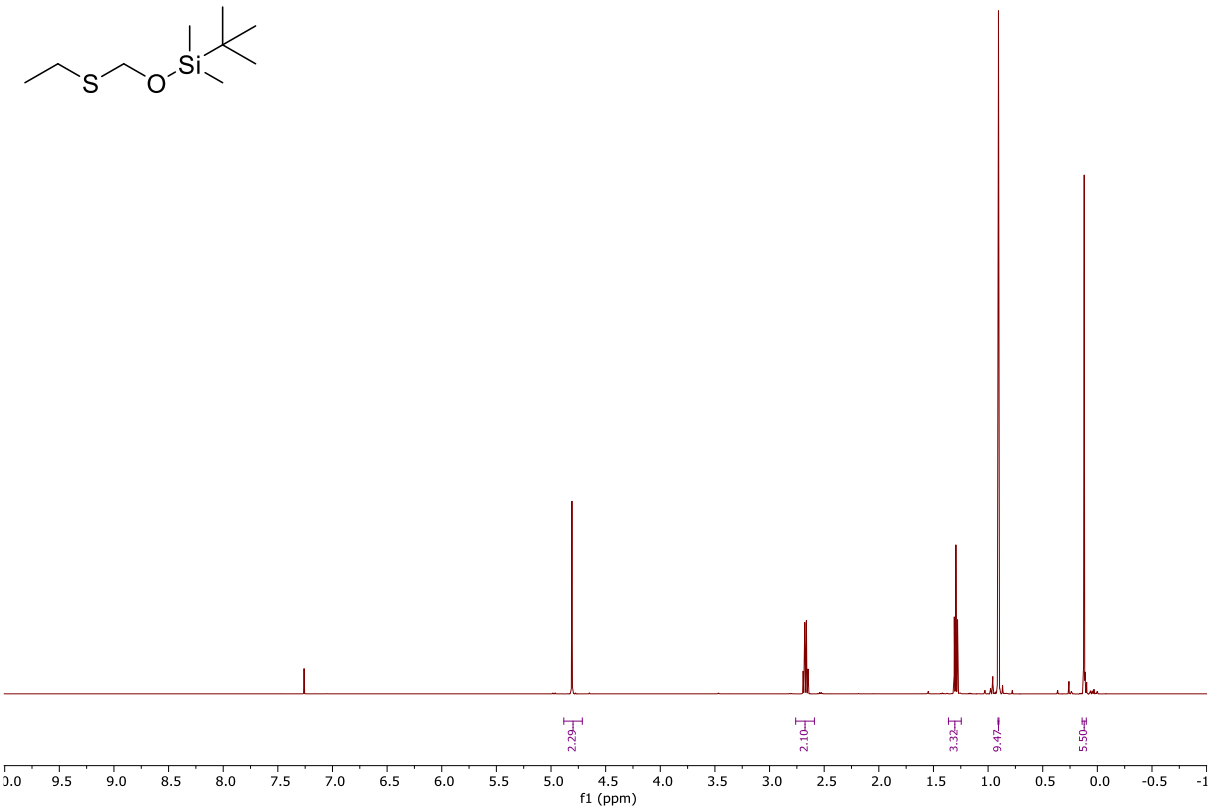

10.2.37 ^{13}C NMR Spectrum of Compound 3.42 (150 MHz, $CDCl_3$)

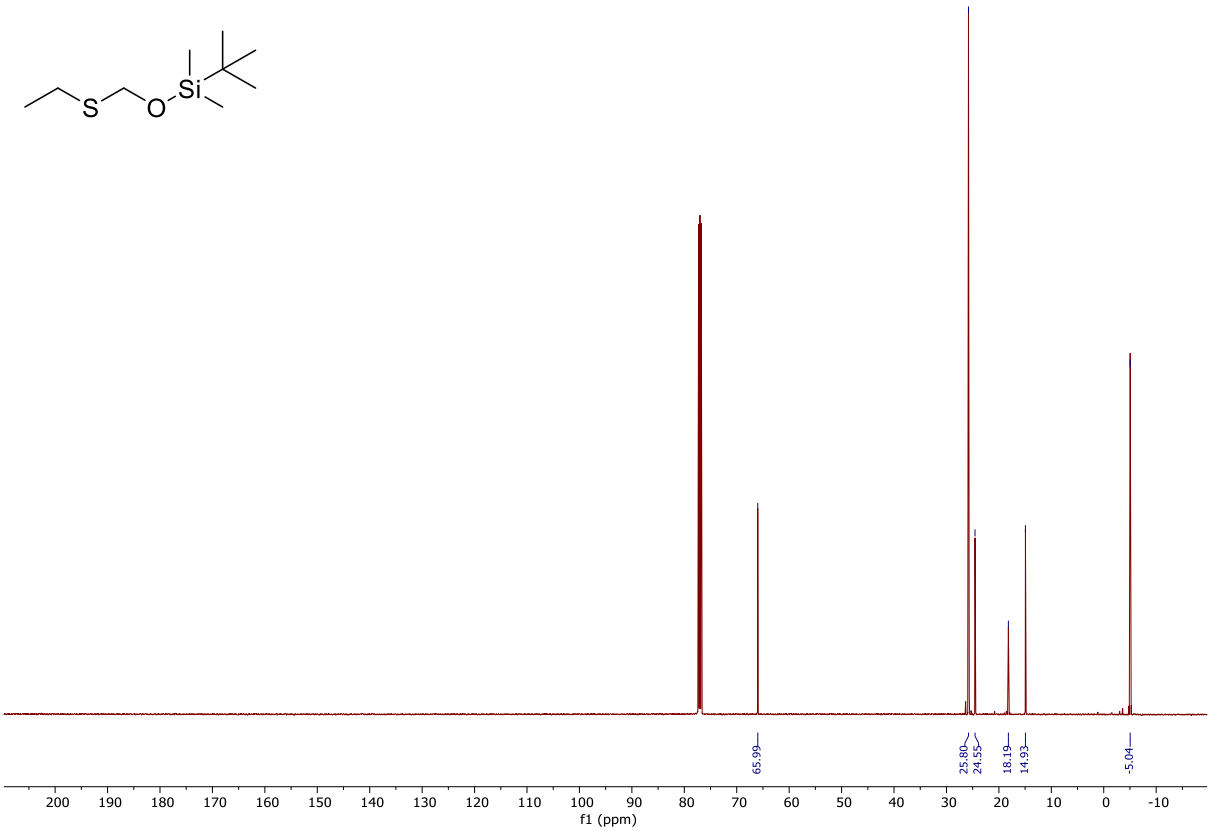

10.2.38 ^{1}H NMR Spectrum of Compound 3.37 (500 MHz $CDCl_3$)

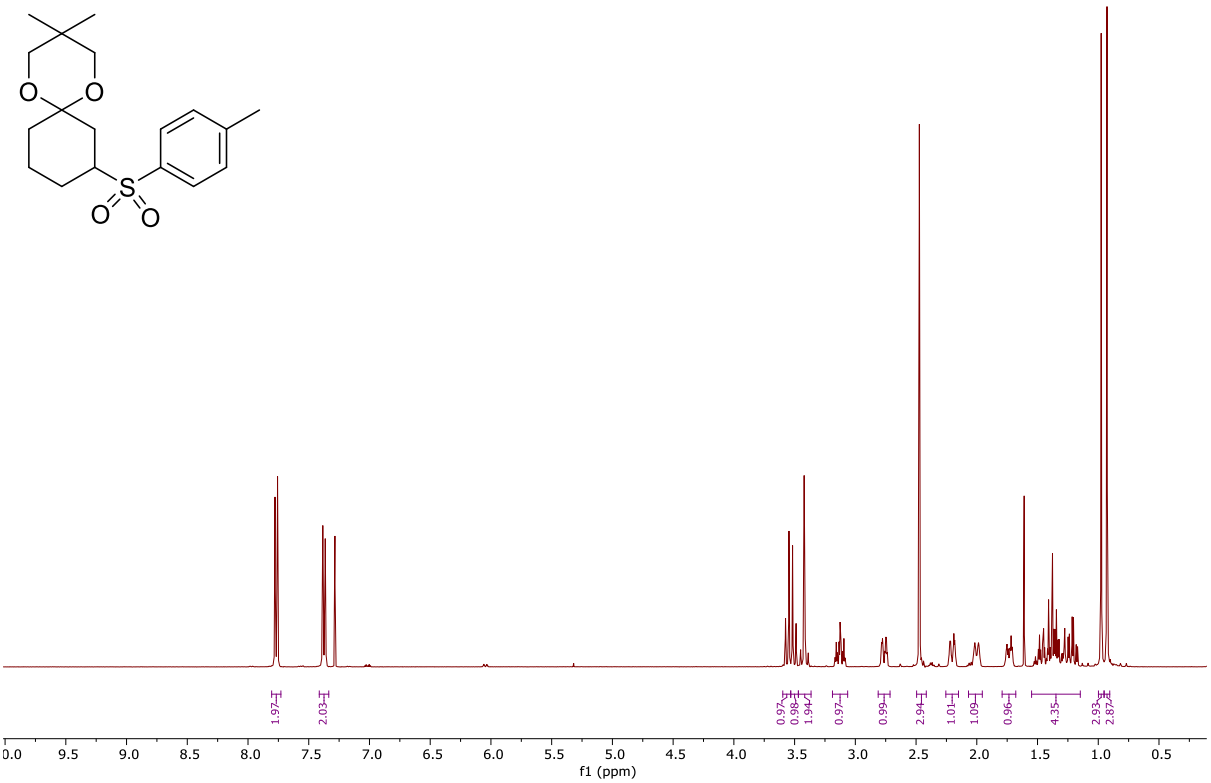

10.2.39 ^{13}C NMR Spectrum of Compound 3.37 (150 MHz, $CDCl_3$)

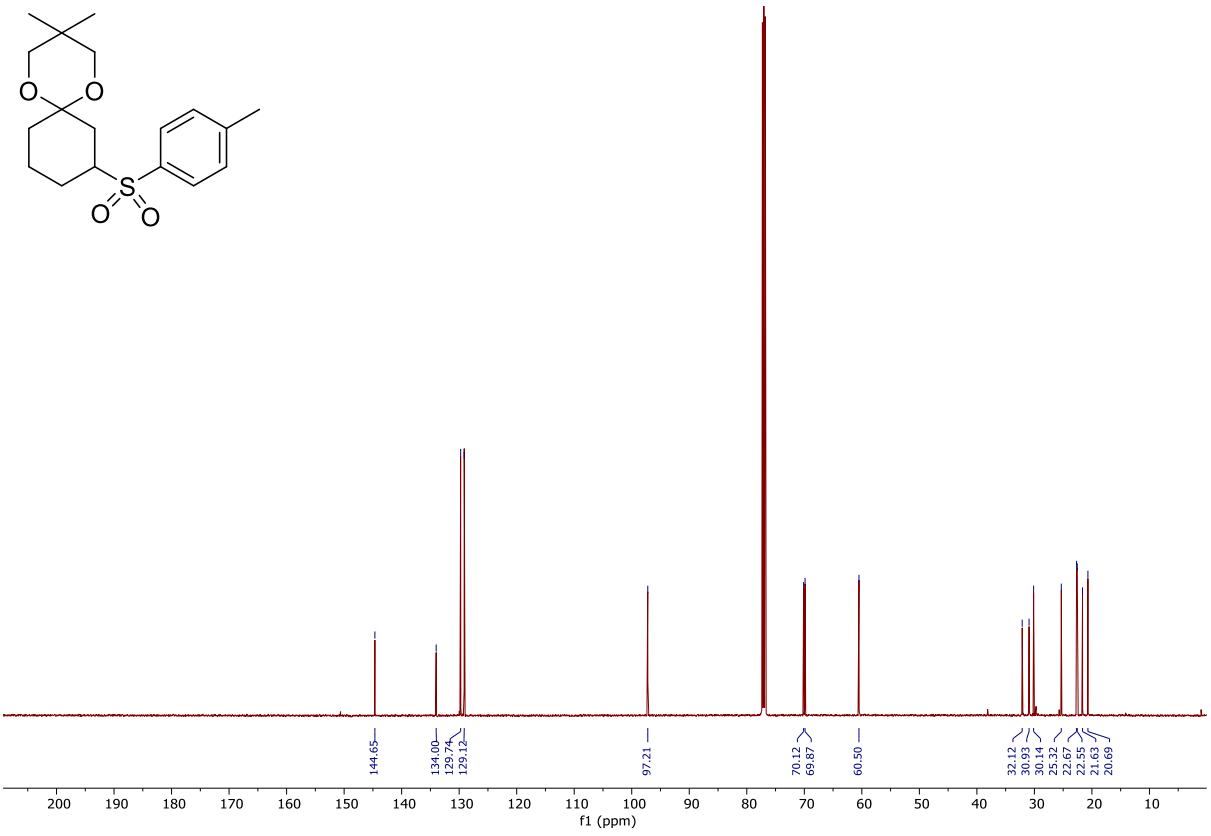

10.2.40 ^{1}H-^{1}H COSY Spectrum of Compound 3.37 ($CDCl_3$)

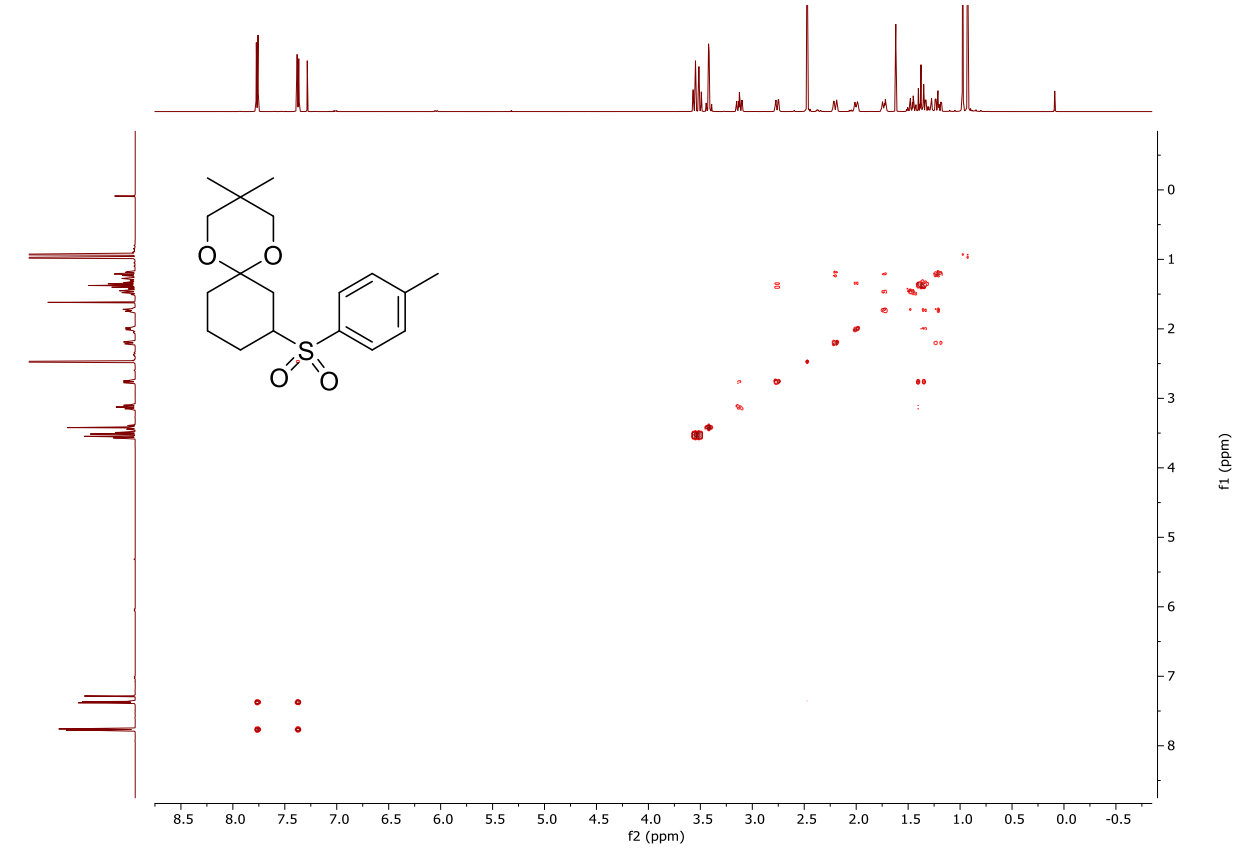

10.2.41 ^{1}H-^{13}C HSQC Spectrum of Compound 3.37 ($CDCl_3$)

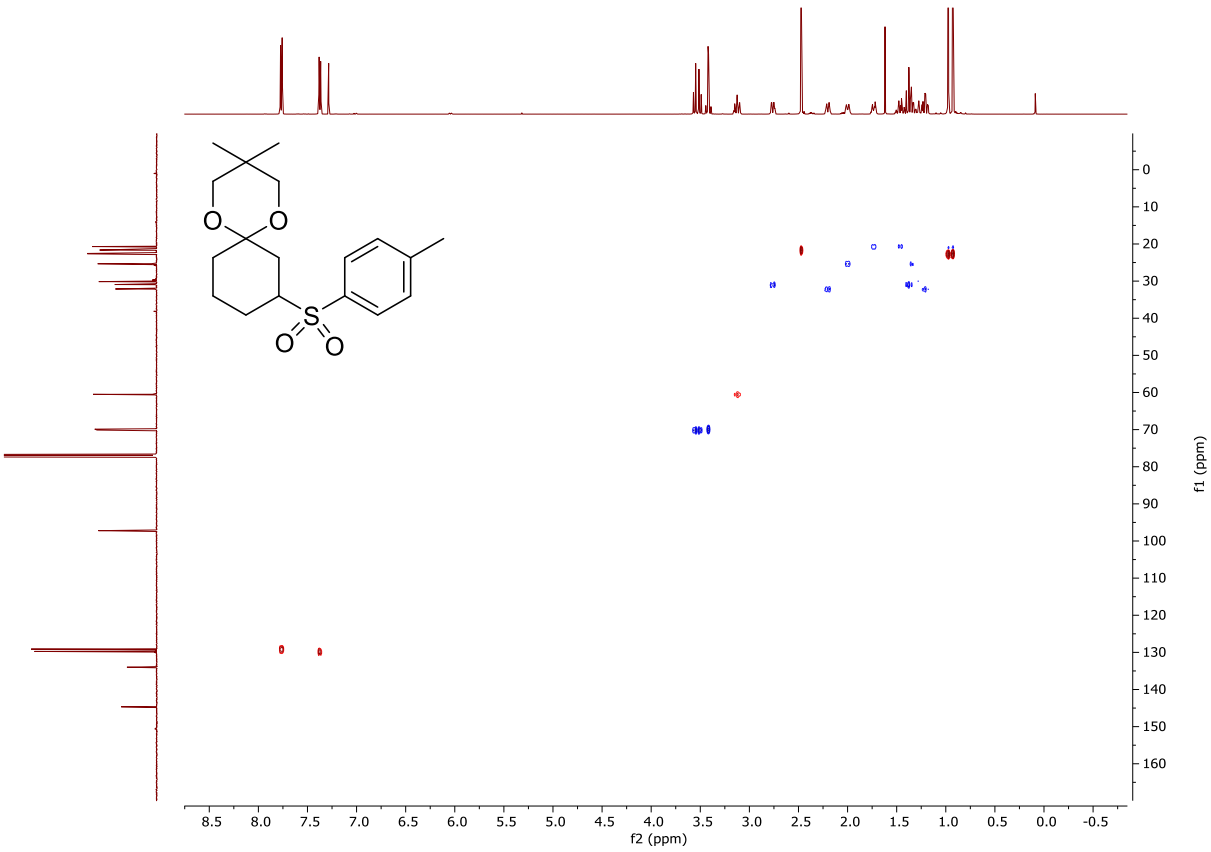

10.2.42 ^{13}C DEPT Spectrum of Compound 3.37 ($CDCl_3$)

10.2.43 ^{1}H NMR Spectrum of Compound (–)-3.51 (600 MHz $CDCl_3$)

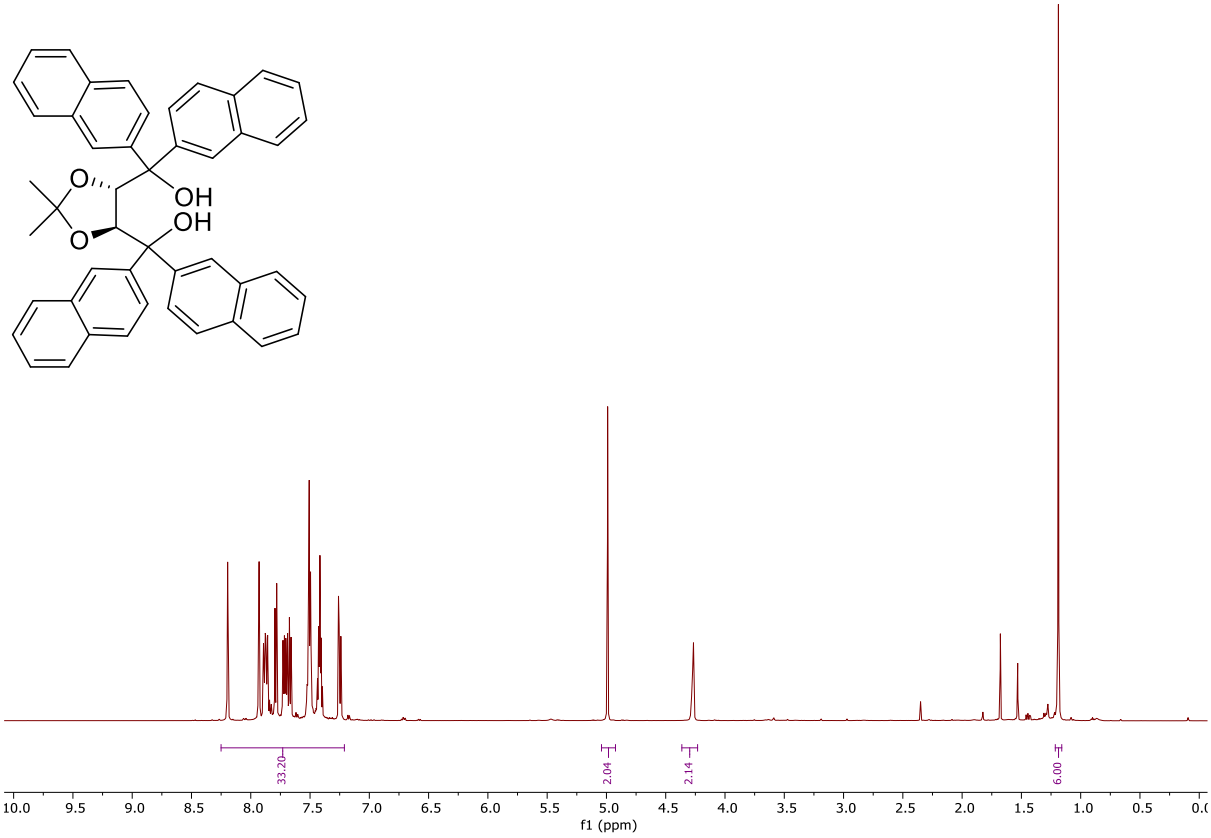

10.2.44 ^{13}C NMR Spectrum of Compound (–)-3.51 (150 MHz, $CDCl_3$)

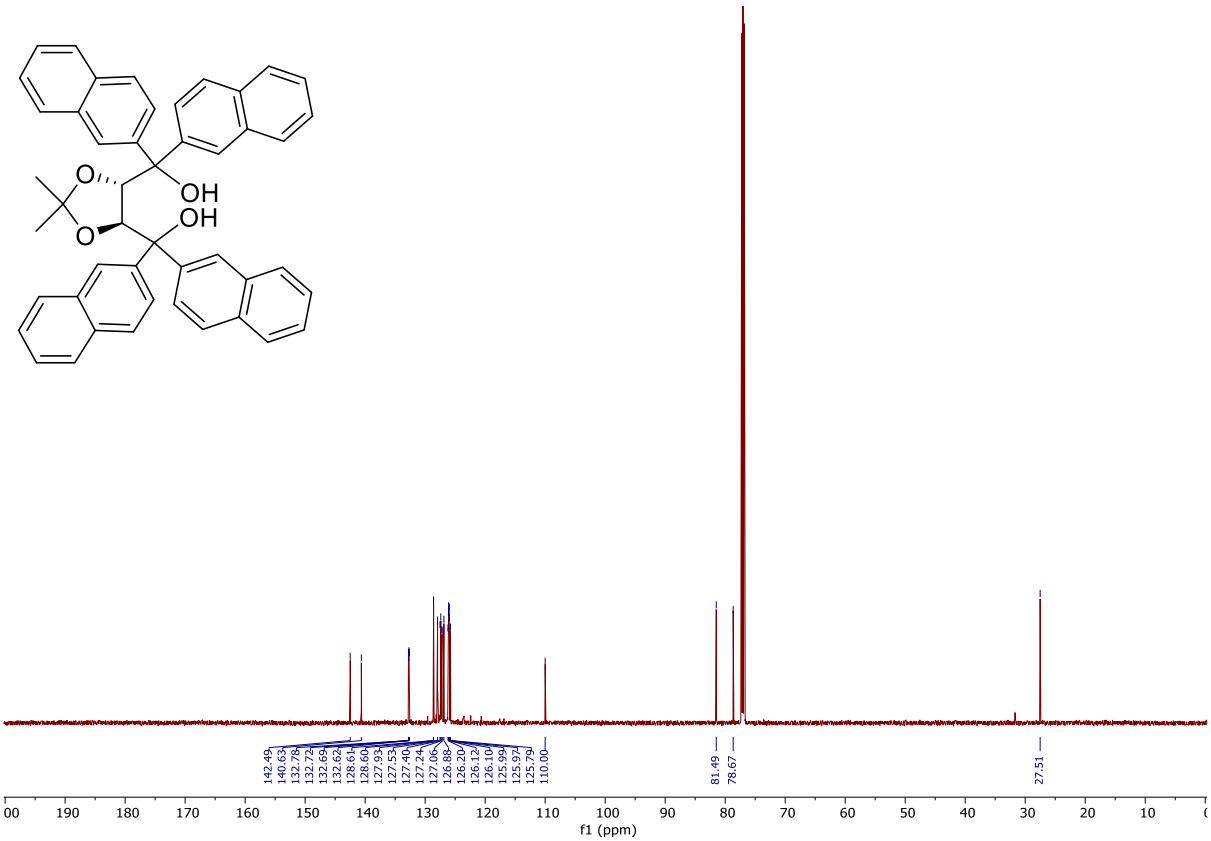

10.2.45 ^{1}H NMR Spectrum of Compound (–)-3.50 (600 MHz $CDCl_3$)

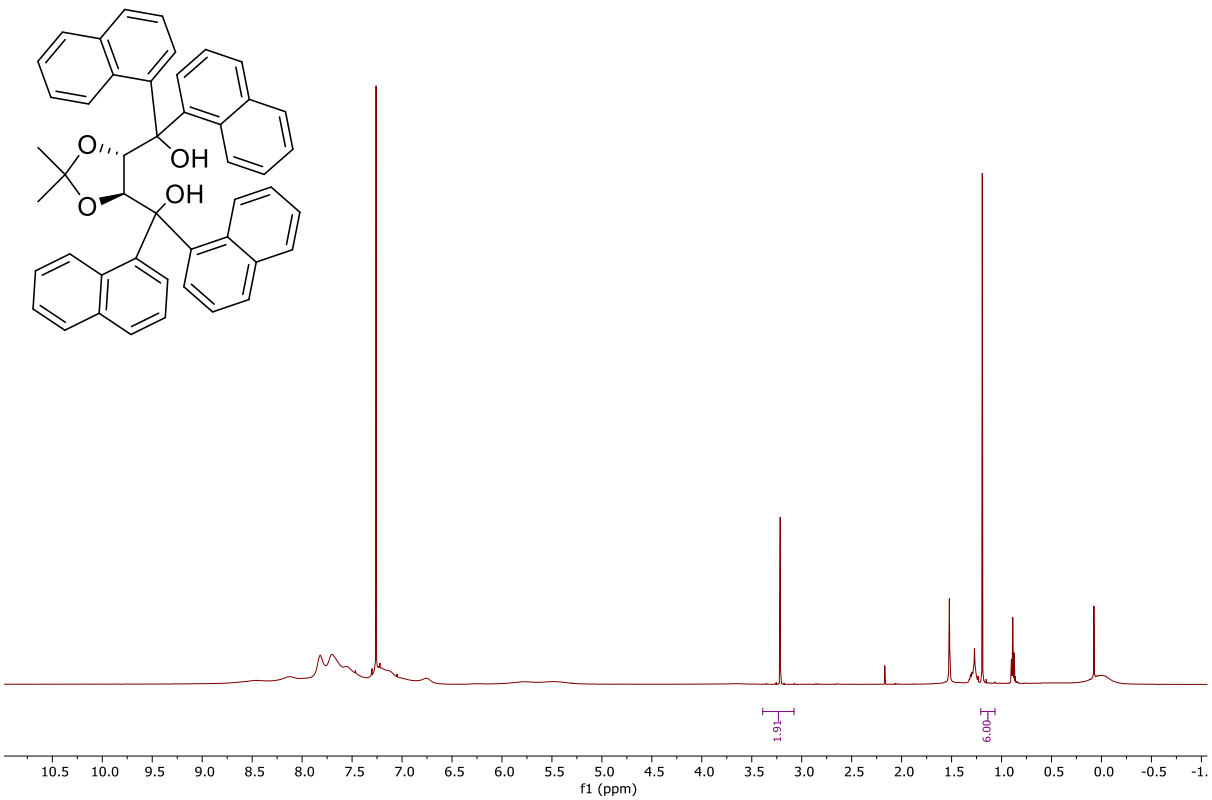

*NMR spectra is poorly resolved due to restricted conformation.

10.2.46 ^{1}H NMR Spectrum of Compound (–)-3.56 (600 MHz $CDCl_3$)

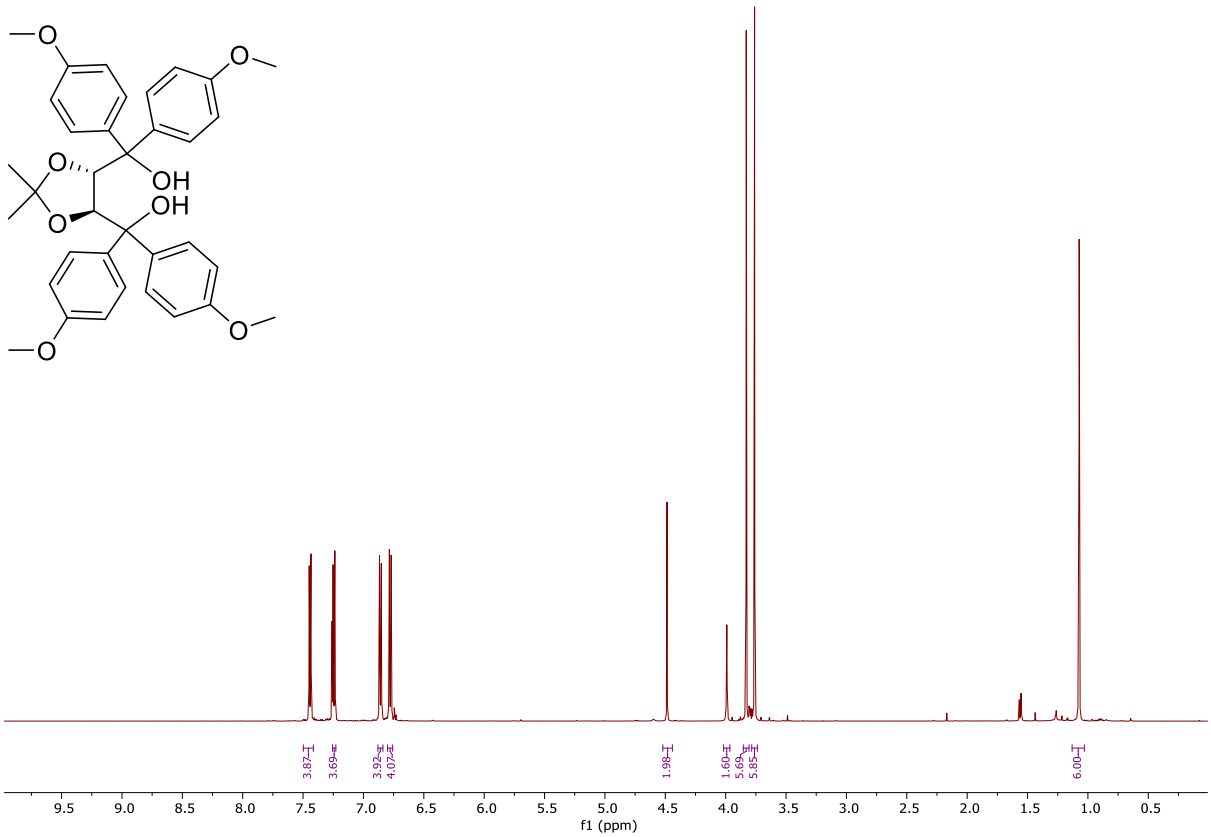

10.2.47 ^{13}C NMR Spectrum of Compound (–)-3.56 (150 MHz, $CDCl_3$)

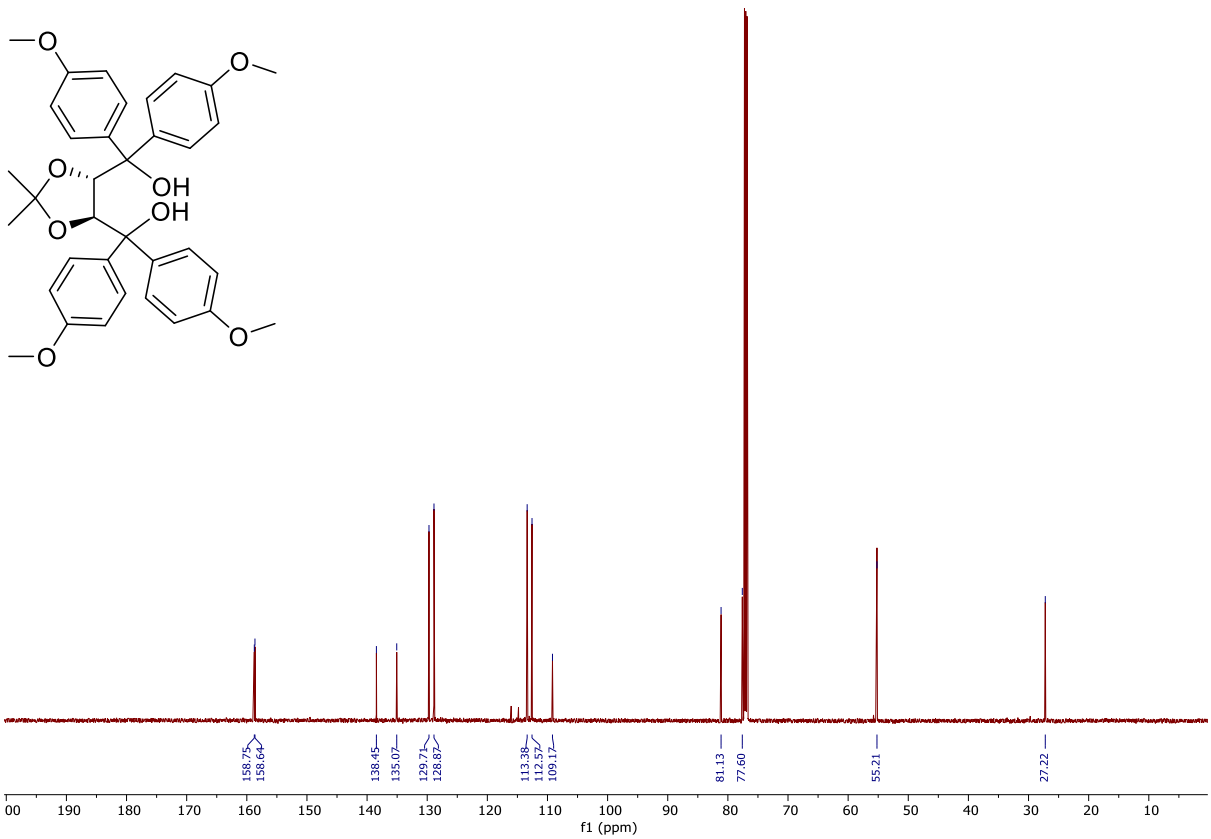

10.2.48 ^{1}H NMR Spectrum of Compound (–)-3.52 (600 MHz $CDCl_3$)

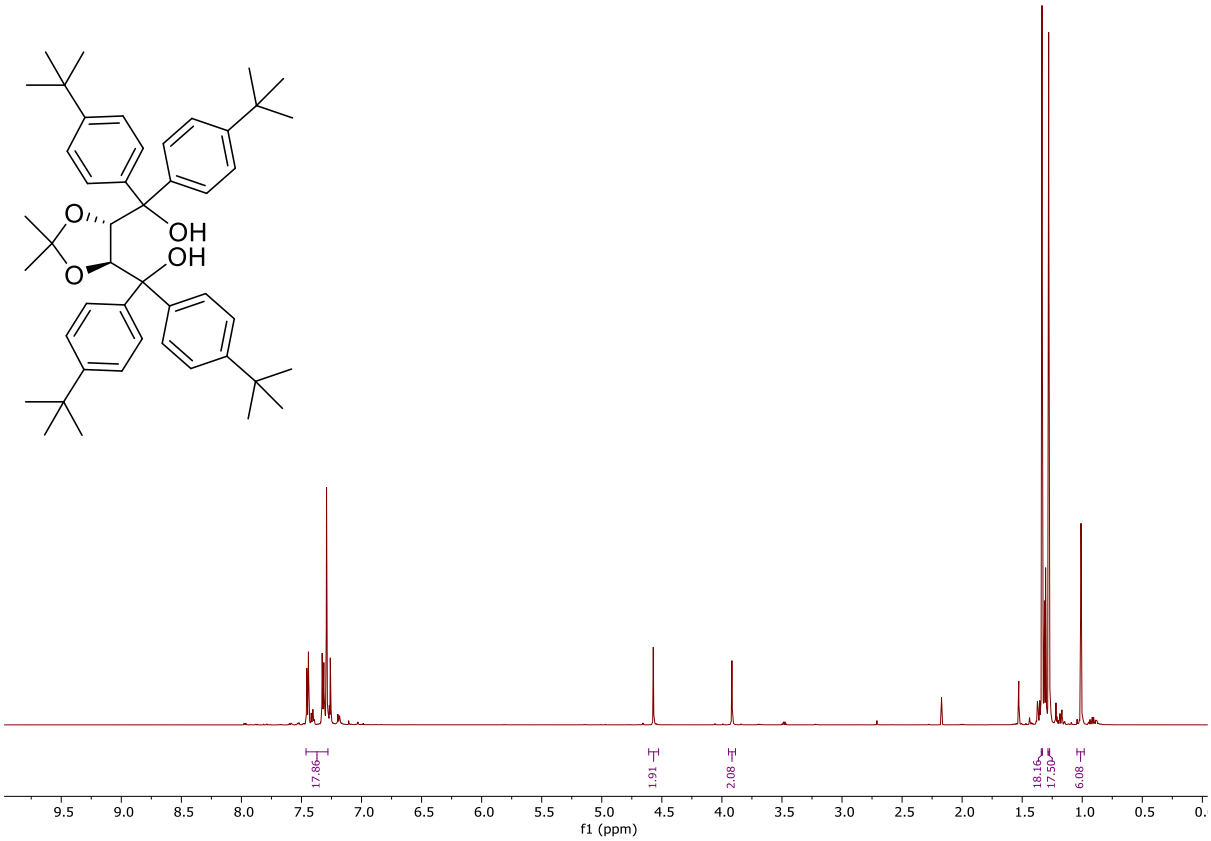

10.2.49 ^{13}C NMR Spectrum of Compound (–)-3.52 (150 MHz $CDCl_3$)

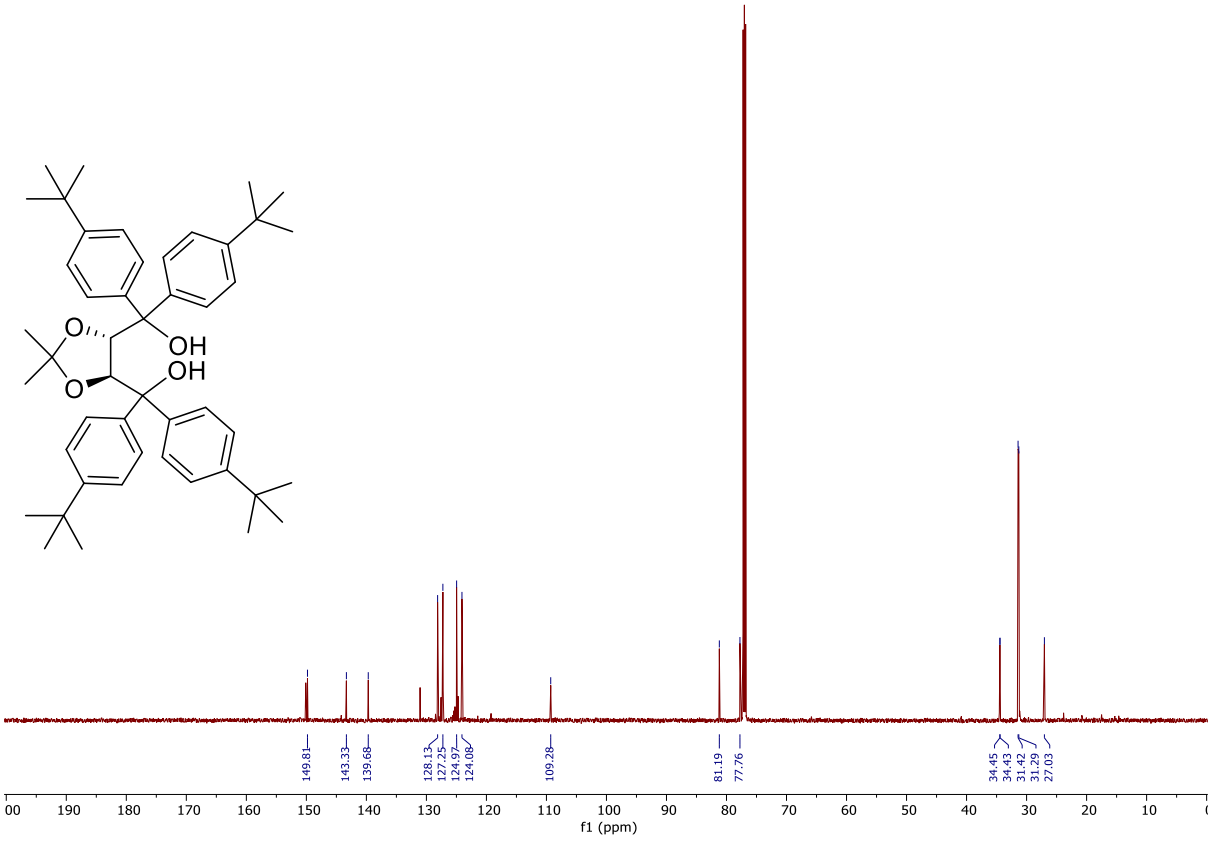

10.2.50 ^{1}H NMR Spectrum of Compound (–)-3.48 (500 MHz $CDCl_3$)

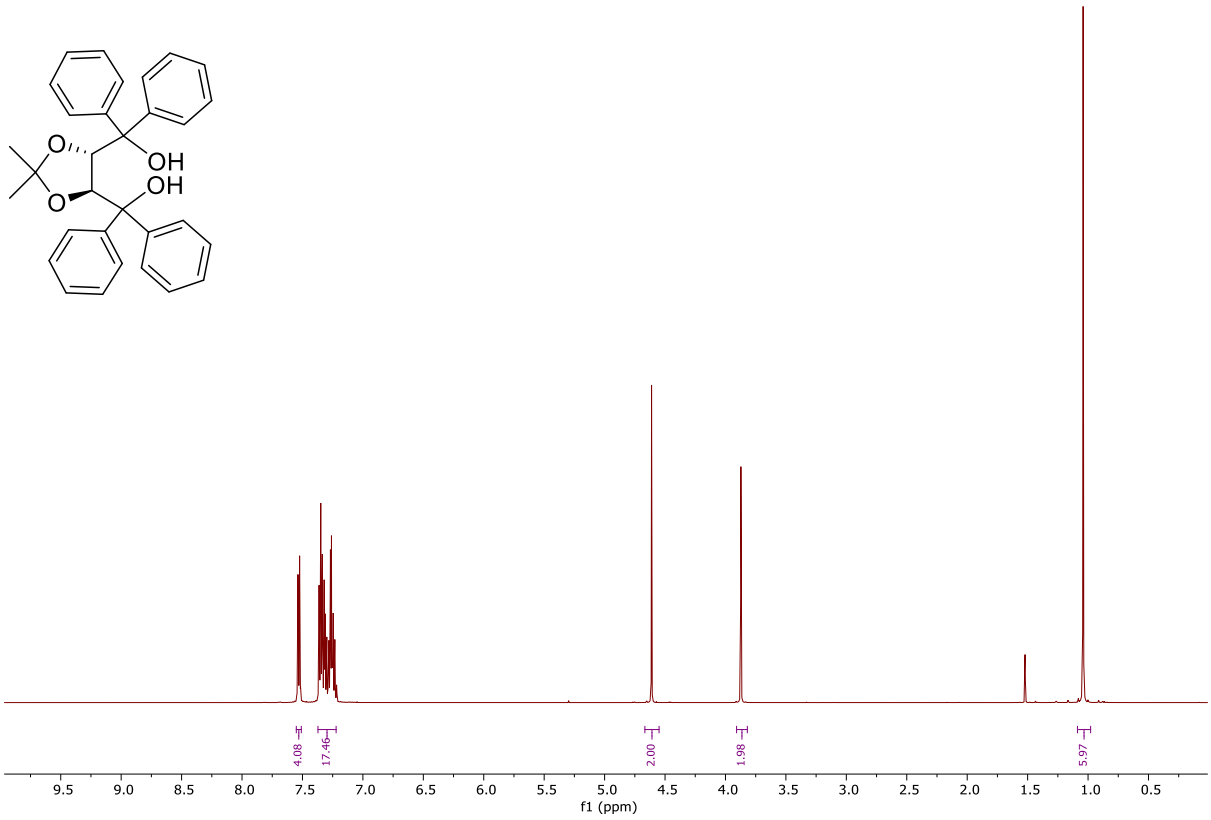

10.2.51 ^{13}C NMR Spectrum of Compound (–)-3.48 (125 MHz, $CDCl_3$)

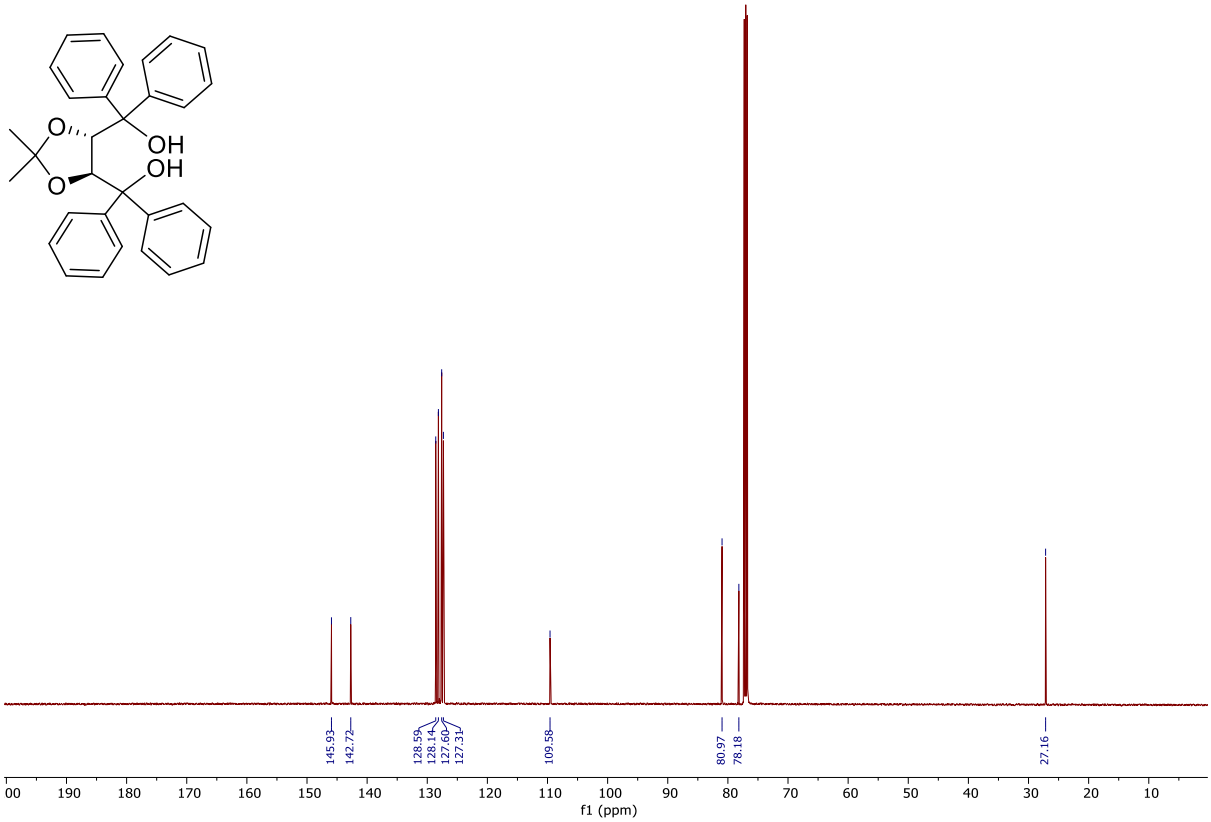

10.2.52 ^{1}H NMR Spectrum of Compound (–)-3.55 (500 MHz $CDCl_3$)

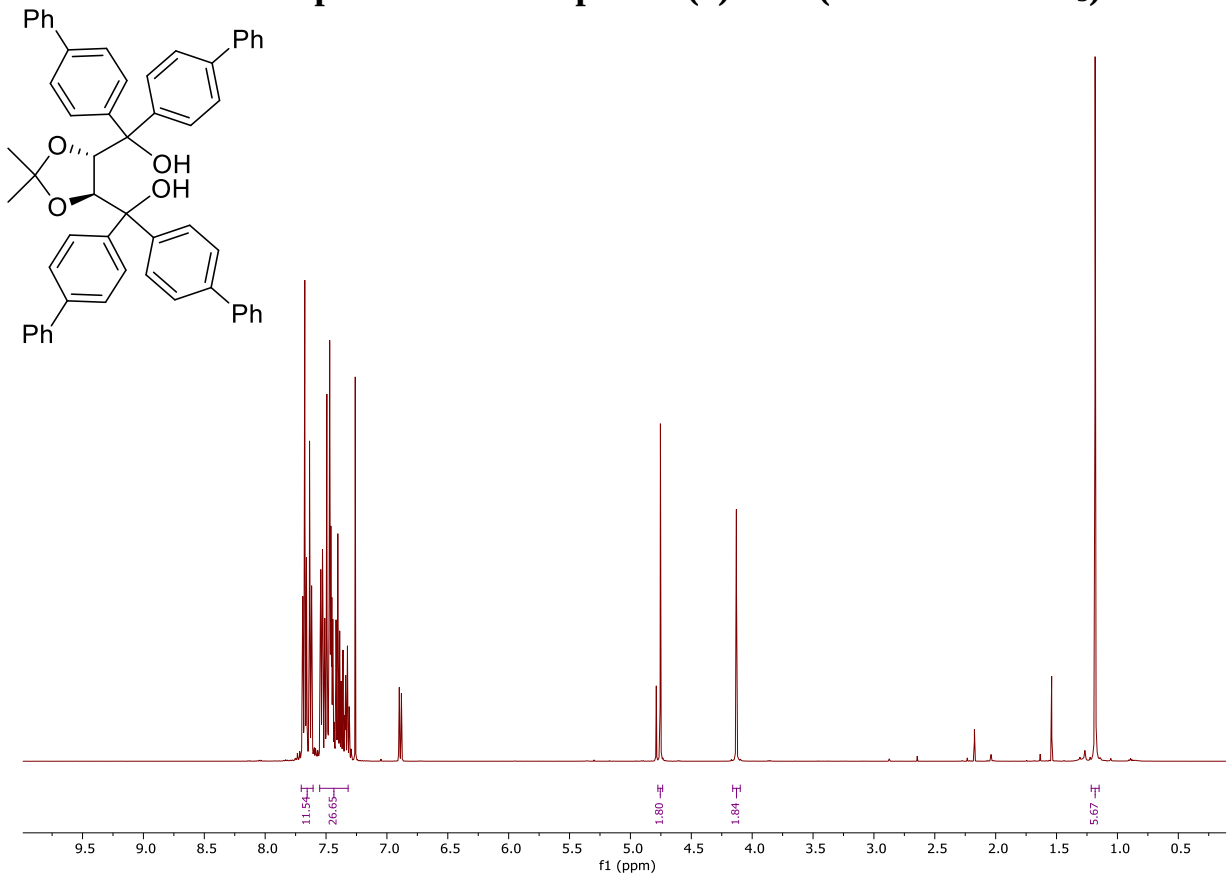

10.2.53 ^{13}C NMR Spectrum of Compound (–)-3.55 (125 MHz, $CDCl_3$)

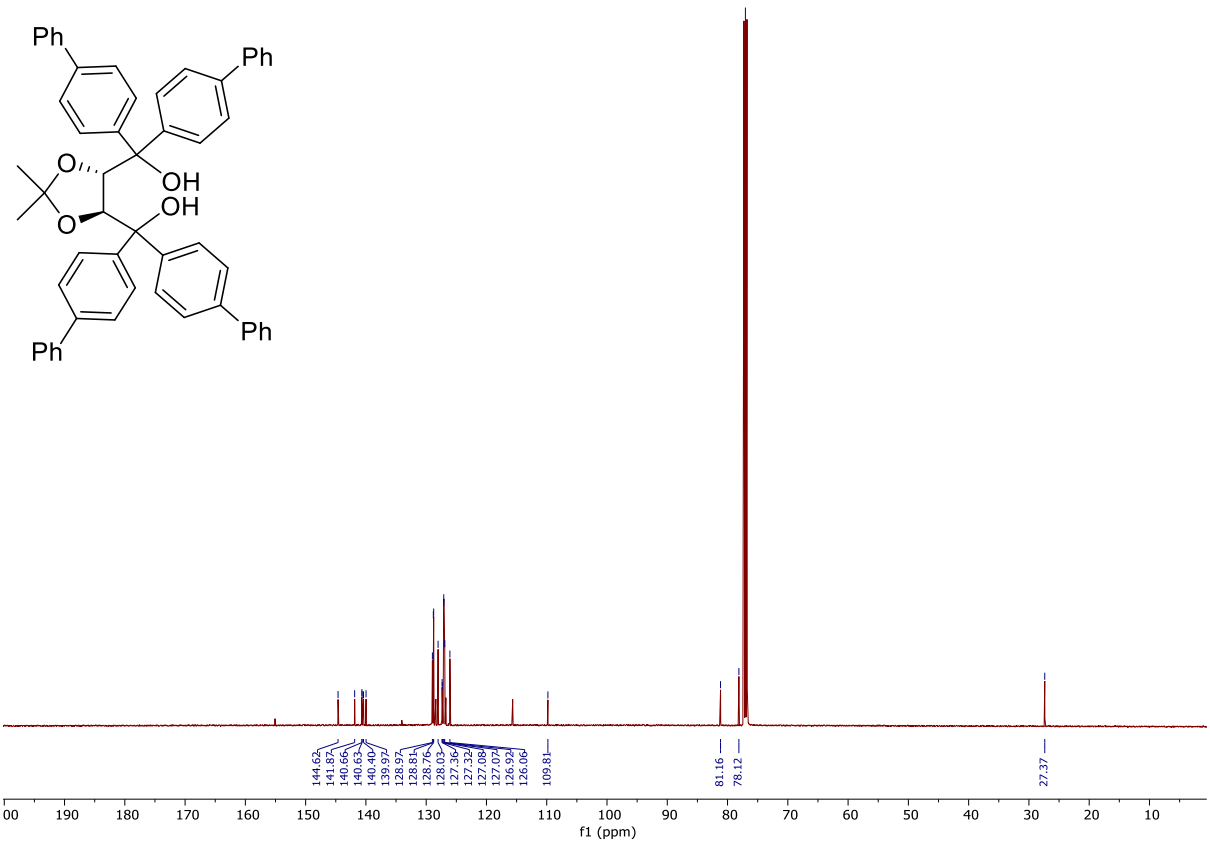

10.2.54 ^{1}H NMR Spectrum of Compound (–)-3.57 (500 MHz $CDCl_3$)

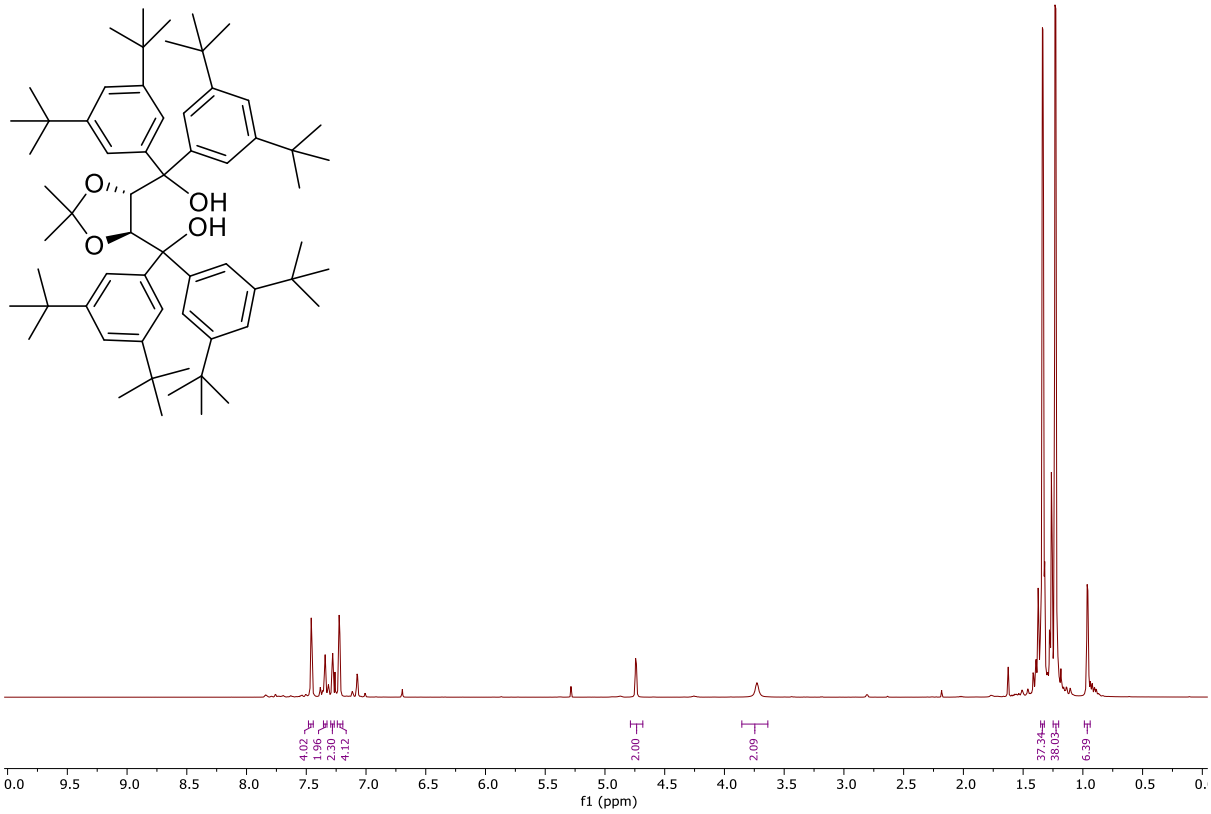

10.2.55 ^{13}C NMR Spectrum of Compound (–)-3.57 (125 MHz, $CDCl_3$)

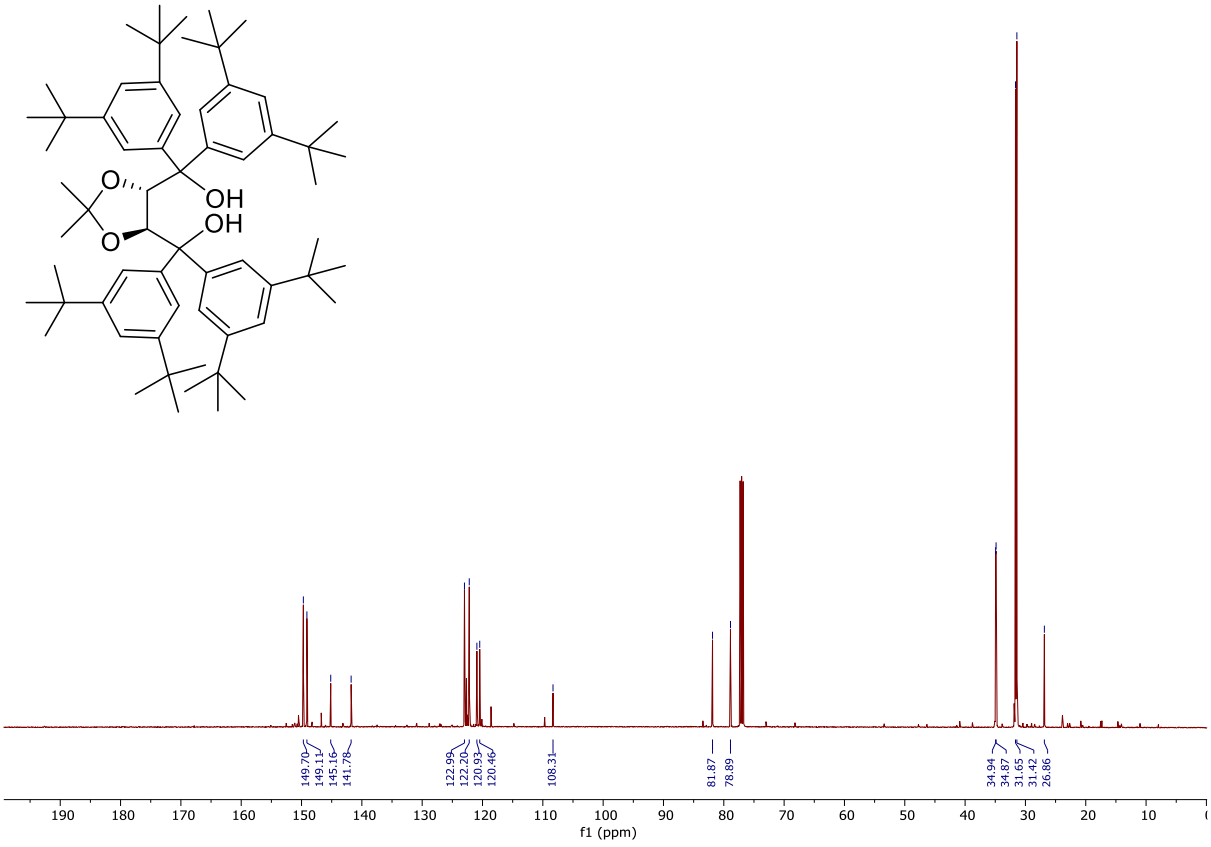

10.3 NMR Spectra Chapter 5

10.3.1 ^{1}H NMR Spectrum of Compound 5.12 (600 MHz, $CDCl_3$)

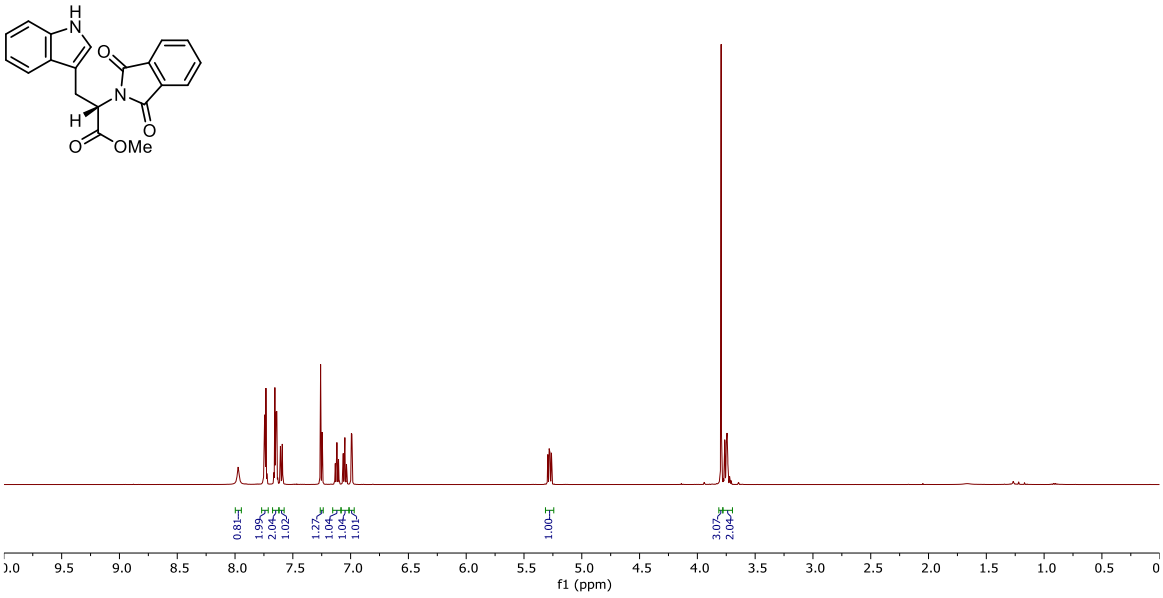

10.3.2 ^{13}C NMR Spectrum of Compound 5.12 (150 MHz, $CDCl_3$)

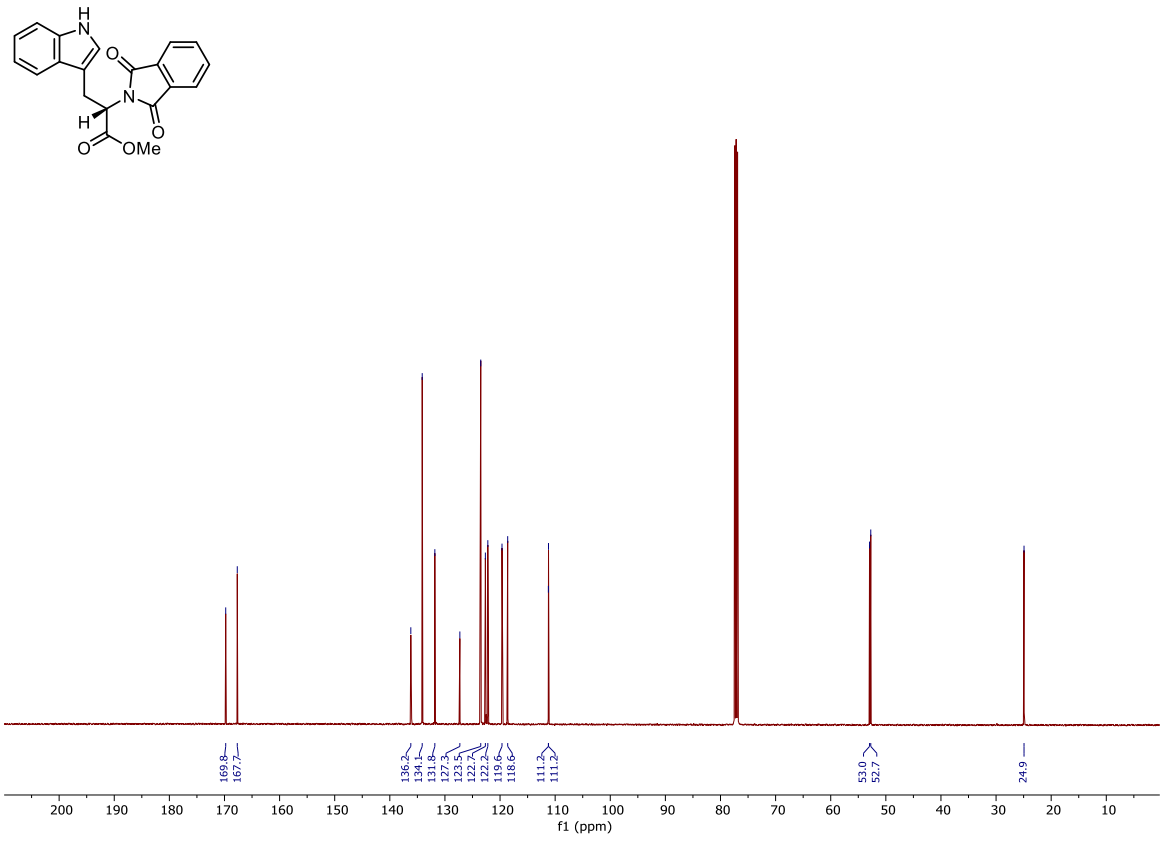

10.3.3 ^{1}H NMR Spectrum of Compound 4.72 (600 MHz, $CDCl_3$)

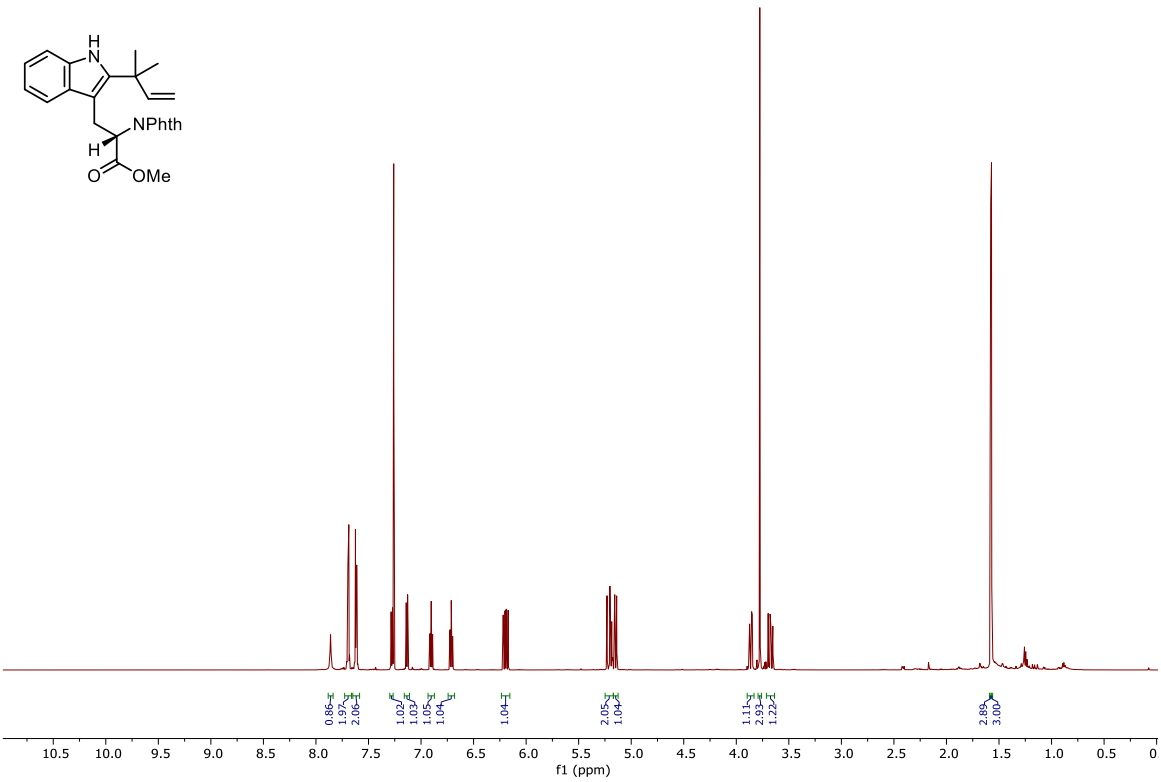

10.3.4 ^{13}C NMR Spectrum of Compound 4.72 (150 MHz, $CDCl_3$)

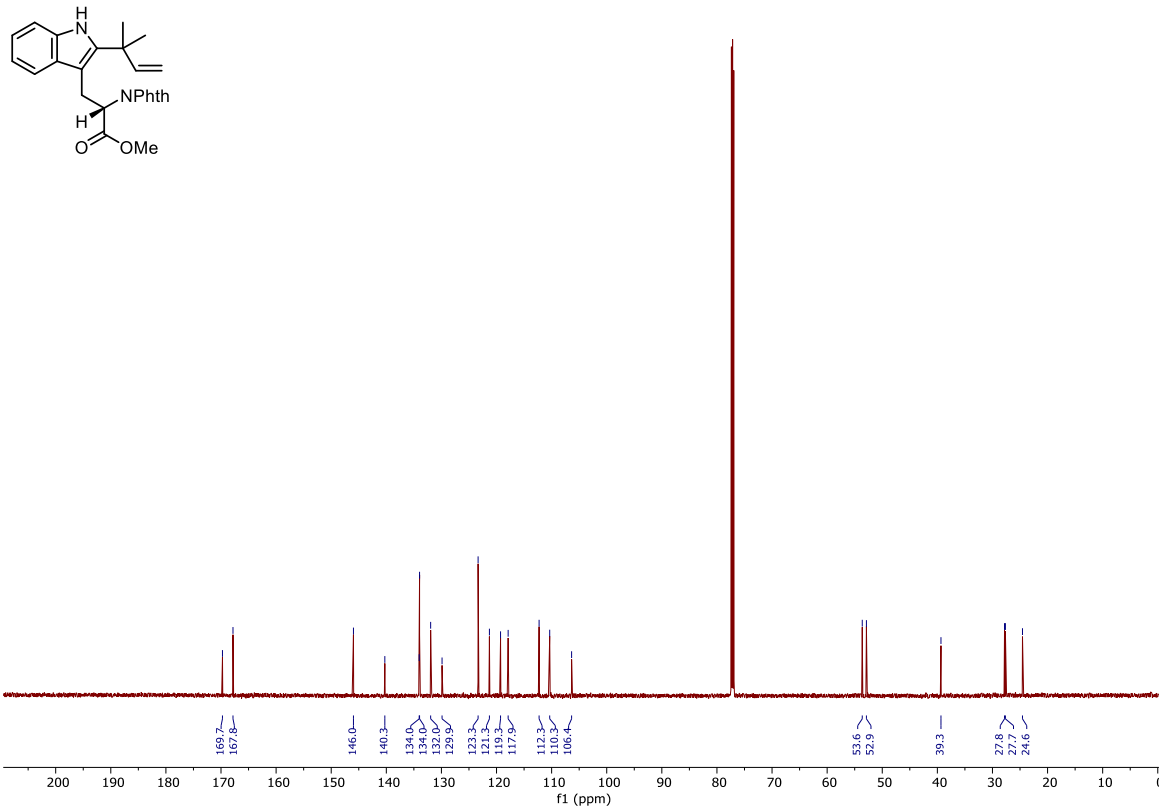

10.3.5 ^{1}H NMR Spectrum of Compound 4.73 (500 MHz, CD_3OD)

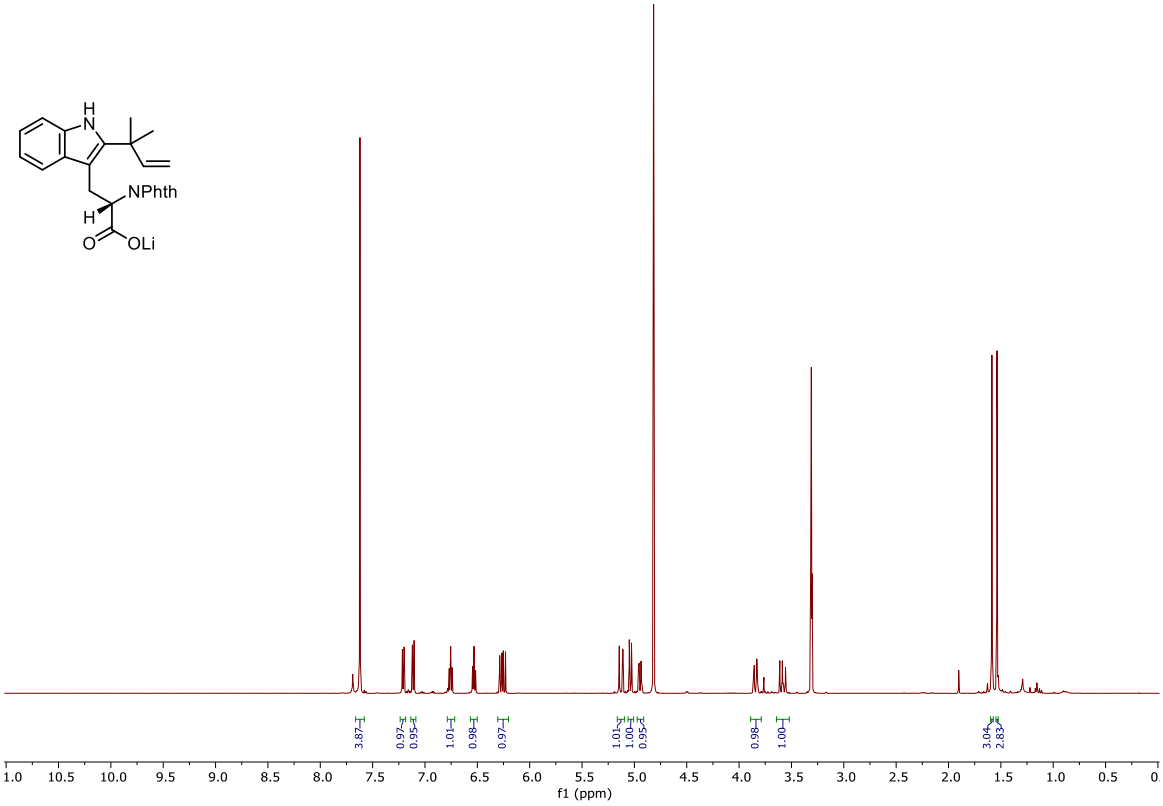

10.3.6 ^{13}C NMR Spectrum of Compound 4.73 (125 MHz, CD_3OD)

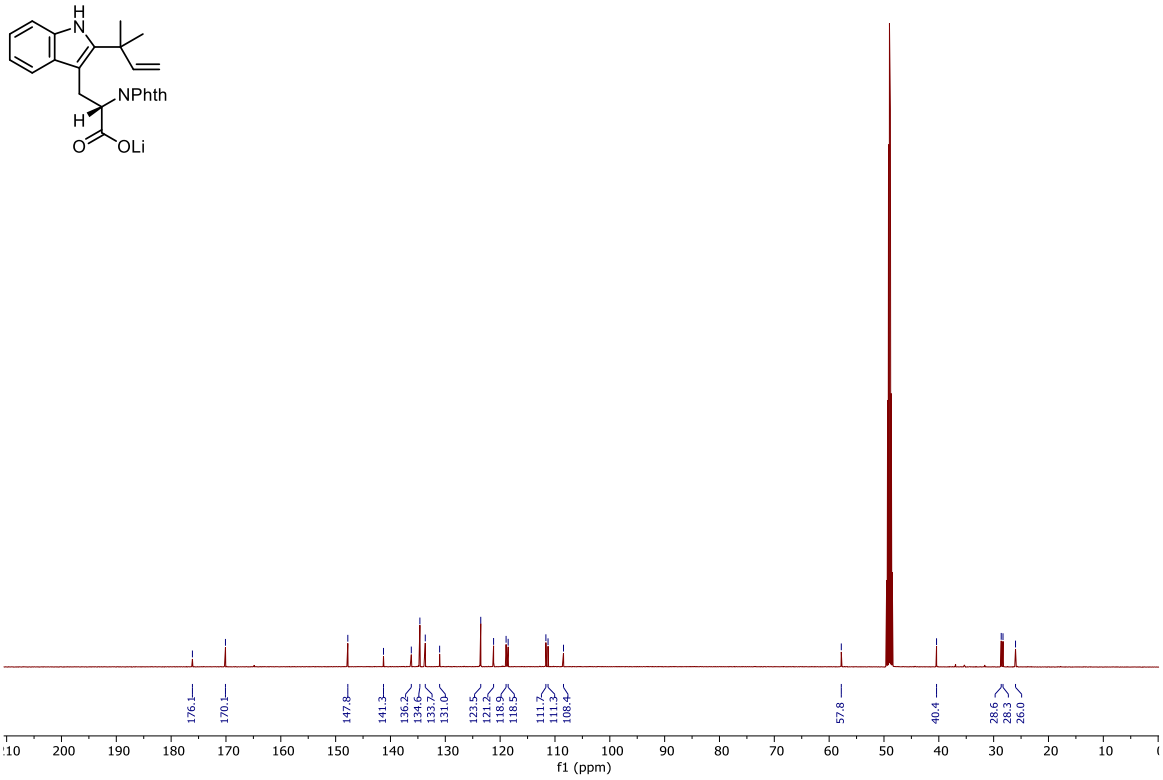

10.3.7 ^{1}H NMR Spectrum of Compound 4.75 (500 MHz, CD_2Cl_2)

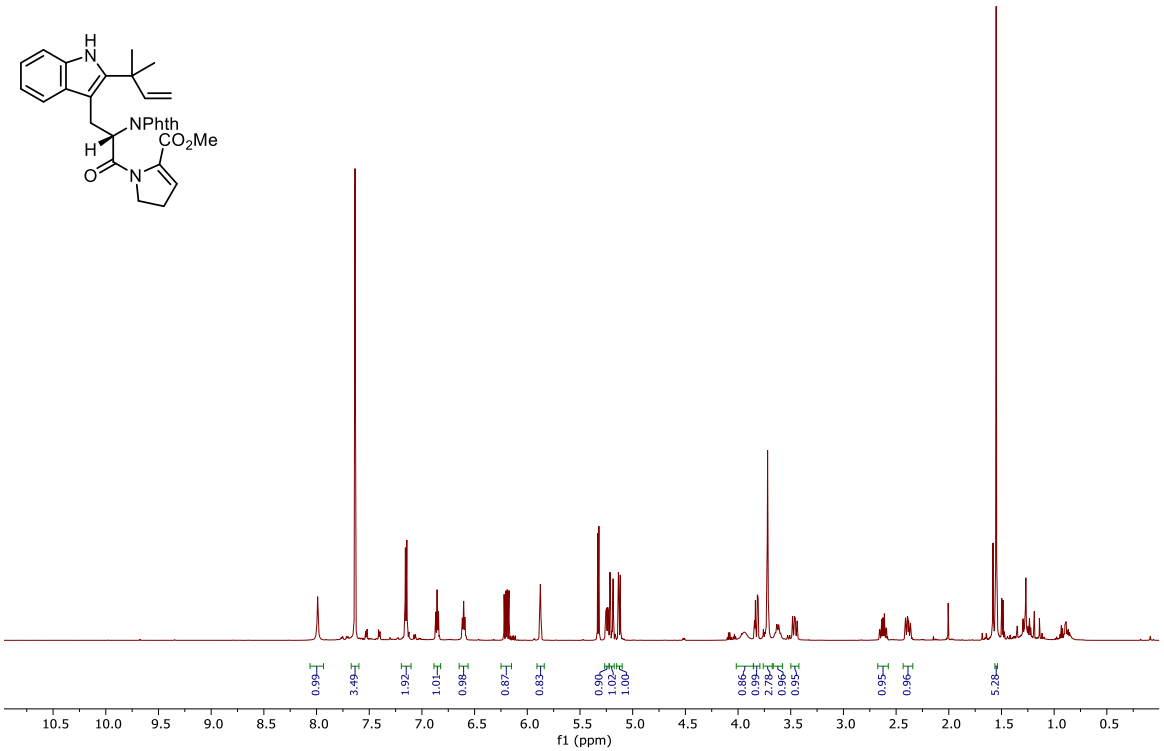

10.3.8 ^{13}C NMR Spectrum of Compound 4.75 (150 MHz, CD_2Cl_2)

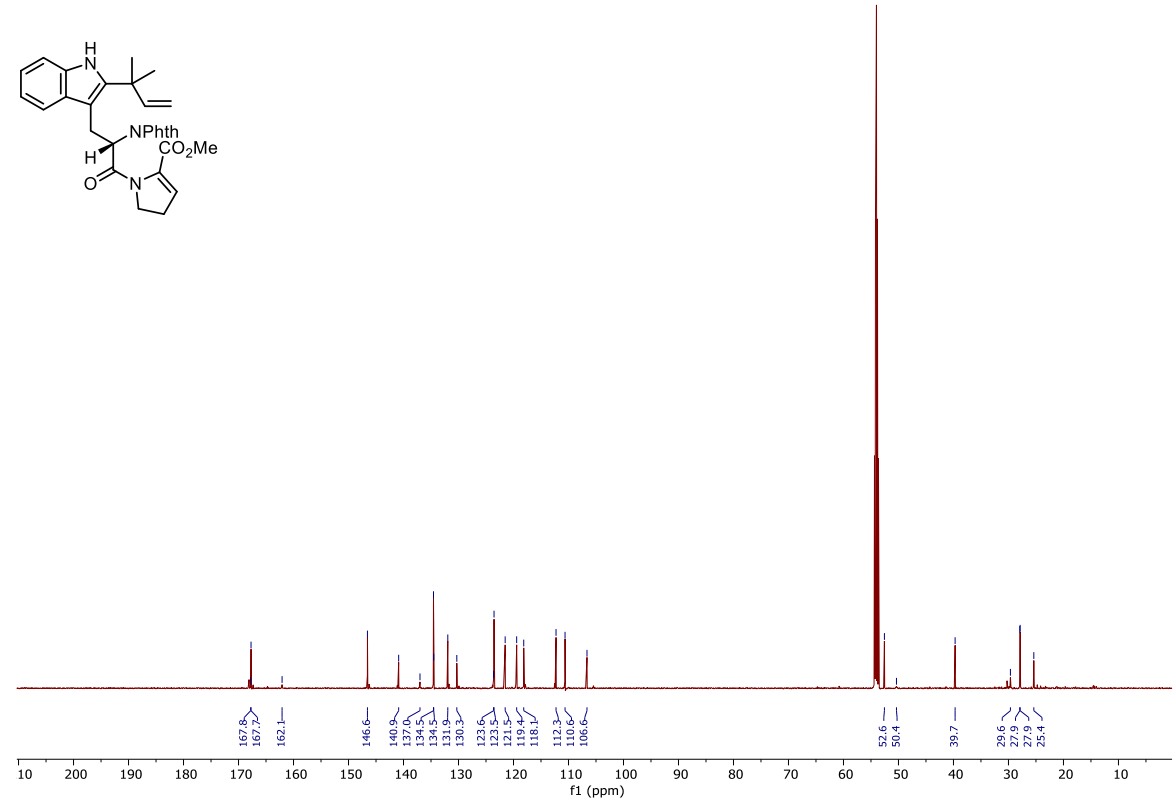

10.3.9 ^{1}H NMR Spectrum of (+)-Dehydrodeoxybrevianamide E 4.45 (500 MHz, $CDCl_3$)

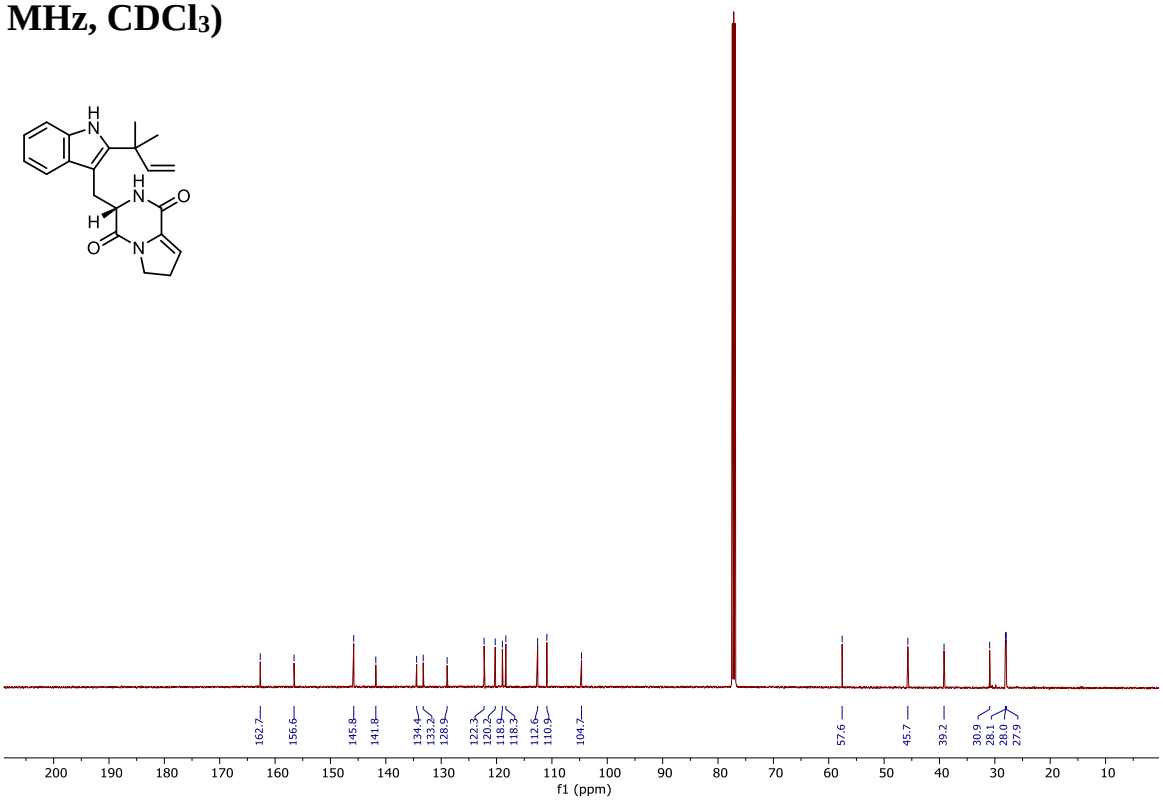

10.3.10 ^{13}C NMR Spectrum of (+)-Dehydrodeoxybrevianamide E 4.45 (125 MHz, $CDCl_3$)

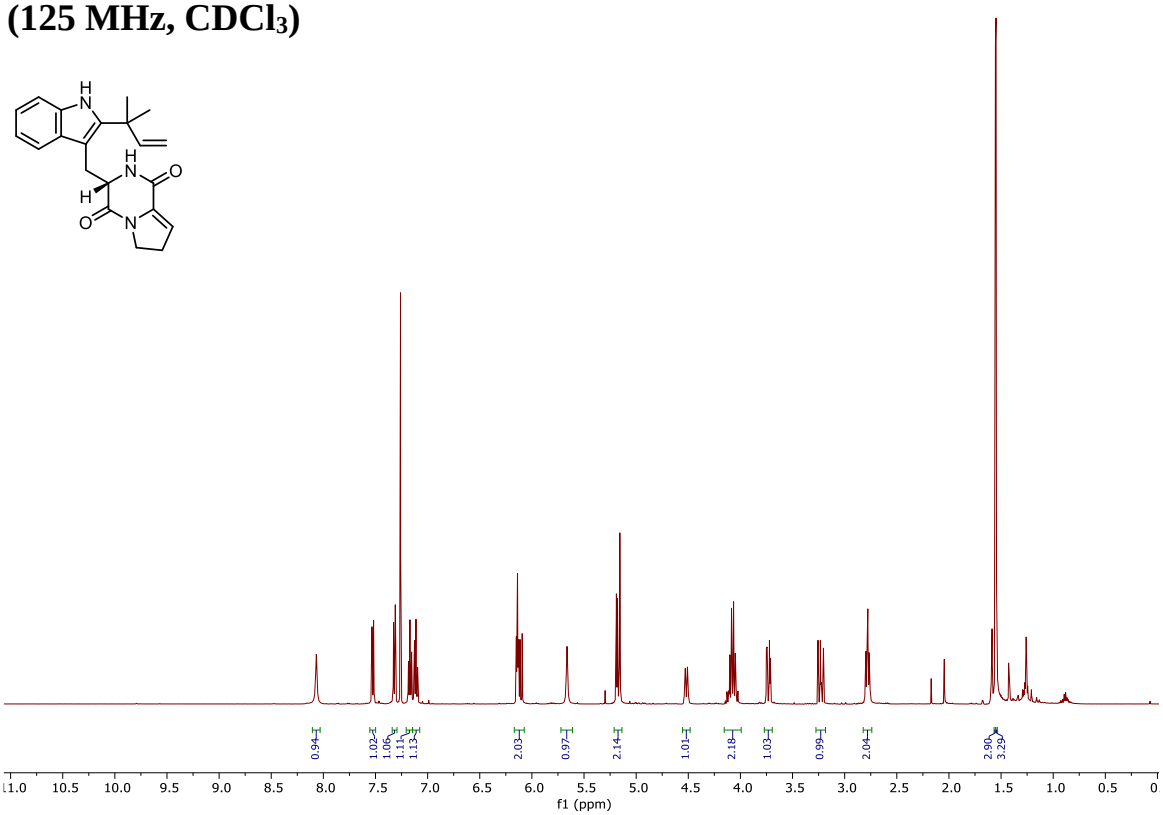

10.3.11 ^{1}H NMR Spectrum of Compound 4.74 (500 MHz, $CDCl_3$)

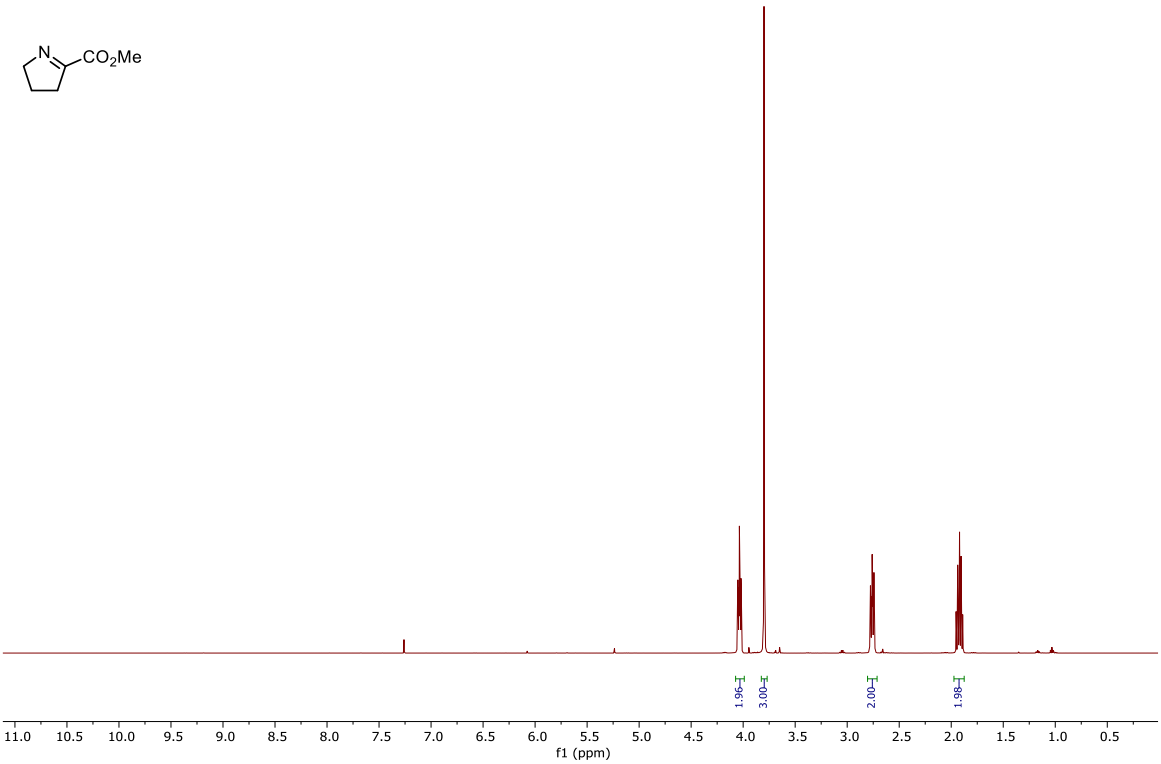

10.3.12 ^{13}C NMR Spectrum of Compound 4.74 (125 MHz, $CDCl_3$)

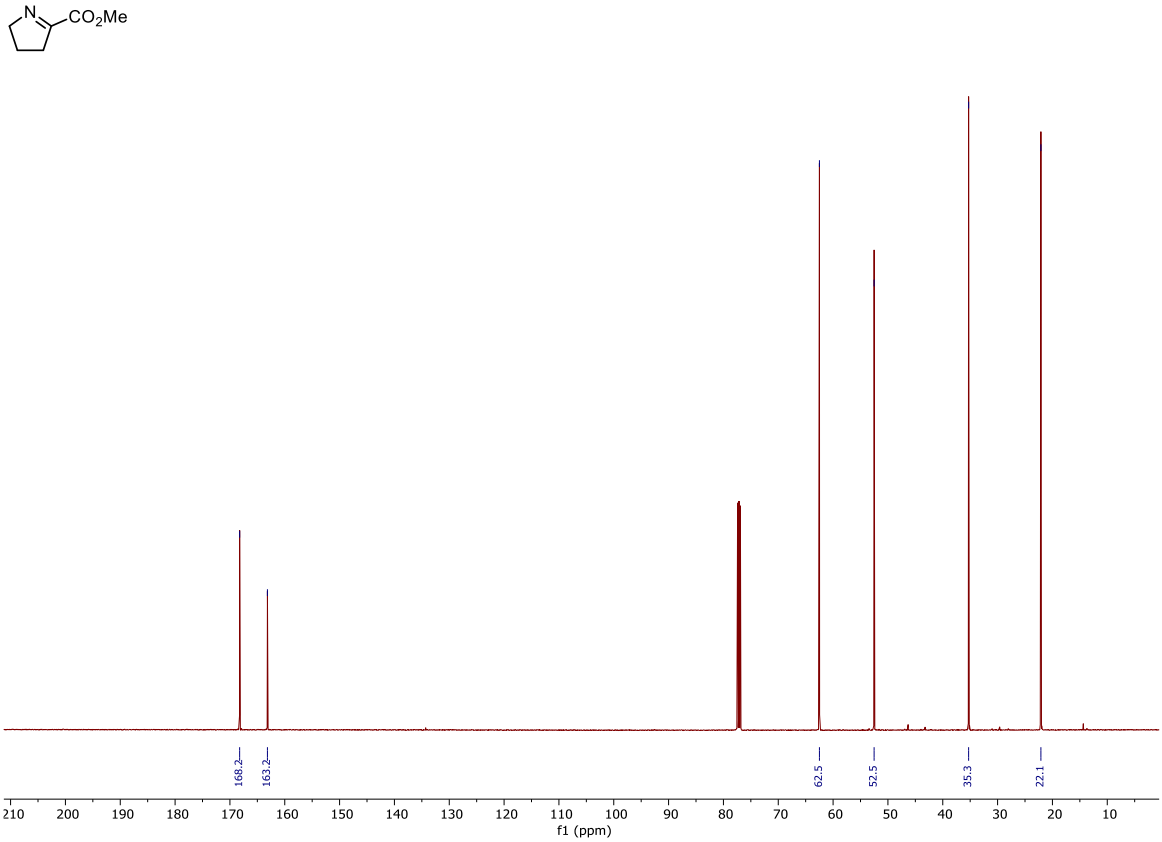

10.3.13 ^{1}H NMR Spectrum of 3-Chloro-3-methyl-1-butyne (5.16) (500 MHz, $CDCl_3$)

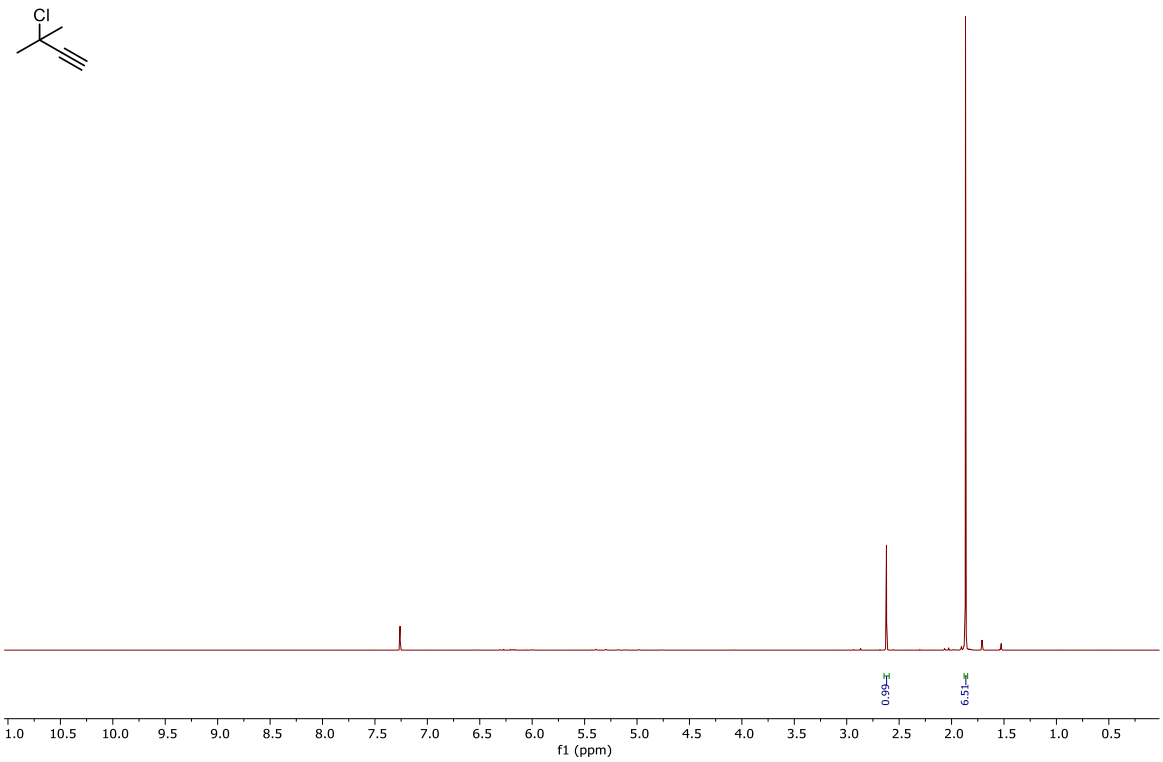

10.3.14 ^{13}C NMR Spectrum of 3-Chloro-3-methyl-1-butyne (5.16) (100 MHz, $CDCl_3$)

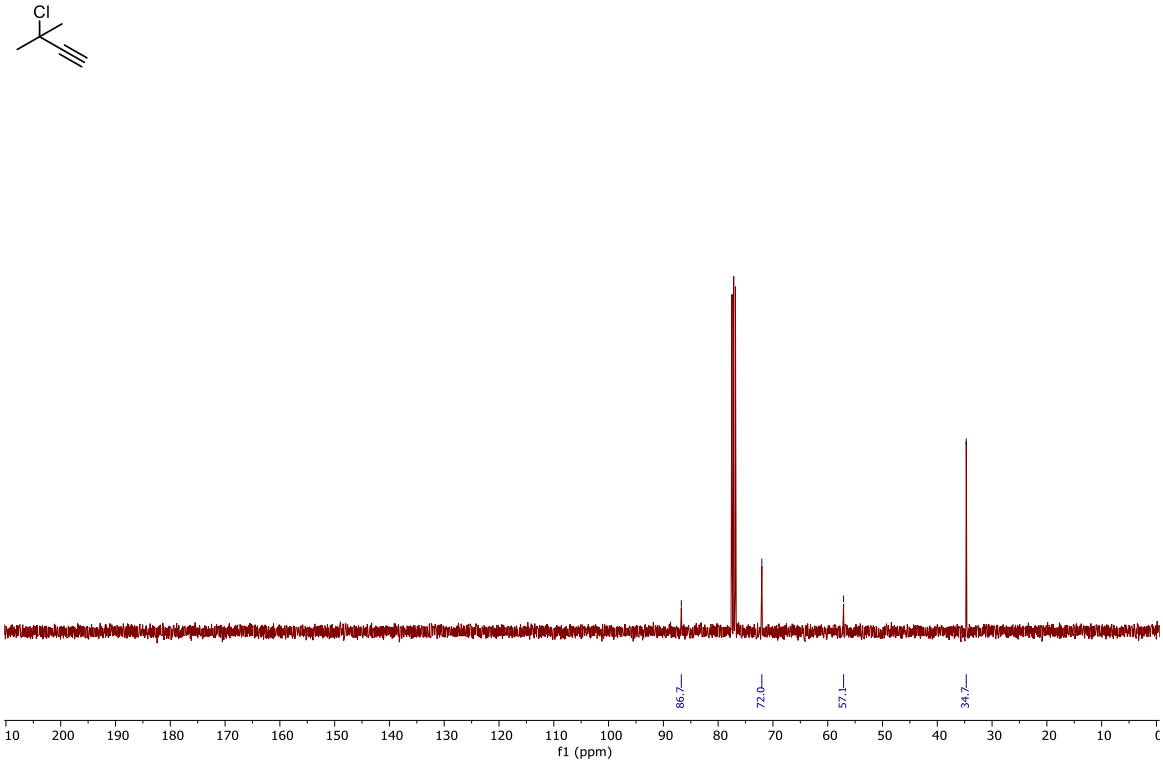

10.3.15 ^{1}H NMR Spectrum of 1,1-Dimethylallene (5.17) (500 MHz, $CDCl_3$)

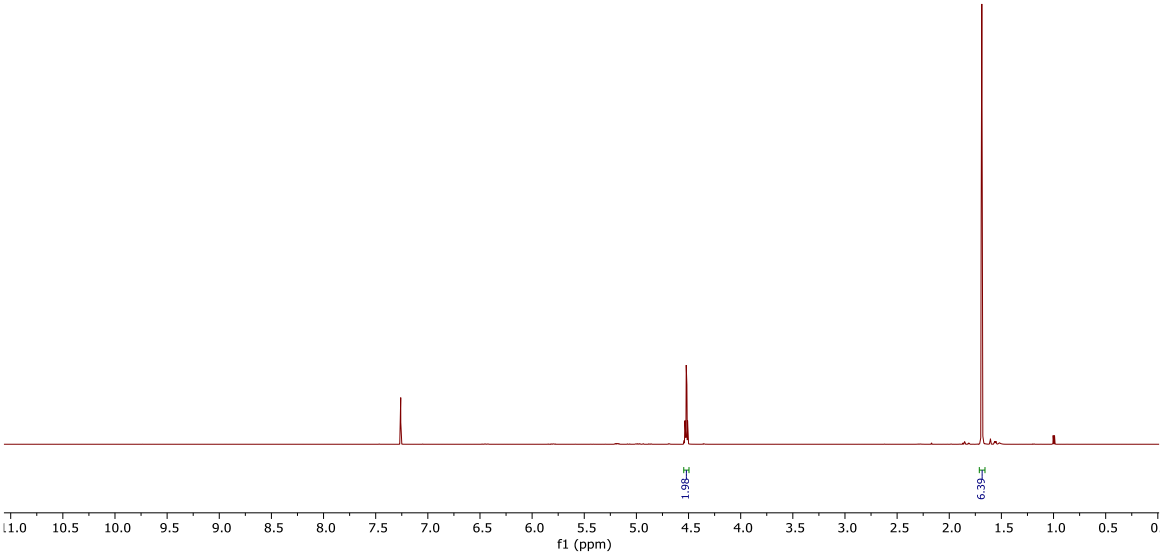

10.3.16 ^{13}C NMR Spectrum of 1,1-Dimethylallene (5.17) (150 MHz, $CDCl_3$)

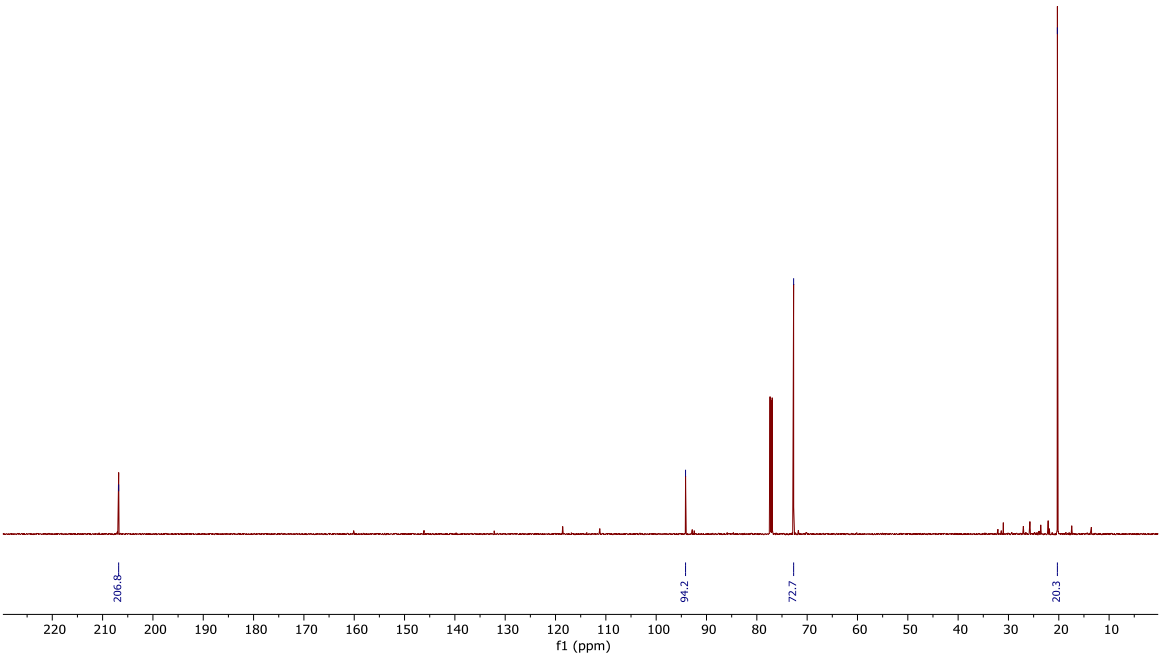

10.3.17 ^{1}H NMR Spectrum of *t*-BuOCl (500 MHz, $CDCl_3$)

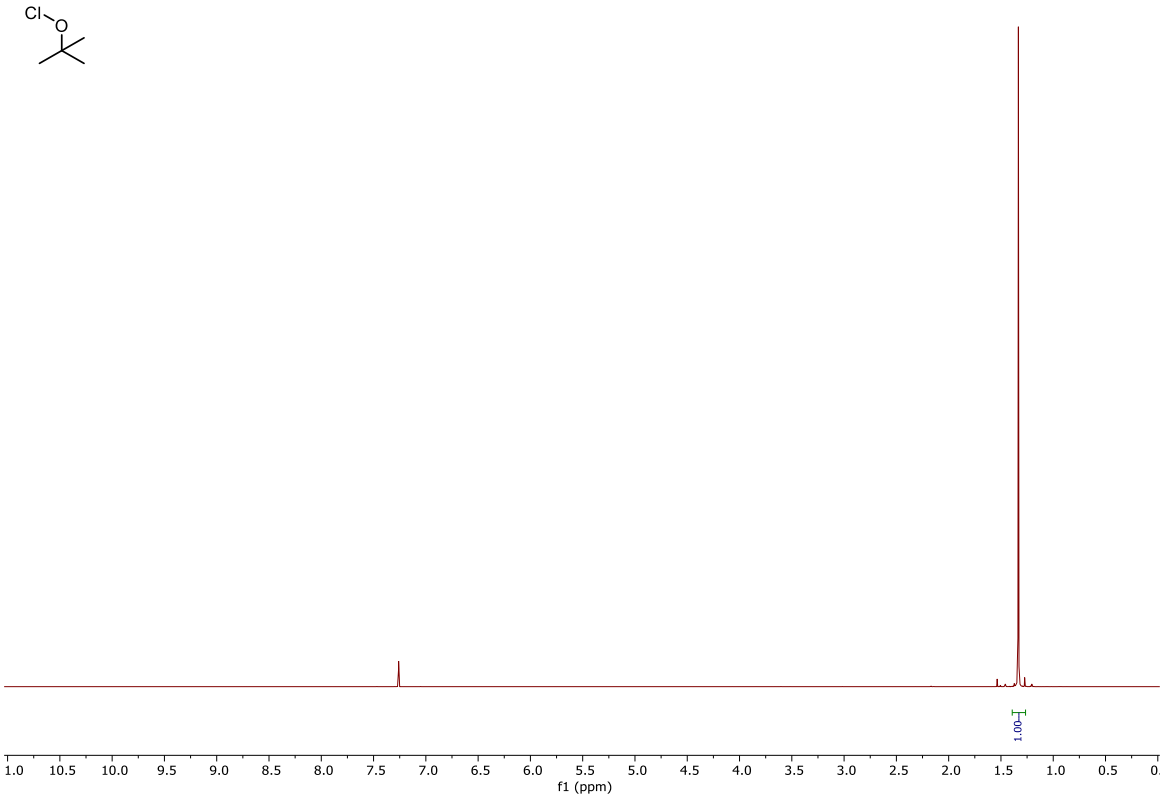

10.3.18 ^{13}C NMR Spectrum of *t*-BuOCl (125 MHz, $CDCl_3$)

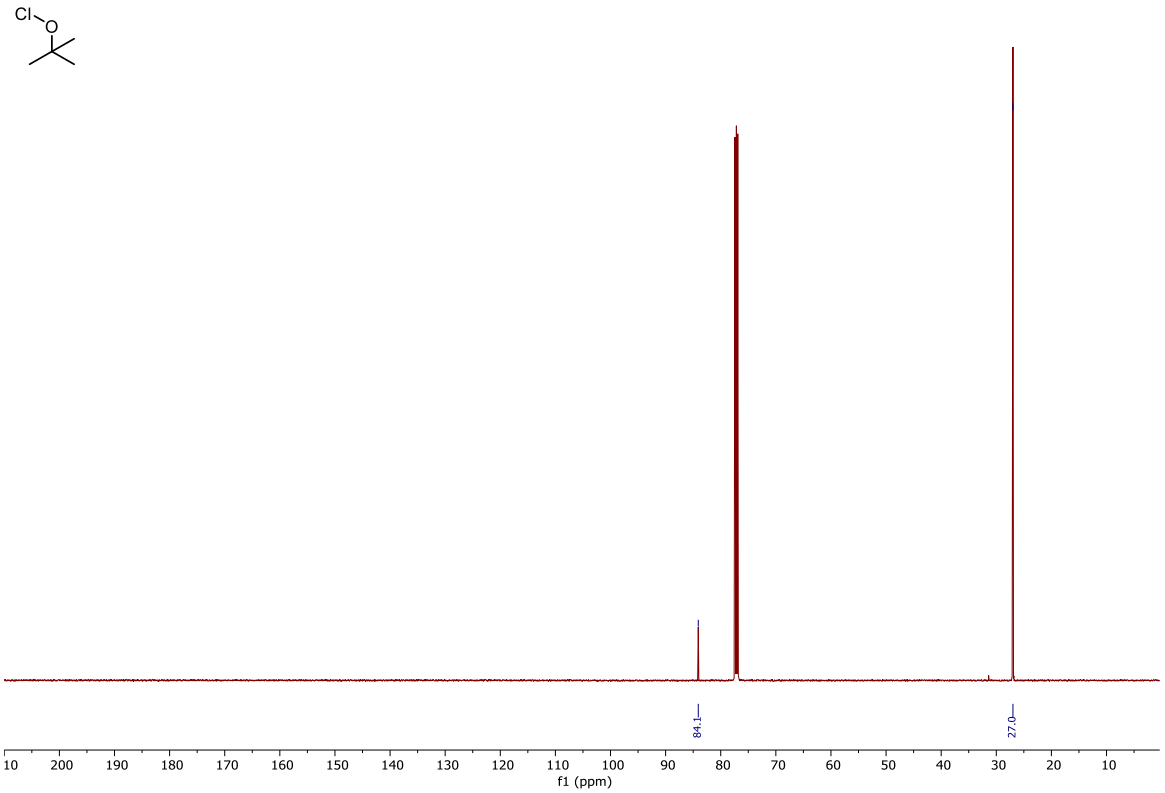

10.3.19 ^{1}H NMR Spectrum of (+)-Dehydrobrevianmide E (4.69) (500 MHz, $CDCl_3$)

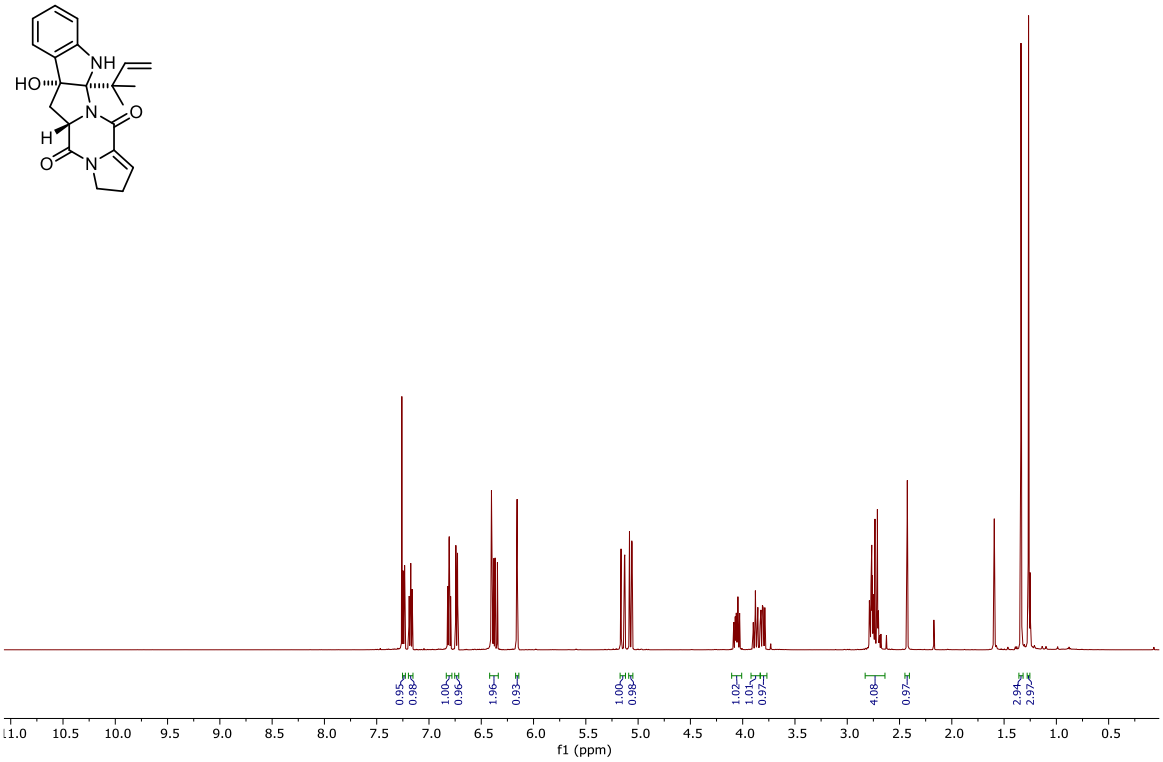

10.3.20 ^{13}C NMR Spectrum of (+)-Dehydrobrevianmide E (4.69) (125 MHz, $CDCl_3$)

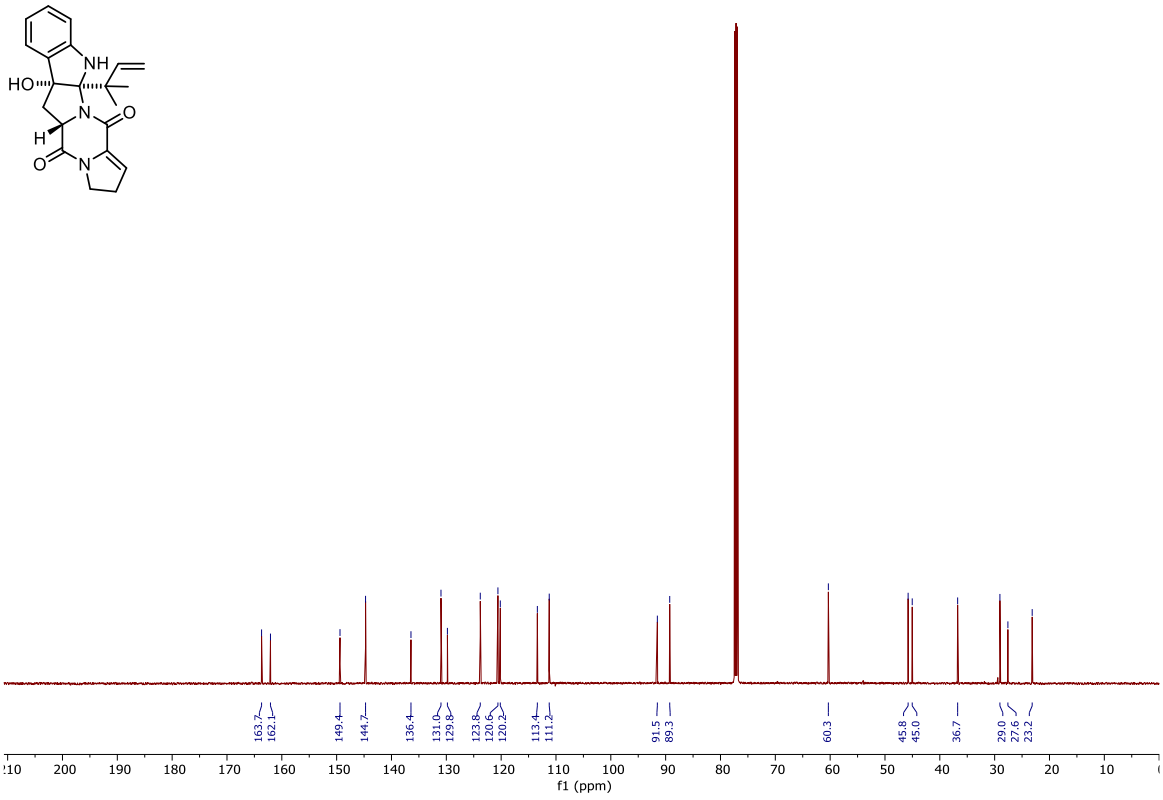

10.3.21 ^{1}H NMR Spectrum of Compound 5.23 (500 MHz, $CDCl_3$)

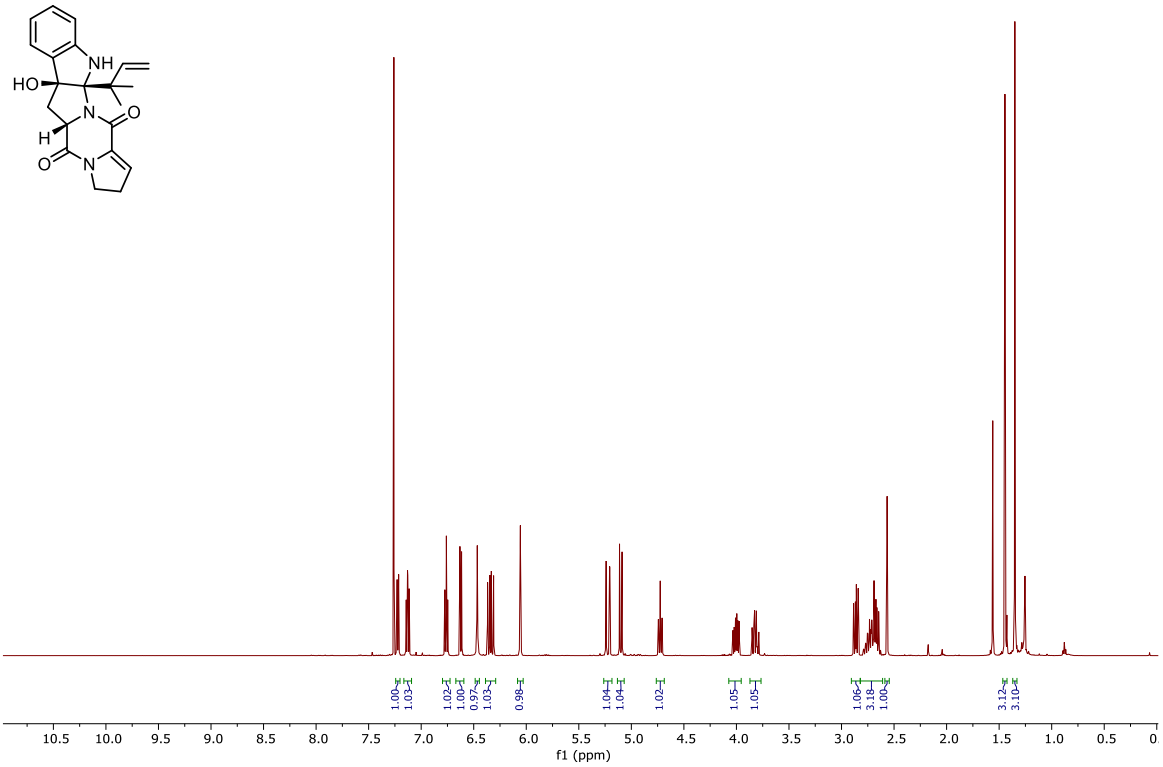

10.3.22 ^{13}C NMR Spectrum of Compound 5.23 (125 MHz, $CDCl_3$)

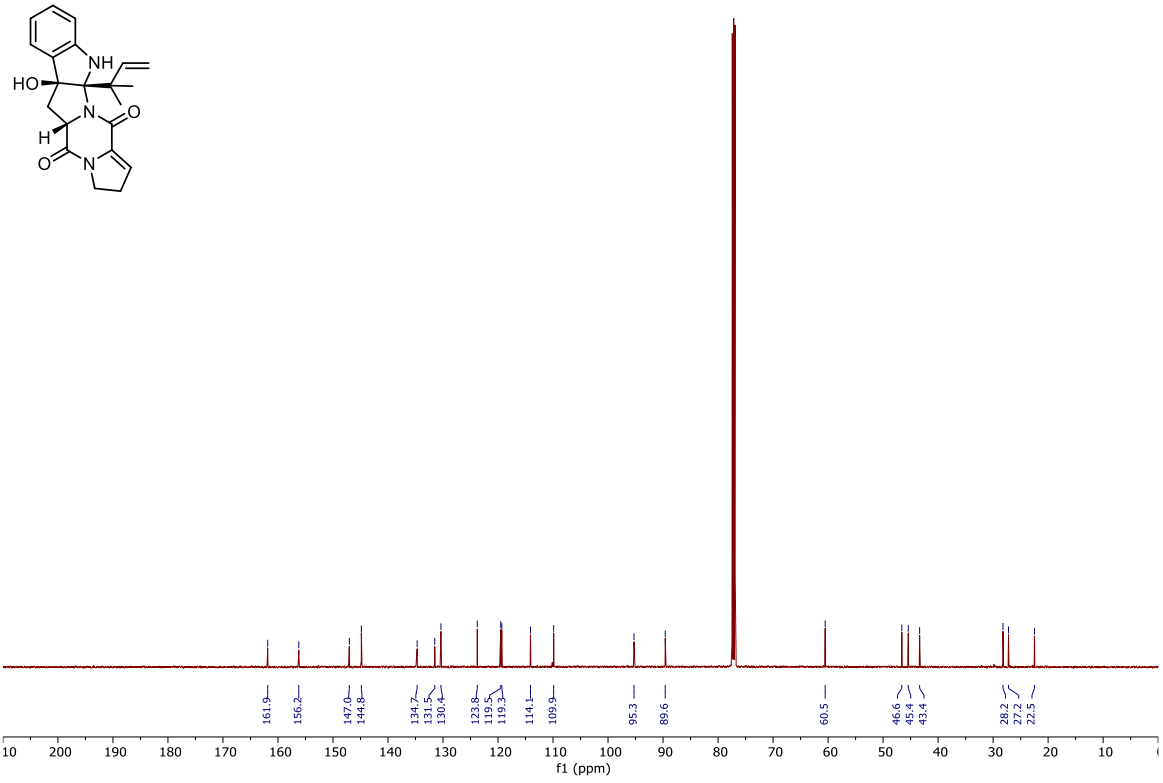

10.3.23 ^{1}H NMR Spectrum of Compound 5.23 (500 MHz, $(CD_3)_2SO$)

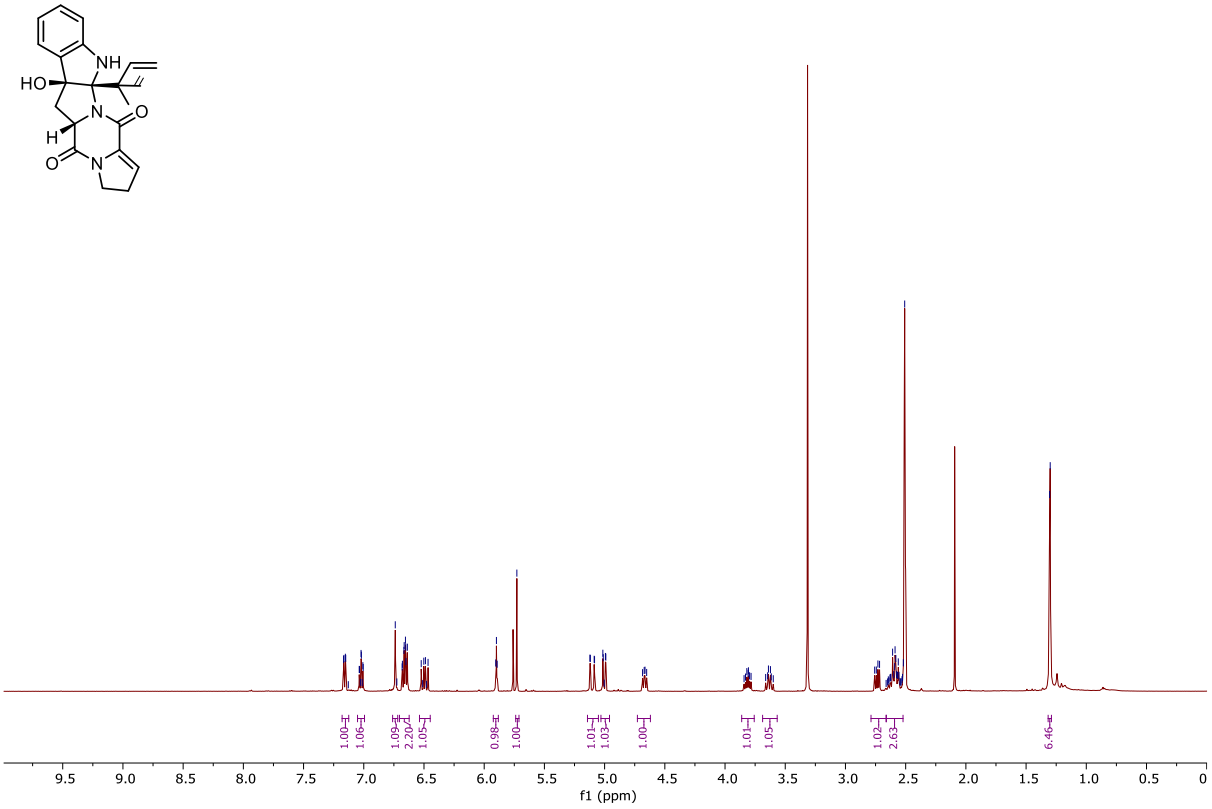

10.3.24 ^{13}C NMR Spectrum of Compound 5.23 (125 MHz, $(CD_3)_2SO$)

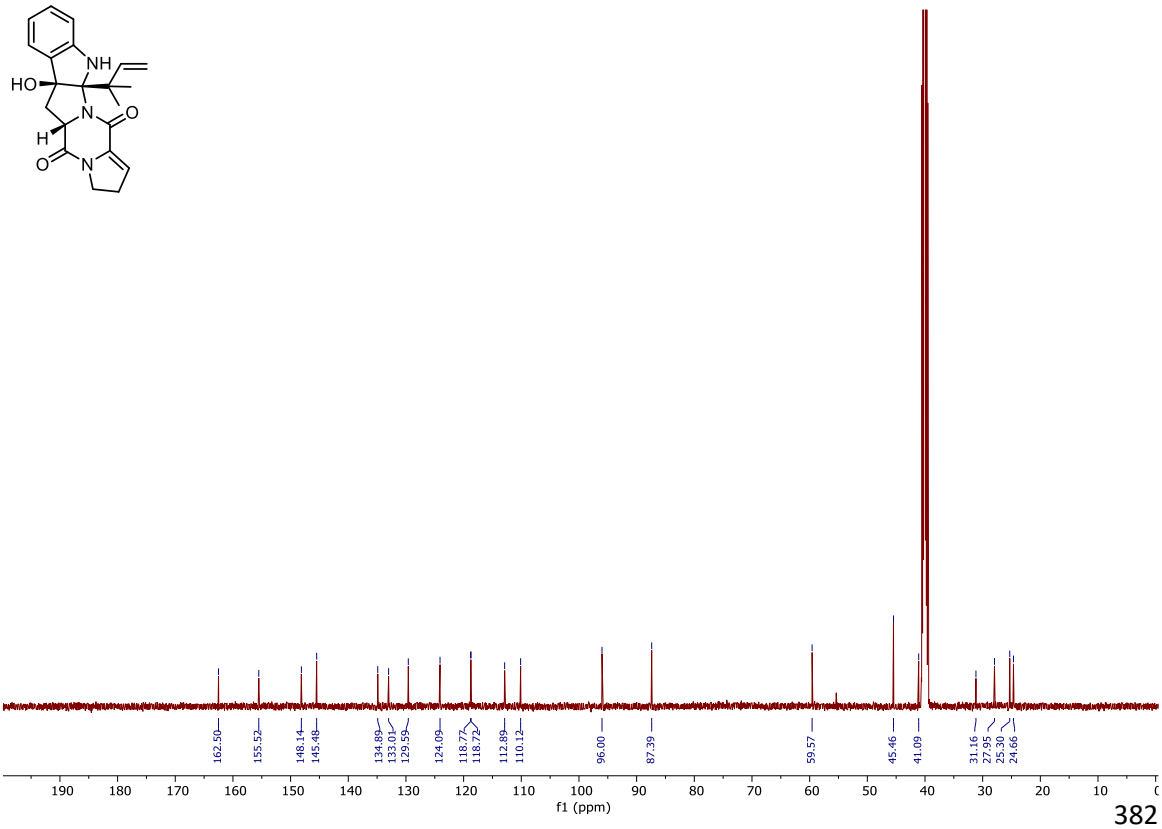

10.3.25 ^{1}H NMR Spectrum of Compound 5.24 (500 MHz, $CDCl_3$)

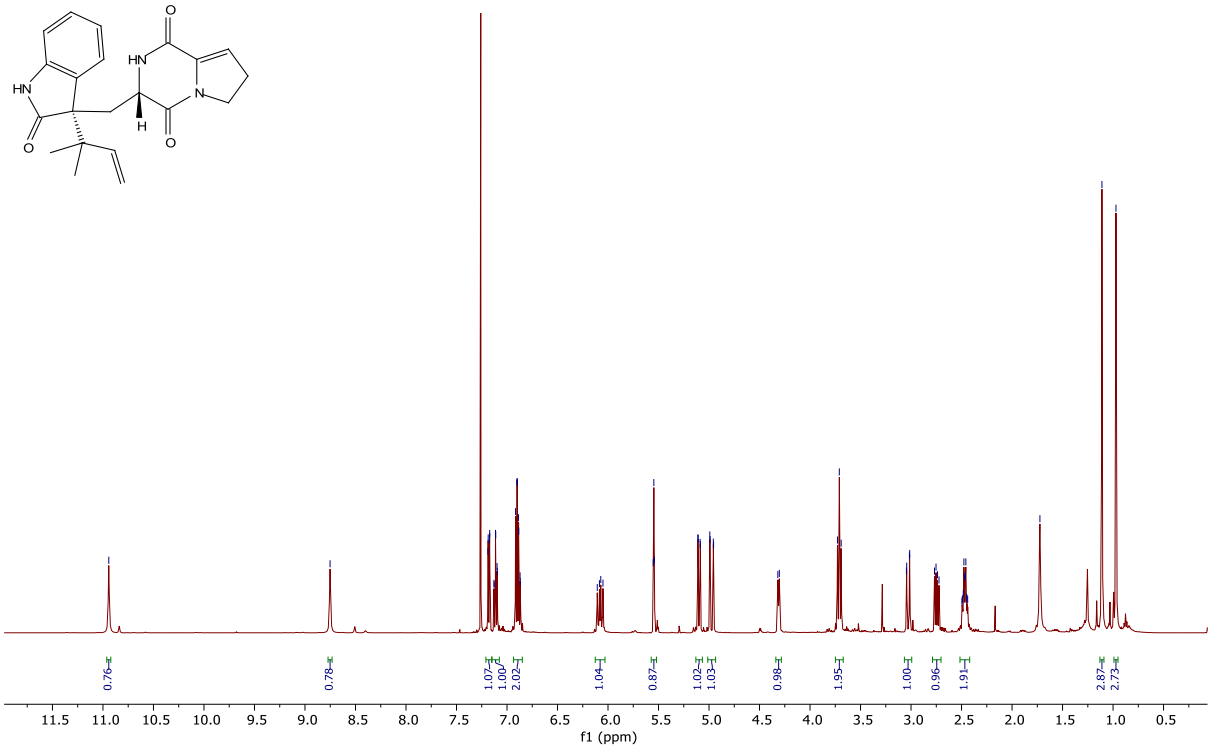

10.3.26 ^{13}C NMR Spectrum of Compound 5.24 (125 MHz, $CDCl_3$)

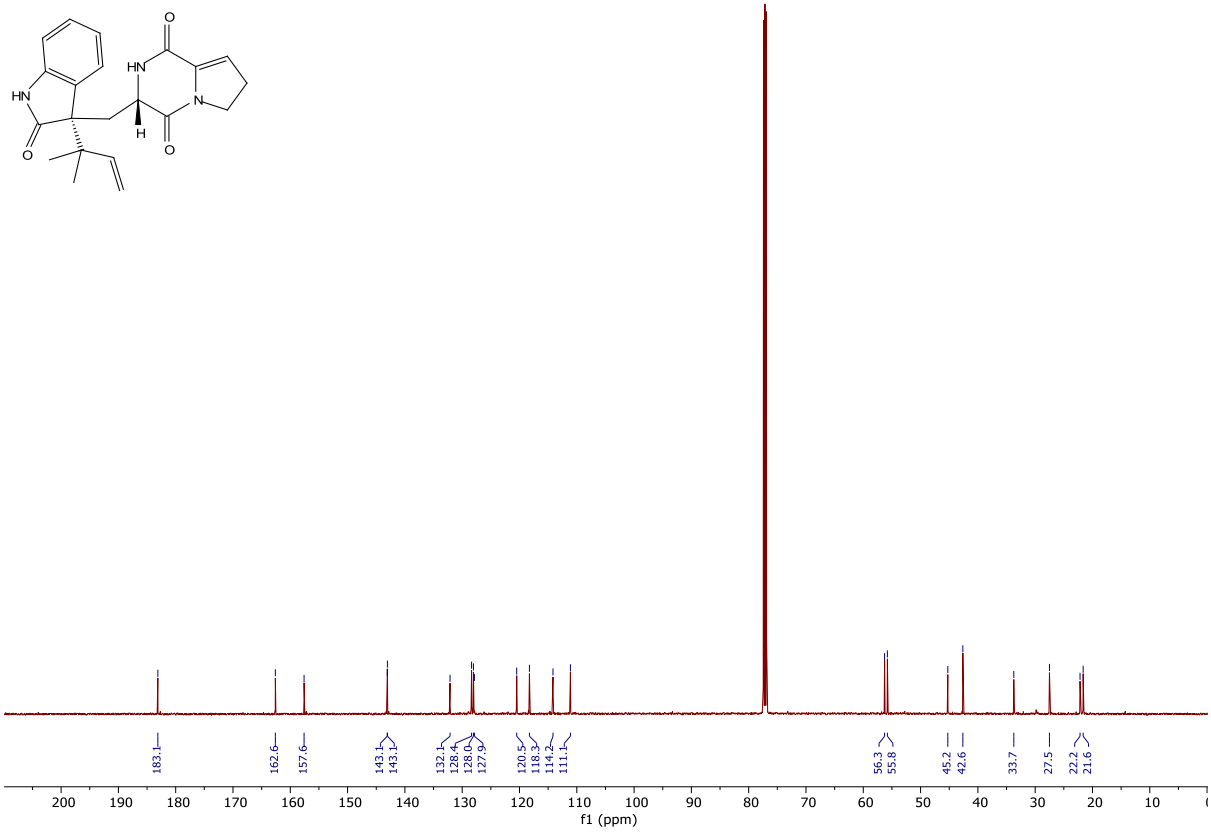

10.3.27 ^{1}H-^{1}H COSY Spectrum of Compound 5.24 ($CDCl_3$)

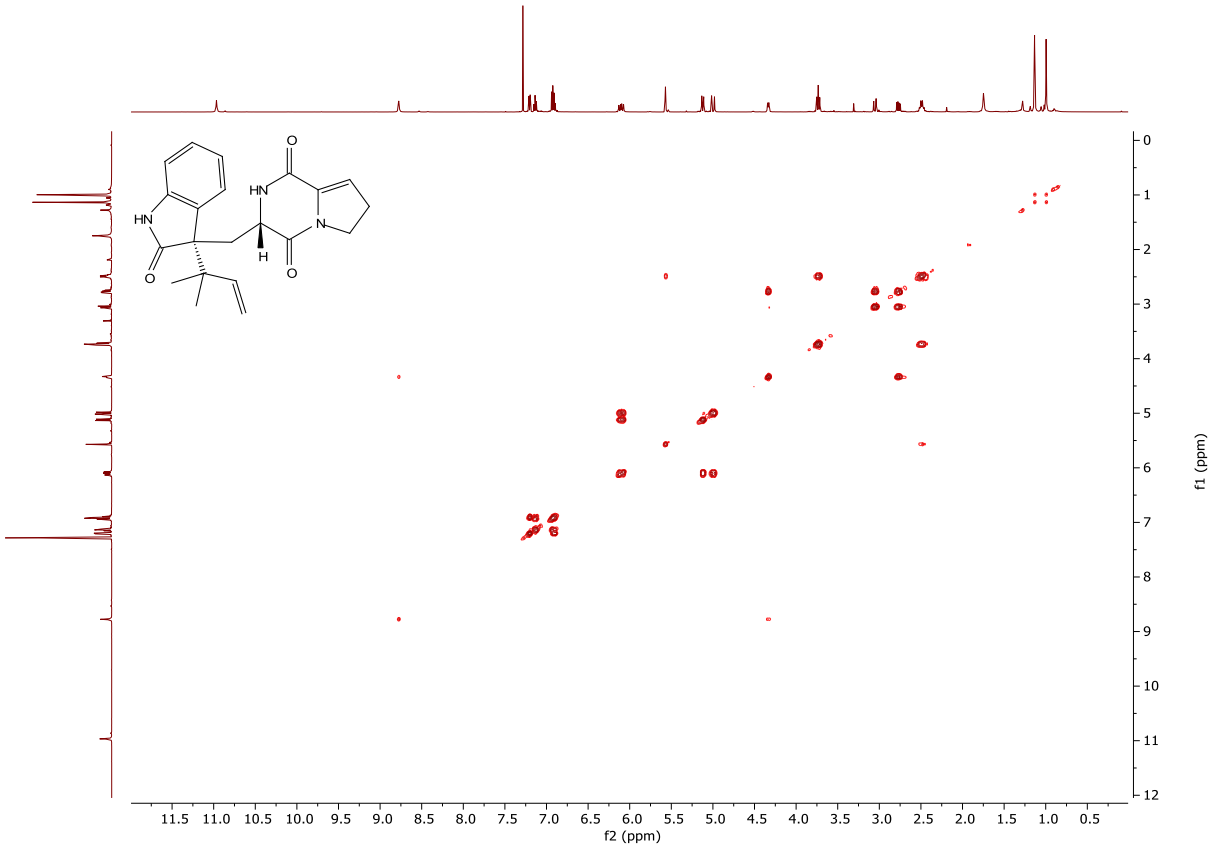

10.3.28 ^{1}H-^{13}C HSQC Spectrum of Compound 5.24 ($CDCl_3$)

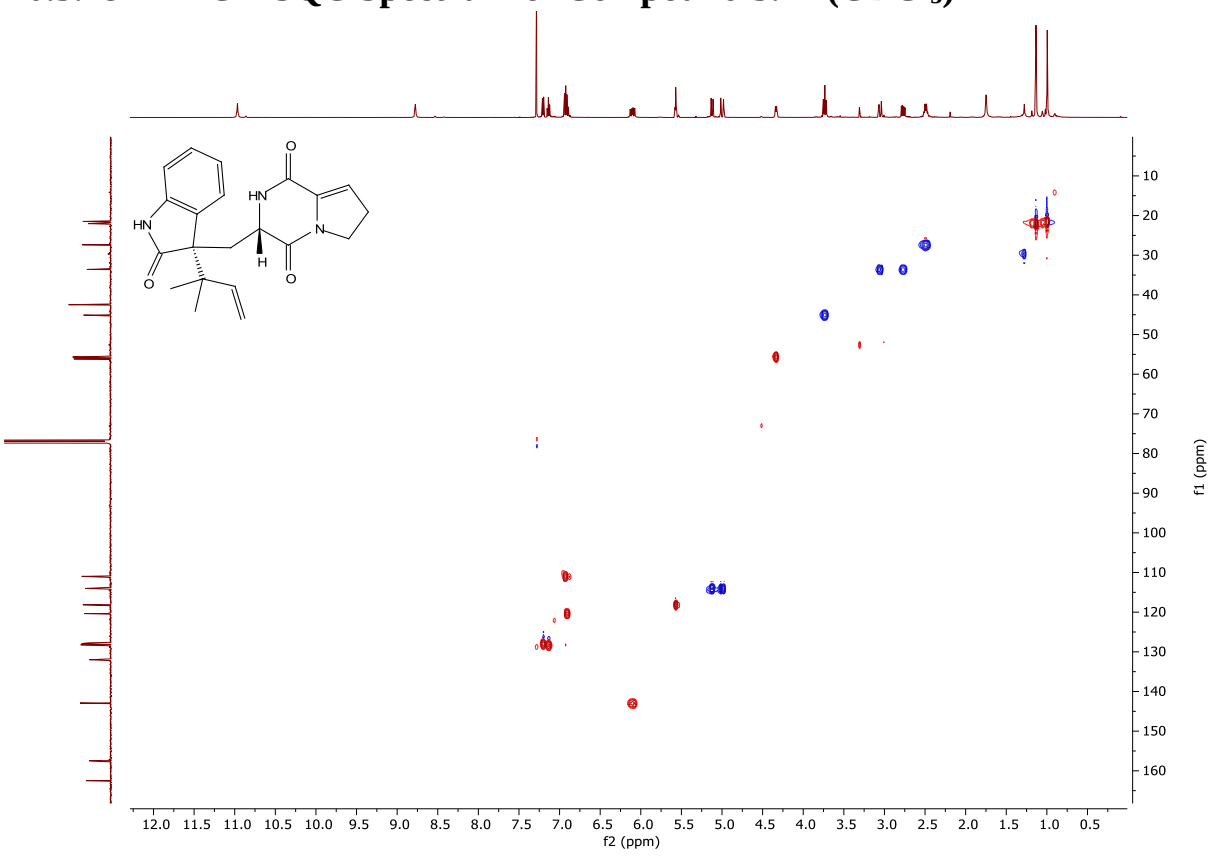

10.3.29 ^{1}H-^{13}C HMBC Spectrum of Compound 5.24 ($CDCl_3$)

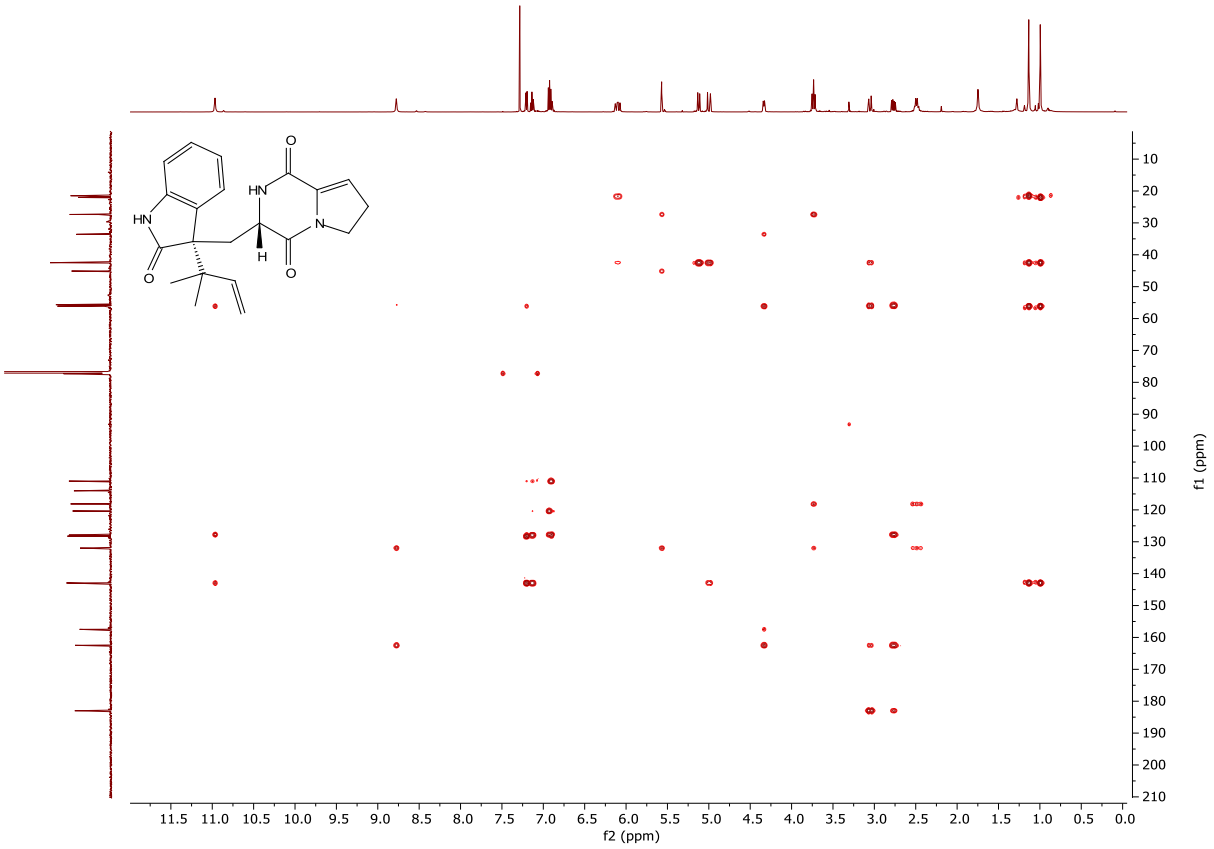

10.3.30 ^{1}H-^{1}H NOESY Spectrum of Compound 5.24 ($CDCl_3$)

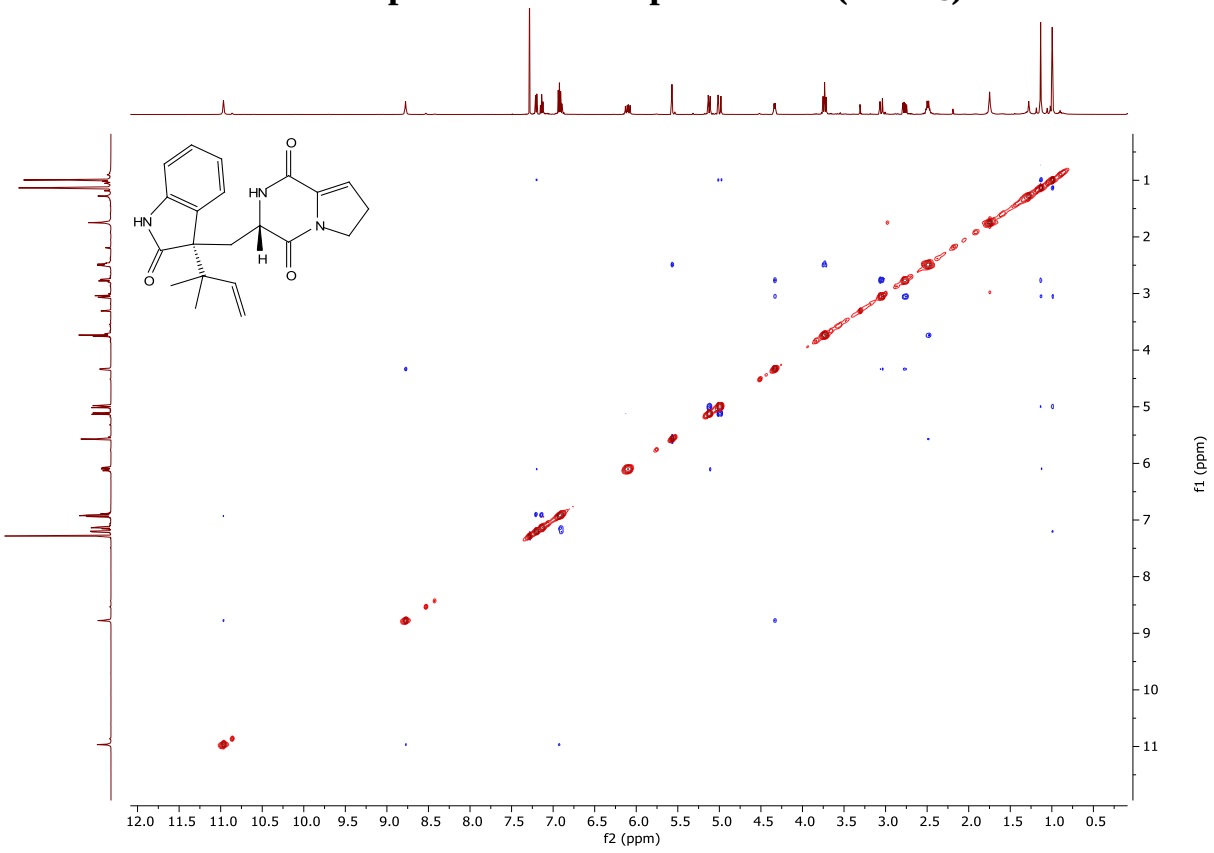

10.3.31 ^{1}H NMR Spectrum of Compound 5.25 (500 MHz, $CDCl_3$)

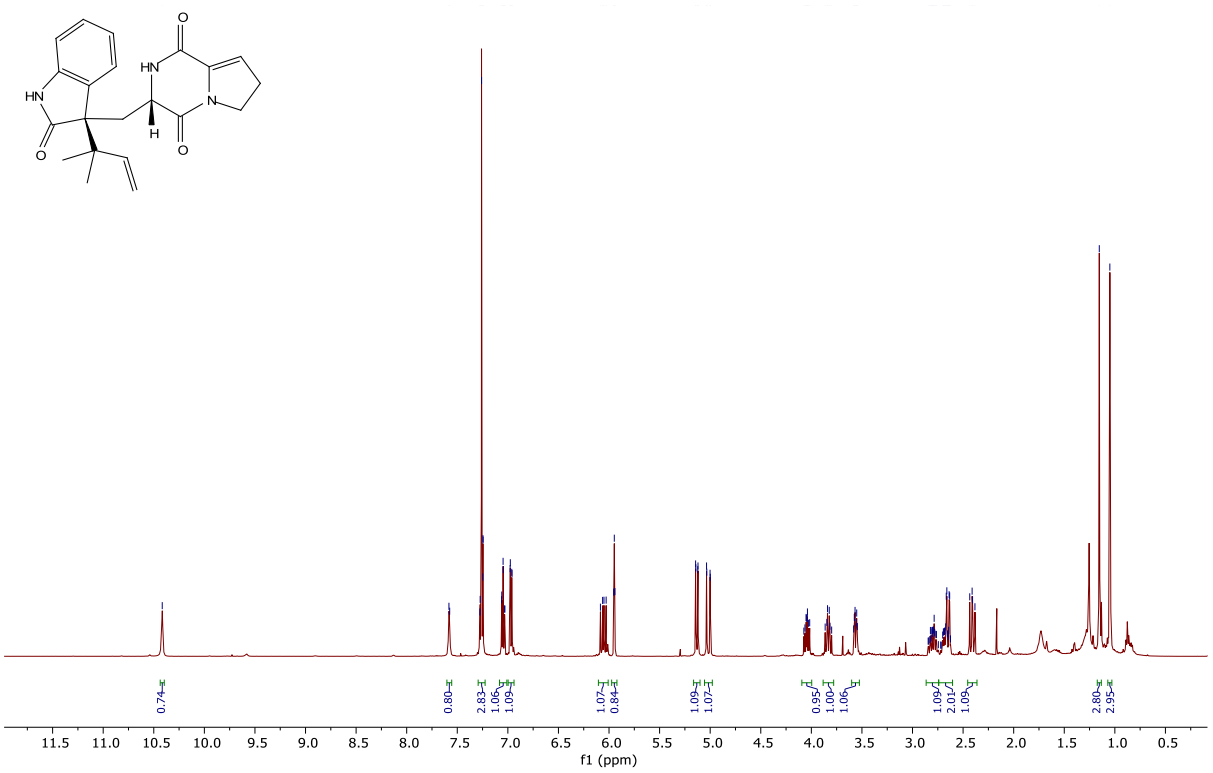

10.3.32 ^{13}C NMR Spectrum of Compound 5.25 (125 MHz, $CDCl_3$)

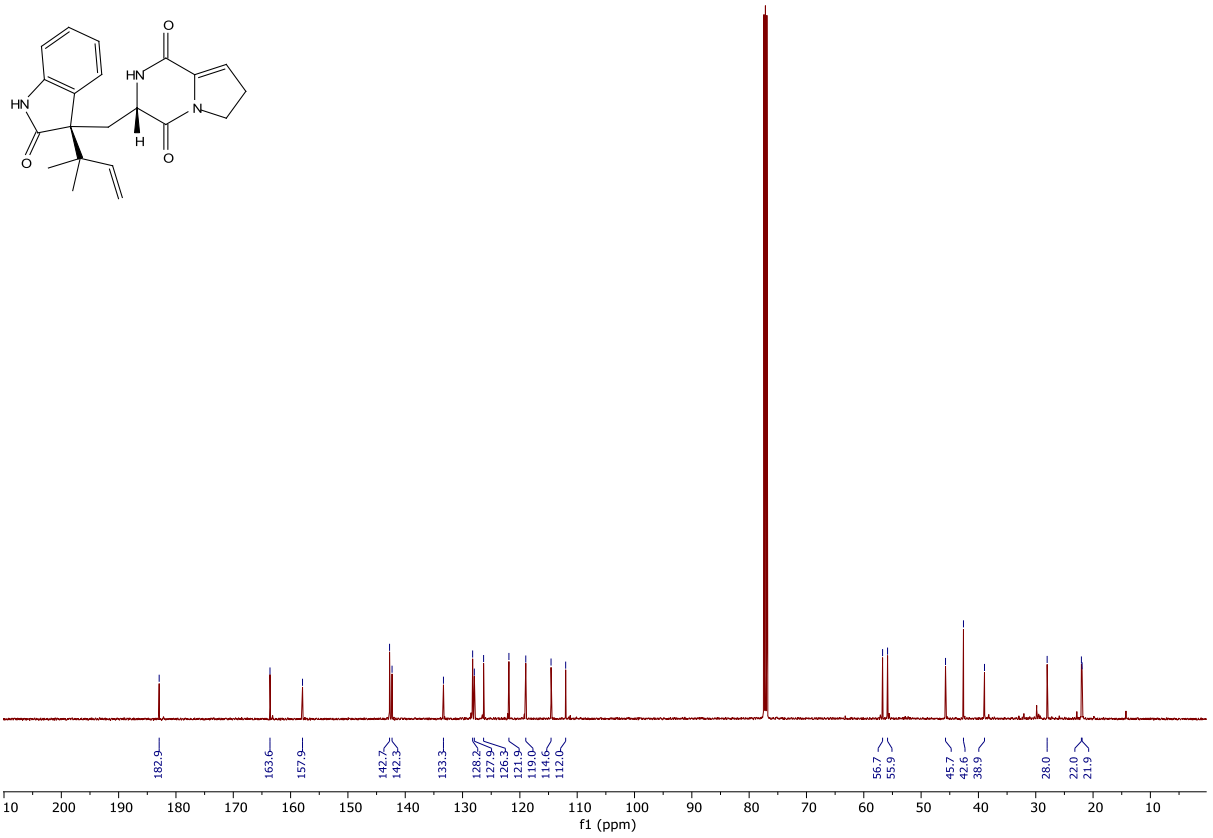

10.3.33 ^{1}H-^{1}H COSY Spectrum of Compound 5.25 ($CDCl_3$)

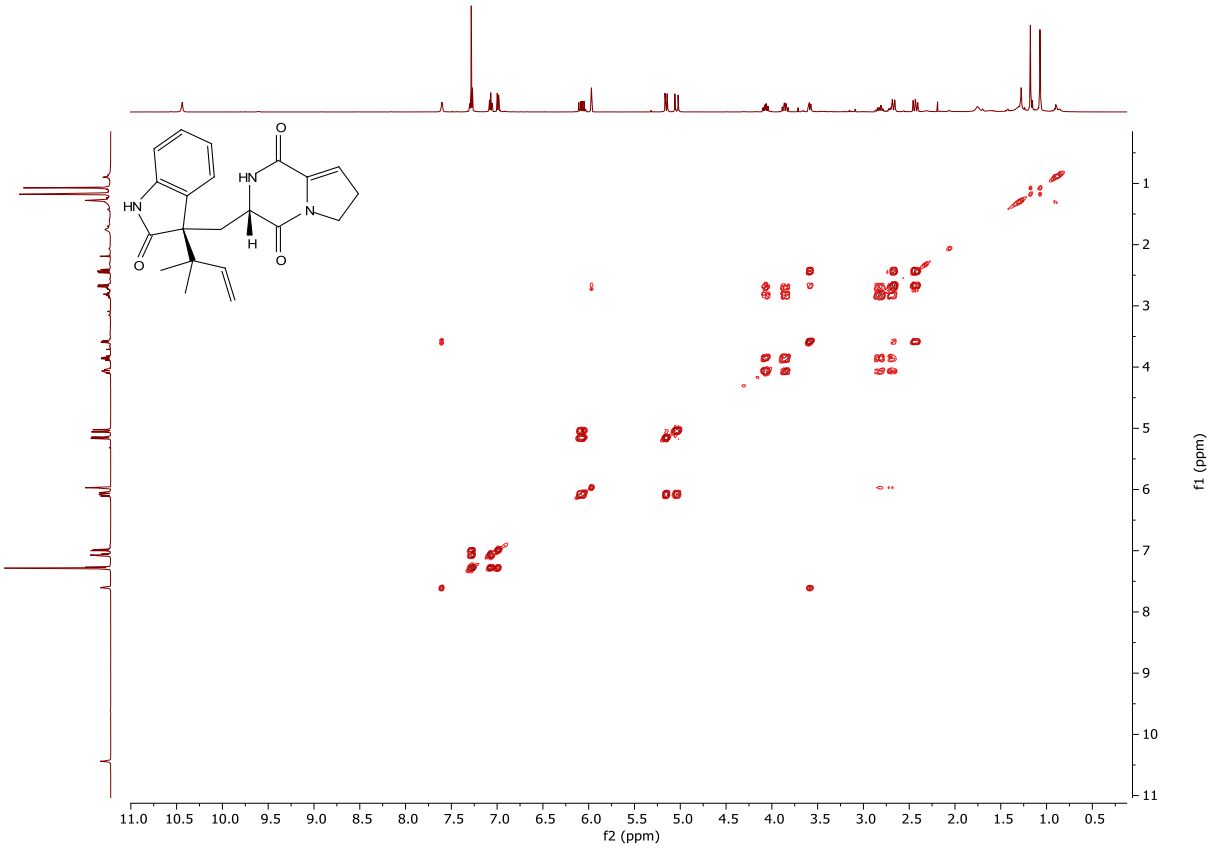

10.3.34 ^{1}H-^{13}C HSQC Spectrum of Compound 5.25 ($CDCl_3$)

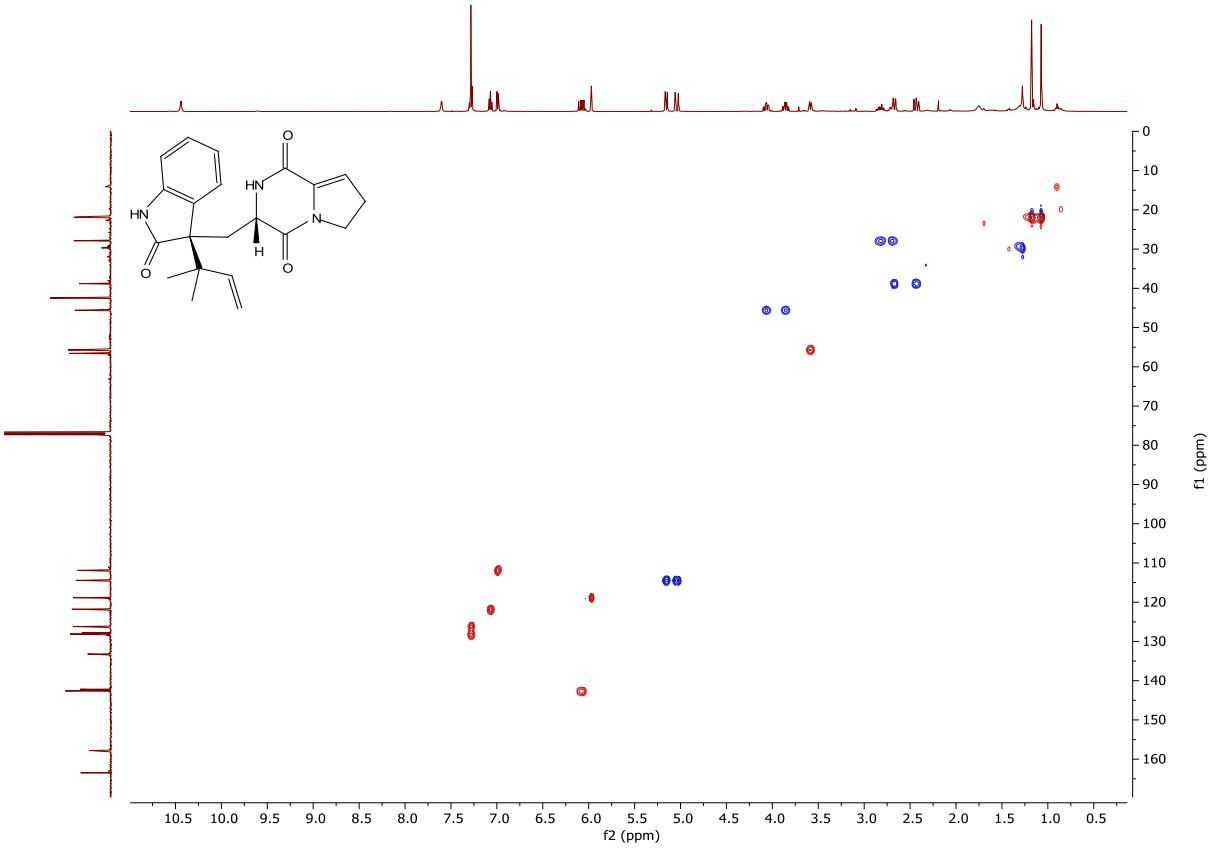

10.3.35 ^{1}H-^{13}C HMBC Spectrum of Compound 5.25 ($CDCl_3$)

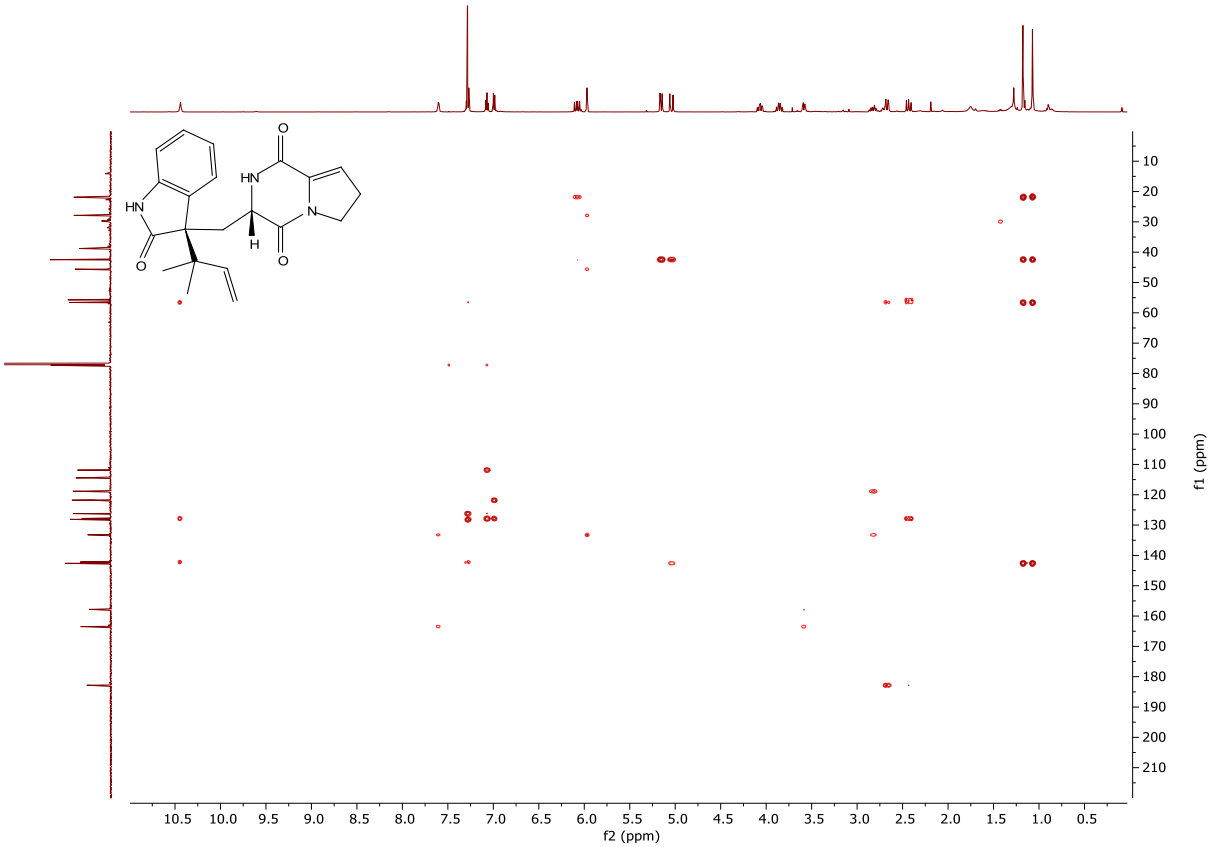

10.3.36 ^{1}H-^{1}H NOESY Spectrum of Compound 5.25 ($CDCl_3$)

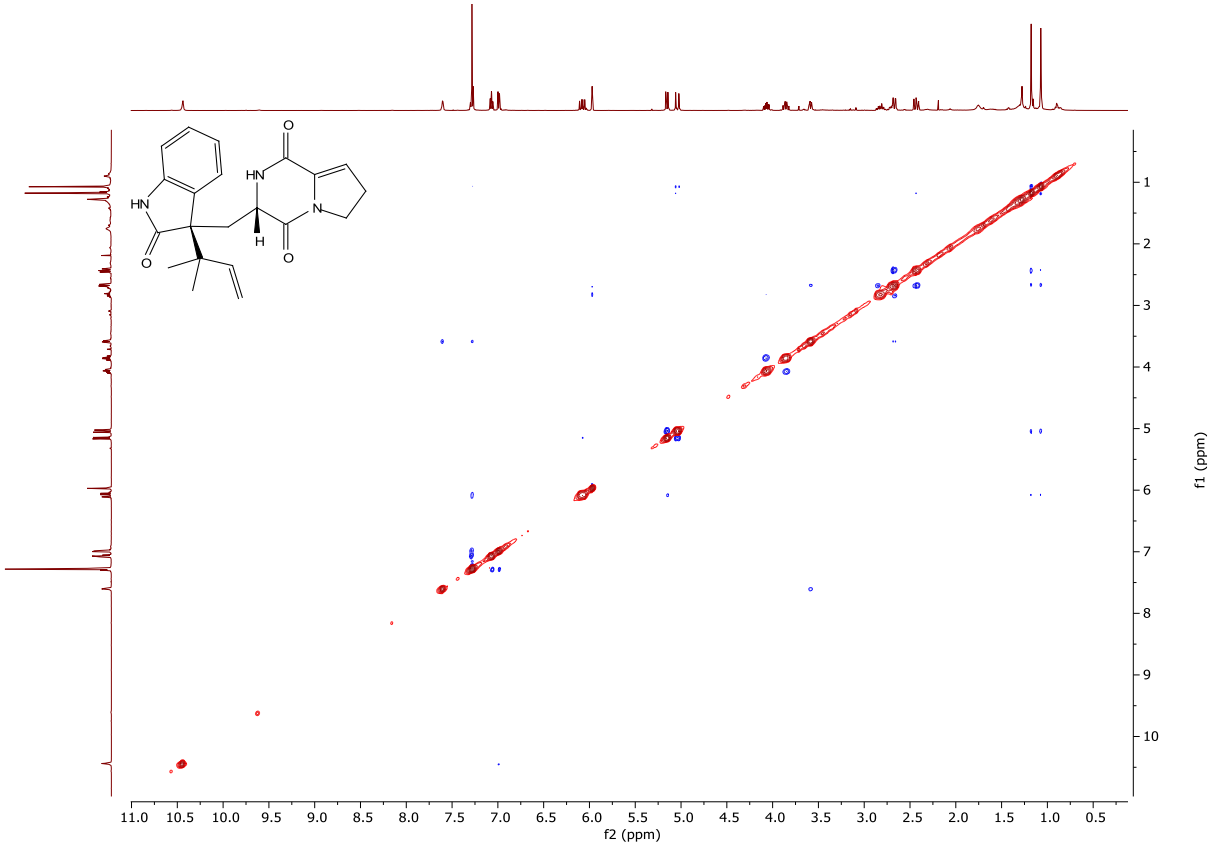

10.3.37 ^{1}H NMR Spectrum of Brevianamide Y (4.4) (500 MHz, $(CD_3)_2SO$)

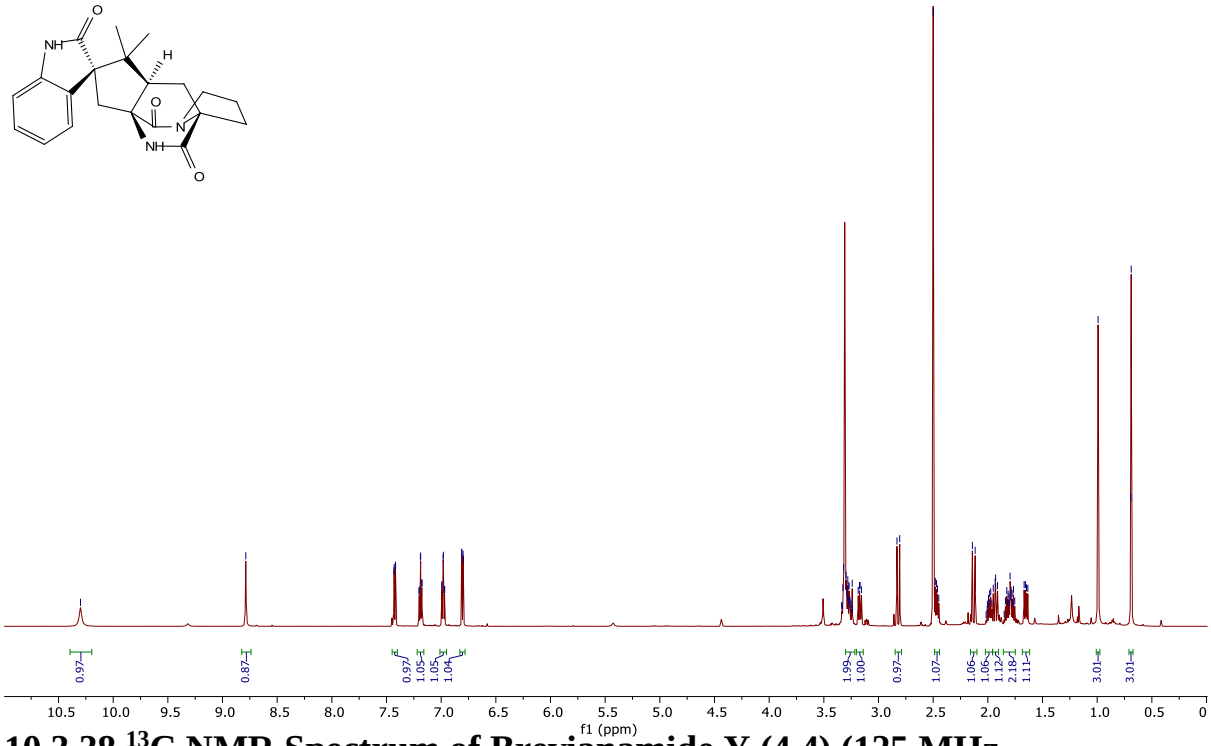

10.3.38 ^{13}C NMR Spectrum of Brevianamide Y (4.4) (125 MHz, $(CD_3)_2SO$))

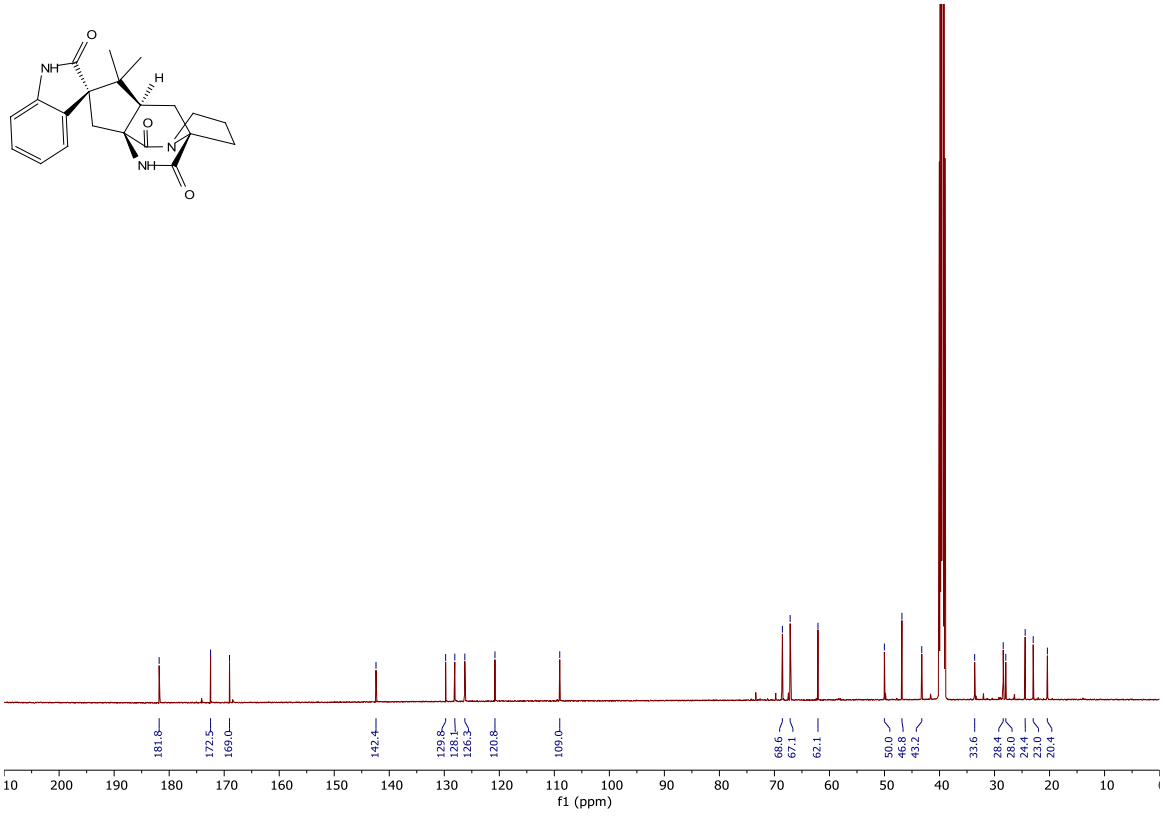

10.3.39 ^{1}H-^{1}H COSY Spectrum of Brevianamide Y (4.4) ($(CD_3)_2SO$)

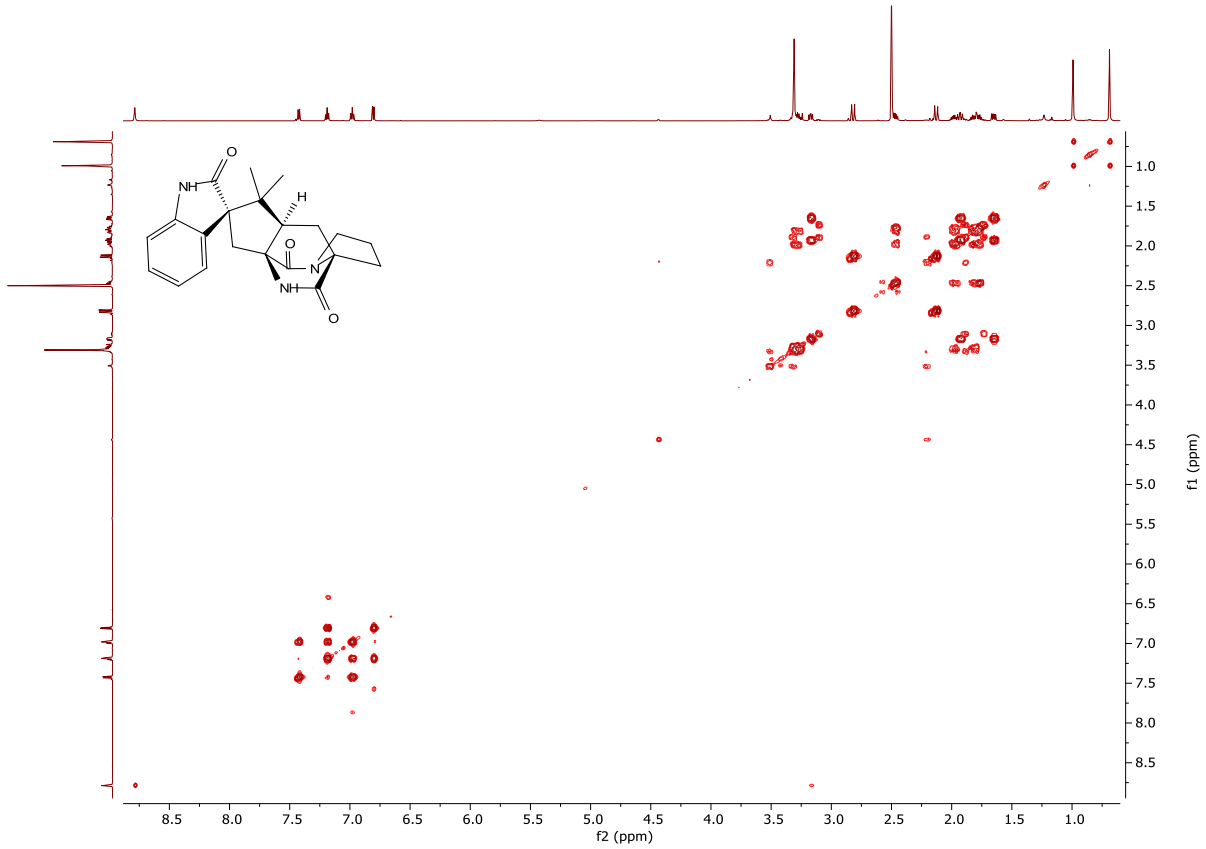

10.3.40 ^{1}H-^{13}C HSQC Spectrum of Brevianamide Y (4.4) ($(CD_3)_2SO$)

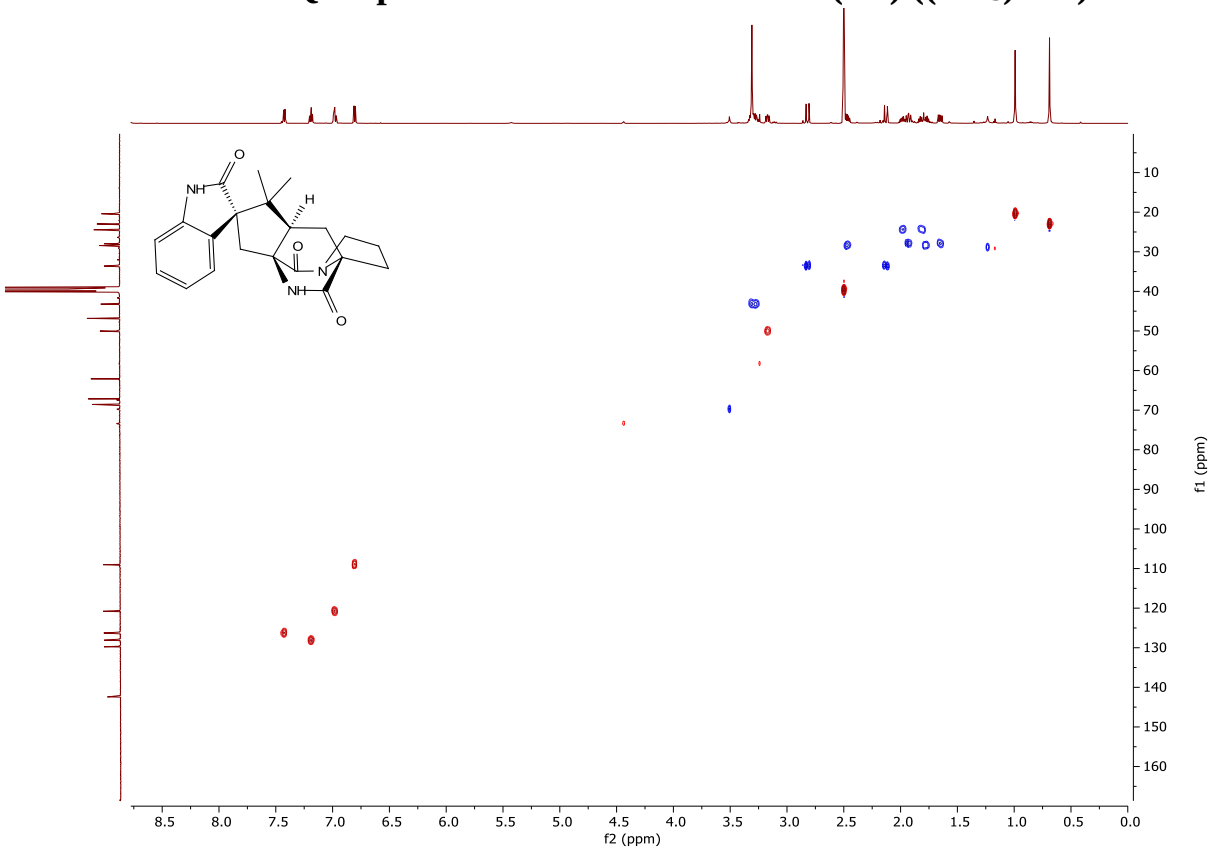

10.3.41 ^{1}H-^{13}C HMBC Spectrum of Brevianamide Y (4.4) ($(CD_3)_2SO$)

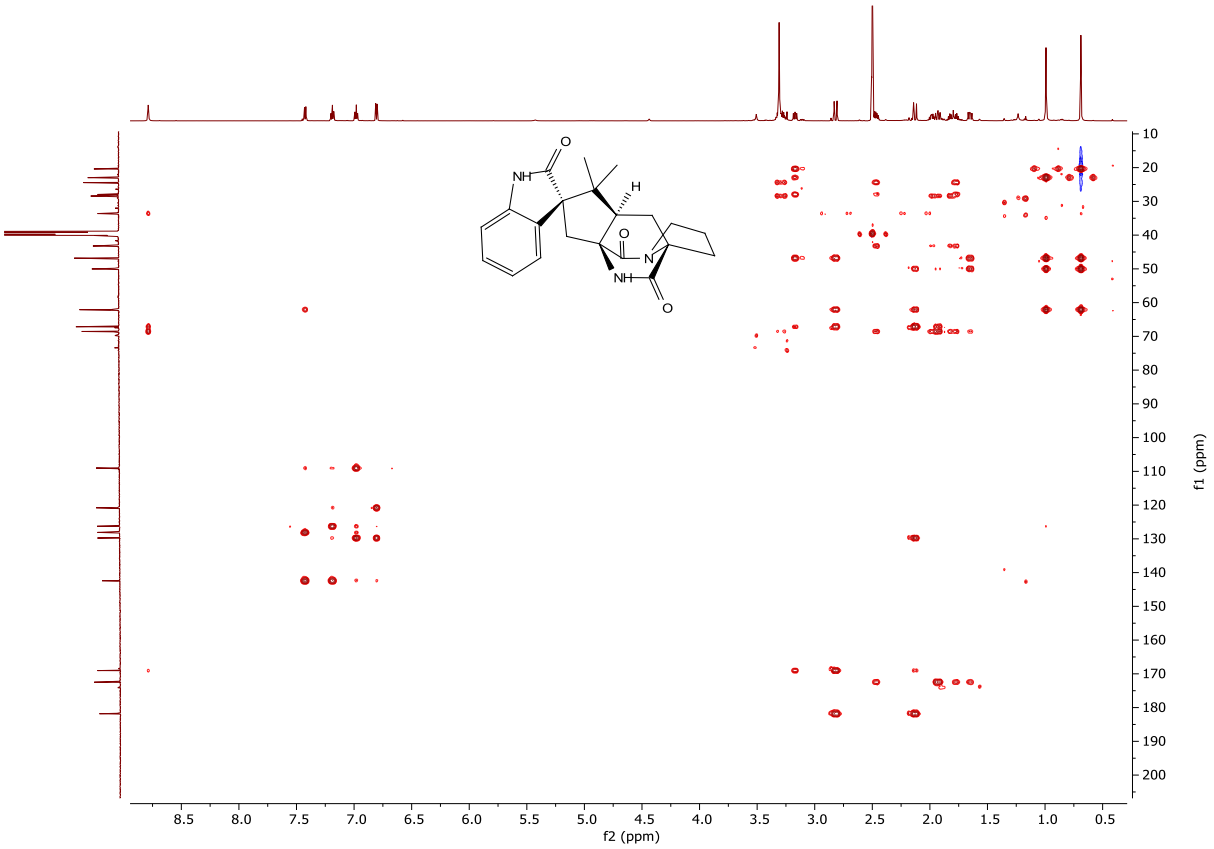

10.3.42 ^{1}H-^{1}H NOESY Spectrum of Brevianamide Y (4.4) ($(CD_3)_2SO$)

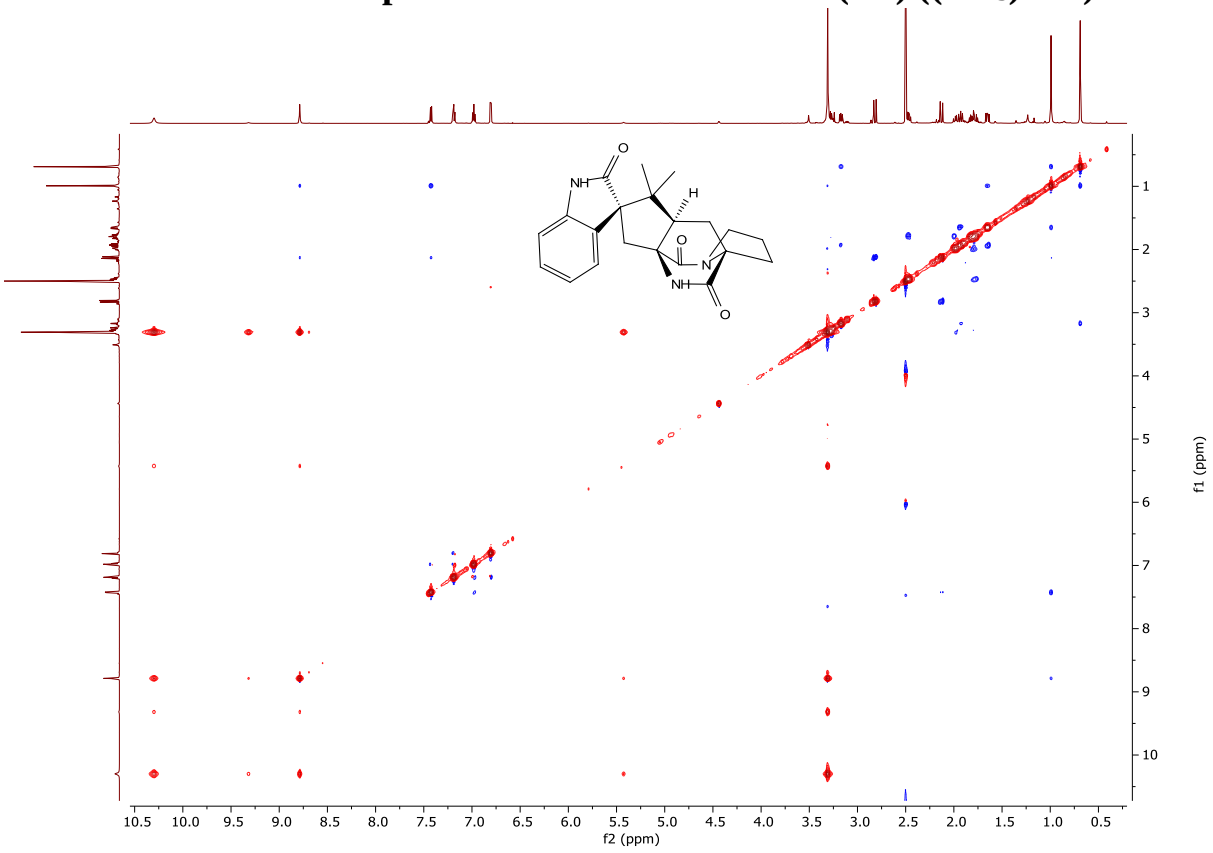

10.3.43 ^{1}H NMR Spectrum of Brevianamide Z (5.3) (500 MHz, $(CD_3)_2SO$)

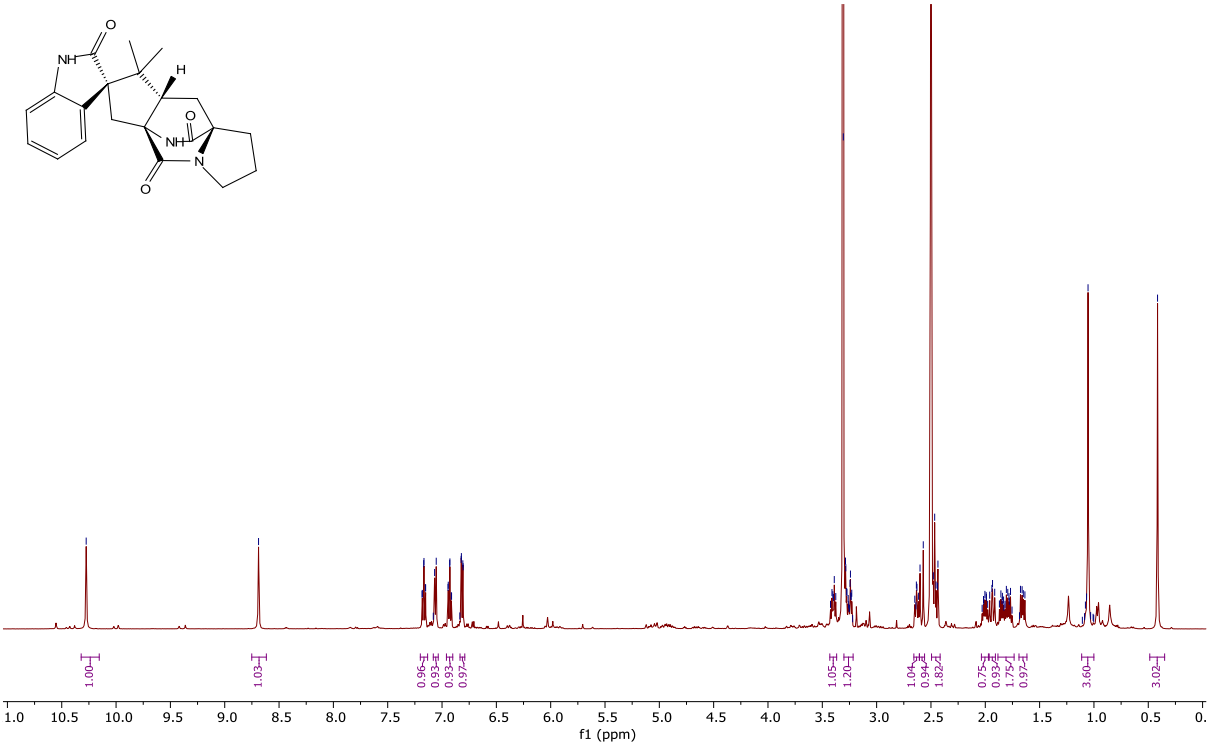

10.3.44 ^{13}C NMR Spectrum of Brevianamide Z (5.3) (125 MHz, $(CD_3)_2SO$)

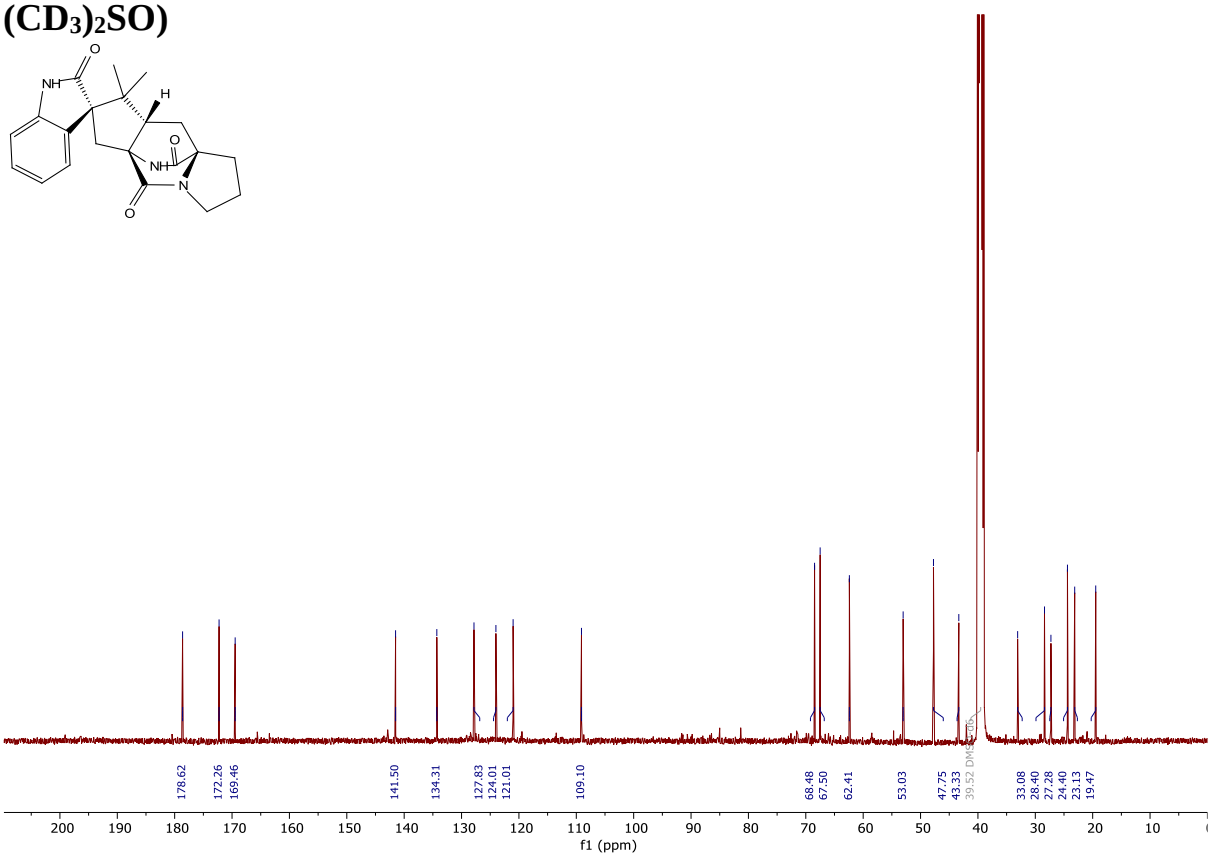

10.3.45 ^{1}H-^{1}H COSY Spectrum of Brevianamide Z (5.3) ($(CD_3)_2SO$)

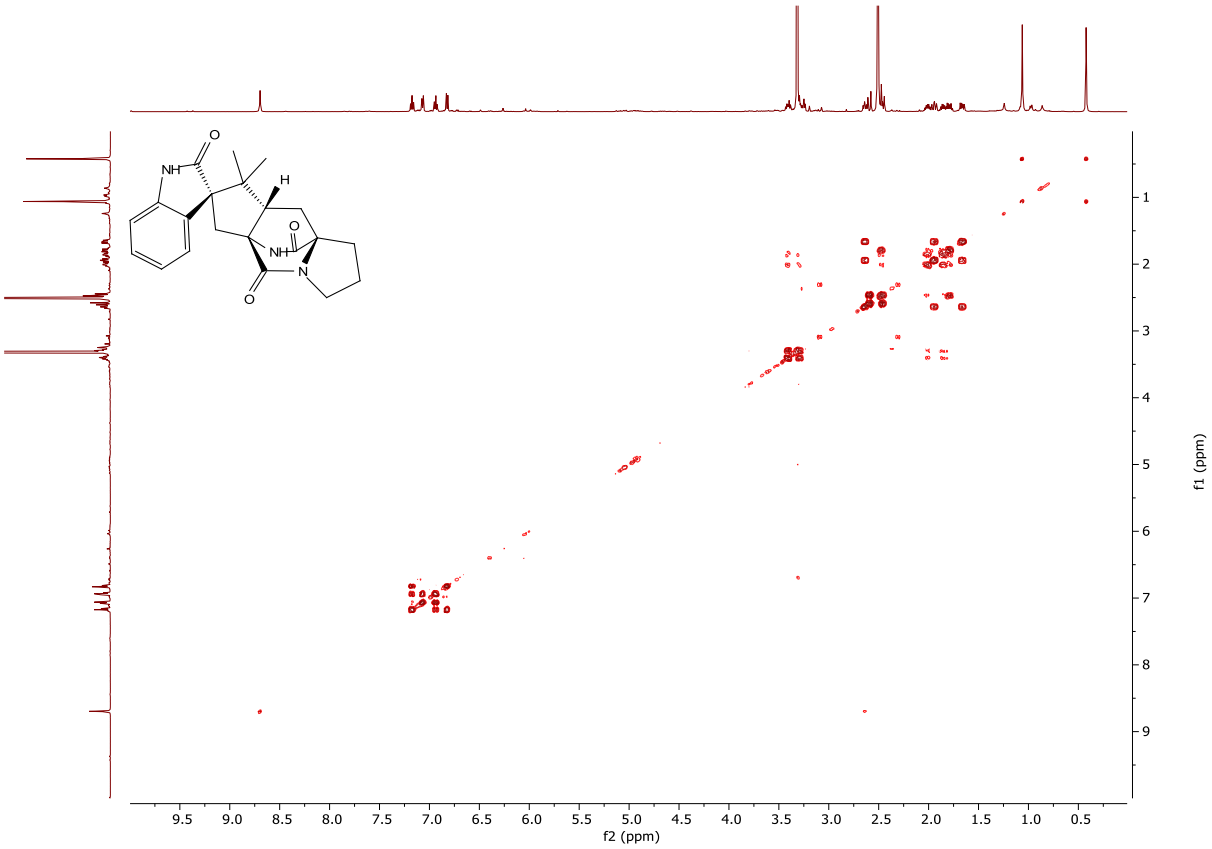

10.3.46 ^{1}H-^{13}C HSQC Spectrum of Brevianamide Z (5.3) ($(CD_3)_2SO$)

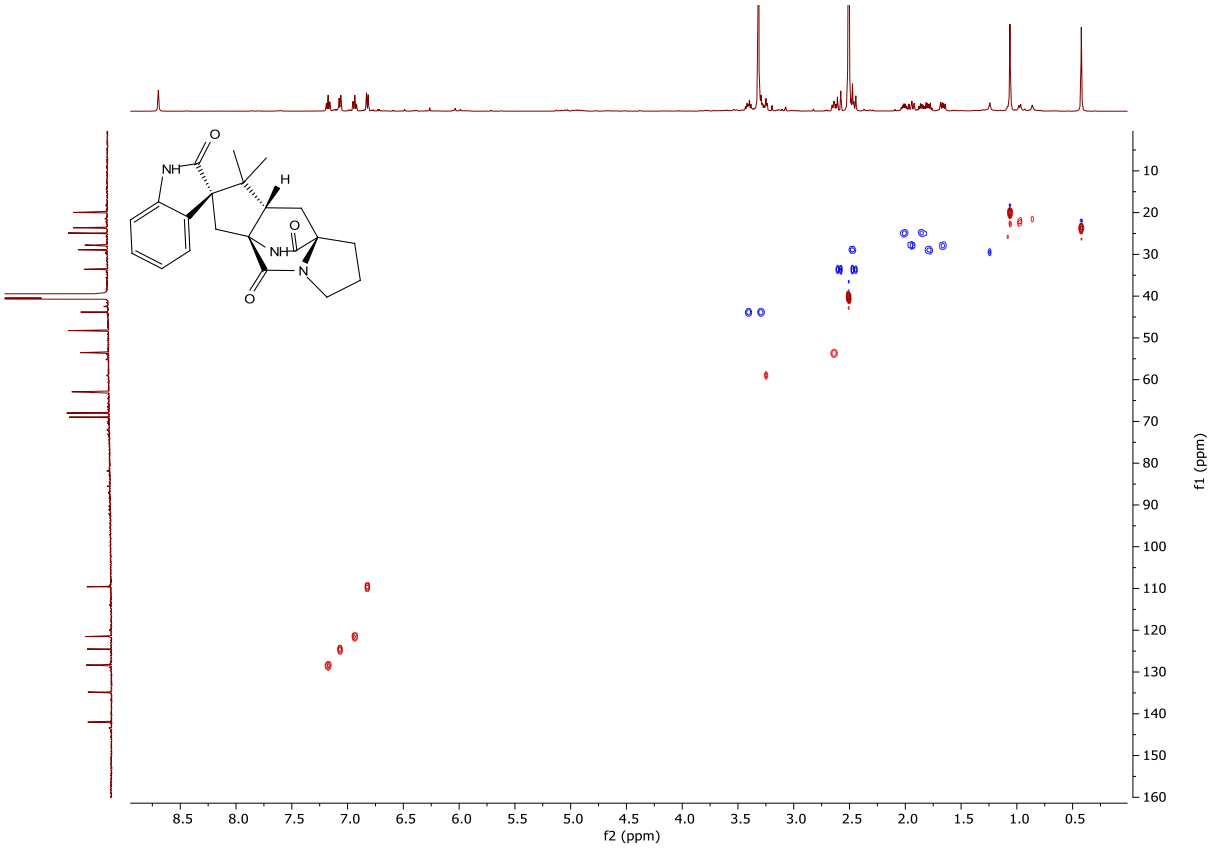

10.3.47 ^{1}H-^{13}C HMBC Spectrum of Brevianamide Z (5.3) ($(CD_3)_2SO$)

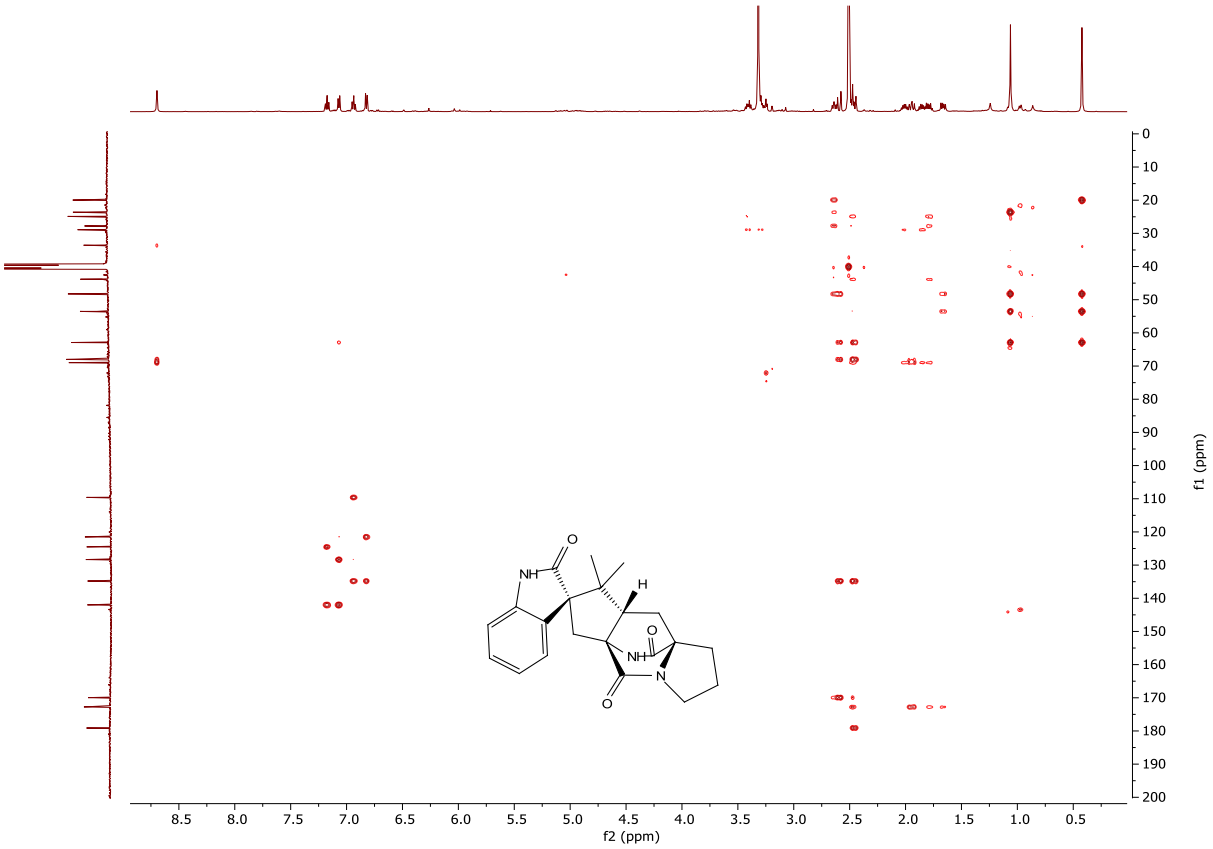

10.3.48 ^{1}H-^{1}H NOESY Spectrum of Brevianamide Z (5.3) ($(CD_3)_2SO$)

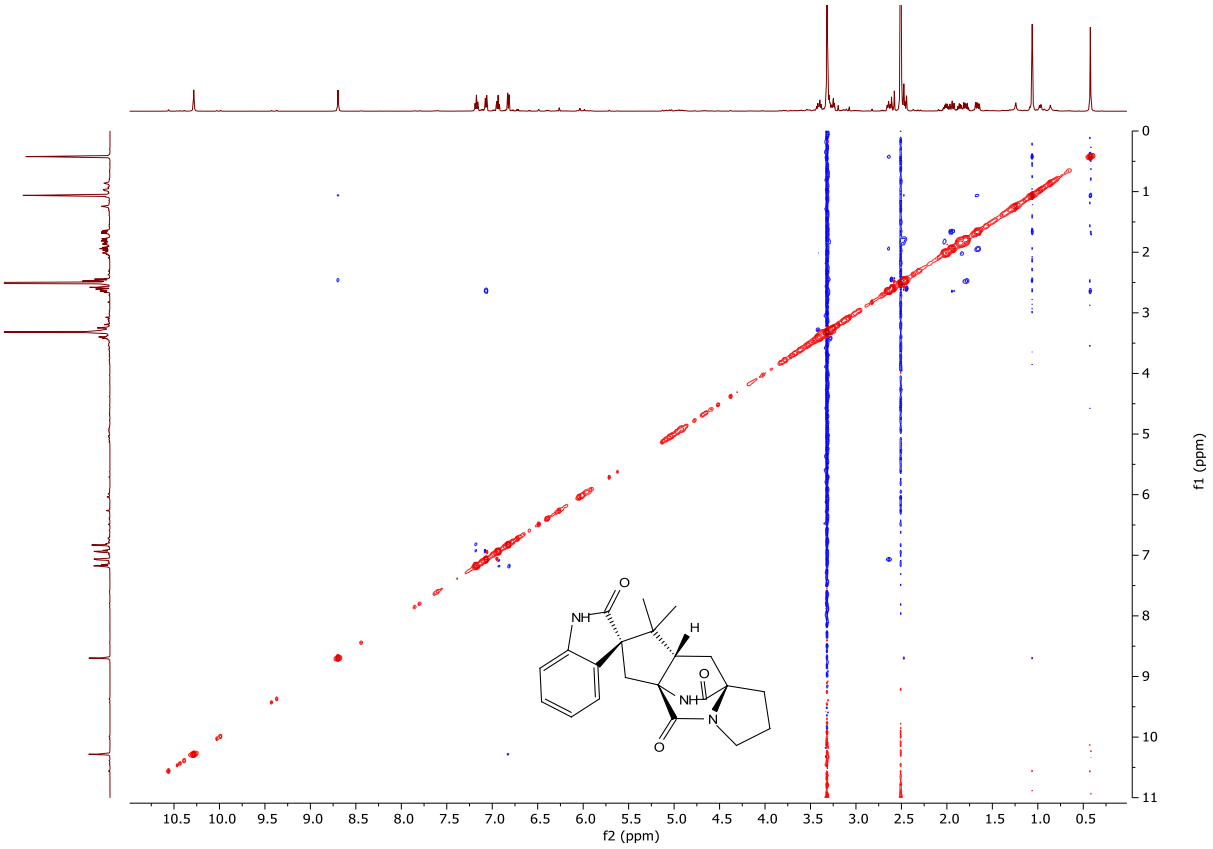

10.4 NMR Spectra Chapter 6

10.3.23 ^{1}H NMR Spectrum of Compound 6.1 (500 MHz, $CDCl_3$)

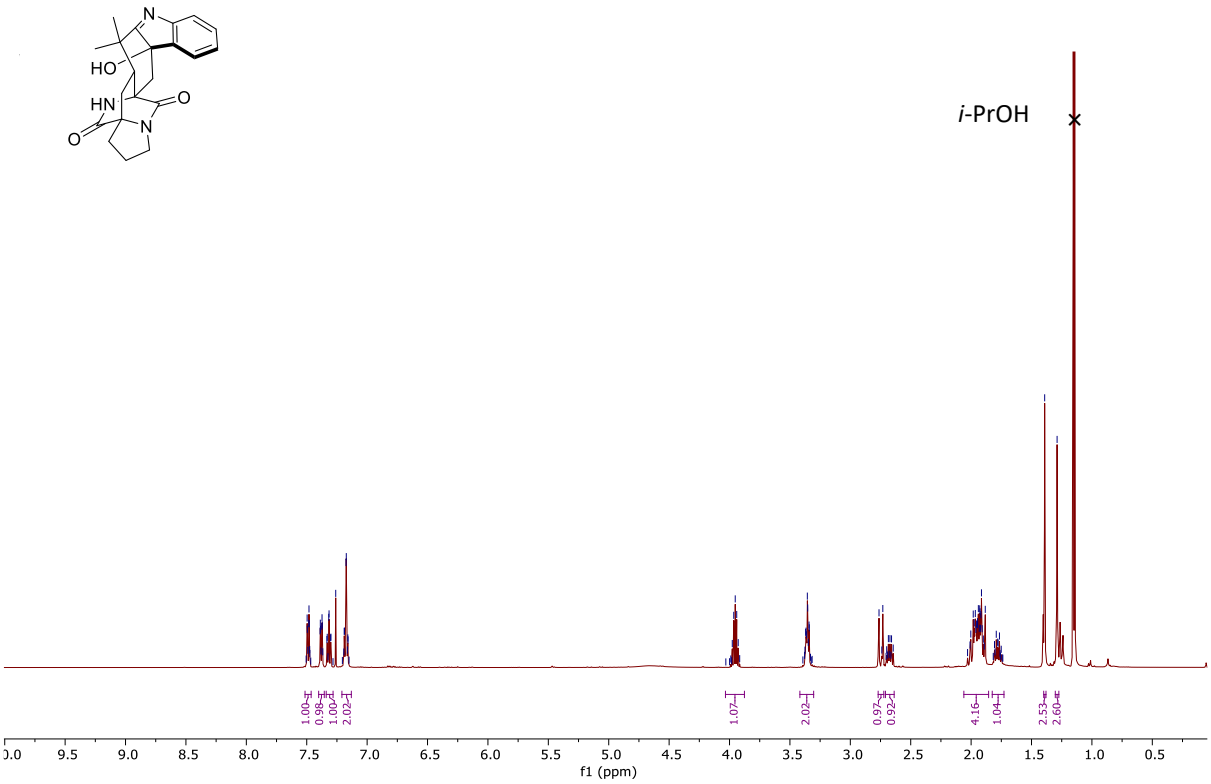

10.3.24 ^{13}C NMR Spectrum of Compound 6.1 (125 MHz, $CDCl_3$)

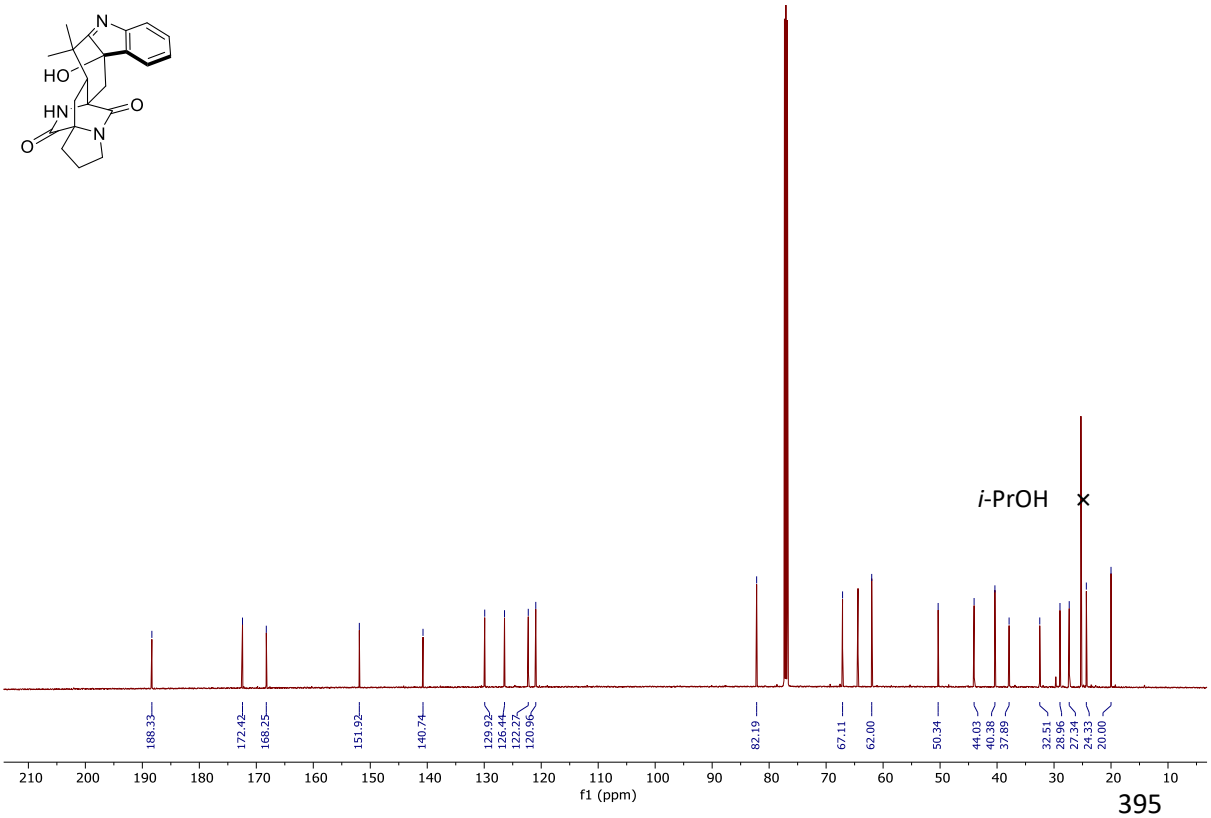

10.3.25 ^{1}H NMR Spectrum of Compound 6.1 (500 MHz, $(CD_3)_2SO$)

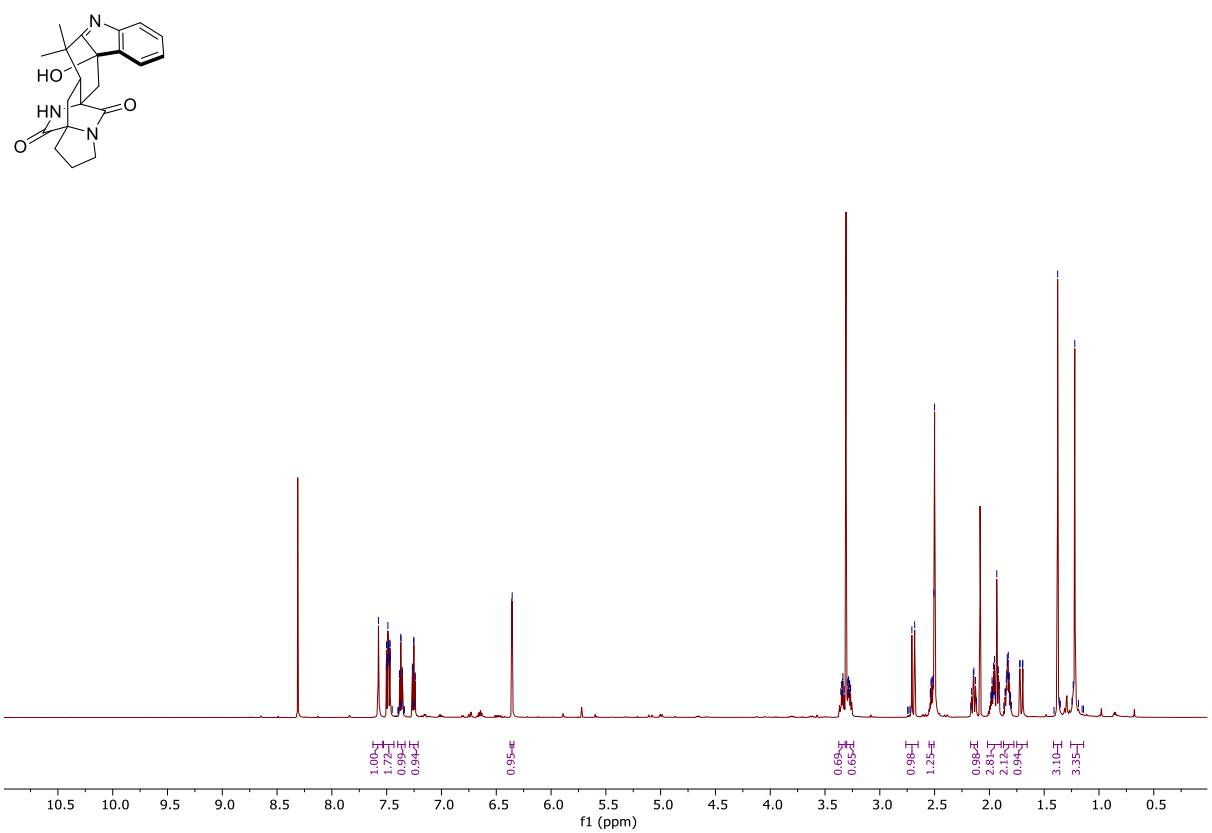

10.3.26 ^{1}H NMR Spectrum of Compound 6.5 (500 MHz, $CDCl_3$)

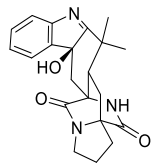

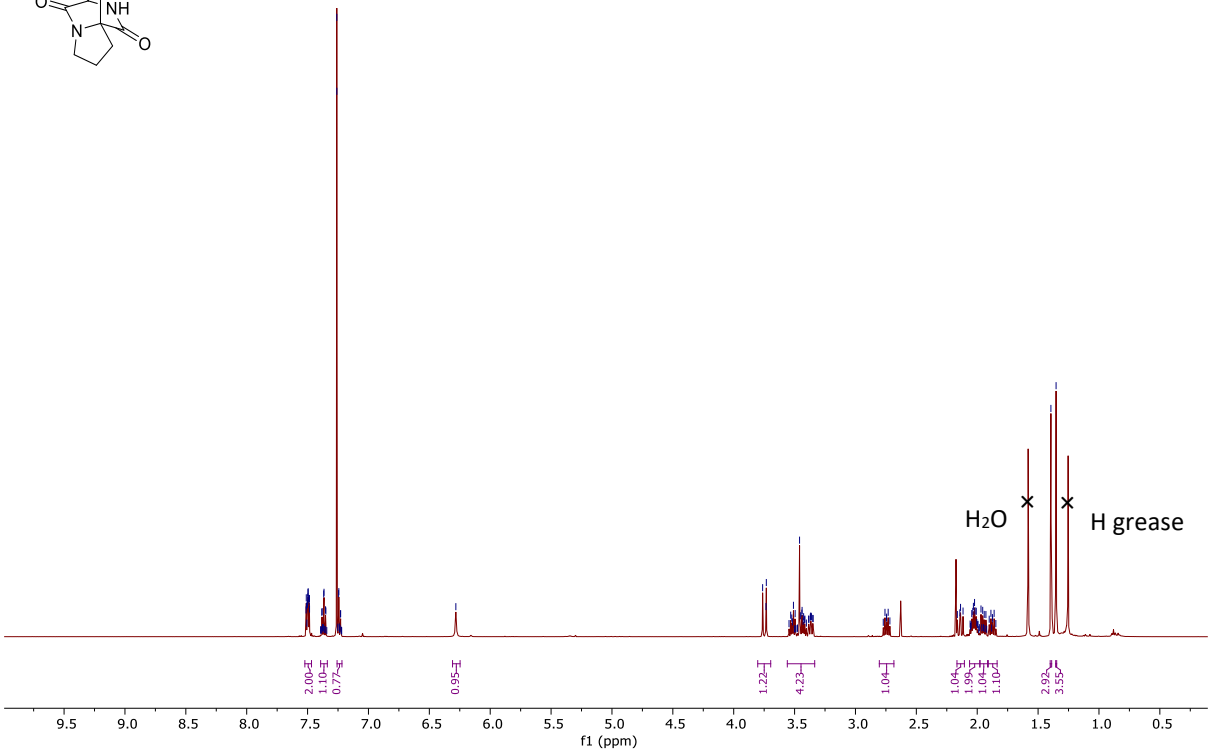

10.3.27 ^{13}C NMR Spectrum of Compound 6.5 (125 MHz, $CDCl_3$)

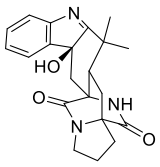

10.3.28 ^{1}H NMR Spectrum of Compound 6.5 (500 MHz, $(CD_3)_2SO$)

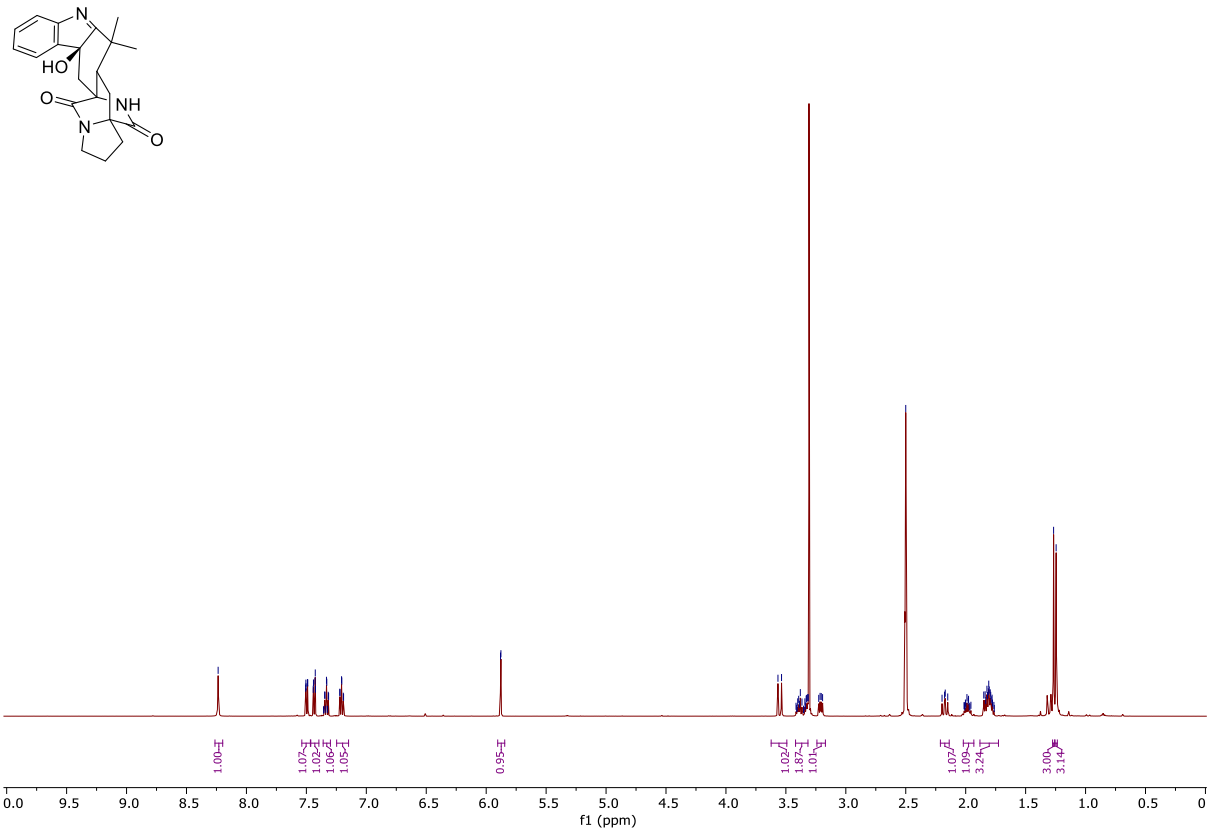

10.3.29 ^{13}C NMR Spectrum of Compound 6.5 (125 MHz, $(CD_3)_2SO$)

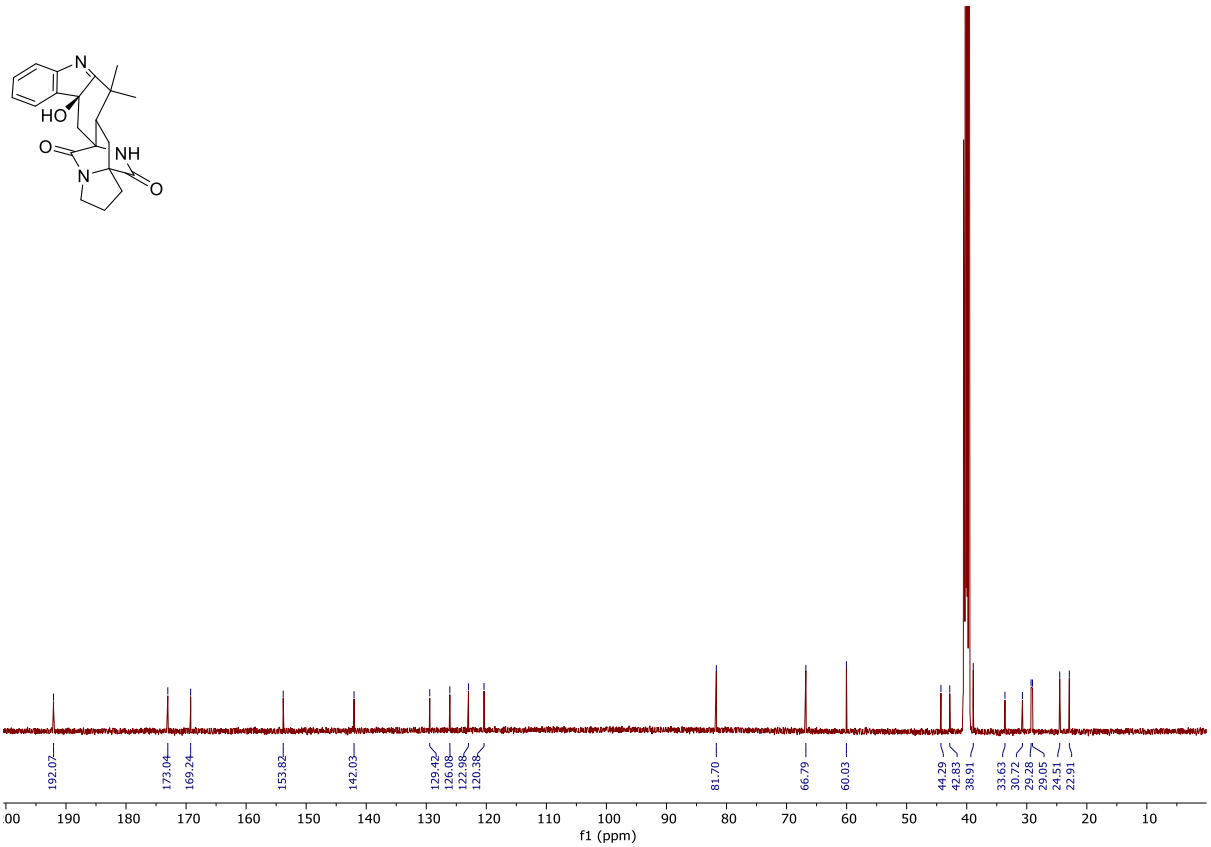

10.3.30 ^{1}H-^{1}H COSY Spectrum of Compound 6.5 ($CDCl_3$)

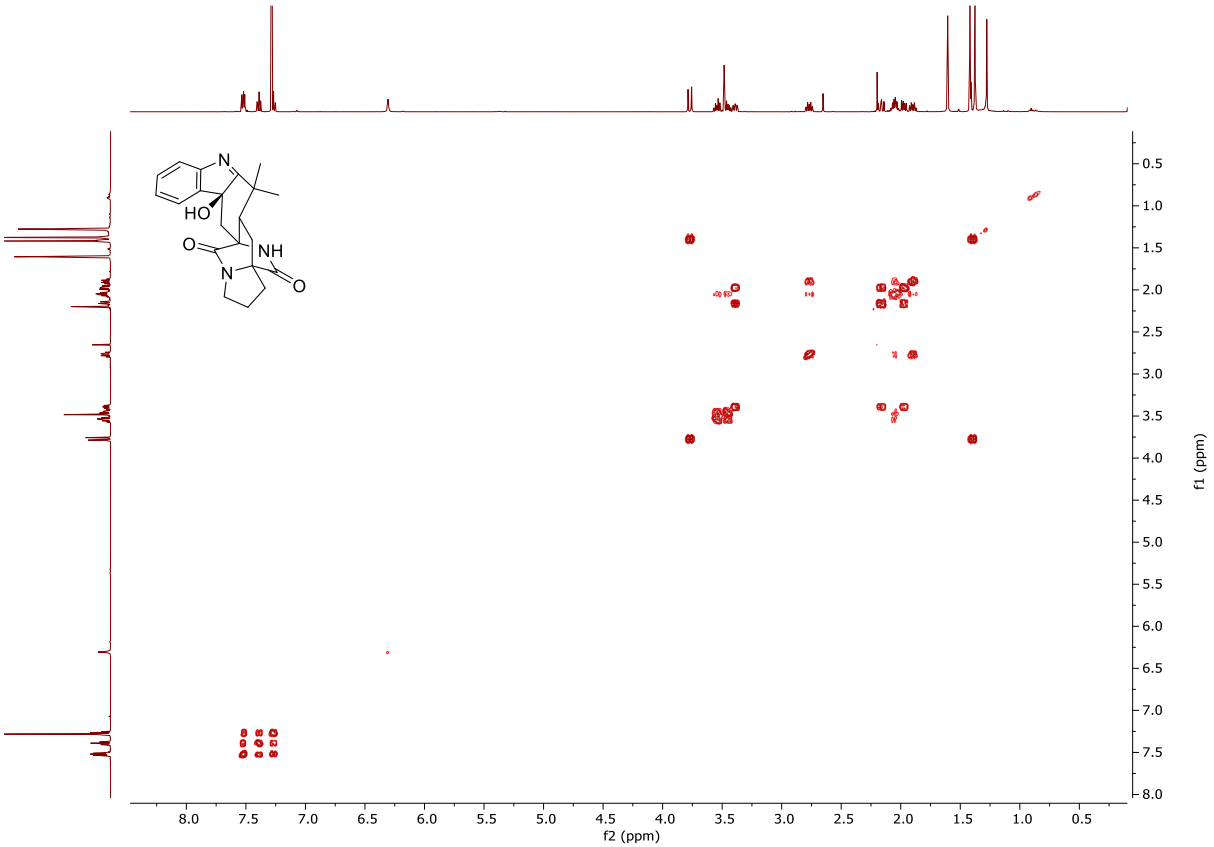

10.3.31 ^{1}H-^{13}C HSQC Spectrum of Compound 6.5 ($CDCl_3$)

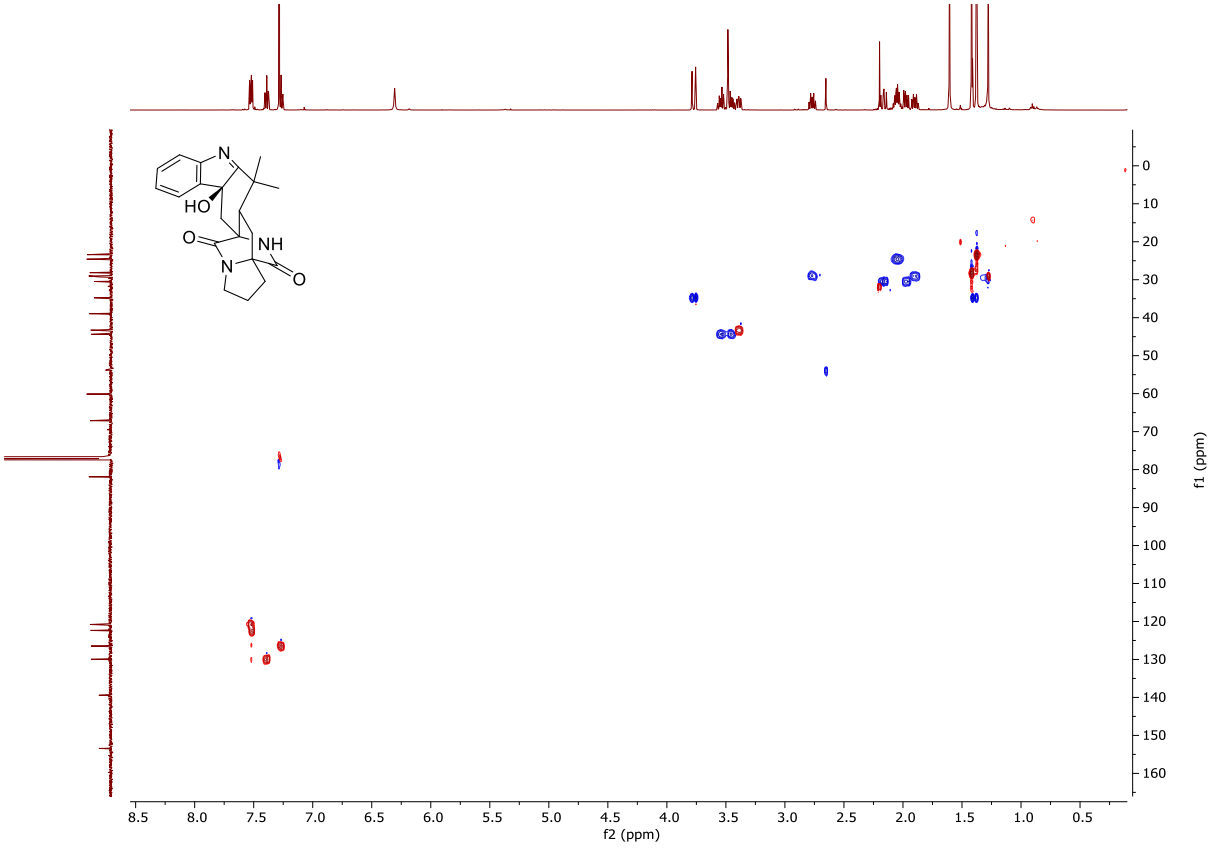

10.3.32 ^{1}H-^{13}C HMBC Spectrum of Compound 6.5 ($CDCl_3$)

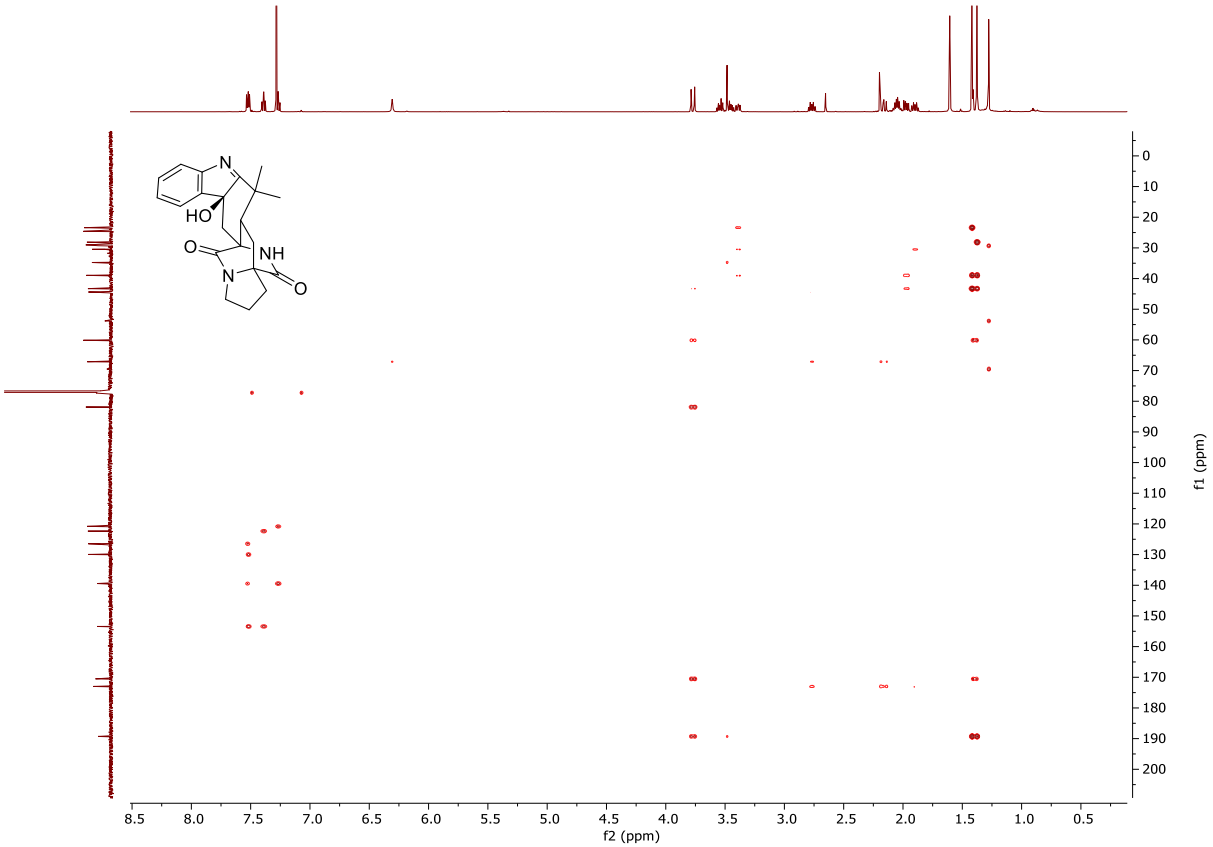

10.3.33 ^{1}H-^{1}H NOESY Spectrum of Compound 6.5 ($CDCl_3$)

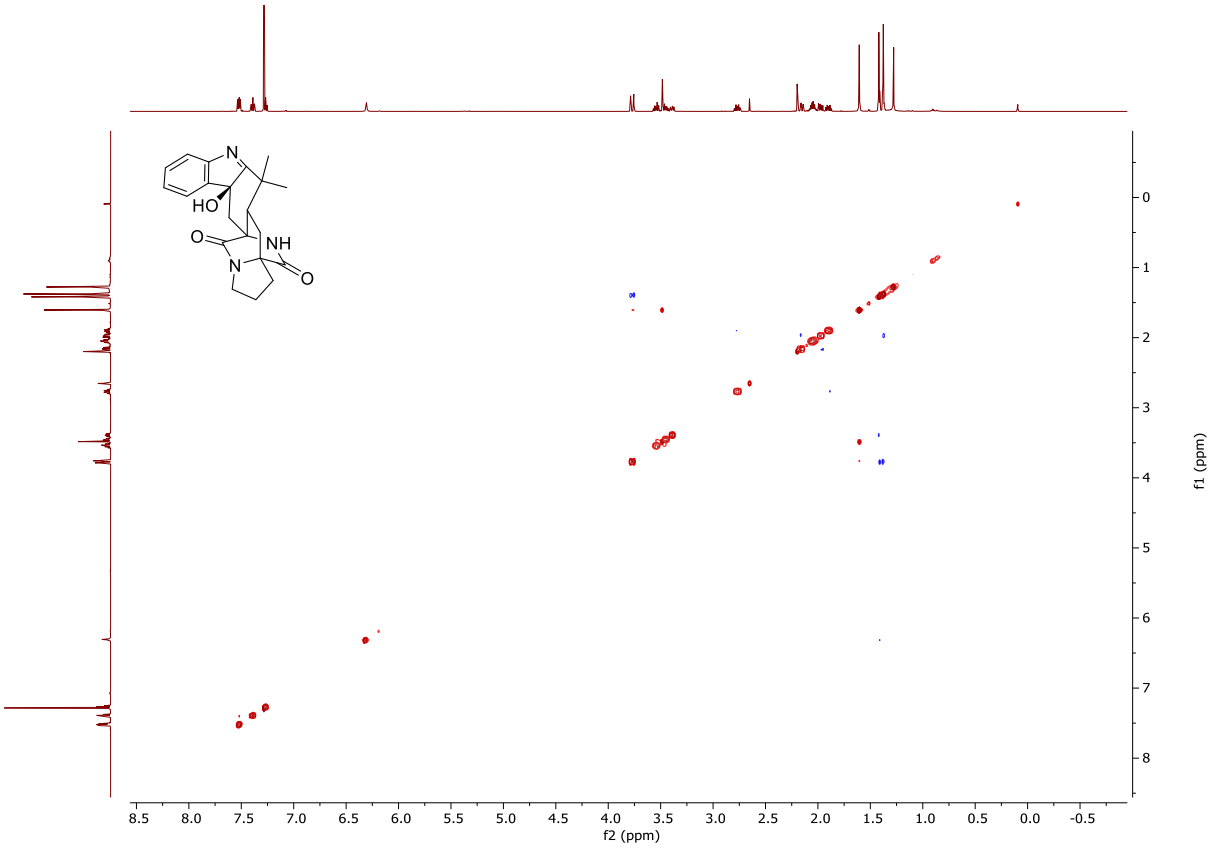

10.5 NMR Spectra Chapter 7

10.5.1 ^{1}H NMR Spectrum of Compound 7.15 (500 MHz, $CDCl_3$)

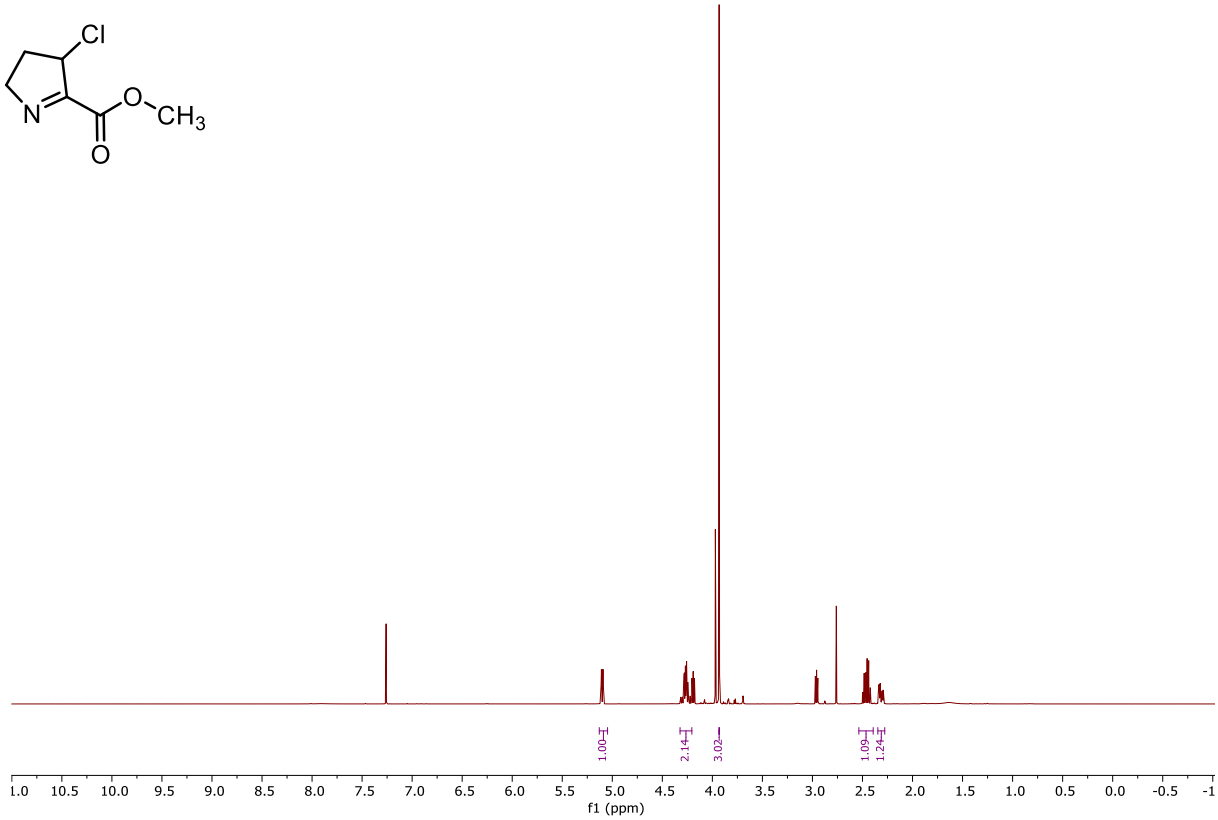

10.5.2 ^{13}C NMR Spectrum of Compound 7.15 (125 MHz, $CDCl_3$)

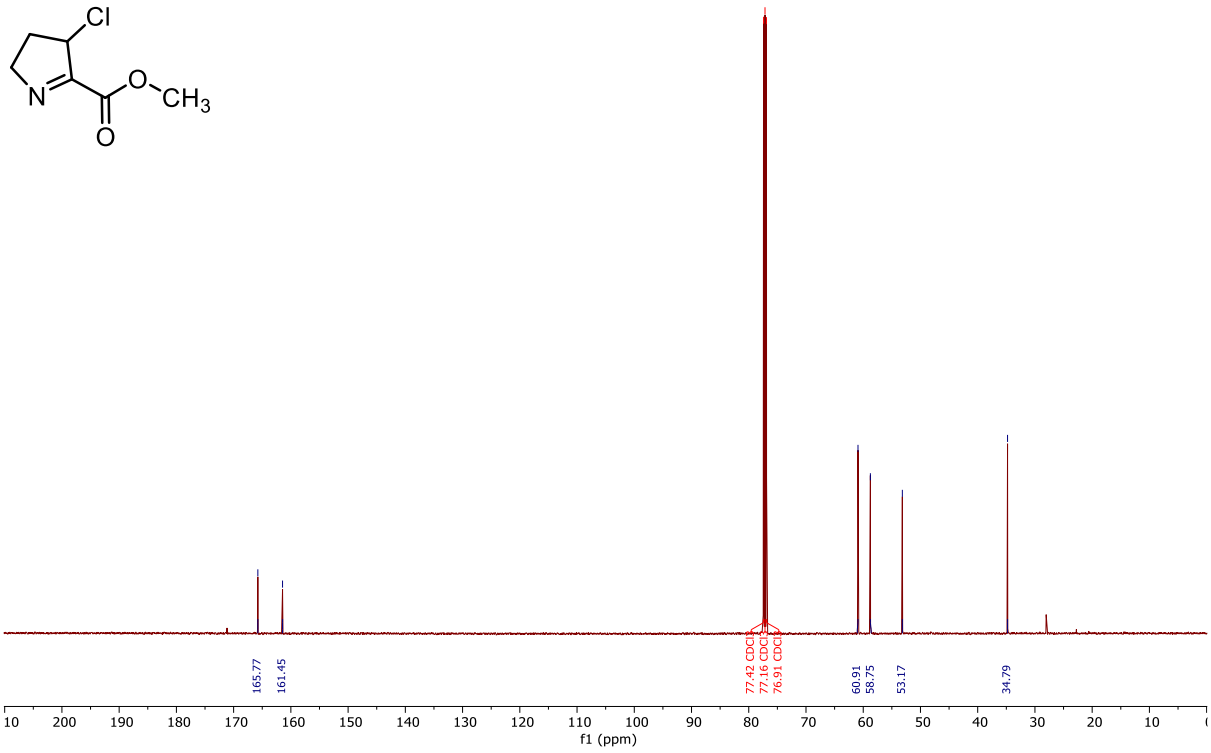

10.5.3 ^{1}H NMR Spectrum of Compound 7.14 (500 MHz, $CDCl_3$)

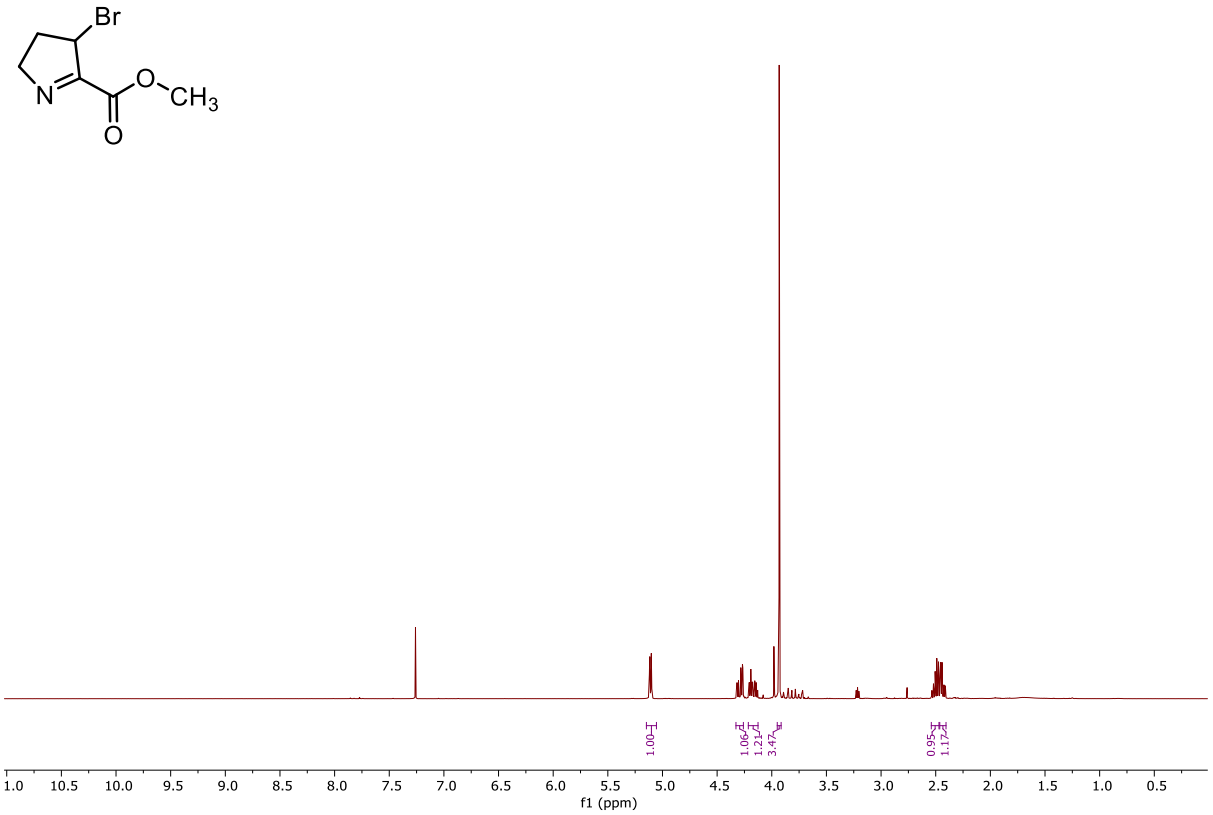

10.5.4 ^{1}H NMR Spectrum of Compound 7.16 (500 MHz, $CDCl_3$)

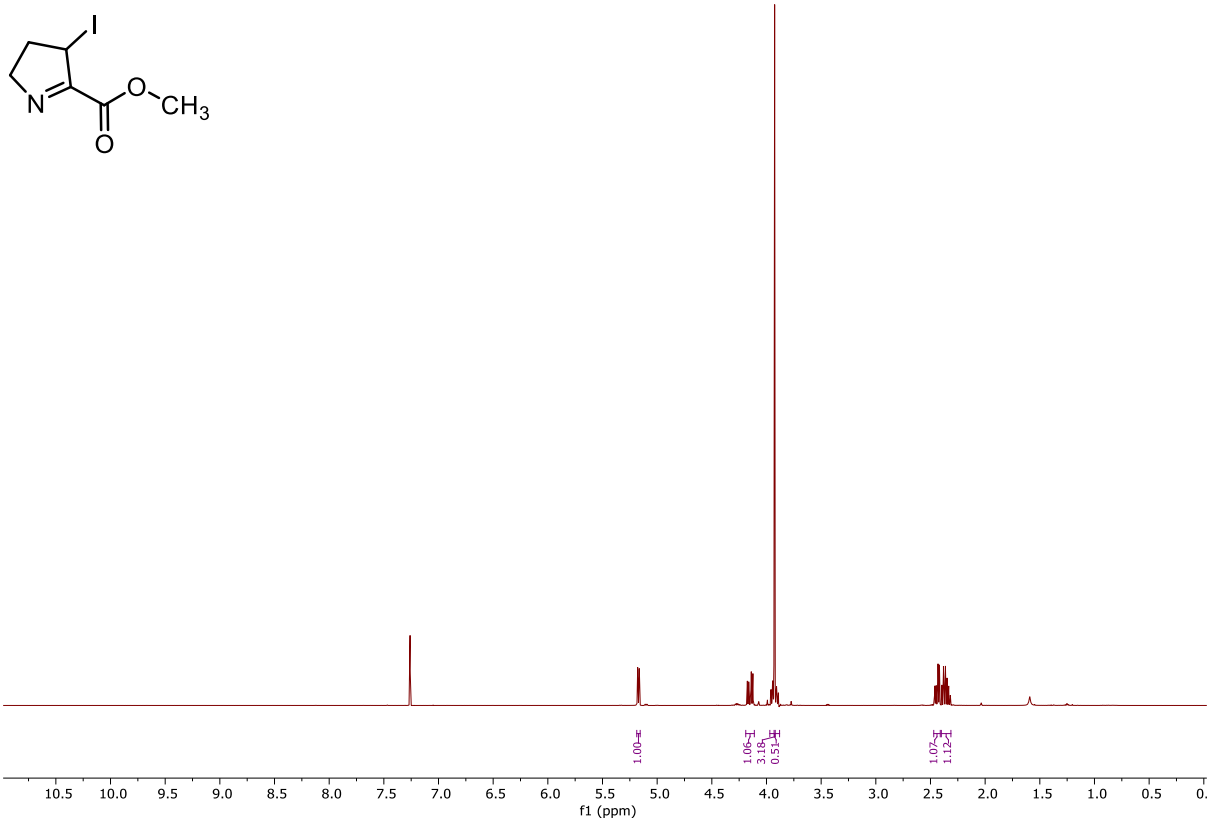

10.5.5 ^{13}C NMR Spectrum of Compound 7.16 (125 MHz, $CDCl_3$)

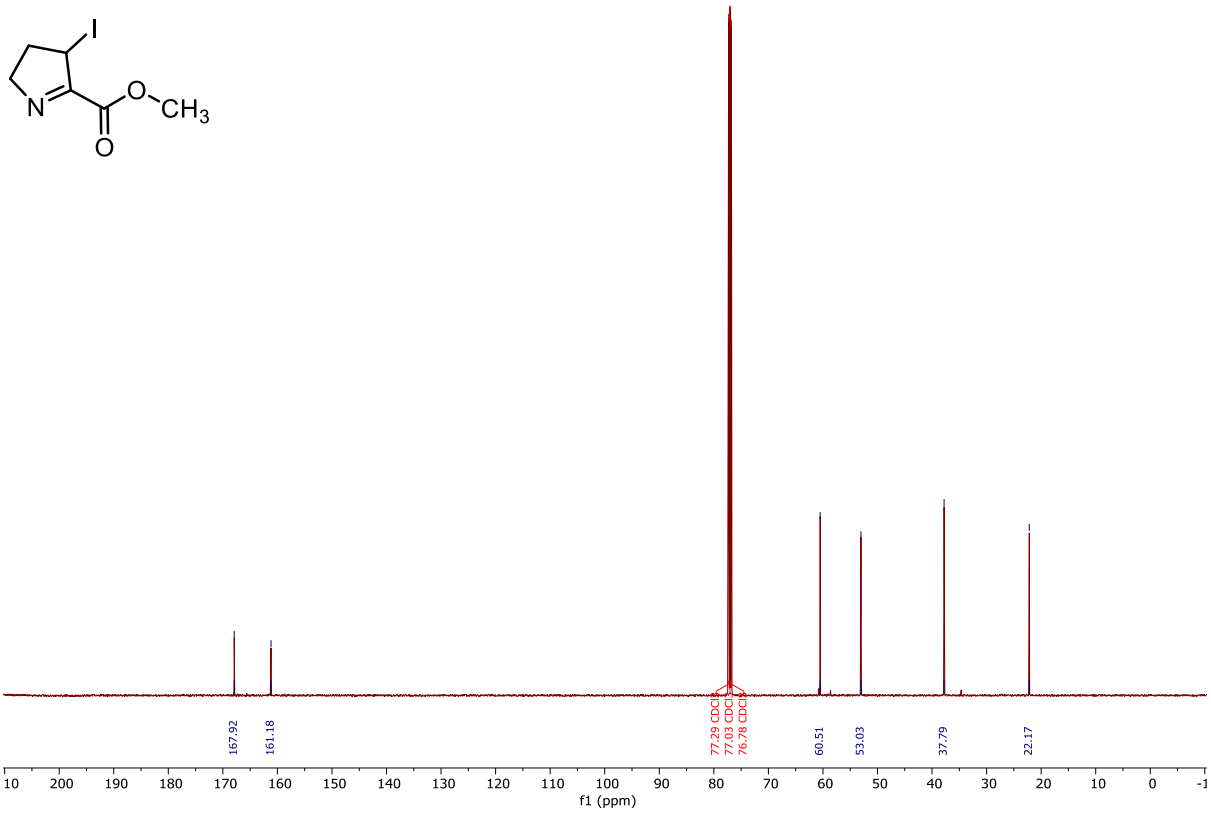

10.5.6 ^{1}H NMR Spectrum of Compound 7.24 (500 MHz, $CDCl_3$)

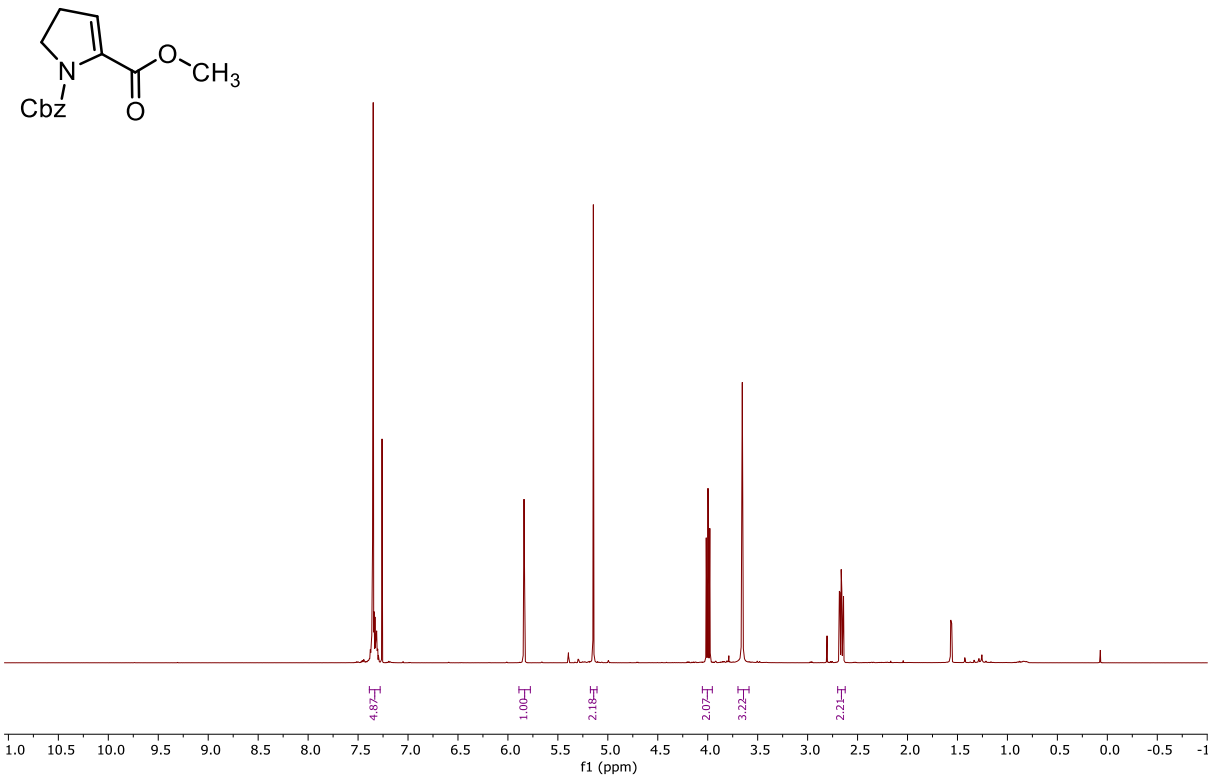

10.5.7 ^{13}C NMR Spectrum of Compound 7.24 (125 MHz, $CDCl_3$)

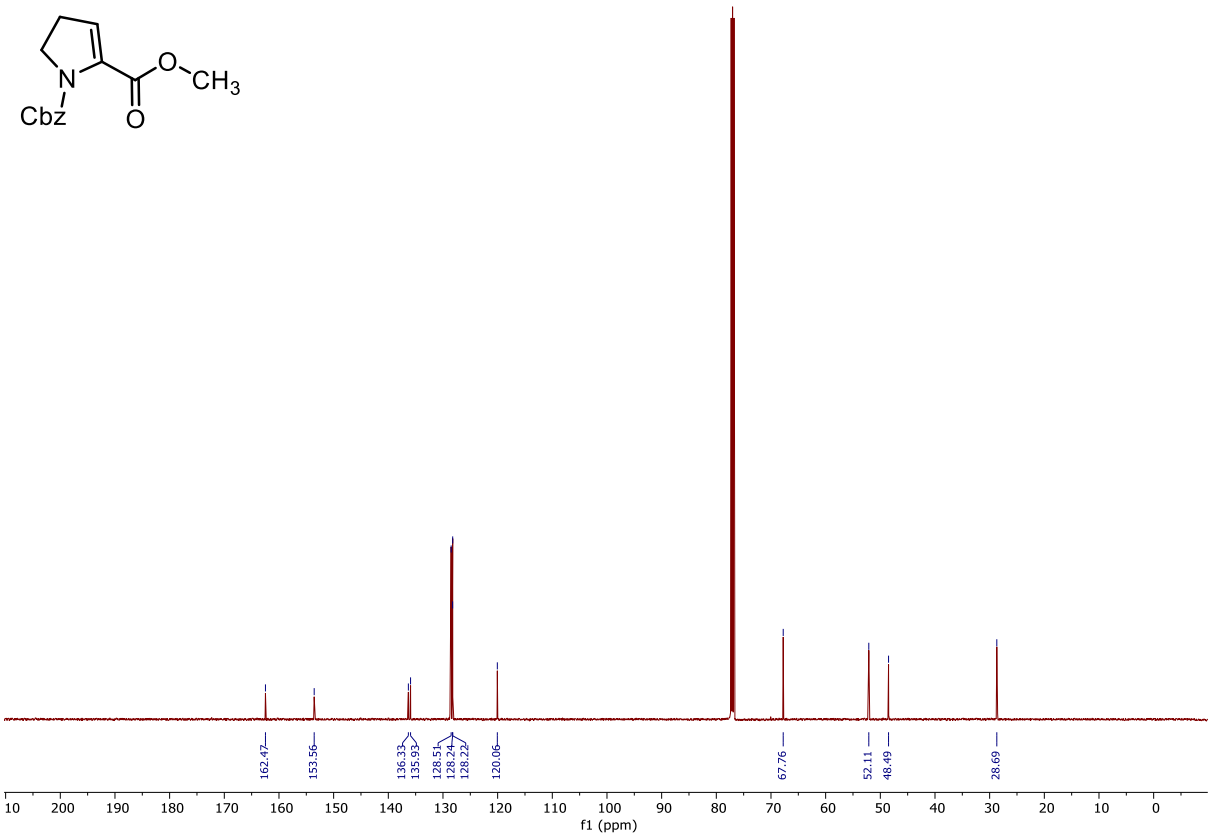

10.5.8 ^{1}H NMR Spectrum of Compound 7.25 (500 MHz, $CDCl_3$)

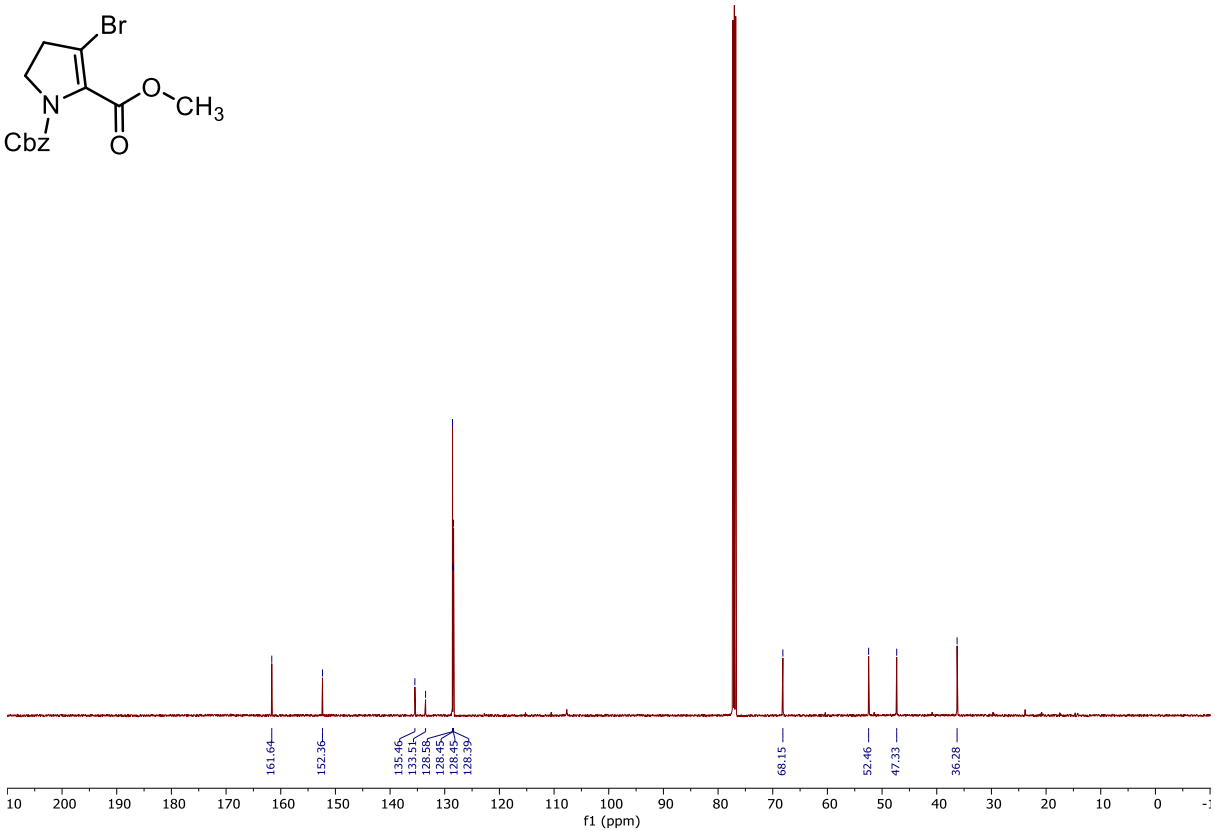

10.5.9 ^{13}C NMR Spectrum of Compound 7.25 (125 MHz, $CDCl_3$)

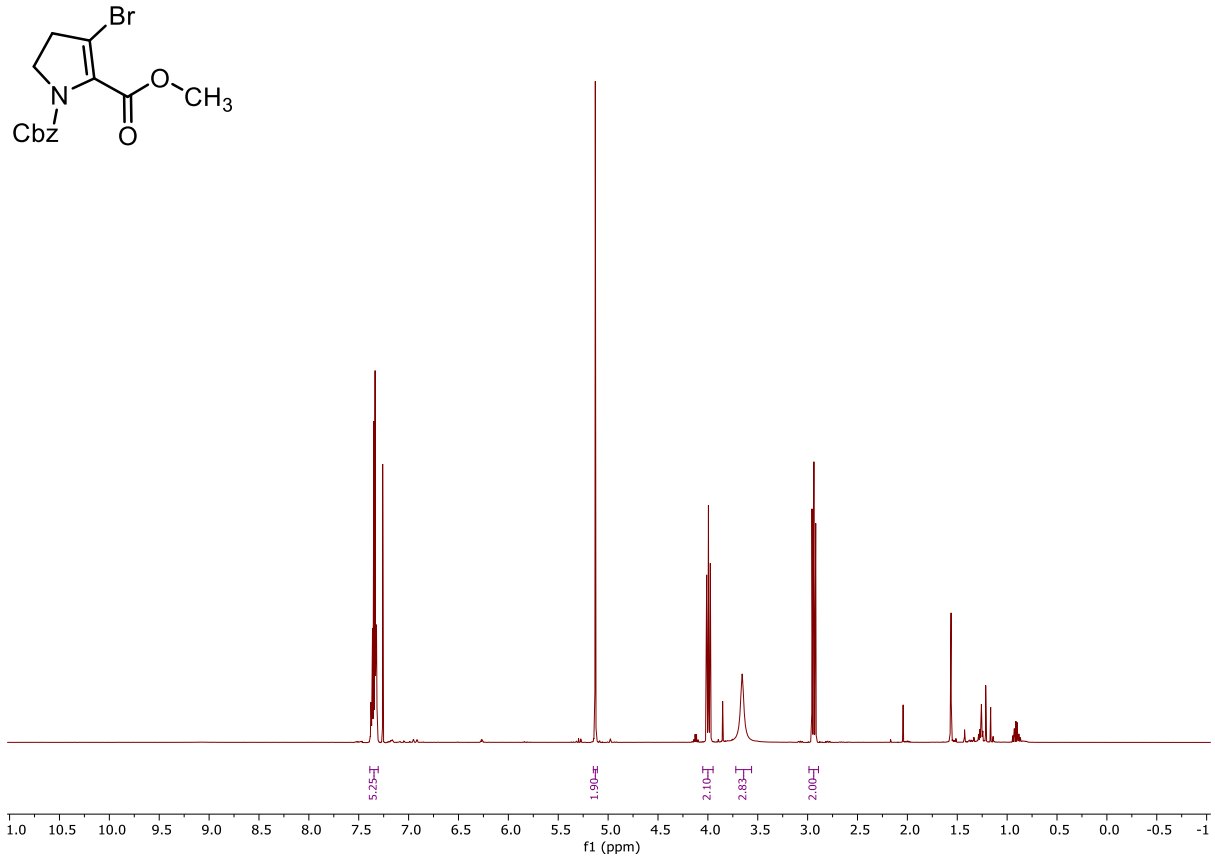

10.5.10 ^{1}H NMR Spectrum of Compound 7.32 (600 MHz, $CDCl_3$)

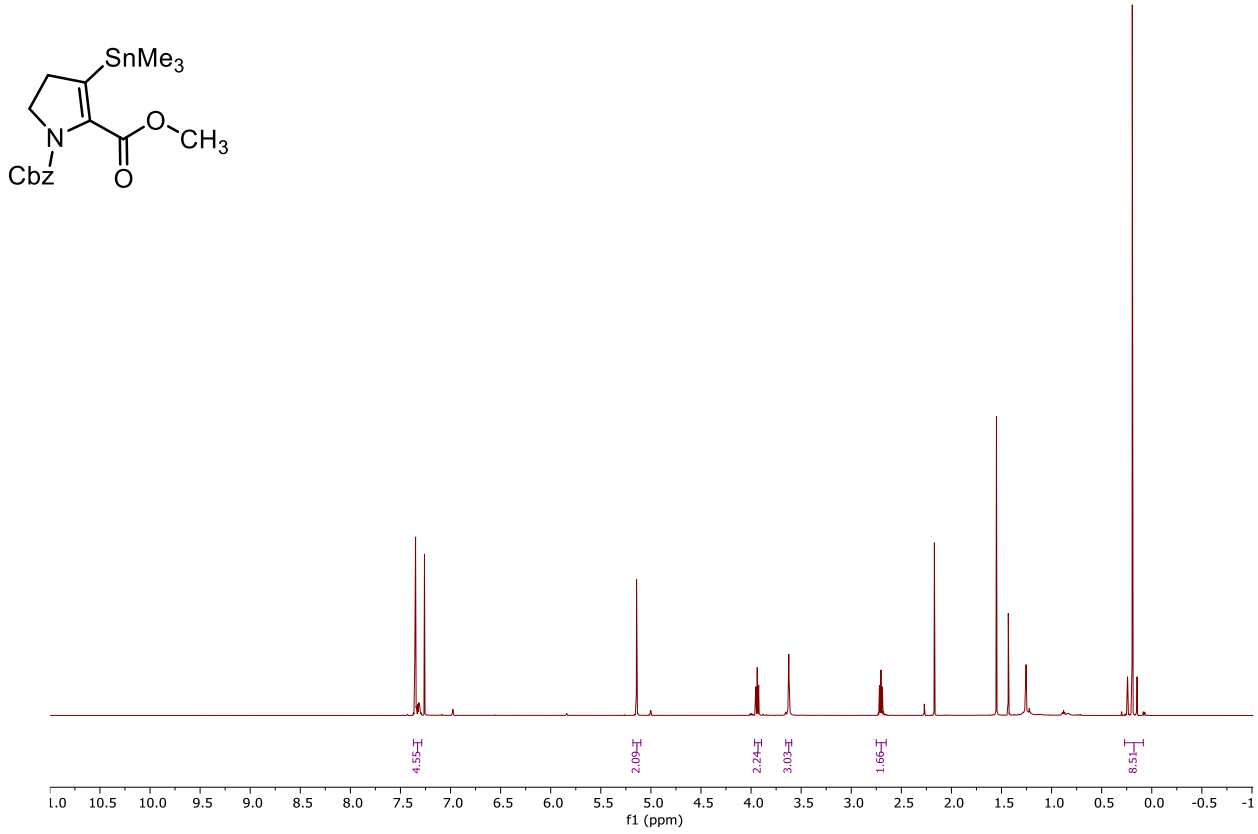

10.5.11 ^{13}C NMR Spectrum of Compound 7.32 (125 MHz, $CDCl_3$)

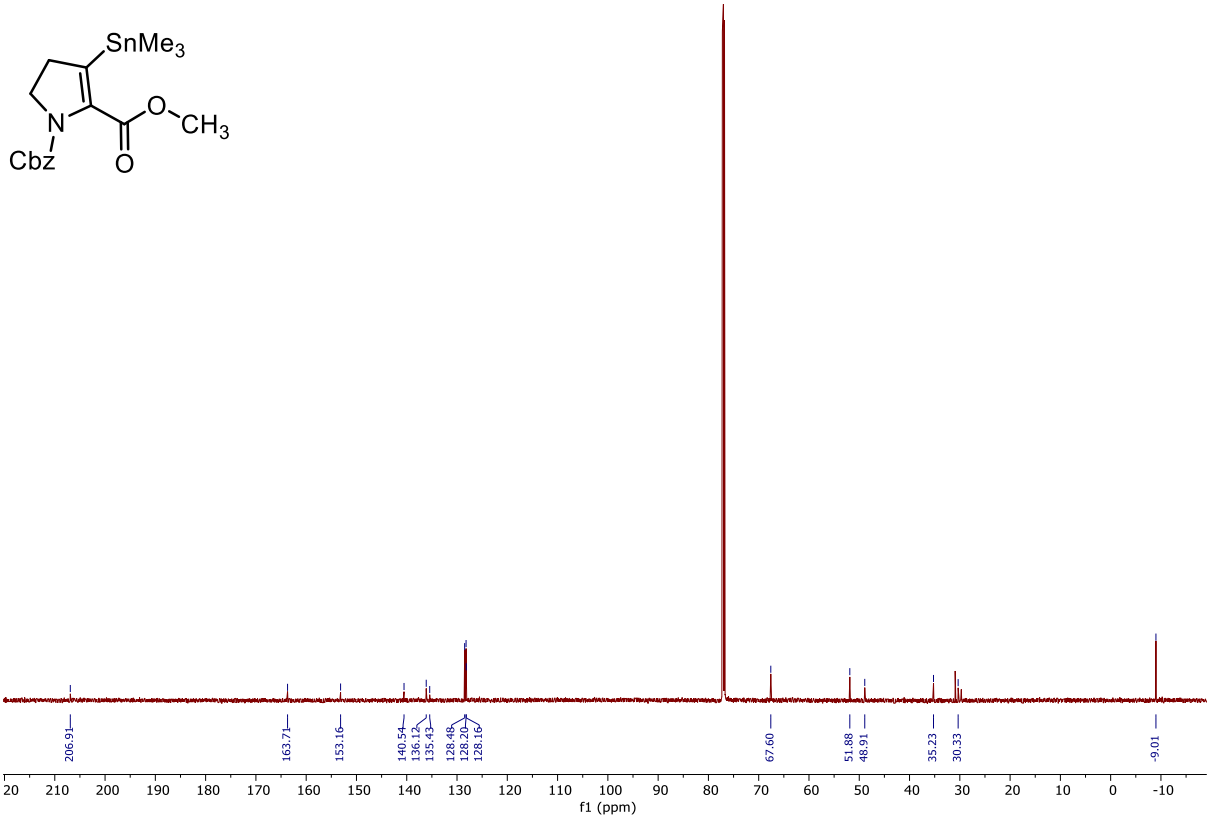

10.5.12 ^{1}H NMR Spectrum of Compound 7.56 (500 MHz, $CDCl_3$)

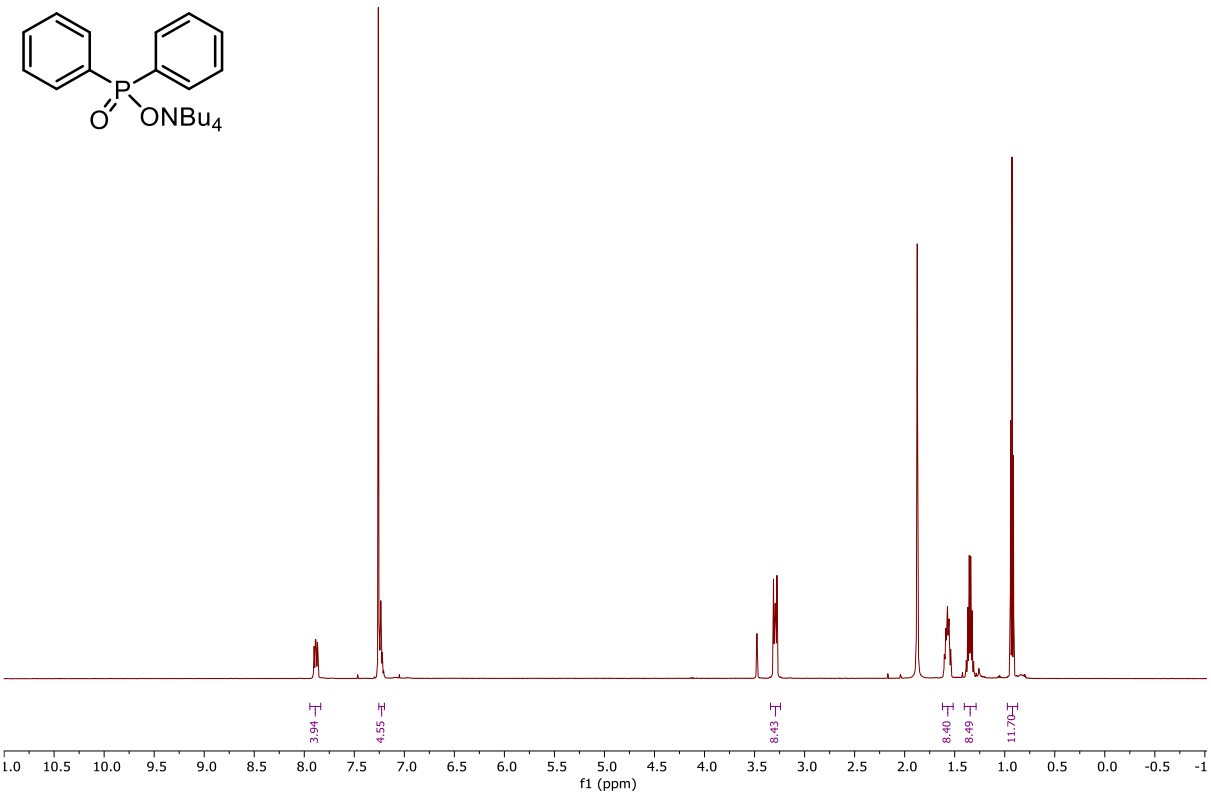

10.5.13 ^{13}C NMR Spectrum of Compound 7.56 (150 MHz, $CDCl_3$)

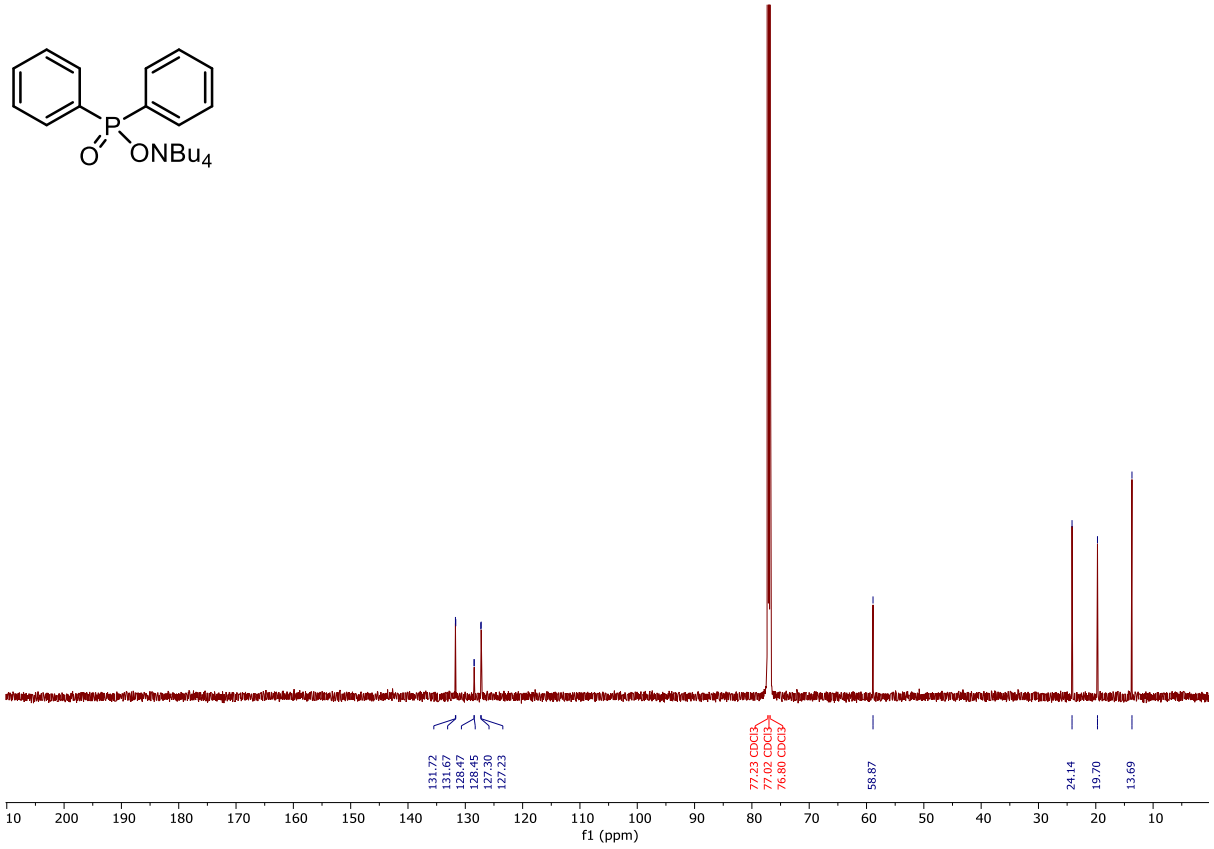

10.5.14 ^{31}P NMR Spectrum of Compound 7.56 (200 MHz, $CDCl_3$)

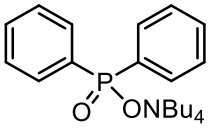

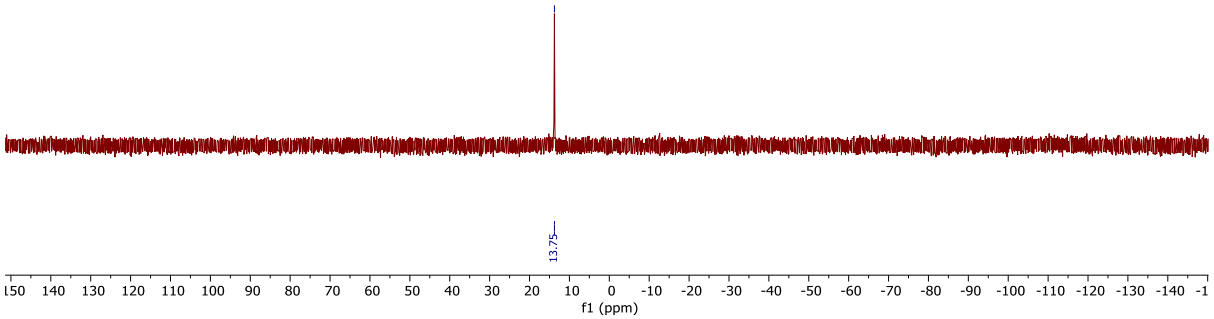

10.5.15 ^{1}H NMR Spectrum of Compound 7.41 (500 MHz, $CDCl_3$)

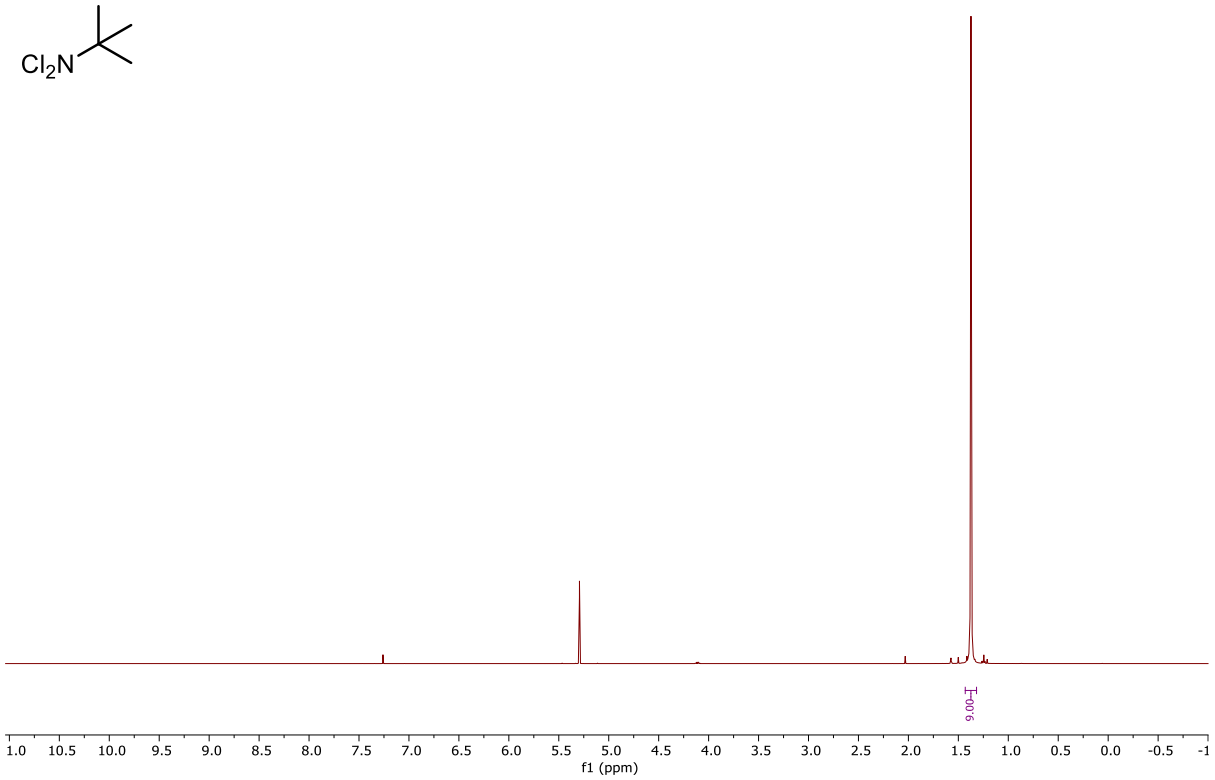

10.5.16 ^{13}C NMR Spectrum of Compound 7.41 (125 MHz, $CDCl_3$)

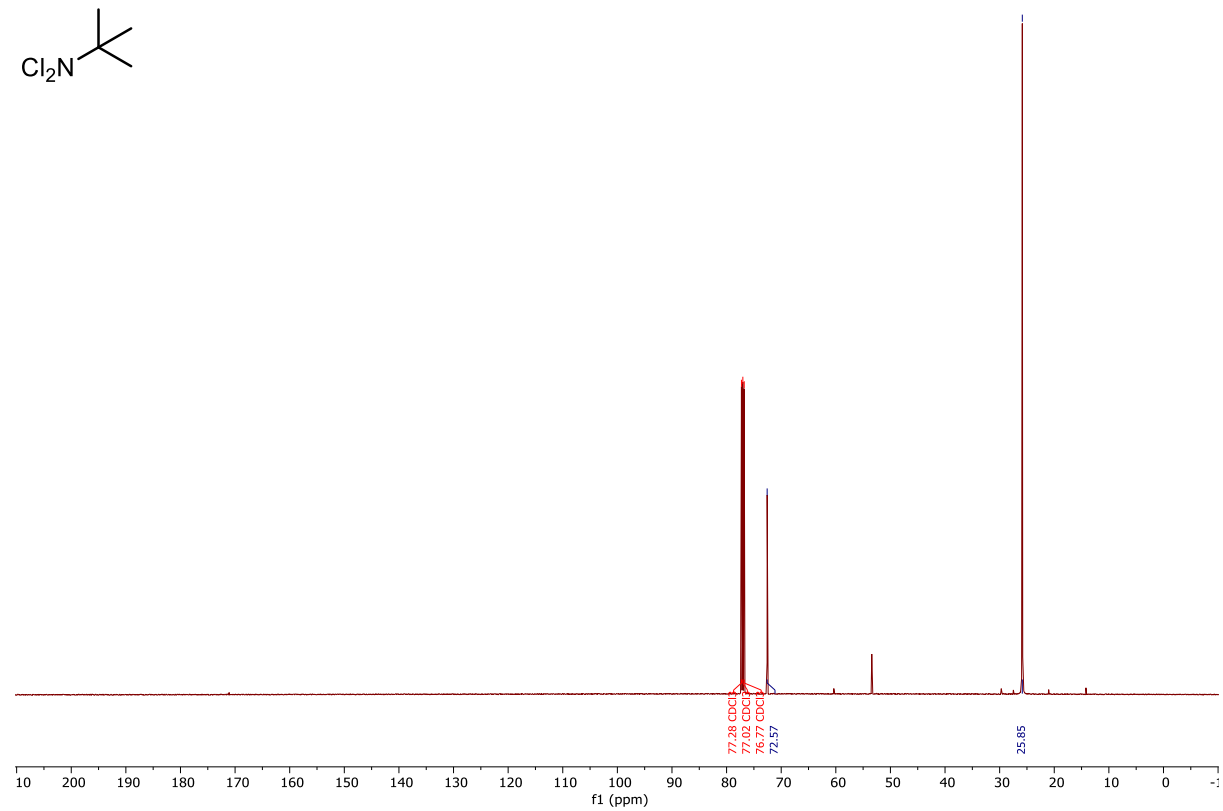

10.5.17 ^{1}H NMR Spectrum of Compound 7.37 (500 MHz, $CDCl_3$)

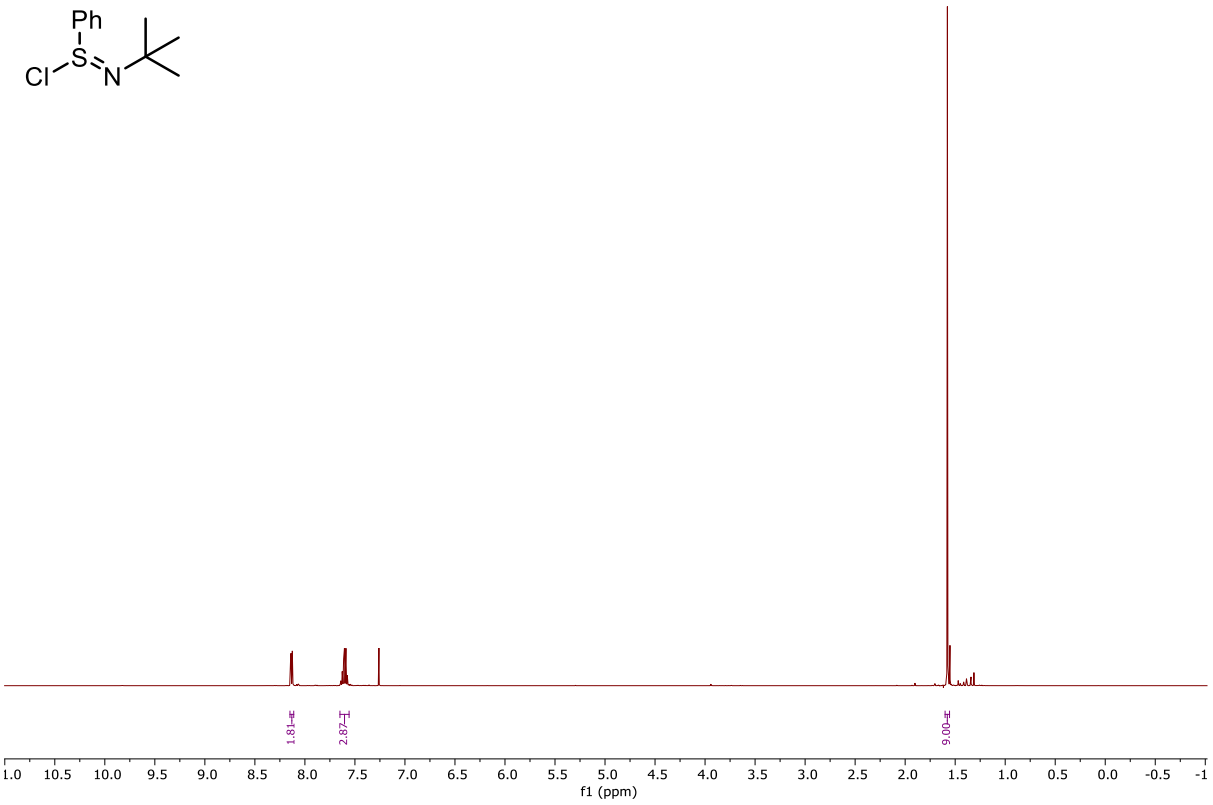

10.5.18 ^{1}H NMR Spectrum of Brevianamide K (7.4) (500 MHz, $CDCl_3$)

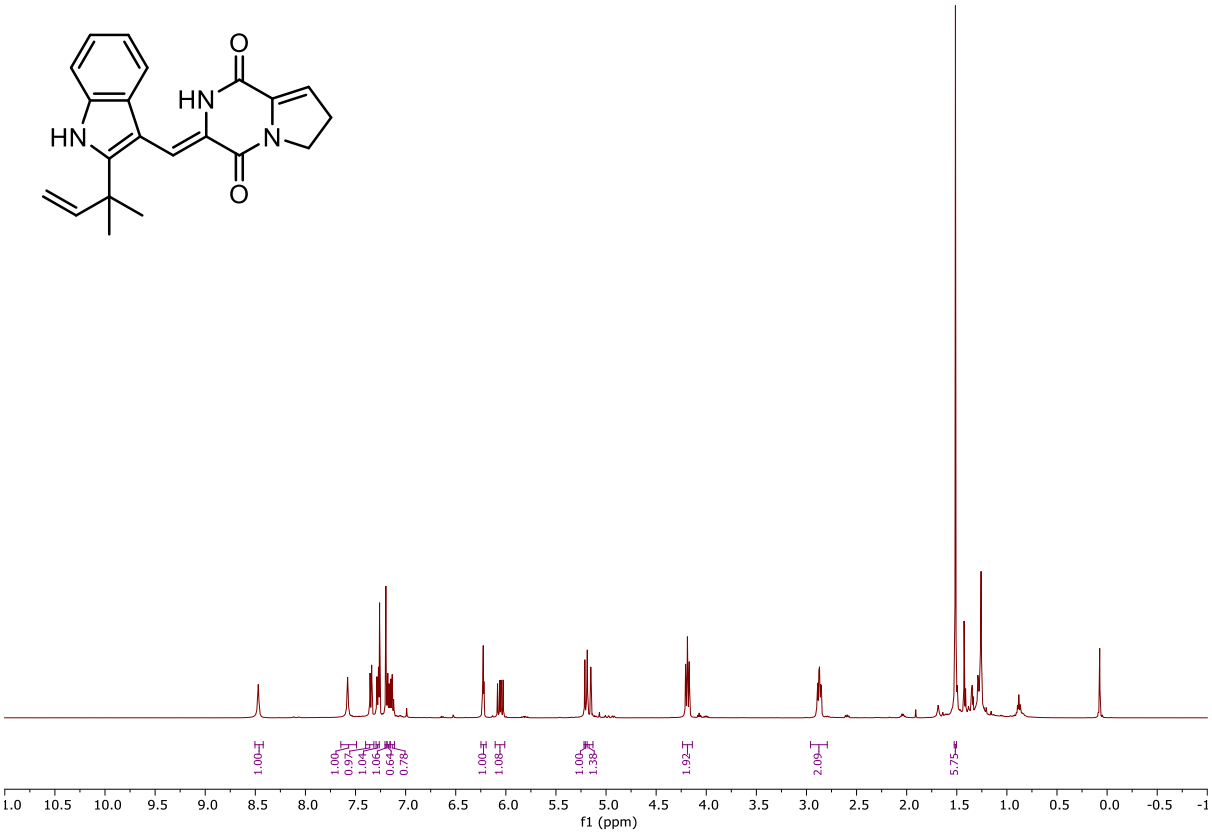

10.5.19 ^{13}C NMR Spectrum of Brevianamide K (7.4) (125 MHz, $CDCl_3$)

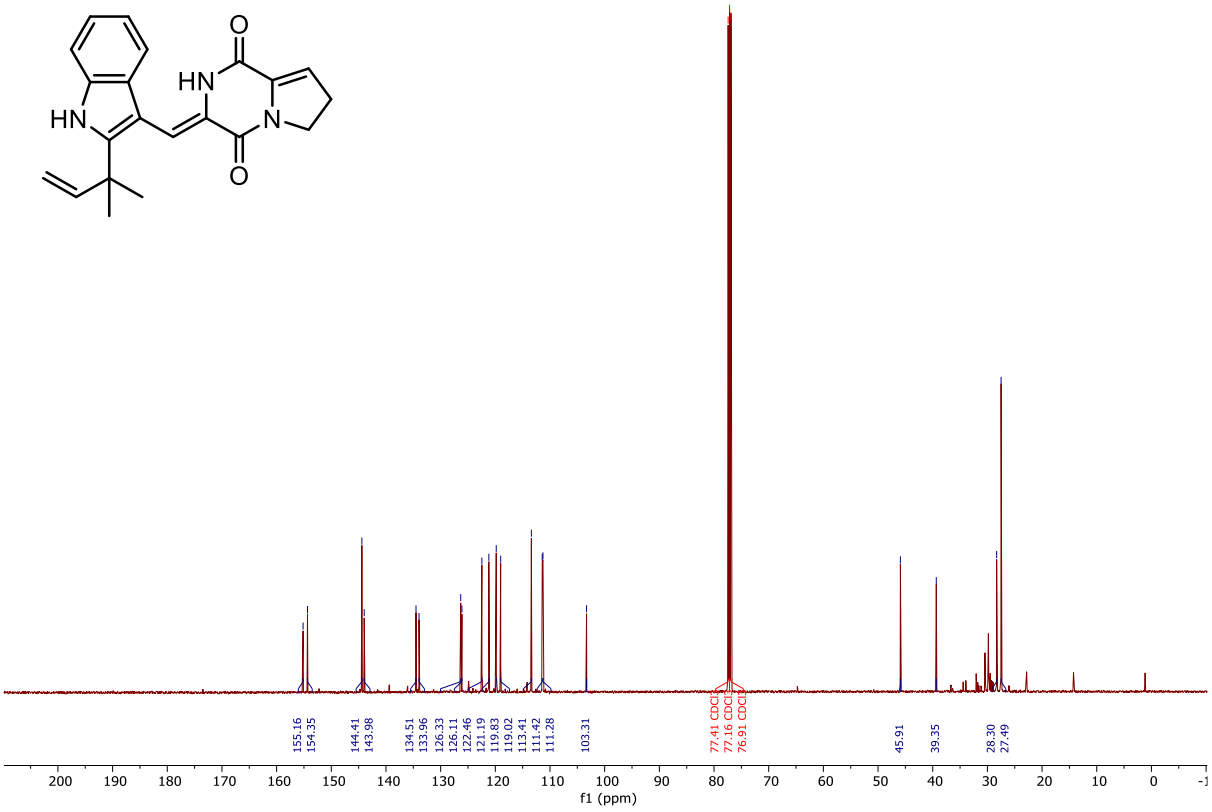

10.5.20 ^{1}H-^{1}H COSY Spectrum of Brevianamide K (7.4) ($CDCl_3$)

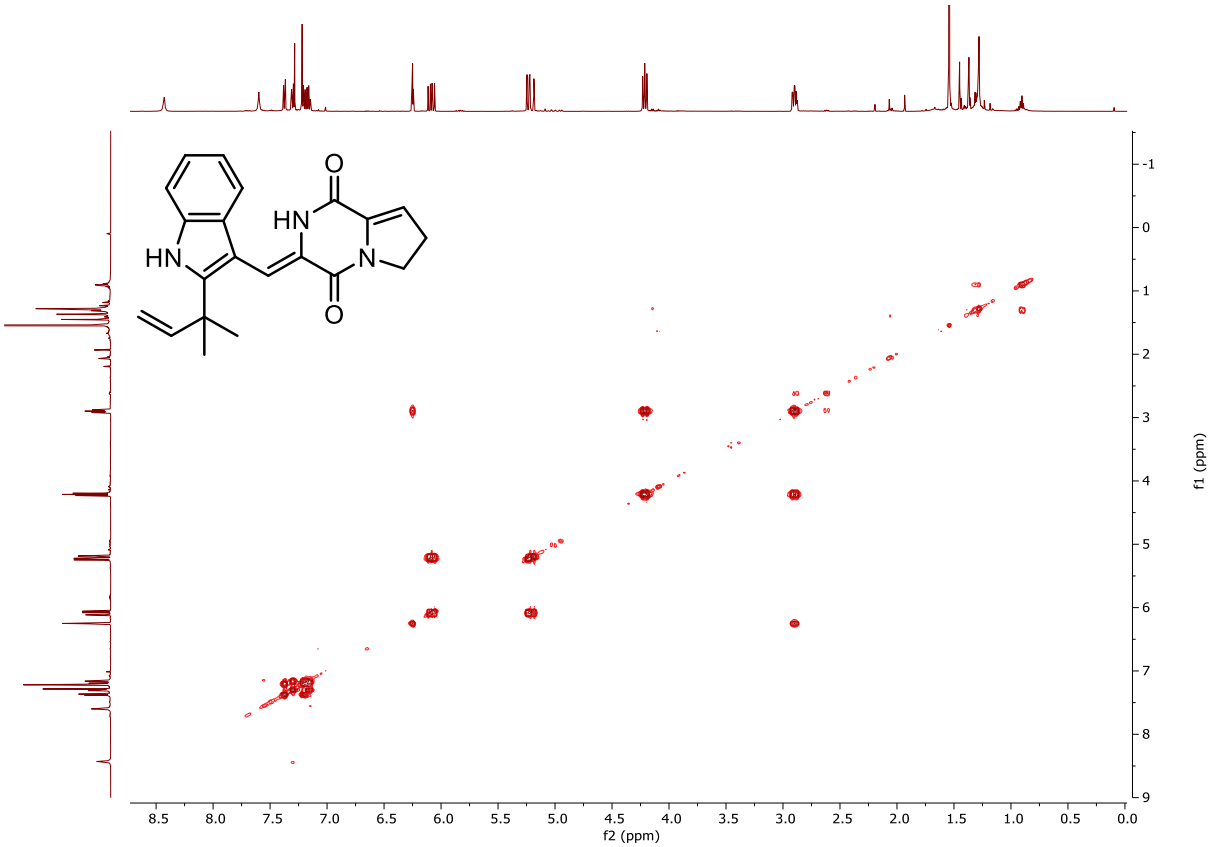

10.5.21 ^{1}H-^{13}C HSQC Spectrum of Brevianamide K (7.4) ($CDCl_3$)

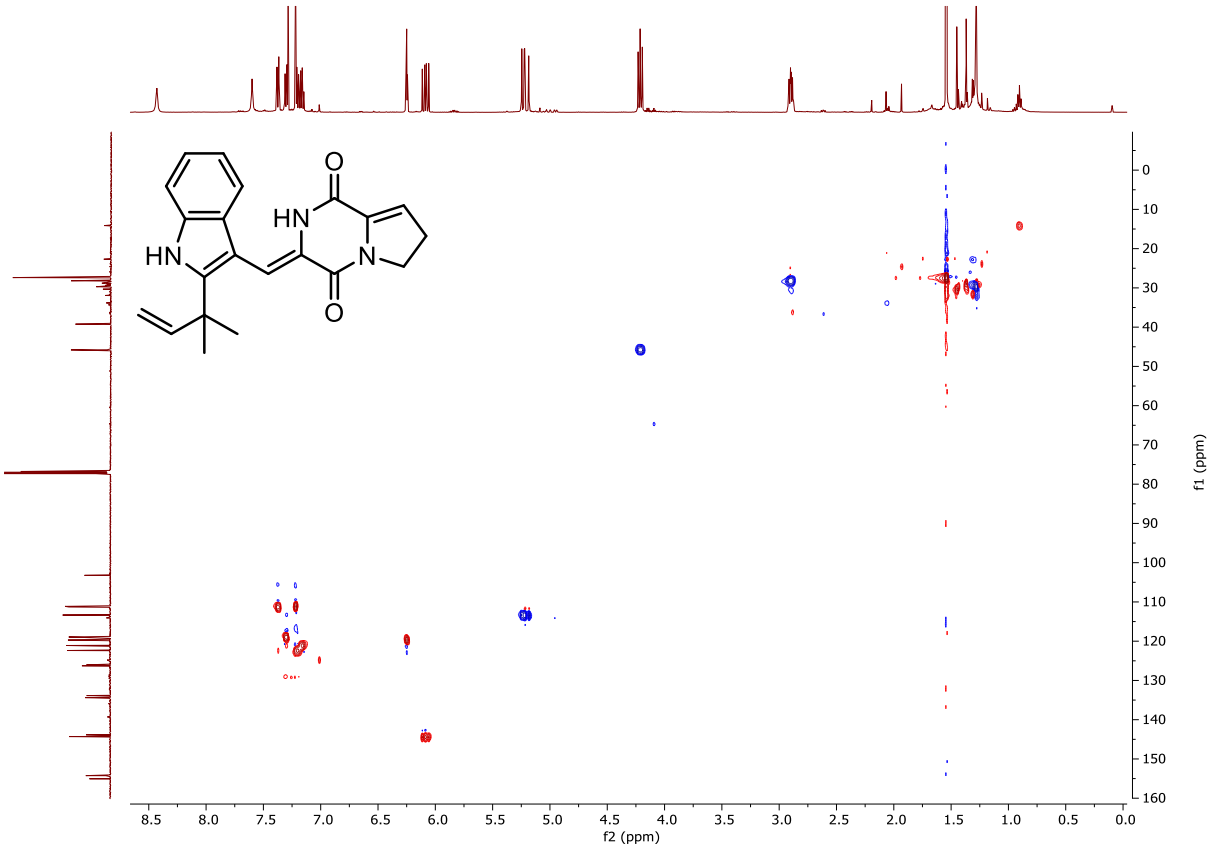

10.5.22 ^{1}H-^{13}C HMBC Spectrum of Brevianamide K (7.4) ($CDCl_3$)

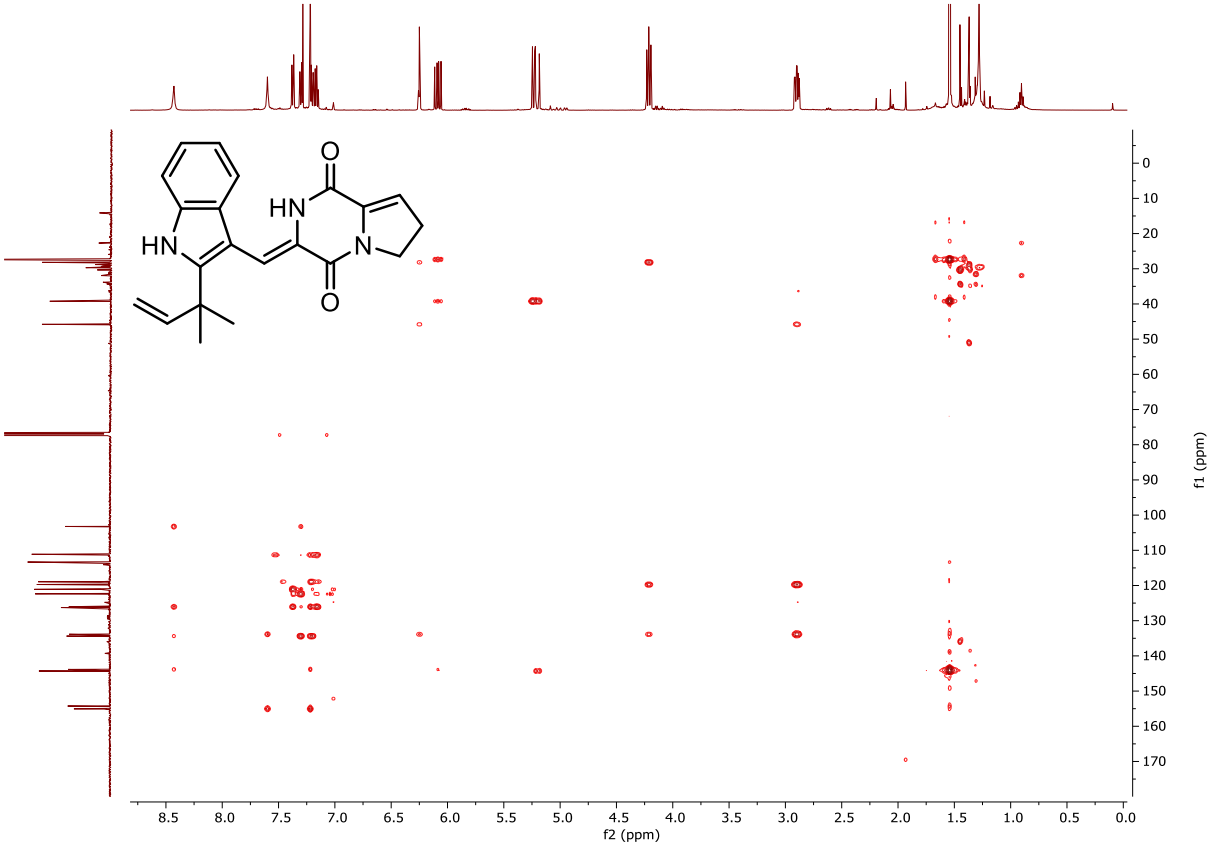

10.5.23 ^{1}H NMR Spectrum of Compound 7.36 (500 MHz, $CDCl_3$)

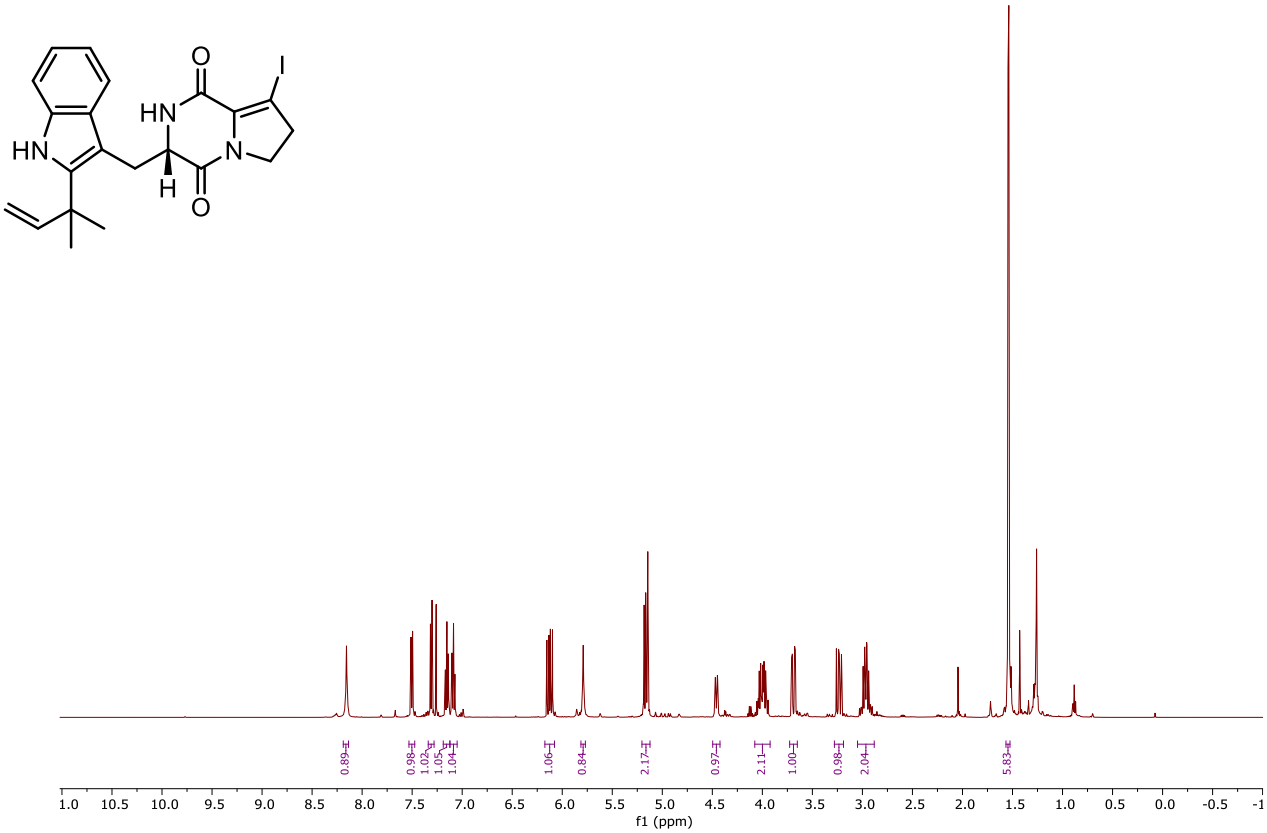

10.5.24 ^{13}C NMR Spectrum of Compound 7.36 (125 MHz, $CDCl_3$)

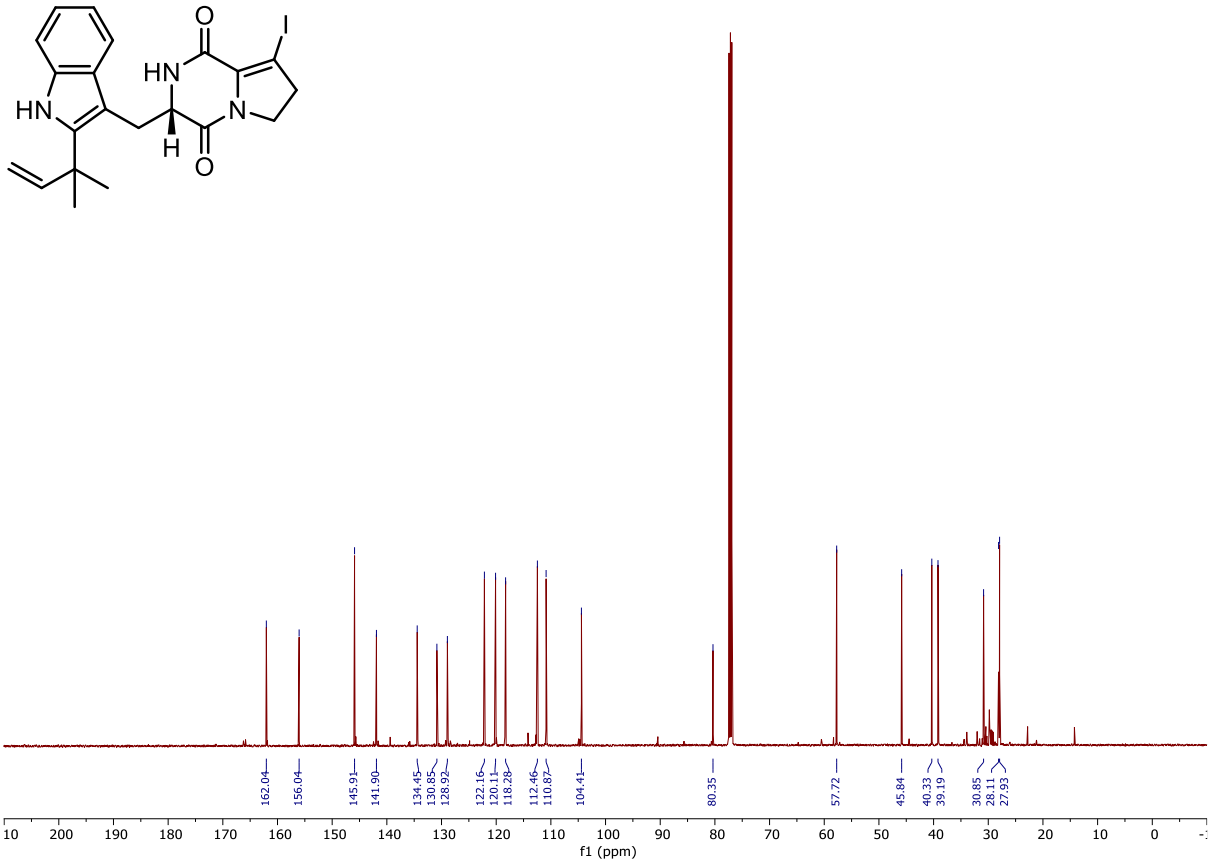

10.5.25 ^{1}H-^{1}H COSY Spectrum of Compound 7.36 ($CDCl_3$)

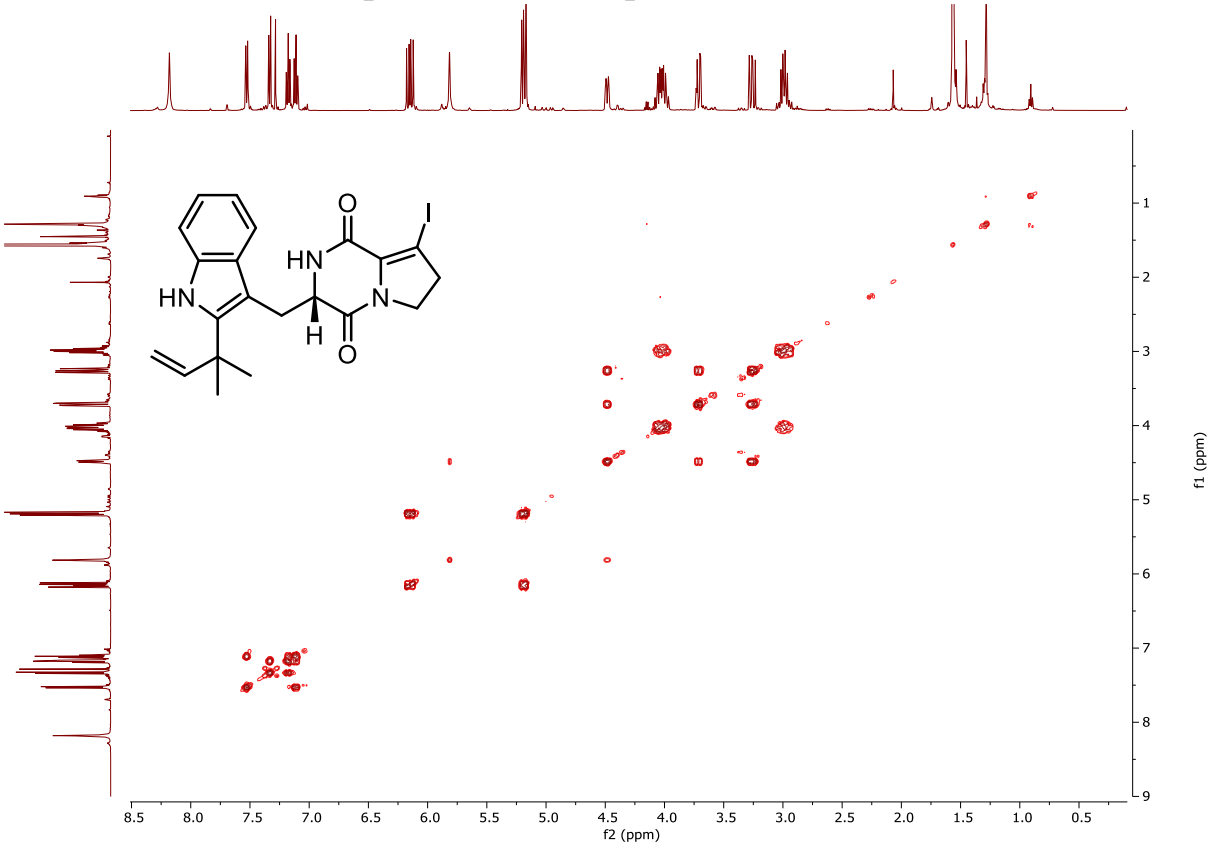

10.5.26 ^{1}H-^{13}C HSQC Spectrum of Compound 7.36 ($CDCl_3$)

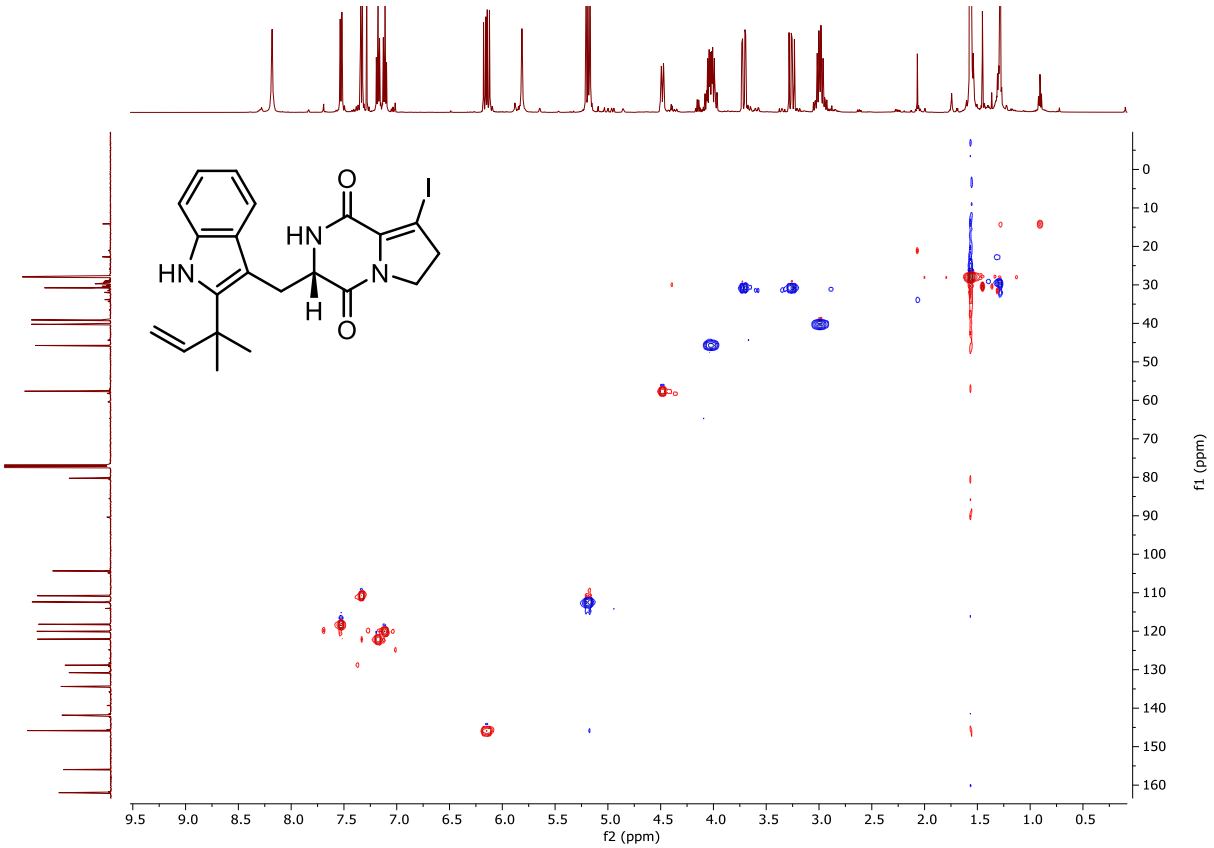

10.5.27 ^{1}H-^{13}C HMBC Spectrum of Compound 7.36 ($CDCl_3$)

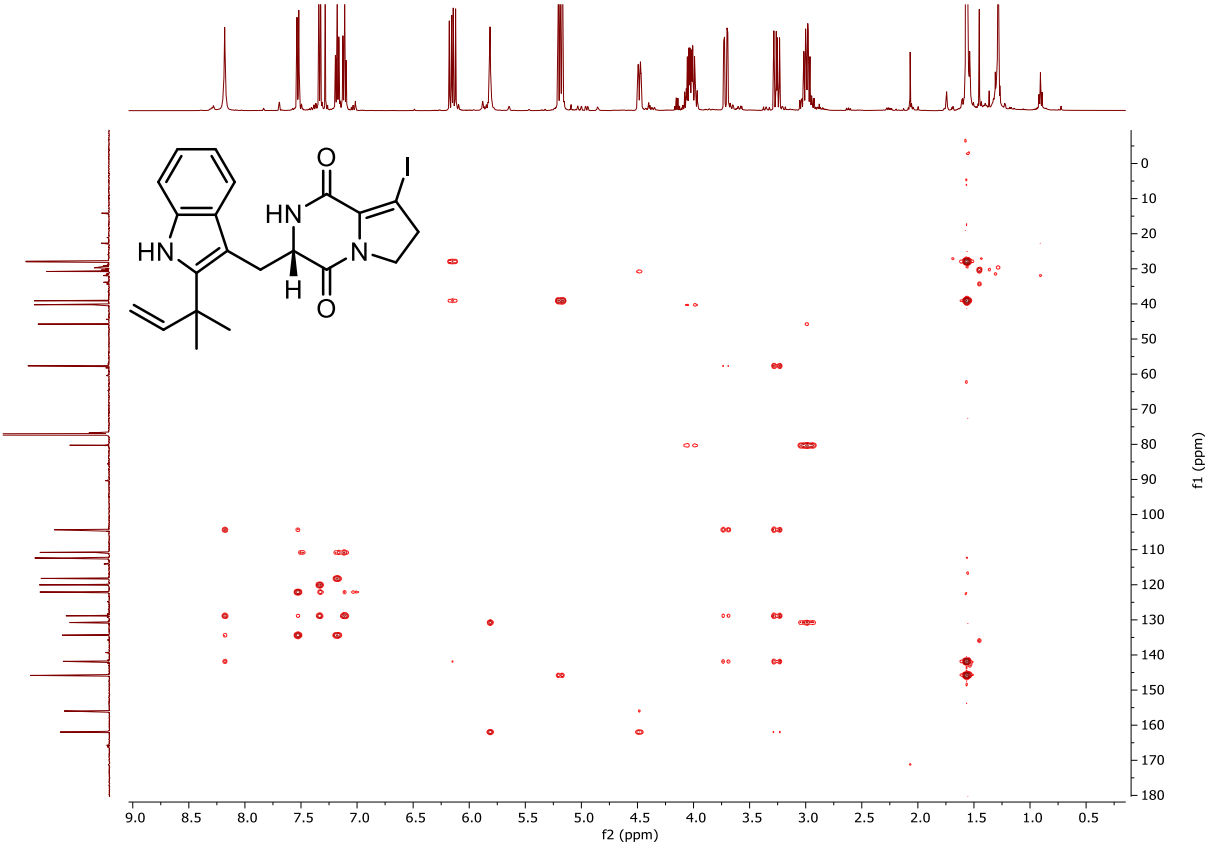

10.5.28 ^{1}H NMR Spectrum of Compound 7.57 (500 MHz, $CDCl_3$)

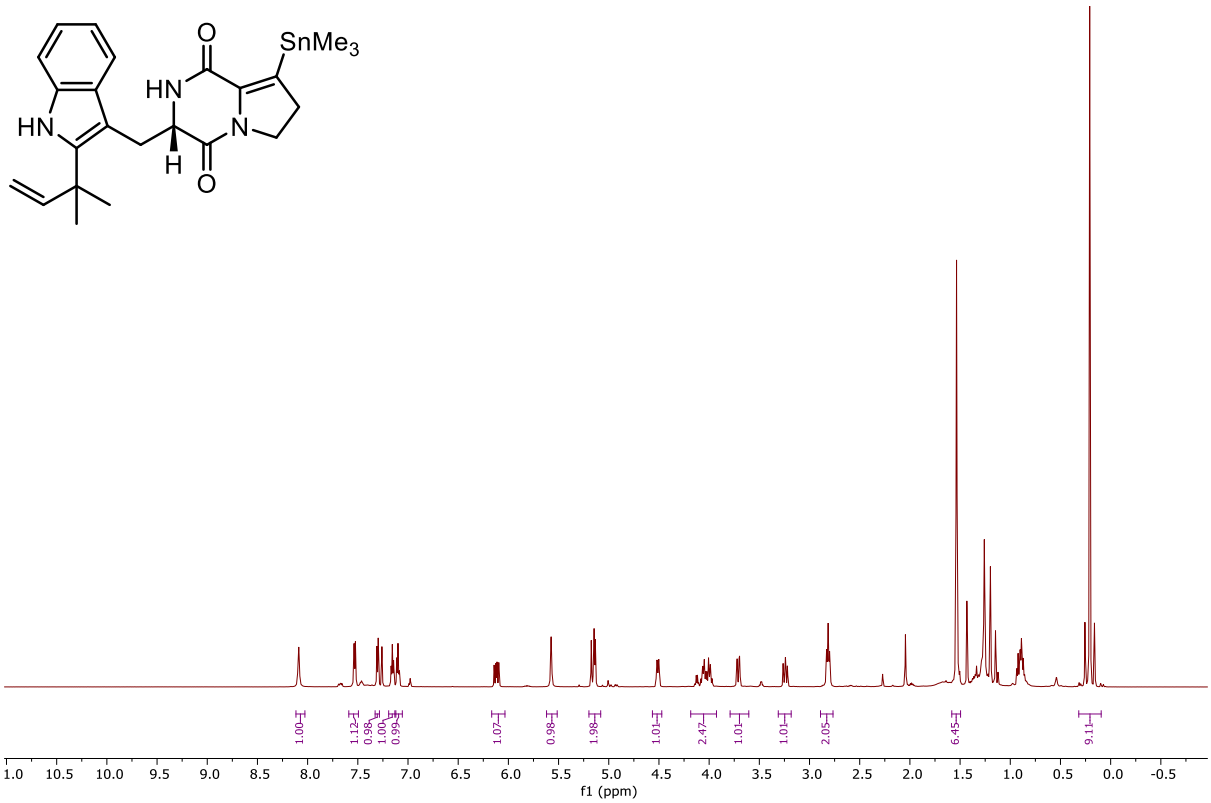

10.5.29 ^{13}C NMR Spectrum of Compound 7.57 (125 MHz, $CDCl_3$)

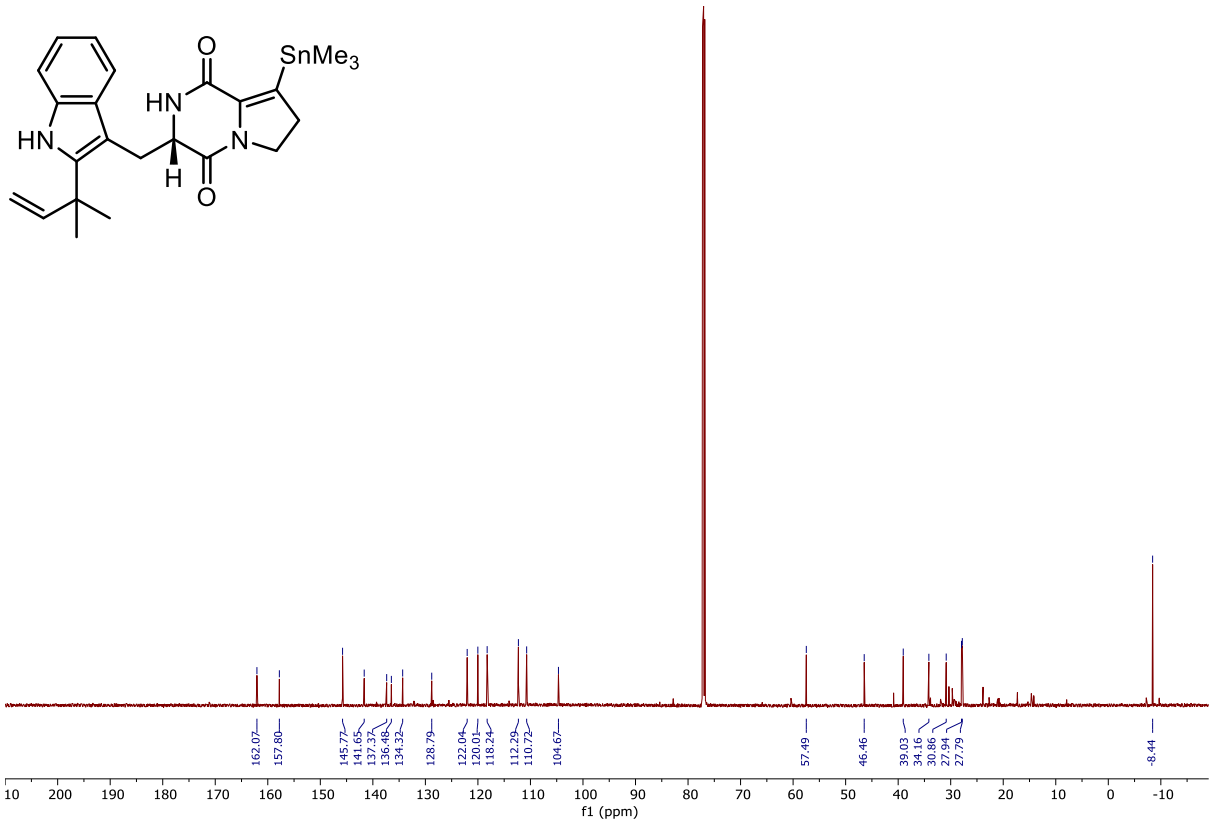

10.5.30 ^{1}H-^{1}H COSY Spectrum of Compound 7.57 ($CDCl_3$)

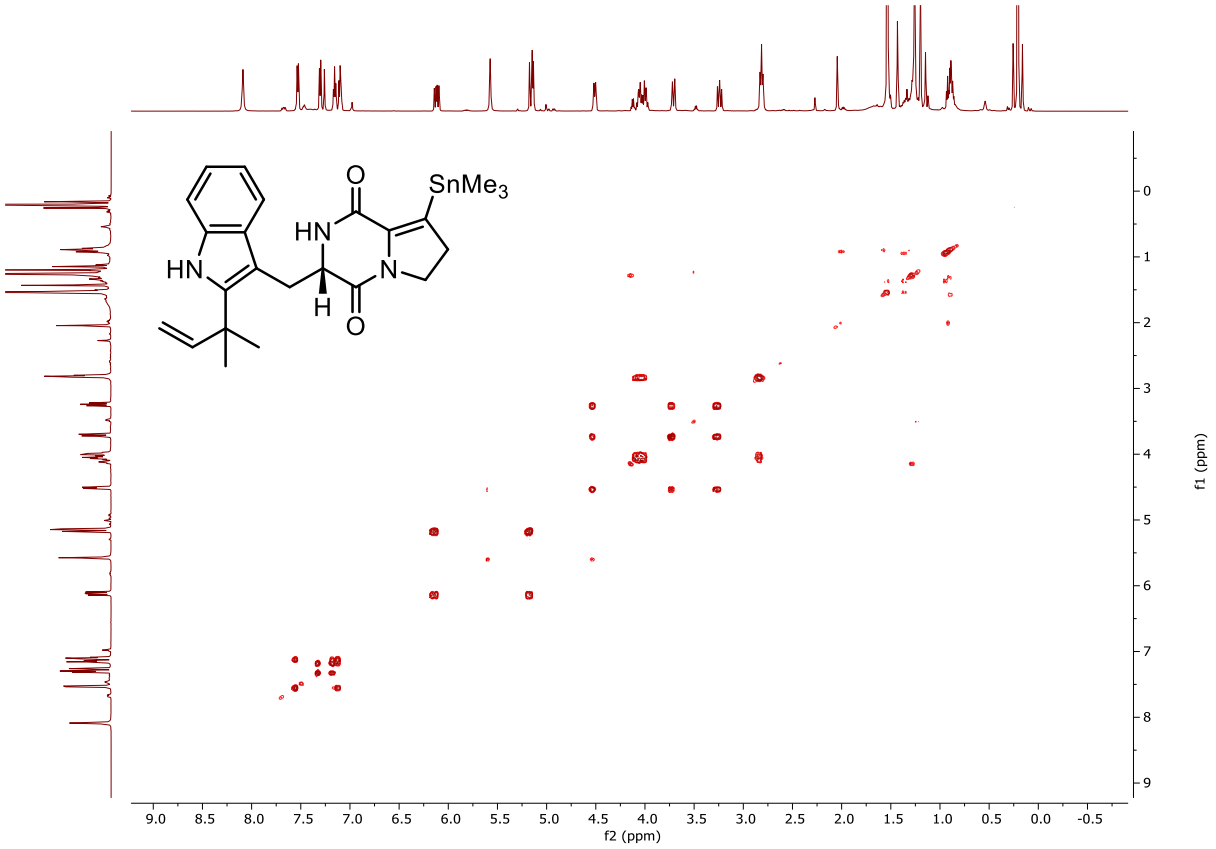

10.5.31 ^{1}H-^{13}C HSQC Spectrum of Compound 7.57 ($CDCl_3$)

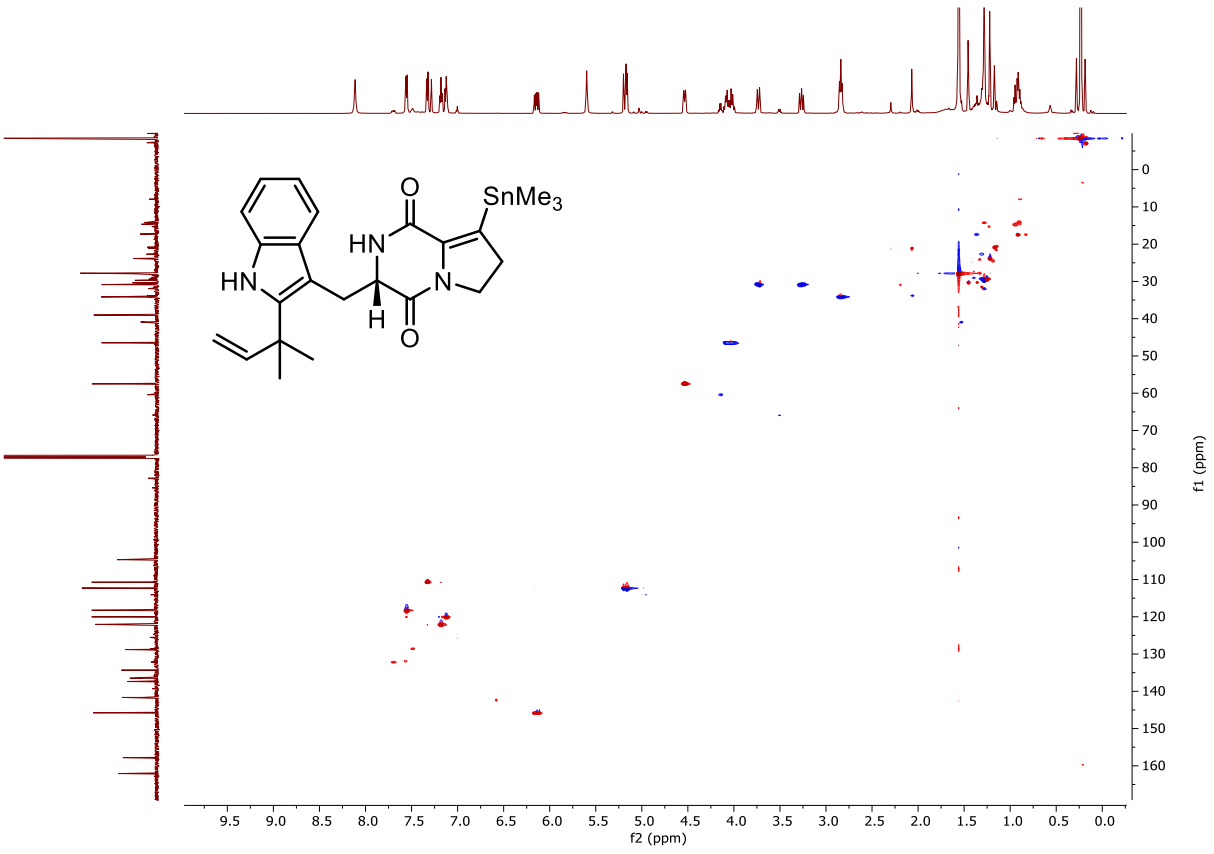

10.5.32 ^{1}H-^{13}C HMBC Spectrum of Compound 7.57 ($CDCl_3$)

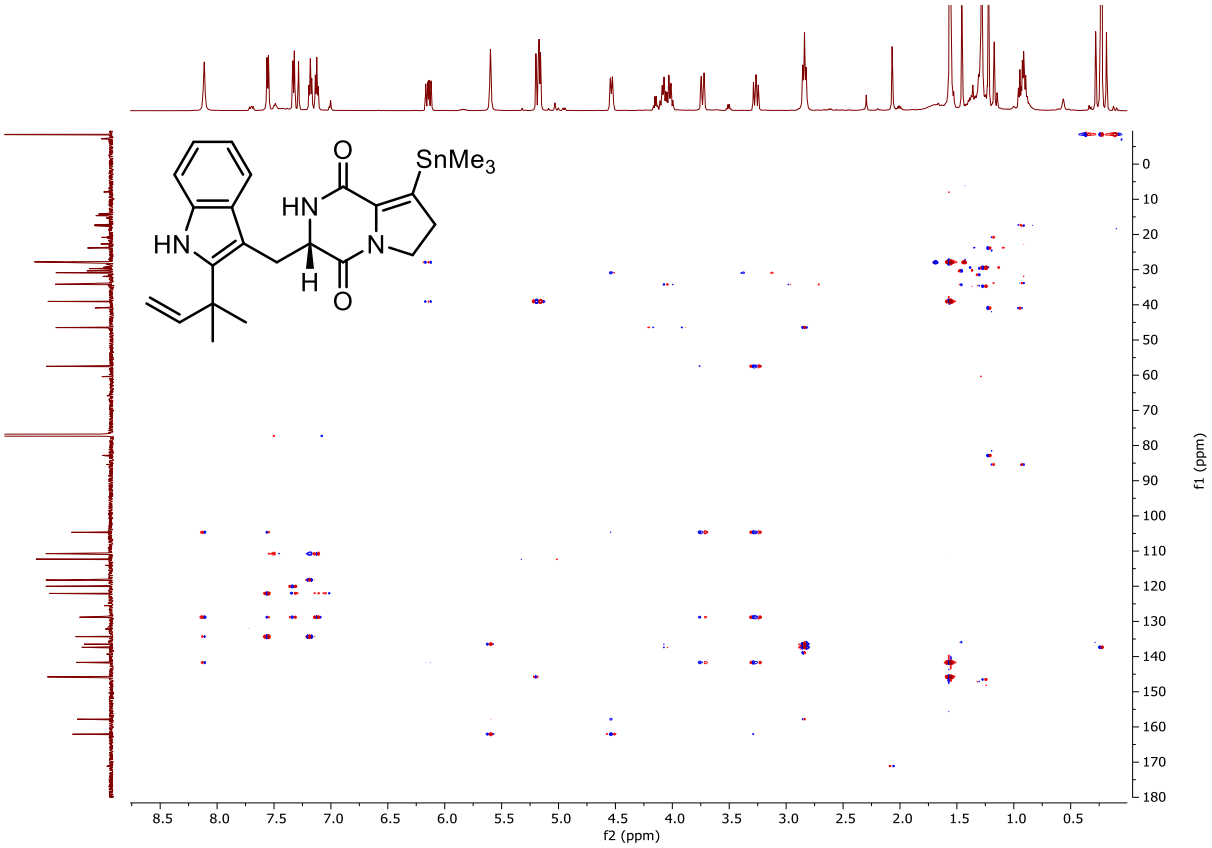

10.5.33 ^{13}C DEPT Spectrum of Compound 7.57 ($CDCl_3$)

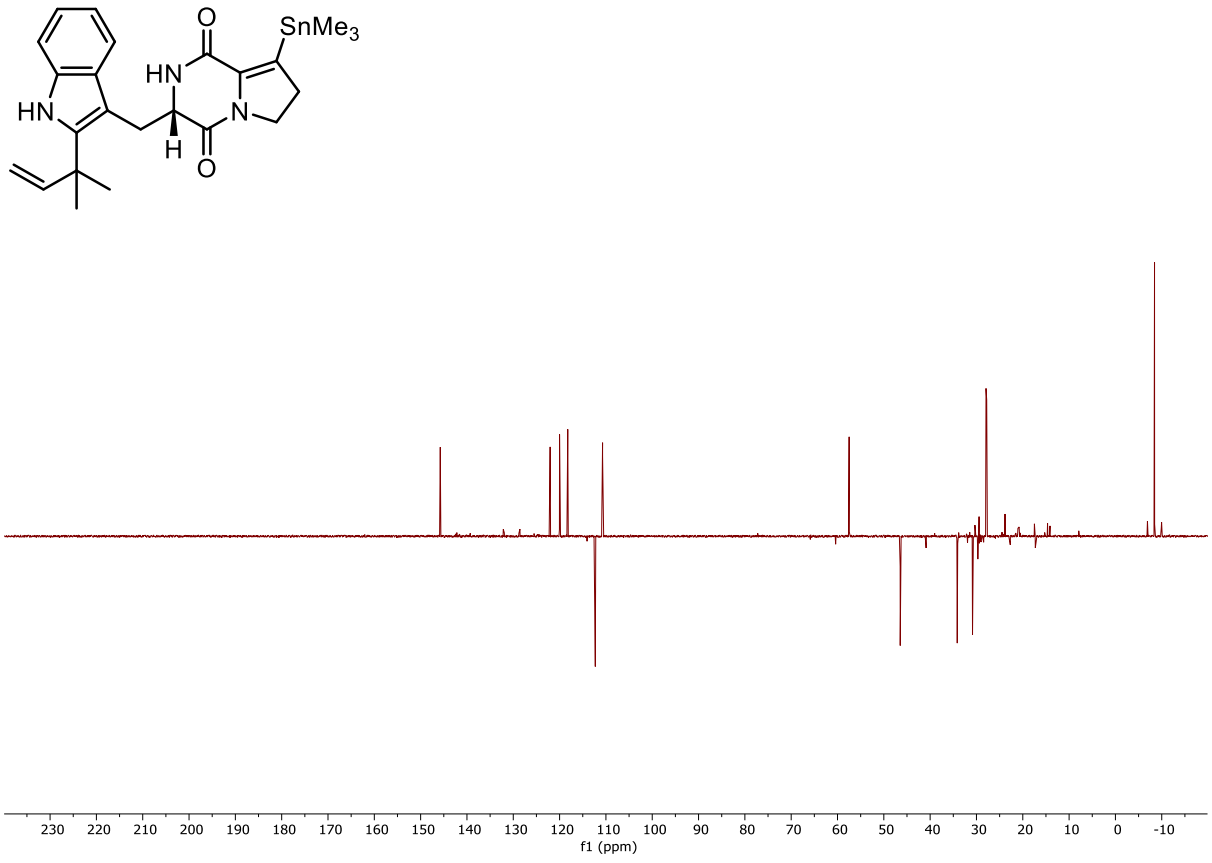

10.5.34 ^{1}H NMR Spectrum of Compound 7.5 (600 MHz, $CDCl_3$)

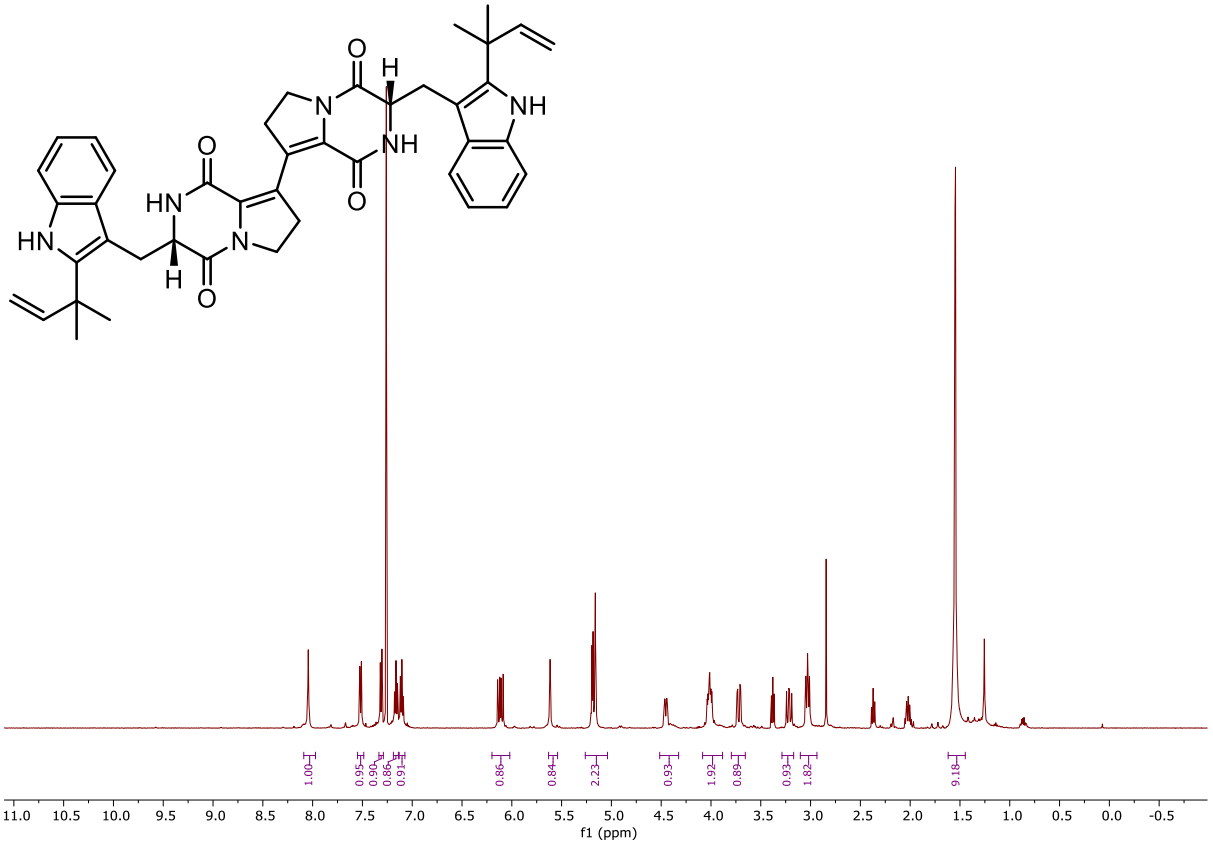

10.5.35 ^{13}C NMR Spectrum of Compound 7.5 (125 MHz, $CDCl_3$)

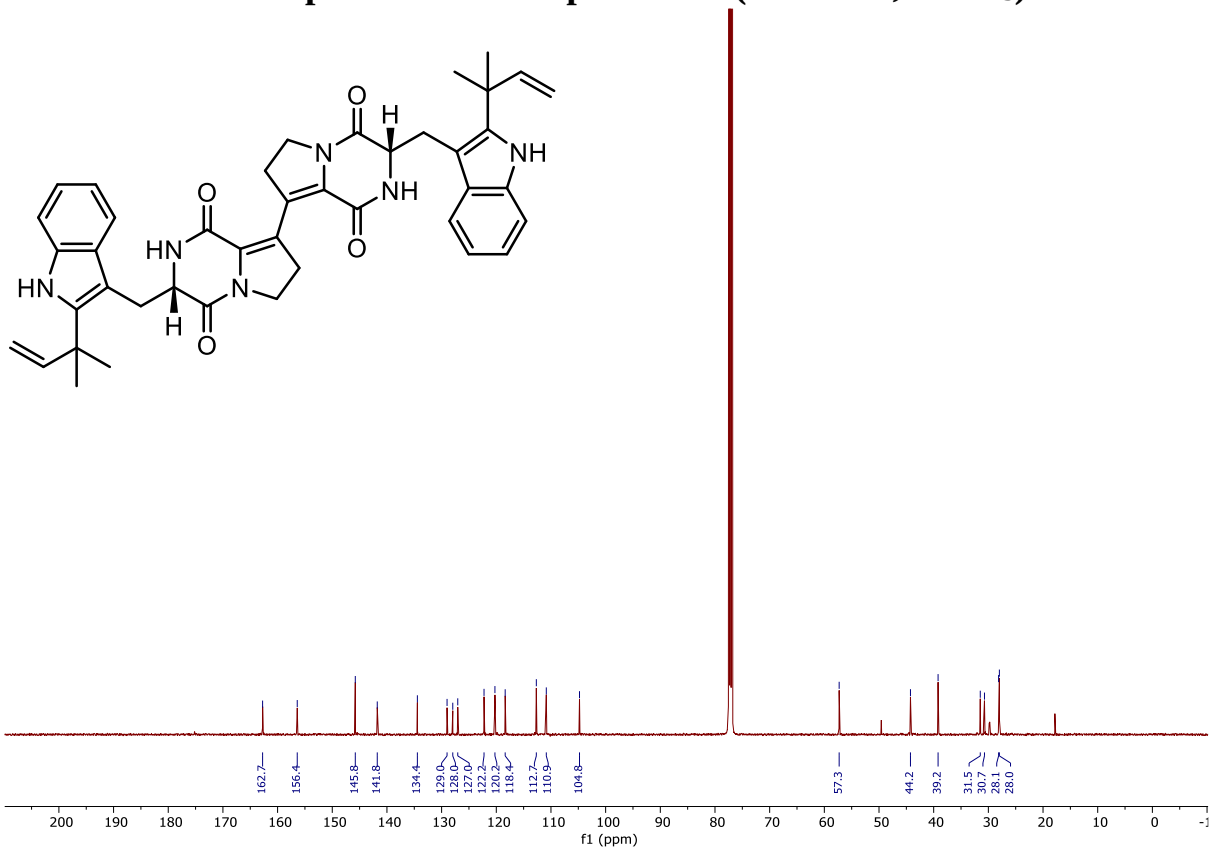

10.5.36 ^{1}H-^{1}H COSY Spectrum of Compound 7.5 ($CDCl_3$)

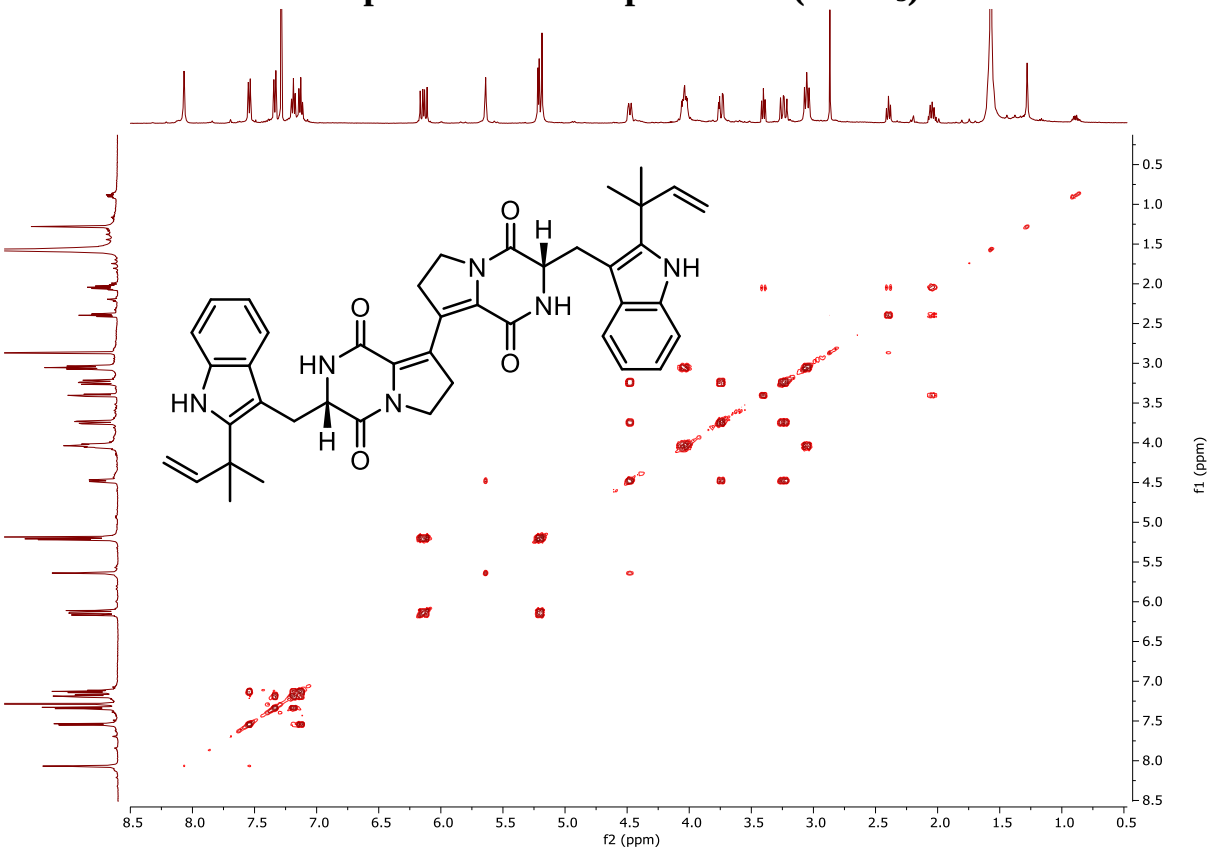

10.5.37 ^{1}H-^{13}C HSQC Spectrum of Compound 7.5 ($CDCl_3$)

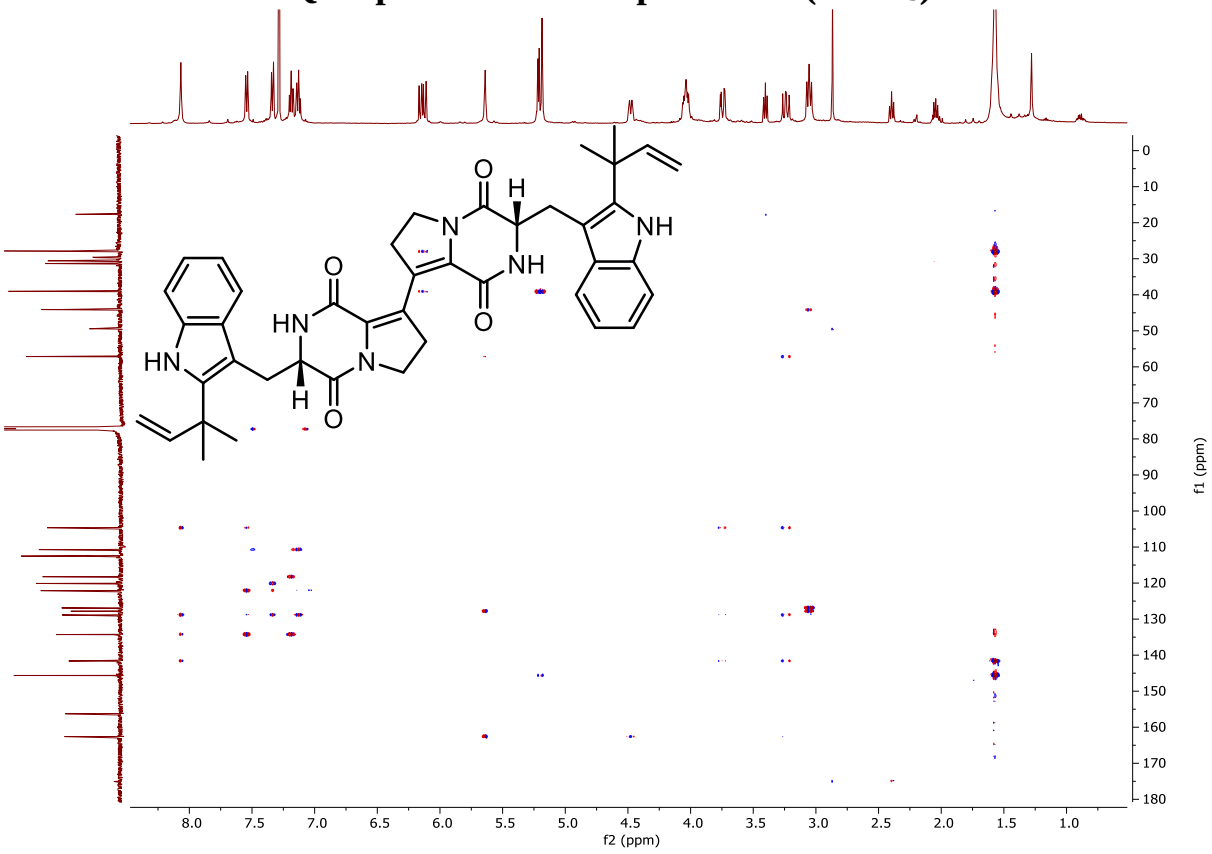

10.5.38 ^{1}H-^{13}C HMBC Spectrum of Compound 7.5 ($CDCl_3$)

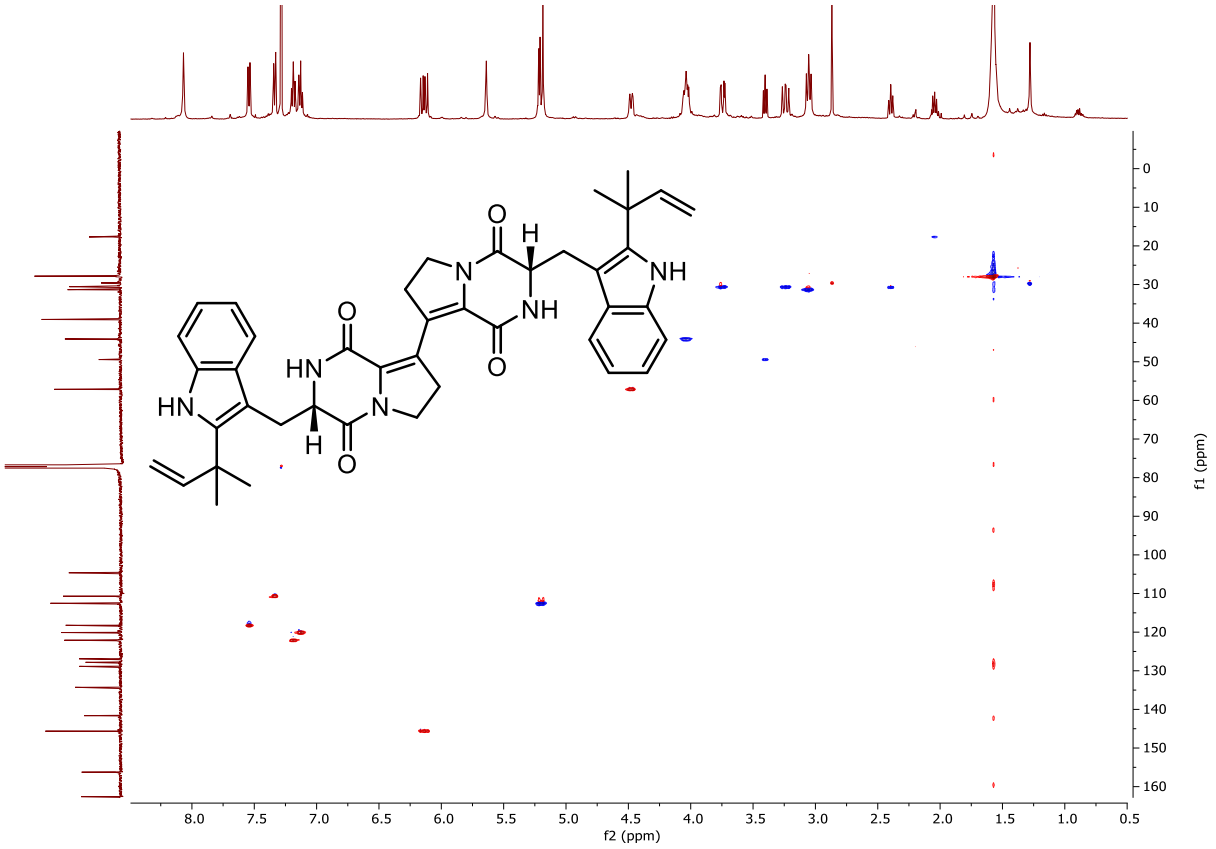

10.5.39 ^{1}H NMR Spectrum of Compound 7.52 (600 MHz, $CDCl_3$)

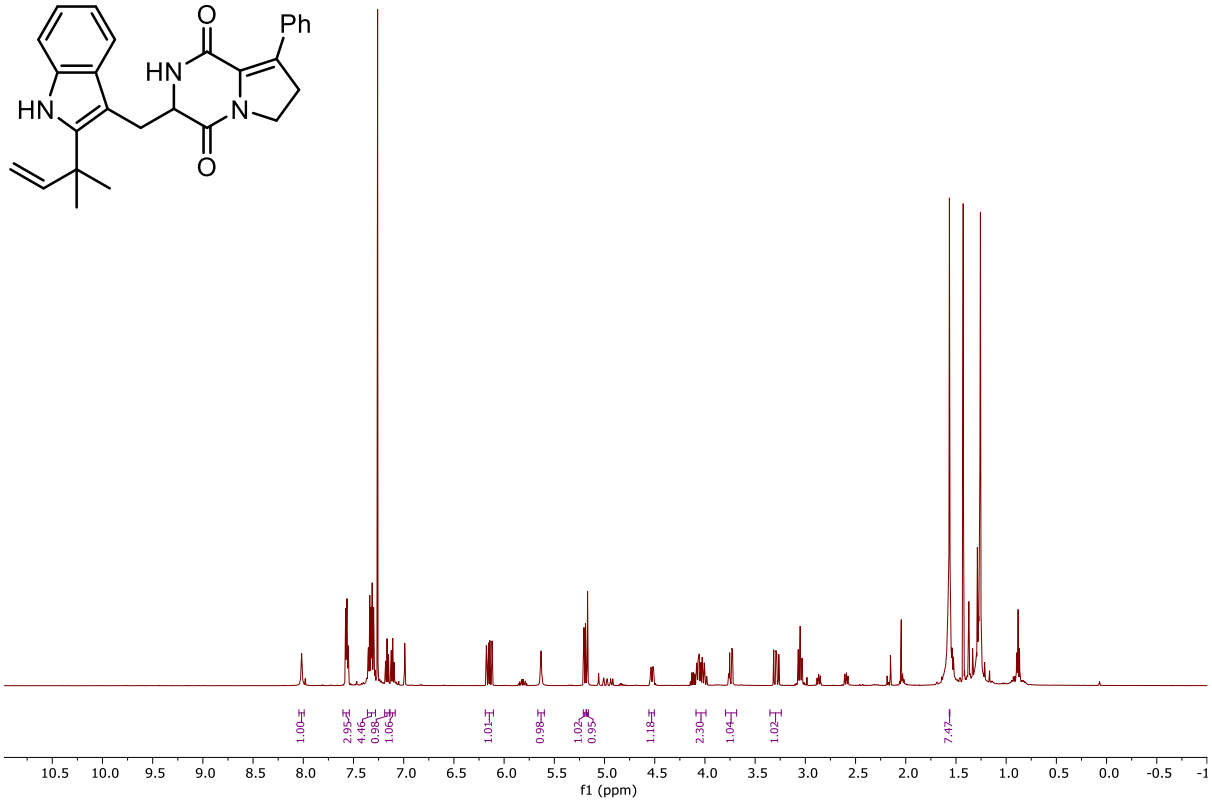

10.5.40 ^{13}C NMR Spectrum of Compound 7.52 (150 MHz, $CDCl_3$)

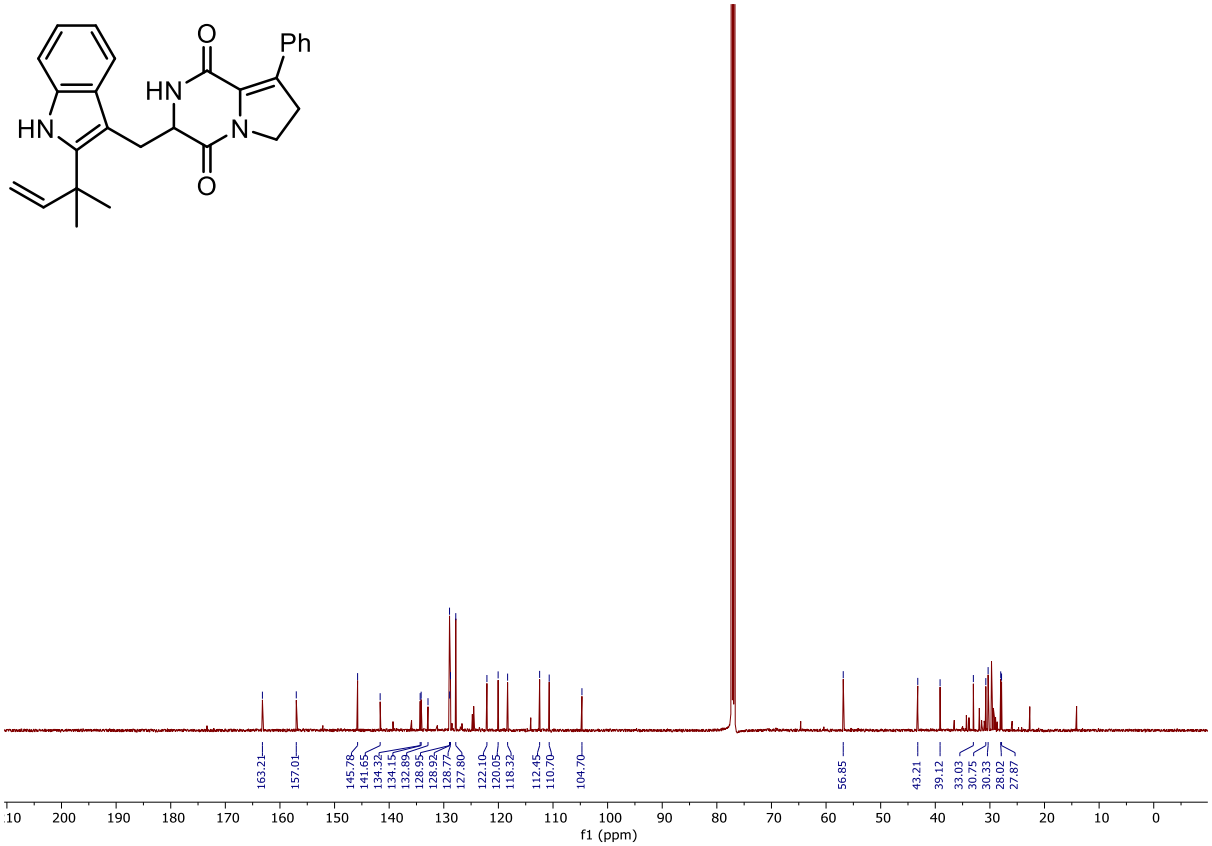

10.5.41 ^{1}H-^{1}H COSY Spectrum of Compound 7.52 ($CDCl_3$)

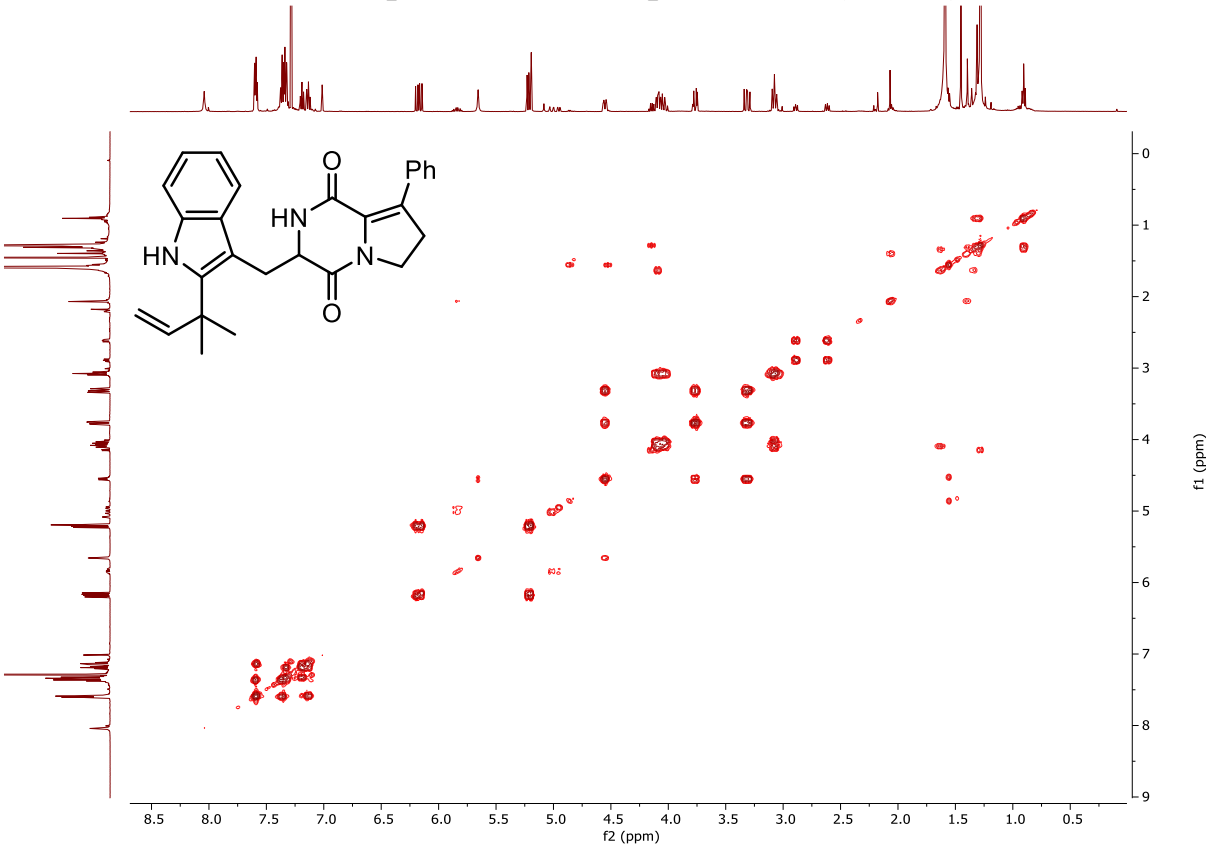

10.5.42 ^{1}H-^{13}C HSQC Spectrum of Compound 7.52 ($CDCl_3$)

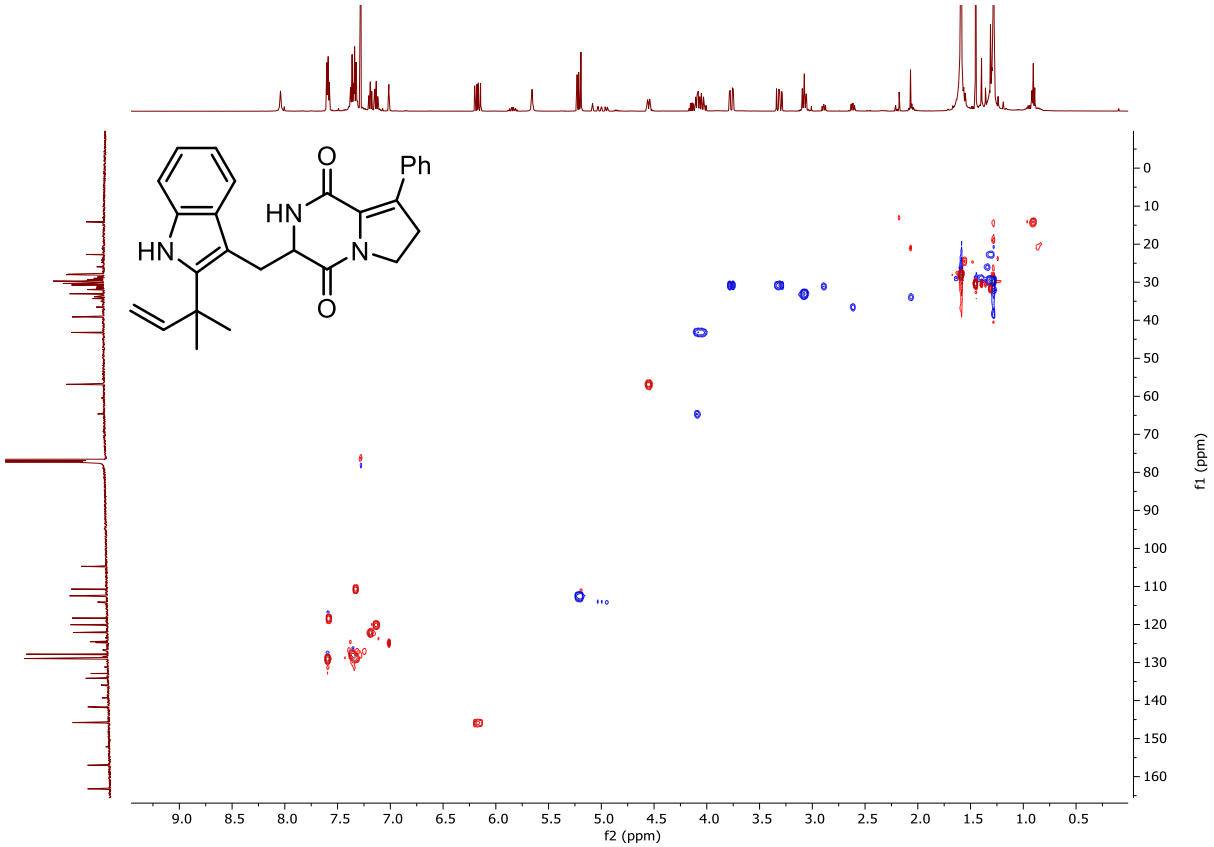

10.5.43 ^{1}H-^{13}C HMBC Spectrum of Compound 7.52 ($CDCl_3$)

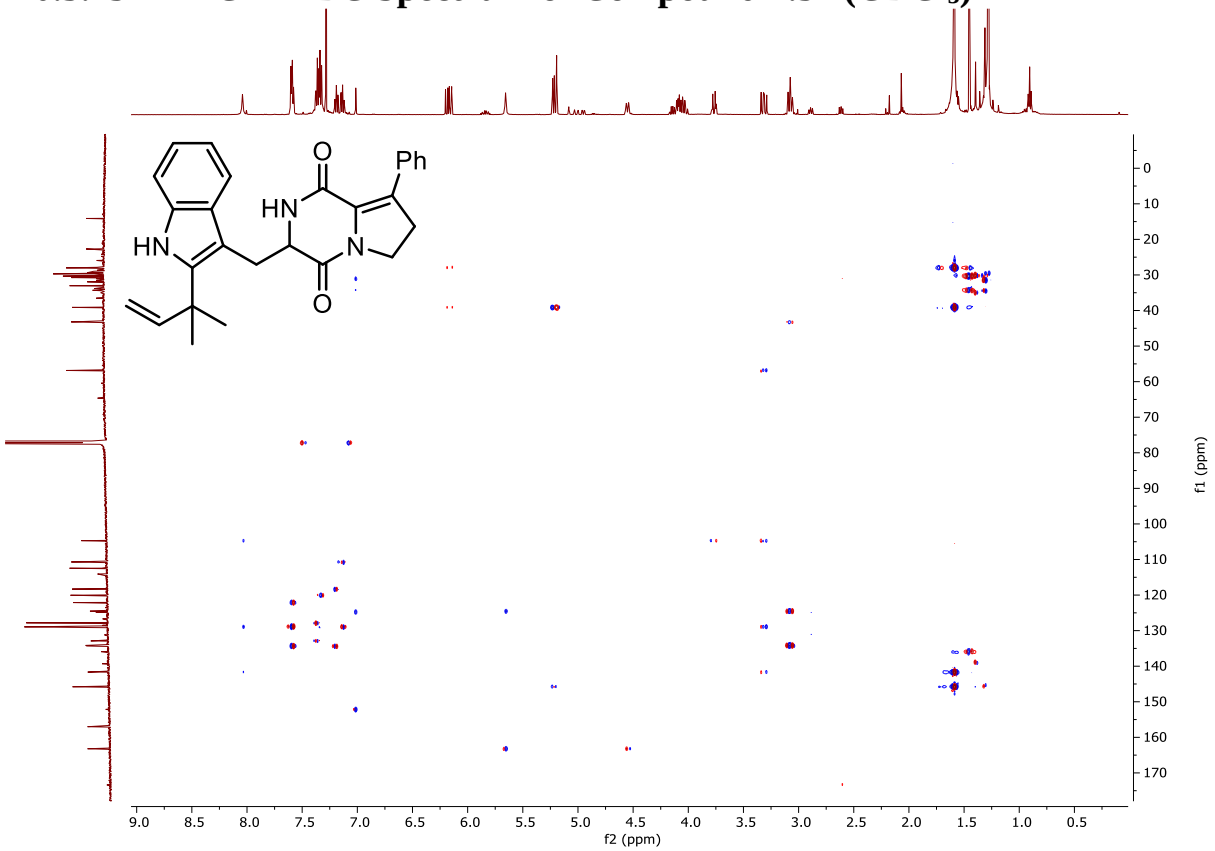

10.5.44 ^{13}C DEPT Spectrum of Compound 7.52 ($CDCl_3$)

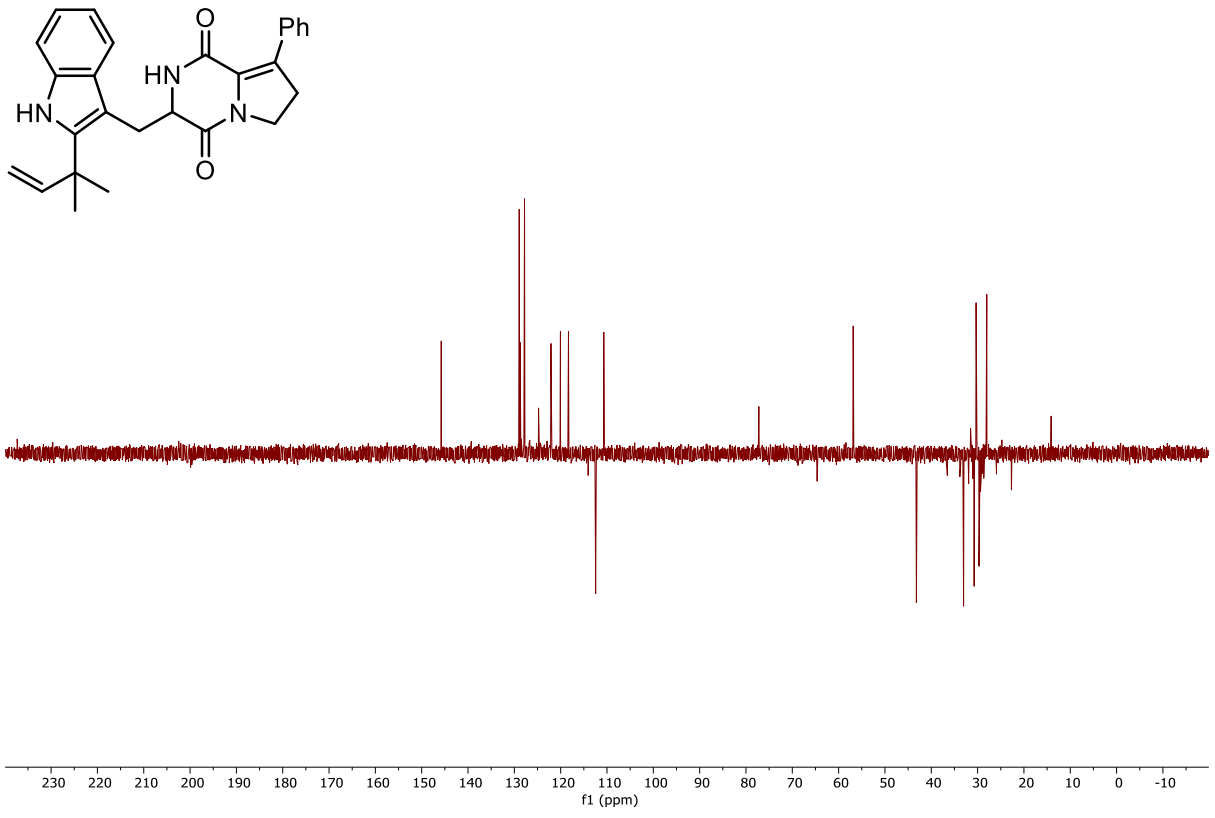

10.5.45 ^{1}H NMR Spectrum of Compound 7.48 (600 MHz, $CDCl_3$)

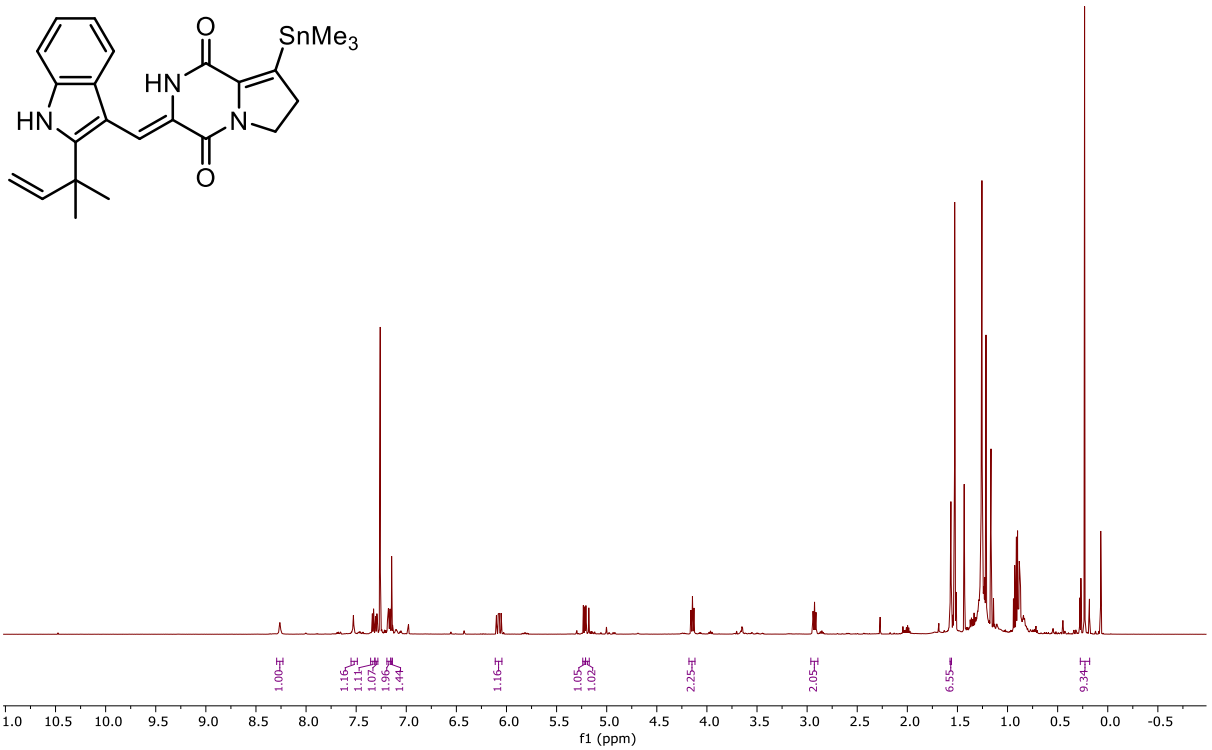

10.5.46 ^{13}C NMR Spectrum of Compound 7.48 (150 MHz, $CDCl_3$)

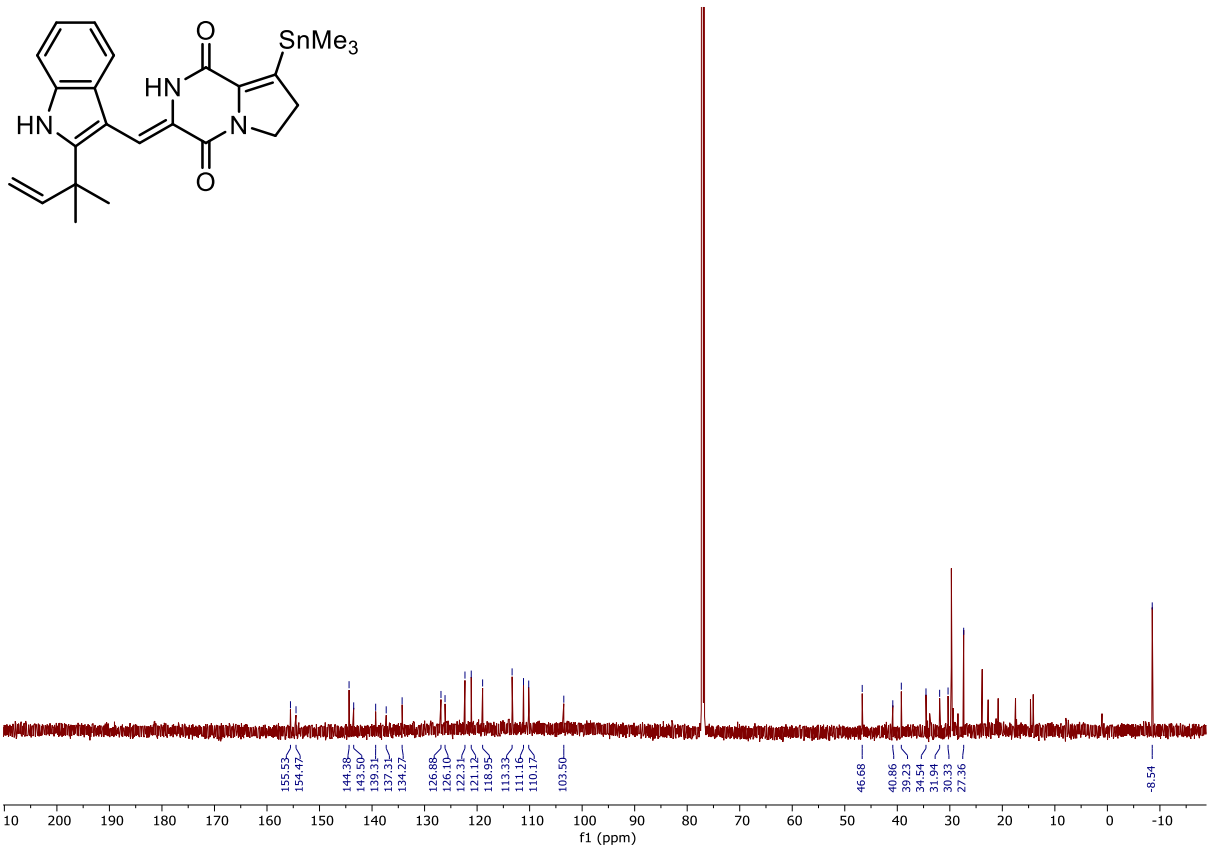

10.5.47 ^{1}H-^{1}H COSY Spectrum of Compound 7.48 ($CDCl_3$)

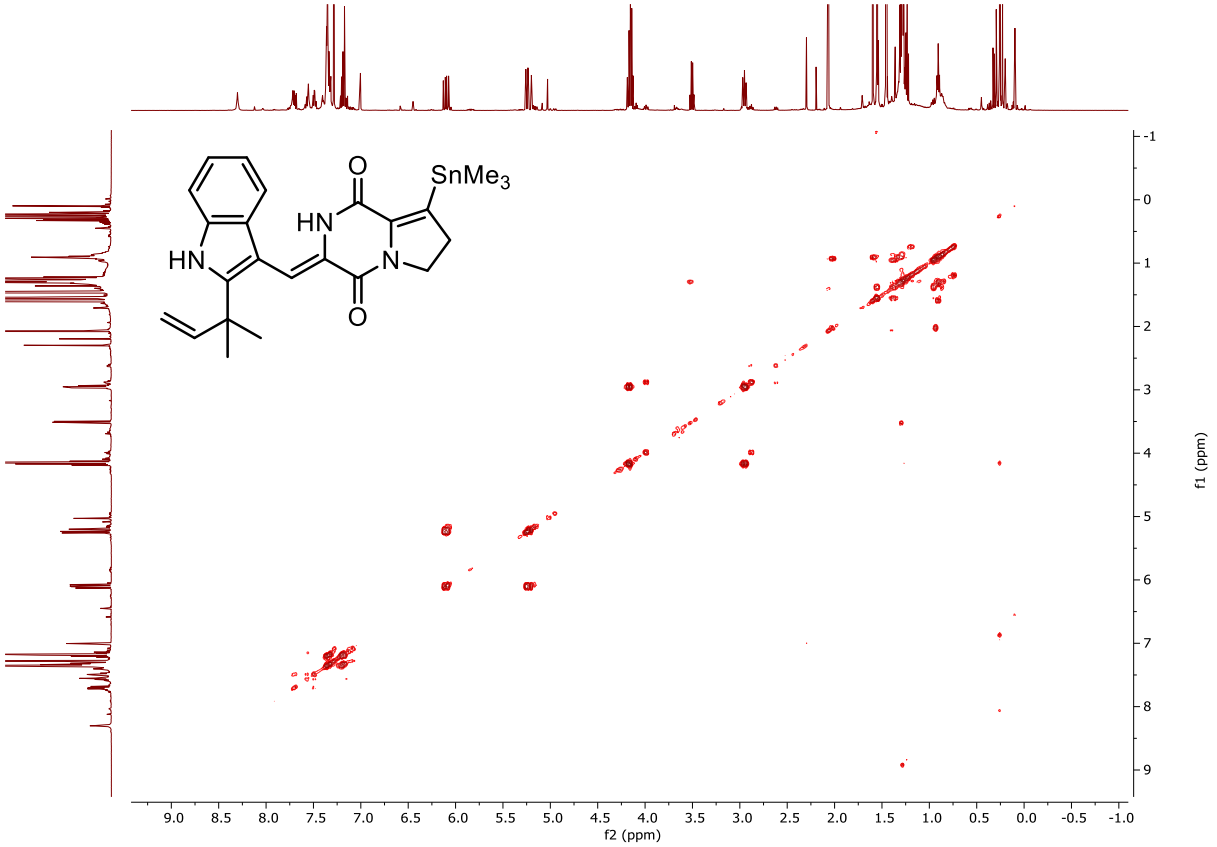

10.5.48 ^{1}H-^{13}C HSQC Spectrum of Compound 7.48 ($CDCl_3$)

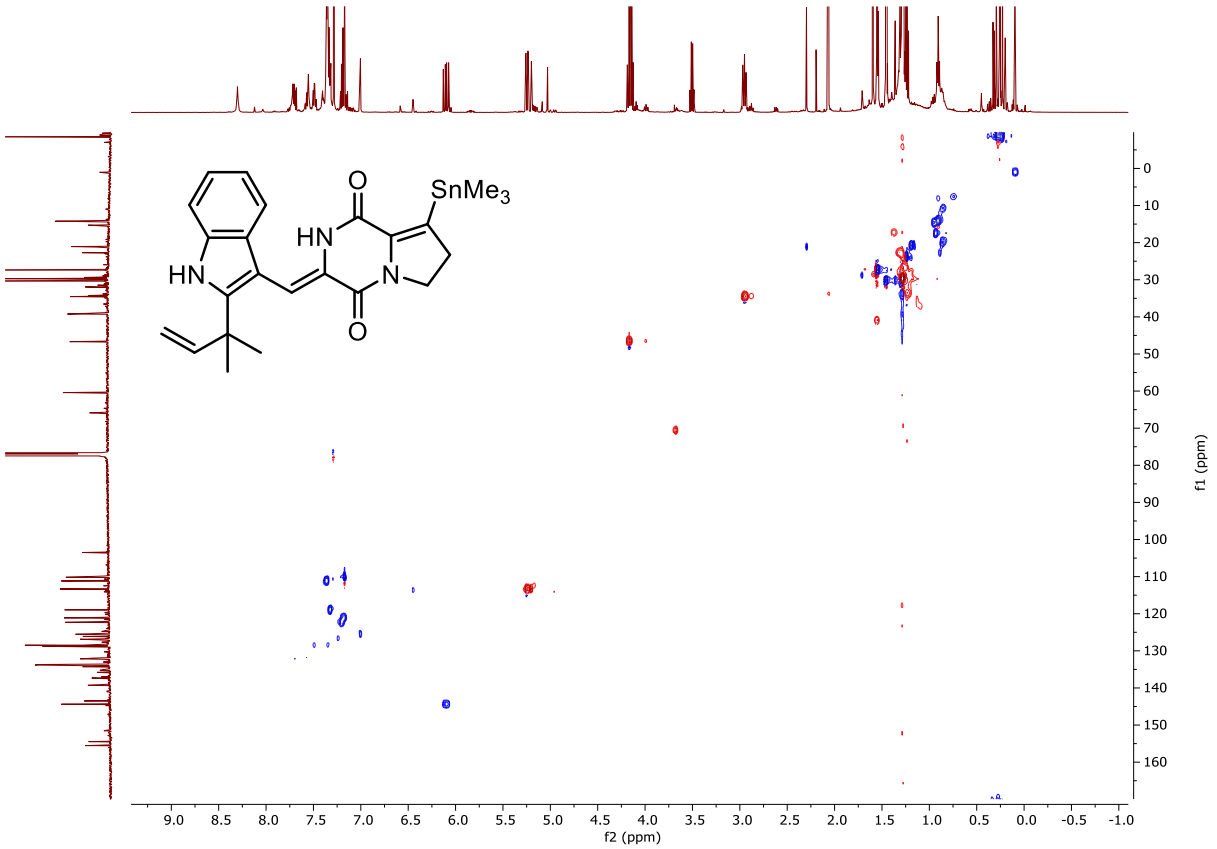

10.5.49 ^{1}H-^{13}C HMBC Spectrum of Compound 7.48 ($CDCl_3$)

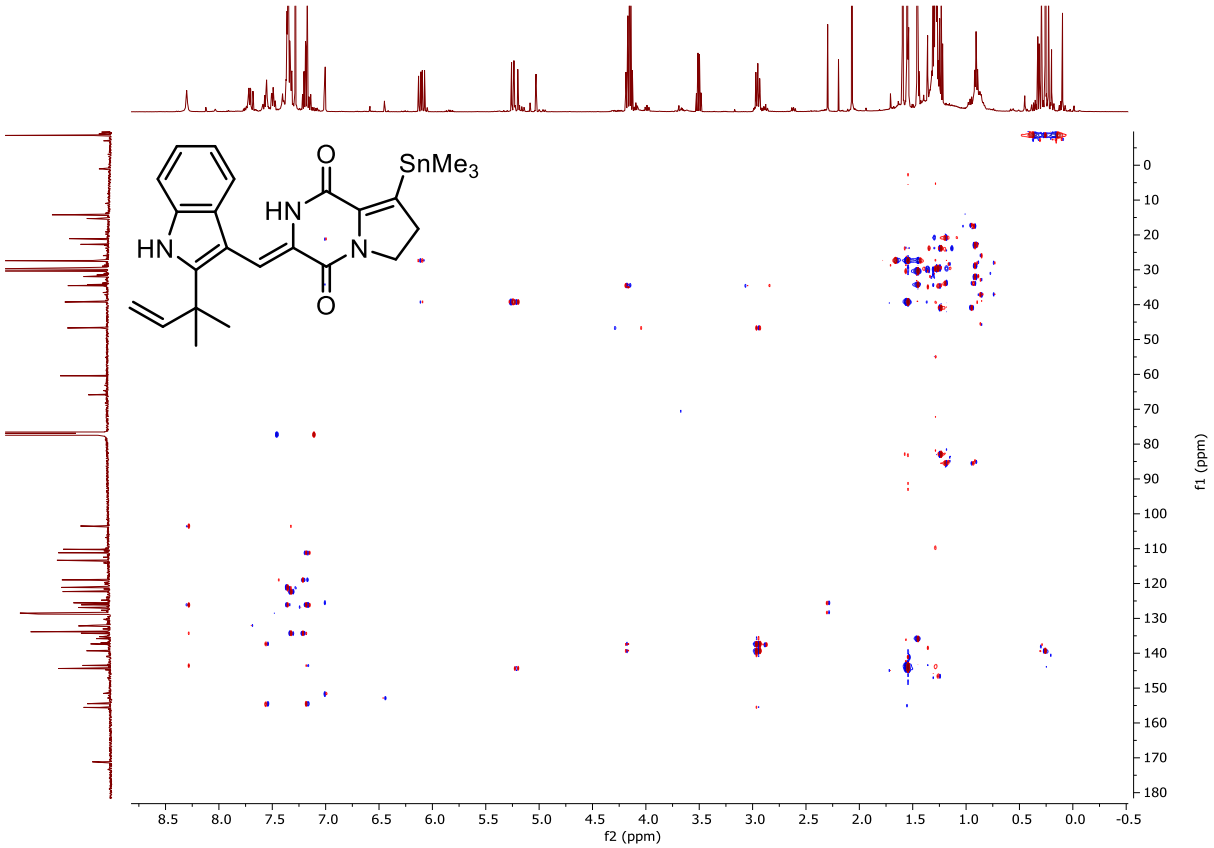

10.5.50 ^{13}C DEPT Spectrum of Compound 7.48 ($CDCl_3$)

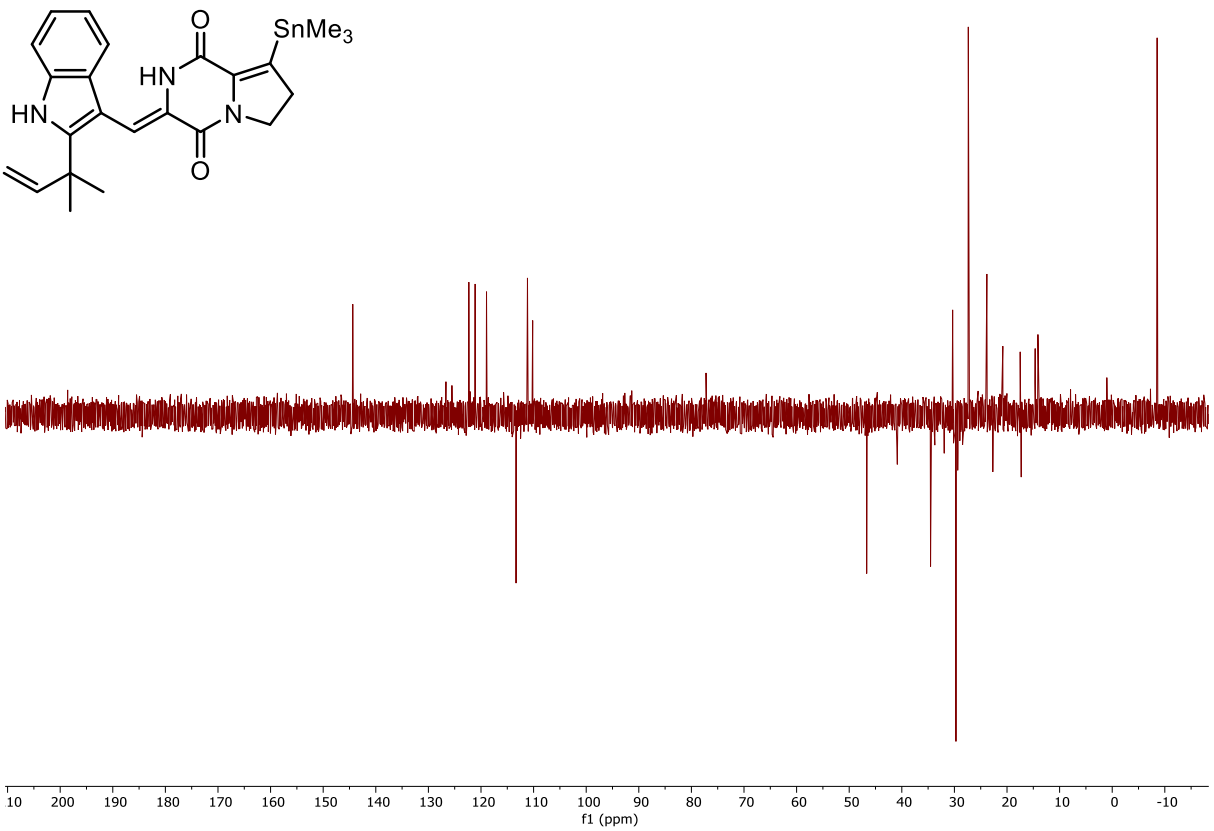

10.5.51 ^{1}H NMR Spectrum of Compound 7.42 (500 MHz, $CDCl_3$)

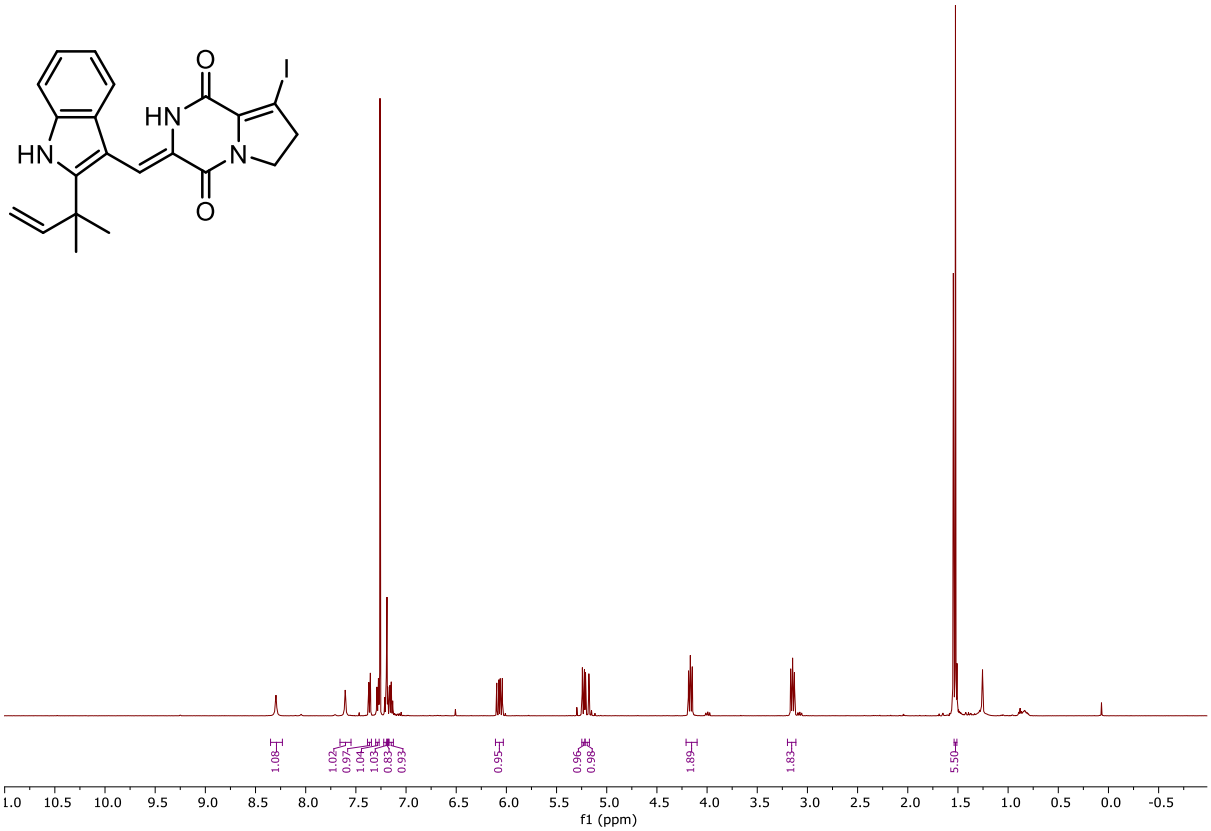

10.5.52 ^{13}C NMR Spectrum of Compound 7.42 (125 MHz, $CDCl_3$)

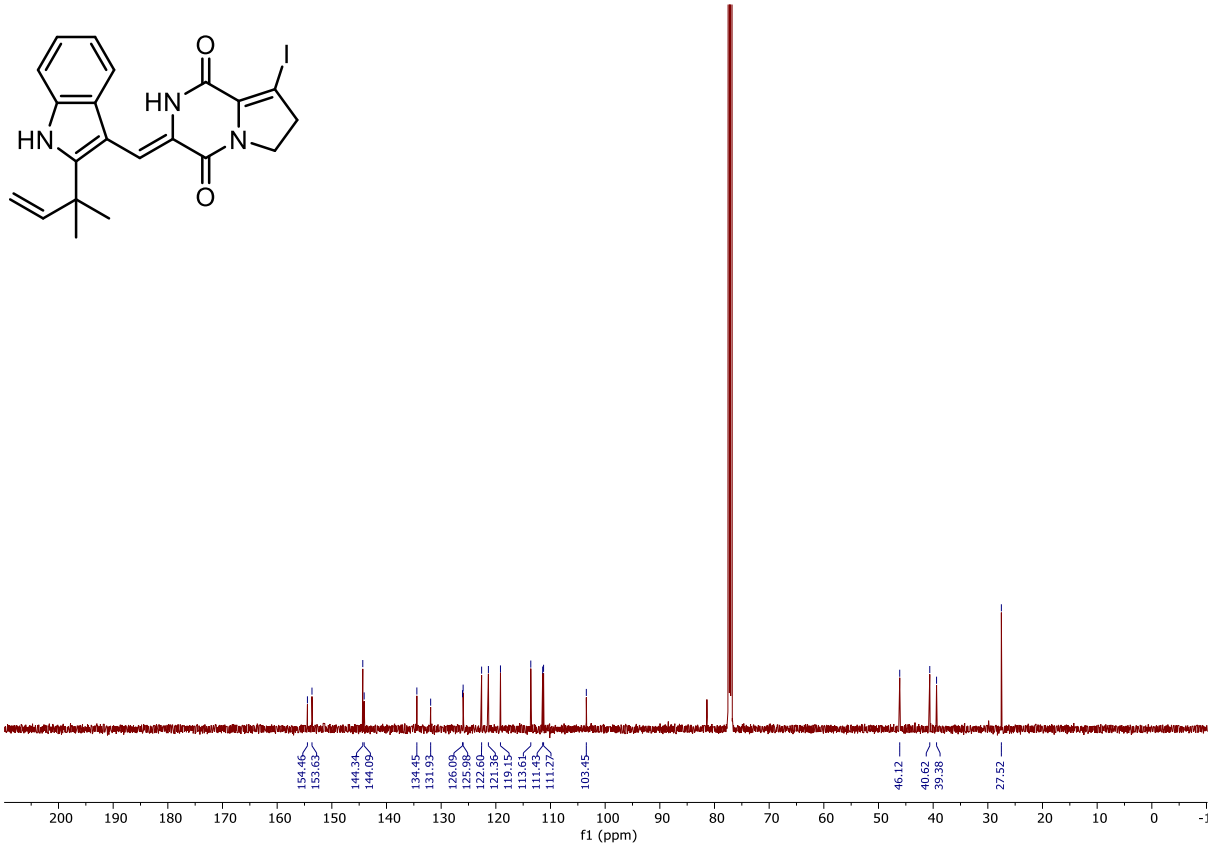

10.5.53 ^{1}H-^{1}H COSY Spectrum of Compound 7.42 ($CDCl_3$)

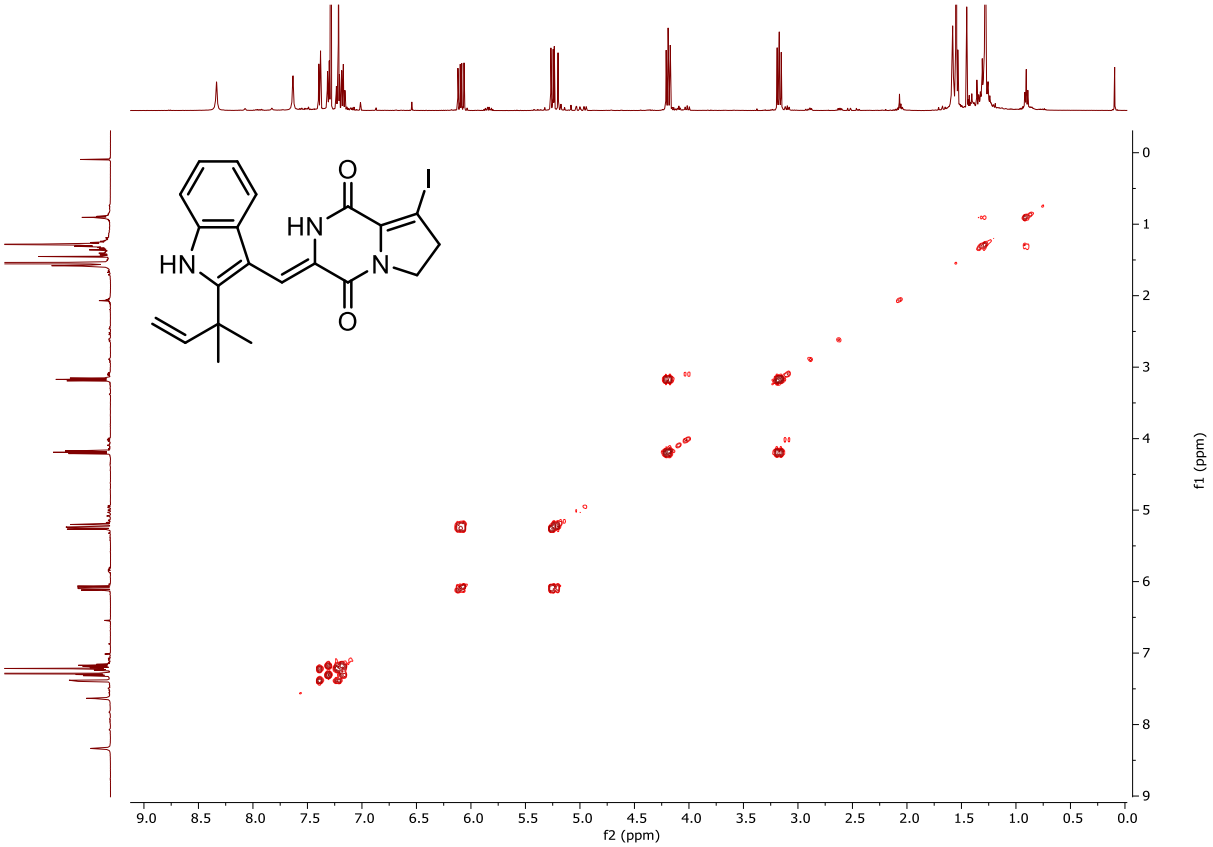

10.5.54 ^{1}H-^{13}C HSQC Spectrum of Compound 7.42 ($CDCl_3$)

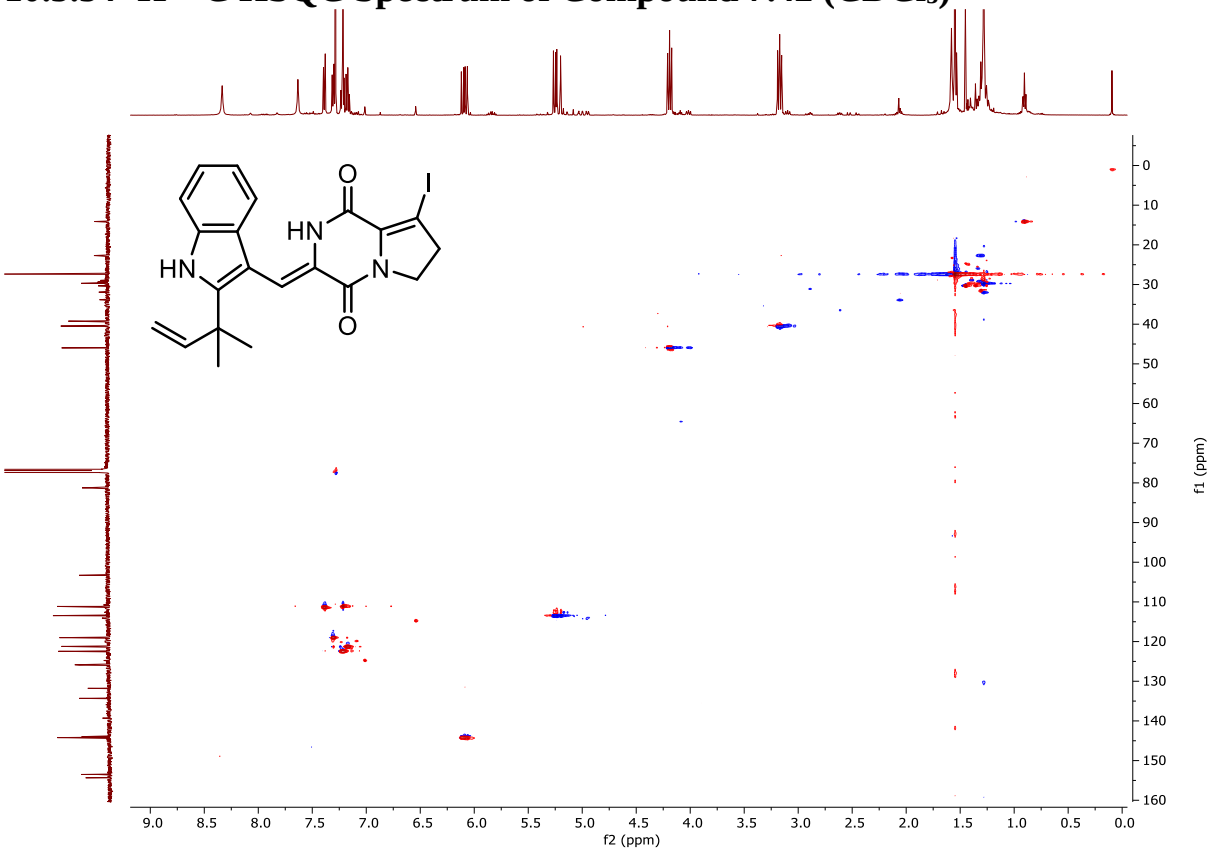

10.5.55 ^{1}H-^{13}C HMBC Spectrum of Compound 7.42 ($CDCl_3$)

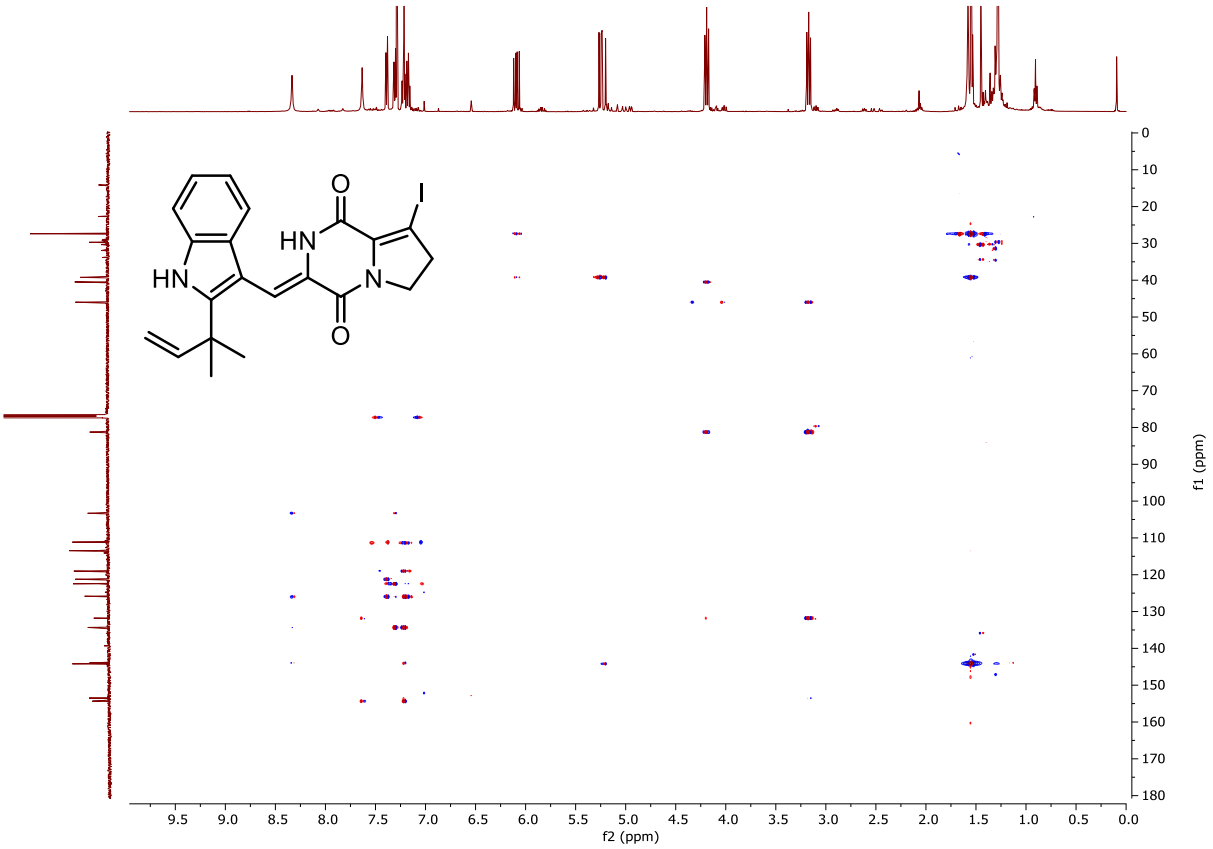

10.5.56 ^{13}C DEPT Spectrum of Compound 7.42 ($CDCl_3$)

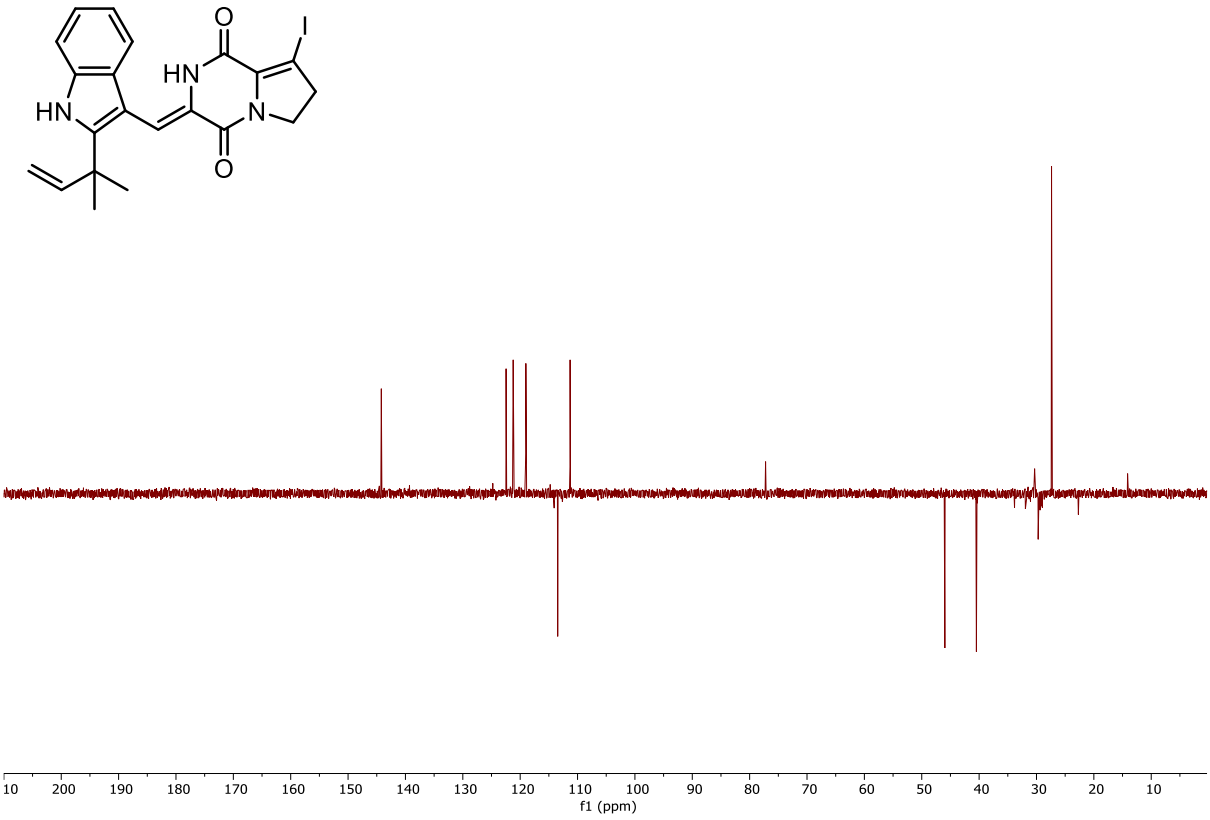

Chapter 11: X-ray Crystal Structures

11.1 X-ray Crystal Structure Data of compound (±)-1.24

AL21001

THE UNIVERSITY of EDINBURGH
Crystal Structure Service

Dr Gary S. Nichol
Crystallography Service Manager
Phone: +44 (0)131 650 4806
E-mail: g.s.nichol@ed.ac.uk

R_1=3.56%

Submitted by: **Helen Jones**

Solved by: **Gary S Nichol**

Submitted by: **None**

Compound HJ-6036 was provided as colourless crystals suitable for single crystal X-ray diffraction, yielding structure AL21001.

Crystal Data and Experimental

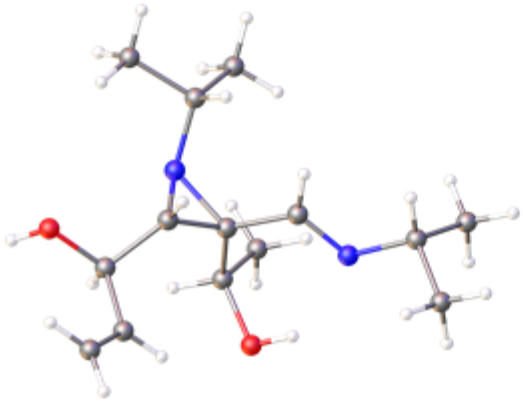

Compound	**AL21001**
Formula	$C_{14}H_{26}N_2O_2$
$D_{calc.}$/ g cm^{-3}	1.108
μ/mm^{-1}	0.074
Formula Weight	254.37
Colour	colourless
Shape	block
Size/mm^3	0.32×0.24×0.15
T/K	100.0
Crystal System	triclinic
Space Group	P-1
a/Å	8.2594(7)
b/Å	8.8832(8)
c/Å	11.3757(9)
α/°	76.581(3)
β/°	75.343(3)
γ/°	73.362(3)
V/Å^3	762.11(11)
Z	2
Z'	1
Wavelength/Å	0.71073
Radiation type	MoKα
Θ_{min}/°	2.429
Θ_{max}/°	33.168
Measured Refl's.	55392
Indep't Refl's	5689
Refl's I≥2 σ(I)	5167
R_{int}	0.0287
Parameters	267
Restraints	0
Largest Peak	0.593
Deepest Hole	-0.256
GooF	1.039
wR_2 (all data)	0.1008
wR_2	0.0980
R_1 (all data)	0.0391
R_1	0.0356

Experimental. Single colourless block crystals of **AL21001** recrystallised from a mixture of dichloromethane and 40-60 petroleum ether by slow evaporation. A suitable crystal with dimensions 0.32 × 0.24 × 0.15 mm^3 was selected and mounted on a MITIGEN holder in Paratone oil. on a Bruker D8 VENTURE diffractometer. The crystal was kept at a steady T = 100.0 K during data collection. The structure was solved with the ShelXT 2018/2 (Sheldrick, 2018) solution program using dual methods and by using Olex2 (Dolomanov, et al., 2009) as the graphical interface. The model was refined with ShelXL 2018/3 (Sheldrick, 2015) using full matrix least squares minimisation on F^2.

Crystal Data. $C_{14}H_{26}N_2O_2$, M_r = 254.37, triclinic, P-1 (No. 2), a = 8.2594(7) Å, b = 8.8832(8) Å, c = 11.3757(9) Å, α = 76.581(3)°, β = 75.343(3)°, γ = 73.362(3)°, V = 762.11(11) Å^3, T = 100.0 K, Z = 2, Z' = 1, μ(MoKα) = 0.074, 55392 reflections measured, 5689 unique (R_{int} = 0.0287) which were used in all calculations. The final wR_2 was 0.1008 (all data) and R_1 was 0.0356 (I≥2 σ(I)).

Structure Quality Indicators

Reflections:	d min (Mo) 2θ=66.3° 0.65	I/σ(I) 49.3	Rint 2.87%	Full 50.5° 98% to 66.3° 99.9
Refinement:	Shift 0.001	Max Peak 0.6	Min Peak -0.3	GooF 1.039

A colourless block-shaped crystal with dimensions 0.32 × 0.24 × 0.15 mm^3 was mounted on a MITIGEN holder in Paratone oil.. Data were collected using a Bruker D8 VENTURE diffractometer equipped with an Oxford Cryosystems Cryostream 800 low-temperature device operating at T = 100.0 K.

Data were measured using ϕ and ω scans using MoKα radiation. . The maximum resolution that was achieved was Θ = 33.168° (0.65 Å).

. The unit cell was refined using SAINT (Bruker, V8.40A, after 2013) on 9718 reflections, 18% of the observed reflections.

Data reduction, scaling and absorption corrections were performed using SAINT (Bruker, V8.40A, after 2013). The final completeness is 99.90 % out to 33.168° in Θ. A multi-scan absorption correction was performed using SADABS-2016/2 (Bruker, 2016/2) was used for absorption correction. wR_2(int) was 0.1226 before and 0.0428 after correction. The Ratio of minimum to maximum transmission is 0.9510. The λ/2 correction factor is Not present. . The absorption coefficient μ of this material is 0.074 mm^{-1} at this wavelength (λ = 0.71073Å) and the minimum and maximum transmissions are 0.710 and 0.747.

The structure was solved and the space group P-1 (# 2) determined by the ShelXT 2018/2 (Sheldrick, 2018) structure solution program using using dual methods and refined by full matrix least squares minimisation on F^2 using version 2018/3 of ShelXL 2018/3 (Sheldrick, 2015). All non-hydrogen atoms were refined anisotropically. Hydrogen atom positions were calculated geometrically and refined using the riding model.

_refine_special_details: H atoms were identified from a difference map and freely refined.

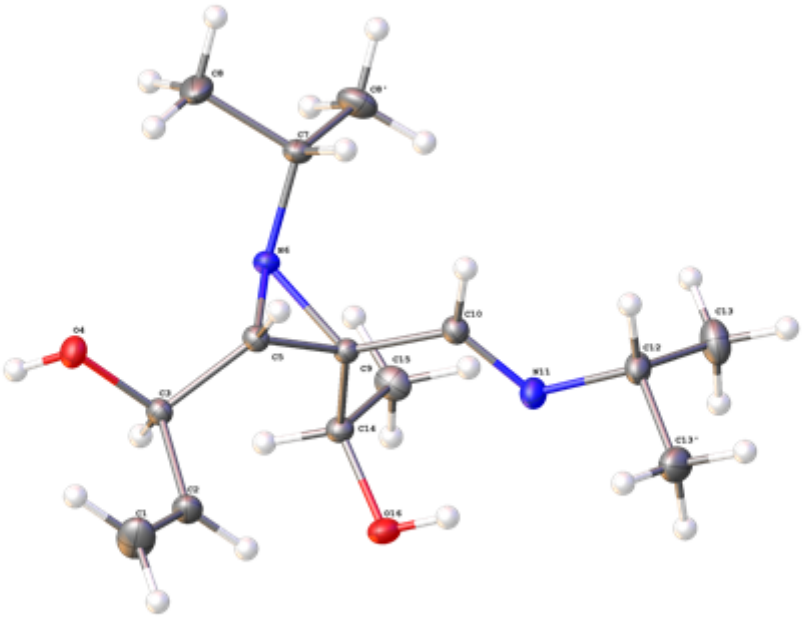

Figure 1: The molecular structure of AL21001. Displacement ellipsoids are at the 50% probability level.

11.2 X-ray Crystal Structure Data of (±)-Brevianamide Y (±)(4.4)

al20001x1

THE UNIVERSITY of EDINBURGH
Crystal Structure Service

Dr Gary S. Nichol
Crystallography Service Manager
Phone +44 (0)131 650 4806
E-mail g.s.nichol@ed.ac.uk

R_1=4.57%

Submitted by: **Helen Jones**

Solved by: **Gary S Nichol**

Submitted by: **None**

Compound Brevianamide Y was provided as colourless prism crystals suitable for single crystal X-ray diffraction, yielding structure AL20001x1. Some needle crystals, AL20001x2, were also present. These were found to have the same unit cell parameters as AL20001x1.

Crystal Data and Experimental

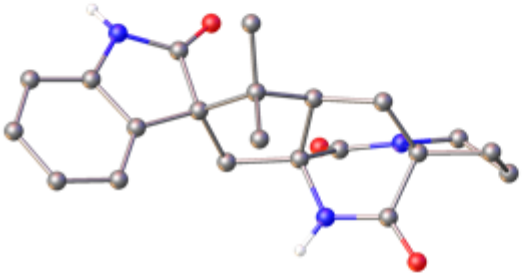

Experimental. Single colourless prism crystals of **al20001x1** recrystallised from a mixture of methanol and 40-60 petroleum ether by slow cooling. A suitable crystal with dimensions 0.30 × 0.24 × 0.08 mm^3 was selected and mounted on a MITIGEN holder in Paratone oil on a Rigaku Oxford Diffraction SuperNova diffractometer. The crystal was kept at a steady T = 119.99(10) K during data collection. The structure was solved with the ShelXT 2018/2 (Sheldrick, 2018) solution program using dual methods and by using Olex2 (Dolomanov et al., 2009) as the graphical interface. The model was refined with ShelXL 2018/3 (Sheldrick, 2015) using full matrix least squares minimisation on F^2.

Crystal Data. $C_{21}H_{23}N_3O_3$, M_r = 365.42, monoclinic, $I2/a$ (No. 15), a = 20.7355(2) Å, b = 7.34090(10) Å, c = 24.6076(3) Å, β = 108.2420(10)°, α = γ = 90°, V = 3557.45(8) Å^3, T = 119.99(10) K, Z = 8, Z' = 1, μ(Cu Kα) = 0.750, 34103 reflections measured, 3700 unique (R_{int} = 0.0555) which were used in all calculations. The final wR_2 was 0.1231 (all data) and R_1 was 0.0457 (I≥2 σ(I)).

Compound	**al20001x1**
Formula	$C_{21}H_{23}N_3O_3$
D_{calc}/ g cm^{-3}	1.365
μ/mm^{-1}	0.750
Formula Weight	365.42
Colour	colourless
Shape	prism
Size/mm^3	0.30×0.24×0.08
T/K	119.99(10)
Crystal System	monoclinic
Space Group	$I2/a$
a/Å	20.7355(2)
b/Å	7.34090(10)
c/Å	24.6076(3)
α°	90
β°	108.2420(10)
γ°	90
V/Å^3	3557.45(8)
Z	8
Z'	1
Wavelength/Å	1.54178
Radiation type	Cu Kα
Θ_{min}°	4.884
Θ_{max}°	75.948
Measured Refl's.	34103
Indep't Refl's	3700
Refl's I≥2 σ(I)	3613
R_{int}	0.0555
Parameters	254
Restraints	0
Largest Peak	0.342
Deepest Hole	-0.249
GooF	1.047
wR_2 (all data)	0.1231
wR_2	0.1225
R_1 (all data)	0.0463
R_1	0.0457

Structure Quality Indicators

Reflections:	d min (Cu)	0.79	I/σ(I)	29.4	Rint	5.55%	complete	100%
Refinement:	Shift	0.001	Max Peak	0.3	Min Peak	-0.2	GooF	1.047

A colourless prism-shaped crystal with dimensions 0.30 × 0.24 × 0.08 mm^3 was mounted on a MITIGEN holder in Paratone oil. Data were collected using a Rigaku Oxford Diffraction SuperNova diffractometer equipped with an Oxford Cryosystems Cryostream 700+ low-temperature device operating at T = 119.99(10) K.

Data were measured using ω scans using Cu Kα radiation. The diffraction pattern was indexed and the total number of runs and images was based on the strategy calculation from the program CrysAlisPro (Rigaku, V1.171.40.61a, 2019). The maximum resolution that was achieved was Θ = 75.948° (0.79 Å).

The diffraction pattern was indexed and the total number of runs and images was based on the strategy calculation from the program CrysAlisPro (Rigaku, V1.171.40.61a, 2019). The unit cell was refined using CrysAlisPro (Rigaku, V1.171.40.61a, 2019) on 27945 reflections, 82% of the observed reflections.

Data reduction, scaling and absorption corrections were performed using CrysAlisPro (Rigaku, V1.171.40.61a, 2019). The final completeness is 99.60 % out to 75.948° in Θ. A multi-scan absorption correction was performed using SADABS-2016/2 (Bruker, 2016/2) was used for absorption correction. wR_2(int) was 0.0984 before and 0.0819 after correction. The Ratio of minimum to maximum transmission is 0.8037. The $\lambda/2$ correction factor is Not present. . The absorption coefficient μ of this material is 0.750 mm^{-1} at this wavelength (λ = 1.54178Å) and the minimum and maximum transmissions are 0.606 and 0.754.

The structure was solved and the space group $I2/a$ (# 15) determined by the ShelXT 2018/2 (Sheldrick, 2018) structure solution program using using dual methods and refined by full matrix least squares minimisation on F^2 using version 2018/3 of ShelXL 2018/3 (Sheldrick, 2015). All non-hydrogen atoms were refined anisotropically. Hydrogen atom positions were calculated geometrically and refined using the riding model. Most hydrogen atom positions were calculated geometrically and refined using the riding model, but some hydrogen atoms were refined freely.

refine_special_details: N-bound H atoms were identified from a difference Fourier map and freely refined.

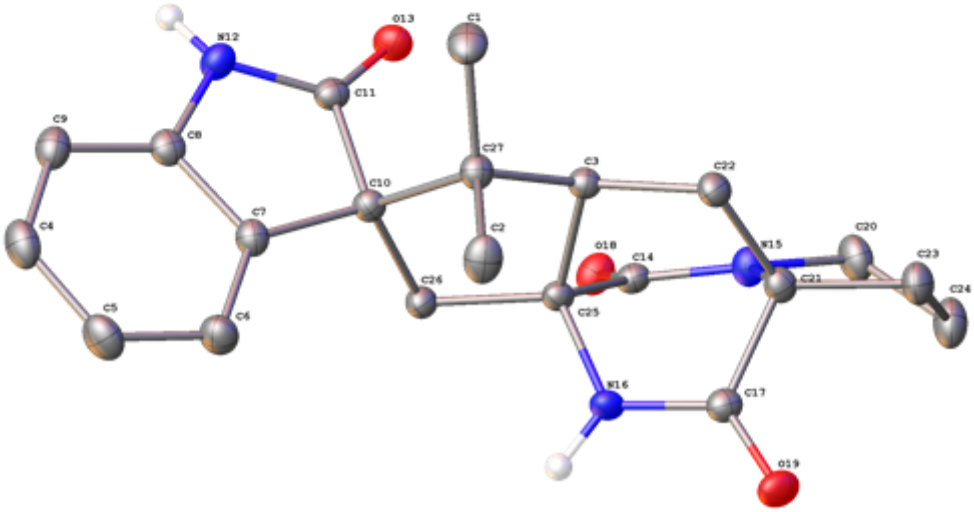

Figure 1: The molecular structure of AL20001x1. Displacement ellipsoids are at the 50% probability level and

Chapter 12: Appendix

12.1 Coaxial NMR Tube

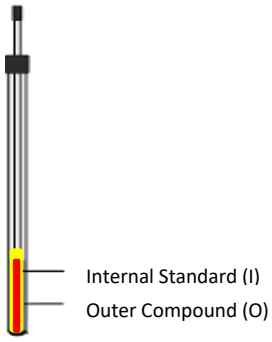

I volume = 0.05 mL

O volume = 0.45 mL

V_I/V_O = NMR active volume

(V_I/V_O) = 0.167-0.184 experimentally determined.

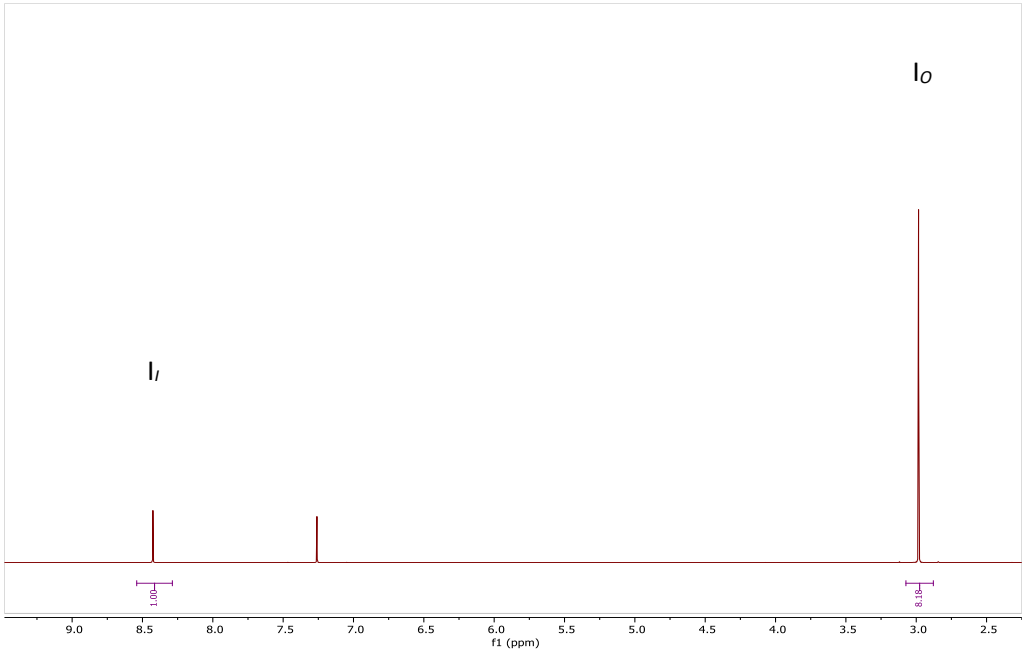

I_O = ^{1}H integration of compound

I_I = ^{1}H integration of internal standard

$n_O = I_O$/no. protons

$n_I = I_I$/no. protons

$x = n_I/n_O$

$V_I/V_O = x(M_O/M_I)$

$((V_I/V_O)M_I)/x = M_O$

12.2 Overview of Previous Total and Formal Syntheses of Brevianamide B.

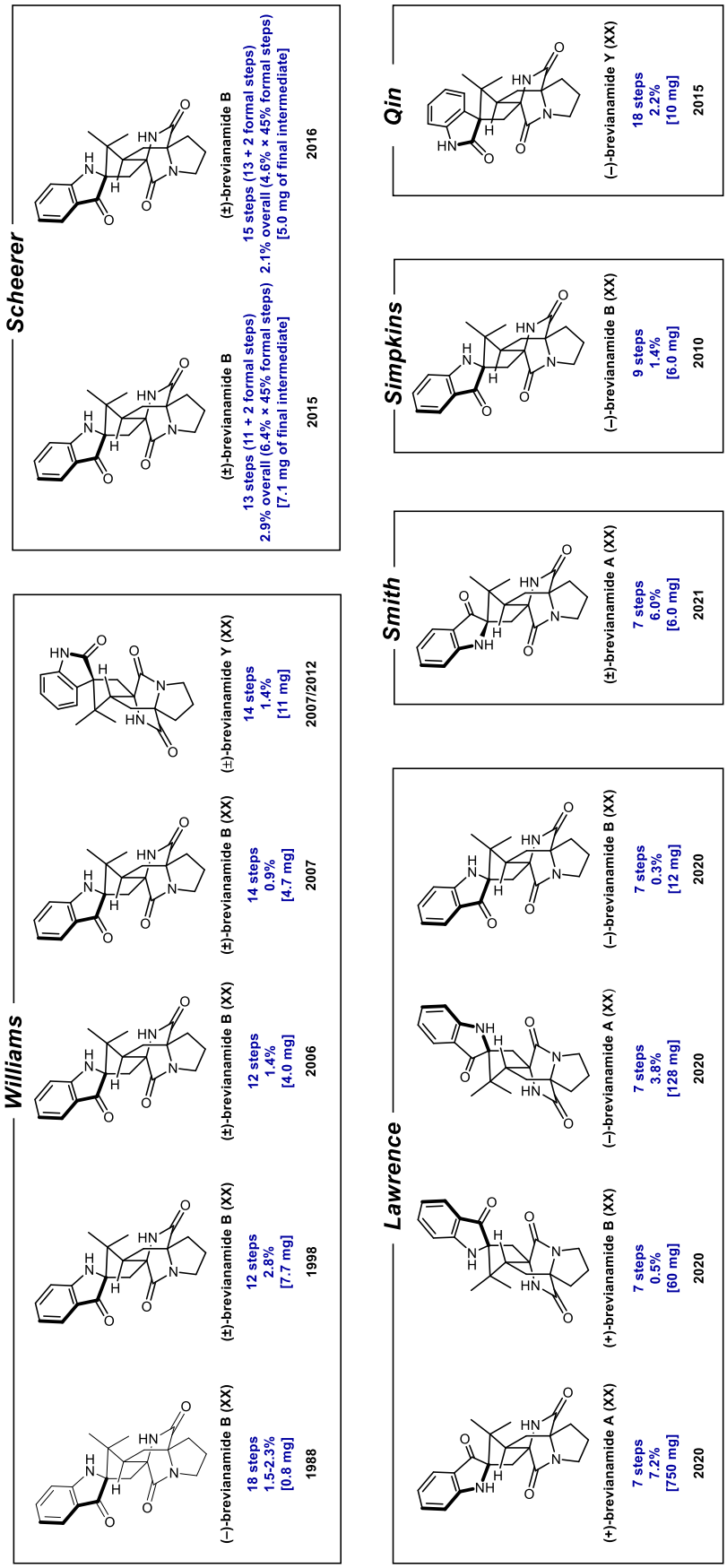

12.3 Williams' 1988 Total Synthesis of (−)-Brevianamide B

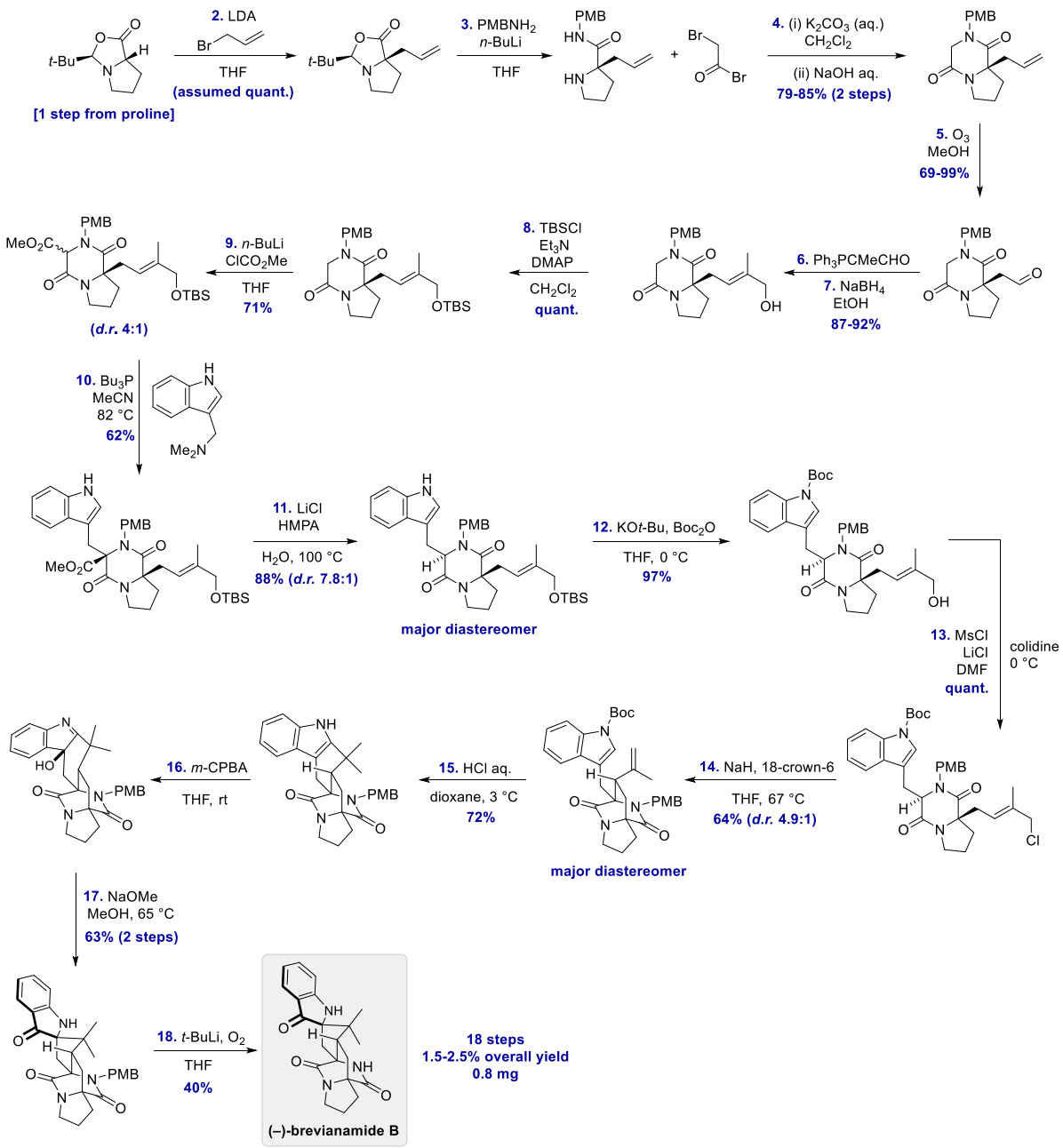

References:

1. Williams, R. M., Glinka, T. & Kwast, E. Facial selectivity of the intramolecular S_N2' cyclization: stereocontrolled total synthesis of brevianamide B. *J. Am. Chem. Soc.* **110,** 5927–5929 (1988).

2. Williams, R. M. & Kwast, E. Carbanion-mediated oxidative deprotection of non-enolizable benzylated amides. *Tetrahedron Lett.* **30,** 451–454 (1989)

3. Williams, R. M., Glinka, T., Kwast, E., Coffman, H. & Stille, J. K. Asymmetric, stereocontrolled total synthesis of (−)-brevianamide B. *J. Am. Chem. Soc.* **112,** 808–821 (1990).

12.4 Williams' 1998 Total Synthesis of (±)-Brevianamide B

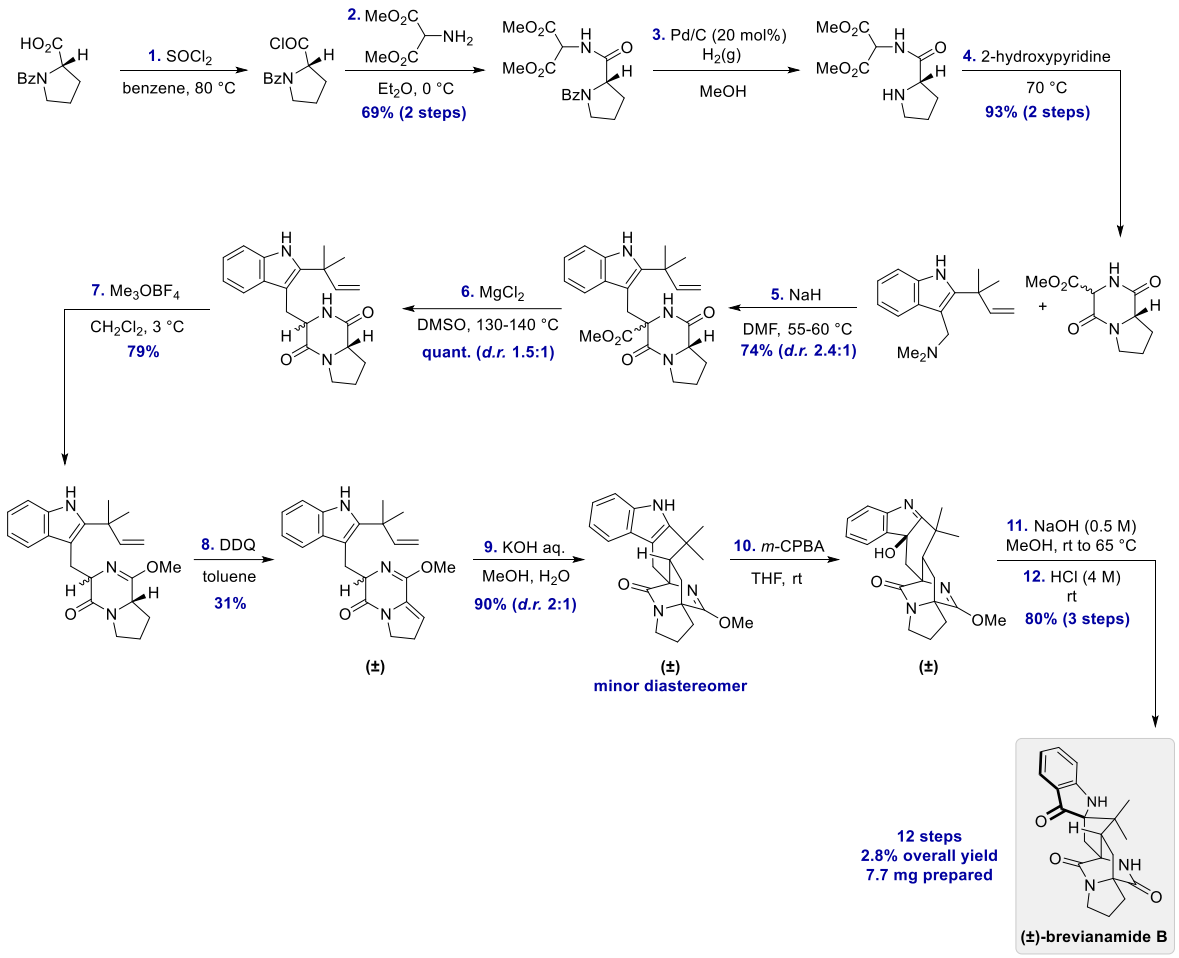

References:

1. Williams, R. M., Sanz-Cervera, J. F., Sancenón, F., Marco, J. A. & Halligan, K. Biomimetic Diels−Alder cyclizations for the construction of the brevianamide, paraherquamide sclerotamide, and VM55599 ring systems. *J. Am. Chem. Soc.* **120,** 1090–1091 (1998).

2. Williams, R. M., Sanz-Cervera, J. F., Sancenón, F., Marco, J. A. & Halligan, K. Biomimetic Diels–Alder cyclizations for the construction of the brevianamide, paraherquamide, sclerotamide, asperparaline and VM55599 ring systems. *Bioorg. Med. Chem.* **6,** 1233–1241 (1998).

3. Steps **1–6** taken from; Kametani, T., Kanaya, N. & Ihara, M. Studies on the syntheses of heterocyclic compounds. Part 876. The chiral total synthesis of brevianamide E and deoxybrevianamide E. *J. Chem. Soc. Perkin Trans. I* 959–963 (1981).

12.5 Williams' 2006 Total Synthesis of (±)-Brevianamide B

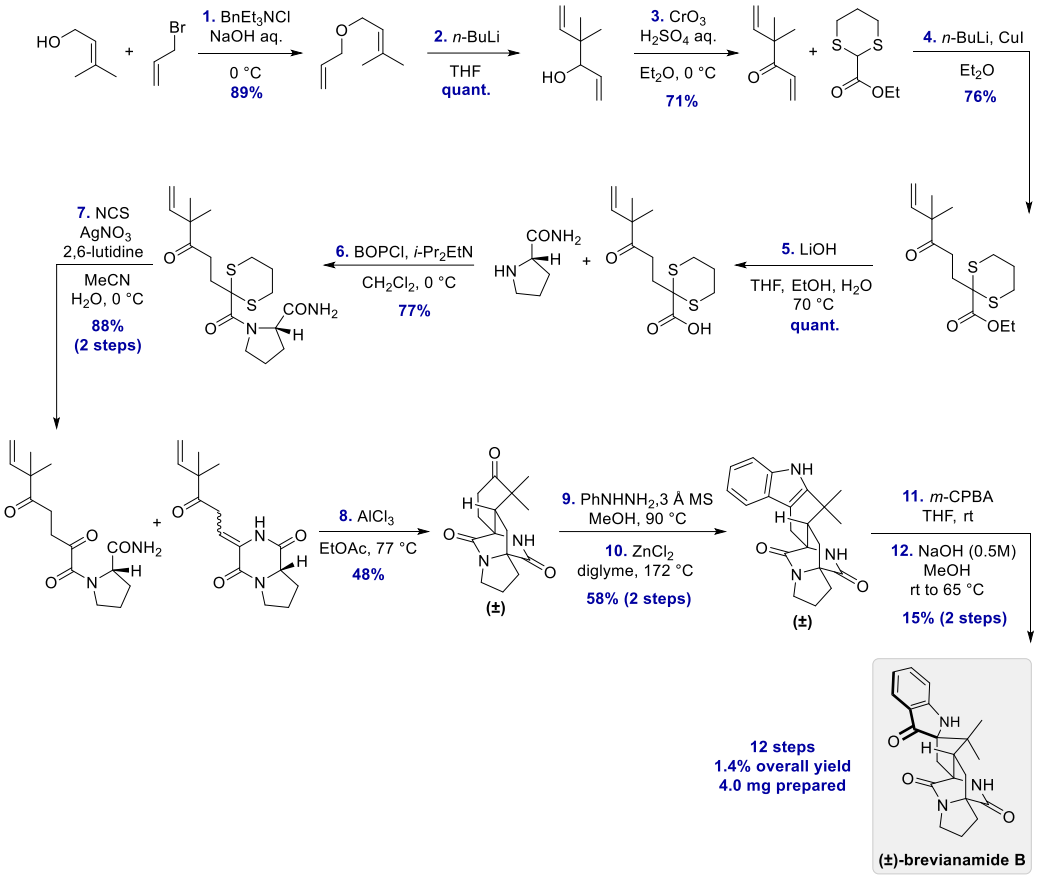

References:

1. Adams, L. A., Valente, M. W. N. & Williams, R. M. A concise synthesis of d,l-brevianamide B via a biomimetically-inspired IMDA construction. *Tetrahedron* **62,** 5195–5200 (2006).

2. Steps **1**–**3** taken from Dauben, W. G., Cogen, J. M., Ganzer, G. A. & Behar, V. Photochemistry of 1,5-hexadien-3-ones: Wavelength-dependent selectivity in intramolecular enone-olefin photoadditions. *J. Am. Chem. Soc.* **113,** 5817–5824 (1991).

12.6 Williams' 2007 Total Synthesis of (±)-Brevianamide B & (±)-Dehydrodeoxybreviaminde E

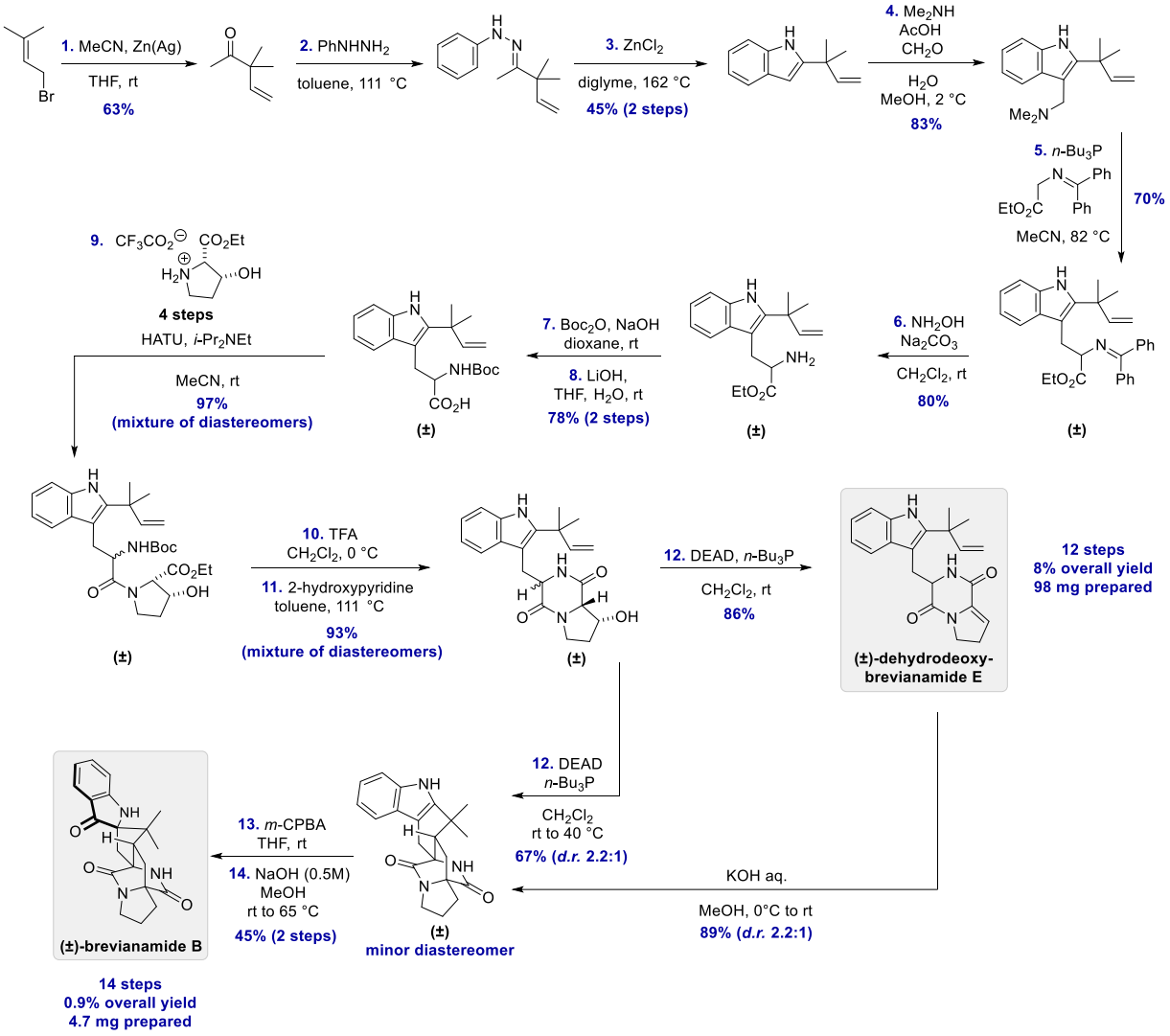

References:

1. Greshock, T. J. & Williams, R. M. Improved biomimetic total synthesis of d,l-stephacidin A. *Org. Lett.* **9,** 4255–4258 (2007).

2. Steps **1–4** taken from; Sanz-Cervera, J. F., Glinka, T. & Williams, R. M. Biosynthesis of brevianamides A and B: In search of the biosynthetic Diels-Alder construction. *Tetrahedron* **49,** 8471−8482 (1993). (which used $^{3}H_2CO$ in step **4**)

3. Steps **5–8** taken from; Stocking, E. M., Sanz-Cervera, J. F. & Williams, R. M. Total Synthesis of VM55599. Utilization of an Intramolecular Diels–Alder Cycloaddition of Potential Biogenetic Relevance. *J. Am. Chem. Soc.* **122,** 1675–1683 (2000).

12.7 Williams' 2007/2012 Total Synthesis of (−)-Brevianamide Y

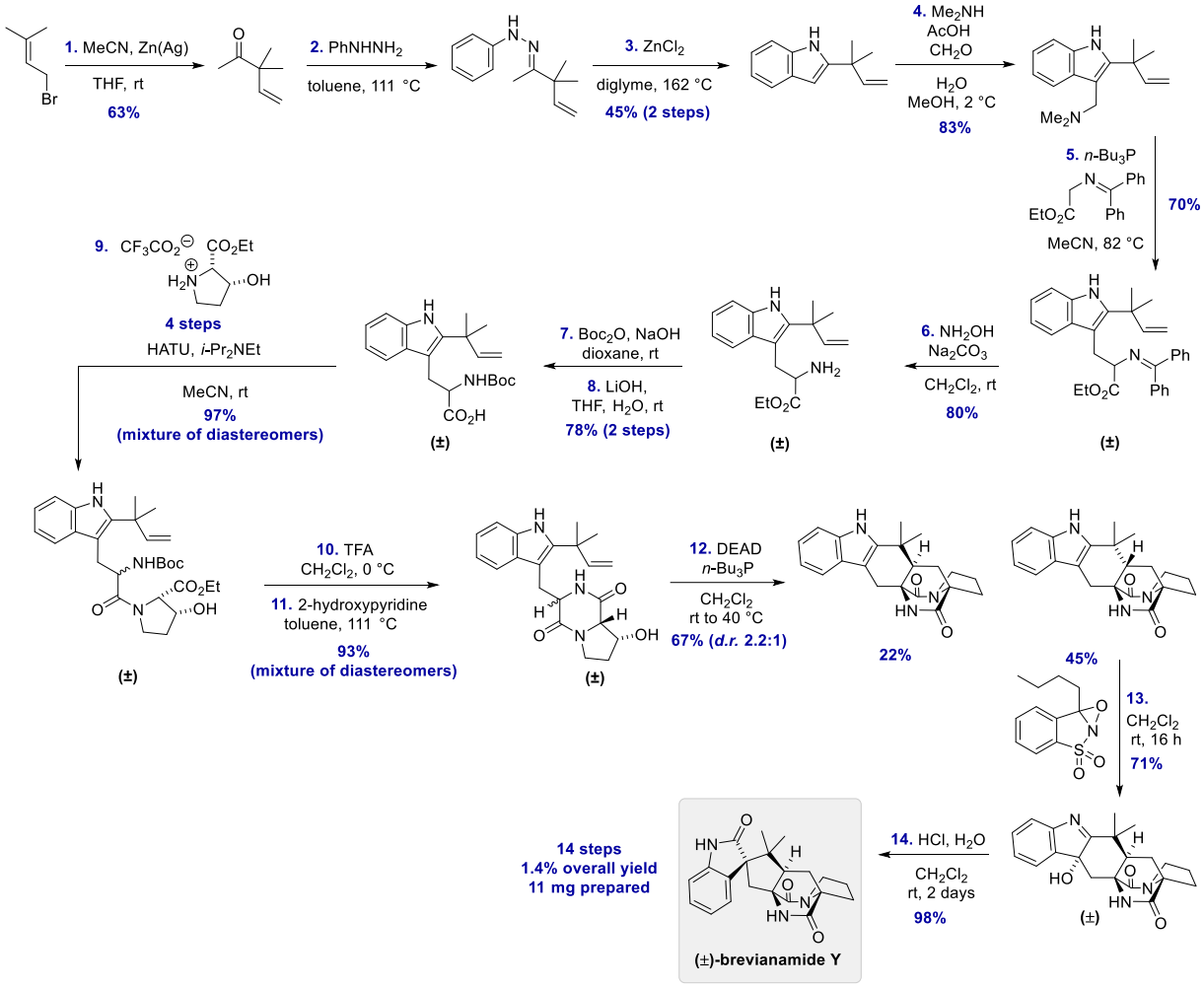

References:

1. Greshock, T. J. & Williams, R. M. Improved biomimetic total synthesis of d,l-stephacidin A. *Org. Lett.* **9,** 4255–4258 (2007).
2. Greshock, T. J. & Williams, R. M. Improved biomimetic total synthesis of d,l-stephacidin A. Correction Notice. *Org. Lett.* **14,** 6377–6378 (2012).

12.8 Simpkins' 2010 Total Synthesis of (−)-Brevianamide B

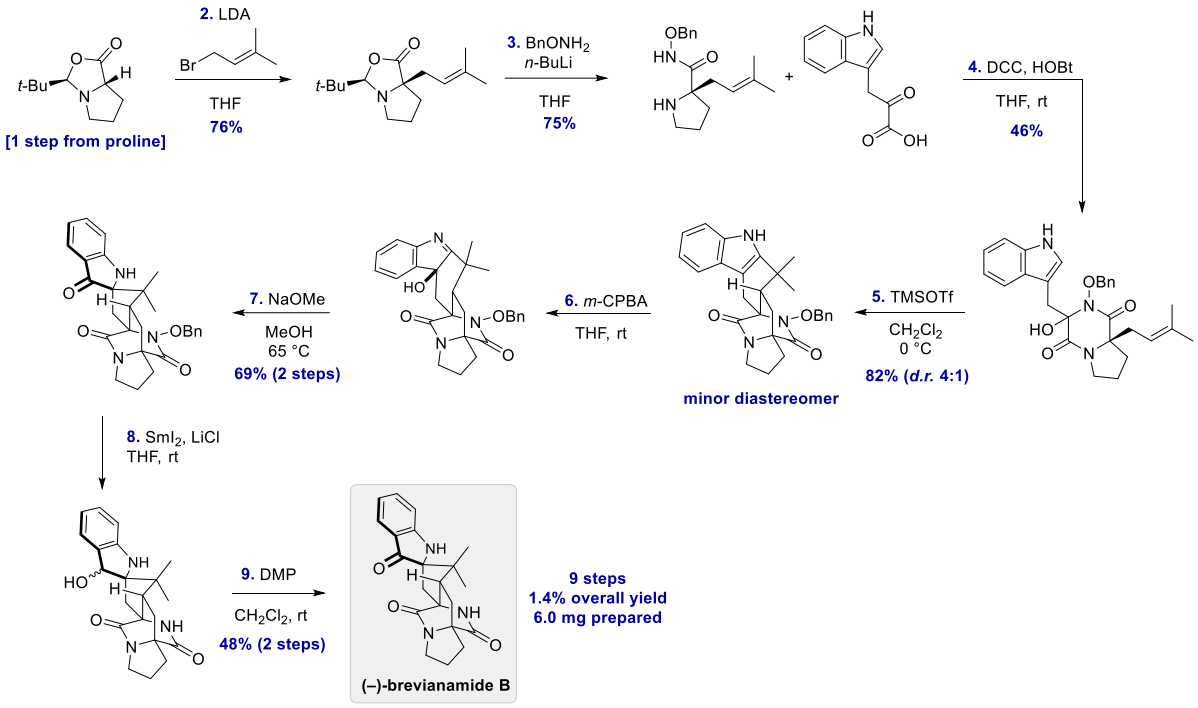

References:

1. Frebault, F. C., Simpkins, N. S., Fenwick, A. A concise enantioselective synthesis of ent-malbrancheamide B. *J. Am. Chem. Soc.* **131,** 4214–4215 (2009).

2. Frebault, F. C., Simpkins, N. S. A cationic cyclisation route to prenylated indole alkaloids: synthesis of malbrancheamide B and brevianamide B, and progress towards stephacidin A. *Tetrahedron* **66,** 6585–6596 (2010).

12.9 Qin's 2015 Total Synthesis of (−)-Brevianamide Y

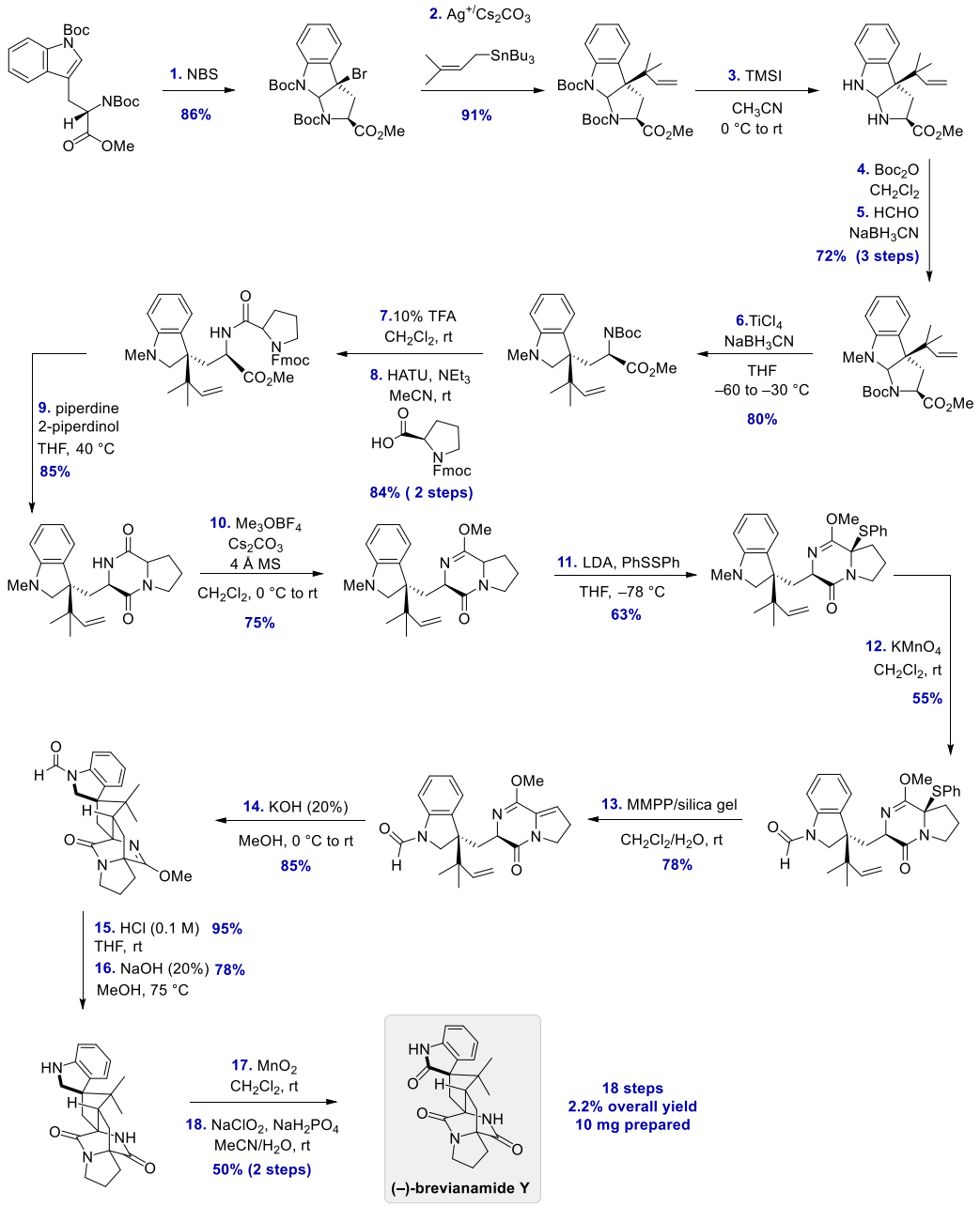

References:

1. Qin, W., Xiao, T., Zhang, D., Deng, L., Wang, Y., Qin, Y. Total synthesis of (–)-depyranoversicolamide B. *Chem. Commun.* **51,** 16143-13146 (2015).

12.10 Scheerer's 2016 Formal Synthesis of (±)-Brevianamide B

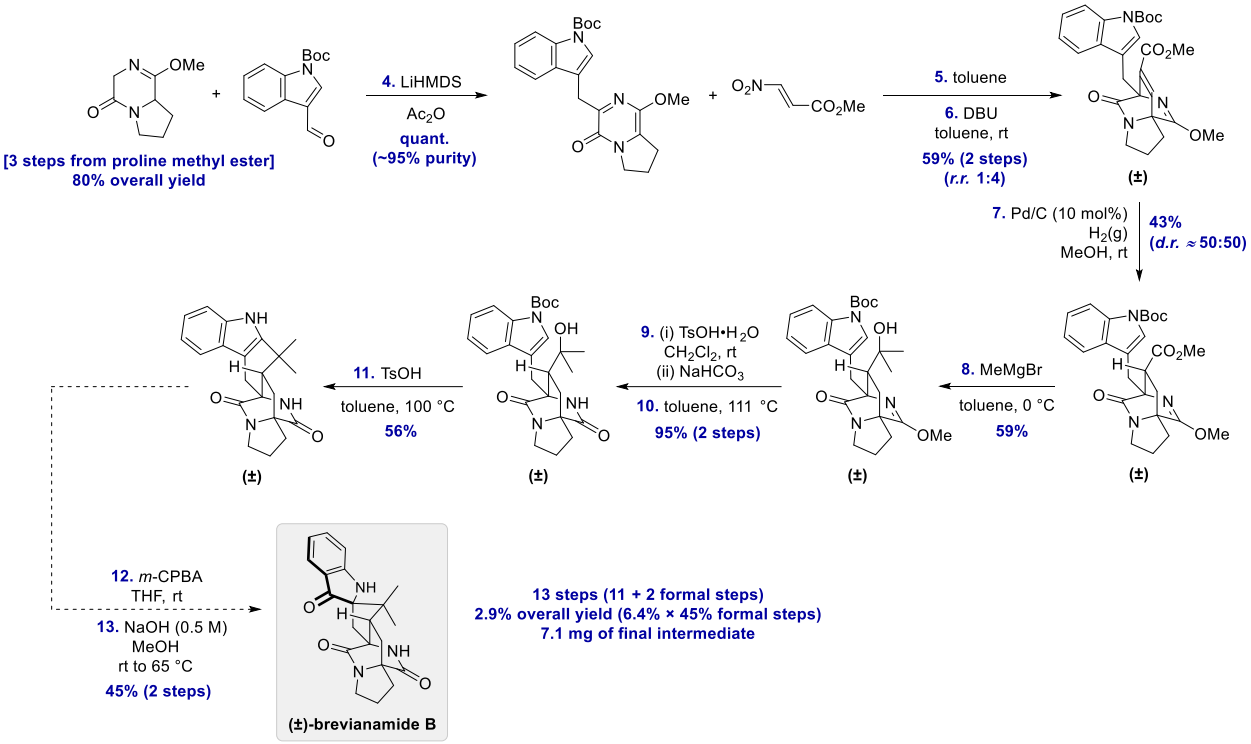

References:

1. Robins, J. G., Kim, K. J., Chinn, A. J., Woo, J. S. & Scheerer, J. R. Intermolecular Diels–Alder Cycloaddition for the Construction of Bicyclo[2.2.2]diazaoctane Structures: Formal Synthesis of Brevianamide B and Premalbrancheamide. *J. Org. Chem.* **81,** 2293–2301 (2016).

2. Steps **1-3** taken from; Laws, S. W. & Scheerer, J. R. Enantioselective Synthesis of (+)-Malbrancheamide B. *J. Org. Chem.* **78,** 2422–2429 (2013).

3. Steps **12-13** taken from; Greshock, T. J. & Williams, R. M. Improved biomimetic total synthesis of d,l-stephacidin A. *Org. Lett.* **9,** 4255–4258 (2007).

12.12 Scheerer's 2017 Total Synthesis of (±)-Brevianamide B

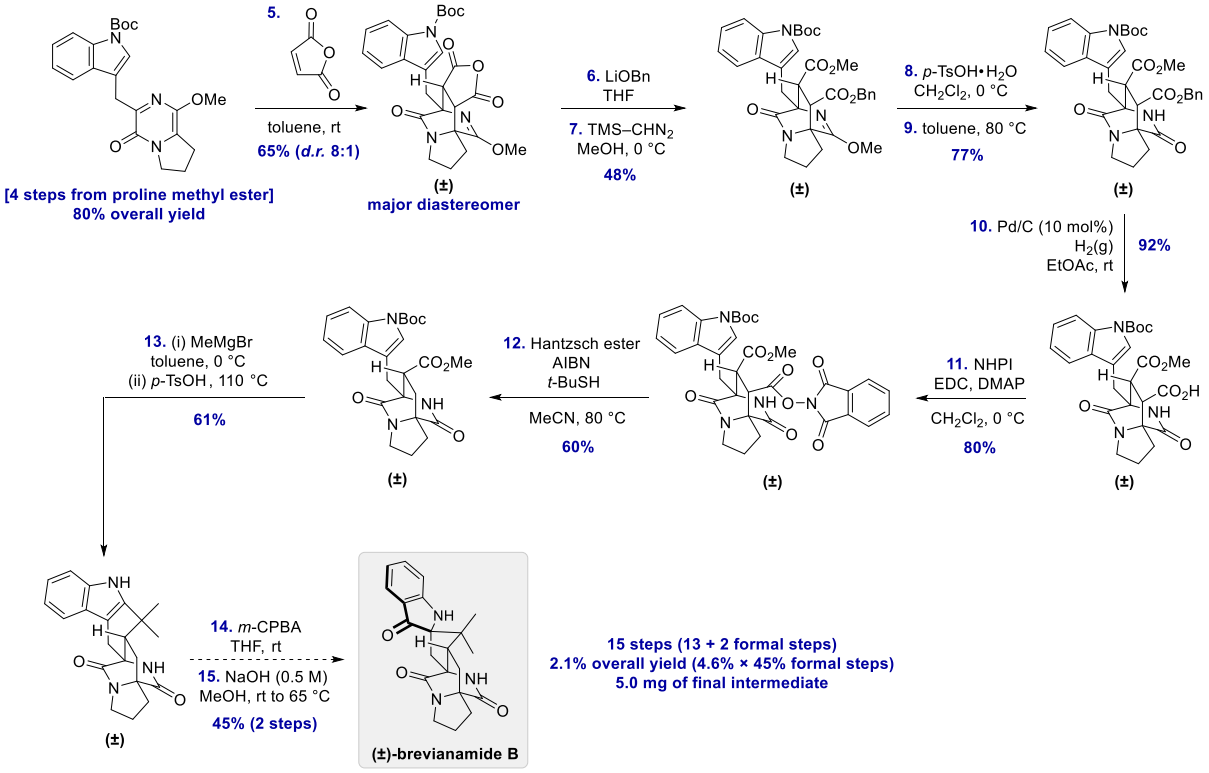

References:

1. Perkins, J. C., Wang, X., Pike, R. D. & Scheerer, J. R. Further investigation of the intermolecular Diels–Alder cycloaddition for the synthesis of bicyclo[2.2.2]diazaoctane alkaloids. *J. Org. Chem.* **82,** 13656–13662 (2017).

2. Steps **1-3** taken from; Laws, S. W. & Scheerer, J. R. Enantioselective Synthesis of (+)-Malbrancheamide B. *J. Org. Chem.* **78,** 2422–2429 (2013).

3. Step **4** taken from; Robins, J. G., Kim, K. J., Chinn, A. J., Woo, J. S. & Scheerer, J. R. Intermolecular Diels–Alder Cycloaddition for the Construction of Bicyclo[2.2.2]diazaoctane Structures: Formal Synthesis of Brevianamide B and Premalbrancheamide. *J. Org. Chem.* **81,** 2293–2301 (2016).

4. Steps **14-15** taken from; Greshock, T. J. & Williams, R. M. Improved biomimetic total synthesis of d,l-stephacidin A. *Org. Lett.* **9,** 4255–4258 (2007).

12.12 Lawrence's 2020 Total Synthesis of (+)/(−)-Brevianamide A and B

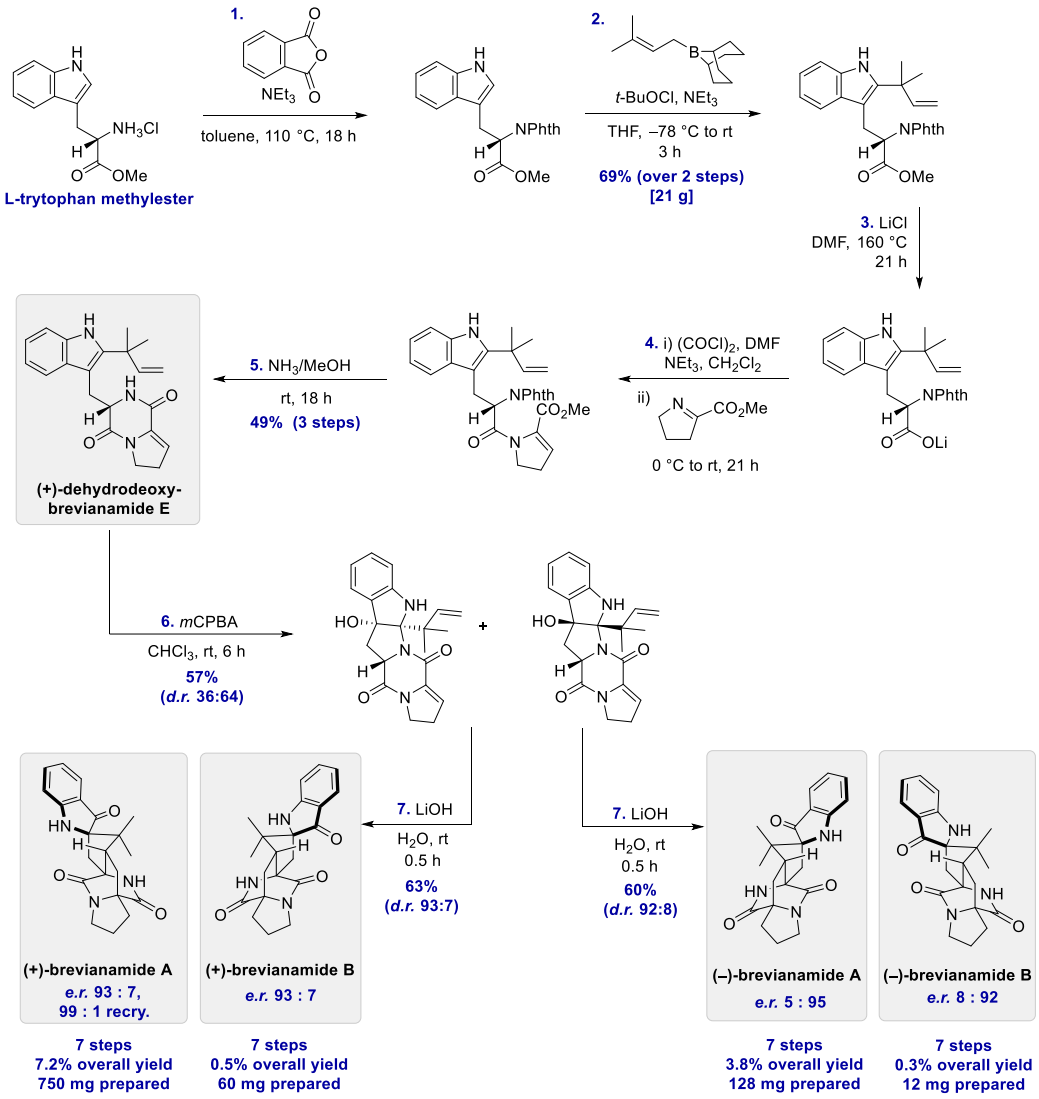

References:

1. Lawrence, A. L., Godfrey, R. C., Green, N. J., Nichol, G. S. Total synthesis of brevianamide A. *Nature Chem.* **12**, 615-620 (2020).

12.13 Smith's 2021 Total Synthesis of (±)-Brevianamide A

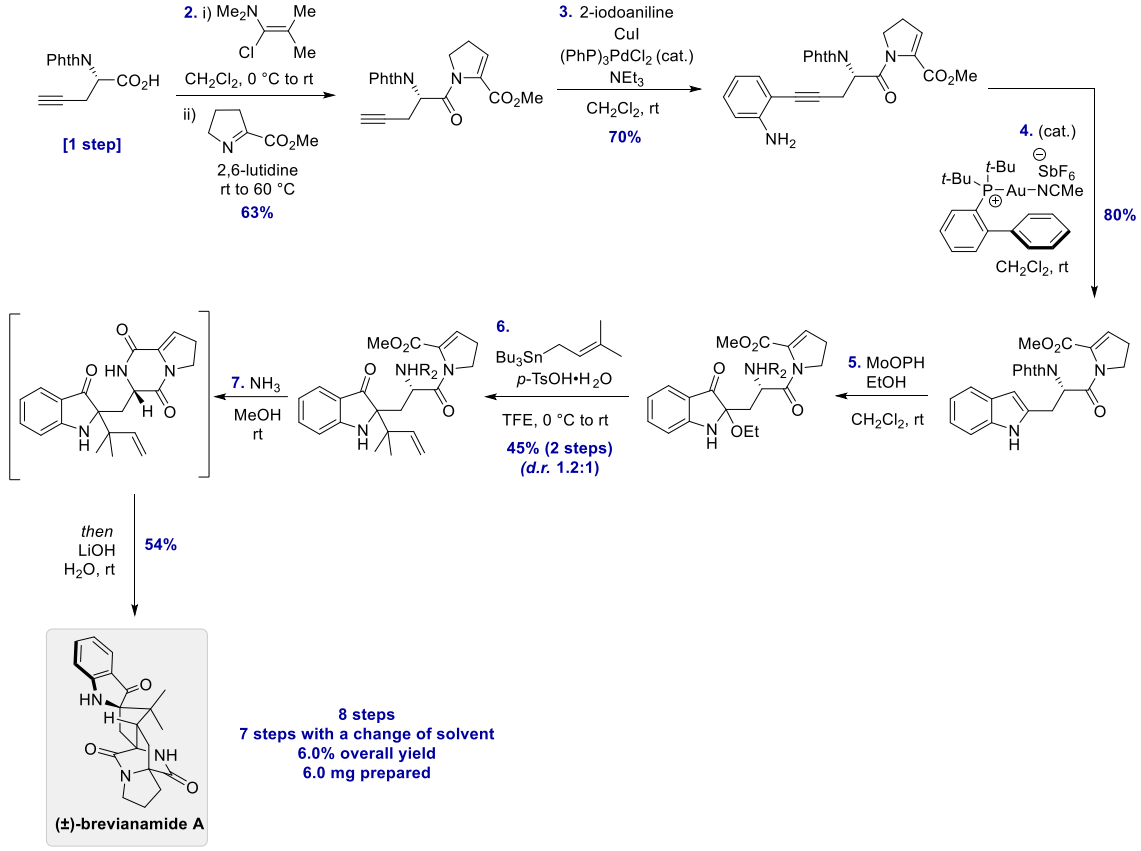

References:

1. Smith, M. W., Wu, F. A General Approach to 2,2-Disubstituted Indoxyls: Total Synthesis of Brevianamide A and Trigonoliimine C. *ChemRxiv* (2021). DOI:10.26434/chemrxiv.14750823.vl.

Chapter 13: References

1. Noyori, R. *et al.* Asymmetric Hydrogenation of β-Keto Carboxylic Esters. A Practical, Purely Chemical Access to β-Hydroxy Esters in High Enantiomeric Purity. *J. Am. Chem. Soc.* **109**, 5856–5858 (1987).

2. Keith, J. M., Larrow, J. F. & Jacobsen, E. N. Practical Considerations in Kinetic Resolution Reactions. *Adv. Synth. Catal.* **343**, 5–26 (2001).

3. Martin, V. S. *et al.* Kinetic Resolution of Racemic Allylic Alcohols by Enantioselective Epoxidation. A Route to Substances of Absolute Enantiomeric Purity. *J. Am. Chem. Soc.* **103**, 6237–6240 (1981).

4. Dong, X., Weickgenannt, A. & Oestreich, M. Broad-spectrum kinetic resolution of alcohols enabled by Cu-H-catalysed dehydrogenative coupling with hydrosilanes. *Nat. Commun.* **8**, 1–7 (2017).

5. Kamble, M. P. & Yadav, G. D. Kinetic Resolution of (R,S)-α-Tetralol by Immobilized Candida antarctica Lipase B: Comparison of Packed-Bed over Stirred-Tank Batch Bioreactor. *Ind. Eng. Chem. Res.* **56**, 1750–1757 (2017).

6. Noyori, R. *et al.* Stereoselective Hydrogenation via Dynamic Kinetic Resolution. *J. Am. Chem. Soc.* **111**, 9134–9135 (1989).

7. Mohr, J. T., Moore, J. T. & Stoltz, B. M. Enantioconvergent catalysis. *Beilstein J. Org. Chem.* **12**, 2038–2045 (2016).

8. Martín-Matute, B. & Bäckvall, J. E. Dynamic kinetic resolution catalyzed by enzymes and metals. *Curr. Opin. Chem. Biol.* **11**, 226–232 (2007).

9. Steinreiber, J., Faber, K. & Griengl, H. De-racemization of enantiomers versus de-epimerization of diastereomers-classification of dynamic kinetic asymmetric transformations (DYKAT). *Chem. - A Eur. J.* **14**, 8060–8072 (2008).

10. Allen, J. V. & Williams, J. M. J. Dynamic kinetic resolution with enzyme and palladium combinations. *Tetrahedron Lett.* **37**, 1859–1862 (1996).

11. Turner, N. J. Controlling chirality. *Curr. Opin. Biotechnol.* **14**, 401–406 (2003).

12. Dunsmore, C. J., Carr, R., Fleming, T. & Turner, N. J. A chemo-enzymatic route to enantiomerically pure cyclic tertiary amines. *J. Am. Chem. Soc.* **128**, 2224–2225 (2006).

13. Trost, B. M., Bunt, R. C., Lemoine, R. C. & Calkins, T. L. Dynamic kinetic asymmetric transformation of diene monoepoxides: A practical asymmetric synthesis of vinylglycinol, vigabatrin, and ethambutol. *J. Am. Chem. Soc.* **122**, 5968–5976 (2000).

14. Trost, B. M., Patterson, D. E. & Hembre, E. J. AAA in KAT/DYKAT processes: First- and second-generation asymmetric syntheses of (+)- and (-)-cyclophellitol. *Chem. - A Eur. J.* **7**, 3768–3775 (2001).

15. Trost, B. M., Patterson, D. E. & Hembre, E. J. Dynamic kinetic asymmetric transformations of conduritol B tetracarboxylates: An asymmetric synthesis of D-myo-inositol 1,4,5- trisphosphate [4]. *J. Am. Chem. Soc.* **121**, 10834–10835 (1999).

16. Pedragosa-Moreau, S., Archelas, A. & Furstoss, R. Microbiological Transformations. 28. Enantiocomplementary Epoxide Hydrolyses as a Preparative Access to Both Enantiomers of Styrene Oxide. *J. Org. Chem.* **58**, 5533–5536 (1993).

17. Alickmann, D., Fröhlich, R. & Würthwein, E. U. Base-Induced Heterochiral Dimerization of an Oxiranyl Carbaldimine: Stereoselective Synthesis of a Highly Functionalized Aziridine. *Org. Lett.* **3**, 1527–1530 (2001).

18. Harrison-Marchand, A. & Maddaluno, J. Chapter 10: Advances in the Chemistry of Chiral Lithium Amides. in *Lithium Compounds in Organic Synthesis* 297–328 (2014).

19. Cox, P. J. & Simpkins, N. S. Asymmetric synthesis using homochiral lithium amide bases. *Tetrahedron:*

Asymmetry **2**, 1–26 (1991).

20. Shoji, M. *et al.* Different Reaction Modes for the Oxidative Dimerization of Epoxyquinols and Epoxyquinones. Importance of Intermolecular Hydrogen-Bonding. *J. Org. Chem.* **69**, 1548–1556 (2004).

21. Shoji, M. *et al.* Total synthesis of epoxyquinols A, B, and C and epoxytwinol A and the reactivity of a 2H-pyran derivative as the diene component in the Diels-Alder reaction. *J. Org. Chem.* **70**, 79–91 (2005).

22. Corey, E. J. Catalytic enantioselective Diels-Alder reactions: Methods, mechanistic fundamentals, pathways, and applications. *Angew. Chemie - Int. Ed.* **41**, 1650–1667 (2002).

23. Alder, A. C. L. D. *et al.* Scheme 1 Department of Organic and Molecular Inorganic Chemistry , Uni V ersity of Groningen Re V ised Manuscript Recei V ed March 16 , 1998 organic reactions . 1 Apart from the obvious economic and effects on many organic transformations . 3 In the field. **7863**, 4238–4239 (1998).

24. Corey, E. J., Shibata, T. & Lee, T. W. Asymmetric diels-alder reactions catalyzed by a triflic acid activated chiral oxazaborolidine. *J. Am. Chem. Soc.* **124**, 3808–3809 (2002).

25. Evans, D., Miller, S., Lectka, T. & von Matt, P. Chiral bis (oxazoline) copper (II) complexes as lewis acid catalysts for the enantioselective Diels-Alder reaction. *J. Am. Chem. Soc.* **121**, 7559–7573 (1999).

26. Sequin, U. & Ceroni, M. Determination of the Relative Configurations in the Side Chains of the Antibiotics Hedamycin and Pluramycin. *Helv. Chim. Acta* **65**, 302–316 (1982).

27. Yoshizawa, R. & Inukai, T. BULLETIN OF THE CHEMICAL SOCIETY OF JAPAN Reactions Acid 1a) of Characterization and Some Ryo YOSHIZAWA and Takashi INUKAI1b) The Central Chisso Corporation , Yokohama acid was prepared from dicrotonyl peroxide by alkaline cleavage and isolated for the . **42**, 3238–3242 (1969).

28. U. Folli, R. Benassi, L. S. and F. T. No Title. *Gazz. Chim. Ital.* **120**, 89–97 (1990).

29. Payne, G. B. & Williams, P. H. Reactions of Hydrogen Peroxide. VI. Alkaline Epoxidation of Acrylonitrile. *J. Org. Chem.* **26**, 651–659 (1961).

30. Glabe, A. R., Sturgeon, K. L., Ghizzoni, S. B., Musker, W. K. & Takahashi, J. N. Novel functionalized acylphosphonates as phosphonoformate analogs. *J. Org. Chem.* **61**, 7212–7216 (1996).

31. Kato, K., Ono, M. & Akita, H. New total synthesis of (^)-, (2)- and (1)-chuangxinmycins. *Tetrahedron* **57**, 10055–10062 (2001).

32. Bedke, D. K. *et al.* Relative stereochemistry determination and synthesis of the major chlorosulfolipid from Ochromonas danica. *J. Am. Chem. Soc.* **131**, 7570–7572 (2009).

33. Harris, R. N., Sundararaman, P. & Djerassi, C. Optical Rotatory Dispersion Studies. 135. Synthesis and Chiroptical Properties of (S)- and (R)-(3-2H1)-2,2-Dimethylcyclobutanone. Evidence for Conformational Effects in Substituted Cyclobutanones. *J. Am. Chem. Soc.* **105**, 2408–2413 (1983).

34. Ley, S. V & Cox, L. R. 1,5-Asymmetric induction of chirality: Highly diastereoselective synthesis of homoallylic tertiary alcohols by the Lewis acid-mediated addition of allylstannanes into ketones in the side-chain of π-allyltricarbonyliron lactone complexes. *J. Chem. Soc. - Perkin Trans. 1* **1**, 3315–3325 (1997).

35. Mori, K., Osada, K. & Amaike, M. Mammalian blood odorant and chirality: synthesis and sensory evaluation by humans and mice of the racemate and enantiomers of trans-4,5-epoxy-(E)-2-decenal. *Tetrahedron Asymmetry* **26**, 861–867 (2015).

36. Ley, S. V *et al.* 1,5-Asymmetric induction of chirality: highly diastereoselective addition reactions of organoaluminium reagents into ketone groups in the side-chain of π-allyltricarbonyliron lactone complexes. *J. Chem. Soc., Perkin Trans. 1* 3299–3314 (1997). doi:10.1039/a704481j

37. Zhao, G. L., Ibrahem, I., Sundén, H. & Córdova, A. Amine-catalyzed asymmetric epoxidation of α,β-unsaturated aldehydes. *Adv. Synth. Catal.* **349**, 1210–1224 (2007).

38. Davis, R. L., Jensen, K. L., Gschwend, B. & Jørgensen, K. A. On the mechanism of the organocatalytic asymmetric epoxidation of α,β-unsaturated aldehydes. *Chem. - A Eur. J.* **20**, 64–67 (2014).

39. Weast, R. C. & Grasselli, J. G. Handbook of Data on Organic Compounds: Supplement. *CRC Press* (1989).

40. Olah, G. A., Vankar, Y. D. & Arvanaghi, M. Synthetic Methods and Reactions; 77. Dimethyl Sulfoxide/chlorosulfonyl Isocyanate: An Extremely Mild Reagent for Oxidation of Alcohols to Carbonyl Compounds. *Synthesis (Stuttg).* 141–142 (1980).

41. Wright, P. & Abbot, J. The oxidation of cinnamaldehyde with alkaline hydrogen peroxide. *Int. J. Chem. Kinet.* **25**, 901–911 (1993).

42. Andrus, M. B. & Poehlein, B. W. Epoxidation of olefins with peracid at low temperature with copper catalysis. *Tetrahedron Lett.* **41**, 1013–1014 (2000).

43. Payne, G. B. Epoxidation of Cinnamaldehyde by Alkaline tert-Butyl Hydroperoxide. *J. Org. Chem.* **25**, 275–276 (1960).

44. Miyashita, M., Suzuki, T. & Yoshikoshi, A. Fluoride-promoted Epoxidation of α,β-unsaturated compounds. *Chem. Lett.* **16**, 285–288 (1987).

45. Aldous, D. J. *et al.* The dihydrofuran template approach to furofuran synthesis. *Org. Biomol. Chem.* **4**, 2912–2927 (2006).

46. Mordini, A., Ben Rayana, E., Margot, C. & Schlosser, M. Facile isomerization of oxiranes to allyl alcohols by mixed metal bases. *Tetrahedron* **46**, 2401–2410 (1990).

47. Whitesell, J. K. & Felman, S. W. Asymmetric Induction. 3. Enantioselective Deprotonation by Chiral Lithium Amide Bases. *J. Org. Chem.* **45**, 755–756 (1980).

48. Duhamel, L. & Plaquevent, J. C. Deracemization by enantioselective protonation IV an improved method for the enantiomeric enrichment of α-aminoacids using metalation by means of chiral amides. *Tetrahedron Lett.* **21**, 2521–2524 (1980).

49. O'Brien, P. Recent advances in asymmetric synthesis using chiral lithium amide bases. *J. Chem. Soc. - Perkin Trans. 1* 1439–1457 (1998). doi:10.1039/a705961e

50. Hodgson, D. M., Buxton, T. J., Cameron, I. D., Gras, E. & Kirton, E. H. M. Enantioselective synthesis of epoxides by alpha-deprotonation--electrophile trapping of achiral epoxides. *Org. Biomol. Chem.* **1**, 4293–301 (2003).

51. Cain, C. M., Cousins, R. P. C., Coumbarides, G. & Simpkins, N. S. Asymmetric deprotonation of prochiral ketones using chiral lithium amide bases. *Tetrahedron* **46**, 523–544 (1990).

52. Aoki, K. & Koga, K. Enantioselective deprotonation of 4-tert-butylcyclohexanone by fluorine-containing chiral lithium amides derived from α-phenethylamine. *Tetrahedron Lett.* **38**, 2505–2506 (1997).

53. Bambridge, K., Begley, M. J. & Simpkins, N. S. Simple synthesis of a C2 symmetric vicinal diamine: Highly diastereoselective Grignard addition to a chiral bis-imine. *Tetrahedron Lett.* **35**, 3391–3394 (1994).

54. Koga, K. *et al.* Stereoselective Reactions. XXII. Design and Synthesis of Chiral Chelated Lithium Amides for Enantioselective Reactions. *Chem. Pharm. Bull.* **42**, 690–693 (1994).

55. O'Brien, P. & Poumellec, P. Chiral base-mediated rearrangement of meso-cyclohexene oxides to allylic alcohols. *Tetrahedron Lett.* **37**, 8057–8058 (1996).

56. Asami, M. An Asymmetric Transformation of Cyclohexene Oxide To (S)-2-Cyclohexen-1-Ol By Chiral Lithium Amides. *Chem. Lett.* **13**, 829–832 (1984).

57. Asami, M. Asymmetric trasformation of symmetrical epoxides to allylic alcohols by lithium (S)-2-(N,N-disubstituted aminomethyl)pyrrolidide. *Bull. Chem. Soc. Jpn.* **63**, 721–727 (1990).

58. Asami, M. & Kirihara, H. An Asymmetric Transformation of Symmetrical Epoxides to Both Enantiomers of Allylic Alcohols by Chiral Lithium Amides. *Chem. Lett.* 389–392 (1987).

59. Aoki, K. & Koga, K. Stereselective Reactions. XXXII. Enantioselective Deprotonation of 4-tert-Butylcyclohexanone by Fluorine-Containing Chiral Lithium Amides Derived from 1-Phenylethylamine and 1-

(1-Naphthyl)ethylamine. *Chem. Pharm. Bull.* **48**, 571–574 (2000).

60. Abe, H., Tsujino, T., Araki, K., Takeuchi, Y. & Harayama, T. Enantioselective construction of bicyclo[3.1.0]hexane derivativesthrough asymmetric deprotonation ofmeso-cyclic ketones. *Tetrahedron Asymmetry* **13**, 1519–1527 (2002).

61. Koga, K., Muraoka, M. & Kawasaki, H. ENANTIOSELECTIVE ALDOL REACTION MEDIATED BY CHIRAL LITHIUM AMIDE BASES. *Tetrahedron Lett.* **29**, 337–338 (1988).

62. Bunn, B. J., Simpkins, N. S., Spavold, Z. & Crimmin, M. J. The effect of added salts on enantioselective transformations of cyclic ketones by chiral lithium amide bases. *J. Chem. Soc. Perkin Trans. 1* 3113–3116 (1993). doi:10.1039/p19930003113

63. Murakata, M., Nakajima, M. & Koga, K. Enantioselective alkylation at the α-position of cyclic ketones using a chiral lithium amide as a base in the presence of lithium bromide. *J. Chem. Soc. Chem. Commun.* **2580**, 1657–1658 (1990).

64. Karasawa, T., Oriez, R., Kumagai, N. & Shibasaki, M. anti-Selective Catalytic Asymmetric Nitroaldol Reaction of α-Keto Esters: Intriguing Solvent Effect, Flow Reaction, and Synthesis of Active Pharmaceutical Ingredients. *J. Am. Chem. Soc.* 12290–12295 (2018).

65. Sugasawa, K., Shindo, M., Noguchi, H. & Koga, K. Solution structures of a monodentate chiral lithium amide in the presence of lithium halide. *Tetrahedron Lett.* **37**, 7377–7380 (1996).

66. Zhou, M. *et al.* Highly enantioselective synthesis of chiral cyclic allylic amines via RH-catalyzed asymmetric hydrogenation. *Org. Lett.* **16**, 3484–3487 (2014).

67. Bhosale, R. S., Bhosale, S. V., Bhosale, S. V., Wang, T. & Zubaidha, P. K. Iodine-catalyzed synthesis of β-keto enol ethers. *Tetrahedron Lett.* **45**, 7187–7188 (2004).

68. Kwon, M. S., Sim, S. H., Chung, Y. K. & Lee, E. Synthetic studies on soft coral norcembranolides: Total synthesis of (+)-10-epigyrosanolide e. *Tetrahedron* **67**, 10179–10185 (2011).

69. Feldman, K. S., Vidulova, D. B. & Karatjas, A. G. Extending Pummerer reaction chemistry. Development of a strategy for the regio- and stereoselective oxidative cyclization of 3-(ω-nucleophile)- tethered indoles. *J. Org. Chem.* **70**, 6429–6440 (2005).

70. Corey, E. J. & Seebach, D. Synthesis of 1,n-Dicarbonyl Derivates Using Carbanions from 1,3-Dithianes. *Angew. Chem. internat. Ed.* **4**, 1077–1078 (1965).

71. Corey, E. J. & Seebach, D. Carbanions of 1,3-Dithianes. Reagents for C -C Bond Formation by Nucleophilic Displacement and Carbonyl Addition. *Angew. Chem. internat. Ed.* **4**, 1075–1077 (1965).

72. Bernasconi, C. F. & Kittredge, I. W. Carbanion stabilization by adjacent sulfur: Polarizability, resonance, or negative hyperconjugation? Experimental distinction based on intrinsic rate constants of proton transfer from (phenylthio)nitromethane and I-nitro-2-phenylethane. *Chemtracts* **12**, 492–493 (1999).

73. Wright, P. M. & Myers, A. G. Methodological advances permit the stereocontrolled construction of diverse fully synthetic tetracyclines containing an all-carbon quaternary center at position C5a. *Tetrahedron* **67**, 9853–9869 (2011).

74. Sikorski, W. H. & Reich, H. J. The regioselectivity of addition of organolithium reagents to enones and enals: The role of HMPA. *J. Am. Chem. Soc.* **123**, 6527–6535 (2001).

75. Dykstram, R. R. Hexamethylphosphoric Triamide. *Encycl. Dict. Polym.* 366–366 (2011). doi:10.1007/978-1-4419-6247-8_5935

76. Brown, C. A. & Yamaichi, A. Induced conjugate addition of simple 2-lithio-1,3-dithians to cyclic αβ-unsaturated ketones. *J. Chem. Soc. Chem. Commun.* 100–101 (1979). doi:10.1039/C39790000100

77. Iwahara, J., Esadze, A. & Zandarashvili, L. Physicochemical properties of ion pairs of biological macromolecules. *Biomolecules* **5**, 2435–2463 (2015).

78. Schlosser, M. *Organometallics in Synthesis*. (Wiley, 1994).

79. Vale, J. R. *et al.* Pot-Economy Autooxidative Condensation of 2-Aryl-2-lithio-1,3-dithianes. *J. Org. Chem.* **83**, 1948–1958 (2018).

80. Cerè, V. *et al.* Preparation of 2-Zincio-1,3-Dithianes and Di(1,3-dithian-2-yl)zinc and Their Reaction with Highly Functionalized Halides and α,β-Unsaturated Carbonyl Compounds. *Synthesis (Stuttg).* 1174–1178 (1997).

81. Birch, A. J. Birch: Reduction by Dissolving Metats. Part I . . 117. Reduction by Dissolving Metals. Part 1. *J. Chem. Soc.* 430–436 (1942). doi:10.1039/jr9440000430

82. Zimmerman, H. E. & Wang, P. A. The Regioselectivity of the Birch Reduction. *J. Am. Chem. Soc.* **115**, 2205–2216 (1993).

83. Adam, J., Gosselain, P. A. & Goldfinger, P. Laws of addition and substitution in atomic reactions of halogens. *Nature* **171**, 704–705 (1953).

84. Incremona, J. H. & Martin, J. C. N-Bromosuccinimide. Mechanisms of Allylic Bromination and Related Reactions. *J. Am. Chem. Soc.* **92**, 627–634 (1970).

85. Clayden, J., Greeves, N. & Warren, S. *Organic Chemistry*. (Oxford Univeristy Press, 2012).

86. Lechuga-Eduardo, H., Romero-Ortega, M. & Olivo, H. F. Synthesis of Functionalized Ring C of Escobarines. *European J. Org. Chem.* **2016**, 51–54 (2016).

87. Wardrop, D. J. *et al.* Template-directed C-H activation: Development and application to the total synthesis of 7-episordidin. *Tetrahedron Asymmetry* **14**, 929–940 (2003).

88. Fringuelli, F., Piermatti, O., Pizzo, F. & Vaccaro, L. Indium Salt-Promoted Organic Reactions. *Curr. Org. Synth.* **3**, 1661–1689 (2003).

89. Smith, B. M. & Graham, A. E. Indium triflate mediated acetalization of aldehydes and ketones. *Tetrahedron Lett.* **47**, 9317–9319 (2006).

90. Lechuga-Eduardo, H., Romero-Ortega, M. & Olivo, H. F. Synthesis of Functionalized Ring C of Escobarines. *European J. Org. Chem.* **2016**, 51–54 (2016).

91. Benhida, R., Blanchard, P., Fourrey, J. & Chimle, I. De. A Mild and Effective Iodination Method Using Iodine in the Presence of Bis- (trifluoroacetoxy) iodobenzene. *Tetrahedron Lett.* **39**, 6849–6852 (1998).

92. Merkushev, E. ., Simakhina, N. . & Koveshnikova, G. . A New, Convenient Iodination Method of Aromatic Compounds. *Synthesis (Stuttg).* **6**, 486–487 (1980).

93. Faust, R. & Gobelt, B. Pd2(dba)3 CHC13/AsPh3 - a Powerful Catalyst System for Pd(0)-Mediated C-C-Bond Formation. *J. fur Prakt. Chemie* **340**, 90–93 (1998).

94. Kirsch, J. F. & Jencks, W. P. Base Catalysis of Imidazole Catalysis of Ester Hydrolysis. *J. Am. Chem. Soc.* **86**, 833–837 (1964).

95. Wang, L. & Clive, D. L. J. Reagent for Divalent Sulfur Protection: Preparation of 4-Methylbenzenesulfonothioic Acid, S-[[[(1,1-Dimethylethyl)-Dimethylsilyl]oxy]methyl] Ester. *Org. Synth.* **90**, 10 (2013).

96. Li, C. *et al.* Angiogenesis inhibitor epoxyquinol A: Total synthesis and inhibition of transcription factor NF-κB. *Org. Lett.* **4**, 3267–3270 (2002).

97. Hu, Y. *et al.* Exploring Chemical Diversity of Epoxyquinoid Natural Products: Synthesis and Biological Activity of (-)-Jesterone and Related Molecules. *Org. Lett.* **3**, 1649–1652 (2001).

98. Thadani, A. N., Stankovic, A. R. & Rawal, V. H. Enantioselective Diels-Alder reactions catalyzed by hydrogen bonding. *Proc. Natl. Acad. Sci. U. S. A.* **101**, 5846–5850 (2004).

99. WeiB, B. & Kuball, H.-G. TADDOLs with Unprecedented Helical Twisting Power in Liquid Crystals. *Helv. Chim. Acta* **80**, 2507–2514 (1997).

100. Seebach, D., Beck, A. K. & Heckel, A. TADDOLs, their derivatives, and TADDOL analogues: Versatile chiral auxiliaries. *Angew. Chemie - Int. Ed.* **40**, 92–138 (2001).

101. Wittkopp, A. & Schreiner, P. R. Metal-free, noncovalent catalysis of Diels - Alder reactions by Neutral hydrogen bond donors in organic solvents and in water. *Chem. - A Eur. J.* **9**, 407–414 (2003).

102. Schreiner, P. R. & Wittkopp, A. H-bonding additives act like lewis acid catalysts. *Org. Lett.* **4**, 217–220 (2002).

103. Sigman, M. S. & Jacobsen, E. N. Schiff base catalysts for the asymmetric strecker reaction identified and optimized from parallel synthetic libraries. *J. Am. Chem. Soc.* **120**, 4901–4902 (1998).

104. Okino, T., Hoashi, Y. & Takemoto, Y. Enantioselective Michael Reaction of Malonates to Nitroolefins Catalyzed by Bifunctional Organocatalysts. *J. Am. Chem. Soc.* **125**, 12672–12673 (2003).

105. Sohtome, Y., Tanatani, A., Hashimoto, Y. & Nagasawa, K. Development of bis-thiourea-type organocatalyst for asymmetric Baylis-Hillman reaction. *Tetrahedron Lett.* **45**, 5589–5592 (2004).

106. Herrera, R. P., Sgarzani, V., Bernardi, L. & Ricci, A. Catalytic enantioselective Friedel-Crafts alkylation of indoles with nitroalkenes by using a simple thiourea organocatalyst. *Angew. Chemie - Int. Ed.* **44**, 6576–6579 (2005).

107. Sigman, M. S., Vachal, P. & Jacobsen, E. N. A general catalyst for the asymmetric strecker reaction. *Angew. Chemie - Int. Ed.* **39**, 1279–1281 (2000).

108. Cao, C. L., Ye, M. C., Sun, X. L. & Tang, Y. Pyrrolidine-thiourea as a bifunctional organocatalyst: Highly enantioselective Michael addition of cyclohexanone to nitroolefins. *Organic Letters* **8**, 2901–2904 (2006).

109. Miyabe, H., Tuchida, S., Yamauchi, M. & Takemoto, Y. Reaction of nitroorganic compounds using thiourea catalysts anchored to polymer support. *Synthesis (Stuttg).* **2**, 3295–3300 (2006).

110. Neudorfl, J., Roland, K. & Berkessel, A. Asymmetric Morita−Baylis−Hillman Reaction Catalyzed by Isophoronediamine-Derived Bis(thio)urea Organocatalysts. *Org. Lett.* **8**, 4195–4198 (2006).

111. Kramer, C. S. & Bräse, S. Thiourea-catalyzed diels-alder reaction of a naphthoquinone monoketal dienophile. *Beilstein J. Org. Chem.* **9**, 1414–1418 (2013).

112. Held, F. E. & Tsogoeva, S. B. Asymmetric cycloaddition reactions catalyzed by bifunctional thiourea and squaramide organocatalysts: Recent advances. *Catal. Sci. Technol.* **6**, 645–667 (2016).

113. Zhang, S. J., Zhang, J., Zhou, Q. Q., Dong, L. & Chen, Y. C. Aminocatalytic asymmetric exo-Diels-Alder reaction with methiodide salts of Mannich bases and 2,4-dienals to construct chiral spirocycles. *Org. Lett.* **15**, 968–971 (2013).

114. Marcantonio, E. *et al.* Direct, Asymmetric Synthesis of Carbocycle-Fused Uracils via [4+2] Cycloadditions: a Noncovalent Organocatalysis Approach. *Adv. Synth. Catal.* **363**, 2625–2633 (2021).

115. Mao, Z. *et al.* Chiral tertiary amine thiourea-catalyzed asymmetric inverse-electron-demand Diels-Alder reaction of chromone heterodienes using 3-vinylindoles as dienophiles. *J. Org. Chem.* **78**, 10233–10239 (2013).

116. Zhao, P. & Beaudry, C. M. Enantioselective and regioselective pyrone Diels-Alder reactions of vinyl sulfones: Total synthesis of (+)-cavicularin. *Angew. Chemie - Int. Ed.* **53**, 10500–10503 (2014).

117. Wu, W., Min, L., Zhu, L. & Lee, C. S. A new class of enantioselective catalytic 2-pyrone Diels-Alder cycloadditions. *Adv. Synth. Catal.* **353**, 1135–1145 (2011).

118. Wang, Y. *et al.* Asymmetric Diels—Alder Reactions of 2-Pyrones with a Bifunctional Organic Catalyst. *ChemInform* **38**, (2007).

119. Min, C. & Seidel, D. Asymmetric Brønsted acid catalysis with chiral carboxylic acids. *Chem. Soc. Rev.* **46**, 5889–5902 (2017).

120. Hatano, M., Goto, Y., Izumiseki, A., Akakura, M. & Ishihara, K. Boron Tribromide-Assisted Chiral

Phosphoric Acid Catalyst for a Highly Enantioselective Diels-Alder Reaction of 1,2-Dihydropyridines. *J. Am. Chem. Soc.* **137**, 13472–13475 (2015).

121. Ahrendt, K. A., Borths, C. J. & MacMillan, D. W. C. New strategies for organic catalysis: The first highly enantioselective organocatalytic diels - Alder reaction. *J. Am. Chem. Soc.* **122**, 4243–4244 (2000).

122. Lelais, G. & MacMillan, D. W. C. Modern strategies in organic catalysis: The advent and development of iminium activation. *Aldrichimica Acta* **39**, 79–87 (2006).

123. Williams, R. M. Total synthesis and biosynthesis of the paraherquamides: An intriguing story of the biological Diels-Alder construction. *Chem. Pharm. Bull.* **50**, 711–740 (2002).

124. Birch, A. J. & Wright, J. J. The brevianamides: A new class of fungal alkaloid. *J. Chem. Soc. D Chem. Commun.* 644–645 (1969). doi:10.1039/C2969000644b

125. Finefield, J. M., Frisvad, J. C., Sherman, D. H. & Williams, R. M. Fungal origins of the bicyclo[2.2.2]diazaoctane ring system of prenylated indole alkaloids. *J. Nat. Prod.* **75**, 812–833 (2012).

126. Kato, H. *et al.* Notoamides A-D: Prenylated indole alkaloids isolated from a marine-derived fungus, Aspergillus sp. *Angew. Chemie - Int. Ed.* **46**, 2254–2256 (2007).

127. Fenical, W., Jensen, P. & Cheng, X. C. Avrainvillamide, a Cytotoxic Marine Natural Product, and the Derivatives thereof. U.S Patent 6,066,635. (2000).

128. Bird, B. A., Remaley, A. T. & Campbell, I. M. Brevianamides A and B are formed only after conidiation has begun in solid cultures of Penicillium brevicompactum. *Appl. Environ. Microbiol.* **42**, 521–525 (1981).

129. Bird, B. A. & Campbell, I. M. Disposition of mycophenolic acid, brevianamide A, asperphenamate, and ergosterol in solid cultures of Penicillium brevicompactum. *Appl. Environ. Microbiol.* **43**, 345–348 (1982).

130. Paterson, R. R. M., Simmonds, M. J. S., Kemmelmeier, C. & Blaney, W. M. Effects of brevianamide A, its photolysis product brevianamide D, and ochratoxin A from two Penicillium strains on the insect pests Spodoptera frugiperda and Heliothis virescens. *Mycol. Res.* **94**, 538–542 (1990).

131. Wilson, B. J., Yang, D. T. C. & Harris, T. M. Production, Isolation, and Preliminary Toxicity Studies of Brevianamide A from Cultures of Penicillium viridicatum. *Appl. Microbiol.* **26**, 633–635 (1973).

132. Xu, X., Zhang, X., Nong, X., Wang, J. & Qi, S. Brevianamides and mycophenolic acid derivatives from the deep-sea-derived fungus penicillium brevicompactum DFFSCS025. *Mar. Drugs* **15**, 4–13 (2017).

133. Steyn, P. S. The structures of five diketopiperazines from Aspergillus ustus. *Tetrahedron* **29**, 107–120 (1973).

134. Maiya, S., Grundmann, A., Li, S. M. & Turner, G. The fumitremorgin gene cluster of Aspergillus fumigatus: Identification of a gene encoding brevianamide F synthetase. *ChemBioChem* **7**, 1062–1069 (2006).

135. Wunsch, C., Mundt, K. & Li, S. M. Targeted production of secondary metabolites by coexpression of non-ribosomal peptide synthetase and prenyltransferase genes in Aspergillus. *Appl. Microbiol. Biotechnol.* **99**, 4213–4223 (2015).

136. Baldas, B. J., Birch, A. J. & Richard, A. Studies in Relation to Biosynthesis. Part X1W1 Incorporation of cyc/o-L-Tryptophyl-L-proline into Brevianamide A. *J. Chem. Soc., Perkin Trans. 1* 50 (1974).

137. Porter, A. E. A. & Sammes, P. G. A diels-alder reaction of possible biosynthetic importance. *J. Chem. Soc. D Chem. Commun.* 1103a (1970). doi:10.1039/C2970001103a

138. Birch, A. J. Terpenoid Compounds of Mixed Biogenetic Origins. *J. Agric. Food Chem.* **19**, 1088–1092 (1971).

139. Birch, A. J. & Russell, R. A. Studies in relation to biosynthesis-XLIV. Structural elucidations of brevianamides-B, -C, -D and -F. *Tetrahedron* **28**, 2999–3008 (1972).

140. Williams, R. M., Kwast, E. & Glinka, T. Facial Selectivity of the Intramolecular SN2' Cyclization: Stereocontrolled Total Synthesis of Brevianamide B. *J. Am. Chem. Soc.* 5927–5929 (1988).

141. Williams, R. M., Glinka, T., Kwast, E., Coffman, H. & Stille, J. Asymmetric, Stereocontrolled Total Synthesis

of (-)-Brevianamide B. *J. Am. Chem. Soc.* 808–821 (1990).

142. Williams, R. M. & Kwast, E. Carbanion-mediated oxidative deprotection of non-enolizable benzylated amides. *Tetrahedron Letters* **30**, 451–454 (1989).

143. Williams, R. M., Sanz-Cervera, J. F., Sancenon, F., Marco, J. A. & Halligan, K. Biomimetic Diels−Alder Cyclizations for the Construction of the Brevianamide, Paraherquamide Sclerotamide, and VM55599 Ring Systems. *Journal of the American Chemical Society* **120**, 1090–1091 (1998).

144. Williams, R. M., Sanz-Cervera, J. F., Sancenón, F., Marco, J. A. & Halligan, K. M. Biomimetic Diels-Alder cyclizations for the construction of the brevianamide, paraherquamide, sclerotamide, asperparaline and VM55599 ring systems. *Bioorganic Med. Chem.* **6**, 1233–1241 (1998).

145. Williams, R. M., Kwast, E., Coffman, H. & Glinka, T. Remarkable, Enantiodivergent Biogenesis of Brevianamide A and B. *J. Am. Chem. Soc.* **111**, 3064–3065 (1989).

146. Kametani, T., Ihara, M. & Kanaya, N. Studies on the syntheses of heterocyclic compounds. Part 876. The chiral total synthesis of brevianamide E and deoxybrevianamide E. *J. Chem. Soc. - Perkin Trans. 1* 959–963 (1981).

147. Sanz-Cervera, J. F., Glinka, T. & Williams, R. M. Biosynthesis of brevianamides A and B: in search of the biosynthetic diels-alder construction. *Tetrahedron* **49**, 8471–8482 (1993).

148. Adams, L. A., Valente, M. W. N. & Williams, R. M. A concise synthesis of d,l-brevianamide B via a biomimetically-inspired IMDA construction. *Tetrahedron* **62**, 5195–5200 (2006).

149. Greshock, T. J. & Williams, R. M. Improved biomimetic total synthesis of d, l-stephacidin A. *Org. Lett.* **9**, 4255–4258 (2007).

150. Greshock, T. J. & Williams, R. M. Additions and Corrections. *Org. Lett.* **14**, 6377–6378 (2012).

151. Domingo, L. R., Sanz-Cervera, J. F., Williams, R. M., Teresa Picher, M. & Alberto Marco, J. Biosynthesis of the brevianamides. An ab initio study of the biosynthetic intramolecular Diels-Alder cycloaddition. *J. Org. Chem.* **62**, 1662–1667 (1997).

152. Stocking, E. M., Sanz-Cervera, J. F. & Williams, R. M. Total synthesis of VM55599. Utilization of an intramolecular Diels - Alder cycloaddition of potential biogenetic relevance. *J. Am. Chem. Soc.* **122**, 1675–1683 (2000).

153. Zipse, H. & Wang, L. H. Bifunctional Catalysis of Ester Aminolysis - A Computational and Experimental Study. *Liebigs Ann.* 1501–1509 (1996). doi:10.1002/jlac.199619961004

154. Scott, P. M., Kennedy, B. P. C., Harwig, J. & Chen, Y.-K. Formation of Diketopiperazines by Penicillium italicum Isolated from Oranges . *Appl. Microbiol.* **28**, 892–894 (1974).

155. Kaur, A., Raja, H. A., Deep, G., Agarwal, R. & Oberlies, N. H. Pannorin B, a new naphthopyrone from an endophytic fungal isolate of Penicillium sp. *Magn. Reson. Chem.* **54**, 164–167 (2016).

156. Williams, R. M. & Cox, R. J. Paraherquamides, brevianamides, and asperparalines: Laboratory synthesis and biosynthesis. An interim report. *Acc. Chem. Res.* **36**, 127–139 (2003).

157. Frebault, F., Simpkins, N. S. & Fenwick, A. Concise enantioselective synthesis of ent-malbrancheamide B. *J. Am. Chem. Soc.* **131**, 4214–4215 (2009).

158. Frebault, F. C. & Simpkins, N. S. A cationic cyclisation route to prenylated indole alkaloids: Synthesis of malbrancheamide B and brevianamide B, and progress towards stephacidin A. *Tetrahedron* **66**, 6585–6596 (2010).

159. Fuchs, J. R., Mitchell, M. L., Shabangi, M. & Flowers, R. A. The effect of lithium bromide and lithium chloride on the reactivity of SmI2 in THF. *Tetrahedron Lett.* **38**, 8157–8158 (1997).

160. Proctor, D. J., Flowers, R. A. & Skrydstrup, T. *Organic Synthesis using Samarium Diiodide: A Practical Guide*. (RSC publishing: Cambridge, 2009).

161. Qin, W. F. *et al.* Total synthesis of (-)-depyranoversicolamide B. *Chem. Commun.* **51**, 16143–16146 (2015).

162. Robins, J. G., Kim, K. J., Chinn, A. J., Woo, J. S. & Scheerer, J. R. Intermolecular Diels-Alder Cycloaddition for the Construction of Bicyclo[2.2.2]diazaoctane Structures: Formal Synthesis of Brevianamide B and Premalbrancheamide. *J. Org. Chem.* **81**, 2293–2301 (2016).

163. Laws, S. W. & Scheerer, J. R. Enantioselective Synthesis of (+)-Malbrancheamide B. (2013).

164. Danishefsky, S. J., Prisbylla, M. P. & Hiner, S. The use of trans-Methyl beta-Nitroacrylate in Diels-Alder Reactions. *J. Am. Chem. Soc.* **100**, 2918–2920 (1978).

165. Baran, P. S., Hafensteiner, B. D., Ambhaikar, N. B., Guerrero, C. A. & Gallagher, J. D. Enantioselective total synthesis of avrainvillamide and the stephacidins. *J. Am. Chem. Soc.* **128**, 8678–8693 (2006).

166. Perkins, J. C., Wang, X., Pike, R. D. & Scheerer, J. R. Further Investigation of the Intermolecular Diels-Alder Cycloaddition for the Synthesis of Bicyclo[2.2.2]diazaoctane Alkaloids. *J. Org. Chem.* **82**, 13656–13662 (2017).

167. Qin, T. *et al.* Nickel-Catalyzed Barton Decarboxylation and Giese Reactions: A Practical Take on Classic Transforms. *Angew. Chemie - Int. Ed.* **56**, 260–265 (2017).

168. Godfrey, R. C., Green, N. J., Nichol, G. S. & Lawrence, A. L. Total synthesis of brevianamide A. *Nat. Chem.* **12**, 615–619 (2020).

169. Fisher, J. W. & Trinkle, K. L. Iodide dealkylation of benzyl, PMB, PNB, and t-Butyl N-acyl amino acid esters via lithium ion coordination. *Tetrahedron Lett.* **35**, 2505–2508 (1994).

170. Fölling, J. *et al.* Photochromic rhodamines provide nanoscopy with optical sectioning. *Angew. Chemie - Int. Ed.* **46**, 6266–6270 (2007).

171. Belov, V. N., Bossi, M. L., Fölling, J., Boyarskiy, V. P. & Hell, S. W. Rhodamine spiroamides for multicolor single-molecule switching fluorescent nanoscopy. *Chem. - A Eur. J.* **15**, 10762–10776 (2009).

172. Xu, F. & Smith, M. W. A General Approach to 2 , 2-Disubstituted Indoxyls : Total Synthesis of Brevianamide A and Trigonoliimine C.

173. Tan, C. J. *et al.* Three new indole alkaloids from trigonostemon lii. *Org. Lett.* **12**, 2370–2373 (2010).

174. Ye, Y. *et al.* Fungal-derived brevianamide assembly by a stereoselective semipinacolase. *Nat. Catal.* **3**, 497–506 (2020).

175. Birch, A. J. & Wright, J. J. Studies in relation to biosynthesis-XLII. The structural elucidation and some aspects of the biosynthesis of the brevianamides-A and -E. *Tetrahedron* **26**, 2329–2344 (1970).

176. Klas, K. R. *et al.* Structural and stereochemical diversity in prenylated indole alkaloids containing the bicyclo[2.2.2]diazaoctane ring system from marine and terrestrial fungi. *Nat. Prod. Rep.* **35**, 532–558 (2018).

177. Han, S., Morrison, K. C., Hergenrother, P. J. & Movassaghi, M. Total Synthesis, Stereochemical Assignment, and Biological Activity of All Known (−)-Trigonoliimines. (2014).

178. Schendera, E., Lerch, S., von Drathen, T., Unkel, L. N. & Brasholz, M. Phosphoric Acid Catalyzed 1,2-Rearrangements of 3-Hydroxyindolenines to Indoxyls and 2-Oxindoles: Reagent-Controlled Regioselectivity Enabled by Dual Activation. *European J. Org. Chem.* **2017**, 3134–3138 (2017).

179. Liu, H., Pattabiraman, V. R. & Vederas, J. C. Stereoselective syntheses of 4-oxa diaminopimelic acid and its protected derivatives via aziridine ring opening. *Org. Lett.* **9**, 4211–4214 (2007).

180. Schkeryantz, J. M., Woo, J. C. G., Siliphaivanh, P., Depew, K. M. & Danishefsky, S. J. Total synthesis of gypsetin, deoxybrevianamide E, brevianamide E, and tryprostatin B: Novel constructions of 2,3-disubstituted indoles. *J. Am. Chem. Soc.* **121**, 11964–11975 (1999).

181. Chengebroyen, J., Linke, M., Robitzer, M., Sirlin, C. & Pfeffer, M. Palladium-mediated intramolecular C-N bond formation involving allyl substituted pyridines. Application to a novel strategy for the synthesis of the skeleton of berberinium derivatives. *J. Organomet. Chem.* **687**, 313–321 (2003).

182. Kuttruff, C. A., Zipse, H. & Trauner, D. Concise total syntheses of variecolortides A and B through an unusual hetero-Diels-Alder reaction. *Angew. Chemie - Int. Ed.* **50**, 1402–1405 (2011).

183. Mintz, M. J. & Walling, C. t-Butyl hypochlorite. *Org. Synth.* **49**, 9 (1969).

184. Ley, S. V., Hewitt, P. R. & Cleator, E. A concise total synthesis of (+)-okaramine C. *Org. Biomol. Chem.* **2**, 2415–2417 (2004).

185. Schkeryantz, J. M., Woo, J. C. G., Siliphaivanh, P., Depew, K. M. & Danishefsky, S. J. Total synthesis of gypsetin, deoxybrevianamide E, brevianamide E, and tryprostatin B: Novel constructions of 2,3-disubstituted indoles. *Journal of the American Chemical Society* **121**, 11964–11975 (1999).

186. Zhao, L., May, J. P., Huang, J. & Perrin, D. M. Stereoselective synthesis of brevianamide e. *Org. Lett.* **14**, 90–93 (2012).

187. Soai, K. & Ookawa, A. Asymmetric Synthesis of Optically Active threo- and erythro-Pyrrolidinylbenzyl Alcohol by the Highly Stereospecific Arylation of (S)-Proline and the Subsequent Highly Diastereoselective Reduction of the a-Amino Ketone. *J. Chem. Soc., Perkin Trans. 1* 1465–1471 (1987). doi:10.1002/recl.19720910713

188. Huy, P., Neudörfl, J. M. & Schmalz, H. G. A practical synthesis of trans -3-substituted proline derivatives through 1,4-addition. *Org. Lett.* **13**, 216–219 (2011).

189. Ding, Y., Greshock, T. J., Miller, K. A., Sherman, D. H. & Williams, R. M. Premalbrancheamide: Synthesis, isotopic labeling, biosynthetic incorporation, and detection in cultures of Malbranchea aurantiaca. *Org. Lett.* **10**, 4863–4866 (2008).

190. David, N., Pasceri, R., Kitson, R. R. A., Pradal, A. & Moody, C. J. Formal Total Synthesis of Diazonamide A by Indole Oxidative Rearrangement. *Chemistry - A European Journal* **22**, 10867–10876 (2016).

191. Meot-Ner, M. The ionic hydrogen bond. *Chem. Rev.* **105**, 213–284 (2005).

192. Hubbard, R. E. & Kamran Haider, M. Hydrogen Bonds in Proteins: Role and Strength. *Encycl. Life Sci.* (2010). doi:10.1002/9780470015902.a0003011.pub2

193. Guthrie, J. P. Short strong hydrogen bonds: Can they explain enzymic catalysis? *Chem. Biol.* **3**, 163–170 (1996).

194. Lin, X. & Grinstaff, M. W. Ionic supramolecular assemblies. *Isr. J. Chem.* **53**, 498–510 (2013).

195. Song, F. *et al.* Brevianamides with antitubercular potential from a marine-derived isolate of aspergillus versicolor. *Org. Lett.* **14**, 4770–4773 (2012).

196. Li, G. Y. *et al.* Brevianamide J, A new indole alkaloid dimer from fungus Aspergillus versicolor. *Org. Lett.* **11**, 3714–3717 (2009).

197. Cai, R. *et al.* (-)- And (+)-Asperginulin A, a Pair of Indole Diketopiperazine Alkaloid Dimers with a 6/5/4/5/6 Pentacyclic Skeleton from the Mangrove Endophytic Fungus Aspergillus sp. SK-28. *Org. Lett.* **21**, 9633–9636 (2019).

198. Green, N. J. *et al.* Bio-inspired Domino oxa-Michael/Diels–Alder/oxa-Michael Dimerization of para-Quinols. *Angew. Chemie - Int. Ed.* **57**, 6198–6202 (2018).

199. De Silvestro, I., Drew, S. L., Nichol, G. S., Duarte, F. & Lawrence, A. L. Total Synthesis of a Dimeric Thymol Derivative Isolated from Arnica sachalinensis. *Angew. Chemie - Int. Ed.* **56**, 6813–6817 (2017).

200. Thomson, M. I., Nichol, G. S. & Lawrence, A. L. Total Synthesis of (−)-Angiopterlactone B. *Org. Lett.* **19**, 2199–2201 (2017).

201. O'Connell, K. M. G., Díaz-Gavilán, M., Galloway, W. R. J. D. & Spring, D. R. Two-directional synthesis as a tool for diversityoriented synthesis: Synthesis of alkaloid scaffolds. *Beilstein J. Org. Chem.* **8**, 850–860 (2012).

202. Hausler, J. Darstellung von cis- und trarts-C-3-substituierten Prolinverbindungen. *Liebigs Ann. der Chemie* 1073–1088 (1981).

203. Movassaghi, M., Ashenhurst, J. & Kim, J. Total Synthesis of (+)-11,11'-Dideoxyverticillin A. *Science (80-.).* **234**, 238–241 (2009).

204. Corbett, D. F. 1,3-Dipolar Addition Reactions of 6-Ethylideneolivanic Acid Derivatives With Diazomethane and Acetonitrile Oxide. *J. Chem. Soc. Perkin Trans. 1* 421–428 (1986). doi:10.1039/p19860000421

205. Kayser, S. *et al.* Stereoselective Synthesis of New (2 S,3 R)-3-Carboxyphenyl)pyrrolidine-2-carboxylic Acid Analogues Utilizing a C(sp3)-H Activation Strategy and Structure-Activity Relationship Studies at the Ionotropic Glutamate Receptors. *ACS Chem. Neurosci.* **11**, 674–701 (2020).

206. Xu, X., Cheng, D. & Pei, W. Iron-Catalyzed Homocoupling of Bromide Compounds. *J. Org. Chem.* **71**, 6637–6639 (2006).

207. Wurtz, A. Ueber eine neue Klasse organischer Stickstoffverbindungen. *Justus Liebigs Ann. Chem.* **129**, 129–149 (1864).

208. Ren, H., Krasovskiy, A. & Knochel, P. Stereoselective preparation of functionalized acyclic alkenylmagnesium reagents using i-PrMgCl-LiCl. *Org. Lett.* **6**, 4215–4217 (2004).

209. Ullman, F. & Bielecki, J. Ueber Synthesen in der Biphenylreihe. *European J. Org. Chem.* **34**, 2174–2185 (1901).

210. Zhang, S., Zhang, D. & Liebeskind, L. S. Ambient Temperature, Ullmann-like Reductive Coupling of Aryl, Heteroaryl, and Alkenyl Halides. *J. Org. Chem.* **62**, 2312–2313 (1997).

211. Yasamut, K., Jongcharoenkamol, J., Ruchirawat, S. & Ploypradith, P. A modified Cu(0)-Cu(I)-mediated Caryl-CarylUllmann coupling for the synthesis of biaryls. *Tetrahedron* **72**, 5994–6000 (2016).

212. Wasserman, H. H. *et al.* Singlei Oxygen in Synthesis. Formation of d,Z- and mew-Isochrysohermidin from a 3,3'-Bipyrrole Precursor. *Tetrahedron* **53**, 8731–8738 (1997).

213. Naora, H., Ohnuki, T. & Nakamura, A. A New Method of Synthesizing 7-(2-Hydroxy-5-oxo-1-cyclopentenyl)heptanoic Acid and Related Compounds. *Bulletin of the Chemical Society of Japan* **61**, 2401–2404 (1988).

214. Kaushik, M., Qi, M., Godt, A. & Corzilius, B. Bis-Gadolinium Complexes for Solid Effect and Cross Effect Dynamic Nuclear Polarization. *Angew. Chemie - Int. Ed.* **56**, 4295–4299 (2017).

215. Jin, B., Liu, Q. & Sulikowski, G. A. Development of an end-game strategy towards apoptolidin: A sequential Suzuki coupling approach. *Tetrahedron* **61**, 401–408 (2005).

216. Wulff, W. D. *et al.* A Regioselective Entry to Vinyllithiums from Unsymmetrical Ketones via Enol Triflates. *J. Org. Chem.* **52**, 277–279 (1986).

217. Paterson, I., Paquet, T. & Dalby, S. M. Synthesis of the macrocyclic core of leiodermatolide. *Org. Lett.* **13**, 4398–4401 (2011).

218. Paterson, I., Kan, J. & Gibson, L. Synthesis of the C1-C13 Tetraenoate Subunit of the Chivosazoles. *Org. Lett.* **12**, 3724–3727 (2010).

219. Farina, V., Kapadia, S., Krishnan, B., Wang, C. & Liebeskind, L. S. On the Nature of the "Copper Effect" in the Stille Cross-Coupling. *J. Org. Chem.* **59**, 5905–5911 (1994).

220. Huwyler, N., Radkowski, K., Rummelt, S. M. & Fürstner, A. Two Enabling Strategies for the Stereoselective Conversion of Internal Alkynes into Trisubstituted Alkenes. *Chem. - A Eur. J.* **23**, 12412–12419 (2017).

221. Mee, S. P. H., Lee, V. & Baldwin, J. E. Significant enhancement of the Stille reaction with a new combination of reagents-copper(I) iodide with cesium fluoride. *Chem. - A Eur. J.* **11**, 3294–3308 (2005).

222. Mukaiyama, T., Matsuo, J. I. & Kitagawa, H. A new and one-pot synthesis of α,β-unsaturated ketones by dehydrogenation of various ketones with n-tert-butyl phenylsulfinimidoyl chloride. *Chemistry Letters* 1250–1251 (2000). doi:10.1246/cl.2000.1250

223. Hara, S., Makino, K. & Hamada, Y. Stereoselective synthesis of protected (2S,3S)-N-methyl-5-

hydroxyisoleucine, a component of halipeptins. *Tetrahedron* **60**, 8031–8035 (2004).

224. Matsuo, J. I., Tanaki, Y. & Ishibashi, H. Oxidative Mannich reaction of N-carbobenzyloxy amines with 1,3-dicarbonyl compounds. *Org. Lett.* **8**, 4371–4374 (2006).

225. Hanessian, S., Dorich, S. & Menz, H. Concise and stereocontrolled synthesis of the tetracyclic core of daphniglaucin C. *Org. Lett.* **15**, 4134–4137 (2013).

226. Li, Y. *et al.* Novel Pyrrolopyridone Bromodomain and Extra-Terminal Motif (BET) Inhibitors Effective in Endocrine-Resistant ER+ Breast Cancer with Acquired Resistance to Fulvestrant and Palbociclib. *J. Med. Chem.* **63**, 7186–7210 (2020).

227. Selva, A., Casnati, G., Barbetta, M. & Pochini, A. NEOECHINULINE: A NEW INDOLE METABOLITE FROM ASPERGILLUS AMSTELODA. *Tetrahedron Lett.* **566**, 4457–4460 (1969).

228. Casnati, G., Pochini, A. & Ungaro, R. No Title. *Gazz. Chim. Ital.* **103**, 141 (1973).

229. Davis, D. A. & Gribble, G. W. DIMERIZATION OF INDOLO[1,2-b][2,7]NAPHTHYRIDINE-5,12-QUINONE. *Heterocycles* **34**, 1613–1621 (1992).

230. Volpin, G., Vepřek, N. A., Bellan, A. B. & Trauner, D. Enantioselektive Synthese und Racemisierung von (−)-Sinoracutin. *Angew. Chemie* **129**, 916–920 (2017).

231. Oikawa, Y. & Yonemitsu, O. Selective Oxidation of the Side Chain at C-3 of Indoles. *J. Org. Chem.* **42**, 1213–1216 (1977).

232. Carbery, D. R. Enamides: Valuable organic substrates. *Org. Biomol. Chem.* **6**, 3455–3460 (2008).

233. Spieß, P., Berger, M., Kaiser, D. & Maulide, N. Direct Synthesis of Enamides via Electrophilic Activation of Amides. *J. Am. Chem. Soc.* **143**, 10524–10529 (2021).

234. Kishi, Y., Nagano, H., Takamatsu, N., Murata, J. & Inoue, S. Synthetic Studies on Echinulin and Related Natural Products. V. : Isolation, Structure and Synthesis of Echinulin-Neoechinulin Type Alkaloids isolated from Aspergillus amstelodami. *Chem. Pharm. Bull.* **97**, 576–581 (1977).

235. Kishi, Y., Takamatsu, N. & Inoue, S. Synthetic Studies on Echinulin and Related Natural Products. III. *Chem. Pharm. Bull.* **97**, 564–568 (1977).

236. Kishi, Y., Takamatsu, N. & Inoue, S. Synthetic Studies on Echinulin and Related Natural Products. II. *Chem. Pharm. Bull.* **97**, 558–563 (1977).

237. Hausler, J., Jahn, R. & Schmidt, U. Radikalisch und photochemisch initiierte Oxidation von Aminosaurederivaten. *Chem. Ber.* **111**, 361–366 (1978).

238. Still, W. C., Kahn, M. & Mitra, A. Rapid Chromatographic Technique for Preparative Separations with Moderate Resolution. *J. Org. Chem.* **43**, 2923–2925 (1978).

239. Ipaktschi, J., Heydari, A. & Kalinowski, H. -O. Chelat-kontrollierte diastereoselektive Addition an α,ß-Epoxy-Aldehyde. *Chem. Ber.* **127**, 905–909 (1994).

240. Nemoto, T., Ohshima, T. & Shibasaki, M. Catalytic asymmetric synthesis of ??,??-epoxy esters, aldehydes, amides, and ??,??-epoxy ??-keto esters: Unique reactivity of ??,??-unsaturated carboxylic acid imidazolides [16]. *J. Am. Chem. Soc.* **123**, 9474–9475 (2001).

241. Piens, N. *et al.* Diastereoselective synthesis of 3-acetoxy-4-(3-aryloxiran-2-yl)azetidin-2-ones and their transformation into 3,4-oxolane-fused bicyclic β-lactams. *Org. Biomol. Chem.* **14**, 11279–11288 (2016).

242. Hoffman, R. V & Kim, H. Synthesis and reactions of 3-hydroxy-2-nosyloxy esters produced by the stereoselective reduction of 2-nosyloxy-3-keto esters. *J. Org. Chem.* **56**, 6759–6764 (1991).

243. Vanga, D. G. & Kaliappan, K. P. Total syntheses of rubiginone A2, C2, and fujianmycin A. *RSC Adv.* **4**, 12716–12722 (2014).

244. Sanz Sharley, D. D. & Williams, J. M. J. Acetic acid as a catalyst for the N-acylation of amines using esters as

the acyl source. *Chem. Commun.* **53**, 2020–2023 (2017).

245. Rodeschini, V., Simpkins, N. S. & Zhang, F. Chiral Lithium Amide Base Desymmetrisation of a Ring Fused Imide: Formation of (3aS,7aS)-2-[2-(3,4-Dimethoxyphenyl)-ethyl]-1,3-dioxo-octahydro-isoindole-3a-carboxylic acid methyl ester. *Org. Synth.* **84**, 306–316 (2007).

246. Callis, D. J., Thomas, N. F., Pearson, D. P. J. & Potter, B. V. L. A Tandem Horner-Emmons Olefination-Conjugate Addition Approach to the Synthesis of 1,5-Disubstituted-6-azabicyclo[3.2.1]octanes Based on the AE Ring Structure of the Norditerpenoid Alkaloid Methyllycaconitine. *J. Org. Chem.* **61**, 4634–4640 (1996).

247. Beck, A. K., Gysi, P., Vecchia, L. & Seebach, D. (4R,5R)-2,2-DIMETHYL-a,a,a',a'-TETRA(NAPHTH-2-YL)-1,3-DIOXOLANE-4,5-DIMETHANOL FROM DIMETHYL TARTRATE AND 2-NAPHTHYL-MAGNESIUM BROMIDE. *Org. Synth.* **76**, 12 (1999).

248. Ding, K., Zhao, D. & Du, H. Enantioselective Catalysis of the Hetero-Diels – Alder Reaction between Brassard s Diene and Aldehydes by Hydrogen-Bonding Activation : A One-StepSynthesis of (S)-(+)-Dihydrokawain. *European J. Org. Chem.* **10**, 5964–5970 (2004).

249. Schmitz, C., Leitner, W. & Franciò, G. Ni-Catalyzed Asymmetric Cycloisomerization of Dienes by Using TADDOL Phosphoramidites. *Chem. - A Eur. J.* **21**, 10696–10702 (2015).

250. Huy, P., Neudörfl, J. M. & Schmalz, H. G. A practical synthesis of trans -3-substituted proline derivatives through 1,4-addition. *Org. Lett.* **13**, 216–219 (2011).

251. Gao, X., Han, J. & Wang, L. Design of Highly Stable Iminophosphoranes as Recyclable Organocatalysts: Application to Asymmetric Chlorinations of Oxindoles. *Org. Lett.* **17**, 4596–4599 (2015).

252. Haeusler, J. Darstellung von cis- und trans-C-3-substituierten Prolinverbindungen. *Liebigs Ann. der Chemie* **6**, 1073–1088 (1981).

253. Huwyler, N., Radkowski, K., Rummelt, S. M. & Fürstner, A. Two Enabling Strategies for the Stereoselective Conversion of Internal Alkynes into Trisubstituted Alkenes. *Chem. - A Eur. J.* **23**, 12412–12419 (2017).

254. Trost, B. M., Masters, J. T., Lumb, J. P. & Fateen, D. Asymmetric synthesis of chiral cycloalkenone derivatives via palladium catalysis. *Chem. Sci.* **5**, 1354–1360 (2014).

255. Sezen, B. & Sames, D. Oxidative C-arylation of free (NH)-heterocycles via direct (sp3) C-H bond functionalization. *Journal of the American Chemical Society* **126**, 13244–13246 (2004).

256. Kametani, T., Kanaya, N. & Ihara, M. Asymmetric Total Synthesis of Brevianamide E. *J. Am. Chem. Soc.* **102**, 3974–3975 (1980).

257. Adam, W., Bosio, S. G. & Wolff, B. T. Chiral-auxiliary-controlled diastereoselectivity in the epoxidation of enecarbamates with DMD and mCPBA. *Org. Lett.* **5**, 819–822 (2003).